Assessment of the *in vitro* and *in vivo* effects of alpha cell toxins on the structure and morphology of the pancreatic islets.

Natalie Klempel, MSc
School of Biomedical Sciences
Faculty of Life and Health Sciences
Ulster University

Thesis submitted for the degree of
Doctor of Philosophy
May 2020

I confirm that the word count of this thesis is less than 100,000 words excluding the title page, contents, acknowledgments, abstract, tables, figures and references.

Contents

Acknowledgements

I would like to express my deepest appreciation and dedicate my thesis to my supervisors, Professor Peter Flatt and Dr. Charlotte Moffett. Thank you for all of the guidance, encouragement, and support offered to me every step of the way. I greatly appreciate the opportunity you have given me to join the Diabetes Research Group at Ulster University. Thank you for strengthening me to become a better researcher.

Thank you to my friends and colleagues, past and present within the DRG: Dr. Neil Tanday, Dr. Shruti Mohan, Dr. Rachelle Perry, Dr. Chris McLaughlin, Dr. Andrew McCloskey, Ryan Lafferty, Sarah Craig, Shaun Sharkey, Ade Owolabi, Mark Campbell, Nathan Scott, and placement students for their support, help, and always providing a laugh. For the Biomedical stores, Lisa, Davey, and Rob, for providing laughter and a listening ear, as well as the much-needed supplies to carry out these projects. A huge thank you to Keith Thomas for all of the help with my cell work and to Dr. Joerg Arnscheidt for help with the German articles.

To my amazing boyfriend, Rob Duff. Thank you for encouragement, support, and belief in me. Thank you for making me laugh and always listening to me when I needed to vent or cry. Thank you for always seeing the positive in life. To my friend, Richard Mullan, a huge thank you for all of your support and belief in me. Thank you for providing a listening ear these past few years. To my mentor and friend, Dr. Collin Thomas; for helping pursue my dream of higher education. A thank you to my best friend, Courtney Bowers, although we are miles apart you never stopped believing and encouraging me. To Tim Morrison and Mike Baughman; a huge thank you for your support, friendship, and belief in me. To those who could not be here to see me accomplish my PhD: Ed and Lois Walsh and Brett Brackett. You are deeply missed, and I know you have been with me every step of the way. To my brother, Zach and his family; Lauren, Tyler, Lane, and Mattie, a huge thank you for the Skype calls to make me laugh, and for your support for the move to Northern Ireland to pursue this degree. To my Aunt Diane and Uncle Blake for supporting me to follow my dreams. To my mom; who always believed, supported, and inspired me every step of the way. I could not have done this without you. Thank you for always being there and encouraging me to do my best. I love you mom.

The studies within this thesis were supported by the Vice-Chancellor Research Scholarship award from the University of Ulster.

Summary

Synthalin A (Syn A) is a pancreatic alpha cell toxin that enjoyed much early research which was discontinued in the early 1950's. As a result, the information to date is limited on this toxin but is reported to display lowering blood glucose levels *in vivo*. There were limited studies on how this toxin only targeted alpha cells and not the pancreatic beta cells and its mechanism. Cobalt chloride, although still being researched today in different avenues, was also reported as being a selective alpha cell toxin in early studies, but such work has also stopped. Both toxins have been said to be species specific, however nothing is mentioned about strain specificity. Tests were coupled with observations with the beta cell toxin, streptozotocin, in the hope to see how the alpha cell toxins compared in terms of mechanism of the destruction of alpha cells. This thesis examines actions in normal and transgenic mice and, normal rats. These different animal models provided insight to the past literature on the changes seen with human subjects given these toxins. Indeed, animals treated with Syn A or cobalt showed alpha cell loss due to apoptosis and dedifferentiation, but also displayed altered beta cell populations likely due to transdifferentiation. Gross anatomical changes, associated with these alpha cell toxins, were also noted in several organs including pallor, blood clots, and stomach distension. Toxicity of Syn A and cobalt was further assed in GLP-1 (GLUTag), insulin (Min-6), and glucagon (Alpha TC) secreting cell lines. Both agents impaired cellular viability across all tested cell lines, with greater effects in alpha and GLUTag cells. In-depth examination uncovered disturbances in gene expression, proliferation, and apoptosis caused by toxin exposure. Collectively, these data confirm that both Syn A and cobalt have detrimental effects on alpha cell function. Contrary to past literature these effects are consistent within rodents.

Abbreviations

AMPK	AMP- activated protein kinase
ARX	Aristaless related homeobox
AUC	Area under the curve
BBRU	Biomedical and Behavioural Research Unit
BSA	Bovine serum albumin
cm	Centimetre
DAPI	4', 6'-diamidino-2-phenylindole
DMSO	Dimethyl sulfoxide
DNA	Deoxyribonucleic acid
FBS	Foetal bovine serum
FITC	Fluorescein isothiocyante
g	Gram
GFP	Green fluorescent protein
GLP-1	Glucagon-like peptide 1
Gcg rec null	Glucagon receptor null
GTT	Glucose tolerance test
HBSS	Hanks balanced salt solution
HCl	Hydrochloric acid
HEPES	4-(2-Hydroxyethyl)-1-piperazineethanesulfonic acid
i.p.	Intraperitoneal injection
Ins	Insulin
KCl	Potassium chloride
kg	Kilogram
KRBB	Krebs Ringer bicarbonate buffer
L	Litre
min	Minute
mg	Milligram
mgm	Milligram
ml	Millilitre

mM	Millimolar
mRNA	Messenger ribonucleic acid
MTT	3-(4,5-dimethylthylthiazol-2-yl)-2,5-diphenytetrazolium bromide
NaCl	Sodium chloride
PBS	Phosphate buffered saline
PC1	Prohormone convertase 1
PCR	Polymerase chain reaction
PFA	Paraformaldehyde
RIA	Radioimmunoassay
STZ	Streptozotocin
Syn A	Synthalin A
Syn A (M)	Syn A multiple dose
Syn A (S)	Syn A single dose
T1D	Type 1 diabetes
T2D	Type 2 diabetes
TRITC	Teramethylrhodamine isothiocyanate
TRIS	Trisaminomethane
TUNEL	Terminal deoxynucleotidyl transferase dUTP nick end labelling
TZD	Thiazolidinediones
UK	United Kingdom
USA	United States of America
µg	Microgram
µl	Microliter
°C	Degrees Celsius
%	Percentage
1°	Primary
2°	Secondary

Declaration

“I hereby declare that for 2 years following the date on which the thesis is deposited in the Research Office of Ulster University, the thesis shall remain confidential with access or copying prohibited. Following expiry of this period I permit:

1. The Librarian of the University to allow the thesis to be copied in whole or in part without reference to me on the understanding that such authority applies to the provision of single copies made for study purposes or for inclusion within the stock of another library

2. The thesis to be made available through the Ulster Institutional Repository and/or EThOSunder the terms of the Ulster eTheses Deposit Agreement which I have signed.

IT IS A CONDITION OF USE OF THIS THESIS THAT ANYONE WHO CONSULTS IT MUST RECOGNISE THAT THE COPYRIGHT RESTS WITH THE UNIVERSITY AND THEN SUBSEQUENTLY TO THE AUTHOR ON THE EXPIRY OF THIS PERIOD AND THAT NO QUOTATION FROM THE THESIS AND NO INFORMATION DERIVED FROM IT MAY BE PUBLISHED UNLESS THE SOURCE IS PROPERLY ACKNOWLEDGED.

Chapter 1
Introduction

1.1 Diabetes Mellitus

Diabetes Mellitus is a bi-hormonal disease characterized by hypoglycemia due to hypoinsulinaemia and hyperglucagonemia predisposed by genetic and environmental factors (Hruban and Iacobuzio-Donahue, 2015; Ashcroft and Rorsman, 2012; Parker *et al.*2002). There are two main types of diabetes: type 1 (T1D); characterized by immune-mediated beta cell destruction and type 2 (T2D); often due to obesity, life style factors, and genetics (Mansur *et al.*2015; Mieczkowska *et al.* 2015; Koh *et al.*2014; Ashcroft and Rorsman, 2012; Pocock and Richards, 2009). In the islets of Langerhans, insulin is a hormone which is secreted from the pancreatic beta cells and lowers an individual's blood glucose levels (Marieb and Hoehn, 2013; Rorsman and Renström, 2003). The pancreatic alpha cells, the main focus of this research, secrete glucagon, a 29-amino acid peptide hormone (Chiras, 2015; Martini *et al.* 2015; Conarello *et al.*2007; Sørensen *et al.*2006; Gelling *et al.*2003). Glucose levels increase when glucagon is released into the blood and act as a counter regulating hormone to insulin (Chiras, 2015; Martini *et al.* 2015; Conarello *et al.*2007; Sørensen *et al.*2006; Lefèbvre, 1995).

1.1.1 Type 2 Diabetes

Type 2 diabetes (T2D) is promoted by obesity, lifestyle factors, and genetics (Koh *et al.* 2014; Ashcroft and Rorsman, 2012; Pocock and Richards, 2009). Individuals who have a relative with first degree T2D are at an increased risk of developing the disease compared to those without a genetic component (Kumar *et al.* 2015). Obesity causes insulin resistance and, in the early phases of T2D, this leads to beta cell hyper-activity and hyperinsulinemia. Eventually, the dysfunctional beta cells become exhausted resulting in overt hyperglycaemia (Hruban and Iacobuzio-Donahue, 2014). T2D is treated by changes in lifestyle, including dietary restrictions, increased physical activity, as well as anti-diabetic medications: biguanides, sulphonylureas, meglitinides, alpha-glucosidase inhibitors, glitazones, GLP-1 mimetics, gliptins, amylin analogues, and SGLT2 inhibitors (Rivas *et al.* 2016; Hruban and Iacobuzio-Donahue, 2014; Halban *et al.* 2014; Nice Guidelines, 2012; Inzucchi, 2009; Modak *et al.* 2007; Bailey and Day, 2004; Seaquist, 2004; Dey *et al.* 2002).

1.2 Prevalence and complications

The prevalence of diabetes is examined within this Section, starting with a worldwide view of prevalence of diabetes. There are several comorbidities and complications that occur with diabetes; blindness, kidney failure, cardiovascular disease, and amputations (WHO, 2016; USRDS, 2014). In individuals with diabetes, the blood vessels and nerves become damaged and in about 2.6% of all cases of blindness is due to diabetes. This is known as diabetic retinopathy (WHO, 2016; Bourne *et al.* 2013). Macrovascular damage also occurs and increases the risk of stroke and myocardial infarctions by 2-3-fold (WHO, 2016; Emerging Risk Factors Collaboration, *et al.*, 2010). Death due to diabetes is relatively high, 1.5 million individuals having died in 2012 and another 2.2 million dying due to elevated blood glucose levels (WHO, 2016). Almost half of those who have a documented death due to elevated blood glucose die before the age of 70 (WHO, 2016). In the space of four years, death by diabetes has increased from 4.6 million in 2011 to 5.0 million in 2015 (IDF, 2015; Ashcroft and Rorsman, 2012).

1.2.1 Worldwide

The World Health Organization (WHO) last published statistics on diabetes in 2014. This organization states that since the 1980's diabetes has increased from 108 million to 422 million, particularly in middle to low income countries (WHO, 2016). Diabetes in those over the age of 18 has increased in this time from 4.7% to 8.5% and is expected to become the 7th leading cause of death in 2030 (WHO, 2016; Mathers and Loncar, 2006). The International Diabetes Federation claims that 463 million people worldwide are living with diabetes and, by the year 2045, 700 million people will have diabetes (IDF, 2019a). As of 2019, Diabetes prevalence was smaller in Africa, with only 4.7% of adults with diabetes. Whereas the Middle East and North Africa, had the highest prevalence at 12.2%. North America and Caribbean, South East Asia, and Western Pacific region displayed about 11% of prevalence. Europe had a prevalence of 6.3% of adults with diabetes (IDF, 2019b).

1.2.2 United Kingdom

In 2013, 6% of people over the age of 17 were diagnosed with diabetes. As obesity is a risk factor for type 2 diabetes (T2D), 90% of the adults aged 16-54 with T2D were also overweight or obese, and in England 12.4% of adults with diabetes are obese (Gatineau *et al.* 2014). The prevalence of diabetes is always increasing within the United Kingdom (UK). In 2015 roughly 3.5 million people were living with diabetes in the UK whereas the number increased to 3.8 million in 2018 (Diabetes UK, 2018a and 2016b). In Table 1.1, the countries within the United Kingdom are listed.

Table 1.1: United Kingdom and diagnosed diabetes in 2017-2018

Prevalence	2017-18
England	3,222,559
Northern Ireland	96,114
Scotland	295,753
Wales	195,693
UK	3,809,119

Table 1.1 above shows the different countries in the United Kingdom and the number of people who have been diagnosed with diabetes in 2018. (Adapted from Diabetes UK, 2018a).

Specifically looking at Northern Ireland, the number of individuals living with T2D is around 96,114 whereas the individuals living with the disease, even those not diagnosed is estimated to be around 104,000. Within the last 5 years, the prevalence of diabetes has increased dramatically by 33% whereas the increase was 25% in England, 20% in Wales, and 18% in Scotland (Diabetes UK, 2018b and 2016a). When broken down by trusts, the Northern trust had the highest prevalence of individuals, 6.5%, living with diabetes, whereas the Southern trust only showed 5.4% of diabetic individuals (Diabetes UK, 2018b).

1.3 Anatomy of the pancreas

Diabetes, whether it is T1D or T2D, is a disease associated with deranged function of the endocrine pancreas. The exocrine section of the pancreas is made up of lobules that contain clusters of tubuloacinar glands, whereas the endocrine pancreas is comprised of the islets of Langerhans. In humans, the islets account for 1-4% of the pancreatic volume, however, in rodents they account for 1-2%. The mesenteric anatomical layout of a rodent pancreas is different from the compact structure of the human pancreas as seen in Figure 1.1 (Liggitt and Dintzis, 2018; Dolenšek *et al.* 2015). This layout of the pancreas allows the main lobes of the rodent pancreas to be separated by different types of tissue, such as adipose and lymphatic (Dolenšek *et al.* 2015). Islet size in humans is roughly 50 ± 29 µm whereas the average diameter of an islet in mice is 116 ± 80 µm. In rats the islet size is 100-200 µm. Beta cells within the human pancreas are not as prominent as they are in mice, and only account for ± 55%. However, the alpha cells in the human pancreas are higher than a mouse and make up about ± 37%. Islet distribution is disproportionate throughout the pancreas, having ± 75% beta cells and ± 18% alpha cells, and the islets are proportionate to the rodent's body mass (Liggitt and Dintzis, 2018).

When comparing the head (the duodenal lobe) to the tail (the splenic lobe), the amount of beta cells is higher in the duodenal lobe (Dolenšek *et al.* 2015; Moffett, 2013; Hörnblad *et al.* 2011; Trimble *et al.* 1982). The way the islet is composed of alpha and beta cells tends to be different between species, which can be found in sections 1.4.2 through 1.4.7 (Steiner *et al.* 2010). Rats and mice have similar pancreatic duct architecture, where the primary duct and the bile duct join before entering the duodenum, however, in humans these two ducts join at the greater duodenal papillae. Rodents have many accessory ducts, whereas humans only have a single one (Liggitt and Dintzis, 2018).

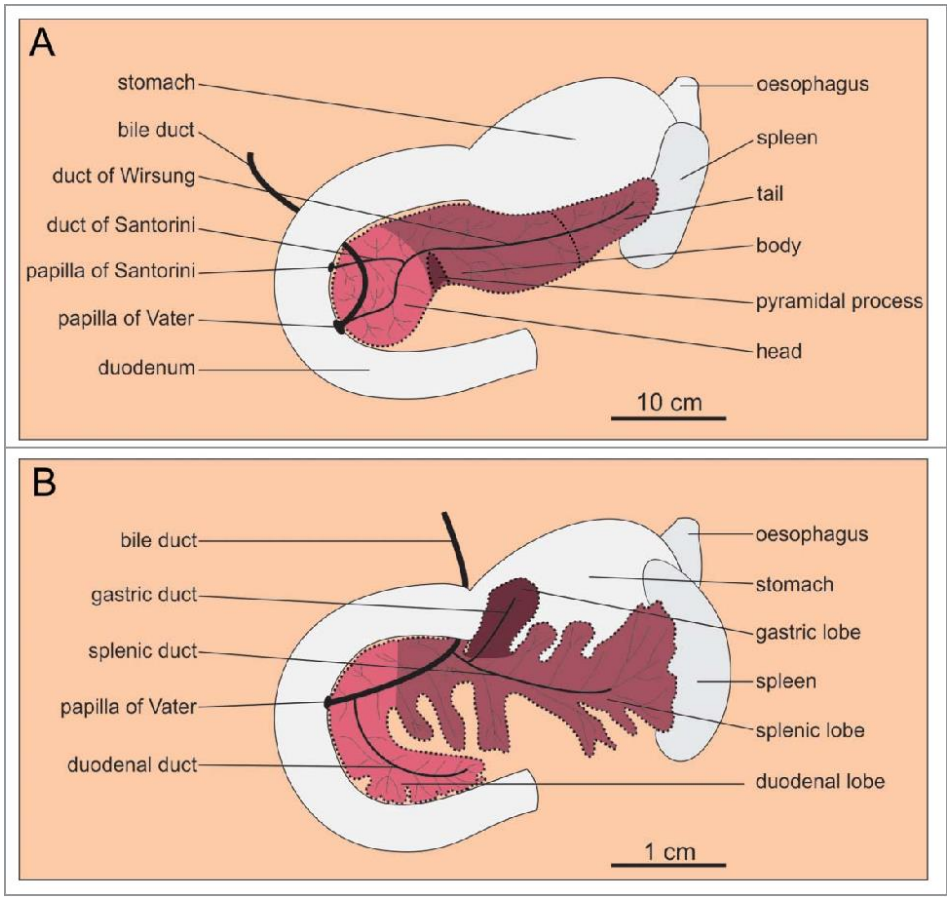

Figure 1.1 shows the anatomical structure of a human pancreas (A) compared to a mouse pancreas (B). The human pancreas is compact and is separated by 3 sections: head, body, and the tail. The mouse pancreas is not as compact and is defined by lobes: the duodenal, gastric, and splenic lobes (Adapted from Dolenšek *et al.* 2015).

1.4 Synthalin A

Synthalin A (Syn A), has been proposed to be a specific alpha cell toxin (Langslow *et al*. 1973; Beekman, 1956; Davis, 1952, Fodden & Read, 1953; Karr *et al*. 1929; Hornung, 1928). It is a derivative of guanidine, has been produced in several forms, including tablets, injections, and a pure salt (Bodo and Marks, 1928; Watanabe, 1918). This compound is different from insulin in two main ways: one, Syn A is effective when taken orally, and secondly, it has a delayed reaction causing the blood sugar to remain at normal levels and then drop to a hypoglycaemia level (Bodo and Marks, 1928). This medication produces a toxic effect causing the patient to become hypoglycaemic (Bodo and Marks, 1928; Watanabe, 1918). There is limited

information regarding Syn A written in English. However, there is an abundance of material in German and many of the research articles referring to Syn do not specify if Syn A or a modified form called Syn B was used. When referring to this toxin, if A or B was not documented, it was referred to as Syn. The purpose of this Chapter is to provide a deeper understanding of why Syn A was discontinued, the history of Syn A, and the anatomical structures that are affected. The focus of this research project is on rodents and Syn A, but also raising awareness of the lack of current research being done using Syn A. Various rodent models; normal, knockout, and transgenic animals, will be used to see if Syn A is possibly strain specific as well as species specific. Three different cell lines, alpha TC 1.9, Min-6, and GLUTag cells will be used with the primary focus on glucagon secreting alpha TC cells.

Proof of concept studies in treating T2D with Syn A is another primary focus of this research project. Many experiments using Syn A also resulted in morphological changes to the alpha cells in the pancreas, which caused the cells to become hydropic, and caused cytoplasmic vacuolation, and affected the nucleus (Östenson, 1983). Some studies propose that an increase in functional activity, along with cell exhaustion, is said to underlie the effect of Syn A on the alpha cells, rather than toxicity, but the exact mechanism of action is unknown (Gunnarsson *et al.* 1969; Creutzfeldt, 1960). It has been suggested that Syn A causes a secondary change to the alpha cells and the pancreas may not be the target tissue (Creutzeldt 1960 and 1957; Langslow and Freeman, 1973; Langslow *et al.* 1973). This provides vital information for the current research project, as existing rodent studies are lacking.

1.4.1 Discovery and discontinuation of Syn A

Syn A is chemically related to biguanides and was proposed as an antidiabetic drug. Figure 1.2 shows the different chemical structures of Syn A and B, along with metformin and phenformin (Bailey and Day, 2004). Frank, Nothmann, and Wagner, first synthesized the drug, showing that Syn A was able to lower a species' blood sugar level when given in specific amounts (Östenson, 1983; Davis, 1952; Frank *et al.*1926). Past research suggests that if Syn A is given in a specific amount, as laid out by Frank, Nothmann, and Wagner, then the effects

are non-toxic (Langslow *et al.*1973; Beekman, 1956; Davis, 1952, Fodden and Read, 1953; Karr *et al.*1929; Hornung, 1928; Graham, 1927; Frank *et al.* 1926). When used in clinical

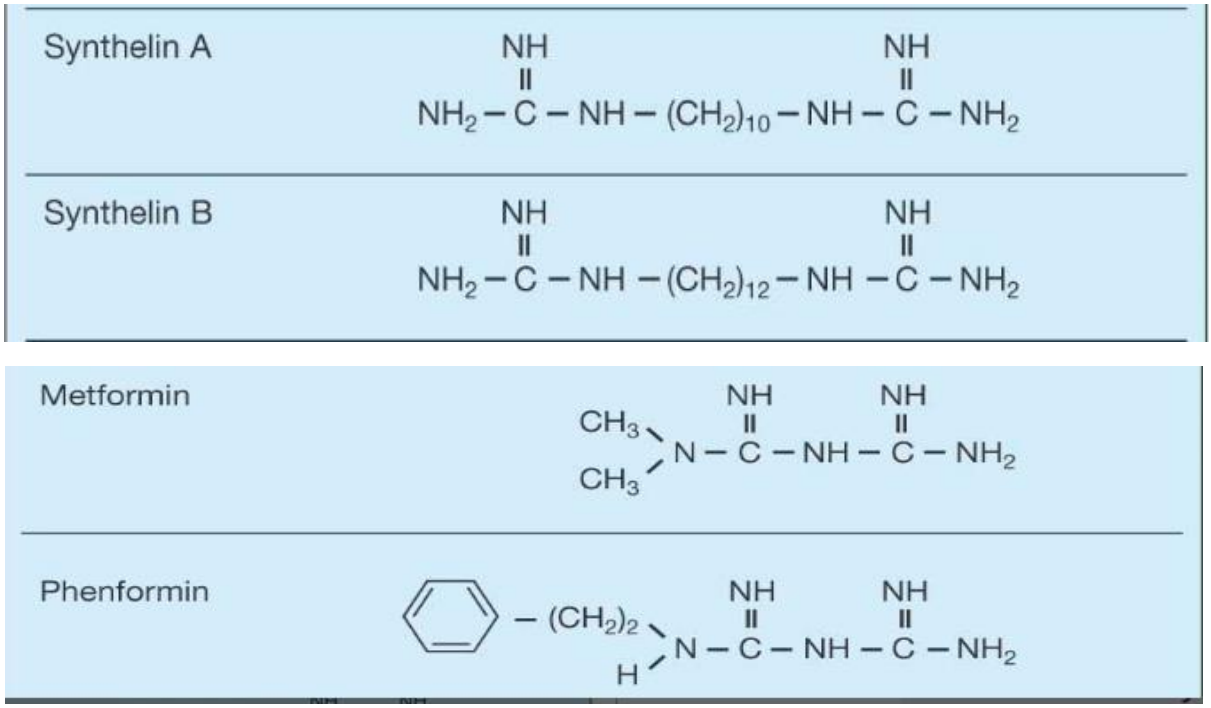

Figure 1.2 shows the chemical structures of a few biguanide drugs: Syn A and B, metformin, and phenformin. (Adapted from Bailey and Day, 2004).

Syn A has been documented to damage alpha cells, with no/limited effect on beta cells, thereby potentially offering a means of decreasing hyperglucagonemia (Martini *et al.* 2015; Langslow *et al.* 1973; Beekman, 1956; Davis, 1952, Fodden and Read, 1953; Karr *et al.* 1929). A focus of this current research project is to discover why Syn A primarily affects alpha cells and not beta cells. However, some research documents slight changes to the beta cells (Östenson, 1983; Davis, 1952; Ferner and Runge, 1955). Even though small effects were found in the beta cells, the damage is not as extensive as in the alpha cells in previous research. Unlike insulin, Syn A is effective when taken orally and causes a progressive lowering of blood sugar (Bodo and Marks, 1928). At high doses, this drug produces adverse effects causing organ toxicity as well as a degeneration of alpha cells (Fodden and Read, 1953; Davis, 1952; Karr *et al.* 1929; Bodo and Marks, 1928; Watanabe, 1918). Within the 1950's and 1960's, research provided insights into the effects of Syn A and the species-

specific toxic effects (Langslow *et al.*1973; Creutzfeldt, 1960 and 1957). Other research states that Syn A was removed from the pharmacological market due to the discovery of insulin (Krishnarth *et al.* 2013; Bailey and Day, 2004; Dey *et al.* 2002; Dale 1927).

1.4.2 Human studies

The human islet has a randomization of alpha and beta cells throughout and tends to contain more alpha cells than beta cells when compared to rodents (Steiner *et al.*2010; Brissova *et al.* 2009; Kharouta *et al.* 2009; Kim *et al.* 2009; Cabrera *et al.* 2006; Grube and Bohn, 1983). However, during early gestation the islet structure is similar to a mouse islet, with the beta cells in the centre, but changes during the 18th week to the random architecture (Steiner *et al.* 2010).

In the late 1920's Syn was already being tested as an anti-diabetic drug on humans (Thomson *et al.* 1932; Graham, 1927; Joslin; 1927; Lawrence, 1927; Rabinowitch, 1927). Joslin (1927) treated 8 individuals with Syn, resulting in positive effects and very limited side effects. One individual reduced their insulin doses from 28 to 16 daily units while maintaining their previous diet but was unsuccessful in decreasing their insulin dosage by another 6 units due to glycosuria appearing. In this individual, 3 mg of Syn replaced one unit of insulin and in the next case 1 mg of Syn replaced one unit of insulin. Another individual was able to completely remove insulin and replace it with Syn, resulting in almost normal levels of blood glucose. This individual was given 50mg of Syn for two consecutive days, it was then withdrawn for one or two days and then the process was repeated. It was repeated until the dose was changed to 30 mg every day for three days and withdrawn for one. One individual had success at their urine becoming sugar-free with diet and insulin and, once the insulin was removed, and their urine remained sugar-free while on Syn. After a surgery for hyperthyroidism, one individual did better with Syn when it replaced insulin, but it is unclear in the document as to how the patient did better. Two older ladies, no age given, started observation with a few grams of sugar in their urine, but were virtually sugar free once Syn was given. One individual was

recorded as disliking Syn, but no other symptoms based on blood sugar were described (Joslin, 1927).

To observe symptoms and monitor blood sugar levels, an in-patient study looked at 8 individuals who were administered Syn. An individual with a mild case of diabetes displayed 40 to 50 grams of sugar in his urine and blood sugar levels over 250 mg. Before Syn was administered, insulin was increased to 20+20 units which reduced the patient's glycosuria, but this increased once insulin was removed. Unfortunately, this study does not state whether the dosage amount is twice a day or a combination of that amount. The patient was then administered 20 + 20 mg for three days followed by a day without medication. The Syn intake showed a decrease in the glycosuria levels with sugar almost untraceable. Syn was then increased to 25 + 25 mg for two days and a one-time dose of 25 mg. The individual had an increase in glycosuria until the third day when the levels became untraceable for three consecutive days. Syn was then withdrawn from the patient and the glycosuria level increased to its initial level but decreased after three days of being re-administered Syn. Blood sugar levels declined throughout the day when the patient was on Syn. The second individual had similar results to patient one, in terms of Syn causing a decline in the individual's blood and urine sugar levels, however, patient two did show signs of no glycosuria (Graham, 1927).

Patient three was a 53-year-old man whose blood sugar levels were sustained at a normal level with diet and 25 + 25 units of insulin. When he was administered the standard 25 +25 mg three-day course of Syn, the insulin units were reduced to 10 +8 and his blood sugar levels remained normal. His dietary intake of carbohydrates was increased by 20 grams when Syn was omitted and no symptoms were documented. Syn was omitted once again for 7 days causing a fluctuation in blood sugar levels. The patient documented feeling well and overall gained 14 lbs causing them to have their 30 units of insulin replaced with Syn. Unlike patient three, patient four, a female, required 15 units of insulin and had fluctuating blood sugar levels; patient four was able to withdraw from insulin altogether and only required Syn to treat her

diabetes. Although she reported feeling well on Syn, she did not gain any weight, unlike patient three (Graham, 1927).

Patient five was a 32-year-old woman who required 35+30 units of insulin and 65 grams of carbohydrates in order to maintain a normal blood sugar level. Once Syn was administered, in the standard form, she was able to reduce her insulin intake; however, after the 7th course of Syn she developed symptoms including nausea and anorexia. Patient six was a teenage boy, age 16, who needed 15 + 15 units of insulin, with the evening dose being reduced once Syn was administered. Upon being discharged from the hospital, the teenager developed nausea, but had normal blood sugar levels. His blood sugar levels remained normal when Syn was re-administered for two days at a time for the majority of the course. At the 13th course of treatment he developed symptoms and on the 20th course his blood sugar increased. Syn was later replaced with insulin which caused blood sugar levels to decline but not to a normal level. Overall, while on Syn he gained 2 lbs, but gained more weight when on insulin the following 5 weeks and stated his refusal to ever be administered Syn A again (Graham, 1927).

Patient 7 was a 60-year-old woman who required 10 + 5 units of insulin and had 25 mg of Syn replace both units of insulin. Her blood sugar levels remained normal and she reported no symptoms until the 13th treatment of Syn when she developed severe urticaria. Due to the hives that were developed, Syn was stopped and her original units of insulin were re-administered. Patient 8 was a 19-year-old female with a history of septic illnesses and had her insulin increased from 10 units to 100 units. After one of her injections she developed an abscess, which complicated the course of her Syn treatments and reduced her insulin intake to 30 + 25 + 5 units. When re-administered at the hospital, her insulin was increased to 40 + 25 +5 units however, when given Syn her insulin was decreased. Syn was withdrawn once she developed the same symptoms as the other patients, however, her insulin was not increased and the patient almost ended up in a coma (Graham, 1927).

Graham (1927) had four other patients whom he treated with Syn, but considered the cases to be failures, having one young girl in the initial stages of becoming comatose. This young child had uncontrollable blood sugar levels and injected 20 +10 units of insulin. Once she was administered 10 +10 mg of Syn, her insulin intake was reduced to 10 + 10 units and increased on day two to 12 + 4 units. Due to still having glycosuria, Syn was increased to 15 + 15 mg and insulin was removed. Once the change in Syn occurred she developed the common symptoms of nausea and vomiting the following morning. She was documented as looking unwell, had deep abdominal breathing, was at the initial stages of falling into a coma, and was positive on the Rothera's test. She recovered through an intake of sugar and insulin throughout the day, and despite the symptoms, Syn was reintroduced again, this time having no effect (Graham, 1927). Regardless of the symptoms documented in this study researchers continued to try to treat diabetes in humans with Syn.

Thompson, *et al.* (1932) looked at a long-term study that focused on a selection of individuals divided into two groups. Overall, researchers found no evidence of Syn being toxic to individuals and the symptoms they experienced were mild. The individuals within the study were given 10mg three times daily following food intake for three consecutive days and skipping the fourth day. The first group looked at 13 individuals: 5 males and 8 females with the combined age average of 58 years. These individuals were given 34mg daily for a total of 16 doses over 4.5 months. Results revealed that, during the treatment, the blood sugar levels decreased during 14 periods, while increasing during the other two. However, during the two periods when the levels increased, the carbohydrate portion of the diet was increased (Thomson *et al.* 1932).

The second group of individuals consisted of four different series. Series A contained 36 individuals 7 males and 29 females, with 14 considered obese, 8 considered normal weight, 14 considered thin (sex not identified), and each were given 30 or 35 mg of Syn, and occasionally 20 mg. Twenty-four were aged between 40 and 60 and 12 individuals were over 60. Thirty of the individuals did not require insulin, while the other 6 required up to 29 insulin

units. Series A was on Syn for a total of 104 months and off Syn for 71 months which resulted in an average weight loss of 1.7 lbs. In terms of toxicity, only two individuals had toxic symptoms, such as pain over the liver, however researchers suggest this may be due to something other than Syn. It was also documented that the individuals in this series had lower levels in blood sugar. Series B contained 12 individuals: 2 males and 10 females, 7 considered obese and 5 considered thin. Ten of the individuals did not require insulin, the other two required up to 29 units of insulin, spent a total of 64.5 months on Syn, and 68.5 off Syn. One was between the ages of 20-40, 8 individuals were between 40-60, and three were over 60 years of age. Syn was removed which resulted in an increase in blood sugar levels (Thomson *et al.* 1932).

Series C consisted of 9 individuals: 2 males and 7 females; 3 considered to be obese and 6 considered to be thin. One individual was aged between 20 and 40, 5 were between the ages of 40 and 60, and 3 were over the age of 60. When Syn was administered to these individuals, their blood sugar levels increased, however the total change in blood sugar levels was less than the first two series and the average weight gain was 0.75 lbs. Four of the individuals did not need insulin, four required 29 units, and one required 30 or more units. Individuals were on Syn for a total of 27 months and Syn was withdrawn for 11 months. Along with two other individuals, there were a few clinical concerns within this series, as one individual showed hyperpiesia and ended up taking insulin later. Another individual reported that they felt unwell when they were taken off Syn even though their blood sugar levels did not decrease. One individual had a poor diet and developed symptoms similar to cholecystitis and felt better on Syn which caused favourable changes in the individual's blood sugar levels. One individual reported to be deteriorating and was likely put on insulin, but nothing else was documented any further on this individual (Thomson *et al.* 1932).

In the last series, Syn was withdrawn from individuals and their blood sugar levels declined. There were 7 individuals: 2 males and 5 females, 4 were considered obese, 1 considered to be of normal weight, and 2 were considered thin. Four of the individuals were

between the ages of 40 and 60 and three were over 60. Three did not require insulin and the remaining four individuals required 29 units of insulin. Individuals were on Syn for 25 months, off Syn for 15 months, and averaged 0.4 lbs weight loss. Within this series one individual also developed severe hyperpiesia, two others did not feel well when Syn was removed, and two other individuals needed insulin later. One individual suffered from ulcerative colitis, but researchers state that this may not have been caused by the Syn but aggravated by the metabolism of carbohydrates. Another individual experienced menstruation delays which may have been the result of the changes in blood sugar levels (Thomson *et al.* 1932).

Rabinowitch (1927) outlines similar symptoms, the previous researchers have documented, with his patient, a male in his late 40's with severe diabetes, was previously not on insulin and excreting 28 grams of sugar. Once he was given insulin, his urine became sugar free, but when the evening dose of insulin was removed, the urine once again contained sugar. The evening dose was replaced with 50 milligrams, causing the blood and urine to become sugar free, but after a few days he experienced nausea and vomited once. When Syn was removed hyperglycaemia and glycosuria returned, however, when Syn was reintroduced the patient described gastrointestinal issues and the drug was removed once more. Insulin was given in increasing amounts causing glycosuria and hyperglycaemia to return. This cycle was repeated several times, until the evening dose of insulin was replaced with 25 mg of Syn, glycosuria was removed, and the blood sugar levels remained stable. Rabinowitch (1927) examined 6 other patients who required insulin, while three patients were able to excrete sugar-free urine. Another patient did not have success on Syn, whereas two other patients were unable to excrete sugar-free urine after a month on Syn. Syn alone was not enough for them to remain sugar free (Rabinowitch, 1927).

With the human studies, it is quite clear that Syn has a positive effect on blood sugar levels along with glycosuria, even when combined with another drug that has toxic effects. Syn has been used in conjunction with glukhorment, which is stated to resemble Syn because of the effects on the pancreas, but does not contain any guanidine derivative (Cameron, 1928;

Lawrence, 1927). In one individual, the combination of these two substances reduced the individual's glycosuria by 10 mg (Lawrence, 1927). Another individual, a young 10-year-old female was able to tolerate the two substances individually but not combined, as she developed nausea and vomiting. Lawrence (1927) concluded that Syn may always have a toxic effect, however, the mechanism of action is uncertain, it cannot be taken consecutively, and does not induce weight gain.

These studies involve Syn used in conjunction with insulin; however, none of these three articles recommend using Syn by itself or in conjunction with another drug, to see if the toxicity could be reduced (Thomson *et al.* 1932; Graham, 1927; Joslin; 1927). Professor Frank, who recommended the standard dosage, said the symptoms experienced by these individuals are common in those dependent on insulin and perhaps Syn would be better for those who refuse to take insulin (Graham, 1927; Lawrence, 1927). When questioned about using Syn for diabetes mellitus treatment, Graham (1927) responds by saying, "for those patients who need insulin and are willing to have it, Syn has no value at present. To those who are unwilling to have more than one dose of insulin, although they really should have two doses, Syn may help" (pp. 534). Overall, researchers state there was little to no evidence of Syn being toxic to individuals and the symptoms they experienced were mild (Thomson *et al.* 1932). Although these studies were human-based and did not look at post-mortem effects, it is important to note the few side effects the individuals did have, such as high blood pressure, sugar-free urine, and incipient coma (Thomson *et al.* 1932; Graham, 1927; Joslin; 1927). Within the human studies, none discuss the effects of Syn on the pancreatic islets unlike the animal studies.

1.4.3 Rabbit studies

Beta cells are the predominant cell type within the rabbit pancreatic islets (Steiner *et al.* 2010). Within the islets there are cells that co-express glucagon and polypeptide (PP), even though only 25% of the islet is made up of alpha cells (Steiner *et al.*2010; Kim *et al.*2009; Jörns *et al.*1988). In a set of experiments that examined Syn A and rabbits, researchers discovered

that by increasing the dose of Syn, the animal had an onset of hypoglycaemia and received very little relief from the hypoglycaemia phase (Bodo and Marks, 1928; Dale, 1927). This set of experiments examined the relation of Syn A and the carbohydrate metabolism of different body systems, such as the muscular skeletal system and hepatic system of different animals (Bodo and Marks, 1928). Although Bodo and Marks (1928) did not look specifically at pancreatic islet cells, it is important to note the toxicity of the antidiabetic drug on the surrounding organs, such as the kidneys or, in this case, the liver. Within this set of experiments, glycogen and insulin were also examined in relation to Syn on the hepatic system. Low levels of glycogen were noticeable when the liver was examined. To determine what caused the hepatic glycogen levels to decrease, food was withheld from rabbits for 24 hours and they were injected with insulin every hour to induce hypoglycaemia. Results showed that when the rabbit was in hypoglycaemia, hepatic glycogen was depleted. However, two of the 12 rabbits that became hyperglycaemic, trace amounts of hepatic glycogen was still available (Bodo and Marks, 1928).

Microscopic examination of the rabbits' liver showed jaundice, liver impairment, and hydropic degeneration of the hepatic cells, but also small sections of necrosis. Researchers in these experiments found that Syn depletes the liver of glycogen during the hypoglycaemic phase. They suggest that the level of the rabbits' blood sugar, after the administration of Syn, is due to the amount of glycogen reserves because Syn possibly inhibits the maintenance of glycogen within the liver. The binding agents in the Syn tablets are believed to cause a possible reduction in blood sugar and more than 20 mg of Syn cannot be injected without killing the animal (Bodo and Marks, 1928). Although these experiments focused only on the effects on the liver, it would be necessary to find out if liver toxicity occurs first, or if it is secondary to alpha cell cytotoxicity, and if they are related in any way, or transferred through the bile or pancreatic duct. It is also of great importance to recognise the effect of Syn on the different body structures, for a broad understanding of how toxic this chemical is.

A large study involving 120 adult rabbits administered Syn was conducted to examine the effects on the liver. Syn or hydrochloride was administered in doses of 1 to 15 mg/kg into a vein in the ear, and 10 additional rabbits were administered 4 to 20 mg/kg of Synthalin B (Syn B). Results showed that Syn B produced lesions on the liver but were less severe when compared to Syn A. The effects of Syn were categorized into two headings: acute damage phase and the repair phase. Within the acute damage phase, results showed that the cells lining the portal tracts were hydropic, pale in colour, and foamy. In the rabbits that were administered Syn, the livers showed the nucleus containing no glycogen and there was a decrease in food intake. Other changes within this first phase included fatty changes and cell necrosis in individual cells within the lobe. Within the necrotic cells, the mitochondria disappeared quickly and was undetectable until hour 16. During the repair phase, the hydropic cells returned to normal size and the necrotic cells were unrecognizable after 48 hours. Some proliferated bile ducts occurred when the hydropic cells began to return to normal and mitoses increased in the Syn treated rabbits around hour 60. Around day 14, the liver tubules had almost become completely repaired, the proliferating bile ducts were repaired and increased in number, and by day 19, the liver cells contained glycogen again (Davis, 1958).

Experiments on rabbits and alpha cell toxicity show that the animals alpha cells underwent hydropic degeneration after the administration of Syn A. Results showed that Syn had an effect on the beta cells as well as the alpha cells in terms of the cells becoming hydropic or degranulating. Outside of biochemical changes and hypoglycaemia resulting from Syn A injections, histological changes to the islets, liver, and kidney also occurred. When Syn A was administered in large doses of 9-12 mg/kg, blood sugar levels were noticeable compared to the smaller doses of 4-6mg/kg. Rabbits experienced a change in blood sugar followed by hypoglycaemia 4-16 hours after Syn A was injected. If the hypoglycaemia was not treated, the animal died of convulsions. Davis (1952) also documented that at 10mg/kg the rabbit usually died from hypoglycaemia and found that at 6mg/kg the animal did not suffer fatal hypoglycaemia, but both dosage amounts caused the alpha cells to become hydropic. It was

also documented that the effects of Syn A were not equally distributed on the alpha cells. Davis (1952) concluded that the alpha cells may have become hydropic due to being overworked. Syn B was also used in this set of experiments, but no alpha cell abnormalities were found, except in a few rabbits, where the alpha cells' nucleus became hydrochromatic and some cytoplasmic vacuolation was also evident (also seen in guinea pigs) (Gunnarsson *et al.* 1969; Davis, 1952). The animal studies did not follow the same dosage pattern as humans, but the effects in animals appear to be more extreme. The rabbit studies provided a comprehensive insight into the effects Syn has on the hepatic system as well as briefly exploring islet destruction.

1.4.4 Guinea pig studies

An article of particular interest is a study that documents the microscopic changes beginning from 2 hours up to 28 days after injection of Synthalin (Herbertson, 1958). Forty-eight adult guinea pigs were administered Syn by a single subcutaneous injection with dosage amounts ranging from 2.5 to 5 mg/kg. Two days after injection, 9 guinea pigs died from convulsions and 6 died due to renal failure. The remaining guinea pigs were sacrificed in intervals from 1 hour up to 30 days after being administered Syn. A gross anatomical autopsy was performed and found that portions of the liver had become pale yellow and other sections were normal colour. After the injection of Synthalin,10-14 days later, the guinea pigs' livers showed a speckled pattern, but no dead hepatic cells remained. It was also documented that the number of hepatic cells in mitosis were back to normal. There was an increase in bile-ducts, lymphocytes, and mononuclear cells and the hepatic glycogen was almost at normal amounts. A yellowish colour was also present in the subcutaneous tissues where urine was also present. The urine contained traces of bile. The kidneys also displayed a pale-yellow colour, especially in the renal cortex, and the medulla showed signs of congestion (Herbertson, 1958).

Within hours two and four the liver cells appeared shrunken, but the nucleus was of normal morphology. There was little to no glycogen present in the cytoplasm and the cytoplasm of the peripheral cells were orange in colour with a small number of adipose droplets. Upon

examination, during hours 8 to 12 after injection, glycogen levels were still absent in the liver lobule peripheral cells, however, some guinea pigs displayed a fair amount of glycogen in the central zone of the liver. The amount of adipose tissue increased unlike before where adipose was hardly detectable. Cells within the portal tract started to undergo necrosis and the nucleus was severely altered. Polymorphonuclear leucocytes are abnormal and present among the sinusoid wall. Eighteen to 24 hours after Syn was given, many of the necrotic liver cells appeared dead and contained a small amount of lipid, but those surviving cells near the necrotic cells appeared enlarged. Most of the adipose droplets disappeared, although the cells in the peripheral areas of the liver lobule that survived still contained adipose droplets. Enlarged epithelial cells were present along the bile ducts and some of the cells were also documented going through mitosis (Herbertson, 1958).

Bile duct proliferation and an increase in the number of cells going through mitosis was evident during the 32 to 36 hours of examination. The portal tract cells began to multiply, and columns were formed in-between the dead hepatic cells, however, the liver cells were not dividing as quickly as the rest of the cells. In the next time frame of 44 to 48 hours, the dead liver cells started to disappear, and other liver cells began to regenerate. Proliferation of the bile duct was still ongoing, new cells created irregular ducts, and some cells still underwent mitosis. The adipose droplets became evenly distributed throughout the cytoplasm of the cells and the bile ducts displayed adipose droplets. The cells located in the peripheral and central zone now displayed a ring of cells which contained a small number of adipose droplets. The liver cells and bile duct proliferation continued as well as mitosis in several cells on day 3 to 4 after Syn A administration. The swollen cells were still present and contained adipose droplets, adipose increasing in the bile ducts and cytoplasm of some cells, and the bile ducts continued to display polymorphonuclear leukocytes (Herbertson, 1958).

During the examination on day 6 to 8, the dead cells were almost completely removed, and regeneration continued to display adipose droplets. Mitosis had decreased along with the number of bile duct divisions. Glycogen was then present in the liver cells in the central zone

and in some cells in the periphery section of the liver. Glycogen remained and increased to a normal level by the time the examination was done between days 10 and 14. The dead hepatic liver cells were gone, and mitosis occurred normally in the hepatic and bile duct. It was suggested that atrophy had occurred within the bile ducts due to the increase in number and structure of ducts. Adipose droplets were still present and continuing to change, however, on day 28, the structure and appearance of the liver had been documented to be within normal limits. With this comprehensive examination of the guinea pig liver, results documented that it was possible that Syn caused the bile ducts to proliferate. Herbertson (1958) also briefly mentions how necrosis was not found in other species such as rats and mice and that the variety of toxicity of the liver due to Syn varies among species.

A similar set of results was obtained in a set of guinea pig studies that used a lower dose of Syn with regards to the fatty appearance of the liver and the kidneys which appeared pale and swollen. Fourteen male guinea pigs were injected three times with 2.0 mg/kg, 22 guinea pigs were administered one injection of 3.0 mg/kg, and the remaining 14 were given 3.5 mg/kg for one injection. The 36 guinea pigs that were given one injection showed a decline in their blood sugar levels after 24 hours and then slowly increased back to normal blood glucose levels. Eight of the guinea pigs had morphological changes in their pancreatic islet cells. The beta cells and A_1 cells displayed no damage and not all of the A_2 cells showed signs of damage. There were no distinguishing factors of these two different A cells in the research article. The cells that were damaged were swollen, vacuolated, and degranulation occurred. Upon further examination of the cells of the Syn treated guinea pigs, the nucleus was enlarged, and the chromatin net had displayed a decrease in density. Seventeen of the 50 guinea pigs that were administered Syn died within 80 hours of receiving the first injection (Gunnarsson *et al.* 1969). An increase in functional activity, along with cell exhaustion, is said to be the effect of Syn on the alpha cells rather than toxicity (Gunnarsson *et al.* 1969; Creutzfeldt, 1960).

Several years after Syn A was discontinued, a study was performed to test the effects of this drug on the alpha cells of the pancreas using incubated islets (Östenson, 1983). Researchers

isolated islets from two groups of guinea pigs; one group was injected with streptozotocin and the other was not. Ten batches of pancreatic islets from the normal group were incubated with a solution that contained different concentrations of Syn A. When the alpha cells were incubated with Syn A, glucagon release increased as the concentration of Syn A was increased. After the islets were incubated, they were washed and plated for three days and then fixed and embedded for further investigation by microscope. Upon examination, islets that were treated with Syn A, presented with a non-destructive ultra-structure. However, the islets that were treated with small doses of Syn A, 5µg/ml, stayed intact, but showed signs of a darker cytoplasm as well as more vacuolization occurring. When examining the islets that were treated with the highest dose of Syn A, 500µg/ml, disintegration was identified as well as the cell showing signs of necrosis in the centre (Östenson, 1983).

Along with the examination of cell morphology, this study looked at glucagon release in the incubated islet cells with Syn A and the effects of glucose, insulin, and somatostatin. When Syn A was increased, the glucagon release was initiated in normal guinea pig islets. At the highest dose of Syn A, secretion of glucagon response was documented as being three times higher than the controlled pancreatic islet glucagon secretion. Syn A also suppressed glucagon oxidation rates in alpha and beta cells by 30 % (Östenson, 1983). Kern (1970) suggests that Syn A should not be used for chronic treatment on guinea pigs due to the toxic effect being extremely high and the fact that this drug affects the alpha cells without damaging the exocrine tissue in any way.

This study showed that, in terms of the pancreatic alpha cells and Syn A, glucose metabolism has a direct effect, as well as causing morphological damage to these cells. Damage to the alpha cells occurred only three days after Syn A was introduced, causing the cells to deteriorate, have increased functional activity, and either cytotoxic degeneration or exhaustion (Östenson, 1983). Researchers concluded that the Syn A showed a significant glucagon release as well as a hyperglycaemia phase within the guinea pigs' islets, which a previous study also documented (Östenson, 1983; Creutzfeldt, 1960). While there is a good description

of what happens to the alpha cells due to Syn A, it is unclear if cytotoxicity would occur if Syn A was combined with another antidiabetic drug and why the other islet cells remained functional. In conjunction with the research project being carried out, the guinea pig studies regarding the incubated islets provide insight on what is to be expected in future tests that will be performed, as stated in the General Discussion Chapter.

1.4.5 Cat and dog studies

The islet architecture is quite different between cats and dogs. The islets within the pancreas of domestic cats, have a centre core of alpha cells surrounded by a layer of beta cells. Alpha and beta cells have been found in the pancreatic ducts as well as connective tissue (Steiner *et al.* 2010). Within the regions, with the exception of the head of the cat pancreas, the alpha cells make up about 30% (Steiner *et al.* 2010; Furuzawa *et al.* 1992). However, in dogs the centre of the islet is primarily beta cells (Steiner *et al.* 2010; Muranishi *et al.* 1999). The tail of the pancreas in dogs tend to contain the majority of the islets which are large in diameter (Steiner *et al.* 2010; Wieczorek *et al.* 1998; Kramer *et al.* 1980).

Eviscerated spinal columns of cats and hind legs from dogs were used to examine the carbohydrate metabolism and Syn effects on these body structures. Cats were given 60mg of Syn caused sugar to disappear from the blood which may have been oxidised and raised some complicating factors such as: glucose drainage from the liver, skeletal muscle twitches, increased tone in these muscles, and effects on the heart (Bodo and Marks, 1928; Dale, 1927). There was limited information on the results from cats treated with Syn, but researchers stated in order to possibly eliminate the complicating factors, they examined Syn on the muscular system of dogs' hind legs. They found that after the blood sugar fell and a second dose of Syn was given vasodilation occurred. Researchers concluded that the administration of Syn A allows the glycogen in the muscle to breakdown (Bodo and Marks, 1928).

Karr *et al.* (1929) looked at the toxic effects of Syn on four dogs. Dog A was given 20 mg of neoSyn for seven non-consecutive days unlike the other dogs who were administered Syn. On the last day of neoSyn, the dog vomited and was found dead the following day. Dog B was administered 10 mg of daily Syn A and on the 10th day increased to 20 mg daily, where it was later discontinued and then re-administered again at 20 mg daily. Dog C was also administered 10 mg of Syn daily, but two days later increased to 20 mg, where it was immediately switched back to 10 mg due to the dog vomiting. Later that month, Syn was increased back to 20 mg and four days later decreased again to 10 mg. Five days later Syn was stopped, but three days later 10 mg of Syn was administered once again, and the dog was found dead the next day. Dog D was given a daily dose of 20 mg of Syn A and 9 days later started to refuse food. 10 days later the dog refused food altogether and was sacrificed shortly after due to being in poor condition. An autopsy and histological studies were performed on the four dogs (Karr *et al.* 1929).

The autopsy of dog A and B were fairly similar, but the pancreas of dog A displayed evidence of pancreatitis such as fat necrosis in several areas along with mild inflammation along the mucus membrane of the stomach. The liver of dog A presented with small vacuoles that contained no fat and no pigment. The heart, spleen and duodenum were also examined but no lesions were found. Findings of the autopsy from dog B were more descriptive than the other dogs stating that the dog looked emaciated and was only slightly rigid. The heart was examined showing no damage except for a small clot within the pericardium. The spleen, bladder, gallbladder, oesophagus, adrenals, and the bowels appeared normal. The kidneys weighed about 15 grams each, and when the capsules were removed the surface of the kidneys remained smooth. The area of the kidney that was dissected displayed a yellow cast and protruded, but the cortex and medulla were normal. The liver also displayed a yellow tint and the rugae of the pyloric area of the stomach was thick and displayed small flecks of what looked like dried blood. Histologically, the kidneys displayed lymphocytes, swollen and granular convoluted tubules, and the nuclei of some cells were pale in colour and pinched.

The cytoplasm of the tubules in the cortex were vacuolated and absent of any adipose tissue. However, the descending portion of the loop of Henle was severely damaged, displayed a fatty degenerated tubule, the glomeruli were overfilled, but blood vessels remained undamaged. The liver displayed degeneration of the parenchyma and appeared granular, vacuolized, and fatty. Large black granules, similar to bile, were displayed in the bile capillaries and in the Kupffer cells, but the bile ducts appeared normal. The pancreas, which was also similar in dogs C and D, displayed characteristics of degeneration and the acinar cells were found to be regenerated, but the islets appeared to be less affected. The stomach of dog B showed superficial necrosis of the mucosa lining. The autopsy of dog C showed that the liver and kidneys were both congested and had a yellow colour to the organs as well as the pancreas displaying a yellow tint. The rugae was similar to dog B and the kidneys in this dog did not display any fat within the renal cells or the hepatic cells. The autopsy on dog D was performed immediately and revealed that the dog had a kidney infection. The other organs that were examined, were described as being the same as the other dogs (Karr *et al.* 1929). It is unclear if the high dose of Syn caused the toxic effects on these dogs or if the inconsistency in dosage amount could have contributed to the severity of organ damage. The studies on cats and dogs give valuable insight into how the different organs are affected by Syn.

1.4.6 Avian studies

There are three main types of islets; dark, light, and mixed islets that have been observed in birds (Steiner *et al.* 2010; Epple, 1968; Epple and Farner, 1967). Dark islets primarily consist of alpha and delta cells, light islets consist of beta cells that are located near capillaries with delta cells on the outside, and mixed islets consisting of all three cell types (Steiner *et al.* 2010). Depending on the strain of bird, the distribution of islets changes. For instance, in the rose-ringed parakeet, beta cells are found in all four pancreatic lobes, but the alpha cells are only located in the splenic lobe (Steiner *et al.* 2010; Gupta and Kumar, 1980). Whereas the zebra finch pancreas contains more delta cells and very few beta cells (Steiner *et al.* 2010; Kim *et al.* 2009). Chicken pancreas have been observed to show that the majority of the

hormones, insulin, glucagon, and somatostatin, are present in the splenic lobe (Weir *et al.* 1976). Glucagon is lower in the dorsal and ventral lobes of the pancreas, and insulin is lower in chickens when compared to other mammals (Weir *et al.* 1976; Langslow *et al.* 1973).

In an aviary study that looked at Syn A and the effects on blood sugar and alpha cells in roosters, researchers administered a single dose of 1.0, 5.0 and 10.0 mg.kg of Syn subcutaneously. Ten roosters were given 10 mg/kg and were sacrificed shortly after due to convulsions starting (Beeckman, 1956). This article is one of three that documented convulsions as a side effect of Syn, to which the rooster died 10 to 30 minutes after experiencing convulsions (Herbertson, 1958; Beekman, 1956; Fodden and Read, 1953). A set of researchers also examined the mode of action of Syn A in newly hatched birds. There were three groups of birds tested, one which had been starved before the injection of Syn A, the other group that were fully fed, and a group of normal birds (Langslow and Freeman, 1973). The experiments showed that the group of starving birds were protected from the effects of the intraperitoneal injection (i.p.) 10mg/kg of Syn A and the full fed birds died, possibly due to hypoglycaemia (Langslow and Freeman, 1973; Langslow *et al.* 1973). The liver and the pectoral muscles of the birds showed a significant amount of glycogen depletion after the antidiabetic drug was administered. The normal birds presented with a higher level of glucose uptake within the gut compared to the birds treated with Syn A (Langslow and Freeman, 1973).

Langslow and Freeman (1973) concluded that one of the factors that was responsible for the hypoglycaemia that developed in the full fed birds, was the loss of glycogen within the liver and voluntary muscles. The level of hypoglycaemia was considerably less in the full fed birds compared to starved birds. The researchers concluded that the primary site for Syn A is not the pancreas, since upon examination the animals showed significant hyperglycaemia and a reduction of plasma free fatty acids and Syn A did not change this (Langslow and Freeman, 1973; Langslow *et al.* 1973). Researchers suggested that Syn A probably does not affect glucagon within the pancreas but is a powerful modifier of carbohydrate and lipid metabolism

in full fed birds (Langslow and Freeman, 1973). They also stated that Syn A possibly interacts only with the animals' intestinal system and it appears that different animals respond differently to the administration of Syn A (Langslow *et al.* 1973).

1.4.7 Rodent studies

Rodent islets are well defined and consist of approximately 60-80% beta cells in the centre surrounded by a layer of alpha cells (Steiner *et al.* 2010; Brissova *et al.* 2005; Kharouta *et al.* 2009; Kim *et al.* 2009; Wieczorek *et al.* 1998; Reddy *et al.* 1985). Different strains of rodents, the islet architecture changes, for instance, the African ice rat has two to three layers of alpha cells where as other rodents have one layer (Steiner *et al.* 2010; Brissova *et al.* 2005; Kharouta *et al.* 2009; Kim *et al.* 2009; Quesada *et al.* 2008; Wieczorek *et al.* 1998; Reddy *et al.* 1985). The tail of the rodent pancreas contains more islets as well as the majority of the alpha cells (Steiner *et al.* 2010; Ku and Lee, 2006; Elayat *et al.* 1995; Park and Bendayan, 1992).

The research involving Syn A and the effects on islets involving rodents is limited, and the few studies that were conducted were performed in the 1950's. In 1938, research was conducted on mice and the effects of this drug along with several others on cancer (Boyland, 1938). Researchers determined the toxicity of each substance and concluded that Syn A became toxic at 0.2mg. Mice survived 37 days with the oral Syn A treatment, but some of the mice grew mammary tumours (Boyland, 1938). No further examination took place and the pancreas was not examined during this experiment but provides insight that Syn A possibly affects other organs besides the pancreas. Another study looked at cancer and Syn A and examined if the hypoglycaemic effects of Syn A were related to the antitumor activity. The Swiss mice in this experiment were given Syn A in three different ways: it was administered orally, injected intraperitoneally, or injected subcutaneously each at different amounts. The i.p. injection of Synthalin showed antitumor activity as well as the mice living longer. Results of this study concluded that the antitumor effect of Syn A may not necessarily correlate with the drug's hypoglycaemic effects but may be limited to the glucose lowering effects as well as the route of administration (Mihich *et al.* 1959).

In an experiment that used new-born albino rats, Syn A was used to determine the toxicity on alpha cells. A subcutaneous injection was given containing 10 mg/kg and the rats were sacrificed 12 to 18 hours after the injection. The pancreas was observed, and results showed that it contained large islets that were well-defined, and the beta cells were encompassed by a layer of alpha cells which varied in thickness. Upon examining the alpha cells, researchers observed that the granules were coarser, and the beta cells did not increase as much as the alpha cells. It was also concluded that none of the new-born rats given Syn A had any altered alpha cells and none of the cells showed lesions. With mitosis being the main focus for the experiment, results showed that the alpha cells in the Syn treated rats had a decreased mitotic frequency and, once in the late prophase and early to middle metaphase, the alpha cells displayed pyknotic degeneration (Ferner and Runge, 1955).

In another study that used rats, 4 mg/kg of Syn was injected subcutaneously, along with another alpha cytotoxic compound, cobaltous chloride. Results showed that Syn A increased ascorbic acid and glutathione within the liver, but the levels decreased in the kidneys. Upon microscopic examination, portions of the kidneys displayed degenerative changes leading to severe kidney damage. Alpha cell damage was documented but the type of damage was not recorded (Hultquist, 1956). One study using rats isolated the rat diaphragm and incubated the hemi-diaphragms in Krebs-Ringer bicarbonate buffer with insulin or saline buffer, an animal serum, or a hypoglycaemic agent. Although the experiment did not look at the alpha cells, it is important to note that results showed that Syn was not affected by the insulin antiserum that was added to the diaphragms. Results show that the insulin extracted from one animal pancreas ends the stimulant effect of extracted insulin from another animal (Wright, 1959).

In another study that looked at other substances with Syn A, Lundbaek and Nielsen (1958) looked at rats and three hypoglycaemic compounds – carbutamide, tolbutamide, and p-aminobenzole (IPTD) and the effects on the pancreas, but only Syn A produced alpha cell damage. Syn A was injected intraperitoneally and contained 20mg in a single dose prior to the rats being sacrificed, and the pancreas, peritoneal cavity, liver, kidneys, and adrenals were

examined further. Degenerative changes within the liver and kidneys in the rats that were given Syn A have been shown in three research studies. The pancreas showed abnormal alpha cells which were severely degranulated while the beta cells remained unharmed. The alpha cells had changed in structure, the granules of some cells were replaced with a substance of pale or greyish colour, while the nuclei of some cells were unaffected and the alpha cells appeared normal (Lundbaek and Nielsen, 1958).

Past research on rodents provided results showing how the alpha cells were affected by the Syn A, whereas the other studies did not examine the cells, but produced more anatomical effects on organs (Lundbaek and Nielsen, 1958; Hultquist, 1956; Ferner and Runge, 1955). These anatomical findings will be important to the animal studies in this thesis and will act as a guideline on what to expect the other organs will look like when extracting tissue from the mice. Some studies suggest that Syn A affects different species in different ways and therefore that this chemical is species specific (Langslow *et al.* 1973; Creutzfeldt, 1960 and 1957).

1.4.8 Other studies

The recent material that mentions Syn A focuses on alternative therapies for diabetes, such as herbs, other antidiabetic drugs, as well as life style changes, such as exercise, changes in diet, and bariatric surgery (Rivas *et al.* 2016; Halban *et al.* 2014; Nice Guidelines, 2012; Thaler and Cummings, 2009; Hawley and Lessard, 2008; Modak *et al.* 2007; Bailey and Day, 2004; Dey *et al.* 2002; Wojtaszewski *et al.* 2000). However, some studies that used Syn A recently used it to test the effects on bacteria and certain diseases like sleeping sickness. Experiments on four different bacteria; *Escherichia coli*, *Staphylococcus aureus*, *Enterococcus faeclis,* and *Pseudomonas aeruginosa* and tested them against antiseptics, Syn A, and anti-trypansomal compounds. As stated previously, Syn A has a toxic effect on organs and alpha cells, however, researchers found that was not the case against bacteria, until 168 hours after exposure (Grare *et al.* 2007). There was very little research carried out in the 1980's and 1990's on Syn A as it has been discontinued for quite some time due to the toxic effects on

the renal and hepatic system (Östenson, 1983). Presently, one can see that the research on Syn is still scarce, especially when it comes to diabetes and the effects on the islets in any species.

Syn A caused toxicity to many organ systems, such as the hepatic and the renal system (Bailey and Day, 2004; Dey *et al.* 2002; Langslow and Freeman, 1973; Creutzfeldt, 1960; Davis, 1952; Bodo and Marks, 1928; Frank *et al.* 1926). Many experiments using this antidiabetic drug also resulted in morphological changes to the alpha cells in the pancreas causing the cells to become hydropic, cytoplasmic vacuolation, and the nucleus was affected (Östenson, 1983). It has been suggested that Syn causes a secondary change to the alpha cells and the pancreas may not be the target tissue (Creutzeldt 1960 and 1957; Langslow and Freeman, 1973; Langslow *et al.* 1973). This provides vital information for the current research project as the lack of current rodent studies is not being addressed, along with a lack of understanding as to why Syn only affects alpha cells whilst the beta cells remain unharmed.

1.5 Cobalt Chloride

Cobalt chloride is an alpha cell toxin that is species specific (Creutzfeldt, 1957; Volk *et al.* 1953). However, it has been suggested that it is not as destructive against the pancreatic alpha cells as Syn A (Ito *et al.* 1958). The research on this toxin is scarce and the primary animals used were guinea pigs and rabbits. It has been suggested that once multiple doses of cobalt were administered, the alpha cells were damaged and not able to stabilize blood sugar levels which then caused hyperglycaemia. One hypothesis about the mechanism of action suggest that the alpha cell damage that occurs with the hyperglycaemia are independent of the cobalt treatments, but of extrapancreatic origin (Volk *et al.* 1953).

1.5.1 Rabbit studies

One study using rabbits, looked at the optimal dosage and cobalt toxicity by intravenously injecting rabbits with different amounts of $CoCl_2$ ranging from 20 to 200mg. Results showed that the animals that received a dosage of higher than 100mg, developed multiple symptoms

including seizures and respiratory difficulty. Very few side effects were observed at the other doses, but it was stated that 40mg and 50mg are the optimal doses for rabbits. Upon finding the optimal dose, rabbits were given a single injection of 50mg of cobalt and sacrificed at various times and days after injection. A second group of rabbits received an additional four doses of cobalt, each an hour after the initial one. A third group received up to three doses of cobalt every 2 hours and a fourth group received repeated injections at various times during a daily interval. Within two hours after a single dose of cobalt, the blood sugar levels increased to maximum value and the levels returned to normal four hours after the initial injection (Volk *et al.*1953).

Histologically, the alpha cells after one hour of injection were considerably decreased in number, size, and appearance. The islets that were examined that were taken after two to three hours of injection mainly consisted only of beta cells and the seldom alpha cells that were seen were viewed as debris. Volk *et al.* (1953) noted that around day 6 after injection the cellular damage was still present, but the alpha cells that were intact were increasing. By the 10^{th} day, regeneration of the alpha cells was even more noticeable. Although changes in alpha cells occurred, the anatomical changes did not seem to differentiate between the number of doses and that the livers of the cobalt treated rabbits were depleted of glycogen (Volk *et al.*1953).

Alloxan diabetic rabbits were given a single dose of 50mg cobalt or a daily dose for several days and repeated for up to 14 days in several animals. When looking at the islets for the control diabetic animals, the central portion showed degeneration of beta cells surrounded by an intact layer of alpha cells. The alpha cells became shapeless and was more noticed in the diabetic animals then the control group. After an injection of cobalt, a prolonged period of hyperglycaemia occurred. After a repeated dose of cobalt, fasting blood glucose levels declined in some of the rabbits and lasted for several days. However, it was noted that if the rabbit received four or five doses of cobalt the glucose levels eventually returned to prior the cobalt injections. Results show that the diabetic animal appeared to be more sensitive to the

cobalt due to not being able to tolerate two or three daily doses resulting in a decline in blood glucose levels and not surviving (Volk *et al.*1953).

In another study that looked at rabbit pancreases following injection with cobalt, showed a high number of alpha cells that had been damaged or had completely disappeared (Goldner *et al.*1953). Telib (1972) found that the number of alpha cells from rabbits treated with cobalt varied from islet to islet within the same subject as well as alpha cells being destroyed near the capillaries. Degranulation and vacuolization were also observed in alpha cells during the first four hours of injection, however, the beta cells remained intact and healthy. The total number of islets as well as the ratio of alpha to beta cells also changed within one to four days after injection showing an increase in alpha cells. However, one week after injections of cobalt resulted in an increase in alpha cells, but no other changes to alpha and beta cells were documented (Telib, 1972). Volk *et al.* (1953) also found an increase in alpha cells within 6-10 days after cobalt was administered.

1.5.2 Guinea pig studies

When examining guinea pigs that had been treated with cobalt chloride, researchers found that the pancreatic alpha cells appeared swollen and hardly damaged. These researchers state that the effects cobalt has on guinea pigs is not necessarily the same effects it has on other species, making this alpha cell toxin, species specific (Creutzfeldt, 1960 and1957; Van Campenhout and Cornells, 1951). However, in another research study, it was discovered that complete vacuolization of the alpha cells only occurs in guinea pigs and is accompanied by glucagon loss (Creutzfeldt, 1957; Bencosme and Feri, 1955). It has been stated that cobalt has selective toxicity properties towards alpha cells within the guinea pig pancreas (Goldner *et al.*1953; Avezzu and Luise, 1951; Van Campenhout and Cornells, 1951). Hultquist and Sundqvist (1961) subcutaneously injected guinea pigs with two different types of cobalt; cobalt chloride and cobalt nitrate for four days. The nucleus of the cells was measured, and results showed that the nucleus in the alpha cells had increased in size where the beta cell nucleus slightly decreased. When comparing the two different types of cobalt, cobalt nitrate affected

the alpha cell nuclei more than the cobalt chloride. Alpha cells also showed more vacuolization when compared to beta cells, but less overall when compared to other animals. A conclusion was made that the alpha cell vacuolization suggested an increase in cellular activity (Hultquist and Sundqvist, 1961).

1.5.3 Rodent studies

One study that used 3 to 6-month-old mice, treated with cobalt chloride, looked at the difference of non-obese and obese mice. Four different groups of mice were used within the experiment; 14 obese mice treated with 2.5 to 10 mg of cobalt, 8 obese mice treated with 1.25 mg of cobalt, and 8 non-obese animals treated with the same dosages as the obese mice. The mice given 2.5 to 10 mg displayed signs of significant hyperglycaemia two hours after the initial injection. Of the 14 mice, four survived 24 hours after the injection, but 3 still were in hyperglycaemia, but only 1 survived past 4 days still at a hyperglycaemic level. One mouse became hypoglycaemic after 24 hours of the cobalt injection. The second group of 8 obese mice that were given 1.25mg of cobalt all survived even though the majority of the mice were at a hyperglycaemic level 2 to 24 hours after injection. Blood glucose levels became lower than the starting level, between days 4 and 7, and the mice were then re injected with cobalt. After the second dose, the blood glucose levels increased, however, not as significantly high as after the initial dose. However, when looking at the non-obese mice that were injected with similar amounts of cobalt, all of the mice became hyperglycaemic and failed to survive 24 hours. Histological results are seldom, and researchers state that the observations with the cobalt were not easy to interpret. However, one observation they did make was that beta cell proliferation, degranulation, regranulation, hypertrophy, and trabecular arrangement occurred in the mice that were given the lower doses of cobalt (Mayer *et al.*1953).

1.6 Proglucagon Gene and Glucagon like peptide-1 (GLP-1)

The primary peptide hormone secreted for the islet alpha cells is glucagon. It is derived from the proglucagon gene, which encodes various peptide hormones within the pancreas, small

and large intestine, distal ileum, and neuronal cells within the brain (Jin, 2008; Drucker, 1998). Specifically examining the pancreas, the proglucagon gene products inhibits insulin, increases fasting, and hypoglycaemia and generates glucagon (Moffett, 2013; Baggio and Drucker, 2007). Within the intestine, the proglucagon gene is stimulated when fasting and is decreased when refeeding occurs and produces glucagon like peptide-1 (GLP-1) (Chiang *et al*. 2012; Baggio and Drucker, 2007; Hoyt *et al.* 1996).

GLP-1 stimulates insulin and somatostatin secretion, inhibits glucagon release, delays gastric emptying, and normalizes fasting and postprandial glycemia levels (Cantini *et al.* 2016; Whalley *et al.* 2011; Jin, 2008; Baggio and Drucker, 2007; Kjems *et al.*2003; Drucker, 2002; Drucker, 1998; Ahen *et al.* 1997; Rachman *et al.*1997; Nauck *et al.*1996; Gutniak *et al.*1994; Nauck *et al.*2003). GLP-1 is secreted from the L-cells from the small intestine and increases prehepatic insulin secretion in those diagnosed with T2D (Cantini *et al*. 2016*;* Whalley *et al.* 2011; Baggio and Drucker, 2007; Kjems *et al.*2003). GLP-1 receptor (GLP-1R) is located in several tissues within the body, for instance, lungs, heart, kidneys, stomach, small intestine, regions of the central nervous system, and the beta cells in the pancreas (Moffett, 2013; Baggio and Drucker, 2007; Drucker and Nauck, 2006). Figure 1.3 below shows GLP-1 and the physiology on the different organs (Baggio and Drucker, 2007).

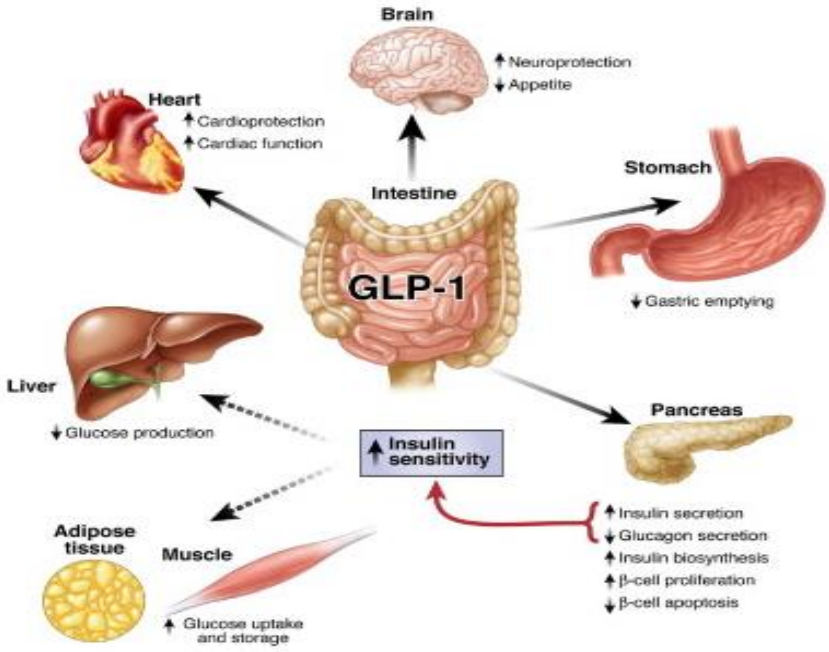

Figure 1.3 shows the physiology of GLP-1 and the impact it has on different areas within the body. Specifically examining the pancreas, GLP-1 increases insulin secretion, biosynthesis of insulin, and increases beta cell proliferation, as well as decreasing beta cell apoptosis and glucagon secretion (Adapted from Baggio and Drucker, 2007).

1.7 Aims and hypotheses

The problem is that currently, there are no therapies that specifically decrease glucagon levels in T2D and address hyperglycaemia, as well as the selective destruction of alpha cells, which would be an interesting therapeutic approach to T2D (Bagger *et al.* 2011; Parker *et al.* 2000; Brand *et al.* 2000; Brand *et al.*1994; Johnson *et al.* 1982). Consequently, this research aims to investigate the role of Syn A and cobalt chloride and to understand if and why the alpha cells are primarily affected. Even though it was found to have caused organ toxicity, the mechanism of action of these agents is still unknown. Understanding this is necessary for investigating if it can be used in developing treatments and so this is a central concern in this research. There are five aims and three hypotheses for this research project, which have been identified below and demonstrated throughout the experiments described in this thesis.

Aims

1. To evaluate Syn A and cobalt chloride as alpha cell toxins, their mechanism of actions, and why they are only toxic to alpha cells, but not beta cells.
2. To determine the effects of glucagon deficiency in glucagon receptor null mice on metabolic regulation and beta cell morphology.
3. To evaluate the effects of Syn A and cobalt chloride on disturbed blood glucose control and in islet morphology in animal models of diabetes.
4. To assess alpha cell production of GLP-1 and other products of the proglucagon gene in Syn A and cobalt chloride exposed clonal alpha cells and the change in *in vivo* models.
5. To conduct preliminary studies to determine the mechanism of action of Syn A and cobalt chloride.

Hypotheses

1. Alpha cells contribute to the development of diabetes and can determine the severity of this disease.
2. The reduction of alpha cells and excess glucagon secretion may provide a novel way of treating diabetes.
3. Local production of glucagon-like peptide-1 (GLP-1) and other products of the proglucagon gene, instead of glucagon in alpha cells, may be beneficial in supporting neighboring beta cells.

Chapter 2
Materials and Methods

2.1 Chemicals and materials

Distilled water, produced by a Milli-Q water purification system, was used in all experiments (Millipore, Millford, MA, USA). Suppliers of chemicals that were used in experiments are outlined below.

Abcam (Cambridge, UK): Goat polyclonal antibody to GFP, mouse monoclonal to insulin, and rabbit polyclonal antibody to Ki-67. Table 2.1 show antibodies and what they were stained for.

Analab (Lisburn, Northern Ireland, UK): BF3-Butanol solution (10%), boron trifluoride-1 butanol solution (approximately 10% in 1-butanol), dimethyl sulfoxide (DMSO), sodium iodide, superoxide dismutase.

BDH Chemicals Ltd (Poole, Dorset, UK): Acetic acid (glacial), calcium chloride ($CaCl_2.6H_2O$), dichloromethane (CH_2Cl_2), di-sodium hydrogen orthophosphate (Na_2HPO_4), ethanol, D-glucose, hydrochloric acid (HCl), magnesium sulphate ($MgSO_4.7H_2O$), paraformaldehyde (PFA), potassium dihydrogen orthophosphate (KH_2PO_4), sodium bicarbonate ($NaHCO_3$), sodium chloride (NaCl), tri-sodium citrate ($C_6H_5Na_3O_7.2H_2O$) and sodium dihydrogen orthophosphate (NaH_2PO_4).

Bio-Techne/RandD Systems (Abingdon, UK): Synthalin A

Gibco Life Technologies Ltd (Paisley, Strathclyde, UK): Antibiotics (100U/ml penicillin and 0.1g/L streptomycin), Dulbecco's Modified Eagle Medium (DMEM) (25mM glucose) supplemented with 4500mg/L glucose, L-glutamine and without pyruvate, foetal bovine serum (FBS), Hanks buffered saline solution (HBSS 10x stock) and trypsin/EDTA (10x stock).

Invitrogen (Paisley, UK): Alexa Fluor 488 goat anti-mouse IgG (H+L), Alexa Fluor 488 goat anti-guinea-pig IgG (H+L), Alexa Fluor 488 goat anti-rabbit IgG (H+L), Alexa Fluor 488 donkey anti-goat IgG (G+L), Alexa Fluor 594 goat anti-mouse IgG (H+L), Alexa Fluor 594 anti-guinea pig IgG (H+L), Alexa Fluor 594 goat anti rabbit IgG (H+L), Alexa Fluor 488 goat anti-rabbit

IgG (H+L), and Alexa Fluor 488 donkey anti-goat IgG (H+L). Table 2.1 show antibodies and what they were stained for.

Oxoid (Basingstoke, England, UK): Phosphate buffered saline (PBS) tablets.

Perkin Elmer (Cambridge, UK): Sodium iodide- ^{125}I (74Mbq/200µl stock)

Roche Diagnostics (Germany): LightCycler 480 Multiwell Plates 50 plates with sealing foils), LightCycler 480 SYBR Green 1 Master mix (5ml)

Sigma-Aldrich Chemical Company Ltd. (Poole, UK): 1,3,4,6-tetrachloro-3α, 6 α -diphenylglycouril (iodogen), 2-mercaptoethanol, 4', 6-diamidino-2-phenylindole (DAPI), C,N-diphenyl-N'-4,5-dimethyl thiazol 2 yl tetrazolium bromide (MTT), N-2-hydroxyethyl-peprazine-N'- 2-ethane-sulphonic acid (HEPES), acetonitrile, benzamide (99%), bovine insulin (crystalline), bovine serum albumin (BSA, essentially fatty acid free, endotoxin free), catalase from bovine liver, charcoal (activated/untreated), chloramine T trihydrate, cobalt chloride ($CoCl_2$), dextran T-70, dimethyl sulphoxide (DMSO), ethylene diaminetetraacetic acid (EDTA), glycerol, hydrogen peroxide (H_2O_2; 30% v/v), *In Situ* Cell Death detection kits Fluorecein, isopropanol, nicotinamide, potassium chloride (KCl), sodium benzoate (Reagent Plus 99%), sodium hydroxide (NaOH), sodium metabisulphite, superoxide dismutase from bovine erythro, streptozotocin (STZ), thimerosol, Tri Reagent, triton x-100, trizma base, trizma hydrochloride, trypan blue (0.4%), tween -20.

ThermoFisher Scientific (United Kingdom): Dead cell apoptosis kit with Annexin V Alexa Fluor 488 and Propidium iodide (PI) for Flow Cytometry

VWR International (Lutterworth, UK): Microslide Polysine Ground Edges^{TM}, Microtome blades DB80 LX, premium low profile, for dense samples

2.2 Animals

2.2.1 Glucagon receptor null mice (Gcg rec null mice)

Glucagon receptor knockout mice were bred in house at the Ulster University Biomedical and Behavioural Research Unit. Details regarding these mice and parameters measured during the study can be found in Chapter 3.

2.2.2 Sprague Dawley Rats

Sprague Dawley rats were obtained from Envigo. Details regarding these rats and parameters measured during the study can be found in Chapter 4.

2.2.3 NIH Swiss and Swiss TO mice

Swiss mice were obtained from Envigo. Details regarding these mice and parameters measured during the study can be found in Chapter 5.

2.2.4 Glu^{Cre} Rosa mice

Glu ^{Cre} Rosa mice were bred in house at the Ulster University Biomedical and Behavioural Research Unit from the original colony which was maintained at the University of Cambridge. Details regarding these mice and parameters measured during the study can be found in Chapter 6 and 7.

2.3 Parameters measured

Daily measurements of body weight, fluid intake, and food intake were carried out, and blood glucose was monitored on alternating days. Rodents were placed in individual cages in an air-conditioned room at 22 ± 2°C with a 12-hour light: 12-hour dark cycle in the Biomedical Behavioural Research Unit (BBRU) at Ulster University in Coleraine. Rodents were given a standard diet consisting of 10% fat, 30% protein, and 60% carbohydrate (Trouw Nutrition, Cheshire, UK) and water *ad libitum*. All animal experiments were carried out in accordance with the rules and regulations of the UK Animals (Scientific Procedures) Act of 1986.

2.3.1 Glucose tolerance test (GTT)

Intraperitoneal (i.p.) glucose tolerance tests were performed on the last day of the study on fasted NIH Swiss and Gcg rec null mice. This test involved the administration of glucose solution (18 mmol/kg body weight). Heparinised microcentrifuge tubes (Sarstedt, Numbrecht, Germany) were used to collect blood from the tail vein of conscious animals at 0, 15, and 30 minutes and centrifuged using a Beckman microcentrifuge (Beckman Instruments, Galway, Ireland). Plasma was extracted and stored at -20°C in 500 µl Eppendorf tubes until used for hormone content assays.

2.3.2 Pancreatic insulin and protein content

Pancreases that were snap frozen at the end of the *in vivo* studies were kept for protein extraction. The tissue was weighed and homogenised using a VWR VDI 12 handheld tissue homogenizer (VWR, UK) in ice cold ethanol (75% (v/v), distilled water (23.5% (v/v), and 12N HCl (1.5% (v/v)) within 8ml bijou tubes. Samples were then centrifuged at 3000RPM at 4° C for 20 minutes. Supernatant was then transferred to a 15 ml centrifuge tube and pH neutral TRIS buffer was added. Samples were then added to the speedvac overnight to allow them to dry out resulting in a fine powder. Once dried, the protein samples were resuspended in 2ml of TRIS buffer and stored at -20° C until required. For total protein content measurements, a Bradford assay was carried out. Triplicates of bovine serum albumin (BSA) standards were prepared ranging from 0-2mg/ml (0, 0.13, 0.17, 0.23, 0.3, 0.4, 0.55, 0.75, 0.96, 1.31, 1.75 and 2mg/ml) concentrations in distilled water. 5 µl of samples were diluted and added in duplicate to a 96 well plate. 250 µl of 1:8 distilled water diluted Bradford reagent (Sigma Aldrich, Poole, Dorset, UK) was pipetted into a 96- well plate and incubated at room temperature for 30 minutes. After the absorbance was read at 595 nm wavelength using a microplate reader (Molecular Devices, Sunnyvale, USA), the total amount of protein was estimated using a reference curve of BSA standards (Figure 2.1). For insulin content measurements, 20 µl of test sample was diluted with 180 µl of working radioimmunoassay (RIA) buffer (1:10 dilution) and measured using RIA as outlined below in Section 2.5.

2.3.3 Iodination of insulin for Radioimmunoassay

In-house radioimmunoassay (RIA) protocol was carried out to quantify the insulin levels in rat and mouse plasma samples. In a fume hood, the iodogen (1,3,4,6-tetrachloro-3 α, 6 α - diphenylcoluril) solution of 100 µl was prepared in a dichloromethane solution (100 µl/ml) and left overnight to create a uniform coating on the tubes when evaporated. The following day, bovine insulin, 1 mg, was dissolved in 10 mM HCl before being diluted in a buffer (125µg/ml (1:8 dilution in 500 mM sodium phosphate buffer (pH 7.4)). First, 20 µl of bovine insulin solution followed by 5 µl of sodium iodide (Na125I 100 mCi/ml stock, Perkin Elmer, Cambridge, UK) was added to the coated iodogen tubes and placed on ice for 15 minutes with occasional agitation to allow solution to mix. The solution was then placed into a new Eppendorf which contained 500µl of 50mM sodium phosphate buffer. In order to separate the reaction mixture, reverse phase high performance liquid chromatography was performed (LKB, Bromma, Sweden). Solvent A (0.12% (v/v) trifluoroacetic acid (TFA) in water) and solvent B (0.1% (v/v) TFA in 70% acetonitrile dissolved in 30% (v/v) water made up the mobile phase of the reaction. The 4.6 37 x250mm Vydar C-8 analytical reverse HPLC column (Hesperia, Ca, USA) was first washed with solvent A. The reaction mixture was then added, and the concentration of solvent B raised in the following stages: 0% - 40% duration 10 minutes, 40% - 80% duration 40 minutes, 80% - 100% duration 10 minutes. At the minute mark, over the next 60 minutes, 1ml of eluent was collected. 5µl from each of the 60 fractions was analysed on the gamma counter (1261 Multigamma counter LKB Wallac, Finland) for radioactivity. The fractions that were deemed suitable for binding affinity were kept at 4° C.

2.3.4 Insulin radioimmunoassay

Flatt and Bailey (1981) developed dextran-coated charcoal RIA to assess insulin release. Protocol as described by Flatt (1977) is written as follows: working RIA buffer was prepared by dissolving BSA (0.5 g/100 ml) in stock 40 mM sodium phosphate buffer – containing 0.3 % (w/v) sodium chloride, 0.02 % (w/v) thimerosal (preservative) and adjusted to pH 7.4 with 40 mM sodium dihydrogen orthophosphate. Triplicates of rat insulin standards were serial diluted

in working RIA buffer from 20ng/ml to 0.039ng/ml in LP3 tubes. Duplicates of unknown samples were combined with 200µl of sample, 100µl guinea pig anti-porcine insulin anti-serum (IAS PID, 1:30,000-1:45,000 dilution, and 100µl of labelled I125 insulin (~10,000 counts per minute per 100µl in working RIA buffer). The samples were then placed in 4° C for 48 hours in order for equilibrium between labelled and unlabelled insulin to occur. Dextran coated charcoal (DCC) stock solution was prepared as follows: 5g dextran T70 and 50g charcoal and dissolved in 1L stock RIA buffed and placed in 4° C until required. A dilution of 1:4 of the DCC stock with RIA buffer stock was used to generate working DCC with the addition of 1ml to every standard and sample tube with the exception for total counts and incubated at 4° C for 20 minutes. The tubes were centrifuged at 2500 rpm for 20 min at 4 °C (Model J-6B centrifuge, Beckmann instruments Inc, UK). The supernatant was decanted, and the remaining charcoal pellet counted using gamma counter (1261 multigamma counter, LKB Wallac, Finland) to asses for radioactivity. The concentration of insulin in unknown samples was determined using the spline curve-fitting algorithm (Figure 2.3).

2.3.5 Tissue processing for Immunohistochemistry

Mice were sacrificed at the end of the study by cervical dislocation. The pancreas was removed and dissected longitudinally or in half separating the head and the tail. Half of the pancreatic tissue was wrapped in aluminium foil and snap frozen in liquid nitrogen and the other half was placed in a beaker containing 4% (w/v) PFA. Frozen samples were stored at -70°C and tissue in PFA were used for immunohistochemistry. The tissues that were placed in PFA during tissue extraction were kept in the solution for 48 hours to allow the preserving of cellular architecture and cross-link proteins to occur. Tissue processing was carried out overnight using an automated tissue processor (Leica Biosystems, Nussloch, Germany). The steps included dehydrating tissues in various concentrations of ethanol, 70-100% before xylene and embedding of paraffin wax took place. Once the tissues were embedded and cooled, the tissues were sectioned into 5-7µm using a microtome (Leica Biosystems, Nussloch, Germany), and left to dry overnight on polysine coated slides (VWR).

2.4 Immunohistochemistry (fluorescence immunoreactivity)

Fluorescence immunoreactivity staining for insulin, glucagon, GFP, Ki-67, and TUNEL was assessed by the following protocol. The pancreases were paraffin embedded using an automatic tissue processor, and 5-7µm thick sections were cut using a microtome and placed on glass slides for staining. Twelve to 20 slides per animal group were processed and mounted resulting in 100-200 islets being analysed per treatment group. Each slide was dewaxed in xylene and then rehydrated using various amounts of ethanol. Slides were rinsed in deionised water and then placed in sodium citrate which was heated to 91 ^{o}C (10mM sodium citrate, 0.05% Tween 20, and a pH of 6.0) for 20 minutes and then left to cool at room temperature for 20 minutes. Next, slides were blocked in a 3% BSA/PBS (Sigma Aldrich) solution for 60 minutes. Next, they were incubated overnight at 4^{o}C with primary antibody, using primary antibodies laid out in Table 2.1. The next day, slides were rinsed in PBS two times and then incubated for one hour at 37^{o}C with secondary antibodies (Table 2.1). Excess antibody was removed by washing the slides twice in PBS for 5 minutes. DAPI (4, 6-diamidino-2-phenylindole) was added, to stain the nucleus of the cells and incubated at 37 ^{o}C for 15 minutes followed by rinsing in PBS. Finally, the slides were mounted with 50:50 glycerine/PBS, covered with a coverslip and painted with nail varnish to hold the coverslip in place. To asses alpha and beta cell apoptosis, a TUNEL assay was performed following manufacture's protocol (*In situ* cell death kit, Fluorescein, Roche Diagnostics, UK). Slides were viewed under the DAPI (350 nm), FITC (488 nm) and TRITC (594 nm) filters using a fluorescent microscope (Olympus system microscope, model BX51) and photographed using 10, 20, or 40x objective lens using the DP70 digital camera adapter system attached to the microscope.

2.4.1 Image analysis

Analysis of each islet was carried out using the Cell^F software program. This program assessed: islet area, beta and alpha cell area (expressed as µm^2), number of islets (expressed as mm^2), and alpha and beta cell percentage. Islet size distribution was defined as small,

medium, and large if they were <10,000 μm^2, 10,000-25,000 μm^2, or 25,000 μm^2. Do determined, apoptosis, transdifferentiation/dedifferentiation, and proliferation, ImageJ software was used. To determine alpha to beta cell transdifferentiation, insulin and GFP staining was used and quantified by the number of insulin positive, GFP positive cells. Alpha cell dedifferentiation was determined through, glucagon and GFP staining was quantified by the number of GFP positive, glucagon positive cells. Alpha and beta cell apoptosis was determined by TUNEL staining and quantified by counting the number of insulin or glucagon positive and TUNEL positive cells. Alpha and beta cell proliferation was determined by Ki-67 antibody along with insulin or glucagon and quantified by the number of positive insulin or glucagon, and Ki-67 cells.

2.5 Cell lines

2.5.1 Cell culture

All three cell lines, Alpha TC 1.9, Min-6, and GLUTag, were cultured in pre-warmed DMEM high glucose growth media containing 10% (v/v) foetal bovine serum (FBS) and 1% (v/v) antibiotics (100 U/ml penicillin and 0.1 mg/ml streptomycin) in 75 cm^2 sterile tissue culture flasks (Greiner bio-one, UK) and maintained at 37°C and 5% CO_2, in a LEEC incubator (Laboratory technical engineering, Nottingham, UK). Min-6 also required 2µl of 2-mercaptoethanol added to normal culture media. Every two days, cells were re-suspended in fresh media (25 ml) and maintained at 37° C till 70-80% confluent. Before experimentation, media was discarded from flasks and cells were washed with 10 ml HBSS. Cells were harvested from the surface of the flask by using 3 ml 0.025% (w/v) trypsin/EDTA. Once in 3-5ml of trypsin, cells were incubated for 3-4 min to allow trypsinization to occur. Once the cells have detached, fresh culture media (7 ml) was added to the detached cells and gently pipetted continuously until a single suspension was formed. The cell suspension was then transferred to a 50 ml Sterilin tube (Sterilin Ltd., Hounslow, UK) and centrifuged at 900 rpm for 5 min (1200 rpm for alpha TC cells). The supernatant was discarded, and pellet re-suspended in a

known volume of cell media. Cells were counted using trypan blue (Sigma Aldrich, Poole, Dorset, UK) and a histocytometer and seeded according to the assay being performed.

2.6 Cellular assays

2.6.1 MTT Assay

Three cell lines; MIN-6, Alpha TC, and GLUTag, were used to carry out the cellular viability assay. Cells were grown in flasks and incubated until confluent and then seeded on a 96 well plate at 125,000 cells/well. Seeded wells were incubated until confluent. 5mM of Syn A plus 1.5ml of media to create the stock. 10mM of cobalt was measured on a weighing scale and mixed with 3ml of media to create the stock. Serial dilution was carried out into several bijous containing culture media and added into each well. Various concentrations allowed for the treatment to penetrate the cell lines followed by a 2 or 8-hour incubation period. The appropriate media for each cell line was used as a control. 125µl of MTT was then added to each well, covered in foil, and incubated for two more hours. 100µl of DMSO was added to each well and the well plates were read at the Flex station using the Softmax Pro program. Analysis was then carried out in GraphPad Prism. Further MTT assays were carried out at the 2 or 8-hour time point with media containing FBS with 2.5 mM treated alpha cells in addition to specific inhibitors. The inhibitors, that inhibit DNA strand breaks, concentrations that were used are as followed: nicotinamide (10mM), theophlylline (5mM), benzamide (1mM), and the inhibitors that scavenge OH radicals; high glucose (20mM), sodium benzoate (50mM), DMSO (28mM), butanol (22mM), superoxide dismutase (2000u/ml), and catalase (250u/ml).

2.6.2 RNA extraction from alpha cells

RNA was isolated from cells and tissues using TRI reagent (TRIZOL; Sigma, UK). The procedure was followed according to the suppliers' protocol. Briefly, cells were seeded into 6 well plates (Nunc) and left to grow overnight at 37^{o}C. The cells were washed the next day with HBSS and media removed. They were treated with 1ml/well of ice-cold TRI reagent and left to incubate for 10-15 min. The lysed cell solution was mixed and transferred into a 1.5ml

Eppendorf and centrifuged at 12,000g for 10 min at 4°C. 200 µL of chloroform per mL of TRI reagent was added to the lysed cells and mixed vigorously before being centrifuged at 12,000g for 15 minutes at 4 °C Three visible layers appeared and the top aqueous layer was extracted and mixed with isopropanol (500µl) followed by another centrifuge spin at 14,000g for 20 minutes. This caused the RNA to precipitate. The precipitate was washed three times in 75% ethanol followed by adding 20 µL of RNA-free water. To quantify the purity of the RNA was then tested on a NanoDrop ND-1000 UV/Vis spectrophotometer. Samples which produced OD260/OD280 ratio >1.8 were considered pure and were then used for cDNA conversion.

2.6.3 RNA to cDNA conversion

The mRNA sample that was obtained from cells was converted into cDNA for Polymerase chain reaction (PCR) to check the expression of various genes. 1 -3 µg of mRNA (each separate sample) was converted to cDNA. OligoDT was added to the RNA samples and placed in the thermocycler (Thermocycler, Bio-Rad, UK) at 70° C to cause the secondary structure of RNA to denature and anneal. A mastermix was created using the first strand buffer, dNTPs, DTT, and superscript reverse transcriptase. Then placed back in the thermocycler at 42°C for one hour. After this hour, the solution was heated to 70°C causing the transcriptase enzyme to inactivate. The samples were then quantified by the NanoDrop ND-1000 UV/Vis spectrophotometer and stored at -20° C.

2.6.4 Real Time Polymerase Chain Reaction (RT-PCR)

The reaction mixture for RT – PCR was prepared by making a master mix for each gene depending on the number of reactions. The master mix contained 9 µL SYBR green (Roche), 1 µL each of the forward primer and reverse primer of the gene, 6 µL of RNA-free water. This 17 µL was prepared for one reaction. After adding this master mix to the PCR wells a 96 well plate, 1 µL of cDNA was added. The PCR run was started after centrifugation on plates containing negative control for each primer and the housekeeping gene β - actin. The amplification conditions were carried out on the LightCycler 480 machine (Roche Diagnostics Ltd., Switzerland) at 95° C for 10 minutes. This was followed by 55 additional cycles at 95° C

for 10 seconds each. The annealing condition was set to 60ºC for 30 seconds followed by 72ºC for 1 second. A melting curve analysis with the temperature range set from 60ºC to 90ºC was generated for each run. The results were analysed by the ΔΔCt method and the mRNA obtained for all genes were normalized with the housekeeping gene β – actin control.

Table 2.2. outlines the mouse primers that were used in PCR assay.

2.6.5 Immunocytochemistry

Alpha TC cells were stained for proliferation after being incubated for 2 hours in the respected treatments. Cells were seeded overnight in a 12 well plate with sterilized 16mm round coverslips at the bottom of each well. After incubation in the conditions, media was discarded, and wells were washed in PBS. Each well was then fixed in a 4% paraformaldehyde for 30 minutes. Antigen retrieval was carried out by adding 1ml sodium citrate buffer to each well and incubation for 20 minutes at 90°C followed by a further 20 minutes at room temperature to cool. Blocking was then carried out by addition of 1ml of 3% (w/v) BSA solution in PBS and left to incubate at room temperature for 45 minutes. The same antibodies used for immunohistochemistry for Ki67 and glucagon double stained were used in immunocytochemistry. Coverslips were placed cell side down on the slide, covered in foil and stored in -20° C until analysis occurred. Stained sections were viewed at 20x and 40x objective lens. FITC (488 nm) and TRITC (594 nm) filters on a fluorescent microscope (Olympus system microscope, model BX51) and photographed using the DP70 digital camera adapter system connected to the microscope. A total of 150 cells per treatment were analysed.

2.6.6 Trypan Blue

Alpha TC cells were seeded into a 6-well plate, three wells per treatment and left overnight to incubate. The following day, specific treatments were added to the cells for 2 hours to assess cellular death. Cells were trypsinised and fresh media was added and spun down with a centrifuge to create a pellet. Fresh media was added and once the pellet was disrupted, 200µl

was placed in an Eppendorf with trypan blue and alive and dead cells were counted on the histocytometer. Analysis was carried out by creating a percentage of dead cells and graphed using GraphPad Prism.

2.6.6 Flow Cytometry

Alpha TC cells were grown overnight in a 6-well plate, one plate per treatment. Treatments were added to the wells and incubated for 2 hours. Flow cytometry was carried out according to suppliers' protocol (Dead cell apoptosis kit with Annexin V Alexa Fluor 488 and Propidium iodide (PI), ThermoFisher Scientific, UK). Waste media was discarded into a universal and the wells were washed with PBS. Discarded PBS was added to the waste universal. The wells were then trypsinised and once the cells detached, fresh media was added and then discarded into the waste universal. The waste universals were then centrifuged and the supernant was discarded. The pellet was resuspended in ice cold PBS and placed back in the centrifuge. Next the PBS was discarded and the 1X annexin-binding buffer is prepared and cells resuspended in this buffer. Next, Alexa Fluor 488 annexin V was added to the cells and they were incubated at room temperature for 15 minutes. The 1X annexin- buffer was added once again and kept on ice. Flow cytometry was performed to detect the different stages of apoptosis and necrosis.

2.7 Statistics

GraphPad Prism v.5 software and Image J software was used to analyse results and generate graphs with data presented as mean plus or minus standard error of the mean (SEM). Statistical analysis was carried out using a two-way Repeated Measures ANOVA test followed by a Bonferroni post-test or an unpaired student t-test was carried out. Any p-value <0.05 was deemed statistically significant.

Table 2.1 Antibodies used for immunohistochemistry and immunocytochemistry

Primary Antibodies

Target	Host	Clonality	Dilution	Used for	Source
Insulin	Mouse	Monoclonal	1:400	Beta cells	Abcam (ab6995)
Glucagon	Guinea-pig	Polyclonal	1:400	Alpha cells	Raised in house (PCA2/4)
GFP	Goat	Polyclonal	1:1000	Transdifferentiation	Abcam (ab5450)
Ki-67	Rabbit	Polyclonal	1:500	Proliferation	Abcam (ab15580)
TUNEL	N/A	N/A	(450µl buffer: 50µl enzyme)	Apoptosis	Roche

Secondary Antibodies

Target	Host	Reactivity	Dilution	Used for	Source
IgG	Goat	Mouse	1:400	Beta cells	Alexa Fluor 488 or Alexa Fluor 594, Invitrogen
IgG	Goat	Guinea-pig	1:400	Alpha cells	Alexa Fluor 488 or Alexa Fluor 594, Invitrogen
IgG	Goat	Rabbit	1:400	Proliferation	Alexa Fluor 594, Invitrogen
IgG	Donkey	Goat	1:400	Transdifferentiation	Alexa Fluor 488, Invitrogen

Table 2.1. List of mouse primers

Official gene symbol	Alias/common name	Primer sequence (5'-nt-3')	Gene expression category
Pcsk1	PC 1/3, Protein convertase subtilisin/ kexin type 1	**F**: GAATGGGCGGCGGAGATCCC **R**: CGGGACCTCCGAGGATGGCTT	Secretion function
Pcsk2	Pc 2, Proprotein convertase subtilisin/ kexin type 2	**F**: CCGAGGAGGAGCTGAAAATGCAGAT **R**: CTGGCTGGCAGGGGTGCGAAT	Secretion function
Gcg	Proglucagon	**F**: TAACCCCCAGCCCTTAGTGA **R**: ACACACCAGGTAGAGAGCCT	Secretion function
Slc2a2	Glucose transporter 2	**F**: ACCGGGATGATTGGCATGTT **R**: GGACCTGGCCCAATCTCAAA	Secretion function
ERK 1	Extracellular signal-regulated kinases	**F**: GCTTATCAACACCCCCTGC **R**: CGTGCTCAGGGTCAGCAATC	Proliferation
ERK 2	Extracellular signal-regulated kinases	**F**: GACAAGGGCTCAGAGGACTG **R**: CTGAGACGGGCTGAAGACAG	Proliferation
Bax	BCL2-associated X Protein	**F**: TGAGCGAGTGTCTCCGGCGA **R**: CACGCGGCCCCAGTTGAAGT	Apoptosis
Bcl 2	B cell lymphoma	**F**: ATGGCCCCAGCATGCGACCTC **R**: CACTTGTGGCCCAGGTATGCACC	Apoptosis
Nos 2	Nitric oxide synthase 2, inducible	**F**: GCTCGCTTTGCCACGGACGA **R**: AAGGCAGCGGGCACATGCAA	Apoptosis
Nxfb1	Nuclear factor of k light polypeptide gene enhancer in B cells 1	**F**: AGAAGTCTGGGCGCACAGCG **R**: TGGTGGACCCTCTTCCGGCC	Apoptosis
Cat	Catalase	**F**: TCAGGGCCGCCTTTTTGCCT **R**: TCGAGCGCGGTAGGGACAGT	Antioxidant defence
GPX-1	Glutathione peroxidase 1	**F**: CCCCACTGCGCTCATGACCG **R**: CGAAAGCGGCGGCTGTACCT	Antioxidant defence

Sod 1	Superoxide dismutase, soluble	**F**: TTCCGTCCGTCGGCTTCTCGT **R**: CGCACACCGCTTTCATCGCC	Antioxidant defence
Sod 2	Superoxide dismutase 2, mitochondrial	**F**: TTCCCAGGATGCCGCTCCGT **R**: GCGTCTGCTAGGCAGCGTCC	Antioxidant defence
Hspa 4	Hsp 70, heat shock 70-kd protein 4	**F**: GCACTGTGCACTGTACCAGGGGA **R**: TCTCCAGGGAACTGGGCAGCTA	ER Stress
Hspa 5	BiP, heat shock 70-kd protein 5	**F**: TGCGTGTGTGTGAGACCAGAAC **R**: CCCCAAGTCGATGCCGACCAC	ER Stress
Arx	Aristaless-related homeobox	**F**: TCAAGCATAGCCGCGCTGAG **R**: ACACCTCCTTCCCCGTGCTG	Alpha cell marker
Pax 6	Paired box gene 6	**F**: TTTAACCAAGGGCGGTGAGCAG **R**: TCTCGGATTTCCCAAGCAAAGATG	Alpha cell marker
Glut 2	Glucose transporter 2	**F**: TTGGTTTTGAGGAGGTTGGGAA **R**: AAGAGGTAGCCTGACCTGTGG	Beta cell marker
Ins1	Insulin	**F**: TAACCCCCAGCCCTTAGTGA **R**: ACACACCAGGTAGAGAGCCT	Beta cell marker
Pdx 1	Pancreatic and duodenal homeobox 1	**F**: GACCCAGAGTGTGGACGTG **R**: GCTCTCGTGCCCTCAAGAAT	Beta cell marker

Figure 2.1 Quantification of total proteins by Bradford assay using BSA standards

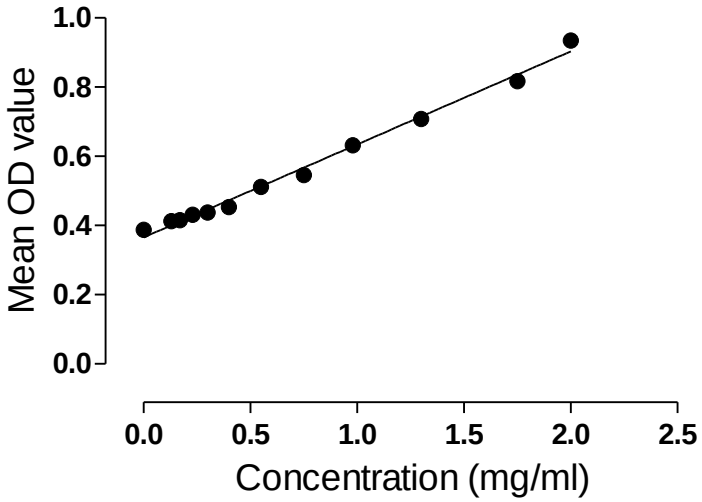

BSA standard curve for the quantification of total protein used in the Bradford assay. BSA as standards from concentrations ranging from 0-2mg/ml. Values are mean ± SEM, n= 3.

Figure 2.2 Iodination of insulin

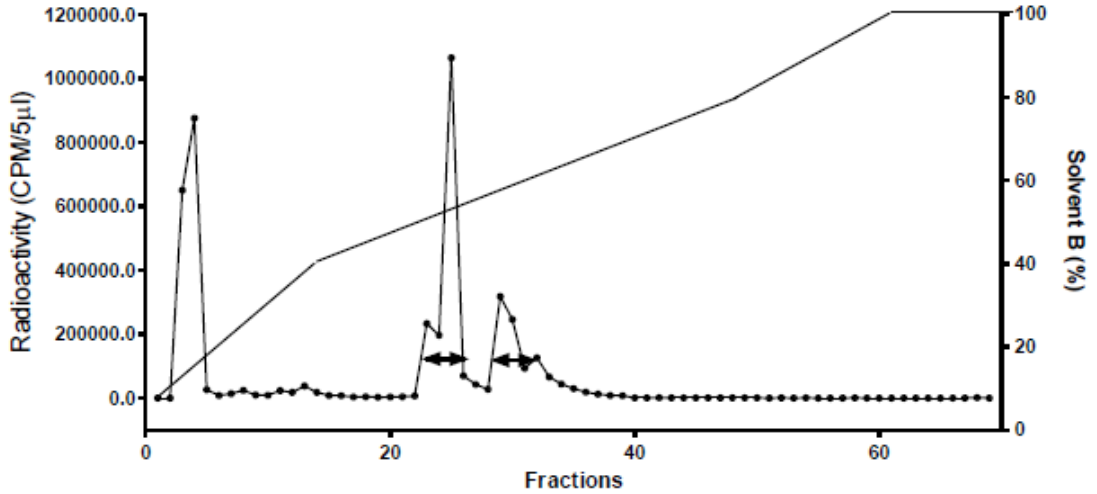

Purification of iodinated insulin using RP-HPLC. Iodination of insulin using a radioactive isotope of iodine, I^{125}. This was prepared by solid phase iodogen method and purified by HPLC. Fractions were collected every minute with the peak fractions between 23-35 minutes which was used for insulin RIA.

Chapter 3

The effects of a single dose of Synthalin A on pancreatic islet function in glucagon receptor knockout mice

3.1 Summary

The absence of the glucagon receptor (Gcg rec) has been reported to result in alpha cell hyperplasia. In a 5-day study, male heterozygous and gcg rec null mice were treated by an intraperitoneal injection (i.p.) with either 0.9% saline or a single dose of 5mg/kg Synthalin A (Syn A). Food and fluid intake were decreased near the end of the study in the Gcg rec null mice given Syn A. An increase in blood glucose levels over a 60-minute glucose tolerance test (GTT) was demonstrated in the Gcg rec null and Gcg rec null mice receiving Syn A mice groups. Histological analysis was performed to evaluate the impact of Syn A, along with possible alpha cell hyperplasia. Gcg rec null mice and Gcg rec null mice with Syn A mice exhibited a decrease in the number of islets per mm^2. The Gcg rec null mice with Syn A also displayed a decrease in islet area. In these mice, the alpha cell area and percentage was decreased when compared to the saline treated mice. Beta cell area and percentages were consistent among all three groups. A decrease was observed in the $Ki67^{+ve}$ $glucagon^{+ve}$ cells in the Gcg rec null and Gcg rec null mice given Syn A. These data indicate that Syn A displays alpha cell toxicity with possible knock-on effects on other islet cell populations.

3. 2 Introduction

As stated previously, glucagon is a hormone that is secreted from the alpha cells of the pancreatic islets and counter-regulates insulin via major effects on hepatic glucose production (Bagger *et al.* 2011; Baggio and Drucker, 2007). The secretion of glucagon from the alpha cells is influenced by several factors such as glucose, amino acids, beta cell products (insulin, amylin), somatostatin, and hormones, such as GLP-1, and activation of autonomic innervation. When glucose levels are decreased, the alpha cells secrete glucagon which helps raise blood glucose levels. In addition to effects on secreted insulin, the activation of the beta cells also causes the release of substances that help regulate glucagon secretion via paracrine interactions. This activity by the beta cells on the alpha cells provides insight into our understanding of how glucose can directly regulate glucagon secretion (*Cantini et al*. 2016; Bagger *et al.* 2011).

The glucagon receptor is expressed in several tissues, muscles, and organs, such as the pancreatic islets, heart, smooth muscle, intestine, kidneys, adipose tissue, and certain areas of the brain. It has been reported that Gcg rec null mice had improved oral glucose tolerance and did not become hypoglycaemic (Cantini *et al*. 2016; Bagger *et al.* 2011; Parker *et al.* 2002). In another study, it was concluded that the Gcg rec null mice not only had improved oral glucose tolerance but also demonstrated enhanced insulin sensitivity (Bagger *et al.* 2011; Sørensen *et al.* 2006; Gelling *et al.* 2003). When these Gcg rec null mice were fasted for 24 hours, glucose levels were lower than the wild type animals. However, the Gcg rec null mice exhibited hyperglucagonemia and the alpha cells became hyperplasic (Bagger *et al.* 2011; Gelling *et al.* 2003).

The aim of this study was to evaluate metabolic characteristics and islet morphology in glucagon receptor knockout mice. A second aim of this study was to examine the effects of Syn A on gcg rec null mice. We have evaluated the effects of Syn A in a heterozygous group and in Gcg rec null mice. The administration of Syn A in Gcg rec null mice is important since Syn A is an alpha cell toxin and these mice have an abundance of alpha cells. Results of the pancreas and islet morphology of this study showed that the Gcg rec null mice treated with Syn A had a decrease in islet cells, specifically the alpha cells.

3. 3 Materials and methods

All materials and methods for this study have been presented briefly in 3.3.1 to 3.3.3. A detailed description of the materials and methods can be found in Chapter 2.

3.3.1 Glucagon receptor null mice

Twenty-one, 12-week-old male mice were bred in-house, at the Biomedical Behavioural Research Unit (BBRU) at Ulster University in Coleraine. Three groups consisting of 7 mice each were used in this animal study and genotyped by ear snips to confirm knockout mice. Group one consisted of 7 heterozygous mice injected with 0.9% saline, group two consisted of 7 Gcg rec null mice injected with 0.9% saline, and group three was made up of 7 Gcg rec

null mice given a one-time Syn A injection of 5 mg/kg. The latter group was intended to test the effects of Syn A in a model devoid of glucagon action. For 5 days, following the initial one-off injection, various parameters were measured, and monitored. On the final day mice were sacrificed, and the pancreas was removed for further analysis involving immunohistochemistry and RIA. Fasting and non-fasting blood was also collected at the end of the study to examine the insulin levels in plasma.

3.3.2 Immunohistochemistry

Twenty-one pancreas were sectioned longitudinally and preserved in paraformaldehyde (PFA). One half was flash frozen for future hormone content and the other half was embedded into paraffin for histological analysis. Immunohistochemistry was carried out on the tissue blocks. Primary antibodies: mouse monoclonal anti-insulin antibody (ab6995, 1:1000; Abcam), guinea-pig anti-glucagon antibody (PCA2/4, 1:200; raised in-house) and Ki67 primary polyclonal anti rabbit- 1:500 (ab15580), were used. Secondary antibodies included: Alexa Fluor 488 or Alexa Fluor 594 goat anti mouse, IgG- 1:400, Alexa Fluor 488 or Alexa Fluor 594 goat anti guinea pig, IgG- 1:400, and Alexa Fluor 594 goat anti rabbit, IgG- 1:400. DAPI was used as nuclei stain. Slides were mounted and analysed using an Olympus fluorescent microscope fitted with DAPI (350nm) FITC (488nm) and TRITC (594nm) filters and a DP70 camera adapter system using Cell^F program.

3.3.3 Statistics

All graphs and figures in this Chapter were generated using GraphPad Prism v.5 software and Image J. A two-way Repeated Measures ANOVA test followed by a Bonferroni post-test or an unpaired student t-test was carried out. Any p-value <0.05 was deemed statistically significant.

3.4 Results

3.4.1 Effects of Syn A on body weight and body weight change in heterozygous and Gcg rec null mice.

Figure 3.1A, shows no significance regarding body weight. No significance was found between any of the groups regarding percentage of weight change (Figure 3.1B).

3.4.2 Effects of Syn A on food and fluid intake in heterozygous and Gcg rec null mice.

After 5 days, the Gcg rec null mice had consumed more food than the other two groups (Figure 3.2A). The Syn A treated mice showed a slight decline ($p<0.01$) on day three of the study, when compared to the other Gcg rec null mice. On day 4, the Gcg rec null mice demonstrated an increase ($p<0.01$) in food intake when compared to the heterozygous mice. Syn A treated mice had a significantly large increase ($p<0.001$) in food amount when compared to the Gcg rec null mice. On the final day of the study, the non-treated Gcg rec null group ($p<0.01$) showed a significant increase compared to the heterozygous mice. When examining the Syn A treated mice ($p<0.05$) against the other Gcg rec null group, there was a significant decrease in food intake.

On day 0, the Gcg rec null mice showed a slight increase ($p<0.05$) in their fluid consumption, when compared to the heterozygous mice (Figure 3.2B). Although, cumulative fluid intake continued to increase for all, no significance was shown until the third day of the study. On days 3 to 5, the only significance ($p<0.05$; $p<0.01$) recorded was when the Syn A treated mice were compared to the heterozygous mice.

3.4.3 Effects of Syn A on blood glucose and during an i.p. GTT in heterozygous and Gcg rec null mice.

As seen in Figure 3.3A, the Gcg rec null group exhibited raised glucose ($p<0.05$) levels which are present on days 1 when compared to heterozygous mice. As seen in Figure 3.3B, when comparing the heterozygous mice with the Gcg rec null mice ($p<0.01$) and Syn A treated mice

(p<0.001) displayed a significant increase which was observed at the 15-minute time point. At the 30-minute mark, Gcg rec null mice displayed another increase (P<0.001) when compared to the heterozygous mice. Also, at this time point, the Syn A treated mice were deemed significant (p<0.01) when compared to the other Gcg rec null mice. At the final time point, 60- minutes, there continued to be a slight significance when the heterozygous and Gcg rec null mice (p<0.05) were compared. Figure 3.3C shows a significant increase in Gcg rec null mice (p<0.001) when compared to heterozygous mice, and in Syn A treated mice (p<0.01) when compared to the un-treated Gcg rec null mice.

3.4.4 Effects of Syn A on non-fasting and fasting plasma insulin in heterozygous and Gcg rec null mice.

As shown in figure 3.4A, Syn A had no significant effect on the non-fasting plasma insulin levels were increased.

3.4.5 Effects of Syn A on the number of islets, islet area, and islet size distribution in heterozygous and Gcg rec null mice.

As shown in Figure 3.5A, the number of islets was significantly decreased in Gcg rec null mice (p<0.01) and Syn A (p<0.05) (Figure 3.5B) when compared to heterozygous mice. When compared to the heterozygous mice, the Syn A mice showed a significant difference (p<0.01) and a significant decrease (p<0.05) in islet area when compared to the Gcg rec null mice. In No significance was found between the three groups regarding size distribution (Figure 3.5C).

3.4.6 Effects of Syn A on alpha cell area and percentage and beta cell area and percentage in heterozygous and Gcg rec null mice.

The alpha cell area was decreased in the Gcg rec null mice once treated with Syn A (p<0.01) when compared to the heterozygous mice (Figure 3.6A). The alpha cell percentage was significantly decreased (p<0.001) by about 10% in the Syn A treated mice when compared to heterozygous and Gcg rec null mice (Figure 3.6B). No significance was found when looking at beta cell area or beta cell percentage (Figure 3.6C and Figure 3.6D). Photo representation

is seen in Figure 3.7A-C. Insulin is represented in green, glucagon in red, and DAPI in blue.

3.4.7 Effects of Syn A on Ki67 positive, insulin positive cells and Ki67 positive, glucagon positive cells in heterozygous and Gcg rec null mice.

As shown in Figure 3.8A, shows no significance regarding beta cell proliferation. Photo representation is displayed in Figures 3.8B-D. Ki67 cells are represented in red, insulin in green, and DAPI in blue. Proliferation of alpha cells was significantly decreased ($p<0.01$) in the Syn A treated mice when compared to heterozygous and un-treated Gcg rec null mice. Photo representation is Figure 3.9B-D. Ki67 cells are represented in red, glucagon in green, and DAPI in blue.

3.5 Discussion

The aim of this study was to evaluate the metabolic and islet morphology effects of Syn A in glucagon (gcg) rec null mice. Past research states that the Gcg rec null mice in their study exhibited normal food consumption as well as body weight, perhaps even reduced body weight (Conarello *et al.* 2007; Gelling *et al.* 2003; Burcelin *et al.* 1996). The control Gcg rec null mice had a slightly higher food consumption.

It has been suggested that Gcg rec null mice exhibited improved oral glucose tolerance and do not become hypoglycaemic (Bagger *et al.* 2011; Parker *et al.* 2002). This was true in the current studies. The Gcg rec null mice with and without the treatment did not enter a hypoglycaemic phase. In another study, it was concluded that the Gcg rec null mice not only exhibited improved oral glucose tolerance, but increased insulin sensitivity (Bagger *et al.* 2011; Conarello *et al.* 2007; Sørensen *et al.* 2006; Gelling *et al.* 2003). Since Syn A is an alpha cell toxin, it can be suggested that the dose given to these mice eliminated some but not all of the alpha cells instead of eliminating all of them. A few of the mice in the Gcg rec null group had higher blood glucose levels than those of the other two groups. This is clear on the increase in Gcg rec null mice blood glucose increase on day one. Previous research states that the Gcg rec null mice displayed lower blood glucose levels due to the Gcg receptor

gene being disrupted (Gelling *et al.* 2003). However, Parker *et al.* (2002) states that the Gcg rec null mice lack glucagon receptors and therefore their glucose levels would be elevated, which confirms our blood glucose results of these mice. Their blood glucose levels remained higher than the other two groups throughout the study. When Gcg rec null mice were fasted for 24 hours, glucose levels were lower than the wild type animals, however this current study shows the heterozygous and the Syn A treated mice had a better GTT results than the Gcg rec null mice (Bagger *et al.* 2011; Gelling *et al.* 2003).

According to Parker *et al.* (2002), plasma insulin levels in these mice appeared lower than the wild type mice and the mice with the Gcg receptor gene. Our fasting data proves to be congruent with Parker *et al.* (2002). However, the non-fasting plasma levels within our study showed that the Gcg rec null mice had no significant change compared to the heterozygous mice.

Results of the pancreas and islet morphology of this study showed that the Gcg rec null mice with and without Syn A had a decrease in islet cells, specifically the alpha cells. Alpha cell hyperplasia did not occur in the islets that have been analysed from the first set of Gcg rec null mice which contradicts the findings in previous research (Conarello *et al.* 2007; Sørensen *et al.* 2006; Gelling *et al.*2003; Parker *et al.* 2002). Similar to Gelling *et al.* (2003), the islets that were analysed from the Gcg rec null mice showed areas that were rich in insulin. This could explain why the beta cell area and percentage was much higher than expected. It has also been documented that the majority of the Gcg rec null mice islets were located next to ducts and within the exocrine tissue (Gelling *et al.* 2003; Bouwens and Blay, 1996; Rall *et al.* 1973). This was not observed in this current study. This is also true when proliferation staining with Ki67 was examined. There was no increase in alpha cell proliferation in the Gcg rec null mice. However, there was an increase in beta cell proliferation in the non-treated Gcg rec null mice. As expected, the mice treated with Syn A showed very little proliferation of the alpha cells when stained for Ki67 and glucagon. The outcome of the immunohistology in the Gcg rec null mice treated with Syn A suggests that like previous studies that it is indeed an alpha

cell toxin (Martini *et al.* 2015; Langslow *et al.* 1973; Beekman, 1956; Davis, 1952; Fodden and Read, 1953; Karr *et al.* 1929).

The major limitation of this study was the dissection of the pancreas. The pancreas that was examined was cut longitudinally and both the head and tail were examined together. This study raises the question, about the anatomical sections of the pancreas in these transgenic mice. Perhaps, if the head and tail were separated it would have provided a clearer picture of the alpha cells in the tail of the pancreas in each of these mice groups, especially the Gcg rec null mice. In conclusion, this is the first study that has been done, to our knowledge that included Gcg rec null mice being treated with Syn A. We can conclude that a treatment with Syn A causes a decrease in food and fluid consumption. We also concluded the effects of this toxin on alpha cell area, percentage, and proliferation.

Figure 3.1 Effects of Syn A on body weight (A) and body weight change (B) in heterozygous and Gcg rec null mice over 5 days following injection.

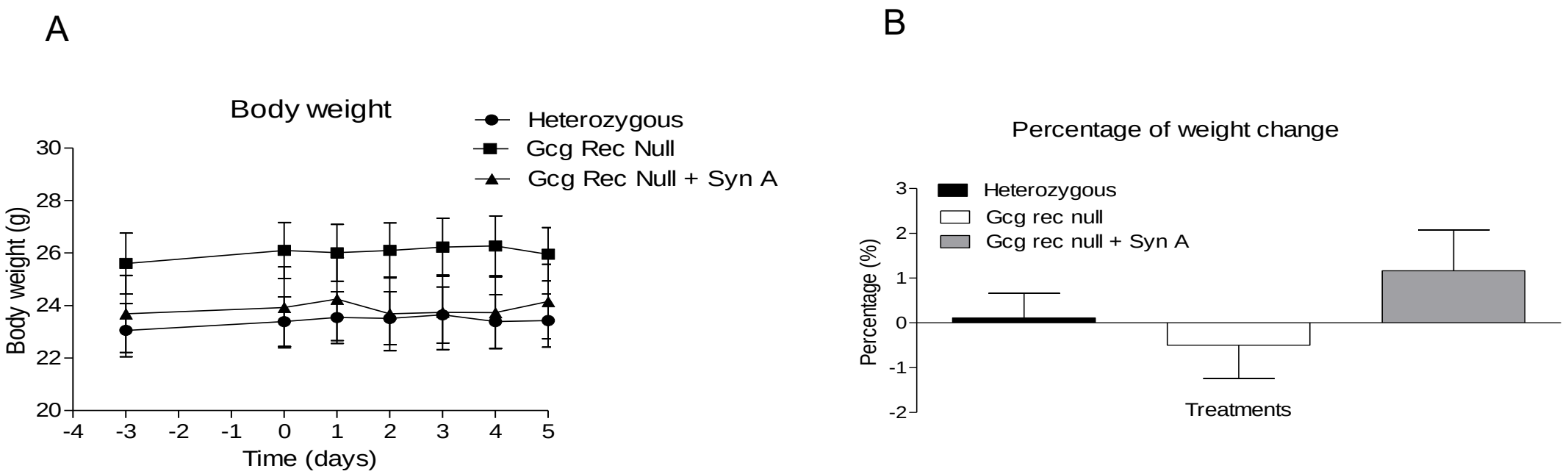

Daily measurements of body weight (A) percentage of weight change over the course of a 5-day study (B). Syn A was administered by i.p. injection at a dose of 5mg/kg on day 0. Values are mean ± SEM (n=7 mice). Changes were deemed significant when p values were $p<0.05$.

Figure 3.2 Effects of Syn A on food (A) and fluid (B) intake in heterozygous and Gcg rec null mice over 5 days following injection.

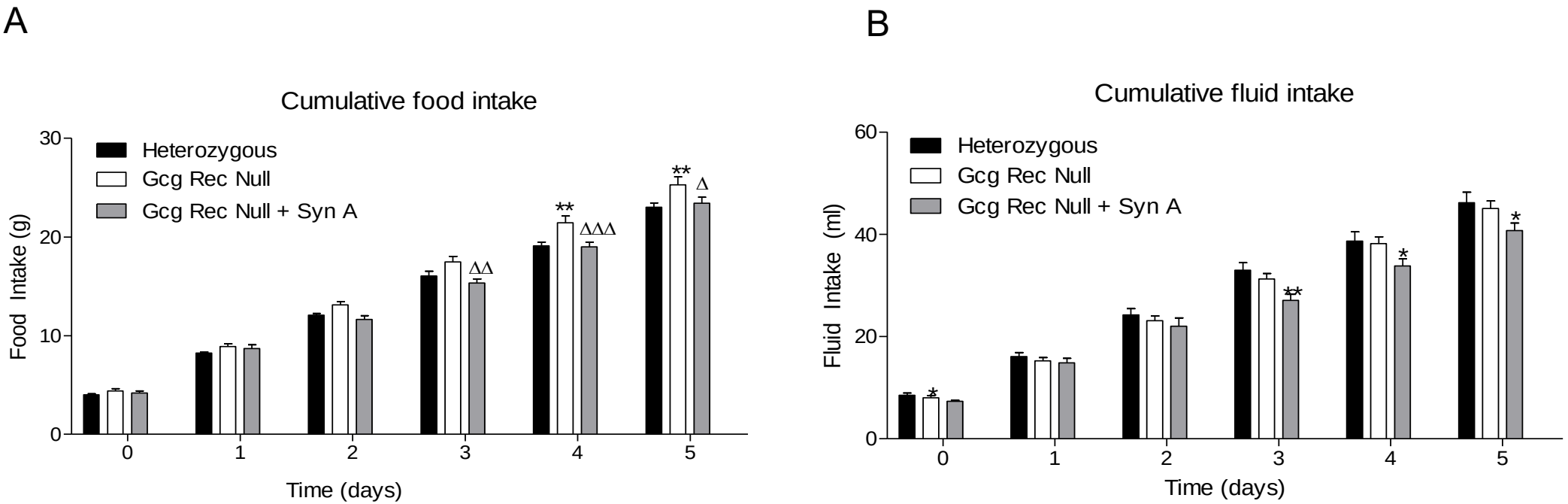

Daily measurements of food (A) and fluid (B) intake throughout the 5-day study. Syn A was administered by i.p. injection at a dose of 5mg/kg on day 0. Values are mean ± SEM (n= 7 mice). Changes were deemed significant when p values were *p <0.05 or **p <0.01 when compared with heterozygous mice. $^{\Delta}$p <0.05, $^{\Delta\Delta}$p <0.01, or $^{\Delta\Delta\Delta}$p <0.001 when Gcg rec null mice were compared with the Syn A treated Gcg rec null mice.

Figure 3.3 Effects of Syn A on blood glucose (A) and during an i.p. GTT (B and C) in heterozygous and Gcg rec null mice over 5 days following injection.

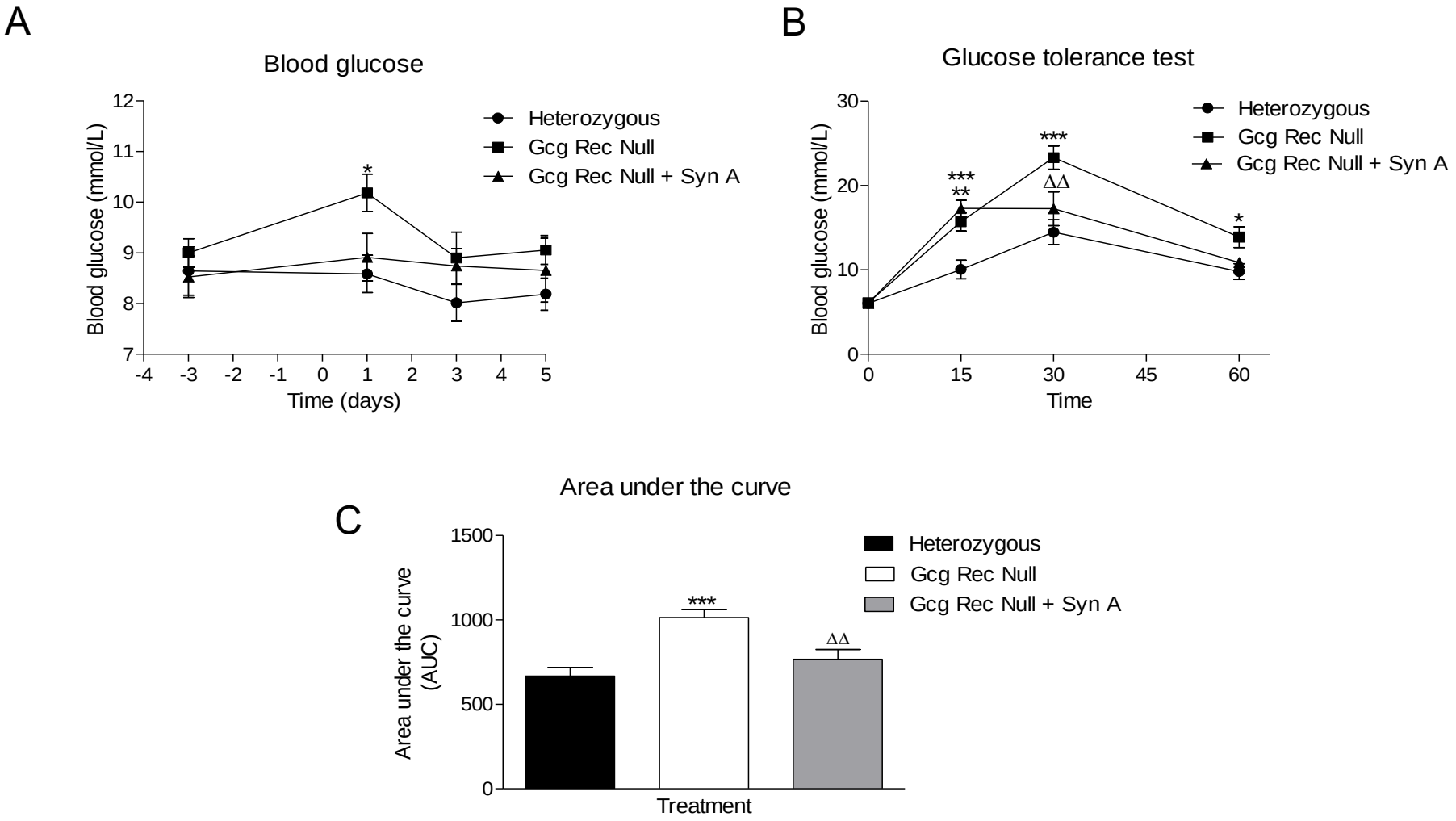

Blood glucose which was measured on alternating days (A) and the GTT (B and C) was performed on the final day of the study. Syn A was administered by i.p. injection at a dose of 5mg/kg on day 0. Values are mean ± SEM (n=7 mice). Changes were deemed significant when p values were $^{*}p < 0.05$, $^{**}p < 0.01$, or $^{***}p < 0.001$ when compared with heterozygous mice. $^{\Delta}p < 0.05$ or $^{\Delta\Delta}p < 0.01$, when Gcg rec null mice were compared with the Syn A treated Gcg rec null mice.

Figure 3.4 Effects of Syn A on nonfasting (A) and fasting (B) plasma insulin in heterozygous and Gcg rec null mice over 5 days following injection.

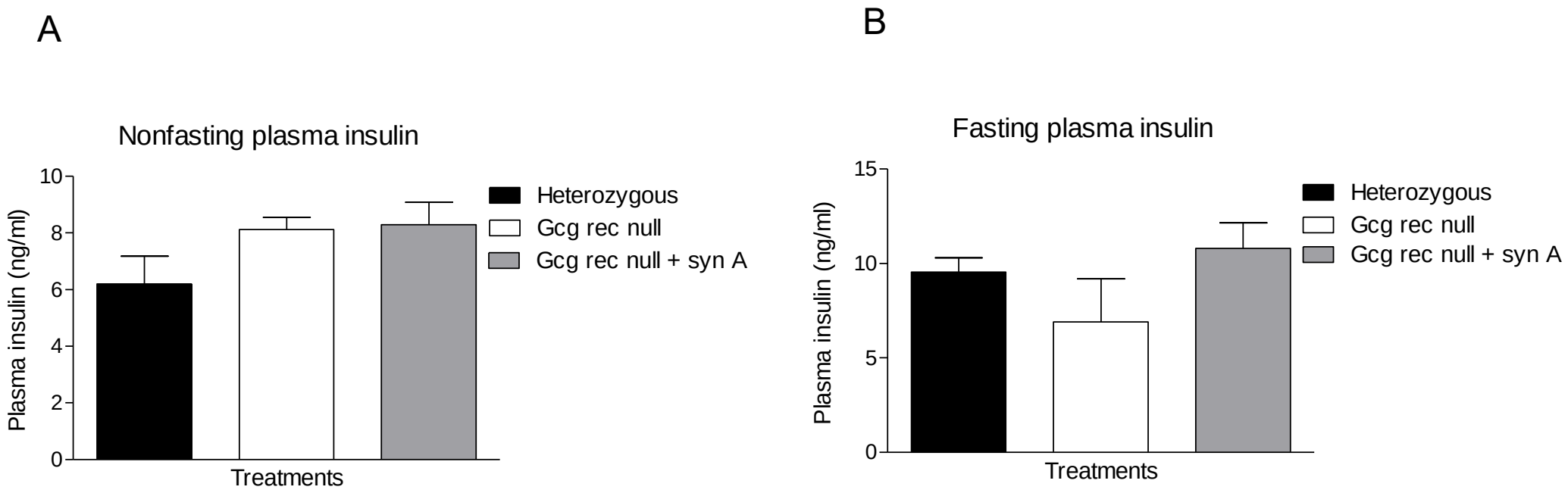

Nonfasting (A) and fasting (B) blood was taken at the end of the study. Plasma and insulin was measured by RIA. Syn A was administered by i.p. injection at a dose of 5mg/kg on day 0. Values are mean ± SEM (n= 7 mice).

Figure 3.5 Effects of Syn A on the number of islets (A), islet area (B), and islet size distribution (C) in heterozygous and Gcg rec null mice over 5 days following injection.

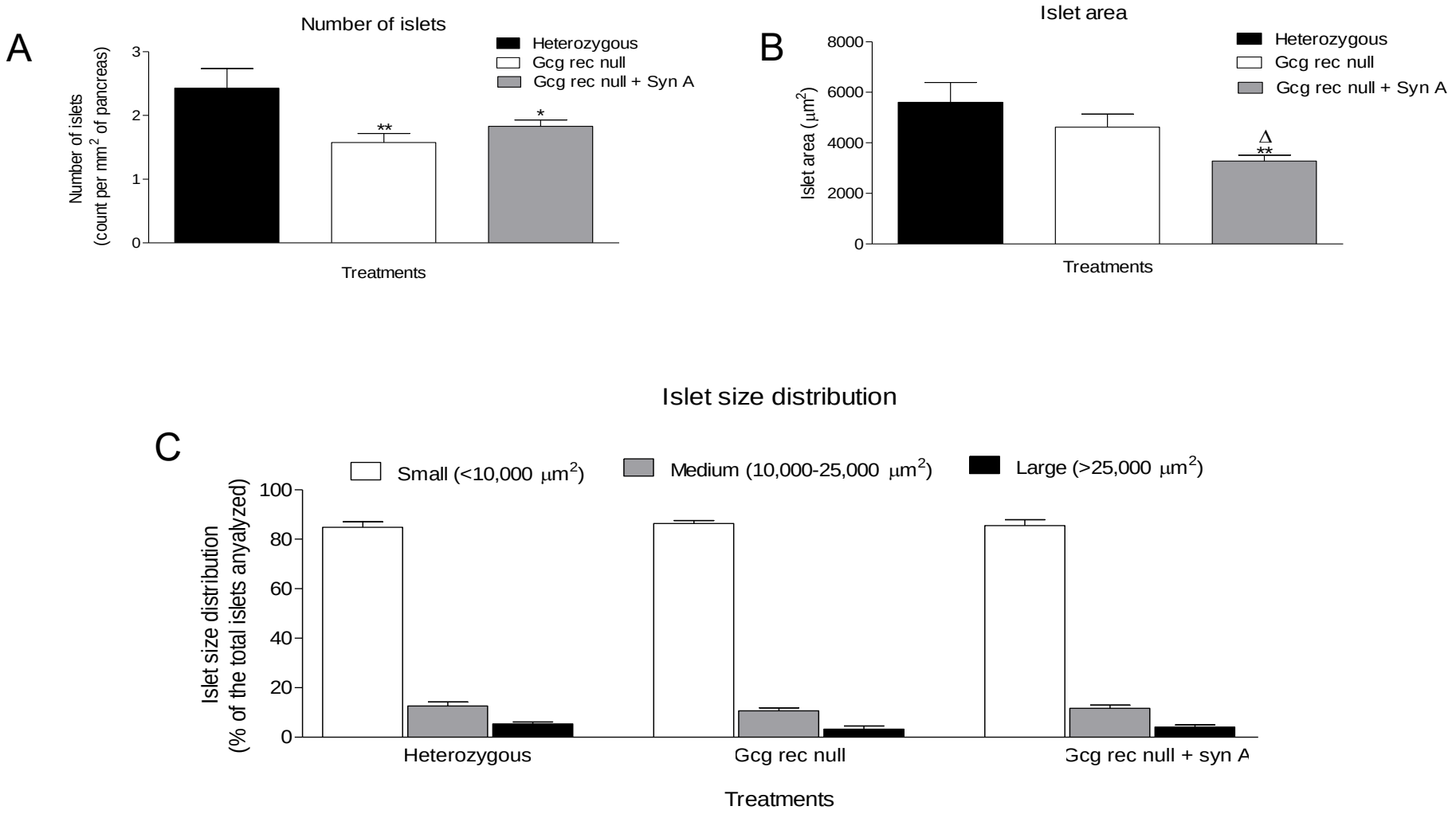

Number of islets (A) islet area (B), and islet size distribution (C) per pancreas. Syn A was administered by i.p. injection at a dose of 5mg/kg on day 0. Values are mean ± SEM (n= 7 mice). Changes were deemed significant when p values were *p<0.05, or **p <0.01 when compared with heterozygous mice. $^{\Delta}$ p <0.05 when Gcg rec null mice were compared with the Syn A treated Gcg rec null mice.

Figure 3.6 Effects of Syn A on alpha cell area and percentage (A and B) and beta cell area and percentage (C and D) in heterozygous and Gcg rec null mice over 5 days following injection.

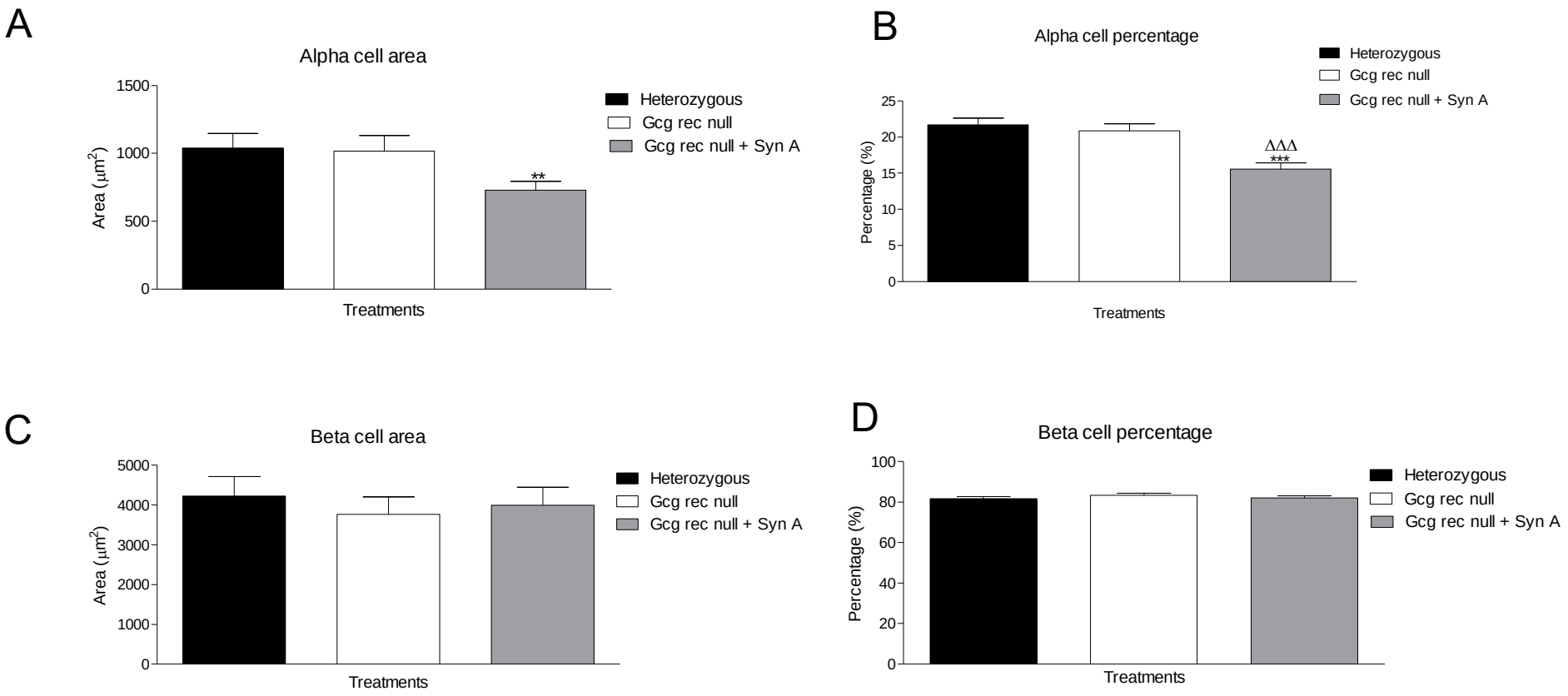

Alpha cell area and percentage (A and B) and beta cell area and percentage (C and D) per pancreas. Syn A was administered by i.p. injection at a dose of 5mg/kg on day 0. Values are mean ± SEM (n=7 mice). Changes were deemed significant when p values were **p <0.01 or ***p<0.001 when compared with heterozygous mice. was compared with Gcg rec null mice. $^{\Delta\Delta\Delta}$p <0.001 when Gcg rec null mice were compared with the Syn A treated Gcg rec null mice.

Figure 3.7 Representative images of heterozygous (A), Gcg rec null (B), and Gcg rec null + Syn A (C) islets from heterozygous and Gcg rec null mice over 6 days following injection.

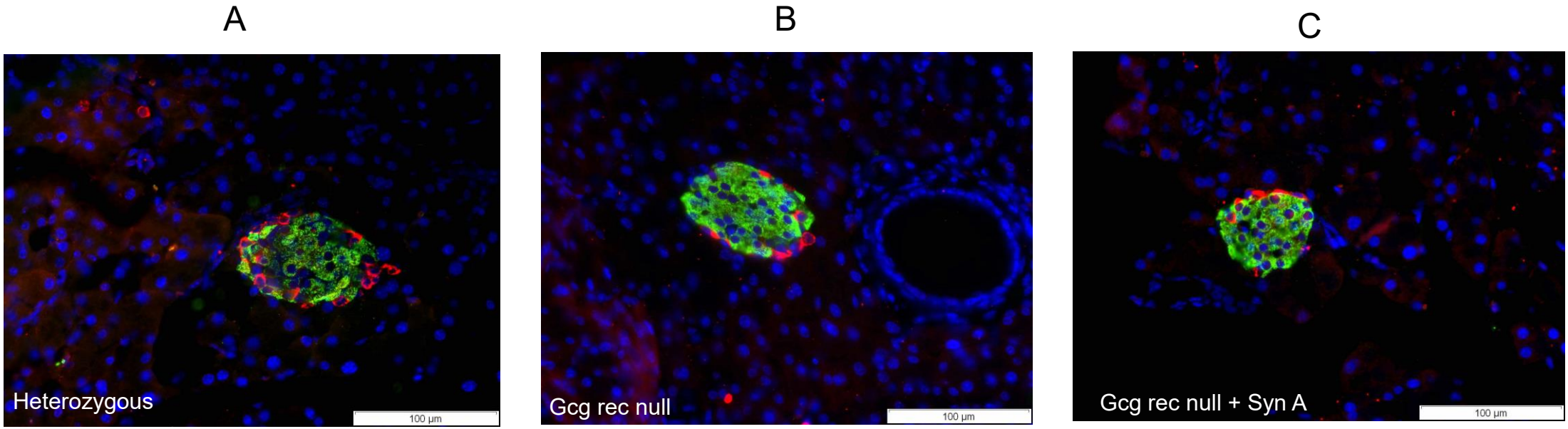

Islet morphology was evaluated at the end of the 5-day study using 7 µm tissue sections. Heterozygous (A), Gcg rec null (B), and Gcg rec null + Syn A (C) islets. Insulin is represented in green, glucagon in red, and DAPI in blue. Photos imaged at 40x objective lens. Total number of 150 islets per treatment group were analysed.

Figure 3.8 Effects of Syn A on Ki67 positive, insulin positive cells (A-D) in heterozygous and Gcg rec null mice over 5 days following injection.

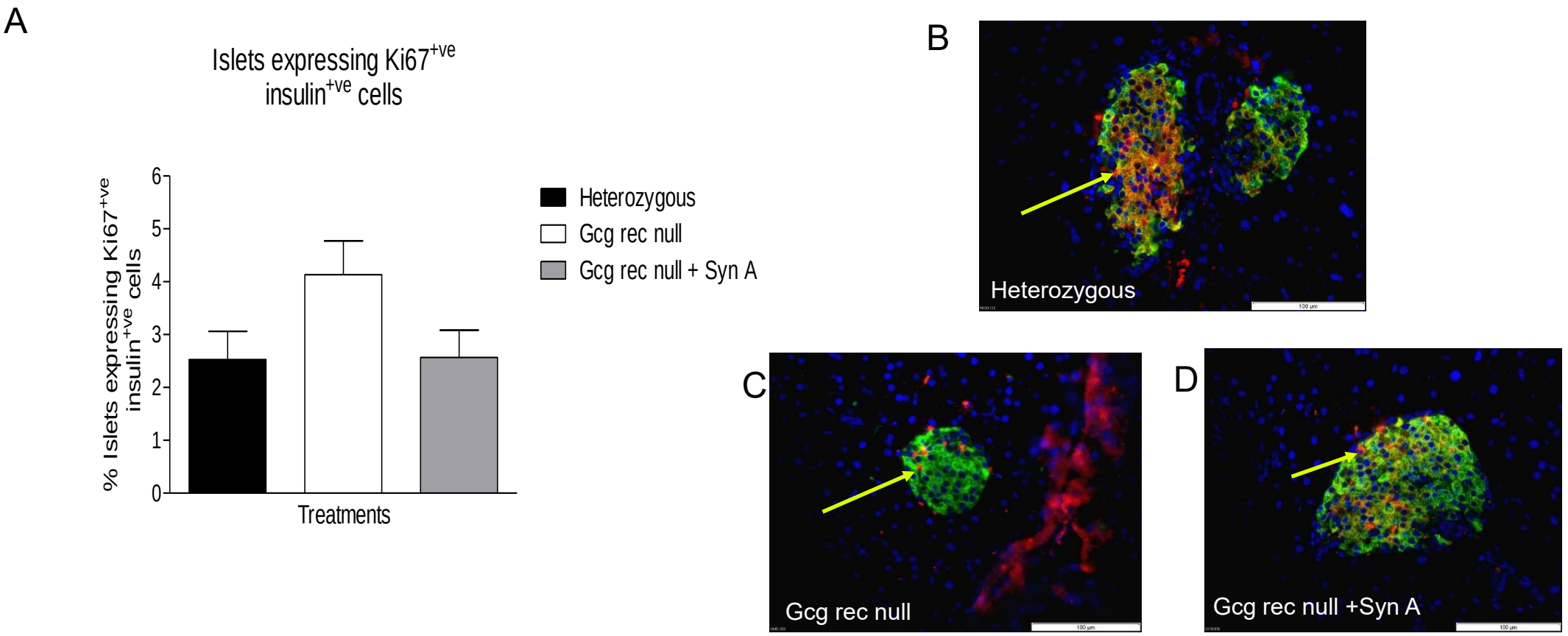

Percentage of beta cell proliferation was determined by the islets expressing Ki67^{+ve}, insulin^{+ve} cells (A) with representative images (B-D). Syn A was administered by i.p. injection at a dose of 5mg/kg on day 0. Values are mean ± SEM (n=7 mice). Changes were deemed significant when p values were ***p <0.001 when compared with heterozygous mice. $^{\Delta\Delta\Delta}$p <0.001 when Gcg rec null mice were compared with the Syn A treated Gcg rec null mice. Insulin is represented in green, Ki67^{+ve} cells in red, and DAPI in blue. Photos were taken at 40x objective lens. Total number of 100 islets were analysed per treatment group.

Figure 3.9 Effects of Syn A on Ki67 positive, glucagon positive cells (A-D) in heterozygous and Gcg rec null mice over 5 days following injection.

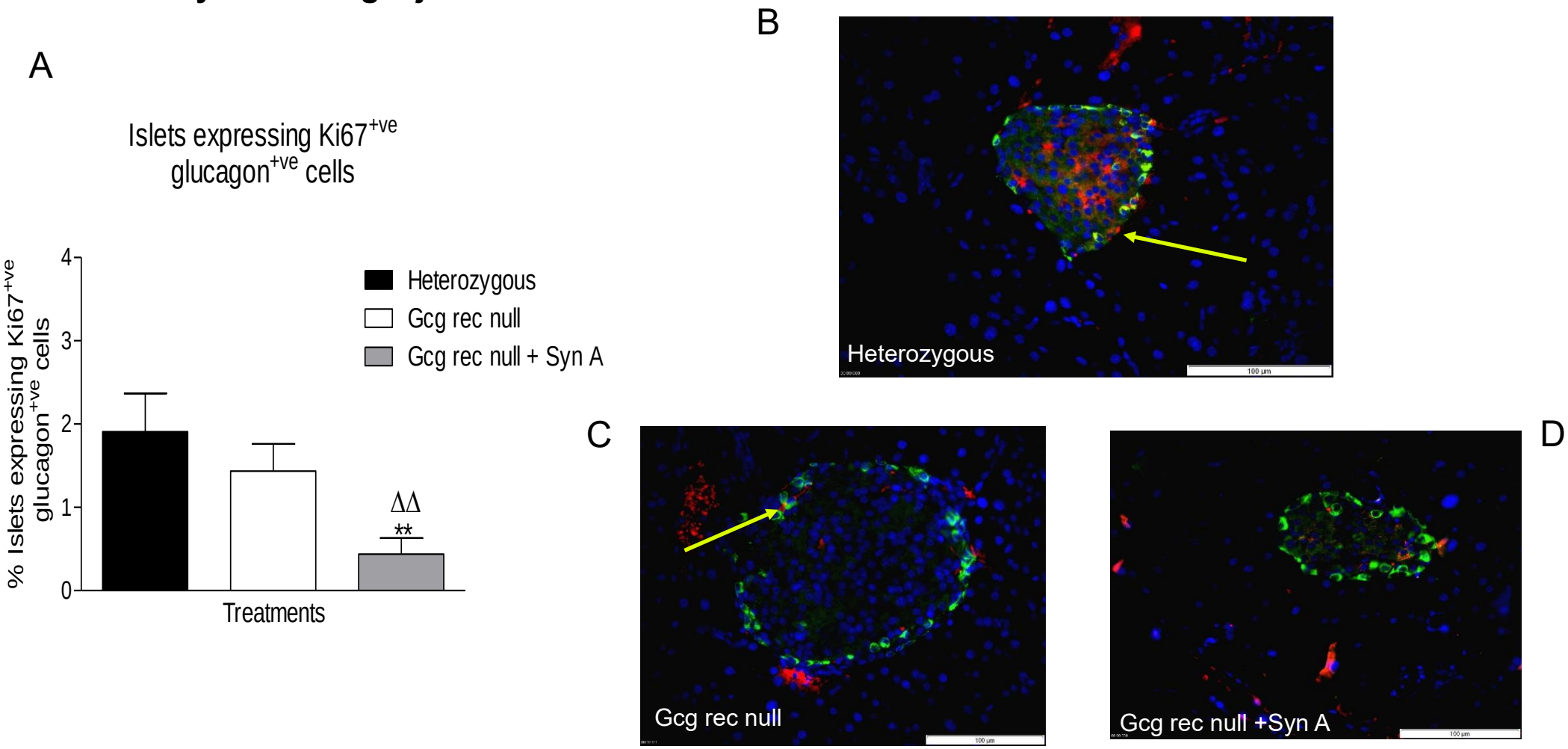

Percentage of alpha cell proliferation was determined by islets expressing Ki67^{+ve}, glucagon^{+ve} cells (A) with representative images (B-D). Syn A was administered by i.p. injection at a dose of 5mg/kg on day 0. Values are mean ± SEM (n=7 mice). Glucagon is represented in green, Ki67^{+ve} cells in red, and DAPI in blue. Photos were taken at 40x. Changes were deemed significant when p values were **p <0.01 when compared with heterozygous mice. $^{\Delta\Delta}$p <0.01 when Gcg rec null mice were compared with the Syn A treated Gcg rec null mice.

Chapter 4

Evaluation of Synthalin A on islet morphology in Sprague Dawley rats

4.1 Summary

Bioanalysis and histological analysis were used to study the *in vivo* effects of Synthalin A (Syn A) in male Sprague Dawley rats. A single low dose (2mg/kg) and high dose (5mg/kg) of Syn A was given to rats to assess effects of single dose over the period of 6 days. The rats treated with the higher dose were more affected by Syn A than the low dose. Both Syn A groups exhibited an increase in blood glucose at the end of the study. Food and fluid intake increased in the lower dose rats, whereas the higher dose rats exhibited an increase in nonfasting plasma insulin levels. Histological analysis resulted in a decrease in the number of islets for the higher dose rats. Alpha cell measurements were decreased and an increase in beta cell measurements were observed in both treatment groups. The rats that were given the lower dose show a similar profile to the higher dose, just not as drastic in some measurements. Proliferation of the alpha and beta cells were significantly decreased when compared to the saline treated rats. However, alpha cell apoptosis was increased in both Syn A groups. As expected, the higher dose of Syn A resulted in alpha cell death. These data indicate that Syn A plays a role in alpha cell toxicity within the pancreas as well as other organs, such as the heart, kidneys, liver, and lungs.

4.2 Introduction

The pancreas in a rat, as well as a mouse, is spread throughout the mesentery. The divisions of the rodent pancreas can be identified as three different sections: duodenal, gastric, and splenic (Liggitt and Dintzis, 2018; Steiner *et al.* 2010; Elayat *et al.* 1995). In humans, the pancreas is more compact and in four different sections: head, neck, body, and tail. In relation to the rodent pancreas divisions, the head would be the duodenal region, the body and neck the gastric region, and the splenic would be the tail. When specifically looking at the islets of Langerhans, the beta cells make up most of the islet. This is different in humans. There are fewer beta cells and more alpha cells in humans. Islets are also unevenly dispersed throughout the rodent, whereas in humans they are evenly spread throughout the pancreas. (Liggitt and Dintzis, 2018). Alpha cells in the rat pancreas are predominantly found in the

splenic lobe and located on the periphery of the islet (Huang *et al.* 2009; Elayat *et al.* 1995; Sacchi and Bani, 1985; Baetens *et al.* 1979*;* Ito *et al.* 1978*;* Sundler *et al.*1977*;* Goldsmith *et al.* 1975). In a study by Elayat *et al.* (1995), the average number of alpha cells was less in the head of the pancreas in comparison to the tail. The number of islets in both rodent and human pancreas is dependent on the body mass (Liggitt and Dintzis, 2018).

Syn A has been recognized as an alpha cell toxin, with little effect on beta cells (Langslow *et al.* 1973; Beekman, 1956; Davis, 1952, Fodden and Read, 1953; Karr *et al.* 1929). Rodent studies are limited when looking at the literature on Syn A. The three rat studies from the 1950's used varying amounts of Syn A, but all consisted of a one-time injection (Lundbaek and Nielsen, 1958; Hultquist, 1956; Ferner and Runge, 1955). This was used as a guide to determine the treatment dose for the current study. Due to this lack of information regarding Syn A and its effects on biological parameters measured; our focus was to examine the alpha cells histologically.

The aim of this Chapter was to see how Syn A affects the alpha cells in rats when compared to the past research and other studies using smaller rodents. This will help us see how a small and large dose of Syn A affects the pancreas. This study was also used to provide a gross inspection of the other anatomical organs that may be affected by the toxin.

4.3 Materials and methods

All materials and methods for this study have been summarised in 4.3.1 to 4.3.3. A detailed description of the materials and methods can be found in Chapter 2.

4.3.1 Sprague Dawley rats

Six, 5-month-old male rats were obtained from Envigo. The rats were separated into three groups for this 6-day study. Each group consisted of two rats. The first day of the study, the rats were given one intraperitoneal (i.p.) injection with their assigned treatment; 0.9% saline, 2mg/kg of Syn A, or 5 mg/kg of Syn A. Following the one-time injection, the rats were

monitored, and various parameters were measured for five days. On the final day they were sacrificed, and the pancreas was dissected for further analysis.

4.3.2 Immunohistochemistry

The pancreas from each rat was taken and preserved in paraformaldehyde (PFA) at the end of the study to analyse morphological changes within the islets. The whole pancreas was embedded into paraffin for histological analysis. Tissue blocks were cut at 7µm thick and placed on polysine coated slides which were double stained using in-house guinea-pig anti-glucagon 1:400, mouse anti-insulin 1:400 as the primary antibodies and rabbit anti-Ki67 1:500 (ab15580). Secondary antibodies for immunohistochemistry included Alexa Fluor 488 or Alexa Fluor 594 goat anti mouse, IgG- 1:400, Alexa Fluor 488 or Alexa Fluor 594 goat anti guinea pig, IgG- 1:400, and Alexa Fluor 594 goat anti rabbit, IgG- 1:400. Rat tissue was also stained for apoptosis using a TUNEL reaction assay. DAPI was used to stain the nuclei of the islets. Once slides were mounted using a 50:50 mixture of glycerol and PBS, they were ready to be analysed using the Olympus fluorescent microscope fitted with DAPI (350nm) FITC (488nm) and TRITC (594nm) filters and a DP70 camera adapter system using Cell^F program.

4.3.3 Statistics

GraphPad Prism 5 software and Image J was used to generate all the graphs and figures within this Chapter. A two-way Repeated Measures ANOVA test followed by a Bonferroni post-test or an unpaired student t-test was performed. Any $p<0.05$ was deemed statistically significant.

4.4 Results

4.4.1. The effects of a single dose of Syn A on body weight, body weight change, and blood glucose in Sprague Dawley rats.

There was no significance regarding body weight (Figure 4.1A). There was no significance regarding percentage of weight change (Figure 4.1B). However, when looking at the blood

glucose levels were significantly increased in the 2mg/kg Syn A ($p<0.01$) and 5mg/kg Syn A ($p<0.001$) treated rats when compared to saline on the final day (Figure 4.1C).

4.4.2. The effects of a single dose of Syn A on food and fluid intake in Sprague Dawley rats.

As shown in Figure 4.2A, the 5mg/kg Syn A ($p<0.001$) rats cumulative food intake was significantly less starting the second day of the study when compared to saline treated rats. The rats treated with the lower dose of Syn A, 2mg/kg also showed significantly increased food intake ($p<0.001$) starting on the third day. The 2mg/kg Syn A rats consumed a larger amount of fluid over the course of the study when compared to the saline rats ($p<0.01$) (Figure 4.2B). The rats that consumed more food also consumed a larger amount of water.

4.4.3. The effects of a single dose of Syn A on nonfasting and fasting plasma insulin levels in Sprague Dawley rats.

The rats that were treated with 5mg/kg of Syn A ($p<0.001$) showed elevated levels of plasma insulin in comparison to the other two groups (Figure 4.3A). However, the nonfasting plasma insulin levels were not different from one another. Significance for fasting plasma levels could not be tested due to the lack of plasma samples from the control group (Figure 4.3B).

4.4.4 The effects of a single dose of Syn A on the number of islets, islet area, and islet size distribution in Sprague Dawley rats.

As shown in Figure 4.4A, the number of islets per mm^2 of pancreas decreased in the higher dose Syn A treated rats ($p<0.01$). Islet area was consistent among the three groups with no appreciable difference (Figure 4.4B). Similar to the previous Chapter on mice, the majority of islets were classified as small (Figure 4.4C). There was no significance difference in islet size distribution in the three groups.

4.4.5 The effects of a single dose of Syn A on alpha cell area and percentage and beta cell area and percentage in Sprague Dawley rats.

Alpha cell area was decreased in 2mg/kg Syn A ($p<0.05$) and in 5mg/kg Syn A ($p<0.01$) treated rats (Figure 4.5A). The percentage of alpha cells in islets was also significantly decreased in both of the Syn A groups: 2mg/kg Syn A ($p< 0.01$) and 5mg/kg Syn A ($p<0.001$) when compared to the rats treated with saline (Figure 4.5B).

Figure 4.5C shows no significance regarding beta cell area. When compared to saline treated rats, the 2mg/kg ($p<0.01$) and the 5mg/kg ($p<0.001$) show a significant increase in beta cell percentage (Figure 4.5D). Photo representation is seen in Figure 4.6A-C. Glucagon is shown in red, insulin in green, and DAPI in blue.

4.4.6. The effects of a single dose of Syn A on Ki67 positive, insulin positive cells and Ki67 positive, glucagon positive cells.

Figure 4.7A shows a large decrease in the percentage of islets expressing both Ki67 positive and insulin positive cells in the 5mg/kg Syn A rat group ($p<0.001$) when compared to saline treated rats. Photo representation is seen in Figures 4.7B-D. Ki67 positive cells are red, insulin in green, and DAPI in blue. Rats treated with 5mg/kg Syn A had significantly lower Ki67 positive glucagon positive cells ($p<0.01$) when compared to saline treated rats. Image representation is seen in Figures 4.8B-D. Ki67 positive cells are red, glucagon in green, and DAPI in blue.

4.4.7. The effects of a single dose of Syn A on TUNEL positive, insulin positive cells and TUNEL positive, glucagon positive cells.

Figure 4.9A shows beta cell apoptosis was increased both Syn A treated rat groups: 2mg/kg Syn A and 5mg/kg Syn A were significantly increased ($p<0.001$) when compared to the saline treated rats. Photo representation is seen in Figure 4.9B-D. Insulin is represented in red and Tunel is represented in green. Figure 4.10A shows the Tunel positive, glucagon positive cells. When compared to saline treated rats, 2mg/kg Syn A ($p<0.05$) and 5mg/kg Syn A ($p<0.001$)

displayed an increase in the percentage of apoptotic cells. Images are represented in Figure 4.10B-D. Glucagon is represented in red and Tunel in Green.

4.5 Discussion

This study has shown that the rats treated with Syn A consumed more food and fluid over the course of the study. This cannot be confirmed or denied by past rat studies as no articles were found that talked about the effects on body weight, food and fluid consumption, or insulin plasma levels. Upon further investigation, these parameters were discussed when examining other species such as dairy bull calves (Mixner *et al.*1957). They examined the blood glucose level and found that it was depressed in the animals treated with Syn A. However, when looking at the islets of Langerhans, no changes were seen in the calves. This could confirm that Syn A is a species-specific toxin (Langslow *et al.*1973; Creutzfeldt, 1960 and 1957).

Past research states that within the first two hours after an injection of Syn A, the blood glucose will increase, and then decline quickly causing the animal to go into a hypoglycaemic state (Bodo and Marks, 1928; Dale, 1927). Our study examined blood glucose levels on the days following the injection and noticed a slight decline days after the injection, but none of the rats ever entered into a hypoglycaemic state. Bodo and Marks (1928) suggest that the reaction to the Syn A on blood glucose could be related to the amount of glycogen within the liver and suggest that glycogen is broken down once Syn A is injected.

Wright (1958), looked at the effects of insulin and insulin antiserum levels, and briefly looked at it in conjunction to Syn A. This study states that the effects of Syn A were not affected by adding insulin antiserum. However, it looked at the stimulant effect of Syn A, and our study looked at insulin levels in the plasma which revealed that at the higher dose of Syn A did have a significant effect. It is possible that our results regarding plasma insulin levels could be to the amount of plasma that was collected at the end of the study. Blood collection was difficult due to clotting in the Syn A rats. It could also be due to the fact that we examined the pancreas and the research from Wright (1958) examined rat diaphragms incubated in insulin.

The aim of this study was to evaluate how the alpha cell toxin, Syn A, affects the pancreatic islets in rats. In the previous research, the alpha cells were documented as either damaged and abnormal (Lundbaek and Nielsen, 1958; Hultquist, 1956). Ferner and Runge (1955), stated that the alpha cells from baby rats were increased yet the ring surrounding the beta cells was incomplete. In the present study, adult male rats that were given the Syn A treatment showed an incomplete layer of alpha cells, and a decrease in the number of alpha cells. It is therefore clear that Syn A does have an impact on the alpha cells of the rodent pancreas at the higher dose. However, when examining the cell damage within the rat and mouse pancreas, the alpha cells from the mouse were affected more. Hultquist (1956) injected the rats in their study at 4mg/kg and found similar effects to alpha cells as this current study. Lundbaek and Nielsen (1958) also found that the alpha cells appeared to be abnormal in colour as well as structure. The Wistar rats' alpha cells appeared to be pale. However, they found that the number, size, and shape of the alpha cells appeared to be normal. This contradicts with what we observed. Although we did not look at the colour of the alpha cells, we did look at the number and size of the alpha cells. The percentage and area of the alpha cells was decreased greatly following a Syn A injection. However, the islet area as a whole was unaffected by the treatment of Syn A. Lundbaek and Nielsen (1958), treated the rats with 20mg of Syn A and found that the beta cells were normal which would confirm the results we found within our study, even at a lower dose of Syn A.

In the present study, anatomical inspection of the organs in the rats showed that the kidneys and pancreas were pale in colour. There were also many blood clots that were discovered around the lungs, heart and kidneys in the rats that were treated with Syn A, with the largest one being around 3 inches. Karr *et al.* (1929), performed an autopsy on the dogs he treated with Syn A. They found lesions on the animals' kidneys and liver as well as a blood clot in the pericardium region, which coincides with one of the areas we found blood clots. However, no histological changes were overserved in the islets upon further examination in their study.

A limitation of this study was the small number of animals studied and the fact that the pancreas was not dissected into a head and tail sections. This would provide more histological detail regarding the effects on alpha versus beta cells. Perhaps further histological methods could be carried out on the Syn A treated rats to examine the colour and structural changes in the alpha cells compared to control.

In conclusion, this study provided a more in-depth account regarding rats and Syn A that had not been documented before. We can conclude that Syn A had an effect on food intake, when given in the smaller amount. Nevertheless, the present results indicate that Syn A decreases alpha cells in rats by decreasing proliferation and increasing their apoptosis.

Figure 4.1 The effects of a single dose of Syn A on body weight (A), body weight change (B), and blood glucose (C) in Sprague Dawley rats over 6 days following injection.

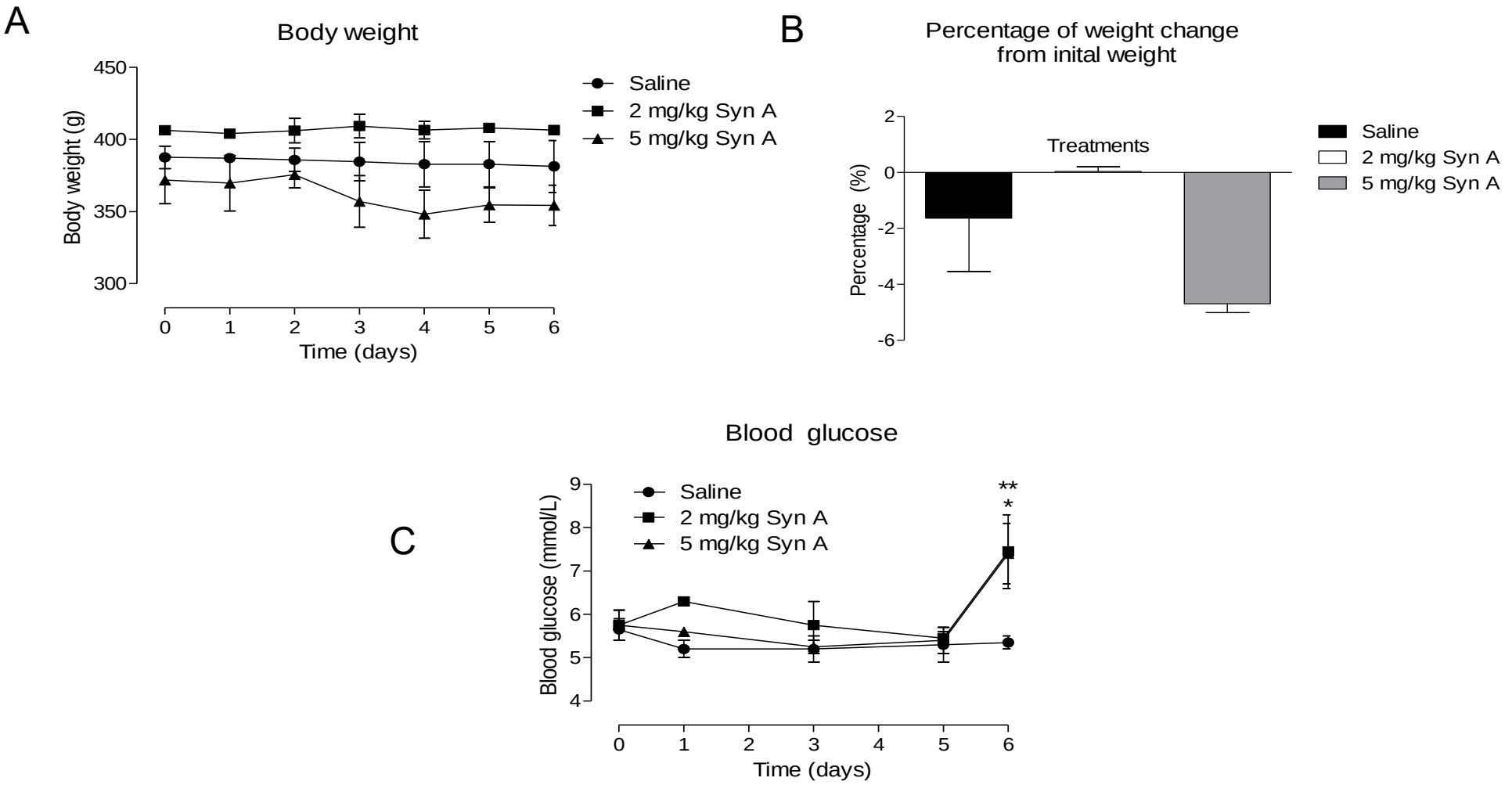

Body weight (A), percentage of body weight change (B), and blood glucose (C) were measured over the course of 6 days in Sprague Dawley rats treated with a single i.p. dose of Syn A on day 1. Values are mean ± SEM (n=2 rats). Changes were deemed significant when p values were *p<0.05 or **p <0.01 when compared saline.

Figure 4.2 The effects of a single dose of Syn A on food (A) and fluid (B) intake in Sprague Dawley rats over 6 days following injection.

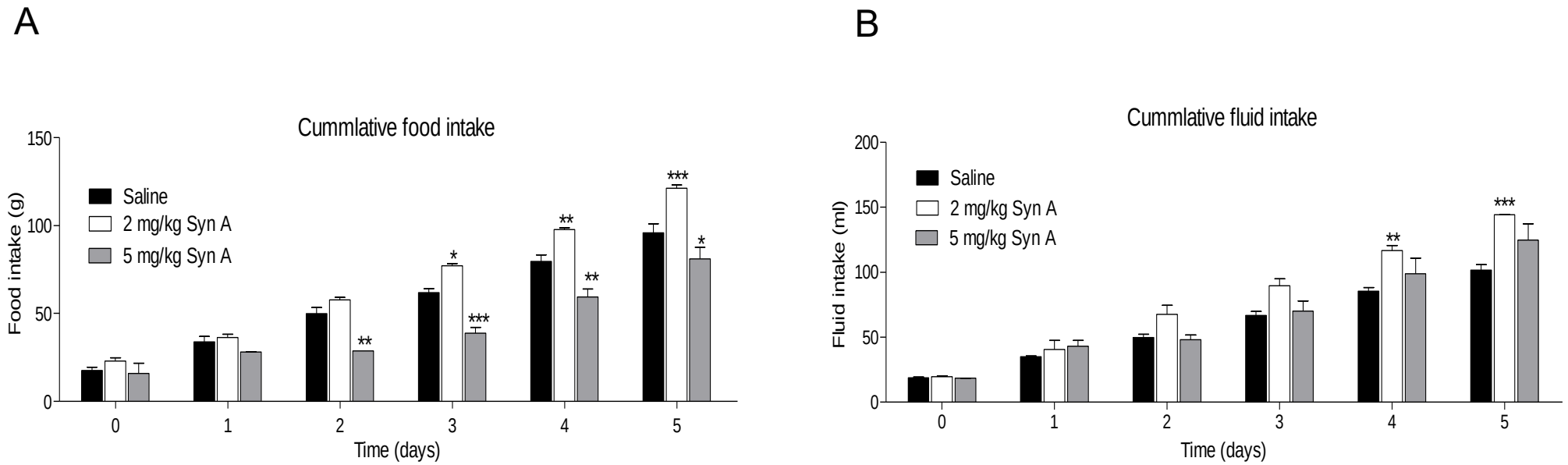

Cumulative food (A) and fluid intake (B) over the course of 6 days in Sprague Dawley rats treated with a single i.p. dose of Syn A on day 1. Values are mean ± SEM (n=2 rats). Changes were deemed significant when p values were *p<0.05, **p <0.01, or ***p<0.001 compared with saline.

Figure 4.3 Effects of a single dose of Syn A on nonfasting (A) and fasting (B) plasma insulin in Sprague Dawley rats over 6 days following injection.

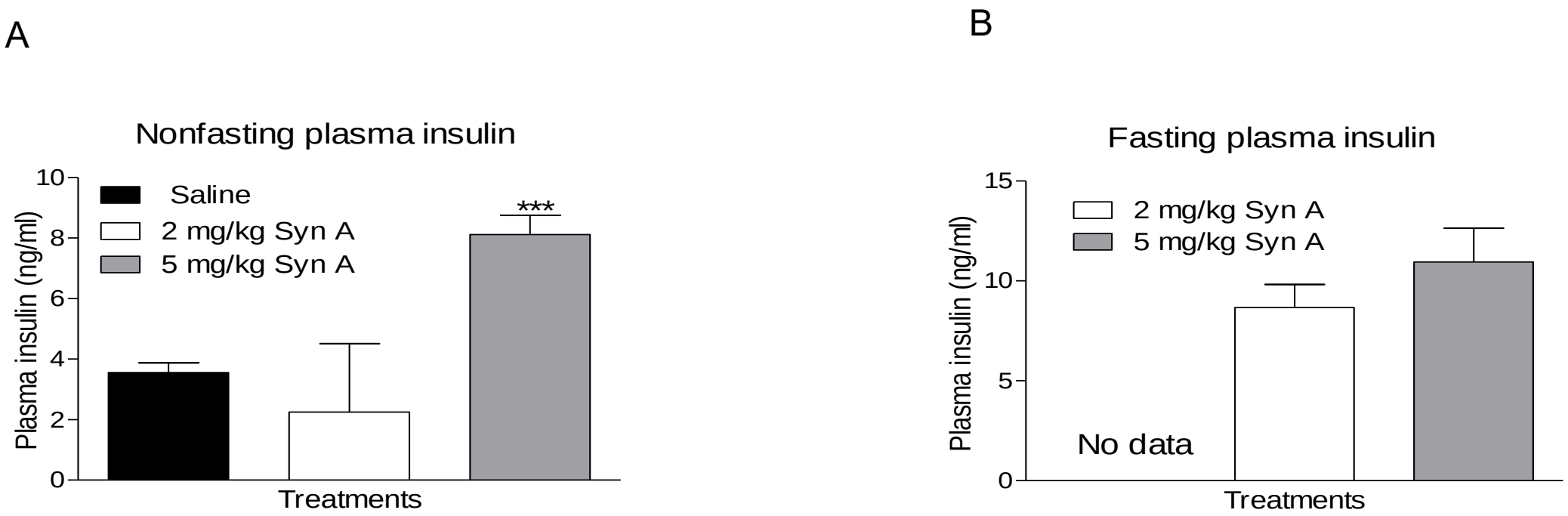

Nonfasting (A) and fasting (B) blood was taken at the end of the 6-day study in Sprague Dawley rats treated with a single i.p. dose of Syn A on day 1. Plasma insulin was measured by RIA. Values are mean ± SEM (n= 2 rats). Changes were deemed significant when p values were ***p<0.001 compared with saline.

Figure 4.4 The effects of a single dose of Syn A on the number of islets (A), islet area (B), and islet size distribution (C) in Sprague Dawley rats over 6 days following injection.

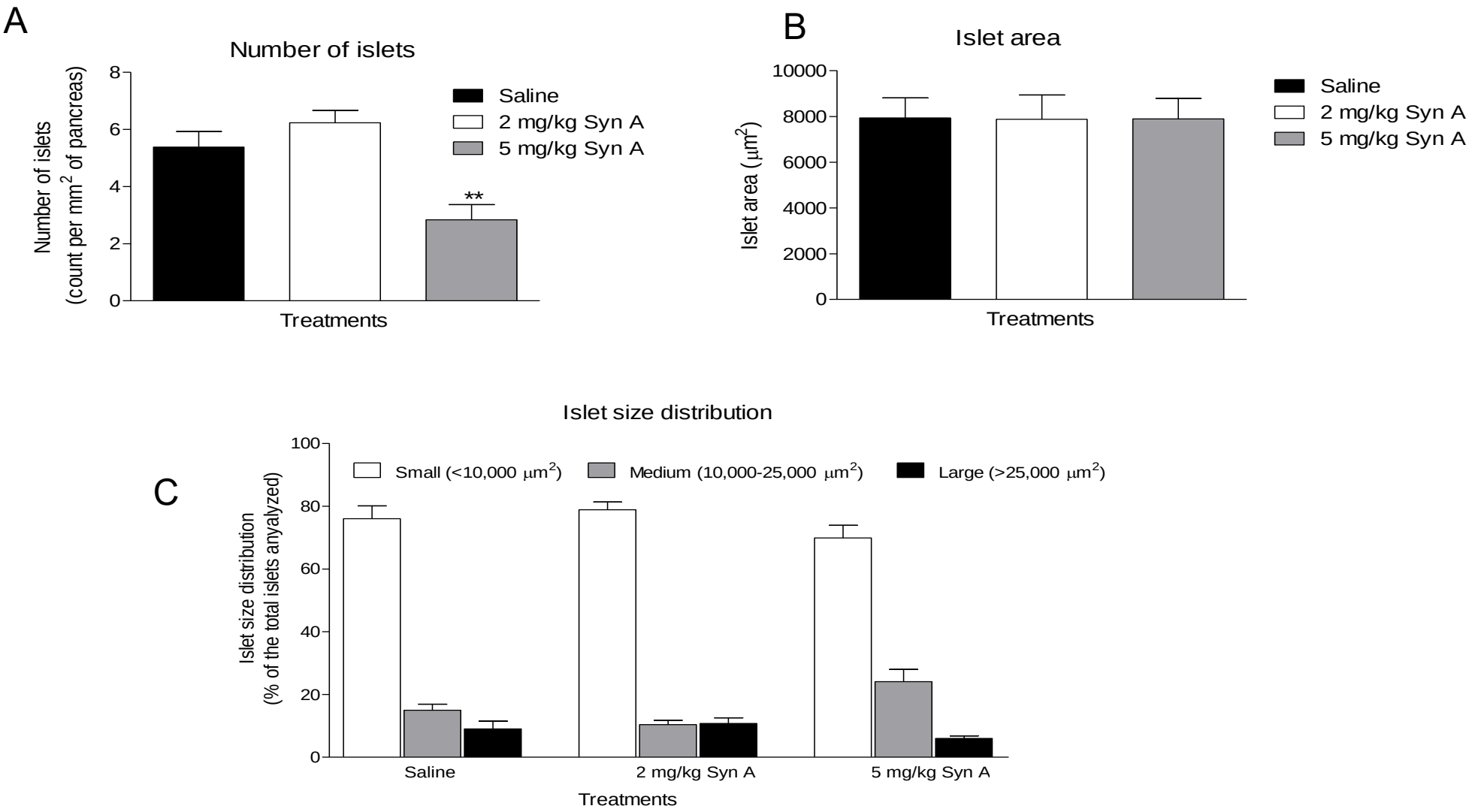

Number of islets (A), islet area (B), and islet size distribution (C) at the end of the 6-day study in Sprague Dawley rats treated with a single i.p. dose of Syn A on day 1. Values are mean ± SEM (n=2 rats). Changes were deemed significant when p values were **p <0.01 compared with saline.

Figure 4.5 The effects of a single dose of Syn A on alpha cell area and percentage (A and B) and beta cell are and percentage (C and D) in Sprague Dawley rats over 6 days following injection.

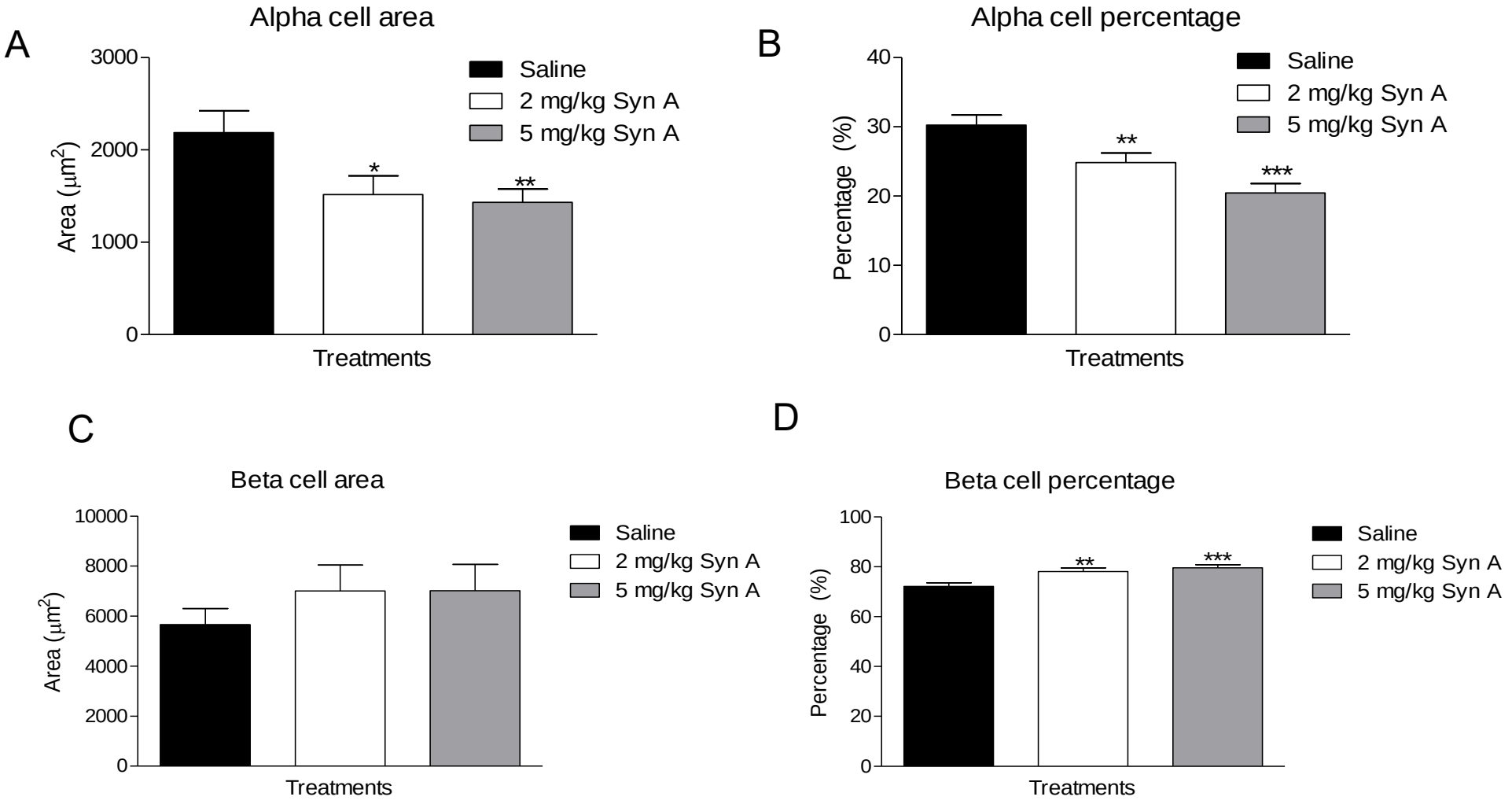

Alpha cell area and percentage (A and B) and beta cell area and percentage (C and D) at the end of the 6-day study in Sprague Dawley rats treated with a single i.p. dose of Syn A on day 1. Values are mean ± SEM (n=2 rats). Changes were deemed significant when p values were *p<0.05, **p <0.01, or ***p<0.001 compared with saline.

Figure 4.6 Representative images of rat islets following a single dose of saline (A), 2mg/kg Syn A (B), and 5mg/kg Syn A (C) islets from Sprague Dawley rats over 6 days following injection.

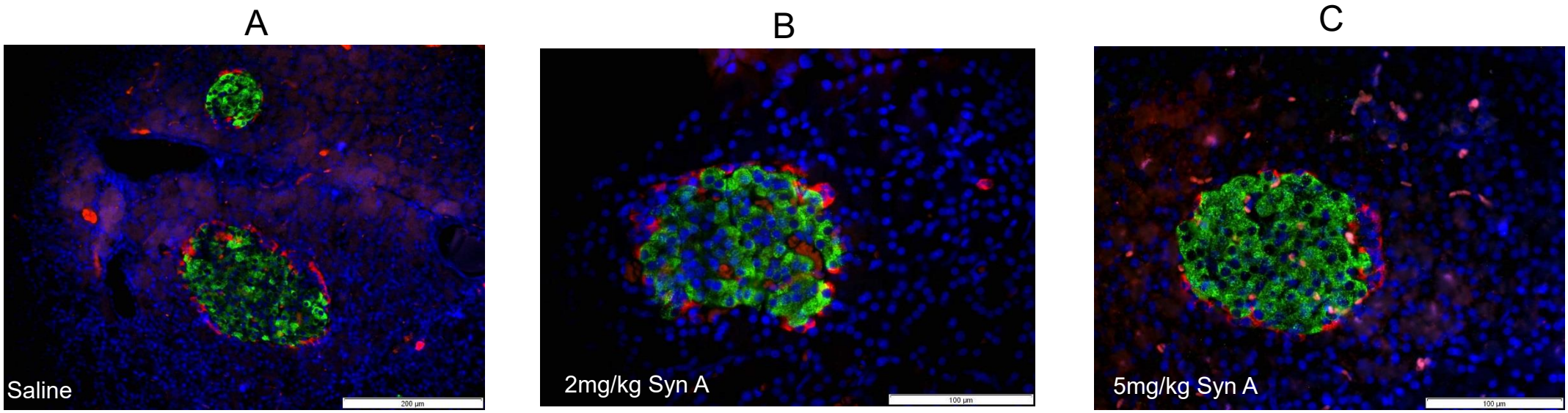

Islet morphology was evaluated at the end of the 6-day study on 7 µm sections. Saline (A), 2mg/kg Syn A (B), and 5mg/kg Syn A (C) islets. Insulin is represented in green, glucagon in red, and DAPI in blue. Photos imaged at 20x and 40x objective lens. Total number of 150 islets were analysed per treatment group.

Figure 4.7 Effects of a single dose of Syn A on Ki67 positive, insulin positive cells (A-D) in Sprague Dawley rats over 6 days following injection.

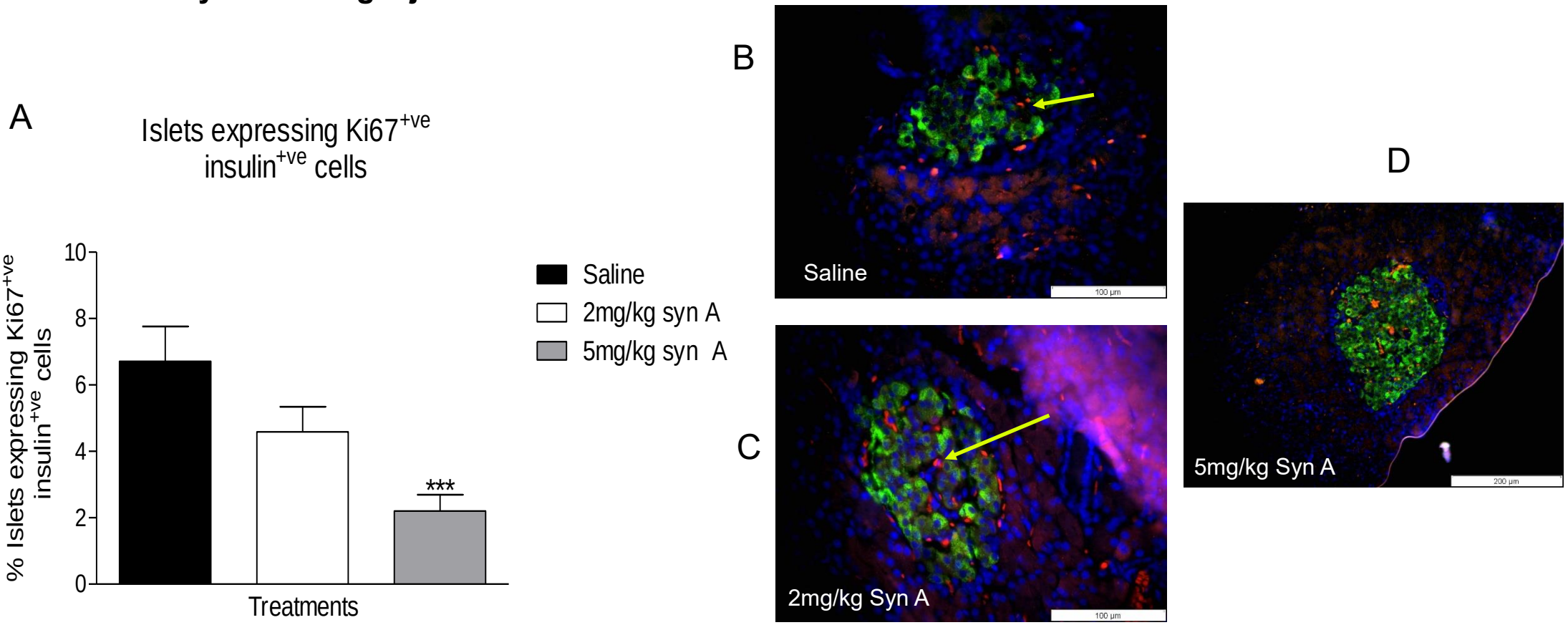

Percentage of beta cell proliferation was determined by islets expressing Ki67^{+ve}, insulin^{+ve} cells (A). Saline Ki67 $^{+ve}$, insulin $^{+ve}$ (B), 2mg/kg of Syn A Ki67^{+ve}, insulin^{+ve} (C), and 5mg/kg of Syn A Ki67^{+ve}, insulin^{+ve} (D) islets. Insulin is represented in green, Ki67 in red, and DAPI in blue. Yellow arrows are pointing to Ki67 positive, insulin positive cells. Images were taken at 20x or 40x objective lens. Sprague Dawley rats treated with a single i.p. dose of Syn A on day 1. Values are mean ± SEM (n=2 rats). Changes were deemed significant when p values were ***p <0.001 compared with saline. Total number of 100+ islets were analysed per treatment group.

Figure 4.8 Effects of a single dose of Syn A on Ki67 positive, glucagon positive cells (A-D) in Sprague Dawley rats over 6 days following injection.

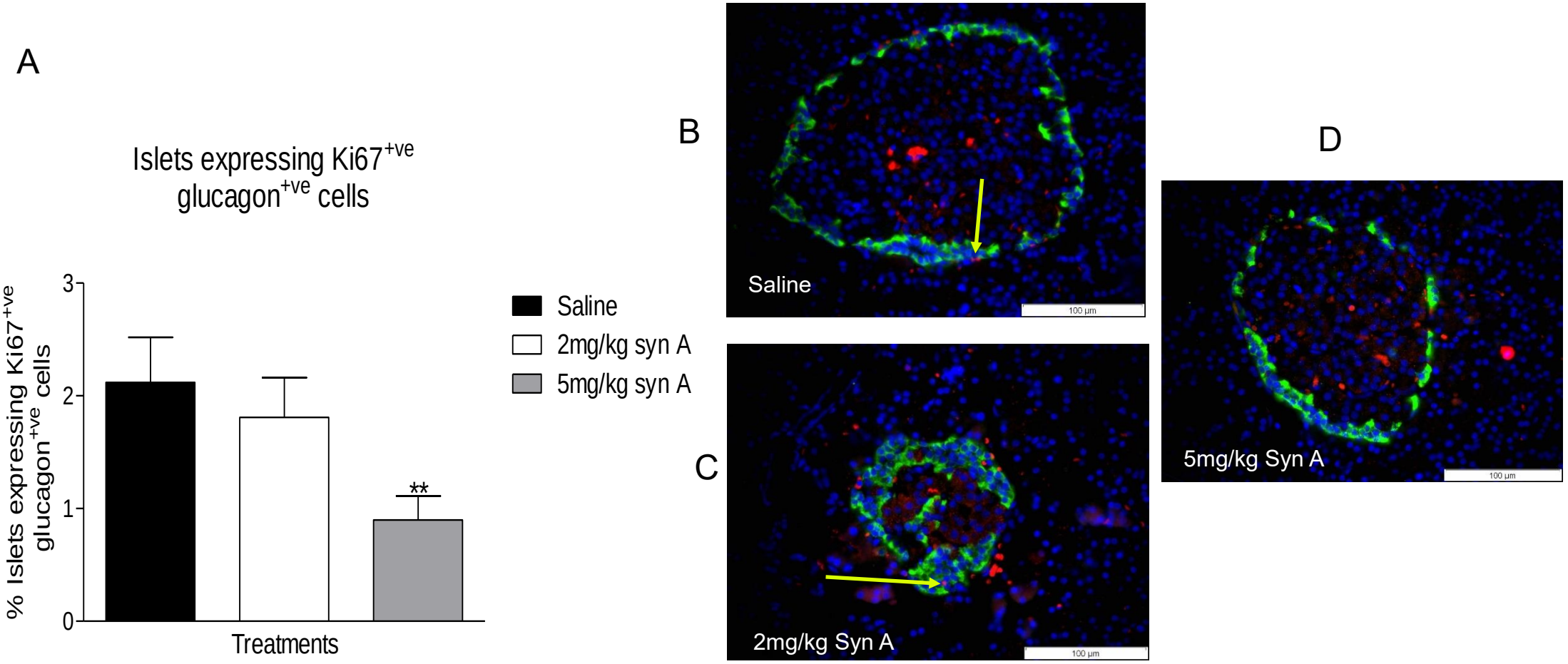

Percentage of alpha cell proliferation was determined by islets expressing Ki67^{+ve}, glucagon^{+ve} cells (A). Saline Ki67 $^{+ve}$, glucagon $^{+ve}$ (B), 2mg/kg of Syn A Ki67^{+ve}, glucagon^{+ve} (C), and 5mg/kg of Syn A Ki67^{+ve}, glucagon^{+ve} (D) islets. Glucagon is represented in green, Ki67 in red, and DAPI in blue. Yellow arrows are pointing to Ki67 positive, glucagon positive cells. Images were taken at 40x objective lens. Sprague Dawley rats treated with a single i.p. dose of Syn A on day 1. Values are mean ± SEM (n= 2 rats). Changes were deemed significant when p values were **p <0.01 compared with saline. Total number of 100+ islets were analysed per treatment group.

Figure 4.9 Effects of a single dose of Syn A on Tunel positive, insulin positive cells (A-D) in Sprague Dawley rats over 6 days following injection.

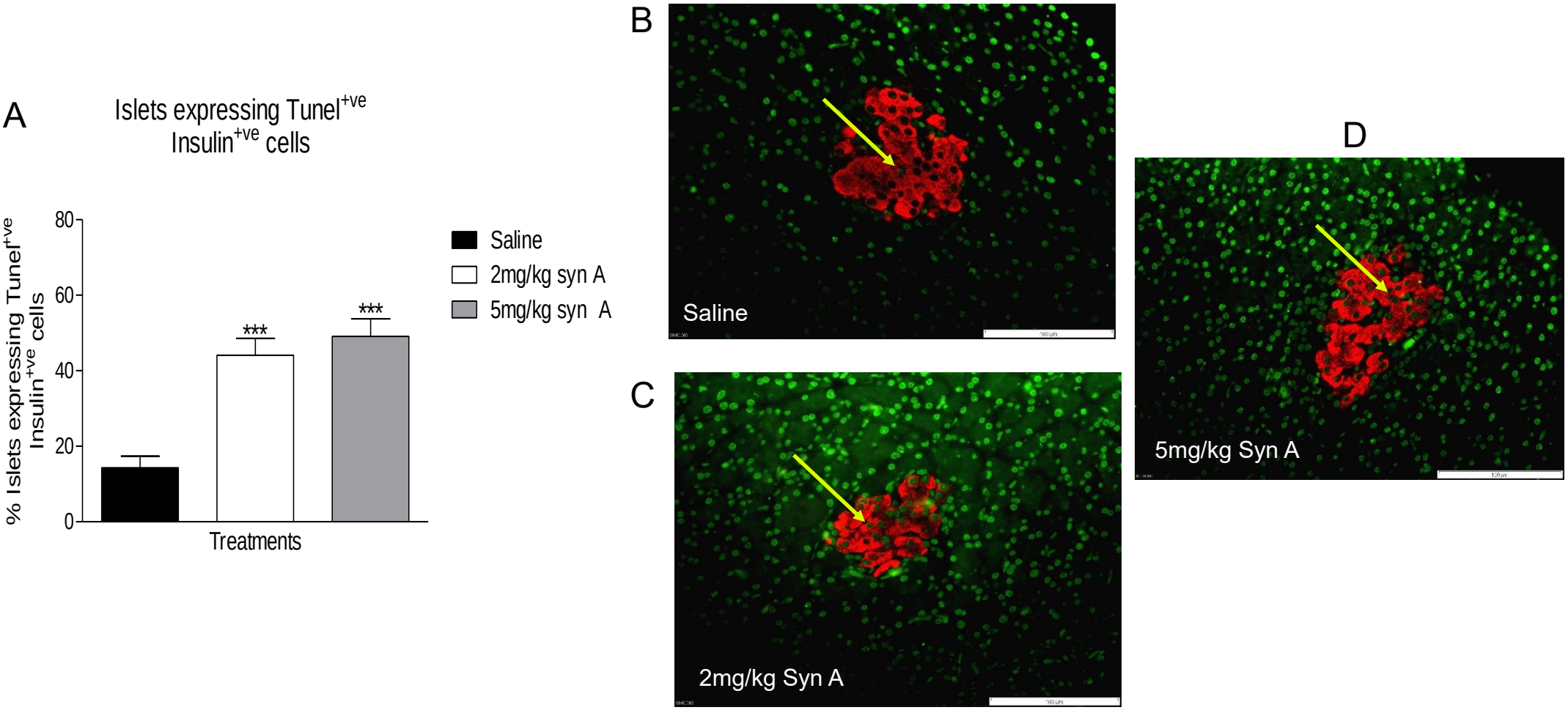

Percentage of beta cell apoptosis was determined by islets expressing Tunel^{+ve}, insulin^{+ve} cells (A). Photo representation of saline (B), 2mg/kg Syn A (C), and 5mg/kg Syn A (D) rats. Sprague Dawley rats treated with a single i.p. dose of Syn A on day 1. Values are mean ± SEM (n=2 rats). Changes were deemed significant when p values were ***p<0.001 compared to saline. Insulin is represented in red and Tunel is represented in green. The yellow arrows are pointing to Tunel^{+ve}, insulin^{+ve} cells. Images taken at 40x objective lens. Total number of 90+ islets were analysed per treatment group.

Figure 4.10 Effects of a single dose of Syn A on Tunel positive, glucagon positive cells (A-D) in Sprague Dawley rats over 6 days following injection.

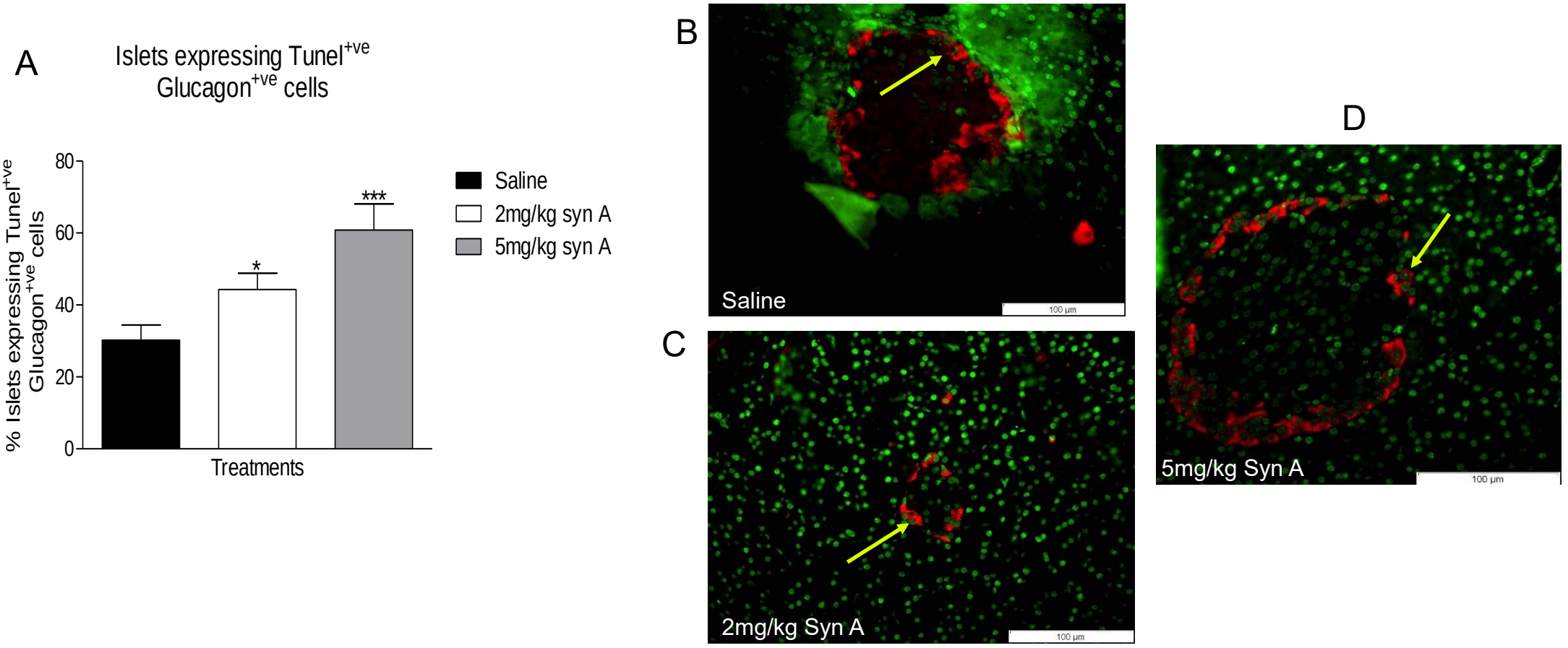

Percentage of alpha cell apoptosis was determined by islets expressing Tunel^{+ve}, glucagon^{+ve} cells (A). Images of saline (B), 2mg/kg Syn A (C), and 5mg/kg Syn A (D) rats. Sprague Dawley rats treated with a single i.p. dose of Syn A on day 1. Values are mean ± SEM (n=2 rats). Changes were deemed significant when p values were *p<0.05 or ***p<0.001 compared to saline. Glucagon is represented in red and Tunel is represented in green. The yellow arrows are pointing to Tunel^{+ve}, glucagon^{+ve} cells. Images taken at 40x objective lens. Total number of 90+ islets were analysed per treatment group.

Chapter 5

Effects of repeated and single doses of Synthalin A compared with multiple doses of Streptozotocin on islet function and morphology in Swiss mice.

5.1 Summary

Synthalin A (Syn A), an alpha cell toxin, is reported to induce hypoglycaemia whilst the beta cell toxin, streptozotocin (STZ), induces overt diabetes associated with hyperglycaemia. The toxicity of these agents in NIH Swiss and Swiss TO mice was evaluated by bioanalysis, histological analysis, and necropsy. NIH Swiss mice received a multiple low doses of 1mg/kg Syn A given for 5 days or a single high dose of 5mg/kg Syn A. The concentration dependent effects of Syn A was also explored in Swiss TO mice which received multiple doses of 1mg/kg, 2mg/kg, 5mg/kg, or 8mg/kg of Syn A over 5 days. Both studies contained mice treated with multiple doses of 0.9% saline or 50mg/kg of STZ for a period of 5 days. Glycaemia was notably lowered in Swiss TO mice treated with high doses of Syn A. Fluid intake was reduced in both NIH Swiss and Swiss TO mice treated with a high dose of Syn A. Histological analysis of pancreatic tissue showed that Syn A elicited concentration dependent destruction of alpha cells. STZ treated mice showed characteristic hyperglycaemia associated with destruction of beta cells in both the head and tail regions of the pancreas. Anatomically, most of the organs removed for a surface inspection were affected by colour, morphology, or surrounded by blood clots in mice treated with Syn A. These data confirm, Syn A and STZ selectively destroy alpha and beta cells, respectively, with the former doing so in a dose-dependent manner.

5.2 Introduction

Syn A, was discovered in the 1920's, the preinsulin era, as a blood glucose lowering treatment. Interest declined in the 1950's due to toxicity plus the discovery of insulin (Krishnarth *et al.* 2013; Bailey and Day, 2004; Dey *et al.* 2002; Östenson, 1983; Davis, 1952; Karr *et al*. 1929; Frank *et al*. 1926). Syn A was claimed to be similar to insulin, except for the fact that Syn A was effective when given orally and had a delayed action on blood glucose levels (Bodo and Marks, 1928). Syn A has been considered to be an alpha cell toxin which has the capacity to decrease high levels of glucagon (Langslow *et al.* 1973; Beekman, 1956; Davis, 1952). The mechanism of Syn A is unknown. However, some researchers state that Syn A may act directly on the hydropic alpha cells when they are overworked (Davis, 1952). Davis (1958) found that the hepatic glycogen disappeared from the periportal cells of the liver once Syn A was administered. Upon further examination of the effects of Syn A, glycogen disappeared from the portal tract in the liver in the majority of the study subjects (Davis, 1958). Mihich *et al.* (1959) state that the life of the mouse was reduced when high doses of Syn A were administered, however there was an anti-tumour effect when this drug was administered by intraperitoneal injection (i.p.). Langslow and Freeman (1973) suggested that the pancreas may not be the primary site of action, due to other tissues and organs being affected. Research suggests that this alpha cell toxin, reduces hyperglucagonemia (Langslow *et al*. 1973; Beekman, 1956; Davis, 1952). Research regarding Syn A is inconclusive regarding the toxic side effects. Past research states that, Syn A produces adverse effects causing various organ toxicity as well as alpha degeneration when given at high doses (Fodden and Read, 1953; Davis, 1952; Karr *et al.* 1929; Bodo and Marks, 1928; Watanabe, 1918). However, Hornung (1928) states that the effects of Syn A are non-toxic if given in a specific amount laid out by Frank, Nothmann, and Wagner.

Streptozotocin (STZ) is a beta cell toxin which impairs the beta cell function by destroying beta cells and depriving the animal of insulin and is commonly used to induce diabetes in animals (Whalley *et al.* 2011; Lenzen, 2008; Szkudelski, 2001). A glucose transporter (GLUT2) in the

cell membrane, which has been found to prevent the diabetic action of STZ when expressed in limited amounts, allows STZ to enter the beta cells, which results in DNA damage (Lenzen, 2008; Szkudelski, 2001; Thulesen *et al*. 1997; Schnedl *et al*. 1994). Within the cells, the toxic action occurs and the damage to DNA is caused by liberation of toxic amounts of nitric oxide from STZ (Lenzen, 2008; Szkudelski, 2001; Karunanayake *et al*. 1976; Tjälve *et al.* 1976). The steps that occur at a cellular level once STZ is injected are shown in Figure 5.1. Arora *et al*. (2009) state that when mice were administered a single high dose of STZ, the mice developed type 1 diabetes (T1D), however, when multiple low doses of STZ were administered, T1D mellitus was associated with beta cell loss due to islet lymphocytic infiltration. The mice used for this Chapter were administered multiple low doses of STZ, to induce diabetes.

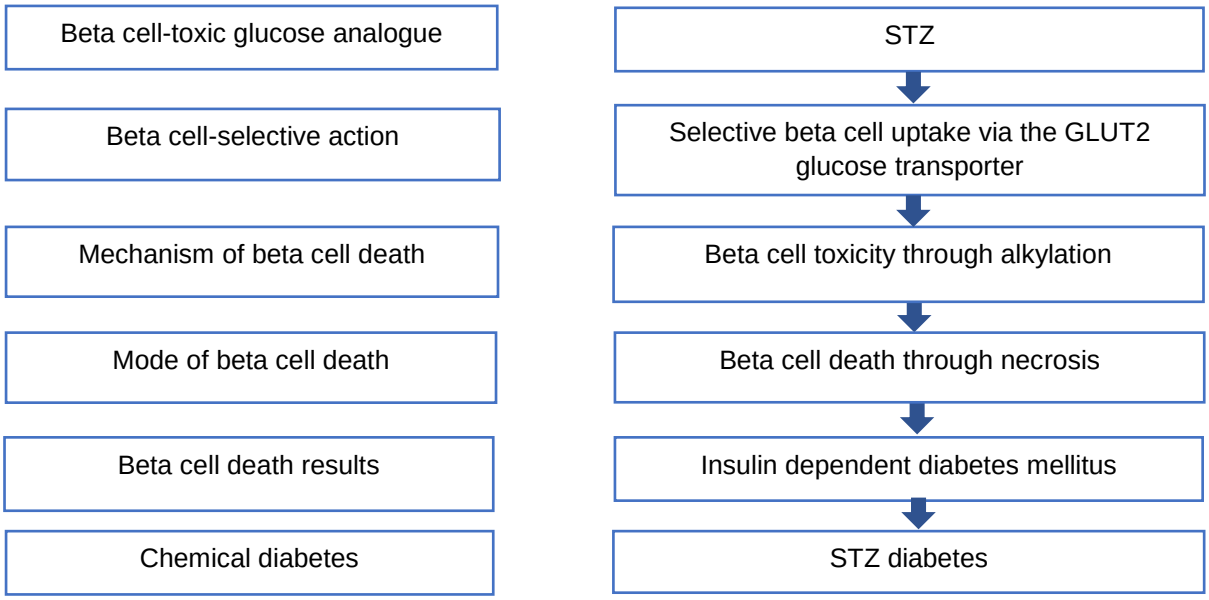

Figure 5.1 Represents the toxic effects of STZ on the pancreatic beta cells which induces diabetes. (Adapted from Lenzen, 2008).

This study examines the metabolic and pancreatic effects of Syn A in comparison with the beta cell toxin streptozotocin in mice. Effects on the two anatomical regions of the pancreas

were examined only in Swiss TO mice. We also aimed to evaluate the effects of Syn A on disturbed blood glucose control and in islet morphology.

5.3 Materials and methods

All materials and methods for this study have been summarised in sections 5.3.1 to 5.3.3. A detailed description of the materials and methods can be found in Chapter 2.

5.3.1 NIH Swiss and Swiss TO mice treated with STZ and Syn A

Twenty-one adult male NIH Swiss mice and 24 two-month-old Swiss TO mice were obtained from Envigo. They were placed in individual cages in an air-conditioned room at 22 ± 2°C with a 12-hour light / 12-hour dark cycle in the Biomedical Behavioural Research Unit (BBRU) at Ulster University in Coleraine. Food and water were provided *ad libitum.* The standard rodent diet consisted of 10% fat, 30% protein, and 60% carbohydrate. This experiment was carried out in accordance with the rules and regulations of the UK Animals (Scientific Procedures) Act of 1986.

The 7-month-old male NIH Swiss mice were separated into four groups and were used in the first set of experiments. The control group contained 5 mice which were injected daily with 0.9% saline, group two contained 5 mice that were injected with 50 mg/kg STZ daily for 5 days, group three consisted of 6 mice that were injected with 1 mg/kg Syn A daily for 5 days, and the last 5 mice received a one-time injection of 5 mg/kg of Syn A. Overall, the four groups were examined over 10 days. On the final day they were sacrificed, and the pancreas was dissected longitudinally for further analysis.

In the second experimental series, 2-month-old male Swiss TO mice were separated into 6 groups, each containing four mice. The first group was injected daily with 0.9% saline solution, group two was injected daily with multiple doses of 50mg/kg of STZ, and the remaining groups were injected daily with various doses of Syn A. The first Syn A group was injected with daily doses of 1mg/kg daily, and the second Syn A group was injected with 2mg/kg daily for 5 days. The third group was injected daily for 5 days with 5mg/kg of Syn A, and the last group was

injected with 8mg/kg once a day, for 5 days. On the final day of the study, body weight and blood glucose were measured, as well as the collection of non-fasting plasma insulin in the morning and fasting plasma insulin levels in the afternoon. Mice were then sacrificed, and the pancreas was extracted for further analysis. The pancreas was dissected in half splitting the head from the tail and then dissected longitudinally to be snap frozen for further use. A necropsy was performed at the end of the study to examine the effects of the different doses of Syn A on the Swiss TO mice.

For both studies' food, fluid, and body weight was measured on a daily basis. Blood glucose was measured on alternating days. Non-fasting and fasting plasma were taken at different time points on the final day of the study.

5.3.2 Immunohistochemistry

The section of the mouse pancreas that was preserved in paraformaldehyde (PFA) was used for immunohistochemistry. The corresponding sections of the pancreas were embedded into paraffin for analysis of morphological changes within the islets. Tissue blocks were cut on the microtome at 5-7µm thick and double stained using in house guinea-pig glucagon 1:400, mouse insulin 1:400 as the primary antibodies, and anti-rabbit Ki67 polyclonal antibodies 1:500 (ab15580). Secondary antibodies for immunohistochemistry included Alexa Fluor 488 or Alexa Fluor 594 goat anti mouse, IgG- 1:400, Alexa Fluor 488 or Alexa Fluor 594 goat anti guinea pig, IgG- 1:400, Alexa Fluor 594 goat anti rabbit, IgG- 1:400, and Alexa Fluor 488 donkey anti goat, IgG- 1:400. The nucleus was then stained with DAPI and a 50:50 mixture of glycerol and PBS was used to mount the coverslips. Images were analysed using the Olympus fluorescent microscope fitted with DAPI (350nm) FITC (488nm) and TRITC (594nm) filters and a DP70 camera adapter system using Cell^F program.

5.3.3 Statistics

All graphs and results were generated using GraphPad Prism 5 and Image J. A two-way Repeated Measures ANOVA statistical test with Bonferroni Multiple Comparison Test or an

unpaired student t-test were carried out. Statistical significance was observed when comparisons between two groups was $p<0.05$.

5.4 Results

5.4.1 Effects of multiple low dose STZ and both multiple and single doses of Syn A on body weight and body weight change in NIH Swiss mice.

As seen in Figure 5.2A, there was no significance regarding body weight. When compared to the saline treated mice, the mice treated with STZ ($p<0.01$), showed significant percentage of weight loss over the course of the 10-day study (Figure 5.2B). Mice treated with 1mg/kg Syn A (m) ($p<0.05$) showed a significant percentage of weight change when compared to saline.

5.4.2 Effects of multiple low dose STZ and both multiple and single doses of Syn A on food and fluid intake in NIH Swiss mice.

Cumulative food intake was similar among all four treatment groups and no significance was found (Figure 5.3A). When examining the cumulative fluid intake, the saline treated mice consumed the largest value of water followed by the mice treated with STZ (Figure 5.3B). On day four, there was a slight decrease ($p<0.05$) in both Syn A groups compared to the saline treated mice. Their significance increased ($p<0.01$; $p<0.001$) for both of the Syn A treated mice throughout the rest of the study when compared to the saline mice.

5.4.3 Effects of multiple low dose STZ and both multiple and single doses of Syn A on blood glucose and during an i.p. GTT in NIH Swiss mice.

Figure 5.4A shows the blood glucose levels of the animals during the 10-day study. Halfway through the study, the blood glucose of the STZ mice increased and continued to increase till the end of the study, displaying statistical significance ($p<0.001$) when compared to saline treated mice. On day 7, there was a slight increase in the blood glucose levels in the mice treated with 5mg/kg Syn A (s) ($p<0.01$), when compared to saline treated mice. During an i.p. glucose tolerance test (GTT), the 5mg/kg Syn A (s) ($p<0.01$) treated mice, showed

significantly raised glucose levels at the 15-minute mark when compared to the saline treated mice (Figure 5.4B). GTTs were not performed in STZ mice as base blood glucose were already 30mmol/L and no significance was found regarding area under the curve (Figure 5.4C).

5.4.4 Effects of multiple low dose STZ and both multiple and single doses of Syn A on nonfasting, fasting, and pancreatic insulin in NIH Swiss mice.

When looking at the nonfasting plasma insulin levels of the four treatment groups, the STZ treated mice ($p<0.05$) showed a significant decrease when compared to the saline treated mice (Figure 5.5A). Mice treated with 5mg/kg Syn A (s) ($p<0.05$) exhibited increased fasting plasma insulin levels when compared to saline (Figure 5.5B). Mice treated with STZ, 1mg/kg Syn A (m) ($p<0.01$) and 5mg/kg Syn A (s) ($p<0.05$) showed significant decreases in pancreatic insulin content when compared to saline treated mice (Figure 5.5C).

5.4.5. Effects of multiple low dose STZ and Syn A on number of islets, islet area, and islet size distribution in NIH Swiss mice.

As seen in Figure 5.6A, the number of islets varied within the treatment groups. When compared to the saline treated mice, the 5mg/kg Syn A (s) mice ($p<0.05$) showed a significant decrease when compared to saline. The STZ treated mice ($p<0.05$) exhibited a decrease, where the 1mg/kg Syn A (m) mice ($p<0.05$) exhibited an increase in their islet area when compared to saline treated mice (Figure 5.6B). The 5mg/kg Syn A (s) mice ($p<0.001$) displayed a significant decrease in islet area when compared to the saline islets. Most of the islets that were analysed were smaller than 10,000μm^2 (Figure 5.6C). Less than 20% of the islets were classified as medium, having an area of 10,000 μm^2 -25,000 μm^2. Significance can be seen in the large islets in the STZ and 5mg/kg Syn A (s) mice ($p<0.05$).

5.4.6. Effects of multiple low dose STZ and both multiple and single doses of Syn A on alpha cell area and percentage and beta cell area and percentage in NIH Swiss mice.

When compared to saline treated mice, mice treated with STZ ($p<0.001$) displayed an increase in alpha cell area (Figure 5.7A). As expected, the alpha cell area was significantly decreased ($p<0.001$) in the 5mg/kg Syn A (s) mice when analysed against the saline mice. Alpha cell percentage was significantly increased in the STZ mice ($p<0.001$) when compared to saline mice (Figure 5.7B). 1mg/kg Syn A (m) and 5mg/kg Syn A (s) treated mice ($p<0.001$) showed a statistically significant decrease in the alpha cell percentage that was observed in the islets analysed.

When compared to saline treated mice, the beta cell area of mice treated with STZ ($p<0.001$) was significantly declined when compared to saline treated mice, which was to be expected (Figure 5.7C). The 1mg/kg Syn A (m) treated mice ($p<0.05$) displayed a significant increase in the beta cell area. The 5mg/kg Syn A (s) mice ($p<0.01$) showed a decrease in beta cell area when compared to saline treated mice. The mice treated with STZ ($p<0.001$) displayed a decrease in beta cell area and percentage when compared to saline treated mice (Figure 5.7D). The mice treated with 1mg/kg Syn A (m) showed an increase ($p<0.001$) in percentage of beta cells when compared to saline. Images are represented in Figure 5.8A-D. Insulin is represented in green, glucagon is represented in red, and DAPI in blue.

5.4.7 Effects of multiple low dose STZ and both multiple and single doses of Syn A on Ki67 positive, insulin positive cells in NIH Swiss mice.

Figure 5.9A, shows the proliferation of Ki67 positive, insulin positive cells within the treatment groups. When compared to saline treated mice, all three treatment groups exhibited a decrease ($p<0.001$) in beta cell proliferation. Photo representation can be seen in Figure 5.9B-E. Insulin is represented in green, Ki67 is represented in red, and DAPI in blue.

5.4.8 Effects of multiple low dose STZ and both multiple and single doses of Syn A on Ki67 positive, glucagon positive cells in NIH Swiss mice.

As seen in Figure 5.10A, the proliferation of Ki67 positive, glucagon positive cells were infrequently observed. When compared to mice treated with saline, STZ treated mice ($p<0.001$) had a significant decrease in Ki67 positive cells. Mice treated with a 1mg/kg of Syn A (m) ($p<0.05$) showed a slight decrease in proliferated alpha cells when compared against saline treated mice. However, the 5mg/kg Syn A (s) ($p<0.001$) had a more significant decrease when compared to the saline treated mice. Images can be seen in Figure 5.10B-E. Glucagon is represented in green, Ki67 is represented in red, and DAPI in blue.

5.4.9 Effects of multiple low dose STZ and varied multiple doses of Syn A on body weight, body weight change, and blood glucose in Swiss TO mice.

Body weight for the Swiss TO mice can be seen in Figure 5.11A. The mice treated with 8mg/kg of Syn A ($p<0.05$) had the highest starting significant weight when compared to saline and declined around day 3, followed by a slight increase, and then decreased near the end. A percentage of body weight change was calculated at the end of the study (Figure 5.11B). The higher doses of Syn A, 5mg/kg ($p<0.05$) and 8mg/kg ($p<0.01$), showed a significant body weight reduction when compared to the saline treated mice. As seen in Figure 5.11C, the blood glucose levels for the STZ mice displayed a significant increase starting at day 5 ($p<0.01$) and continued to increase ($p<0.001$) by day 6. On days 5 and 6, significance ($p<0.05$) was observed in mice treated with 5mg/kg Syn A when compared to the control mice. However, for the high dose of 8mg/kg of Syn A, their blood glucose levels declined after the first day, showing significance ($p<0.05$) on day 3. Their blood glucose levels were stable between day 3 and 5, and then declined on the last day. Statistical significance ($p<0.01$ and $p<0.001$) was also observed on day 5 and 6.

5.4.10 Effects of multiple low dose STZ and varied multiple doses of Syn A on food and fluid intake in Swiss TO mice.

Cumulative food intake for the 1mg/kg and 2mg/kg Syn A treatment groups was similar to the saline treated mice (Figure 5.12A). Starting from the first injection on day 1, the food intake started to decline in the higher dose mice and continued to be lower than the other treatment groups till the end of the study. Significance ($p<0.05$ and $p<0.01$) was observed from day 2 and continued throughout the study with an increase in significance ($p<0.001$) for both groups. As seen in Figure 5.12B, the lower dose treatment Syn A groups showed a decline in fluid intake starting from the start of the study and was consistently lower than the saline group with significance starting on day 2 ($p<0.05$ and $p<0.01$) and increased ($p<0.001$) through the remainder of the study.

5.4.11 Effects of multiple low dose STZ and varied multiple doses of Syn A on nonfasting and fasting plasma insulin levels in Swiss TO mice.

As seen in Figure 5.13A, shows that when compared to saline treated mice, the 8mg/kg Syn A treated mice ($p<0.05$) had significantly lower nonfasting plasma levels. Mice treated with STZ and 1mg/kg Syn A ($p<0.05$) displayed a significant decrease in fasting plasma levels (Figure 5.13B).

5.4.12 Effects of multiple low dose STZ and varied multiple doses of Syn A on pancreatic insulin content in the head, tail, and whole pancreas in Swiss TO mice.

Figure 5.14A, shows that the mice treated with 5mg/kg ($p<0.01$), and 8mg/kg ($p<0.001$) displayed the greatest decrease in pancreatic insulin content in the head of the pancreas. There was a significant decrease in pancreatic insulin content in the tail in the mice treated with 5mg/kg ($p<0.05$), and 8mg/kg ($p<0.01$) Syn A when compared to saline treated mice (Figure 5.14B). A significant decrease was observed in pancreatic insulin content within the whole pancreas in mice treated with 2mg/kg Syn A ($p<0.05$) when compared to saline treated

mice (Figure 5.14C). Mice treated with 5mg/kg Syn A ($p<0.01$) and 8mg/kg Syn A ($p<0.001$) show a significant decrease in pancreatic insulin content in the whole pancreas when compared to mice treated with saline.

5.4.13 Effects of multiple low dose STZ and varied multiple doses of Syn A on number of islets, islet area, and islet size distribution in the head of the pancreas in Swiss TO mice.

The number of islets within the head of the pancreas, can be seen in Figure 5.15A. The STZ treated mice ($p<0.01$), 1mg/kg Syn A treated mice ($p<0.001$), and 8mg/kg Syn A ($p<0.001$) showed a significant increase in the number of islets when compared to the saline treated mice. Figure 5.15B, shows no significance regarding islet area in the head of the pancreas. As shown in Figure 5.15C, medium islets were significantly increased in the mice treated with 8mg/kg of Syn A ($p<0.05$). There was a significant increase in large islets in the 8mg/kg Syn A ($p<0.01$) when compared to the saline treated mice.

5.4.14 Effects of multiple low dose STZ and varied multiple doses of Syn A on number of islets, islet area, and islet size distribution in the tail of the pancreas in Swiss TO mice.

When looking at the tail portion of the pancreas, the number of islets significantly decrease in the three higher doses of Syn A; 2mg/kg, 5mg/kg, and 8mg/kg ($p<0.05$; $p<0.01$) (Figure 5.16A). No significance was found regarding islet area in the tail of the pancreas (Figure 5.16B). As shown in Figure 5.16C, when compared to medium size islets from the saline treated mice, there was a significant decrease in the mice treated with 1mg/kg Syn A ($p<0.01$), 2mg/kg Syn A ($p<0.01$), and 5mg/kg Syn A ($p<0.001$) treated mice. When examining the large islet percentages compared to saline treated mice, mice treated with STZ ($p<0.05$), 1mg/kg Syn A ($p<0.05$), 2mg/kg Syn A ($p<0.01$), and 5mg/kg Syn A ($p<0.001$) exhibited a significant increase.

5.4.15 Effects of multiple low dose STZ and varied multiple doses of Syn A on number of islets, islet area, and islet size distribution in the whole pancreas in Swiss TO mice.

Figure 5.17A, shows that the number of islets in the whole pancreas was decreased significantly in the mice that were treated with 2mg/kg Syn A ($p<0.01$). The islet area within the whole pancreas displayed no significance (Figure 5.17B). As seen in Figure 5.17C, mice treated with 8mg/kg of Syn A, showed a significant decrease ($p<0.001$) in the percentage of islets that were categorized as small when compared to saline treated mice. There was an increase in medium islets in the mice treated with 8mg/kg Syn A ($p<0.05$).

5.4.16 Effects of multiple low dose STZ and varied multiple doses of Syn A on alpha cell area and percentage and beta cell area and percentage in the head of the pancreas in Swiss TO mice.

Figure 5.18A shows that there was a significant increase in the alpha cell area in mice treated with 8mg/kg Syn A ($p<0.01$). There was a large increase in the percentage of alpha cells observed in the mice treated with STZ ($p<0.001$) when compared with the control mice group (Figure 5.18B). As expected, the beta cell area within the STZ mice was significantly decreased ($p<0.01$) in relation to the saline treated mice (Figure 5.18C). There was a significant decrease in the STZ treatment group ($p<0.001$) when compared to saline (Figure 5.18D). Photo representation is shown in Figure 5.19A-F. Insulin is represented in green, glucagon is represented in red, and DAPI is represented in blue.

5.4.17 Effects of multiple low dose STZ and varied multiple doses of Syn A on alpha cell area and percentage and beta cell area and percentage in the tail of the pancreas in Swiss TO mice.

Figure 5.20A, shows the alpha cell area in the tail region of the pancreas. When compared to saline, the STZ treatment group ($p<0.01$), showed an increase in the alpha cell area. In comparison to the mice treated with saline, a significant decrease was observed in the 5mg/kg

Syn A ($p<0.01$) and the 8mg/kg Syn A ($p<0.001$) treated mice. There was a large increase in the percentage of alpha cells in the STZ treatment group ($p<0.001$) when compared to the saline mice (Figure 5.20B). Mice treated with 5mg/kg Syn A ($p<0.01$) and 8mg/kg Syn A ($p<0.001$) exhibited a decrease in the percentage of alpha cells when compared to saline treated mice. As seen in Figure 5.20C, the STZ treated mice ($p<0.05$) had a slight decrease in the beta cell area of the islets observed when compared to the saline mice. Mice treated with 2mg/kg of Syn A ($p<0.05$) showed an increase in the beta cell area of the analysed islets. Analysis of beta cell percentage showed that there was a decrease in the islets of the mice treated with STZ ($p<0.001$) when compared to saline (Figure 5.20D). Mice treated with 5mg/kg Syn A ($p< 0.05$) and 8mg/kg Syn A ($p<0.001$) treated mice displayed an increase in beta cell percentage when compared to the saline treated mice. Photo representation is shown in Figure 5.21 A-F. Insulin is represented in green, glucagon is represented in red, and DAPI is represented in blue.

5.4.18 Effects of multiple low dose STZ and varied multiple doses of Syn A on alpha cell area and percentage and beta cell area and percentage in the whole pancreas in Swiss TO mice.

Mice treated with STZ ($p<0.001$), 1mg/kg Syn A ($p<0.05$), and 2mg/kg Syn A ($p<0.01$) showed a significant increase in alpha cell area in the whole pancreas when compared to the saline group (Figure 5.22A). Alpha cell percentage was increased in mice treated with STZ ($p<0.001$) and decreased in mice treated with 8mg/kg Syn A ($p<0.001$) when compared with saline treated mice (Figure 5.22B). Figure 5.22C, shows the STZ treated mice ($p<0.01$) displayed a decrease in beta cell area when compared to the saline mice. There was an increase in beta cell area in the mice treated with 8mg/kg ($p<0.05$) in contrast to saline. As seen in Figure 5.22D, the percentage of beta cells in STZ mice ($p<0.001$) significantly decreased when assessed against the saline treatment group. There was an increase in beta cell percentage in the 8mg/kg ($p<0.001$) when compared to the saline group.

5.4.19 Effects of multiple low dose STZ and varied multiple doses of Syn A on Ki67 positive, insulin positive cells and Ki67 positive, glucagon positive cells in the whole pancreas in Swiss TO mice.

No significance was found regarding Ki67 positive, insulin positive cells (Figure 5.23A). No significance was observed regarding Ki67 positive, glucagon positive cells (Figure 5.23B). Photo representation is shown in Figure 5.24A-F for Ki67 positive, insulin positive cells. Photo representation is shown in Figure 5.24G-L for Ki67 positive, glucagon positive cells. Insulin or glucagon is represented in green, Ki67 is represented in red, and DAPI is represented in blue.

5.5 Discussion

5.5.1 NIH Swiss Mice bioanalysis

Effects of Syn A on body weight was documented in only two of the past studies (Karr *et al.* 1929; Rabinowitch, 1927). Humans treated with Syn A and/or insulin showed stable body weight during the three-month study (Rabinowitch, 1927). This is similar to the mice we treated with both 1mg/kg Syn A (m) and 5 mg/kg Syn A (s). However, the dogs that were treated with Syn A showed a small decline in body weight within the first few weeks of injection (Karr *et al.*1929). Review of previous articles indicate that no past research examines the food and fluid intake in subjects treated with Syn A. We found that the mice treated with Syn A did not show decreases in food intake. Observation of the two groups treated with Syn A, showed a significant decrease in the cumulative fluid intake. Blood glucose remained stable throughout the study. However, in a study that looked at the effects of Syn A on blood glucose in lizards, severe hypoglycaemia occurred (Miller and Wurster, 1958). Some researchers state that other organs are affected by Syn A, such as the liver, and that the pancreas may not be the sole target site of action (Langslow and Freeman, 1973; Davis, 1958). Unlike the Syn A mice, the mice treated with STZ showed increasing levels of blood glucose. The STZ mice in this study became diabetic by day 5, causing their blood sugar to be too high to partake in the i.p. GTT on the final day. This is a result of the insulin deficiency in these mice (Lenzen,

2008). A study that examined chickens in response to Syn A examined their insulin and glucagon plasma levels along with the free fatty acids and glucagon-like immunoreactives. The plasma insulin levels decreased over a period of 6 hours in chickens that were nonfasted. The highest level of plasma insulin once Syn A was injected was at the 15-minute mark and decreased to starting from the 60-minute mark and stable for the next several hours (Lansglow *et al.*1973). When examining the nonfasted plasma insulin levels in the mice we treated with Syn A, results were similar to the mice treated with saline. We took nonfasting blood on the 10th day, and both Syn A groups were higher than in past research. However, when Langslow *et al*. (1973) examined 48 hour fasting insulin plasma levels, no change was detectable. Nevertheless, the mice treated with Syn A showed an increasing amount in both groups when compared to saline in our study.

5.5.2 NIH Swiss Mice islet morphology

As expected, the STZ revealed beta cell destruction (Vasu *et al.* 2014; Like and Rossini, 1976). When looking at the mice treated with 1mg/kg Syn A (multiple dose) and 5 mg/kg Syn A (single dose), the islets contained a limited number of alpha cells. This has also been documented in the study by Ferner and Runge (1955), who examined pancreas and alpha cells from rats. In the rats used by Lundbaek and Nielsen (1958), it was reported that some of the alpha cells were unaffected by the administration of Syn A, which can also be seen in the present study. Not all of the islets disappeared in the mice that were administered Syn A. In an experiment carried out by Lundbaek and Nielsen (1958), the alpha cells that remained were supposed to be present on the outside of the islet. Histologically, the alpha cells created a rim around the islet in the pancreas of the rats that were administered Syn A (Lundbaek and Nielsen, 1958). However, in the NIH Swiss mice, if the alpha cells were present after the administration of Syn A, the ring on the islet was often incomplete. In the proliferation immunohistochemistry assay, the three treatment groups had very little Ki67 positive, insulin positive cells. Same is true when Ki67 positive, glucagon positive cells were analysed. This is to be expected when examining glucagon positive cells as it was hypothesized that Syn A

is an alpha cell toxin and histologically affects the alpha cells. The NIH Swiss mice study shows that Syn A has an impact on alpha cells as well as the animals' blood glucose levels, by allowing them to remain stable.

5.5.3 Swiss TO mice bioanalysis

Similar to the NIH Swiss mice, body weight remained stable throughout the course of the study for most of the treatment groups: saline, STZ, 1mg/kg, 2mg/kg, and 5mg/kg Syn A. Mice treated with 8mg/kg Syn A had a higher body weight for the first part of the study. The STZ treated mice, also had an increase in their blood glucose levels whereas the higher dose of Syn A had a decrease in their blood glucose. Mihich *et al.* (1959), demonstrated that, when Syn was administered i.p., for the treatment of tumours, at three different doses, 2mg/kg, 4mg/kg, and 8mg/kg, the DBA2 and Ha-ICR Swiss mice lived 6-12 days after injection. However, three of the four animals that were administered 8mg/kg in this Swiss TO study survived five daily doses of 8mg/kg. Three of the four mice in the group that were administered 5mg/kg had stable blood glucose levels throughout the 5-day study. It is quite clear that the higher doses of Syn A have a massive effect on the mouse's blood glucose level. Graham (1927) states that the toxic symptoms of Syn include vomiting, nausea, and anorexia, in a human case study. Although no vomit was present, the higher doses, 5mg/kg and 8mg/kg mice, did show a decrease in the amount of food intake near the end of the five days and three of the 7 mice in these two groups stopped eating after day three of the study. The lack of food intake clearly affected the animals' body weight over the course of the study. However, the mice with the lower dose of 2mg/kg of Syn A also lost weight during the study, just not as much as the higher-dosed mice. Cumulative fluid intake showed a decrease in the higher doses of Syn A, which was similar to the NIH Swiss mice, even though the lower doses showed similar results as the saline treated mice. The nonfasting and fasting plasma insulin levels were the same as the NIH Swiss mice. Due to these differences, Langslow *et al.* (1973) suggest that Syn A only interacts with an active intestinal system.

5.5.4 Swiss TO islet morphology

None of the past research has reported examining the islets located in the different regions of the pancreas regarding action of Syn A. Some studies have looked at the differences in islet morphology in normal animals of different species as well as their islet morphology in different regions of the pancreas (Steiner *et al.* 2014; Kim *et al.* 2009; Elayat *et al.* 1995). This research has found that the number of islets in the tail is higher than the number in the head portion of the pancreas (Steiner *et al.* 2014; Elayat *et al.* 1995). In Swiss TO mice, we found that the head of the pancreas contained more islets than the tail. The Swiss TO mice pancreas were dissected into two sections: head and tail, where a previous article on islet architecture separated the pancreas into four: upper duodenal, lower duodenal, gastric, and splenic (Elayat *et al.* 1995). This difference in head and tail was also true for our mice in relation to islet area. The diameters of the islets were smaller in the tail compared to the head, whereas Elayat *et al*. (1995), found that the diameter of islets was much larger in the gastric and splenic region.

As expected, the beta cells within the head of the pancreas, were mostly affected by the STZ treatment, where-as the number of alpha cells were increased in the head and tail. This was also seen in islets from the tail portion of the pancreas. Interestingly, the Syn A higher dose treatment groups presented with a greater number of alpha cells than suspected from the head of the pancreas. This could be that the alpha cells are hydropic (Davis, 1952). This is supported by our observations in the increased number of islets, islet area, and the islet size distribution in the higher doses of Syn A compared to saline. However, when examining islets from the tail region, there is a decrease in number of islets, diameter, size, alpha and beta cell area/percentage. This is to be expected due to Syn A being an alpha cell toxin. Due to a lack of tissue to separate head and tail for the proliferation staining, all data from each group had to be combined as one. Although this does not give specific data in proliferation in the head vs. tail regions, it does provide expected results in regard to the lack of insulin and glucagon proliferating cells affected by each treatment.

When specifically looking at the organs in the Swiss TO mice, the two higher doses of Syn A were significantly different compared to the others in the study. The head of the pancreas was smaller in size, especially in the 8mg/kg mice. All of the mice in the 5mg/kg and 8mg/kg Syn A groups showed signs of intestinal pseudo obstruction with sections of necrosis being present. The stomachs of these 8 mice were severely distended and measured around 3mm to 3.5mm in length and 2 mm in width. Rabinowitch (1927) stated that the normal and depancreatised dogs showed signs of gastro-intestinal problems but does not specify what disturbances occurred. Mice within these groups also presented with several blood clots around their heart and lungs. Stool and urine were darker in the 8mg/kg mice when compared to the other mice. The autopsy of the mice in the higher treatment groups displayed similar findings as dogs that were administered neoSyn in the 1920's (Karr *et al.*1928). The pancreas in the dogs was hard to identify due to the colour of the pancreas (Karr *et al.*1928). The head of the pancreas of the mice in this study was also difficult to identify, due to the head looking like it had been stretched. It was often hard to distinguish the head from the tail of the pancreas, as well as adipose from pancreatic tissue.

One of the limitations within this study was the small number of mice per group in the Swiss TO study. Perhaps with more mice per group, there would be more tissue to analyse and could carry out the head and tail analysis for the staining experiments. Another limitation within that study was the lack of observation days after the last Syn A treatments to look at potential reversibility. This would have been congruent with the NIH Swiss study as those mice had an observation period, then we could have seen how multiple doses of larger treatments compared to the observation of the NIH Swiss 1mg/kg Syn A multiple dose. Overall, these data show that the high single dose and the higher multiple doses of Syn A have an overall effect on blood glucose levels. We can also conclude that there is a deleterious effect to the islets and the organs in the animals treated with the different doses, especially the higher doses of Syn A.

Figure 5.2 Effects of multiple low dose STZ and both multiple and single doses of Syn A on body weight (A) and body weight change (B) in NIH Swiss mice over 10 days.

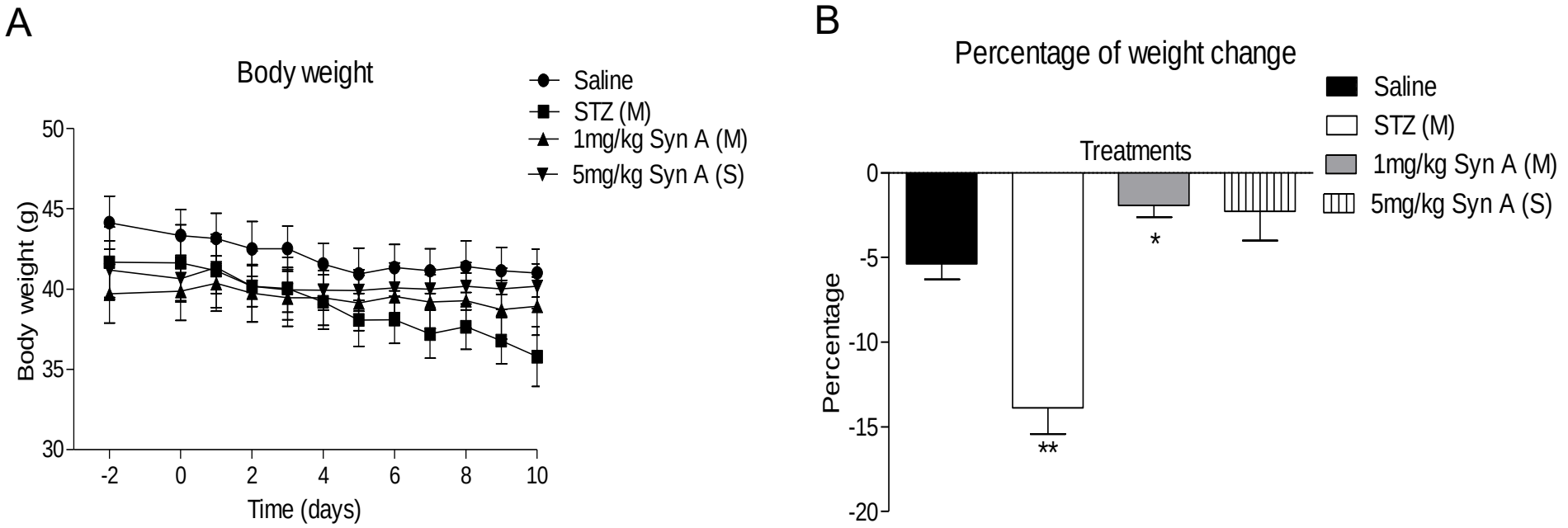

Daily measurements of body weight (A) and percentage of body weight change (B) over the course of the 10-day study. 50mg/kg STZ (m) was administered for 5 daily doses by i.p. starting at day 1. 1mg/kg Syn A (m) was administered for 5 daily doses by i.p. starting at day 1. 5mg/kg Syn A (s) was administered for a single dose by i.p. on day 1. Values are mean ± SEM (n= 5-6 mice). Changes were deemed significant when p values were *$p<0.05$, **$p<0.01$ when compared with saline.

Figure 5.3 Effects of multiple low dose STZ and both multiple and single doses of Syn A on food (A) and fluid (B) intake in NIH Swiss mice over 10 days.

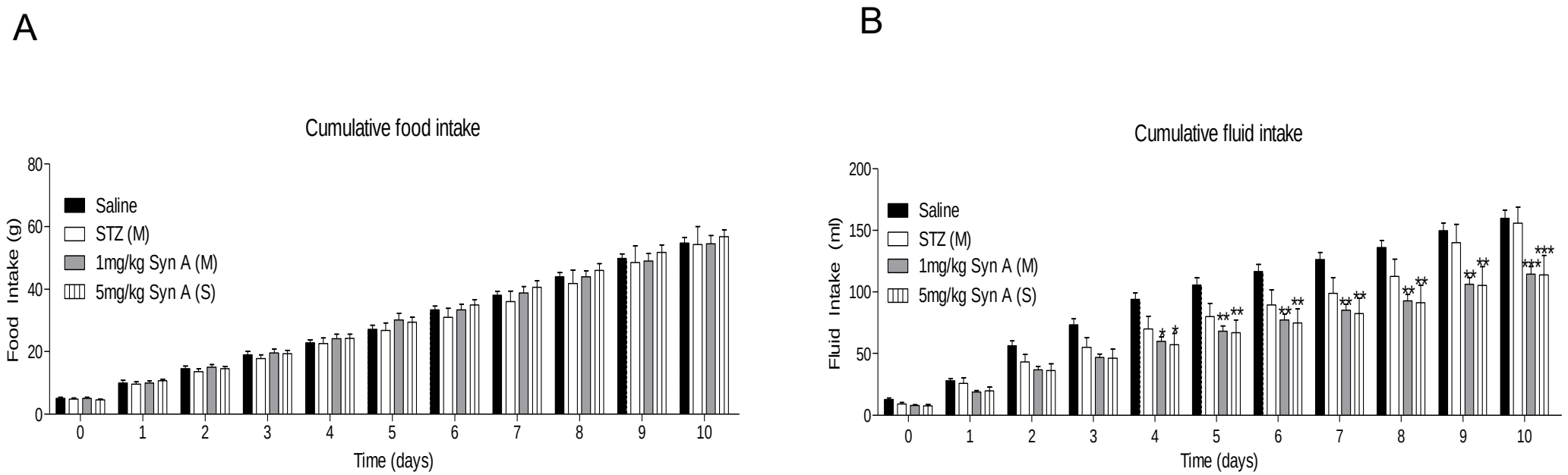

Daily measurements of food (A) and fluid (B) intake over the course of 10 days. 50mg/kg STZ (m) was administered for 5 daily doses by i.p. starting at day 1. 1mg/kg Syn A (m) was administered for 5 daily doses by i.p. starting at day 1. Values are mean ± SEM (n= 5-6 mice). Changes were deemed significant when p values were *p <0.05, **p <0.01, or ***p <0.001 when compared with saline.

Figure 5.4 Effects of multiple low dose STZ and both multiple and single doses of Syn A on blood glucose (A) and during an i.p. GTT (B and C) in NIH Swiss mice over 10 days.

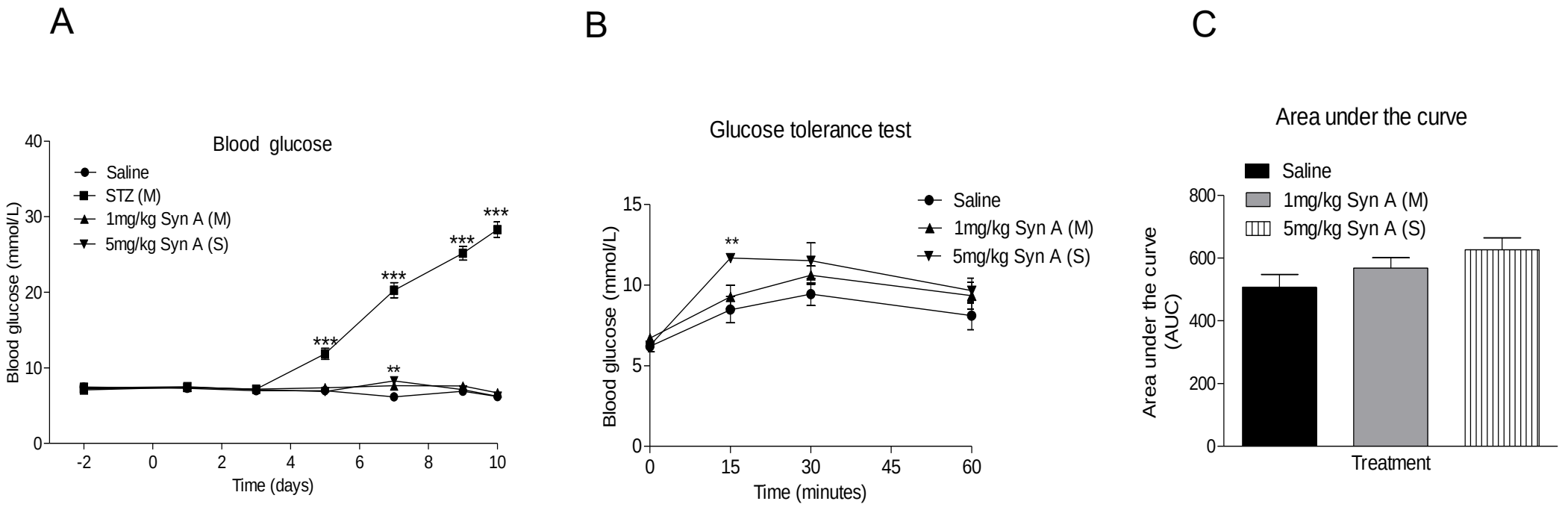

Blood glucose which was measured on alternating days (A) the GTT (B and C) which was performed on the final day of the study. 50mg/kg STZ (m) was administered for 5 daily doses by i.p. starting at day 1. 1mg/kg Syn A (m) was administered for 5 daily doses by i.p. starting at day 1. Values are mean ± SEM (n= 5-6 mice). Changes were deemed significant when p values were *p <0.05, **p <0.01, or ***p <0.001 when compared with saline.

Figure 5.5 Effects of multiple low dose STZ and both multiple and single doses of Syn A on nonfasting plasma insulin (A), fasting plasma insulin (B), and pancreatic insulin content (C) in NIH Swiss mice at the end of 10 days.

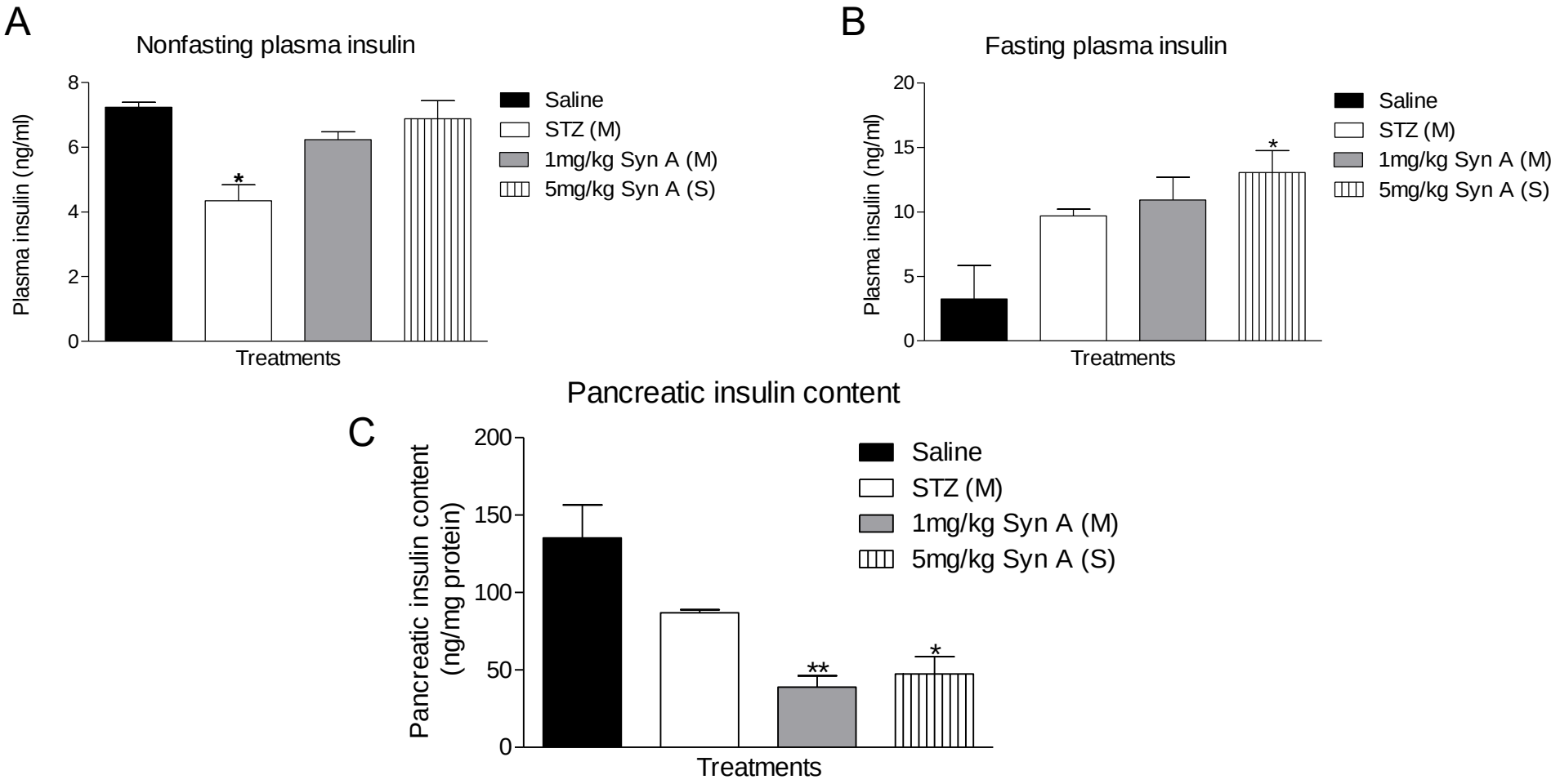

Nonfasting (A) and fasting (B) blood was taken at the end of the study. Plasma insulin levels were measured by RIA. Pancreatic insulin content (C) was measured with flash frozen pancreas. 50mg/kg STZ (m) was administered for 5 daily doses by i.p. starting at day 1. 1mg/kg Syn A (m) was administered for 5 daily doses by i.p. starting at day 1. Values are mean ± SEM (n= 5-6 mice). Changes were deemed significant when p values were *p <0.05 or **p<0.01 when compared with saline.

Figure 5.6 Effects of multiple low dose STZ and both multiple and single doses of Syn A on the number of islets (A), islet area (B), and islet size distribution (C) in NIH Swiss mice after 10 days.

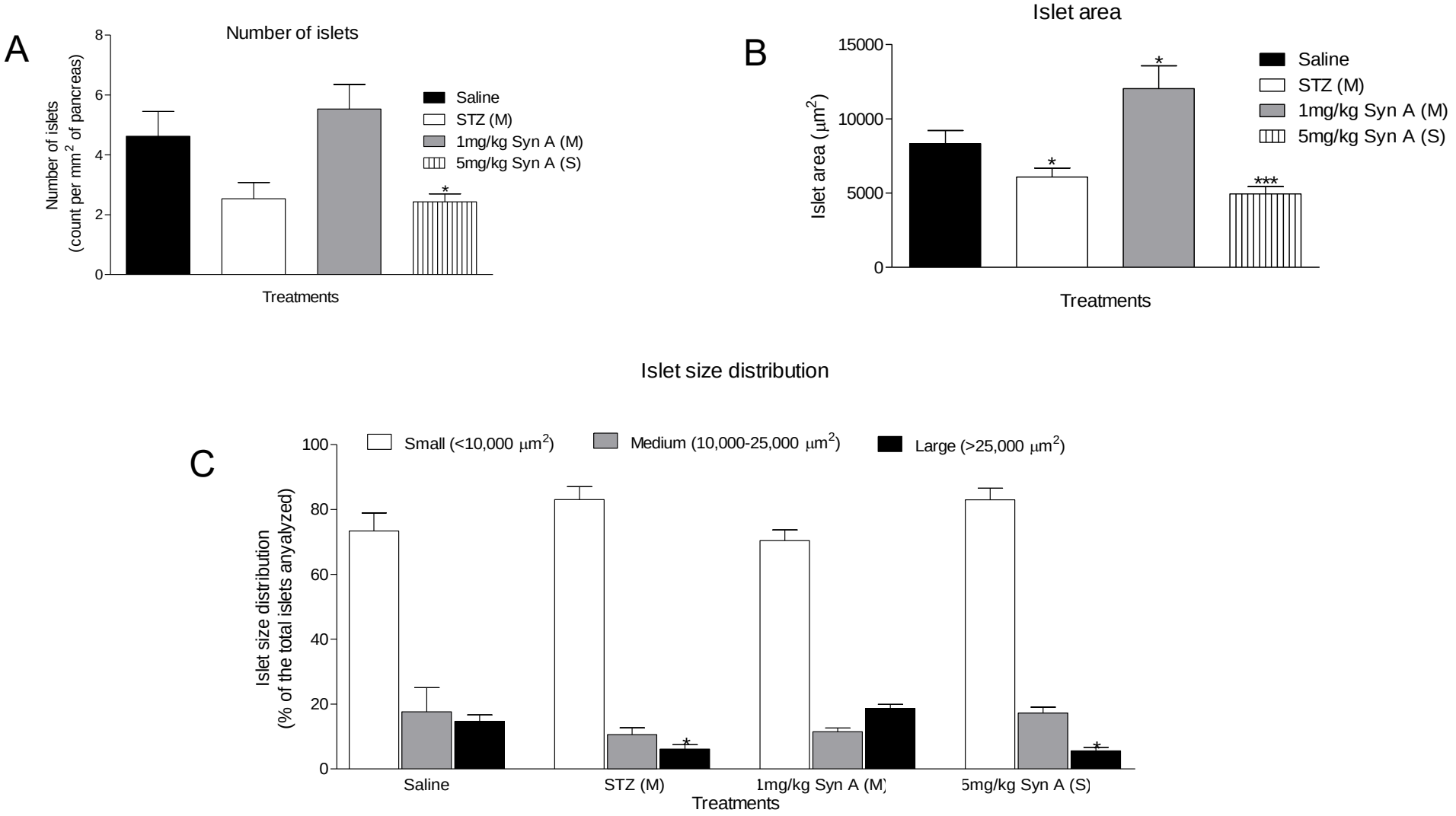

Number of islets per mm^2 (A), islet area (B), and islet size distribution (C). 50mg/kg STZ (m) was administered for 5 daily doses by i.p. starting at day 1. 1mg/kg Syn A (m) was administered for 5 daily doses by i.p. starting at day 1. Values are mean ± SEM (n= 5-6). Changes were deemed significant when p values were *p <0.05 or ***p <0.001 when compared with saline.

Figure 5.7 Effects of multiple low dose STZ and both multiple and single doses of Syn A on alpha cell area and percentage (A and B) and beta cell area and percentage (C and D) in NIH Swiss mice after 10 days.

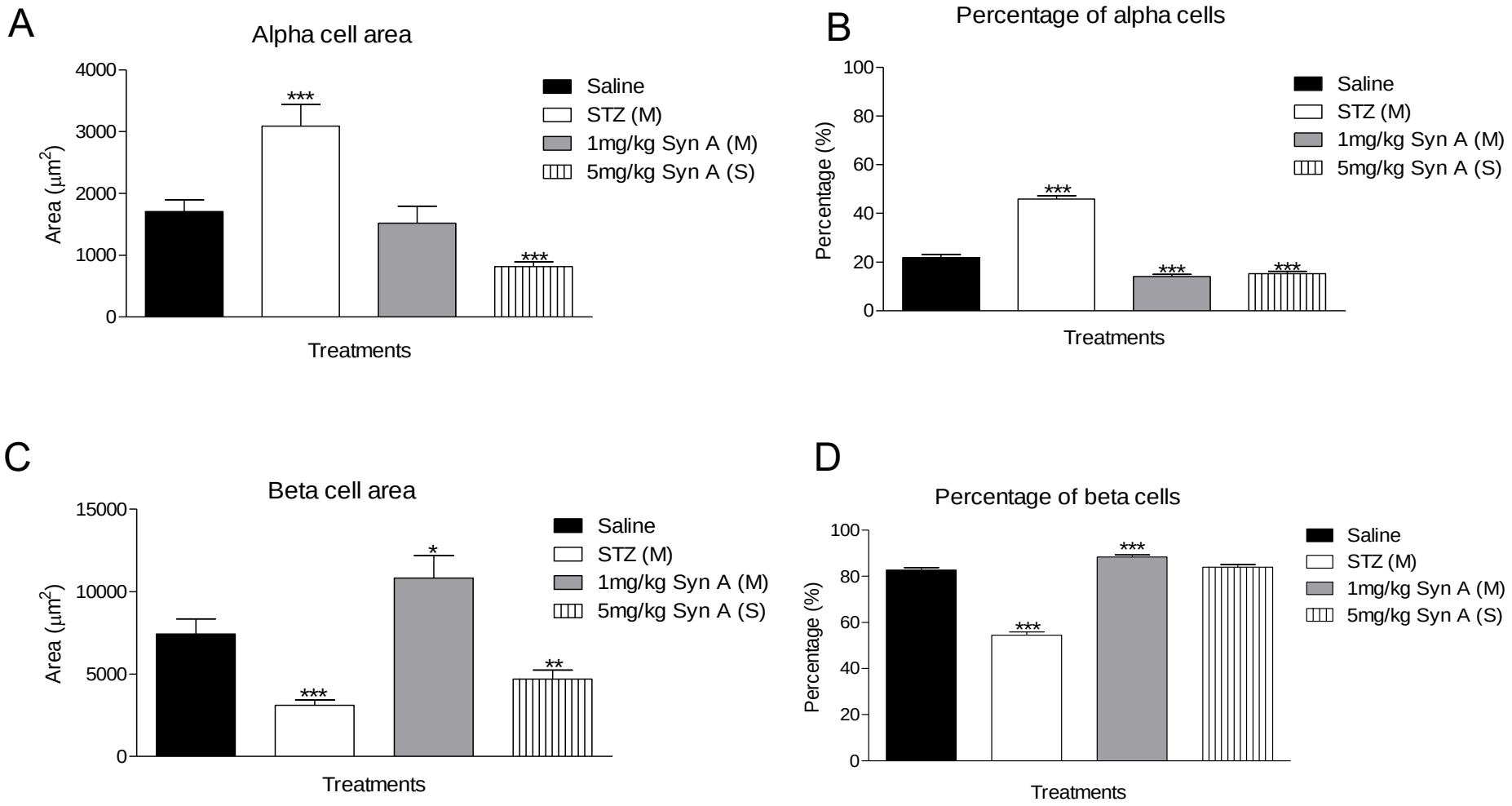

Alpha cell area and percentage (A and B) and beta cell area and percentage (C and D) per pancreas. 50mg/kg STZ (m) was administered for 5 daily doses by i.p. starting at day 1. 1mg/kg Syn A (m) was administered for 5 daily doses by i.p. starting at day 1. Values are mean ± SEM (n= 5-6 mice). Changes were deemed significant when p values were ***p <0.001 when compared with saline.

Figure 5.8 Representative images from saline (A), STZ (B), Syn A multiple dose (C), and Syn A single dose (D) islets from NIH Swiss mice after 10 days.

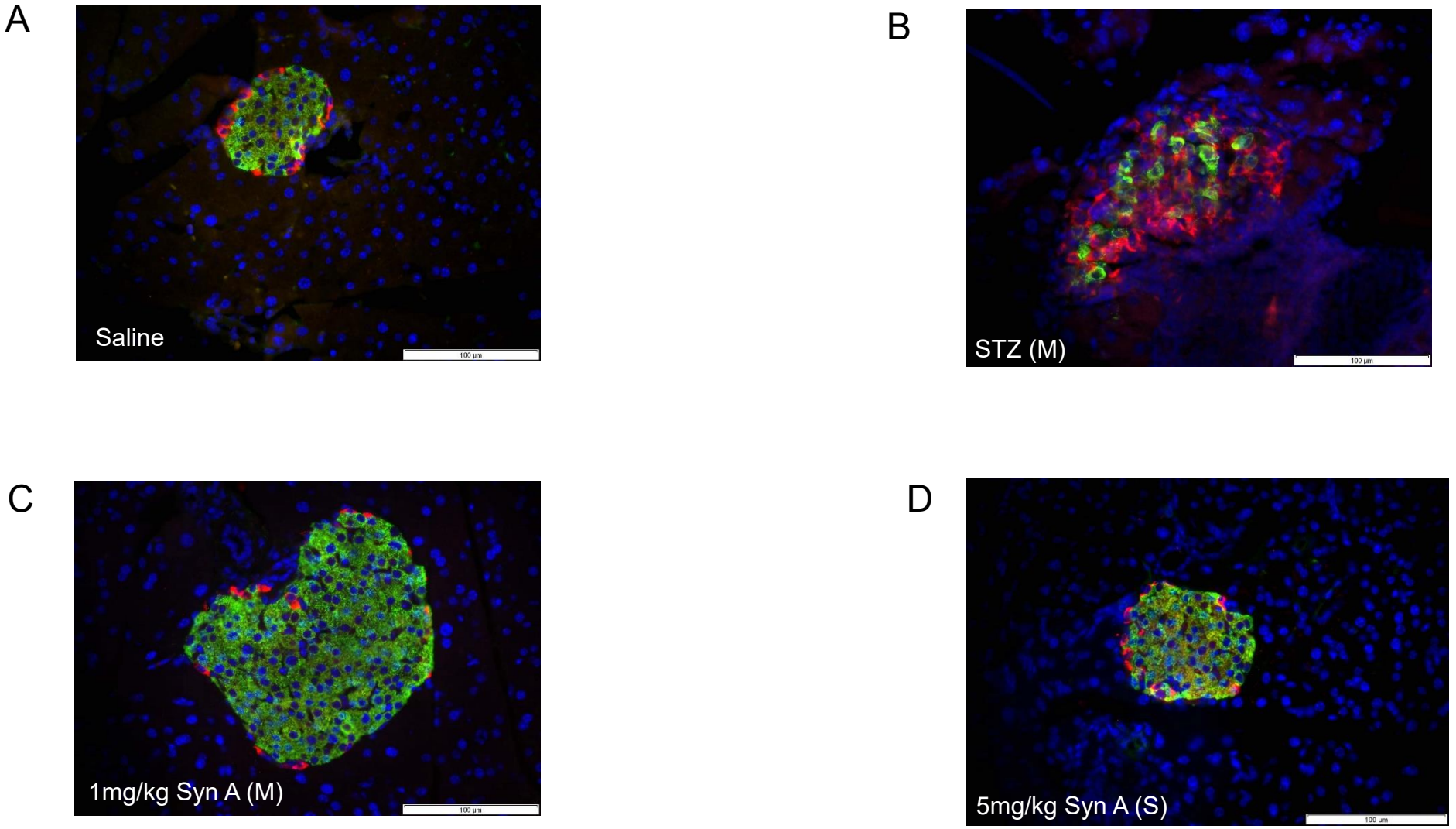

Islet morphology was evaluated at the end of the 10-day study using 5-7 µm tissue sections. Saline (A), STZ (B), 1mg/kg Syn A (m) (C), and 5mg/kg Syn A (s) (D) islets. Insulin is represented in green, glucagon in red, and DAPI in blue. Photos imaged at 40x.

Figure 5.9 Effects of multiple low dose STZ and both multiple and single doses of Syn A on Ki67 positive, insulin positive cells (A-E) in NIH Swiss mice after 10 days.

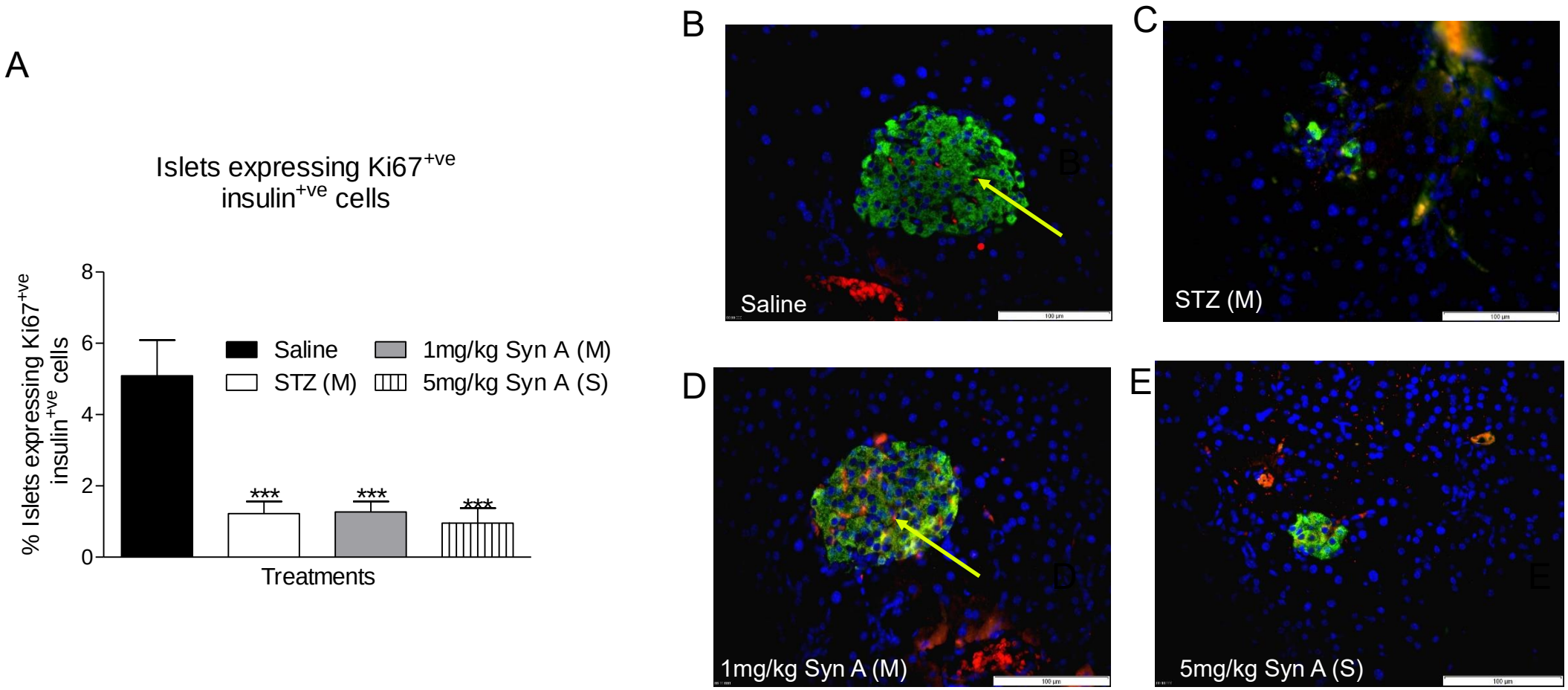

Percentage of beta cell proliferation was determined by islets expressing Ki67^{+ve}, insulin^{+ve} cells (A) with representative images (B-E). Insulin is represented in green, Ki67^{+ve} cells in red, and DAPI in blue. Yellow arrows are pointing at Ki67^{+ve}, insulin^{+ve} cells. Images taken at 40x objective lens. 50mg/kg STZ (m) was administered for 5 daily doses by i.p. starting at day 1. 1mg/kg Syn A (m) was administered for 5 daily doses by i.p. starting at day 1. Values are mean ± SEM (n= 5-6 mice). Changes were deemed significant when p values were *p <0.05 or **p<0.01 when compared with saline.

Figure 5.10 Effects of multiple low dose STZ and both multiple and single doses of Syn A on Ki67 positive, glucagon positive cells (A-E) in NIH Swiss mice after 10 days.

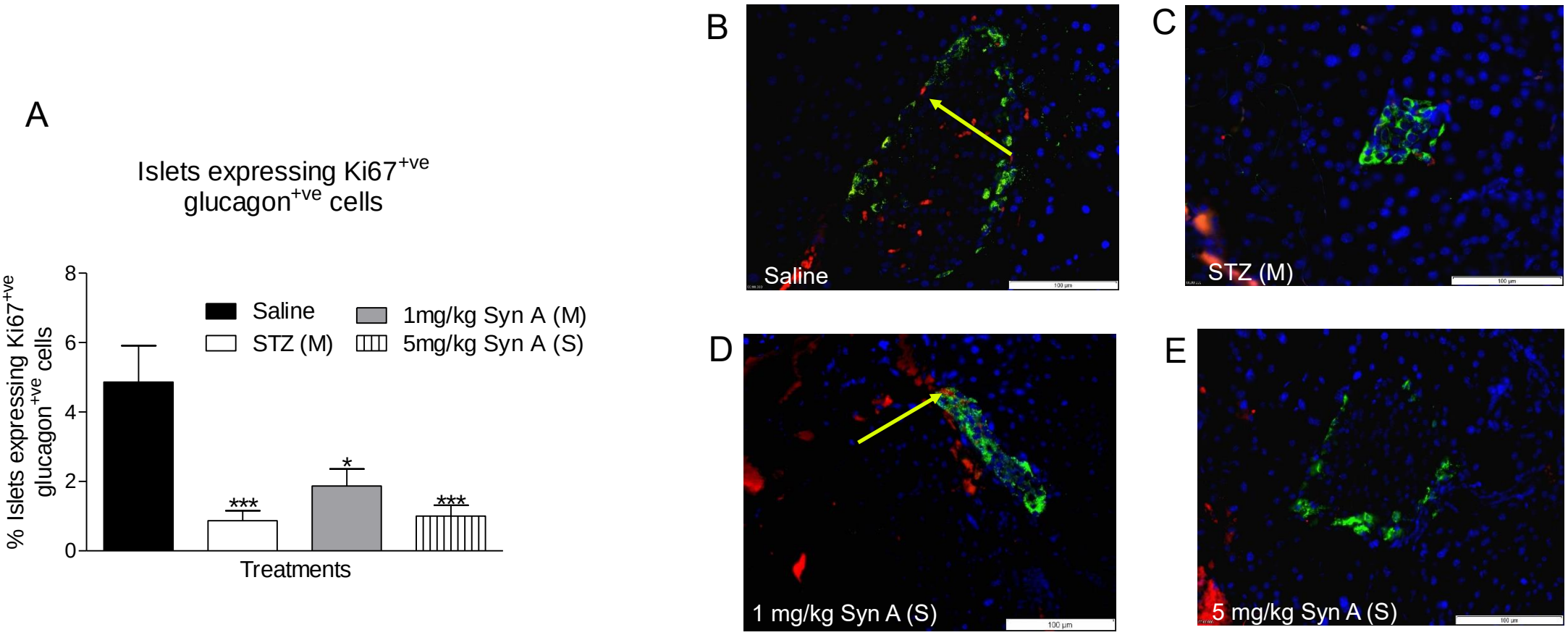

Percentage of alpha cell proliferation was determined by islets expressing Ki67^{+ve}, glucagon^{+ve} cells (A) with representative images (B-E). Glucagon is represented in green, Ki67^{+ve} cells in red, and DAPI in blue. Yellow arrows are pointing to Ki67^{+ve}, glucagon^{+ve} cells. Images taken at 40x objective lens. 50mg/kg STZ (m) was administered for 5 daily doses by i.p. starting at day 1. 1mg/kg Syn A (m) was administered for 5 daily doses by i.p. starting at day 1. Values are mean ± SEM (n= 5-6 mice). Changes were deemed significant when p values were *p <0.05 or **p<0.01 when compared with saline.

Figure 5.11 Effects of multiple low dose STZ and varied multiple doses of Syn A on body weight (A), body weight change (B), and blood glucose (C) in Swiss TO mice over 6 days.

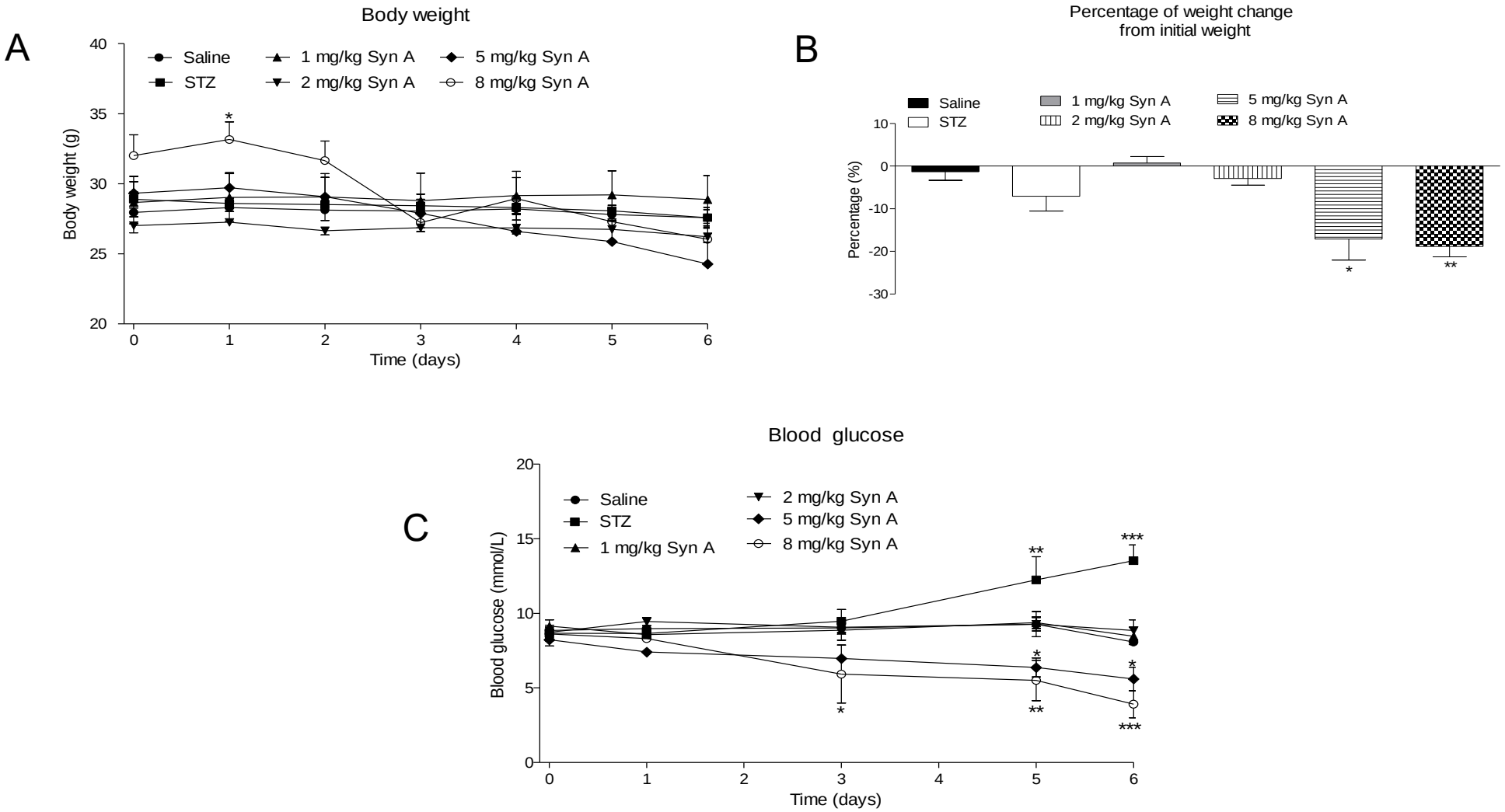

Daily measurements of body weight (A), the percentage of body weight change (B), and blood glucose measurements (C) over the course of the 5-day study. 50mg/kg STZ, 1mg/kg, 2mg/kg, 5mg/kg and 8mg/kg Syn A was administered for 5 daily doses by i.p. starting at day 1. Values are mean ± SEM (n= 4 mice). Changes were deemed significant when p values were *p<0.05, **p<0.01, ***p<0.001 when compared with saline.

Figure 5.12 Effects of multiple low dose STZ and varied multiple doses of Syn A on food (A) and fluid intake (B) in Swiss TO mice over 6 days.

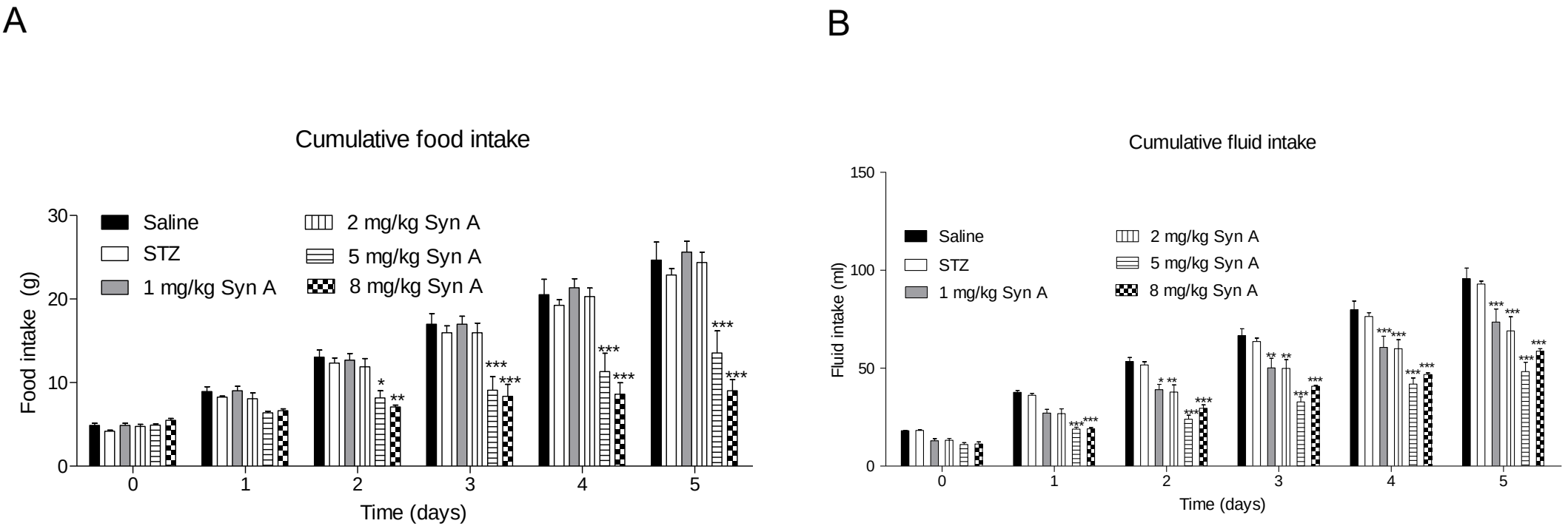

Cumulative measurements of daily intake of food (A) and fluid (B) over the course of the 5-day study. STZ (50mg/kg), 1mg/kg, 2mg/kg, 5mg/kg and 8mg/kg Syn A was administered for 5 daily doses by i.p. starting at day 1. Values are mean ± SEM (n= 4 mice). Changes were deemed significant when p values were *p<0.05, **p<0.01, ***p<0.001 when compared with saline.

Figure 5.13 Effects of multiple low dose STZ and varied multiple doses of Syn A on nonfasting (A) and fasting (B) plasma insulin levels in Swiss TO mice measured at the end of 6 days.

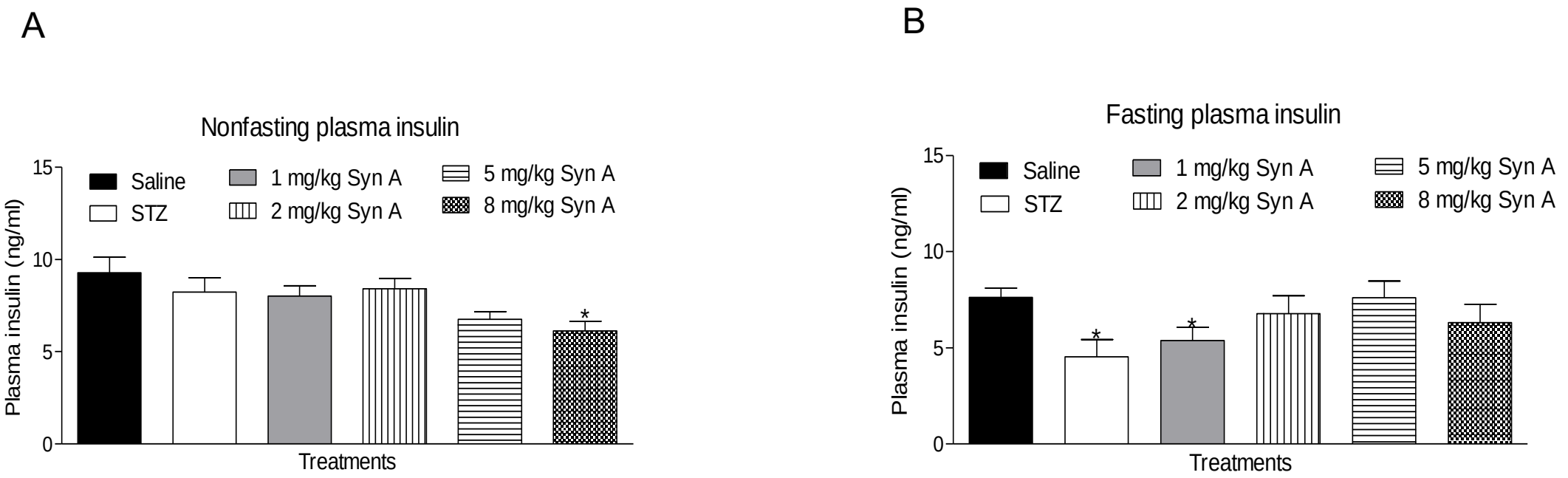

Nonfasting (A) and fasting (B) blood was taken at the end of the study. STZ (50mg/kg), 1mg/kg, 2mg/kg, 5mg/kg and 8mg/kg Syn A was administered for 5 daily doses by i.p. starting at day 1. Plasma insulin was measured by RIA. Values are mean ± SEM (n= 4 mice). Changes were deemed significant when p values were *p <0.05 when compared with saline.

Figure 5.14 Effects of multiple low dose STZ and varied multiple doses of Syn A on pancreatic insulin content from the head (A), and tail (B), and whole pancreas (C) in Swiss TO mice after 6 days.

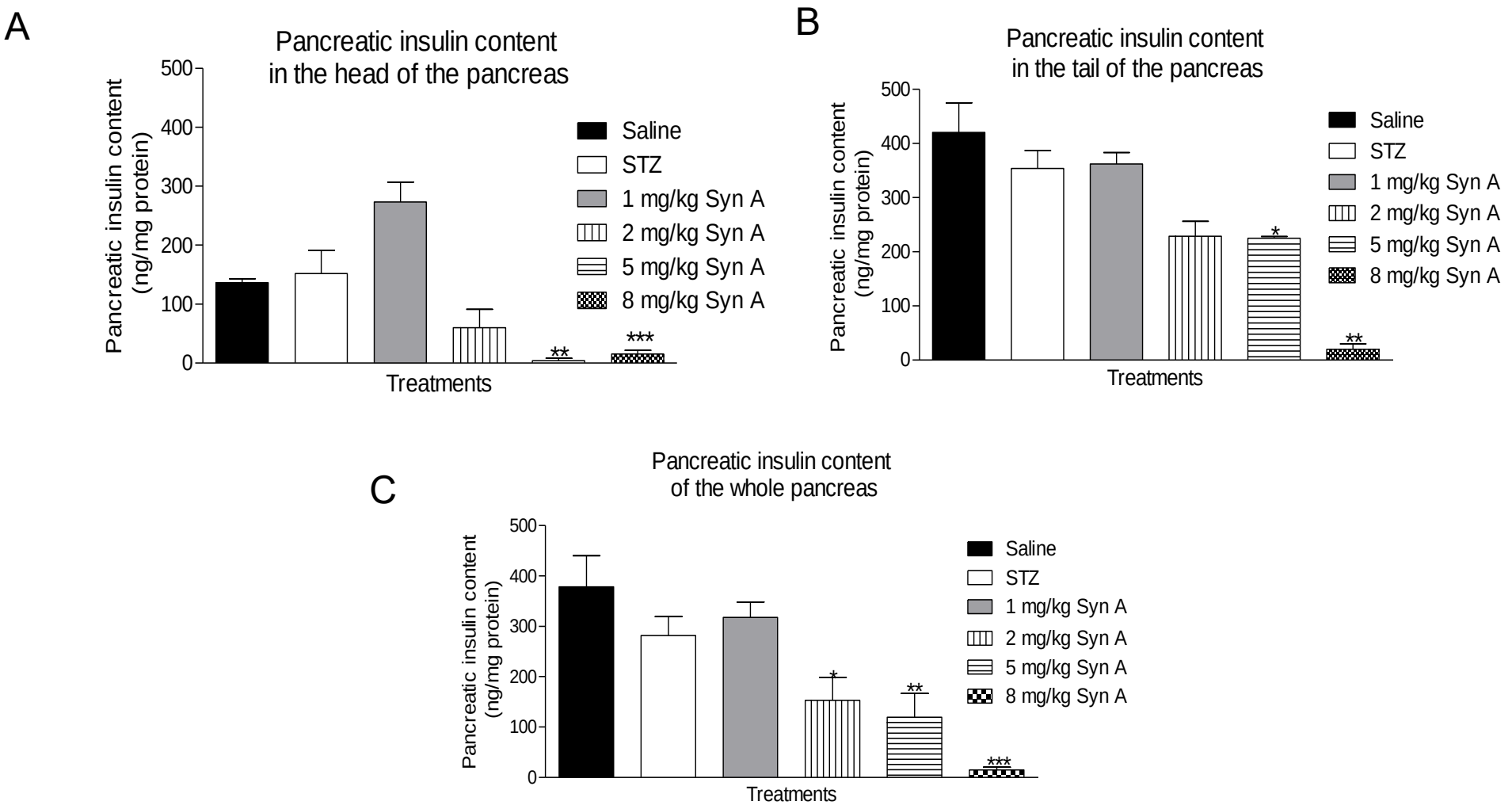

Pancreatic insulin content was measured from the head (A), tail (B), and whole (C) flash frozen pancreas. STZ (50mg/kg), 1mg/kg, 2mg/kg, 5mg/kg and 8mg/kg Syn A was administered for 5 daily doses by i.p. starting at day 1. Values are mean ± SEM (n= 4 mice). Changes were deemed significant when p values were *p <0.05, **p<0.01, or ***p<0.001 when compared with saline.

Figure 5.15 The effects multiple low dose STZ and varied multiple doses of Syn A on the number of islets (A), islet area (B), and size distribution (C) in the pancreatic head of Swiss TO mice after 6 days.

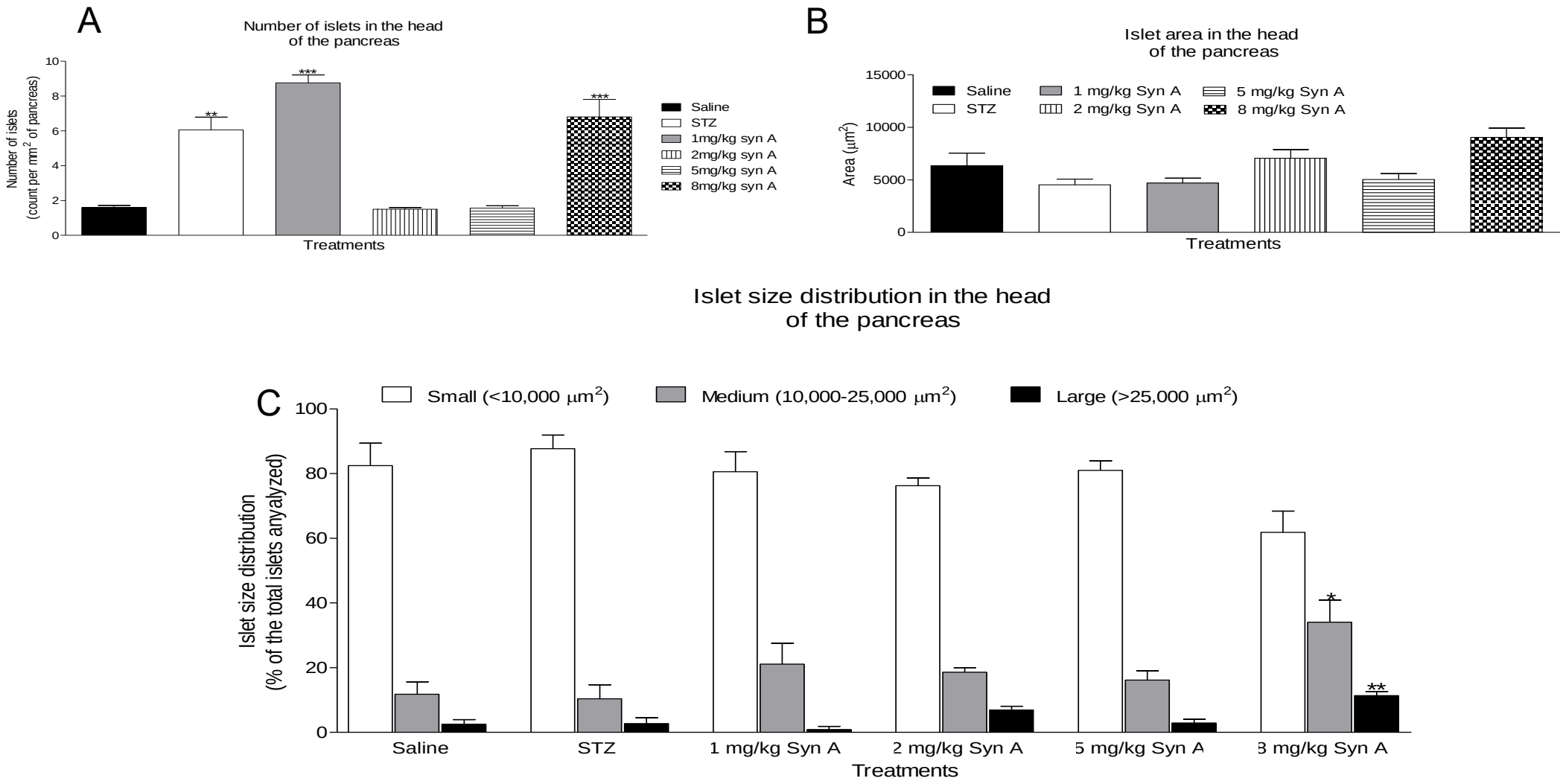

Number of islets per mm^2 (A), islet area (B), and size distribution (C) on the head of the pancreas. STZ (50mg/kg), 1mg/kg, 2mg/kg, 5mg/kg and 8mg/kg Syn A was administered for 5 daily doses by i.p. starting at day 1. Values are mean ± SEM (n=4 mice). Changes were deemed significant when p values were *p<0.05, **p <0.01, ***p<0.001 when compared with saline.

Figure 5.16 The effects multiple low dose STZ and varied multiple doses of Syn A on the number of islets (A), islet area (B), and size distribution (C) in the pancreatic tail of Swiss TO mice after 6 days.

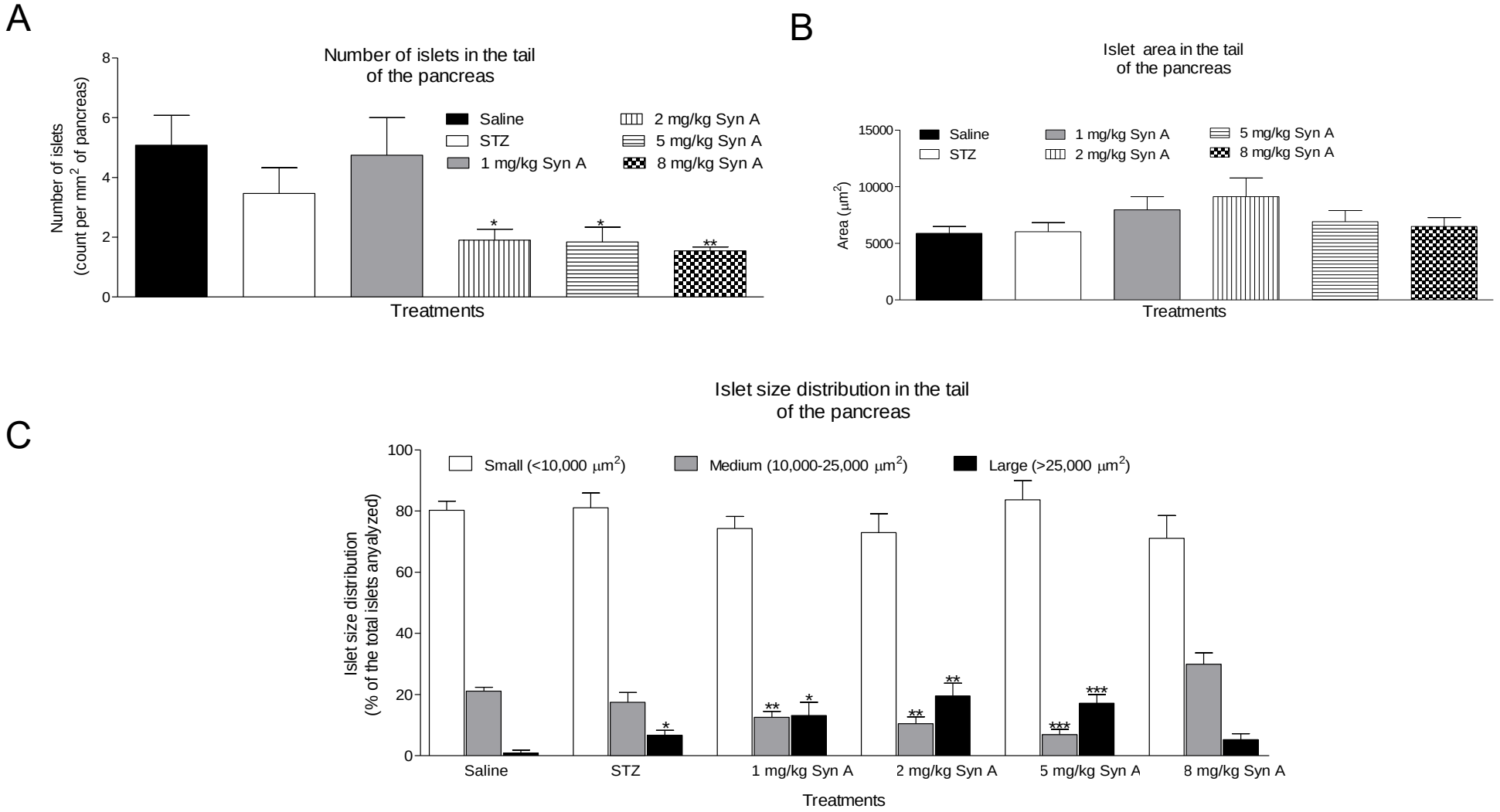

Number of islets per mm^2 (A), islet area (B), and size distribution (C) in the tail of the pancreas. STZ (50mg/kg), 1mg/kg, 2mg/kg, 5mg/kg and 8mg/kg Syn A was administered for 5 daily doses by i.p. starting at day 1. Values are mean ± SEM (n=4 mice). Changes were deemed significant when p values were *p<0.05, **p <0.01, ***p<0.001 when compared to the saline treated mice.

Figure 5.17 The effects multiple low dose STZ and varied multiple doses of Syn A on the number of islets (A), islet area (B), and size distribution (C) in the whole pancreas of Swiss TO mice after 6 days.

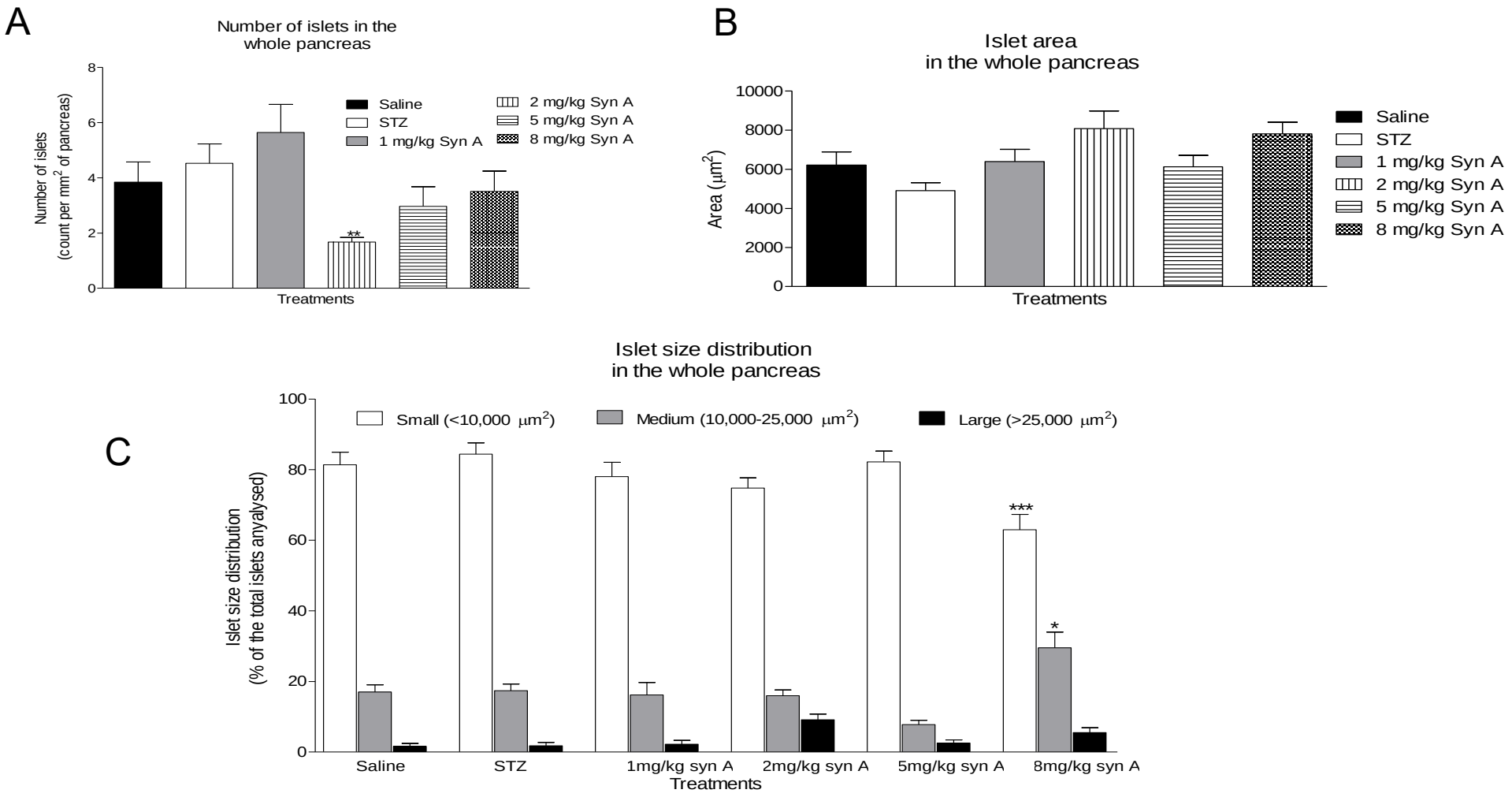

Number of islets per mm^2 (A), islet area (B), and size distribution (C) per pancreas. STZ (50mg/kg), 1mg/kg, 2mg/kg, 5mg/kg and 8mg/kg Syn A was administered for 5 daily doses by i.p. starting at day 1. Values are mean ± SEM (n=4 mice). Changes were deemed significant when p values were **p <0.01 or ***p< 0.001 when compared to the saline treated mice.

Figure 5.18 The effects multiple low dose STZ and varied multiple doses of Syn A on alpha cell area and percentage (A and B) and beta cell area and percentage (C and D) in the pancreatic head of Swiss TO mice after 6 days.

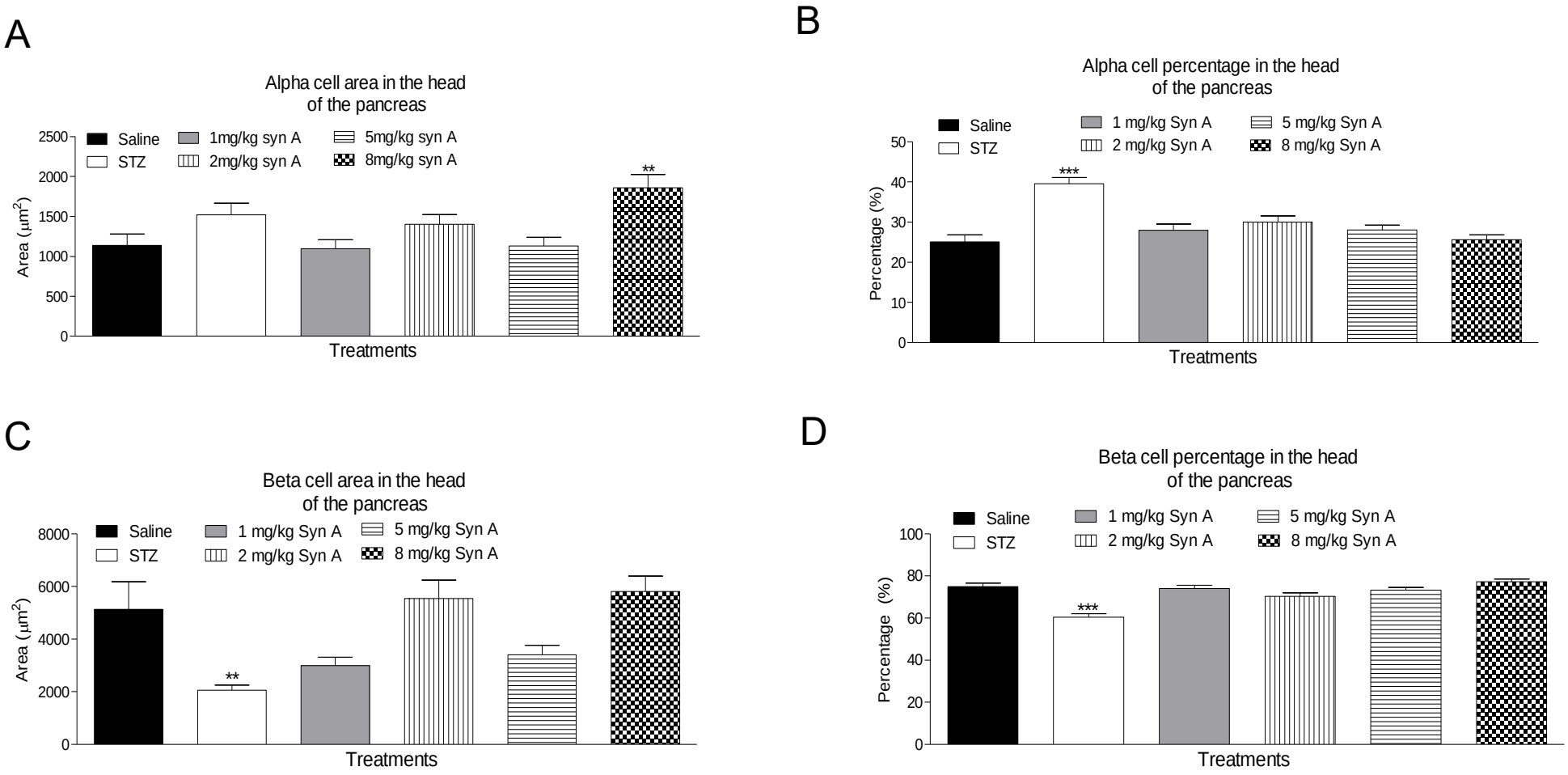

Alpha cell area and percentage (A and B) and beta cell area and percentage (C and D) in the head of the pancreas. STZ (50mg/kg), 1mg/kg, 2mg/kg, 5mg/kg and 8mg/kg Syn A was administered for 5 daily doses by i.p. starting at day 1. Values are mean ± SEM (n=4 mice). Changes were deemed significant when p values were **p <0.01 or ***p<0.001 when compared to the saline treated mice.

Figure 5.19 Representative images of saline (A), STZ (B), 1mg/kg Syn A (C), 2mg/kg Syn A (D), 5mg/kg Syn A (E), and 8mg/kg Syn A (F) islets from the head of Swiss TO mice after 6 days.

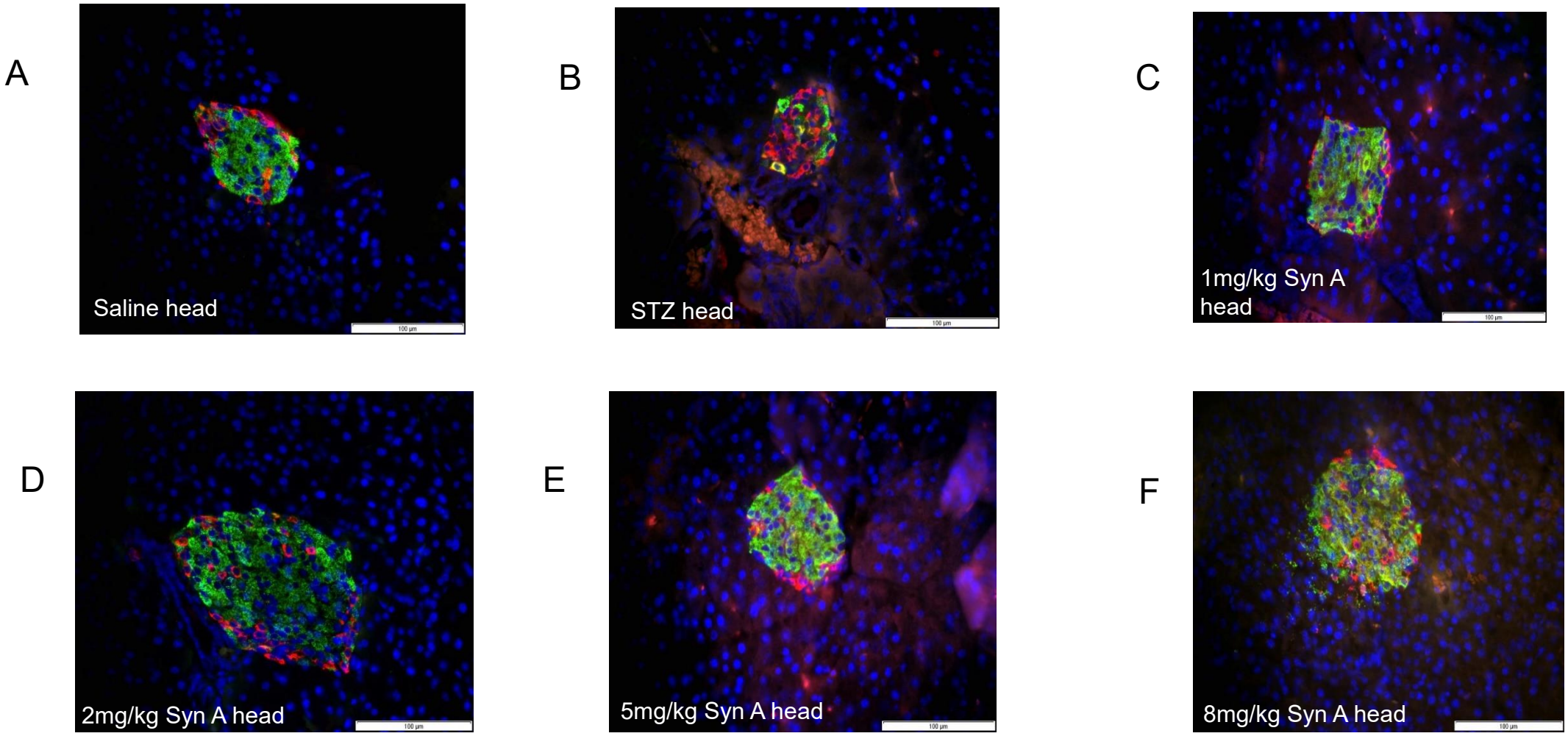

Islet morphology was evaluated at the end of the 6-day study using 5-7 µm tissue sections. Saline (A), STZ (B), 1mg/kg Syn A (C), 2mg/kg Syn A (D), 5mg/kg Syn A (E), and 8mg/kg Syn A (F) islets. Insulin is represented in green, glucagon in red, and DAPI in blue. Photos imaged at 40x.

Figure 5.20 The effects multiple low dose STZ and varied multiple doses of Syn A on alpha cell area and percentage (A and B) and beta cell area and percentage (C and D) in the pancreatic tail of Swiss TO mice after 6 days.

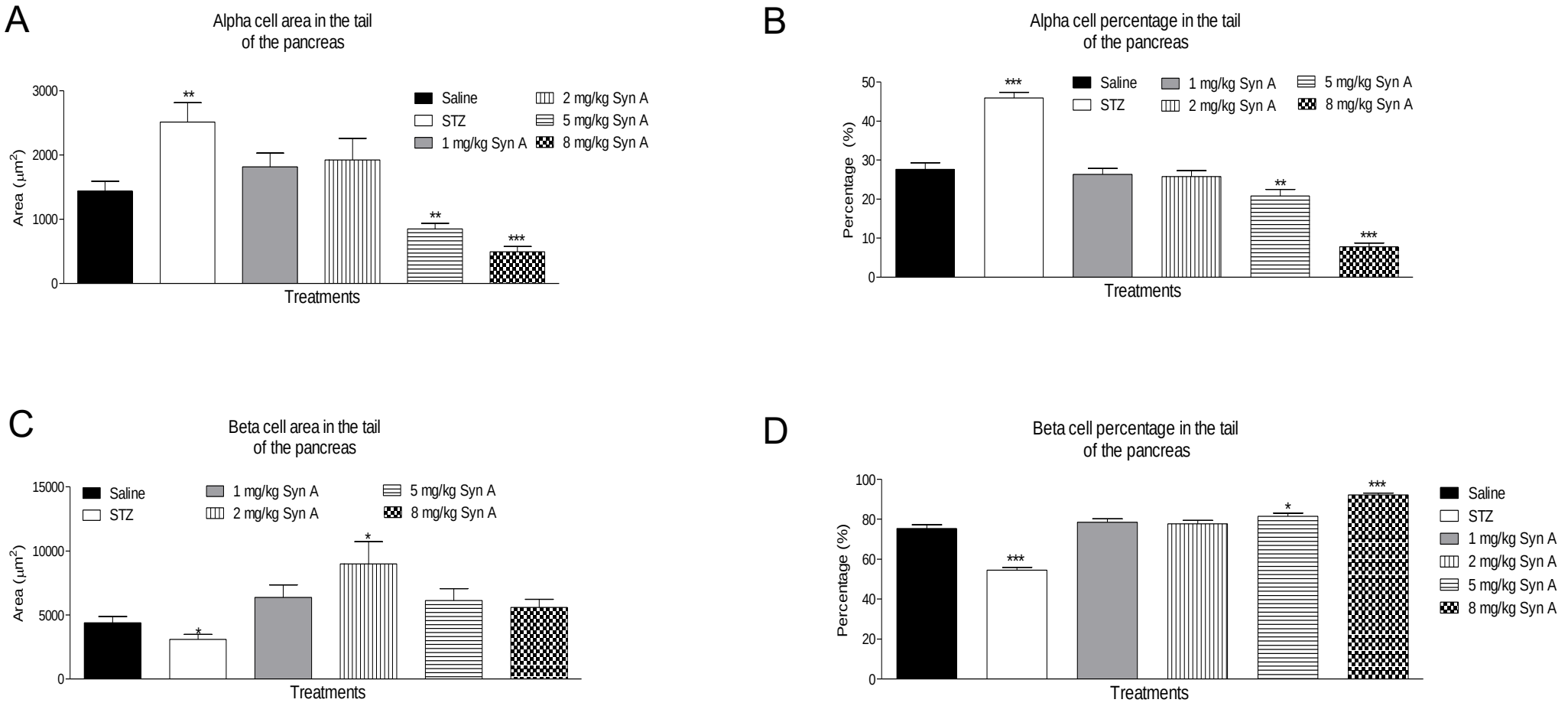

Alpha cell area and percentage (A and B) and beta cell area and percentage (C and D) in the tail of the pancreas. STZ (50mg/kg), 1mg/kg, 2mg/kg, 5mg/kg and 8mg/kg Syn A was administered for 5 daily doses by i.p. starting at day 1. Values are mean ± SEM (n=4 mice). Changes were deemed significant when p values were *p<0.05, **p <0.01, or ***p<0.001 when compared to saline.

Figure 5.21 Representative images of saline (A), STZ (B), 1mg/kg Syn A (C), 2mg/kg Syn A (D), 5mg/kg Syn A (E), and 8mg/kg Syn A (F) islets from the tail of Swiss TO mice after 6 days.

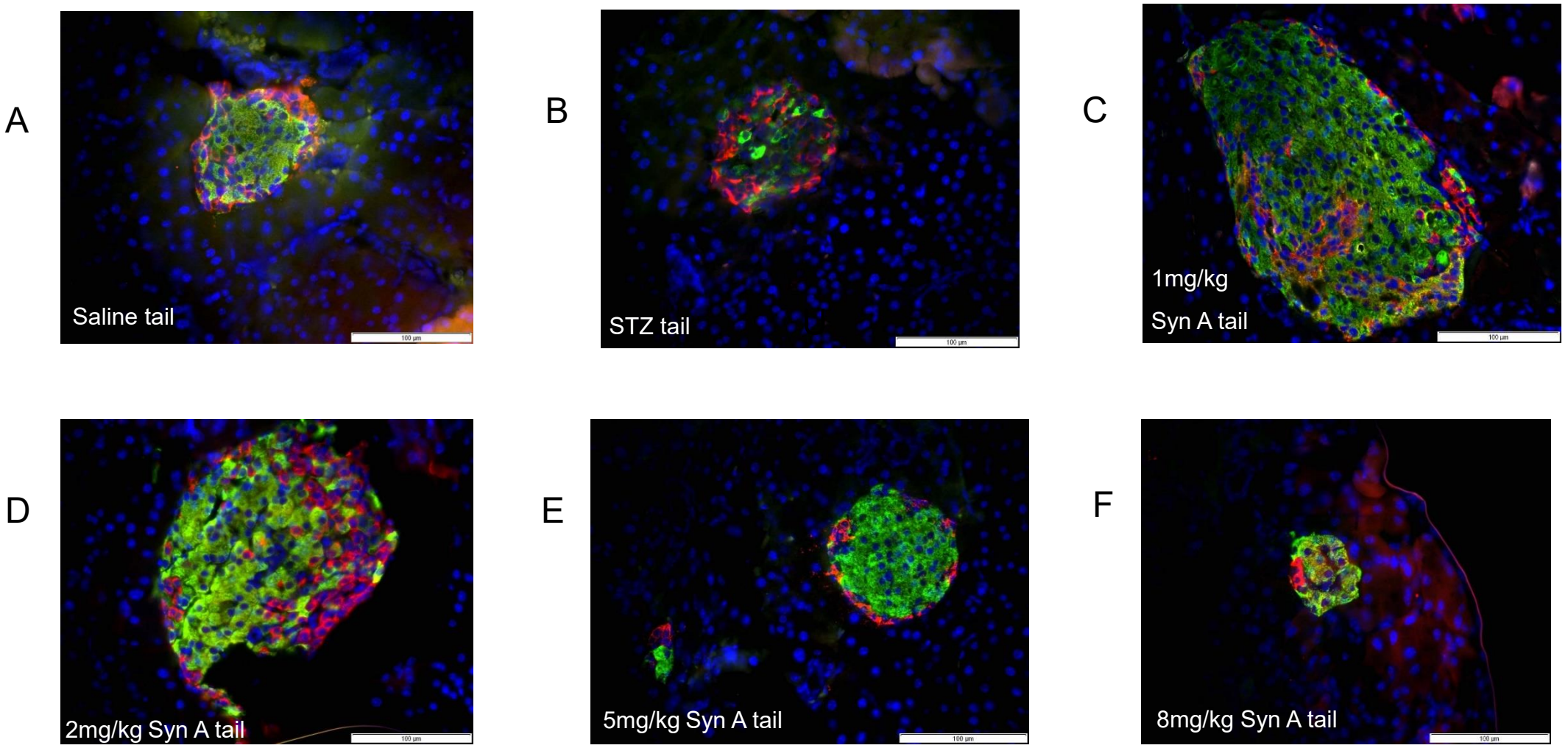

Islet morphology was evaluated at the end of the 8-day study using 5-7 µm tissue sections. Saline (A), STZ (B), 1mg/kg Syn A (C), 2mg/kg Syn A (D), 5mg/kg Syn A (E), and 8mg/kg Syn A (F) islets. Insulin is represented in green, glucagon in red, and DAPI in blue. Photos imaged at 40x.

Figure 5.22 The effects multiple low dose STZ and varied multiple doses of Syn A on alpha cell area and percentage (A and B) and beta cell area and percentage (C and D) in the whole pancreas of Swiss TO mice after 6 days.

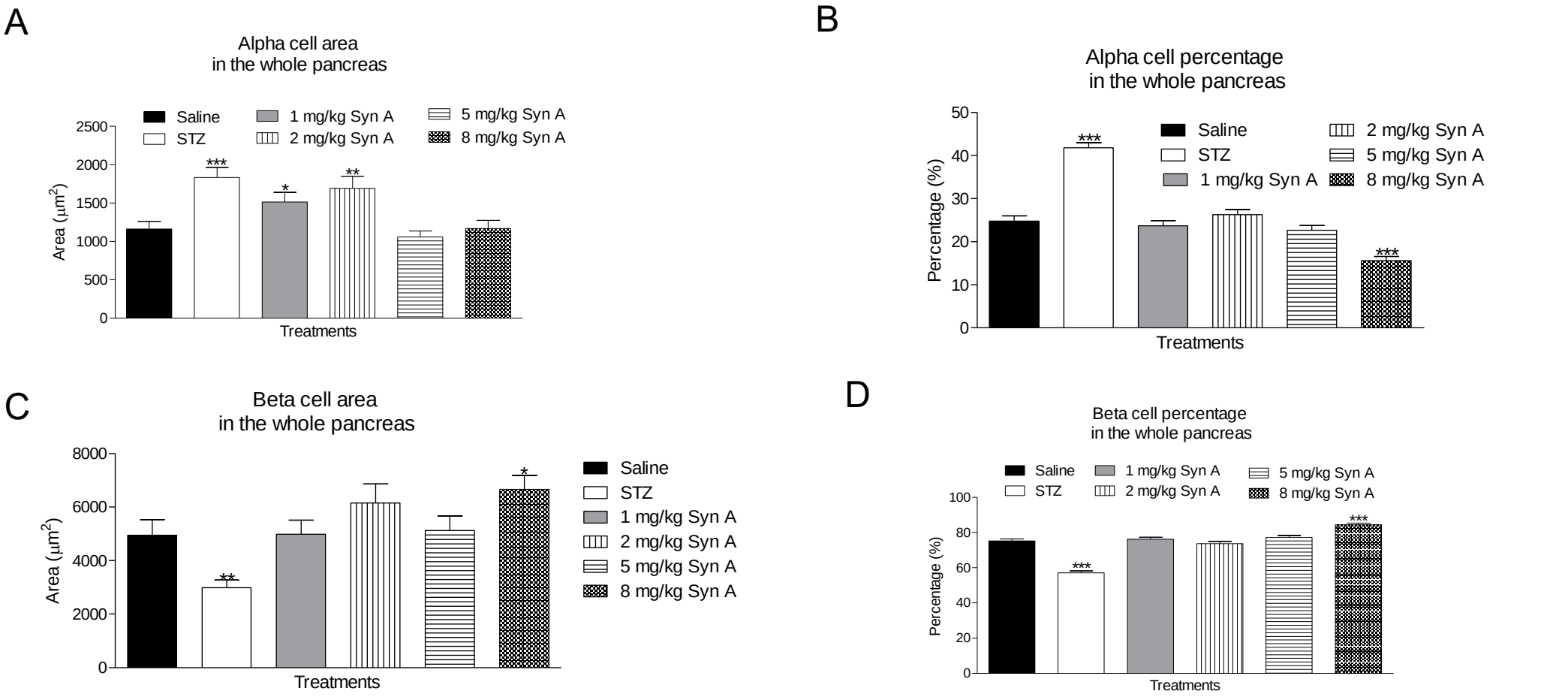

Alpha cell area and percentage (A and B) and beta cell area and percentage (C and D) in the pancreas. STZ (50mg/kg), 1mg/kg, 2mg/kg, 5mg/kg and 8mg/kg Syn A was administered for 5 daily doses by i.p. starting at day 1. Values are mean ± SEM (n=4 mice). Changes were deemed significant when p values were *p<0.05, **p <0.01, or ***p<0.001 when compared to saline.

Figure 5.23 The effects multiple low dose STZ and varied multiple doses of Syn A on Ki67 positive, insulin positive (A) and Ki67 positive, glucagon positive (B) cells in the whole pancreas of Swiss TO mice after 6 days.

A

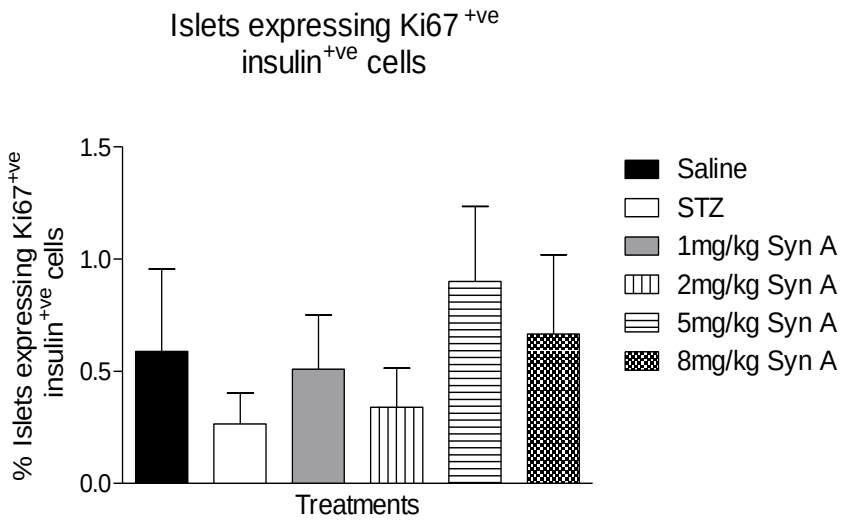

B

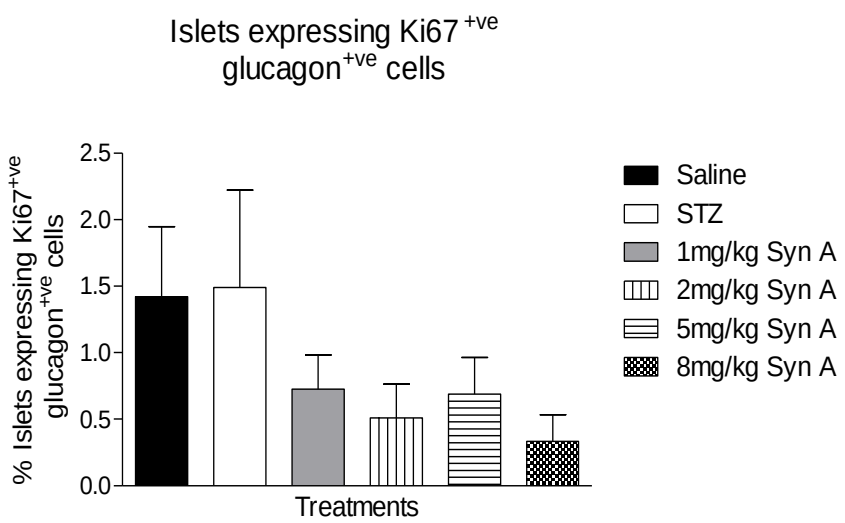

Percentage of beta cell proliferation was determined by islets expressing Ki67^{+ve}, insulin^{+ve} cells. Percentage of alpha cell proliferation was determined by islets expressing Ki67^{+ve}, glucagon $^{+ve}$ cells. STZ (50mg/kg), 1mg/kg, 2mg/kg, 5mg/kg and 8mg/kg Syn A was administered for 5 daily doses by i.p. starting at day 1. Values are mean ± SEM 7 mice. Changes were deemed significant when p values were <0.05.

Figure 5.24 Representative images of multiple low dose STZ and varied multiple doses of Syn A on Ki67 positive, insulin positive cells (A-F) and Ki67 positive, glucagon positive cells (G-L) in the pancreas in Swiss TO mice.

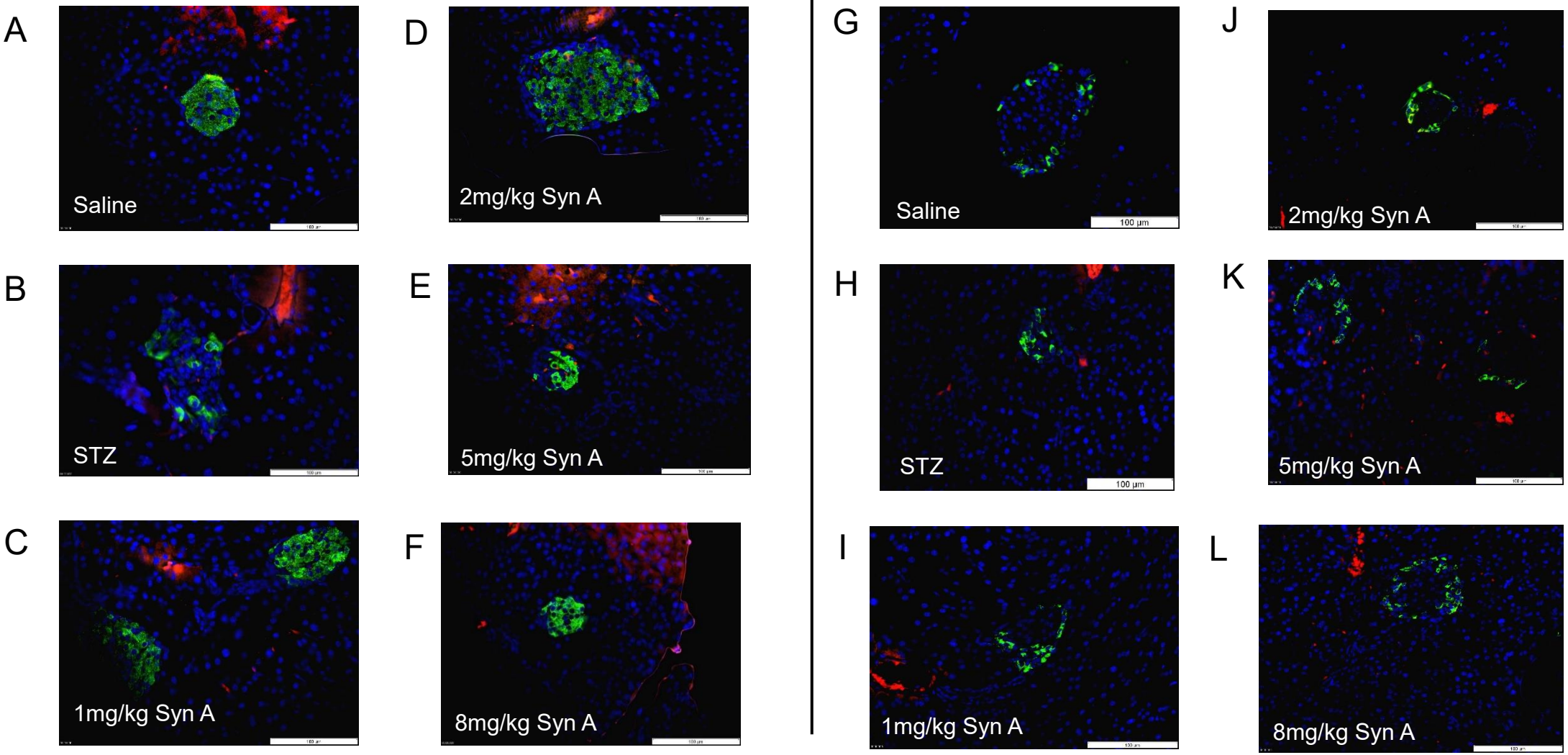

Islet proliferation was evaluated at the end of the 6-day study using 5-7 µm tissue sections. Saline Ki67 $^{+ve}$, insulin $^{+ve}$ (A), STZ Ki67^{+ve}, insulin^{+ve}(B), 1mg/kg Ki67^{+ve}, insulin^{+ve}(C), 2mg/kg Ki67^{+ve}, insulin^{+ve} (D), 5mg/kg Ki67^{+ve}, insulin^{+ve} (E), and 8mg/kg Ki67^{+ve}, insulin^{+ve} (F) islets. Saline Ki67 $^{+ve}$, glucagon $^{+ve}$ (G), STZ Ki67^{+ve}, glucagon^{+ve} (H), 1mg/kg Ki67^{+ve}, glucagon^{+ve} (I), 2mg/kg Ki67^{+ve}, glucagon^{+ve} (J), 5mg/kg Ki67^{+ve}, glucagon^{+ve} (K), and 8mg/kg Ki67^{+ve}, glucagon^{+ve} (L) islets. Insulin or glucagon is represented in green, Ki67 in red, and DAPI in blue. Images were taken at 40x.

Chapter 6

Effects of multiple and single dose Synthalin A on islet morphology and alpha to beta cell transdifferentiation in Streptozotocin diabetic Glu^{Cre} mice

6.1 Summary

The pancreatic islets of Langerhans are complex structures comprised of several cell types, such as alpha, beta, and delta cells. Pancreas formation and development of these different cell types is strictly ordered with hormone-producing cells considered fixed within their specific cell type. Newly identified plasticity of islet cells has been shown to occur through dedifferentiation and transdifferentiation of alpha and beta cells. Transdifferentiation, along with sex differences were evaluated. Transgenic Glu^{cre} mice that express YFP within their alpha cells was used to identify the effect of Syn A on alpha cell transdifferentiation. In addition to this, the impact of sex was examined on the basis that male and female react differently to streptozotocin (STZ), with oestrogen offering protection against this beta cell toxin. We aimed to examine islet morphology and transdifferentiation of the islet alpha cells after treatment with Synthalin (Syn A). Male and female mice were treated with 0.9% saline or 50mg/kg STZ for a minimum of five days. Once diabetic, a multiple dose 3mg/kg of Syn A or a single dose of 8mg/kg Syn A was given. When coupled with an alpha cell toxin, only the male mice displayed extreme levels of hyperglycaemia. Syn A did not counter the expansion in alpha cell mass that occurred in STZ mice of both sexes. Green fluorescent protein (GFP) staining revealed transdifferentiation and dedifferentiation. Proliferating alpha cell percentages were lower in the STZ + 8mg/kg Syn A mice groups in both sexes. Apoptosis of both alpha and beta cells was revealed in all three STZ treatment groups of the male mice, when looking at insulin and glucagon positive cells. These observations reveal the differences in the pancreatic sections and sex differences when evaluating the transdifferentiation of alpha to beta cells.

6.2 Introduction

6.2.1 Transdifferentiation

Transdifferentiation occurs under certain culture conditions and follows one of two pathways causing the islet to change (Graf and Enver, 2009). This could be because the alpha and beta cells are in close proximity and work with contrasting effects to one another (Ye *et al.* 2015). Pathway one, direct transdifferentiation, is when the islet cell expresses a second hormone before the original hormone is loss. Pathway two, indirect transdifferentiation occurs when the cell changes into a different cell within the islets before the transcription factors are reactivated (Tanday, 2019; van der Meulen and Huising, 2015; Wang *et al.* 2014; Talchai *et al.* 2012; Jonas *et al.* 1999). Mice treated with a beta cell toxin have been documented to trigger alpha to beta cell transdifferentiation (Chung *et al.* 2010; Thorel *et al.* 2010). In previous research using transgenic mice, results showed that the Gcg ^{creERT2}; Rosa26eYFP mice do not have any alteration within the function of their alpha and beta islets. These mice will hereafter be referred to as Glu^{Cre} mice. The alpha cells within these mice express the Cre recombinase, making the alpha cells detectable after they start losing their glucagon expression (Quoix *et al.* 2007). This provides an excellent model to examine alpha and beta cell toxins. The Gcg gene is expressed in alpha cells and encodes the proglucagon gene. As stated previously, this gene increases in fasting and hypoglycaemia (Baggio and Drucker, 2007). When looking at alpha cells changing to beta cells, when the yellow fluorescent protein (YFP) was co-expressed with glucagon or insulin, research indicated that these alpha cells had previously expressed insulin. These cells were still present a month after the beta cells were killed. Research showed that when the alpha and beta cells were both injured, the bihormonal cells were not present, even though these cells increase after the loss of only beta cells (Thorel *et al.* 2010). Dedifferentiation may also occur. In terms of the alpha cell, this is when the alpha cell markers exhibit a decrease in gene function (Moin and Butler, 2019). Alpha cell markers are examined in Chapter 8.

6.2.2 Sex differences

STZ has been shown to have a decreased sensitivity in female mice (Deeds *et al.* 2011; Le May *et al.* 2006). This has been said to be a result of the high oestrogen level in the female mice, which allows the beta cells to be protected from apoptosis caused by the STZ (Deeds *et al.* 2011; Le May *et al.* 2006). Deeds *et al.* (2011) states that the dose of STZ not only depends on the sex of the rodent, but also the strain of rodent. Due to the sex hormones in females, diabetes prevalence in females is lower (Le May *et al.* 2006). Very few studies have been conducted on female rodents in combination with Syn A. One study concluded that the female mice developed mammary tumours. These mice were given 0.05mg of Syn A and declared that the toxic dose for these Dilute brown female mice, was 0.2mg. Their survival rate was 37 days, even with mammary tumours. There was no mention of the effects on the pancreas or blood glucose (Boyland, 1938). Lundbaek and Nielsen (1958) treated female Wistar rats with a 20mg solution of Syn A after 14-16 hours of fasting. They found that the outer rim of alpha cells in the islet were degranulated. There were no males included in the study to account for, and the results of the rats treated with Syn A were focused on the organs instead of biochemical analysis (Lundbaek and Nielsen, 1958).

Seldom research has been conducted at pancreatic histological levels in rodents, in terms of effects or a combination of diabetes and Syn A. Past research on humans, as well as the previous mice studies, showed that blood glucose decreased when Syn A was administered. Given this knowledge, it is hypothesized that the blood glucose of these diabetic mice will decrease to normal levels after Syn A has been injected. The aim of these studies was to test this and determine if there is any transdifferentiation present among the islets. Since Syn A has previously shown to reduce the alpha cells within the pancreas, we aim to see if this is a result of alpha to beta cell transdifferentiation. We also aim to determine if there were any sex differences between the male and female mice injected with STZ and STZ + Syn A.

6.3 Materials and methods

All materials and methods for this study have been summarised in Sections 6.2.1 to 6.2.3. A detailed description of the materials and methods can be found in Chapter 2.

6.3.1 Glu^{Cre} Rosa mice treated with STZ and Syn A

Twenty-five two-month-old male and 16 two-month-old female Glu^{Cre} Rosa mice were used. The 25 male mice were divided into four groups; each containing 6 mice and one group containing 7 and the 16 female mice were separated into four groups; each containing four mice, each received their respected treatment by an i.p. injection. To induce gene expression each mouse was administered 7mg/kg of tamoxifen by i.p. injection. Both male and females had the same treatment groups. The control group was treated with 0.9% saline. The three remaining groups were treated with 50 mg/kg of STZ for 5 days after a four-hour fasting period followed by daily monitoring for the next 5 days. Female mice were injected with 120, 180 and 200mg/kg of STZ until they became diabetic. Injections for the two Syn A treated groups followed once the mice were declared diabetic. Two groups were then injected with either multiple (m) daily doses of 3mg/kg or a single (s) dose of 8mg/kg of Syn A. Throughout the study, daily measurements of body weight, food, and fluid intake were made. On alternating days, blood glucose was measured. At the end of the studies, non-fasting and fasting blood was collected, and the animals were sacrificed.

6.3.2 Immunohistochemistry

Head and tail sections of the pancreas that was preserved in paraformaldehyde (PFA) was used for immunohistochemistry to analyse morphological changes within the islets and paraffin embedded for histological analysis. Embedded tissue blocks were cut at 5-7µm thick. Slides were double stained using in-house guinea-pig glucagon 1:400, mouse insulin 1:400 as the primary antibodies, anti-rabbit Ki67 primary polyclonal antibodies 1:500 (ab15580) and goat GFP primary polyclonal antibodies (ab 5450). Secondary antibodies for immunohistochemistry included Alexa Fluor 488 or Alexa Fluor 594 goat anti mouse, IgG- 1:400, Alexa Fluor 488 or Alexa Fluor 594 goat anti guinea pig, IgG- 1:400, Alexa Fluor 594

goat anti rabbit, IgG- 1:400, and Alexa Fluor 488 donkey anti goat, IgG- 1:400. DAPI was then added to the tissues to stain for the nuclei of the islets. A 50:50 mixture of glycerol and PBS was used to mount coverslips to the slides. Images were analysed using the Olympus fluorescent microscope fitted with DAPI (350nm) FITC (488nm) and TRITC (594nm) filters and a DP70 camera adapter system using Cell^F program.

6.3.3 Statistics

All graphs and analysis were generated using GraphPad Prism 5 and Image J. A two-way RM ANOVA statistical test with Bonferroni Multiple Comparison Test or an unpaired t-test were carried out. Comparisons between two groups with $p<0.05$ were deemed statistically significant.

6.4 Results

6.4.1 Effects of single or multiple dose of Syn A on body weight, weight change, and blood glucose in male Glu^{Cre} Rosa mice with multiple low dose STZ diabetes.

Body weight for the three treatment groups declined throughout the study and was significantly lower than the mice treated with saline (Figure 6.1A). Starting from day 6 to the end of the study, the mice treated with STZ fluctuated in significance ($p<0.05$ or $0<0.01$) when compared to saline. Significance ($p<0.01$) varied starting from day 5 till the end of the study. When looking at the mice treated with STZ + 8mg/kg Syn A (s), significance ($p<0.001$) started on day 6 and varied till day 11. From day 12 to 15, significance ($p<0.001$) stayed stable with a slight decline throughout the study, when compared to saline treated mice. This group of mice had the lowest body weight among the treatment groups. When compared to saline, shows the drastic decrease the percentage of body weight change among the three treatment groups increase ($p<0.001$) (Figure 6.1B). Blood glucose continued to increase starting from day 7 in all three treatment groups (Figure 6.1C). The multiple dose of Syn A, STZ + 3mg/kg Syn A (m), and the STZ only group had similar significance ($p<0.001$) starting from day 9 till day 15,

when analysed against the saline treated mice. The mice treated with STZ + 8mg/kg Syn A (s) starting from day 7 ($p<0.05$) and increased till the end of the study ($p<0.001$) when compared to mice treated with saline.

6.4.2 Effects of single or multiple dose of Syn A on food and fluid intake in male Glu^{Cre} Rosa mice with multiple low dose STZ diabetes.

As seen in Figure 6.2A, the cumulative food intake was increased significantly in STZ + 8mg/kg Syn A (s) mice ($p<0.05$) on day 14 and continued to increase ($p<0.01$) on the final day. The multiple dose of Syn A, STZ + 3mg/kg Syn A (m), and STZ only treatment groups consumed similar amounts of food throughout the course of the study. As expected, the fluid intake increased throughout the study for all three treatment groups (Figure 6.2B). Significance ($p<0.001$) was only observed at the end of the study when STZ was compared to saline treated mice. The multiple dose of Syn A, STZ + 3mg/kg (m), showed an increase ($p<0.05$ or $p<0.001$) in cumulative fluid intake, as well as when compared to saline treated mice. However, the increase was not as dominant as the STZ only mice. The single dose of Syn A, STZ + 8mg/kg, significantly ($p<0.001$) increased to a similar result as the STZ only mice when compared to the saline mice. When examining the data with the STZ only mice, no significance was observed.

6.4.3 Effects of single or multiple dose of Syn A on nonfasting and fasting plasma insulin levels in male Glu^{Cre} Rosa mice with multiple low dose STZ diabetes.

Figure 6.3A shows that the mice treated with only STZ ($p<0.05$) had the lowest level of insulin in their nonfasting plasma, compared to saline control. When compared to the STZ only treated mice, the STZ + 3mg/kg Syn A (m) ($p<0.001$) showed a significant decrease in fasting plasma levels (Figure 6.3B).

6.4.4 Effects of single or multiple dose of Syn A on pancreatic insulin content from the head, tail, and the whole pancreas in male Glu^{Cre} Rosa mice with multiple low dose STZ diabetes.

Pancreatic insulin content from the head of the pancreas can be seen in Figure 6.4A. When compared to saline, a decrease in pancreatic insulin was observed in the STZ only mice ($p<0.001$). An increase in pancreatic insulin levels were exhibited in the STZ + 3mg/kg Syn A (m) and STZ+ 8mg/kg of Syn A (s) mice ($p<0.05$) when analysed against the STZ only treated mice. As seen in Figure 6.4B, the pancreatic insulin levels of the tail of the pancreas significantly increased ($p<0.001$) in the mice treated with STZ + 3mg/kg Syn A (m) when compared to saline and STZ only mice. There was a significant decrease in pancreatic insulin content in mice treated with STZ+ 8mg/kg of Syn A (s) ($p<0.001$) when compared to saline and STZ only mice. When looking at the pancreas as a whole, the mice that were treated with STZ+ 3mg/kg Syn A (m) ($p<0.05$) showed an increase in insulin content when compared to saline (Figure 6.4C).

6.4.5 Effects of single or multiple dose of Syn A on number of islets, islet area, and islet size distribution in the head of the pancreas in male Glu^{Cre} Rosa mice with multiple low dose STZ diabetes.

As seen in Figure 6.5A, the number of islets varies from each of the groups. The mice treated with STZ + 3mg/kg Syn A (m) ($p<0.05$) displayed an increase in islets within the head of the pancreas compared to the saline treated mice. Of the islets analysed in the tail of the pancreas, the STZ only islets ($p<0.01$) showed a decrease in islet area when compared to saline (Figure 6.5B). The STZ + 3mg/kg Syn A (m) and STZ + 8mg/kg Syn A (s) ($p<0.001$) treated mice, there was a significant increase when compared to STZ only mice. When looking at the percentage of small islets in comparison to saline, significant increase was observed in the STZ only treated mice ($p<0.05$) (Figure 6.5C). There was a slight decline in the percentage of medium islets in the STZ only treated mice ($p<0.05$) when compared to mice treated with saline. When comparing small islet percentages to STZ, both Syn A groups, STZ + 3mg/kg

Syn A (m) ($p<0.01$) and STZ + 8mg/kg Syn A (s) ($p<0.05$) showed a significant decline. However, when looking at the medium islets, the mice treated with STZ + 3mg/kg Syn A (m) ($p<0.05$) were significantly increased when compared with saline and STZ only treated mice. However, the mice treated with STZ + 8mg/kg Syn A (s) ($p<0.01$) was increased significantly when compared to the STZ only treated mice, when examining the percentage of medium islets.

6.4.6 Effects of single or multiple dose of Syn A on number of islets, islet area, and islet size distribution in the tail of the pancreas in male Glu^{Cre} Rosa mice with multiple low dose STZ diabetes.

When examining the mice treated with STZ + 8mg/kg Syn A (s), there was a significant decline in the number of islets within the pancreatic tail, when compared to saline ($p<0.001$) and STZ only treated mice ($p<0.01$) (Figure 6.6A). When looking at the mice treated with STZ + 3mg/kg Syn A (m), there was a significant decline when compared to saline ($p<0.01$) and STZ only treated mice ($p<0.001$) (Figure 6.6B). As shown in Figure 6.6C, there was an increase in the mice treated with STZ + 3mg/kg Syn A (m) ($p<0.001$) when compared to both the saline and STZ only treated mice. STZ + 8mg/kg Syn A (s) showed a slight increase when the percentage of small islets were compared to saline ($p<0.05$) and STZ only treated mice ($p<0.01$). Mice treated with STZ + 3mg/kg Syn A (m) showed a significant decrease in medium islets when compared to saline ($p<0.01$) and STZ only treated mice ($p<0.001$). STZ + 8mg/kg Syn A (s) mice showed a significant decline ($p<0.001$) when compared to STZ only treated mice.

6.4.7 Effects of single or multiple dose of Syn A on number of islets, islet area, and islet size distribution in the whole pancreas in male Glu^{Cre} Rosa mice with multiple low dose STZ diabetes.

As seen in Figure 6.7A, the mice treated with a single dose of STZ + 8mg/kg Syn A (s), exhibited a significant decrease when compared to saline ($p<0.01$) and when compared to STZ only treated mice ($p<0.05$). No significance was observed in regard to the islet area within

the whole pancreas (Figure 6.7B). STZ + 3mg/kg Syn A (m) mice showed a decrease in medium sized islets ($p<0.05$) when compared to saline treated mice (Figure 6.7C).

6.4.8 Effects of single or multiple dose of Syn A on alpha cell area and percentage and beta cell area and percentage in the head of the pancreas in male Glu^{Cre} Rosa mice with multiple low dose STZ diabetes.

As seen in Figure 6.8A, the mice that were treated with STZ + 3mg/kg Syn A (m) and STZ +8mg/kg Syn A (s) showed a significant increase ($p<0.001$) in alpha cell area when compared to saline and STZ only treated mice. The alpha cell percentage was increased in all three treatment groups ($p<0.01$; $p<0.001$) when compared to saline treated mice (Figure 6.8B). STZ + 3mg/kg Syn A (m) mice and 8mg/kg Syn A (s) showed a significant increase ($p<0.001$) in the percentage of the alpha cells in the head of the pancreas when compared to STZ only treated mice. As expected, the beta cell area in STZ only treated mice was significantly decreased ($p<0.001$) when compared to the saline treated mice (Figure 6.8C). STZ + 3mg/kg Syn A (m) ($p<0.01$) treated mice showed a significant increase when compared to STZ only treated mice. The STZ + 8mg/kg Syn A (s) mice ($p<0.05$) displayed a decrease when compared to the saline treated mice. All three treatment groups showed a decrease ($p<0.01$; $p<0.001$) when compared to saline (Figure 6.8D). Both the STZ+ 3mg/kg Syn A (m) ($p<0.001$) and the mice treated with STZ + 8mg/kg Syn A (s) ($p<0.001$) showed a decrease in beta cell percentages when compared to saline and STZ only treated mice.

6.4.9 Effects of single or multiple dose of Syn A on alpha cell area and percentage and beta cell area and percentage in the tail of the pancreas in male Glu^{cre} Rosa mice with multiple low dose STZ diabetes.

Figure 6.9A shows the variation in alpha cell area within the tail of the pancreas. Mice that were treated only with STZ and STZ + 8mg/kg Syn A (s) ($p<0.001$) show a significant increase in alpha cell area when compared to saline treated mice. The STZ+ 3mg/kg Syn A (m) treatment group ($p<0.001$) showed a decrease in alpha cell area only when compared to the

STZ only treated mice. All three treatment groups displayed an increase ($p<0.001$) in alpha cell percentage when compared to saline (Figure 6.9B). However, the mice treated with STZ + 8mg/kg Syn A (s) showed a significant increase in the alpha cell percentage, when compared to STZ only treated mice ($p<0.01$). When looking at the mice treated with STZ + 3mg/kg Syn A (m) and STZ+ 8mg/kg Syn A (s), beta cell area was significantly decreased ($p<0.001$) when compared to saline as well as when compared to STZ only treated mice ($p<0.05$; $p<0.01$) (Figure 6.9C). All three treatment groups displayed a decrease in beta cell percentage when compared to saline ($p<0.001$) (Figure 6.9D). Mice treated with STZ + 8mg/kg Syn A (s) showed a decrease when compared to STZ only treated mice ($p<0.01$).

6.4.10 Effects of single or multiple dose of Syn A on alpha cell area and percentage and beta cell area and percentage in the whole pancreas in male Glu^{Cre} Rosa mice with multiple low dose STZ diabetes.

Figure 6.10A shows that the STZ only treatment group ($p<0.05$) showed an increase in the area of alpha cells within the whole pancreas when analysed against the saline treatment mice. Both Syn A treatment groups displayed an increase in alpha cell area ($p<0.001$) when compared to saline treated mice. However, the STZ + 8mg/kg Syn A (s) also showed a significant increase to STZ only treated mice ($p<0.01$). All three treatment groups showed an increase in alpha cell percentage ($p<0.001$) when compared to saline treated mice (Figure 6.10B). When compared to STZ only treated mice, the STZ + 3mg/kg Syn A (m) ($p<0.01$) and STZ + 8mg/kg Syn A (s) ($p<0.001$) mice showed an increase in alpha cell percentage. As shown in Figure 6.10C, all three groups; STZ only treated mice ($p<0.01$), STZ + 3mg/kg Syn A (m) treated mice ($p<0.05$), STZ + 8mg/kg Syn A (s) ($p<0.001$) showed a significant decrease in beta cell area when compared to saline treated mice. All three groups showed a decrease ($p<0.001$) in beta cell percentage when compared to mice treated with saline (Figure 6.10D). Mice treated with STZ + 3mg/kg Syn A (m) ($p<0.01$) and STZ + 8mg/kg Syn A (s) ($p<0.001$) treated mice showed the largest decline in beta cell percentages when compared to STZ only

treated mice. Photo representation can be seen in Figure 6.11A-D. Insulin is represented in green, glucagon is represented in red, and DAPI in blue.

6.4.11 Effects of single or multiple dose of Syn A on GFP positive, insulin positive cells in the head, tail, and whole pancreas in male Glu^{Cre} Rosa mice with multiple low dose STZ diabetes.

Figure 6.12A displays an increase in GFP positive, insulin positive cells in the head of the pancreas in the all three treatment groups ($p<0.001$) when compared to saline. Positive cells within the head of the pancreas in mice treated with STZ + 3mg/kg Syn A (m) ($p<0.05$) and STZ + 8mg/kg Syn A (s) ($p<0.001$) showed a decrease when compared to STZ only treated mice. When compared to saline treated mice, the positive cells were increased in mice treated only with STZ ($p<0.01$), STZ + 3mg/kg Syn A (m) ($p<0.001$), and STZ + 8mg/kg Syn A (s) ($p<0.001$) in the tail portion of the pancreas (Figure 6.12B). As seen in Figure 6.12C, all three treatment groups displayed an increase ($p<0.001$) in positive cells within the whole pancreas when compared to saline mice. Images are represented in Figure 6.13 A-D. Insulin is represented in red, GFP is represented in green, and DAPI is represented in Blue.

6.4.12 Effects of single or multiple dose of Syn A on GFP positive, insulin negative cells in the head, tail, and whole pancreas in male Glu^{Cre} Rosa mice with multiple low dose STZ diabetes.

GFP positive, insulin negative cells in the head of the pancreas were decreased in all three groups ($p<0.001$) when compared to saline treated mice (Figure 6.14A). GFP positive, insulin negative cells was increased in the mice treated with STZ + 3mg/kg Syn A (m) ($p<0.05$) and STZ + 8mg/kg Syn A (s) ($p<0.001$) treated mice exhibited an increase when compared to STZ only treated mice. All three groups: STZ only ($p<0.01$), STZ + 3mg/kg Syn A (m) ($p<0.001$), and STZ + 8mg/kg Syn A (s) ($p<0.001$) were decreased when compared to the saline treated mice (Figure 6.14B). As seen in Figure 6.14C, all three groups exhibited a decrease ($p<0.001$) in GFP positive, insulin negative cells within the whole pancreas when compared to saline

treated mice. Images are represented in Figure 6.15A-D. Insulin is represented in red, GFP is represented in green, and DAPI is represented in Blue.

6.4.13 Effects of single or multiple dose of Syn A on GFP positive, glucagon positive cells in the head, tail, and whole pancreas in male Glu^{Cre} Rosa mice with multiple low dose STZ diabetes.

As seen in Figure 6.16A, the STZ + 8mg/kg Syn A (s) mice displayed a decrease in the percentage of positive cells when compared to saline ($p<0.05$) and STZ only treated mice ($p<0.01$). Compared to saline treated mice, there was an increase in positive cells in the tail portion of the pancreas in the mice treated with STZ + 8mg/kg Syn A (s) ($p<0.05$) (Figure 6.16B). As seen in Figure 6.16C, no significance was observed within the whole pancreas. Images are represented in Figure 6.17A-D. Glucagon is represented in red, GFP is represented in green, and DAPI is represented in Blue.

6.4.14 Effects of single or multiple dose of Syn A on GFP positive, glucagon negative cells in the head, tail, and whole pancreas in male Glu^{Cre} Rosa mice with multiple low dose STZ diabetes.

As seen in Figure 6.18A, the mice treated with STZ + 8mg/kg Syn A (s) exhibited an increase in GFP positive, glucagon negative cells in the head of the pancreas when compared to saline ($p<0.05$) and when compared to STZ only treated mice ($p<0.01$). GFP positive, glucagon negative cells were decreased in the pancreatic tail of the mice treated with STZ + 8mg/kg Syn A (s) ($p<0.05$) when compared to saline (Figure 6.18B). There was no significance observed in regard to the whole pancreas (Figure 6.18C). Images are represented in Figure 6.19 A-D. Glucagon is represented in red, GFP is represented in green, and DAPI is represented in Blue.

6.4.15 Effects of single or multiple dose of Syn A on Ki67 positive, insulin positive cells in the head, tail, and whole pancreas in male Glu^{Cre} Rosa mice with multiple low dose STZ diabetes.

No significance was observed in regard to positive cells in the head of the pancreas (Figure 6.20A). A decrease ($p<0.05$) was exhibited in beta cell proliferation in the tail of the pancreas of mice treated only with STZ when compared to saline (Figure 6.20B). No significance was observed in regard to beta cell proliferation within the whole pancreas (Figure 6.20C). Images are represented in Figure 6.21 A-D. Insulin is represented in green, Ki67 is represented in red, and DAPI is represented in Blue.

6.4.16 Effects of single or multiple dose of Syn A on Ki67 positive, glucagon positive cells in the head, tail, and whole pancreas in male Glu^{Cre} Rosa mice with multiple low dose STZ diabetes.

Figure 6.22 A-C displayed no significance in regard to alpha cell proliferation within the head, tail, or whole pancreas. Images are represented in Figure 6.23 A-D. Glucagon is represented in green, Ki67 is represented in red, and DAPI is represented in Blue.

6.4.17 Effects of single or multiple dose of Syn A on Tunel positive, insulin positive cells in the head, tail, and whole pancreas in male Glu^{Cre} Rosa mice with multiple low dose STZ diabetes.

As seen in Figure 6.24A, the percentage of beta cells in the head of the pancreas that presented with Tunel positive, insulin positive cells was significantly in mice treated with STZ + 3mg/kg Syn A (m) ($p<0.05$) when compared to saline and ($p<0.01$) when compared to STZ only treated mice. Positive beta cell apoptosis was increased in the pancreatic tail in mice treated with STZ + 8mg/kg Syn A (s) when compared to saline ($p<0.01$) and ($p<0.001$) when compared to STZ only treated mice (Figure 6.24B). Figure 6.24C, shows the percentage of positive apoptotic cells expressed in the whole pancreas was increased in the mice treated with STZ + 8mg/kg Syn A (s) when compared to saline and STZ only treated mice ($p<0.01$).

Images are represented in Figure 6.25 A-D. Insulin is represented in red and Tunel is represented in green.

6.4.18 Effects of single or multiple dose of Syn A on Tunel positive, glucagon positive cells in the head, tail, and whole pancreas in male Glu^{Cre} Rosa mice with multiple low dose STZ diabetes.

The percentage of positive apoptotic alpha cells in the head of the pancreas significantly decreased in the mice treated only with STZ ($p<0.001$) when compared to saline treated mice (Figure 6.26A). Mice treated with STZ + 3mg/kg Syn A (m) displayed an increase in positive cells when compared to the mice treated with saline ($p<0.01$) and only STZ ($p<0.001$). The STZ + 8mg/kg Syn A (s) treated mice ($p<0.001$) exhibited an increase in apoptotic alpha cells when compared to STZ only treated mice. Figure 6.26B, shows that when compared to saline treated mice, mice treated with STZ only ($p<0.001$) displayed a decrease in the positive apoptotic percentages. There was a significant increase in the STZ + 3mg/kg Syn A (m) ($p<0.001$) and STZ + 8mg/kg Syn A (s) ($p<0.01$) when compared to the STZ only treated mice. STZ only treated mice ($p<0.001$) exhibited a decrease in positive cells when compared to saline treated mice in the whole pancreas (Figure 6.26C). An increase in positive apoptotic alpha cells was observed in the STZ + 3mg/kg Syn A (m) treated mice ($p<0.01$) when compared to saline and ($p<0.001$) when compared STZ only treated mice. Mice treated with STZ + 8mg/kg Syn A (s) ($p<0.05$) showed a decrease in positive cells when compared to saline treated mice and an increase ($p<0.001$) when compared to STZ only treated mice. Images are represented in Figure 6.27 A-D. Insulin is represented in red and Tunel is represented in green.

6.4.19 Effects of single or multiple dose of Syn A on body weight, weight change, and blood glucose in female Glu^{Cre} Rosa mice with multiple low dose STZ diabetes.

As seen in Figure 6.28A, mice treated with STZ only showed a significant decrease when compared to saline, starting at day 4 ($p<0.05$; $p<0.001$) and an increase in body weight after day 7, and significance shown on day 11, when they weighed the most in the study. Day 18 showed a significant decrease ($p<0.01$) on day 18 when compared to saline treated mice, and then increased and was stable throughout the rest of the study. Mice treated with STZ + 3mg/kg Syn A (m) showed a significant decline at the start of the study and showed significance ($p<0.01$; $p<0.001$) when compared to saline treated mice. This was the period of the study where they weighed the least amount. At day 6 and day 8, they were also significant ($p<0.05$; $p<0.01$) when compared to STZ only treated mice. Body weight declined between day 11 and 14 and weight continued to vary till day 20 where it continued on a slight increase. During this time period, mice treated with STZ + 3mg/kg Syn A (m) exhibited a decrease in weight ($p<0.01$) when compared to saline. Mice treated with STZ + 8mg/kg Syn A (s) displayed a decline in body weight ($p<0.01$; $p<0.001$) when compared to the stable weight of the saline treated mice. After their increase in body weight in the middle of the study, significance was observed around day 14 ($p<0.001$) and weight continued to fluctuate till day 20, when it became stable for the course of the study.

Figure 6.28B, shows the mice treated with STZ + 8mg/kg Syn A (s) showed a decrease in the percentage of body weight when compared to saline ($p<0.001$) and a decrease when compared to STZ treated only mice ($p<0.05$). When compared to saline treated mice, an increase in blood glucose can be seen for the STZ+ 8mg/kg Syn A (s) treated mice ($p<0.01$) on day 17 and increased ($p<0.05$) on day 19 and continued to increase ($p<0.001$) for the remainder of the study (Figure 6.28C).

6.4.20 Effects of single or multiple dose of Syn A on food and fluid intake in female Glu^{Cre} Rosa mice with multiple low dose STZ diabetes.

As seen in Figure 6.29A, day 5 through 7 shows that both of the Syn A treatment groups display a decrease in food intake ($p<0.05$; $p<0.01$) when compared to the saline treatment mice. The single dose of Syn A, STZ + 8mg/kg Syn A (s), consumed the least amount of food throughout the course of the study and significance ($p<0.05$) was observed on days 14 -17 and 19-20 when compared to saline treated mice. Significant increase was observed starting from day 7 ($p<0.05$) and day 8 ($p<0.01$) and continued to increase till the end of the study ($p<0.001$) (Figure 6.29B).

6.4.21 Effects of single or multiple dose of Syn A on nonfasting and fasting plasma insulin levels in female Glu^{Cre} Rosa mice with multiple low dose STZ diabetes.

No significance was observed in regard to the nonfasting plasma insulin levels (Figure 6.30A). Figure 6.30B shows the fasting plasma insulin levels are increased in STZ only treated mice when compared to saline treated mice (Figure 6.30B).

6.4.22 Effects of single or multiple dose of Syn A on pancreatic insulin content from the head, tail, and the whole pancreas in female Glu^{Cre} Rosa mice with multiple low dose STZ diabetes.

No significance was observed pancreatic insulin content in the head of the pancreas (Figure 6.31A). Mice treated with STZ + 3mg/kg Syn A (m) ($p<0.05$) and STZ + 8mg/kg Syn A (s) ($p<0.01$) showed a decrease of insulin content within the pancreatic tail when compared to STZ only mice (Figure 6.31B). Pancreatic insulin within the whole pancreas was increased in the STZ only mice ($p<0.01$) when compared to saline mice. (Figure 6.31C). A pancreatic insulin decrease was exhibited in mice treated with STZ + 3mg/kg Syn A (m) ($p<0.01$) and STZ + 8mg/kg Syn A (s) ($p<0.001$) when compared to STZ only treated mice. Mice treated

with STZ + 8mg/kg Syn A (s) also displayed a decrease ($p<0.05$) in the whole pancreas insulin when compared against the saline mice.

6.4.23 Effects of single or multiple dose of Syn A on number of islets, islet area, and islet size distribution in the head of the pancreas in female Glu^{Cre} Rosa mice with multiple low dose STZ diabetes.

As seen in Figure 6.32A, mice treated with STZ + 3mg/kg Syn A (m) ($p<0.05$) and STZ + 8mg/kg Syn A (s) ($p<0.01$) displayed a decrease in the number of islets within the head of the pancreas when compared to STZ only treated mice. The number of islets was decreased in the STZ + 8mg/kg Syn A (s) mice ($p<0.05$) when compared to saline. When compared to saline treated mice, there was an increase in islet area in the head of the pancreas in mice treated with STZ + 3mg/kg Syn A (m) ($p<0.05$) and STZ + 8mg/kg Syn A (s) ($p<0.001$) (Figure 6.32B). When compared to STZ treated mice, the mice treated with STZ + 8mg/kg Syn A (s) ($p<0.001$) showed an increase in the islet area. Mice treated with STZ + 8mg/kg Syn A (s) exhibited a decrease in the percentage of small islets when compared to saline ($p<0.001$) and ($p<0.01$) when compared to STZ treated mice (Figure 6.32C). The percentages of medium islets increased in the STZ + 3mg/kg Syn A (m) ($p<0.05$) and STZ + 8mg/kg Syn A (s) mice ($p<0.01$) in comparison to saline treated mice. Mice treated with STZ + 8mg/kg Syn A (s), displayed an increase ($p<0.05$) in the percentage of medium islets when compared to STZ only treated mice.

6.4.24 Effects of single or multiple dose of Syn A on number of islets, islet area, and islet size distribution in the tail of the pancreas in female Glu^{Cre} Rosa mice with multiple low dose STZ diabetes.

Figure 6.33A shows that the number of islets in the tail of the pancreas in the mice treated with STZ only ($p<0.01$) was increased when compared to saline treated mice. STZ + 8mg/kg Syn A (s) mice ($p<0.05$), exhibited a decrease in the number of islets when compared to STZ only mice. Islet area within the tail of the pancreas significantly decreases in the mice treated

only with STZ ($p<0.01$), when compared to the saline treated mice (Figure 6.33B). STZ + 3mg/kg Syn A (m) ($p<0.01$) showed a significant increase in islet area when compared to the mice treated only with STZ. Figure 6.33C, shows the size distribution among the female mice groups. There was a significant increase in small islets when saline and STZ only treated mice ($p<0.001$) were compared. Small islets in the mice treated with STZ + 3mg/kg Syn A (m) and STZ + 8mg/kg Syn A (s) ($p<0.05$) showed a decrease in the percentage of small islets when compared to STZ only treated mice. Medium islet percentages were significantly decreased in the STZ only treated mice ($p<0.01$) and STZ + 8mg/kg Syn A (s) ($p<0.05$) when compared to saline treated mice. Mice treated with STZ + 3mg/kg Syn A (m) ($p<0.05$) showed a significant increase in the percentage of medium islets when compared to the mice treated only with STZ.

6.4.25 Effects of single or multiple dose of Syn A on number of islets, islet area, and islet size distribution in the whole pancreas in female Glu^{Cre} Rosa mice with multiple low dose STZ diabetes.

Figure 6.34A shows a decrease in the number of islets in the mice treated with STZ + 8mg/kg Syn A (s) ($p<0.01$) when compared to saline and STZ only treated mice ($p<0.001$). STZ+ 8mg/kg Syn A (s) ($p<0.05$) displayed an increase in islet area when compared to saline and an increase ($p<0.001$) when compared to STZ only treated mice (Figure 6.34B). As seen in Figure 6.34C, when compared to saline treated mice, there was an increase in the percentage of small islets in the mice treated with STZ only mice ($p<0.05$). Mice treated with STZ + 3mg/kg Syn A (m) and STZ + 8mg/kg Syn A (s) showed a decrease ($p<0.05$) in small islet percentages when compared to STZ only treated mice. Both Syn A treatment groups: STZ + 3mg/kg Syn A (m) and STZ + 8mg/kg Syn A (s) treated mice showed a significant increase ($p<0.05$) when compared to STZ only medium islet percentages. A small decrease in the percentage of large islets was seen in STZ + 3mg/kg Syn A (m) treated mice ($p<0.05$) when compared to saline treated mice.

6.4.26 Effects of single or multiple dose of Syn A on alpha cell area and percentage and beta cell area and percentage in the head of the pancreas in female Glu^{Cre} Rosa mice with multiple low dose STZ diabetes.

When examined against saline, all three treatment groups showed an increase ($p<0.001$) in alpha cell area within the head of the pancreas (Figure 6.35A). STZ + 3mg/kg Syn A (m) treated mice also showed a significant increase in alpha cell area, when compared STZ treated mice ($p<0.01$). As seen in Figure 6.35B, when compared to saline, all three treatment groups showed a significant increase ($p<0.001$) in alpha cell percentage. Compared to STZ only treated mice, the alpha cell percentage significantly increased in mice treated with STZ + 3mg/kg Syn A (m) ($p<0.001$) and significantly decreased in STZ + 8mg/kg Syn A (s) mice ($p<0.001$).

Mice treated with STZ + 8mg/kg Syn A (s) show a significant increase ($p<0.001$) in the area of the beta cells when compared to saline and STZ only treated mice (Figure 6.35C). All three treatment groups displayed a decrease ($p<0.001$) in the percentage of beta cells when compared against the saline treated mice (Figure 6.35D). STZ + 3mg/kg Syn A (m) mice ($p<0.001$) exhibited a decrease in beta cell percentage and STZ + 8mg/kg Syn A (s) mice exhibited an increase when compared to STZ only treated mice.

6.4.27 Effects of single or multiple dose of Syn A on alpha cell area and percentage and beta cell area and percentage in the tail of the pancreas in female Glu^{Cre} Rosa mice with multiple low dose STZ diabetes.

Figure 6.36A, shows the alpha cell area in the islets from the tail portion of the pancreas were increased in the mice treated with STZ + 3mg/kg Syn A (m) ($p<0.01$) and STZ + 8mg/kg Syn A (s) ($p<0.05$) when compared to the saline treated mice. All three treatment groups showed a significant increase ($p<0.001$) when compared to saline treated mice (Figure 6.36B). Mice treated with STZ + 3mg/kg Syn A (m) and mice treated with STZ + 8mg/kg Syn A (s) showed a decrease ($p<0.001$) when compared to STZ only treated mice.

Figure 6.36C, shows a decrease in the beta cell area in the mice treated with only STZ ($p<0.001$) when compared to saline. Mice treated with STZ + 3mg/kg Syn A (m) ($p<0.01$) and STZ + 8mg/kg Syn A (s) ($p<0.001$) showed a significant decrease in beta cell area when compared to saline treated mice. When compared to STZ only treated mice, STZ + 3mg/kg Syn A (m) ($p<0.001$) and STZ + 8mg/kg Syn A (s) ($p<0.01$) treated mice displayed a significant increase in beta cell area. Compared to saline treated mice, all three treatment groups exhibited a decrease ($p<0.001$) in the percentage of beta cells in the tail of the pancreas (Figure 6.36D). Mice treated with STZ + 3mg/kg Syn A (m) and STZ + 8mg/kg Syn A (s) showed a significant decrease ($p<0.001$) when compared to STZ only treated mice.

6.4.28 Effects of single or multiple dose of Syn A on alpha cell area and percentage and beta cell area and percentage in the whole pancreas in female Glu^{Cre} Rosa mice with multiple low dose STZ diabetes.

As seen in Figure 6.37A, when compared to saline treated mice, all three treatment groups showed a significant increase ($p<0.001$) in the alpha cell area within the whole pancreas. STZ + 3mg/kg Syn A (m) ($p<0.001$) exhibited an increase in alpha cell area when compared to the STZ only treated mice. Compared to saline treated mice, all three treatment groups showed a substantial increase ($p<0.001$) in alpha cell percentage in the whole pancreas (Figure 6.37B). Mice treated with STZ + 8mg/kg Syn A (s) ($p<0.001$) showed a decrease when compared to STZ only treated mice. When analysed against the saline treated mice, STZ only ($p<0.01$) and mice treated with STZ + 3mg/kg Syn A (m) ($p<0.001$) showed a significant decrease in the beta cell area (Figure 6.37C). STZ + 8mg/kg Syn A (s) ($p<0.001$) treated mice displayed an increase in beta cell area when compared to STZ only treated mice. When compared to saline treated mice, all three treatment groups showed a significant decrease ($p<0.001$) in the percentage of beta cells (Figure 6.37D). STZ + 8mg/kg Syn A (s) treated mice showed a significant increase when compared to STZ only treated mice ($p<0.001$). Images are represented in Figure 6.38 A-D. Insulin is represented in green, glucagon is represented in red, and DAPI in blue.

6.4.29 Effects of single or multiple dose of Syn A on GFP positive, insulin positive cells in the head, tail, and whole pancreas in female Glu^{Cre} Rosa mice with multiple low dose STZ diabetes.

STZ only treated mice ($p<0.01$) displayed an increase in positive cells when compared to saline (Figure 6.39A). Mice treated with STZ + 3mg/kg Syn A (m) showed an increase of positive GFP and insulin cells in the head of the pancreas when compared to saline ($p<0.001$) and STZ only mice ($p<0.01$). As seen in Figure 6.39B, STZ + 8mg/kg Syn A (s) treated mice exhibited a decrease in the positive cells, within the pancreatic tail, compared to saline ($p<0.01$) and STZ only ($p<0.001$) treated mice. Mice treated with STZ only ($p<0.05$) and STZ + 3mg/kg Syn A (m) ($p<0.001$) displayed an increase of positive cells within the whole pancreas when compared to saline (Figure 6.39C). A significant decrease was observed in STZ + 8mg/kg Syn A (s) ($p<0.01$) treated mice when compared with STZ only treated mice. Image representation is shown in Figure 6.40A-D. Insulin is represented in red, GFP is represented in green, and DAPI is represented in blue.

6.4.30 Effects of single or multiple dose of Syn A on GFP positive, insulin negative cells in the head, tail, and whole pancreas in female Glu^{Cre} Rosa mice with multiple low dose STZ diabetes.

STZ only treated mice ($p<0.01$) and STZ + 3mg/kg Syn A (m) ($p<0.001$) displayed a significant decrease in insulin negative cells when compared to saline (Figure 6.41A). STZ + 3mg/kg Syn A (m) ($p<0.05$) displayed a decrease in GFP positive, insulin negative cells in the pancreatic head when compared to STZ only treated mice. In Figure 6.41B, an increase in the percentage of GFP positive, insulin negative cells in the tail of the pancreases of STZ + 8mg/kg Syn A (s) treated mice were increased ($p<0.01$) when compared to saline and ($p<0.001$) when compared to STZ only mice. Mice treated with STZ only ($p<0.05$) and STZ + 3mg/kg Syn A (m) displayed a decrease when compared to saline and ($p<0.001$) (Figure 6.41C). An increase in cells were observed in STZ + 8mg/kg Syn A (s) mice ($p<0.01$) when

compared to saline treated mice. Image representation is shown in Figure 6.42A-D. Insulin is represented in red, GFP is represented in green, and DAPI is represented in blue.

6.4.31 Effects of single or multiple dose of Syn A on GFP positive, glucagon positive cells in the head, tail, and whole pancreas in female Glu^{Cre} Rosa mice with multiple low dose STZ diabetes.

When compared to the mice treated with saline, STZ only ($p<0.05$) and STZ + 3mg/kg Syn A (m) treated mice ($p<0.001$) showed an increase in the percentage of GFP positive, glucagon positive cells in the head of the pancreas (Figure 6.43A). STZ + 8mg/kg Syn A (s) treated mice ($p<0.05$) showed a decrease in positive cells when compared to STZ only treated mice. As shown in Figure 6.43B, STZ only and STZ + 8mg/kg Syn A (s) treated mice displayed a decrease ($p<0.001$) in positive cells when compared to saline treated mice. Mice treated with STZ + 3mg/kg Syn A (m) ($p<0.001$) showed a significant increase in positive cells when compared to STZ only treated mice. A decrease was observed in positive cells in mice treated with STZ + 8mg/kg Syn A (s) ($p<0.05$) when compared to STZ only treated mice. STZ + 3mg/kg Syn A (m) treated mice showed a significant increase in percentage of positive cells when compared to saline ($p<0.01$) and STZ only treated mice ($p<0.001$) (Figure 6.43C). A decrease was observed in the STZ + 8mg/kg Syn A (s) mice ($p<0.001$) when compared to saline ($p<0.01$) and ($p<0.01$) when compared to STZ only treated mice. Image representation is shown in Figure 6.44 A-D. Glucagon is represented in red, GFP is represented in green, and DAPI is represented in blue.

6.4.32 Effects of single or multiple dose of Syn A on GFP positive, glucagon negative cells in the head, tail, and whole pancreas in female Glu^{Cre} Rosa mice with multiple low dose STZ diabetes.

There was a significant decrease in GFP positive, glucagon negative cells in mice treated with STZ only ($p<0.05$) and STZ + 3mg/kg Syn A (m) ($p<0.001$), when compared to saline (Figure 6.45A). Mice treated with STZ + 8mg/kg Syn A (s) ($p<0.05$) showed a significant increase in

GFP positive, glucagon negative cells when compared to STZ only mice. When compared to saline treated mice, STZ only and STZ + 8mg/kg Syn A (s) treated mice showed an increase ($p<0.001$) in the percentage of GFP positive, glucagon negative cells tail of the pancreas (Figure 6.45B). Mice treated with STZ + 3mg/kg Syn A (m) ($p<0.001$) showed a significant decrease in cells when compared to STZ only treated mice. GFP positive, glucagon negative cells in mice treated with STZ + 8mg/kg Syn A (s) ($p<0.05$) displayed an increase when compared with STZ only treated mice. STZ + 3mg/kg Syn A (m) treated mice exhibited a decrease in GFP positive, glucagon negative cells in the whole pancreases when compared with saline ($p<0.01$) and STZ only treated mice ($p<0.001$) (Figure 6.45C). Mice treated with STZ + 8mg/kg Syn A (s) exhibited an increase in these cells when compared to saline treated mice ($p<0.001$) and STZ only mice ($p<0.01$). Image representation is shown in Figure 6.46A-D. Glucagon is represented in red, GFP is represented in green, and DAPI is represented in blue. Photos were taken at 40x objective lens and a total of 100+ islets were analysed per treatment group.

6.4.33 Effects of single or multiple dose of Syn A on Ki67 positive, insulin positive cells in the head, tail, and whole pancreas in female Glu^{Cre} Rosa mice with multiple low dose STZ diabetes.

No significance was exhibited regarding beta cell proliferation in the head, tail, or whole pancreas (Figure 6.47A-C). Image representation is shown in Figure 6.48A-D. Ki67 is represented in red, insulin is represented in green, and DAPI is represented in blue. Photos were taken at 40x objective lens and a total of 100+ islets were analysed per treatment group.

6.4.34 Effects of single or multiple dose of Syn A on Ki67 positive, glucagon positive cells in the head, tail, and whole pancreas in female Glu^{Cre} Rosa mice with multiple low dose STZ diabetes.

No significance was exhibited regarding alpha cell proliferation in the head, tail, or whole pancreas (Figure 6.47A-C). Image representation is shown in Figure 6.50A-D. Ki67 is

represented in red, glucagon is represented in green, and DAPI is represented in blue. Photos were taken at 40x objective lens and a total of 100+ islets were analysed per treatment group.

6.5 Discussion

The aim of this study was to examine the effects of Syn A in mice with multiple dose STZ, as well as the use of the enhanced yellow fluorescent protein (EYFP) as a marker for easy alpha cell detection. All three treatment groups exhibited signs of diabetes, such as an increase in fluid intake and frequent urination. The adult male mice became diabetic with their blood glucose continuing to increase after the Syn A treatment started. Male and female mice are different in their susceptibility to STZ, allowing only the male mice to go into a severe hyperglycaemic phase (McEvoy *et al.* 1984; Leiter, 1982; Paik *et al.* 1982; Maclaren *et al.* 1980; Rossini *et al.* 1978). The female mice in our study were resistant to the multiple low dose STZ. After the multiple low doses, some female mice showed an increase in blood glucose, but then the levels returned to normal after the observation period. The female mice were resistant to becoming diabetic when given 50mg/kg for two of the three groups. Mice treated with STZ + 8mg/kg Syn A (s) became diabetic after the fifth day dose of STZ. Syn A treatment followed. The STZ only and STZ + 3 mg/kg Syn A (m) only reached a diabetic state once 200mg/kg STZ was given. These two groups were treated with 50mg/kg, 150mg/kg, 180mg/kg, and 200mg/kg, which could explain for the fluctuation in blood glucose levels in these female treatment groups. Some mice became diabetic after the higher doses; however, the blood glucose dropped the following days causing the blood glucose levels to return to normal and a higher dose of STZ to be needed.

In male mice treated with STZ only, oestrogen only, and STZ + oestrogen, the plasma glucose levels were lower in these males treated with STZ + oestrogen by the end of the study compared to the other treatment groups (Paik *et al.* 1982). We confirmed that the male's pancreatic insulin content was decreased (Dusaulcy *et al.* 2016; Paik *et al.* 1982). When looking at females treated with STZ only, testosterone only, and STZ + testosterone, the plasma glucose levels increased in each of the groups. The male mice had no problems

becoming diabetic. The change in blood glucose levels in mice receiving STZ, STZ + opposite sex hormone, or the opposite sex hormone that they normally produce shows that sex hormones can be the issue of susceptibility to STZ (Paik *et al.* 1982).

Deeds *et al.* (2011) states that the response to STZ in the different sexes of mice and rats can be drastic causing severe hyperglycaemia in males, and little effect, if any, in female rodents. Nonfasting and fasting insulin levels could not test significance due to not having more than one number in the saline nonfasting and one number in the STZ + 8mg/kg Syn A (s) fasting female mice. This is because there was not enough blood taken from these groups during those phases.

Similar amounts of islets per mm^2 within the head of the pancreas were seen in both the STZ only treated male and female mice. This is backed up by research stating that the number of islets decreases after the last dose of STZ (Bonnevie-Nielsen *et al.* 1981). However, when looking at the islet area, male mice with STZ showed a significant decrease compared to females. Both Syn A groups in the female mice islet area were significantly larger than the males. However, the male mice showed that the multiple dose of Syn A increased the islet area, whereas in the females, the single dose of Syn A, STZ + 8mg/kg Syn A (s) had the largest islet area. Bonnevie-Nielsen *et al.* (1981), also showed there was a significant decline in islet area over the course of their study which confirmed our results. There were differences in the size distribution as well, showing that the female mice contained islets that were larger than 25,000μm^2. When looking at the alpha and beta cell area in the head portion of the pancreas, female mice contained a larger amount of alpha and beta cells. The female mice treated with the single dose of Syn A, STZ + 8mg/kg Syn A (s), showed large amount of beta cells, perhaps due to the mice only being treated with 5 doses of 50mg/kg STZ. Normal islet architecture when looking at the beta and alpha cells, was seen in wild type female mice, who were treated with a single dose of 150mg/kg STZ. Le May *et al*. (2006) found that wild type and transgenic mice treated with oestrogen showed a decrease in the destruction of beta cells. However, in the mice that were bred to be oestrogen resistant, pancreatic insulin content

remained stable after the injection of STZ (Le May *et al.* 2006). This is different from previous research on Syn A in female rats. The past literature states that the number of islets, and the size of alpha cells remained unchanged. The same was true for the beta cells (Lundbaek and Nielsen, 1958).

When looking at the sex differences on islets within the tail of the pancreas, male mice showed larger amounts of islets than the female mice. However, when looking at the islet area of the analysed islets in the tail, the female mice that were treated with Syn A show an increase in the islet area. Like the head of the pancreas, the islets within the tail show differences in size distribution among the male and female mice. Surprisingly, the alpha cell area increased in the islets from the tail of the pancreases in the mice, both sexes, treated with Syn A. In male mice, the multiple dose of Syn A showed the suspected effect of decreasing the alpha cells in the tail. However, very little effect was observed on the female alpha cell area. In fact, there was an increase in the mice treated with multiple doses of Syn A. Dusaulcy *et al.* (2016) states that once the beta cells are killed off, then there is a decrease in beta cell mass. This was only seen in the male mice due to STZ treatments.

When analysing the head of the pancreas that was stained for GFP positive, insulin cells in male mice, it shows alpha to beta transdifferentiation within the head and tail of the pancreas. When looking at GFP positive, glucagon cells in the head of the pancreas it appears that the alpha cells in the mice treated with STZ+ 8mg/kg Syn A (s) are dedifferentiating. However, in the tail, the STZ + 8mg/kg Syn A (s) seems to reduce the process of dedifferentiation. Perhaps this process is only occurring within the head due to the small percentage of alpha cells located there.

However, when examining the head of the pancreas in the GFP positive, insulin cells, the alpha cells are transdifferentiating to beta cells in the female STZ only and STZ + 3mg/kg Syn A (m) mice. However, in the pancreatic tail, the female mice treated with STZ + 8mg/kg Syn A (s) shows that the process of transdifferentiation is reduced. In the GFP positive, glucagon cells, there is an increase in alpha cells maintaining their identity in the head of the pancreas

in mice treated with STZ + 3mg/kg Syn A (m). In the tail of the pancreas, the STZ is causing the alpha cells to dedifferentiate, however, the mice treated with 3mg/kg Syn A prevents this process from occurring, but the higher dose of STZ + 8mg/kg Syn A (s) does not. Thorel *et al*. (2011), stated that with the destruction of the alpha cells, regulation of blood glucose would remain unaffected. However, this was not the case in the majority of the Syn A groups. Both Syn A groups of male mice exhibited an increase in blood glucose levels. The mice treated with STZ +8 mg/kg Syn A (s) had levels higher than the STZ only treated mice near the end of the study. The female mice exhibited lower blood glucose levels then the males. The Syn A female mice groups as well as the STZ mice were lower than 25mmol/L. The mice treated with STZ + 3mg/kg Syn A (m) displayed a blood glucose slightly higher than the saline mice, which is consistent with the study by Thorel *et al* (2011). Perhaps there are sex differences in the way the alpha cells transdifferentiate or dedifferentiate with the alpha cell toxin.

It has been documented that the alpha cells within the islet will proliferate in mice treated with STZ (Takeda *et al.* 2012). However, when looking at the male and female mice in this study, the male mice treated with STZ only showed an increase in proliferated alpha cells, but only within the head of the pancreas. Female mice did not show much of an increase in alpha cell proliferation in any section of the pancreas. When looking at proliferation of beta cells in female rats that received an oestrogen treatment, it was observed that oestrogen did not cause the lack of proliferating beta cells (Le May *et al.* 2006). It was expected to see a decline in alpha cell proliferation due to the Syn A destroying the alpha cells. It was surprising to see an increase in beta cell proliferation in the STZ + Syn A in sections of the male and female mice.

A Tunel assay kit, was used to detect cells that have become apoptotic due to DNA degradation (Kyrylkova *et al.* 2012). When looking at apoptotic cells in the male mice, it was surprising to find that the multiple dose of Syn A; STZ + 8 mg/kg, showed extremely high levels of apoptosis in the beta cells in the head and the tail. This could be due to the STZ treatments first. However, when looking at the multiple dose of Syn A, STZ + 3mg/kg Syn A (m), the beta cells in the pancreas were lower than expected. Perhaps the multiple dose of Syn A protected

the beta cells or creates new beta cells through transdifferentiation. When focusing on the glucagon and Tunel positive cells, it was interesting to find that the mice treated with a higher dose of Syn A, had lower percentages than the saline treated mice. Possibly, this could be due to the multiple dose of Syn A and having a more drastic effect on the alpha cells then just one large dose or that the cells are undergoing dedifferentiation. In a paper that examined beta cell dedifferentiation and transdifferentiation, results showed that when dedifferentiation occurs in the beta cell, it does not become apoptotic (Moin and Butler, 2019). This can be seen in the NIH Swiss and Swiss TO mice. The positive apoptotic cells indicate that the alpha cells are being destroyed, as expected by the alpha cell toxin. However, this assay shows that the DNA within these alpha and beta cells is breaking due to the toxic effect of Syn A (Kyrylkova *et al.* 2012). Le May *et al.* (2006) looked at apoptosis using the Tunel assay and found that males treated with STZ showed an increase in apoptotic cells.

When attempting to stain for apoptosis using the Tunel assay, the female pancreas tissue would not adhere to the stain. There was also very little tissue left over from these mice. This could be due to the fact that when dissecting out the pancreas of these female mice, the tissue was often hard to differentiate, especially in the mice treated with a higher dose of STZ and the multiple doses of Syn A.

The male mice treated with STZ and Syn A had pale kidneys, however, the spleen and liver were very dark in colour. Blood clots were found around the lungs and heart on the mice, which is similar to the Swiss TO mice, just less in quantity. The stomachs did not appear to be distended but the intestines were congested. The lungs and spleen showed some dark spotting on the outer surface in the mice treated with STZ + 8mg/kg Syn A (s). However, within the cages of these mice there tended to be a lot more urine output then the saline mice. STZ + 3mg/kg Syn A (m) mice had urine and colour of the bladder were a darker yellow then the saline mice. The bile duct of mice treated with STZ + 3mg/kg Syn A (m) appeared larger than the other mice groups. The pancreas of some of the male mice treated with STZ + Syn A was similar in colour and the shape of fatty tissue.

The female mice also displayed some blood clots around the lungs and heart. One female mouse that was injected with 50mg/kg, 180mg/kg, and 200mg/kg STZ and 3mg/kg Syn A had a distended stomach, no blood to collect for fasting phases, and the pancreas resembled the colour and consistency of fatty tissue. The heart, kidneys, and liver were all a pale brown colour in the mice treated with STZ + 3mg/kg Syn A (m). The female mice treated with STZ + 8mg/kg Syn A (s) showed very little blood clots, but the kidneys, spleen, and liver were all pale in colour.

Limitations within the female study, due to the different doses in STZ. It would be beneficial to start the female mice at a higher dose of STZ. This would have provided a clearer picture to the destruction of the islets by STZ and by the different Syn A doses. This would also allow for a shorter experiment to have the same number of days between the male and female studies which would allow for a more consistent comparison.

In conclusion, we were able to anatomically identify the different organs that were affected with Syn A. We can also conclude that Syn A does drive the alpha to beta cell transdifferentiation as well as dedifferentiation. We can also determine that given the treatment to STZ induced diabetic male mice, the blood glucose did not decrease, as we had hoped it would.

Figure 6.1 Effects of single or multiple dose of Syn A body weight (A), weight change (B), and blood glucose (C) in male Glu^{Cre} Rosa mice with multiple low dose STZ diabetes over 15 days.

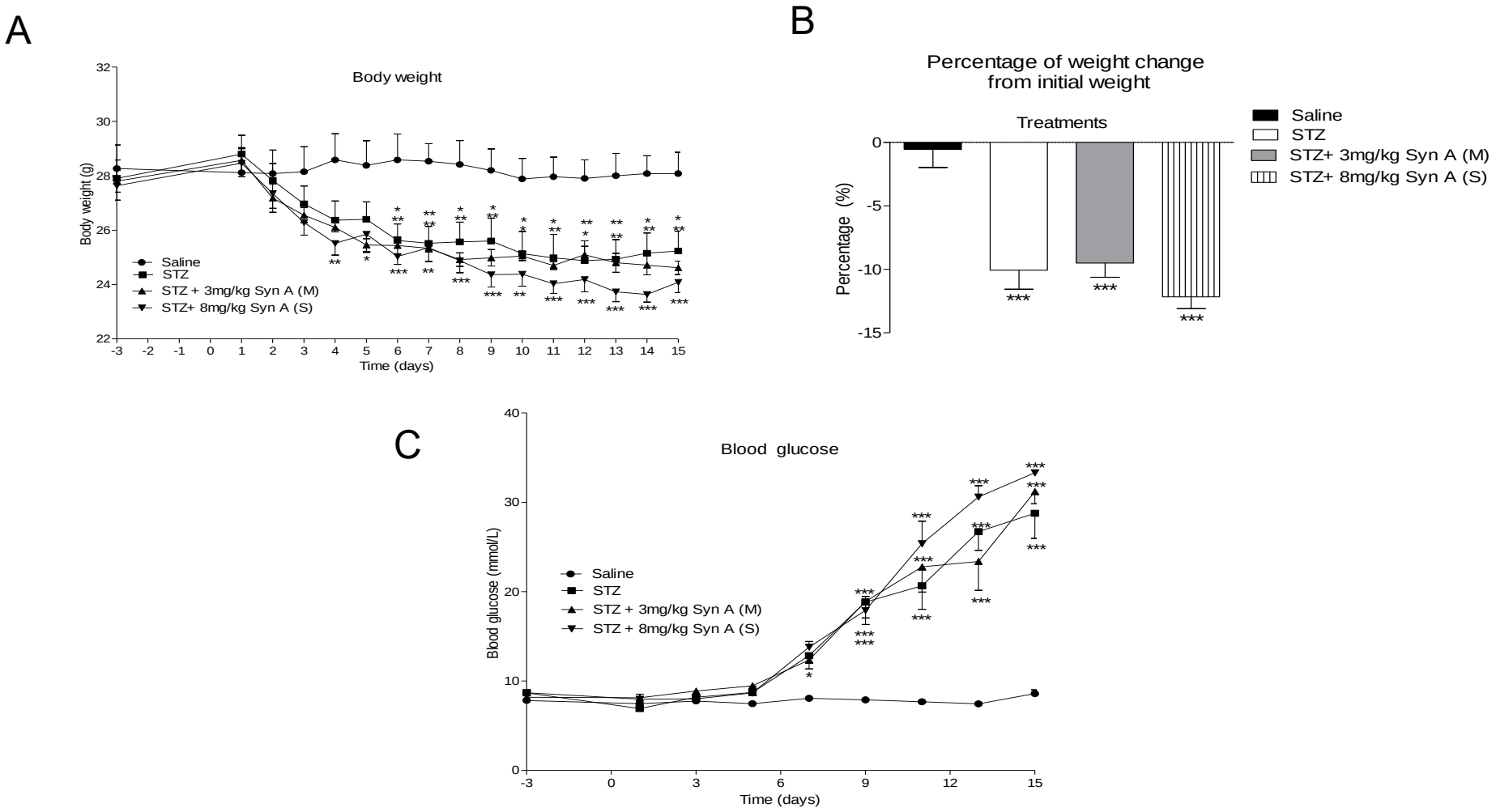

Body weight (A), percentage of body weight change (B), and blood glucose (C) over the course of 15 days in Glu^{Cre} mice. STZ (50mg/kg) administered by i.p. on days 1-5, 3mg/kg Syn A (m) administered on days10-14, and 8mg/kg (s) administered on day 10. Values are mean ± SEM (n=6 mice). Changes were deemed significant when p values were *p<0.05, **p <0.01, or ***p< 0.001 when compared with saline.

Figure 6.2 Effects of single or multiple dose of Syn A on food (A) and fluid (B) intake in male Glu^{Cre} Rosa mice with multiple low dose STZ diabetes over 15 days.

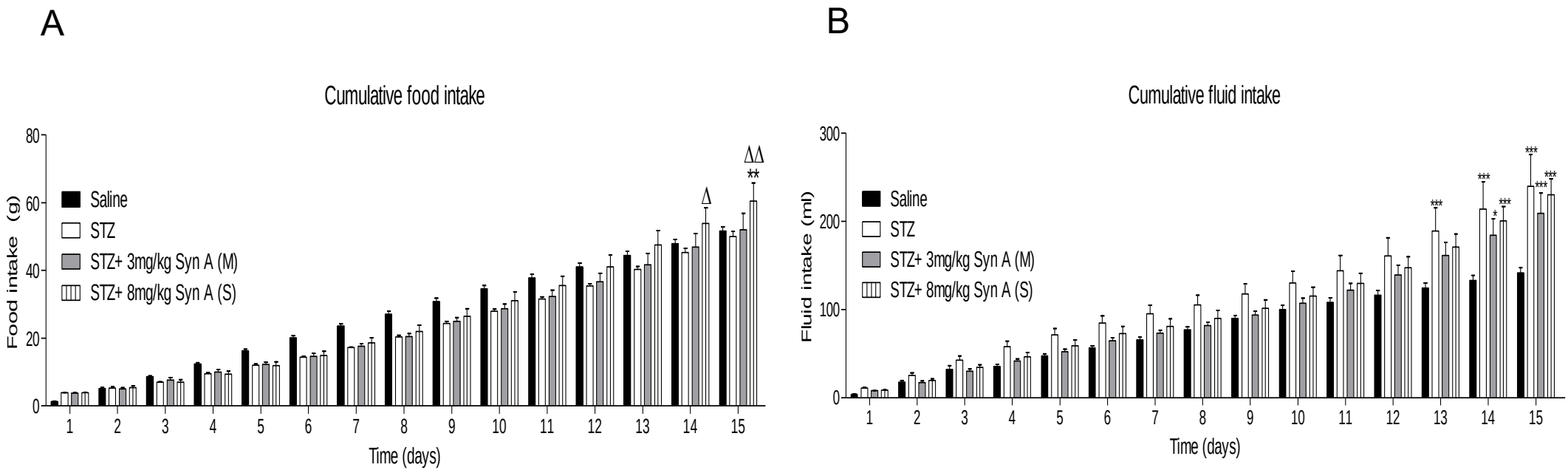

Cumulative food (A) and fluid (B) intake over the course of 15 days in Glu^{Cre} Rosa mice. STZ (50mg/kg) administered by i.p. on days 1-5, 3mg/kg Syn A (m) administered on days10-14, and 8mg/kg Syn A (s) administered on day 10. Values are mean ± SEM (n=6 mice). Changes were deemed significant when p values were *p<0.05, **p <0.01, or ***p<0.001 when compared with saline. $^{\Delta}$ p <0.05 or $^{\Delta\Delta}$ p <0.01 when STZ was compared with Syn A treated mice.

Figure 6.3 Effects of single or multiple dose of Syn A on nonfasting (A) and fasting (B) plasma insulin levels in male Glu^{Cre} mice with multiple low dose STZ diabetes at the end of the study.

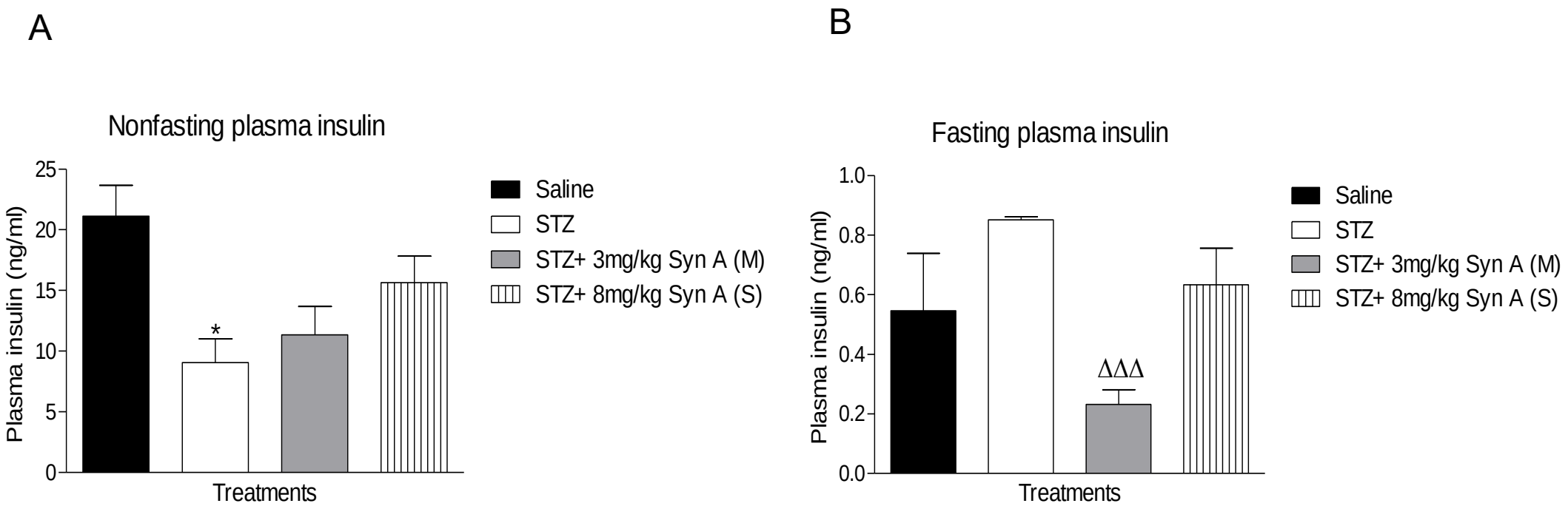

Nonfasting (A) and fasting (B) blood was taken at the end of the study. STZ (50mg/kg) administered by i.p. on days 1-5, 3mg/kg Syn A (m) administered on days 10-14, 8mg/kg (s) administered on day 10. Plasma insulin was measured by RIA. Values are mean ± SEM (n= 6 mice). Changes were deemed significant when p values were *p <0.05 when compared with saline. $^{\Delta\Delta\Delta}$ p <0.001 when STZ was compared with the Syn A treated mice.

Figure 6.4 Effects of single or multiple dose of Syn A on pancreatic insulin content from the head (A), tail (B), and whole (C) of the pancreas in male Glu^{Cre} mice with multiple low dose STZ diabetes after 15 days.

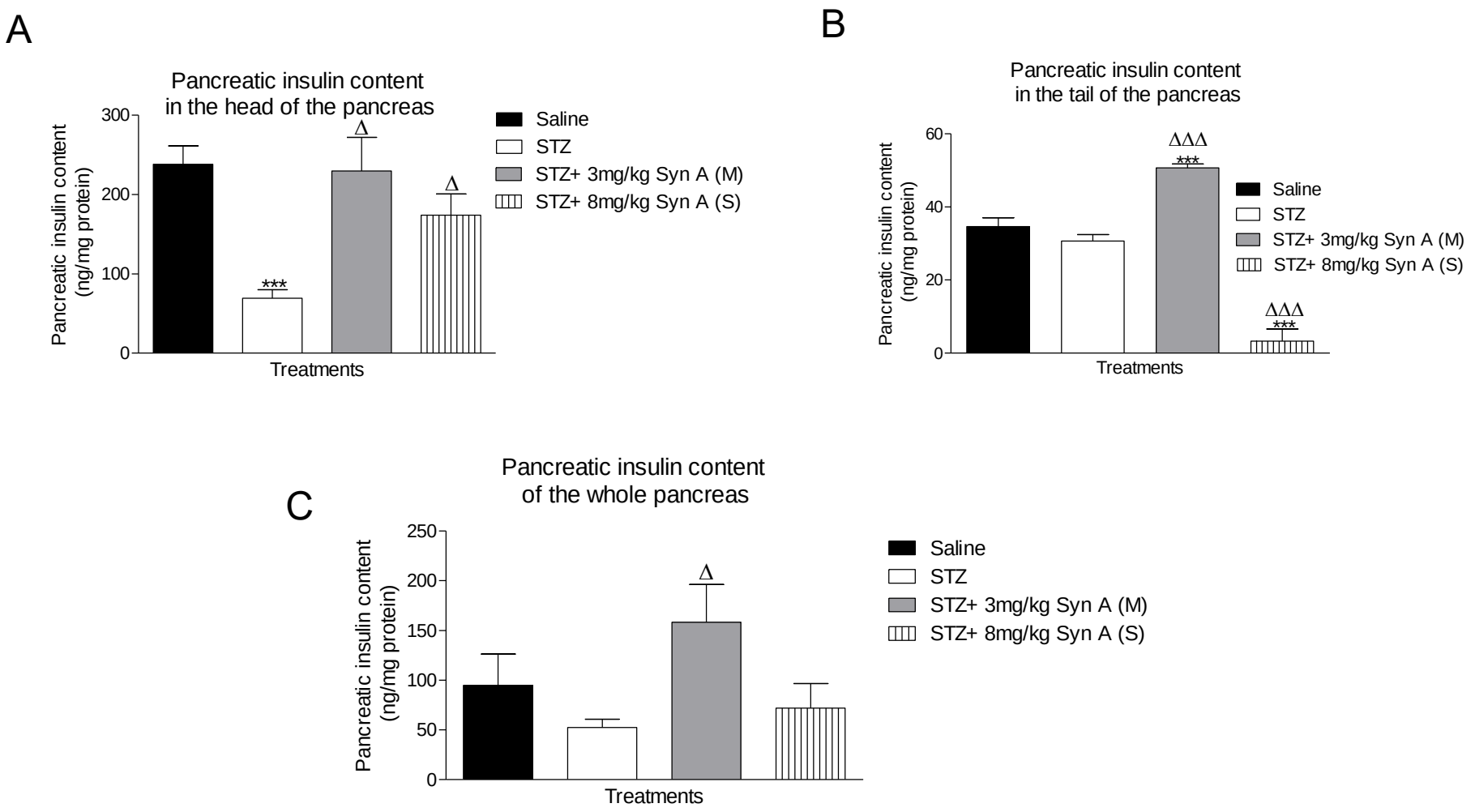

Pancreatic insulin content was measured from the head (A), tail (B), and whole (C) flash frozen pancreas. STZ (50mg/kg) administered by i.p. on days 1-5, 3mg/kg Syn A (m) administered on days10-14, and 8mg/kg (s) administered on day 10. Values are mean ± SEM (n= 6 mice). Changes were deemed significant when p values were ***p <0.001 when compared with saline. $^{\Delta}p<0.05$ or $^{\Delta\Delta\Delta}p<0.001$ when STZ was compared with Syn A treated mice.

Figure 6.5 Effects of single or multiple dose of Syn A on number of islets (A), islet area (B), and islet size distribution (C) in the head of the pancreas in male Glu^{Cre} Rosa mice with multiple low dose STZ diabetes after 15 days.

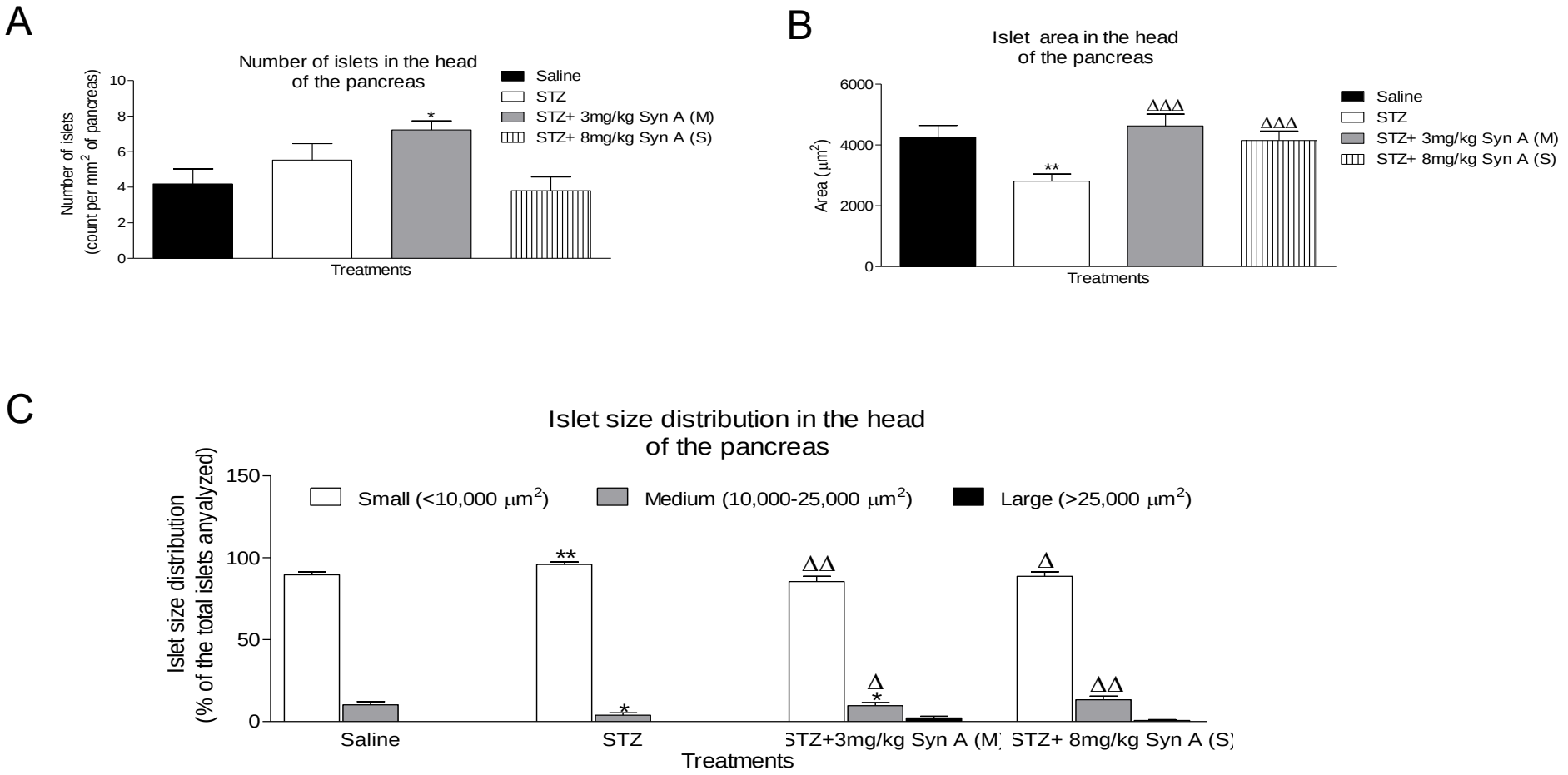

Number of islets (A), islet area (B), and islet size distribution (C) per pancreas in male Glu^{Cre} Rosa mice. STZ (50mg/kg) administered by i.p. on days 1-5, 3mg/kg Syn A (m) administered on days10-14, and 8mg/kg (s) administered on day 10. Values are mean ± SEM (n=6 mice). Changes were deemed significant when p values were *p<0.05 or **p <0.01 when compared with saline. $^{\Delta}$p<0.05, $^{\Delta\Delta}$ p<0.01, or $^{\Delta\Delta\Delta}$p<0.001 when STZ was compared with Syn A treated mice.

Figure 6.6 Effects of single or multiple dose of Syn A on number of islets (A), islet area (B), and islet size distribution (C) in the tail of the pancreas in male Glu^{Cre} Rosa mice with multiple low dose STZ diabetes after 15 days.

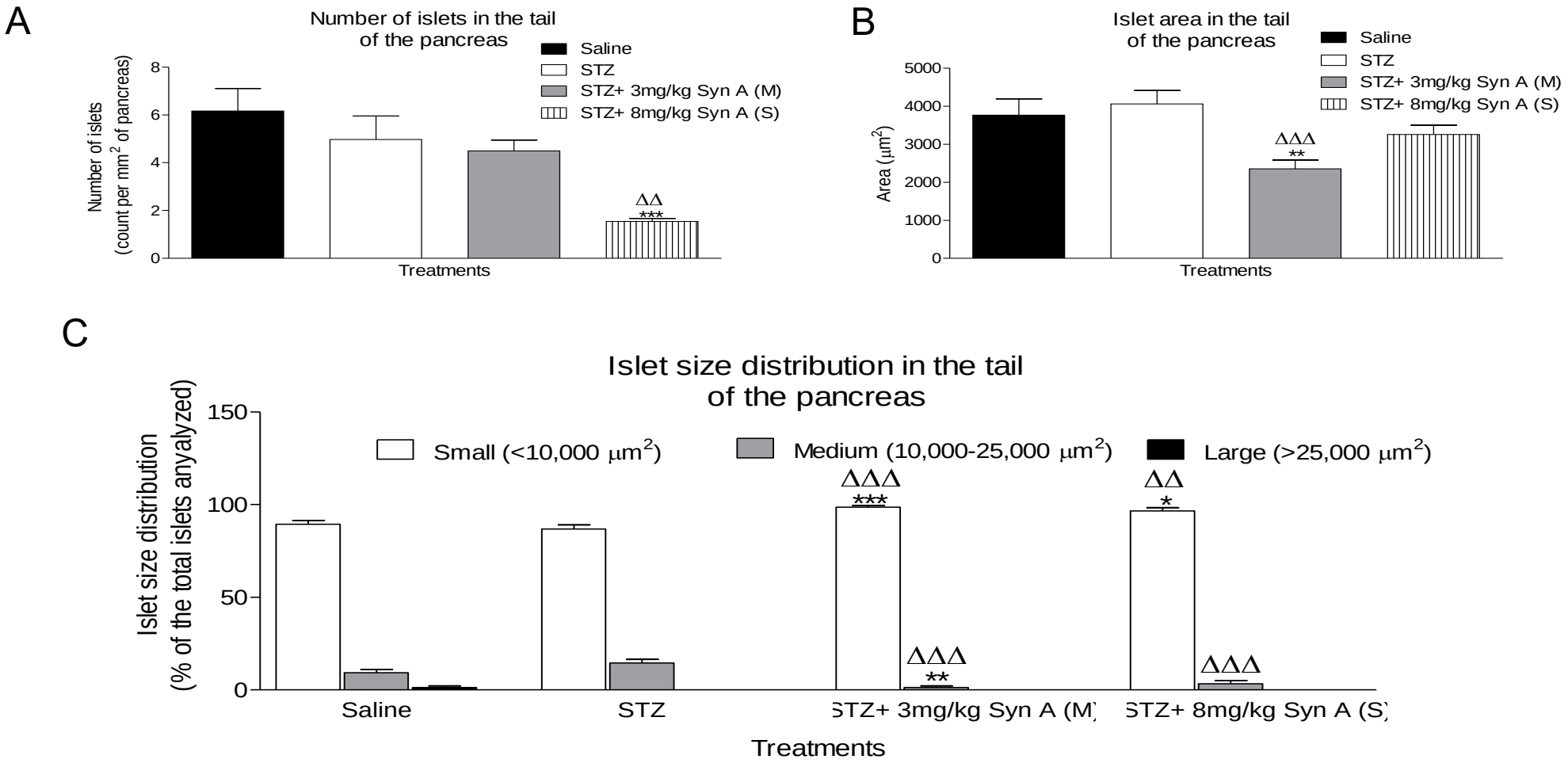

Number of islets (A), islet area (B), and islet size distribution (C) per pancreas in male Glu^{Cre} Rosa mice. STZ (50mg/kg) administered by i.p. on days 1-5, 3mg/kg Syn A (m) administered on days10-14, and 8mg/kg (s) administered on day 10. Values are mean ± SEM (n=6 mice). Changes were deemed significant when p values were *p<0.05, **p <0.01, or ***p<0.001 when compared with saline. $^{\Delta\Delta}$ p<0.01 or $^{\Delta\Delta\Delta}$p<0.001 when STZ was compared with Syn A treated mice.

Figure 6.7 Effects of single or multiple dose of Syn A on number of islets (A), islet area (B), and islet size distribution (C) on the whole pancreas in male Glu^{Cre} Rosa mice with multiple low dose STZ diabetes after 15 days.

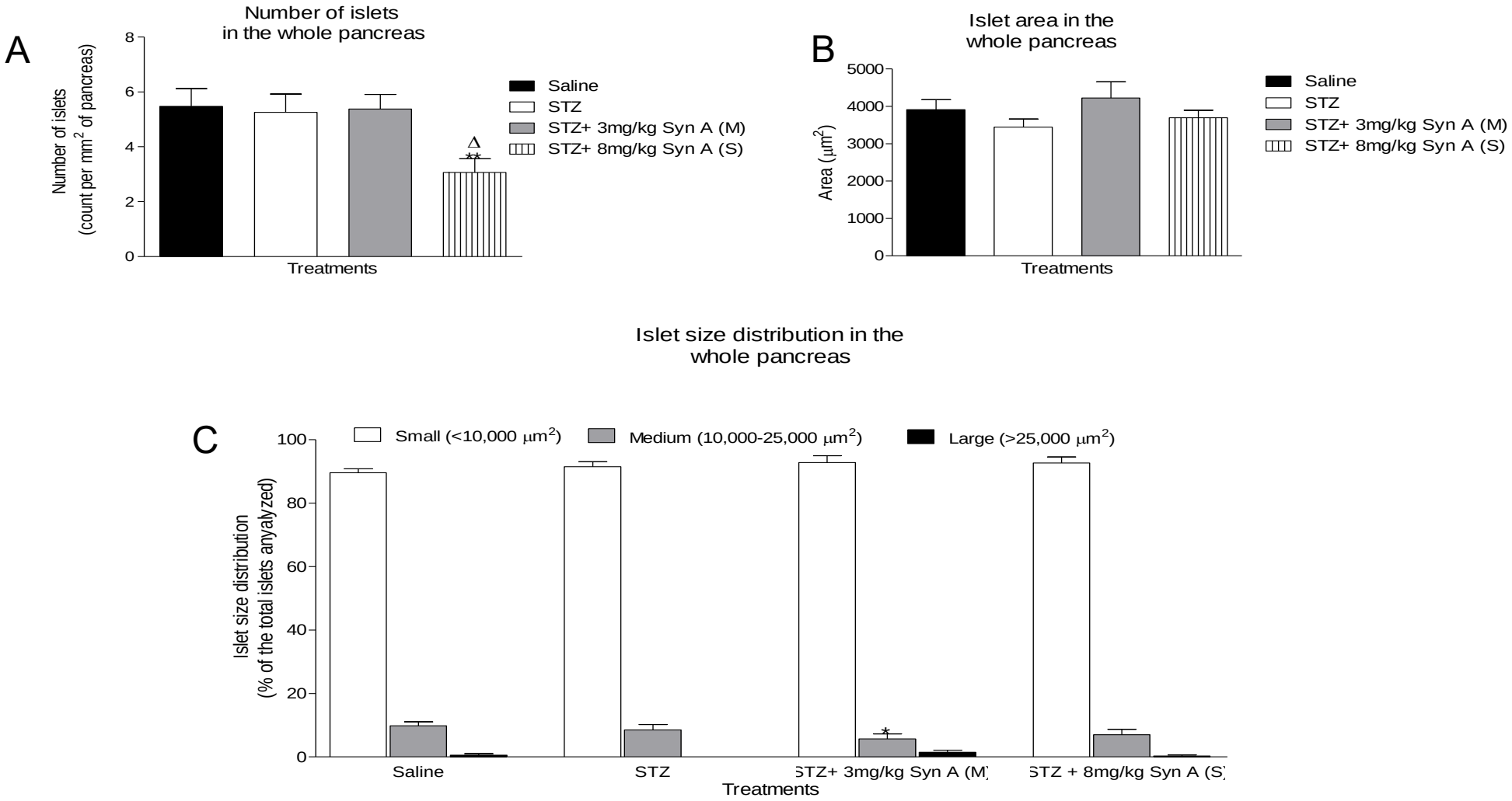

Number of islets (A), islet area (B), and islet size distribution (C) per pancreas in male Glu^{Cre} Rosa mice. STZ (50mg/kg) administered by i.p. on days 1-5, 3mg/kg Syn A (m) administered on days10-14, and 8mg/kg (s) administered on day 10. Values are mean ± SEM (n=6 mice). Changes were deemed significant when p values were *p<0.05 or **p <0.01 when compared with saline. $^{\Delta}$p<0.05 when STZ was compared with Syn A treated mice.

Figure 6.8 Effects of single or multiple dose of Syn A on alpha cell area and percentage (A and B) and beta cell area and percentage (C and D) in the head of the pancreas in male Glu^{Cre} Rosa mice with multiple low dose STZ diabetes after 15 days.

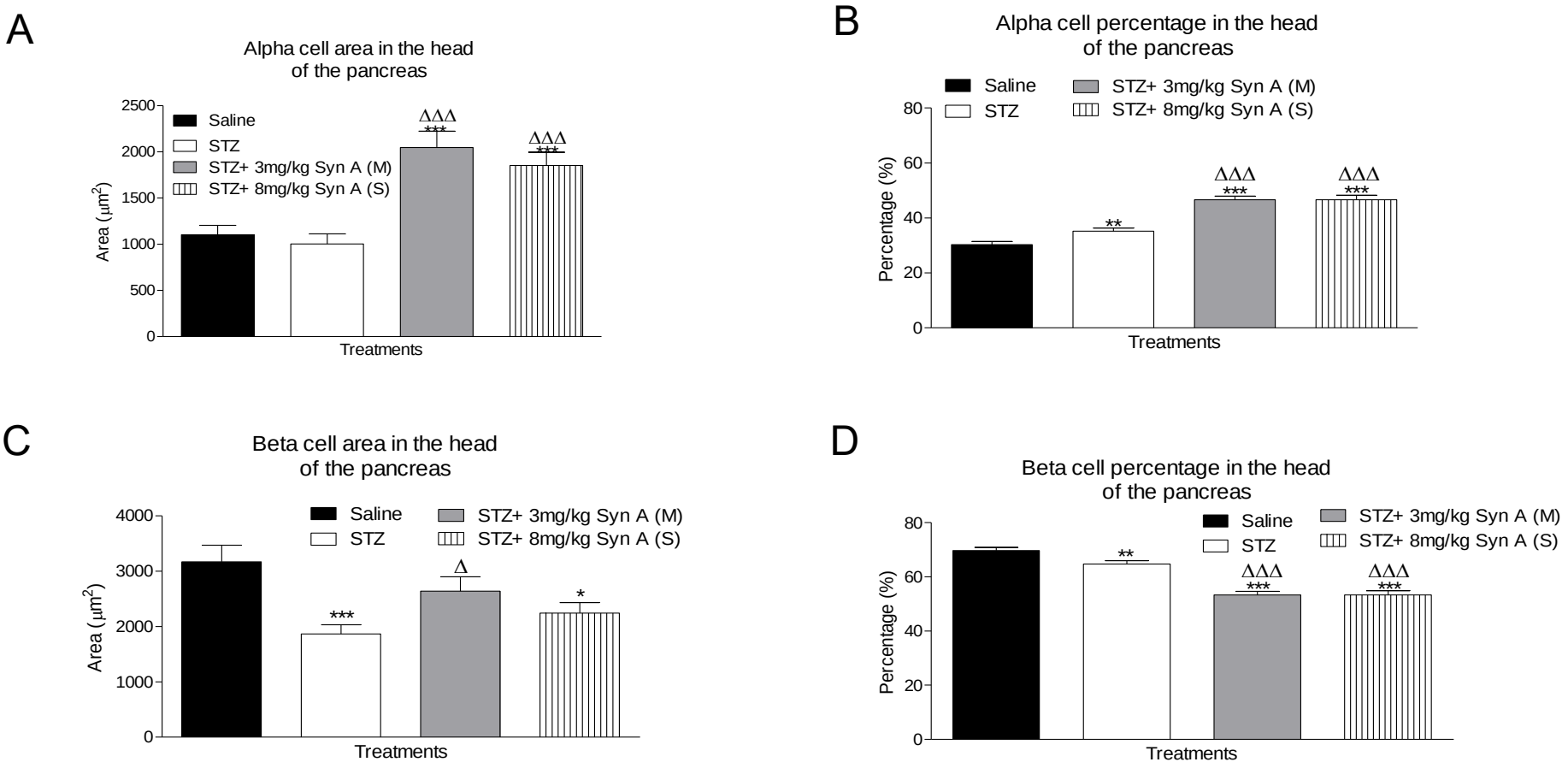

Alpha cell area and percentage (A and B) and beta cell area and percentage (C and D) per pancreas in male Glu^{Cre} Rosa mice. STZ (50mg/kg) administered by i.p. on days 1-5, 3mg/kg Syn A (m) administered on days10-14, and 8mg/kg (s) administered on day 10. Values are mean ± SEM (n=6 mice). Changes were deemed significant when p values were *p<0.05, **p <0.01, or ***p<0.001 when compared with saline. $^{\Delta}$p<0.01 or $^{\Delta\Delta\Delta}$p<0.001 when STZ was compared with Syn A treated mice.

Figure 6.9 Effects of single or multiple dose of Syn A on alpha cell area and percentage (A and B) and beta cell area and percentage (C and D) in the tail of the pancreas in male Glu^{Cre} Rosa mice with multiple low dose STZ diabetes after 15 days.

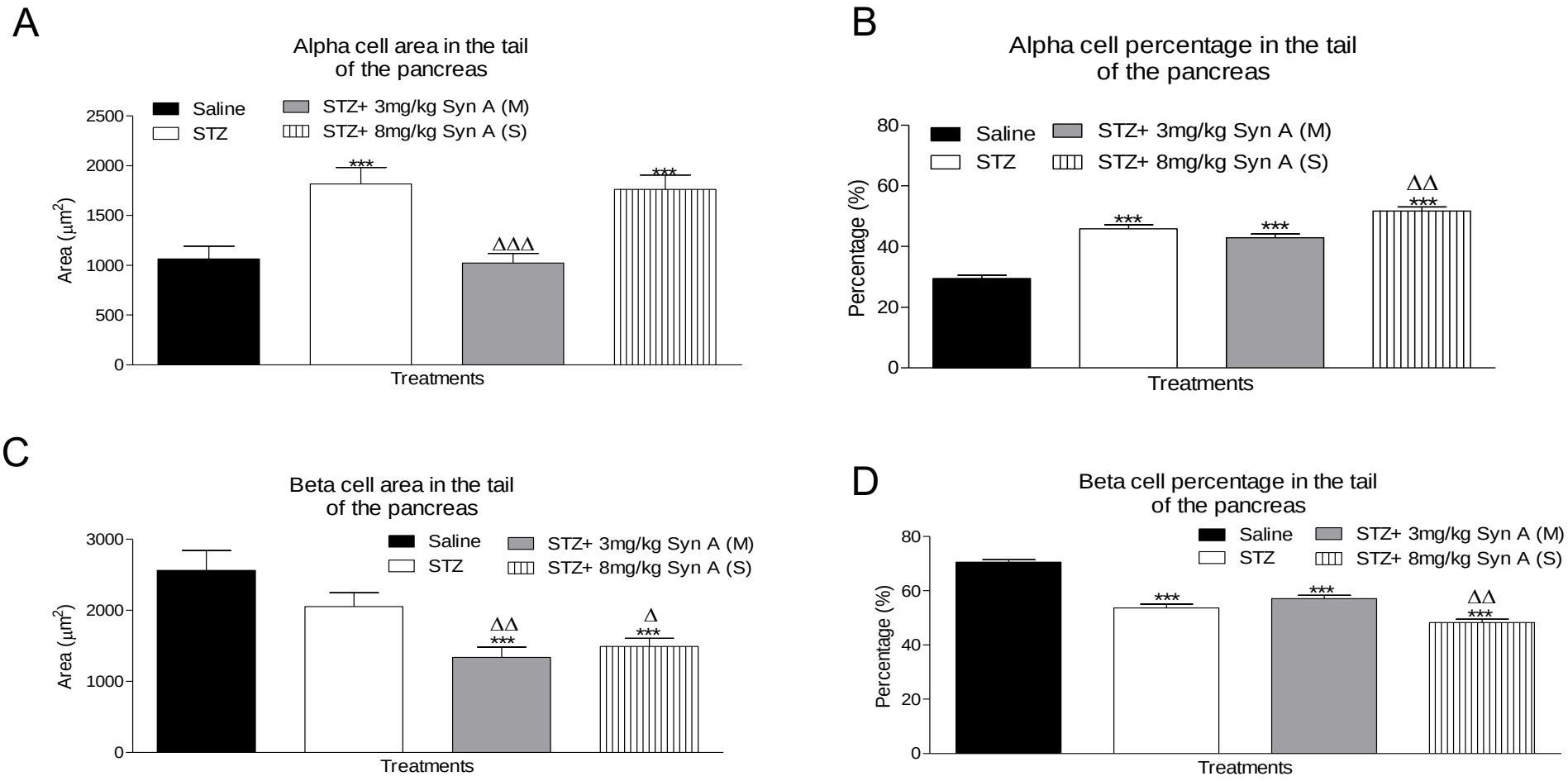

Alpha cell area and percentage (A and B) and beta cell area and percentage (C and D) per pancreas in male Glu^{Cre} Rosa mice. STZ (50mg/kg) administered by i.p. on days 1-5, 3mg/kg Syn A (m) administered on days10-14, and 8mg/kg (s) administered on day 10. Values are mean ± SEM (n=6 mice). Changes were deemed significant when p values were ***p<0.001 when compared with saline. $^{\Delta}$p<0.05, $^{\Delta\Delta}$p<0.01, or $^{\Delta\Delta\Delta}$p<0.001 when STZ was compared with Syn A treated mice.

Figure 6.10 Effects of single or multiple dose of Syn A alpha cell area and percentage (A and B) and beta cell area and percentage (C and D) in the whole pancreas in male Glu^{Cre} Rosa mice with multiple low dose STZ diabetes after 15 days.

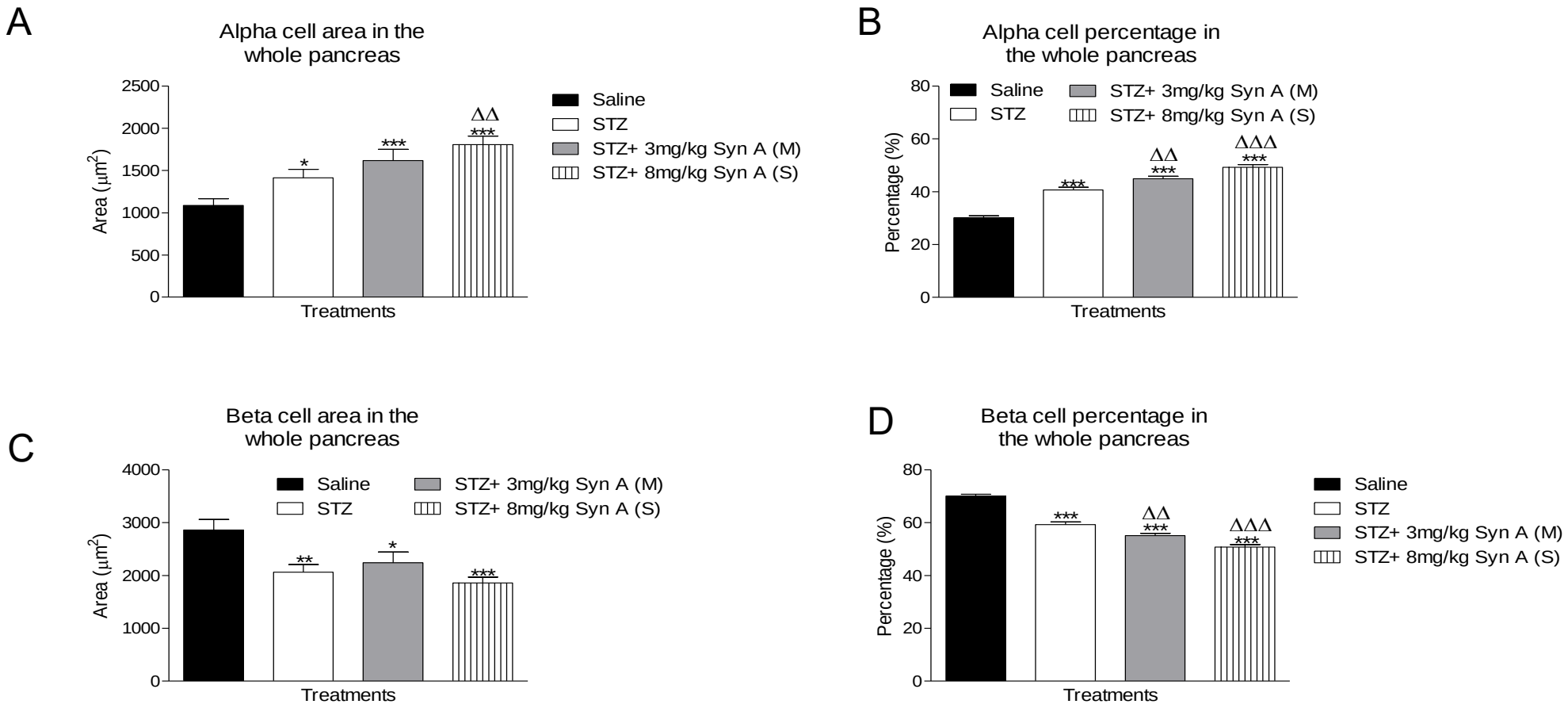

Alpha cell area and percentage (A and B) and beta cell area and percentage (C and D) per pancreas in male Glu^{Cre} Rosa mice. STZ (50mg/kg) administered by i.p. on days 1-5, 3mg/kg Syn A (m) administered on days10-14, and 8mg/kg (s) administered on day 10. Values are mean ± SEM (n=6 mice). Changes were deemed significant when p values were *p<0.05 or ***p<0.001 when compared with saline. $^{\Delta\Delta}$p<0.01 or $^{\Delta\Delta\Delta}$p<0.001 when STZ was compared with Syn A treated mice.

Figure 6.11 Representative images of saline (A), STZ (B), STZ+ 3mg/kg Syn A (C), and STZ+ 8mg/kg Syn A (D) islets from the tail of the pancreas in male Glu^{Cre} mice.

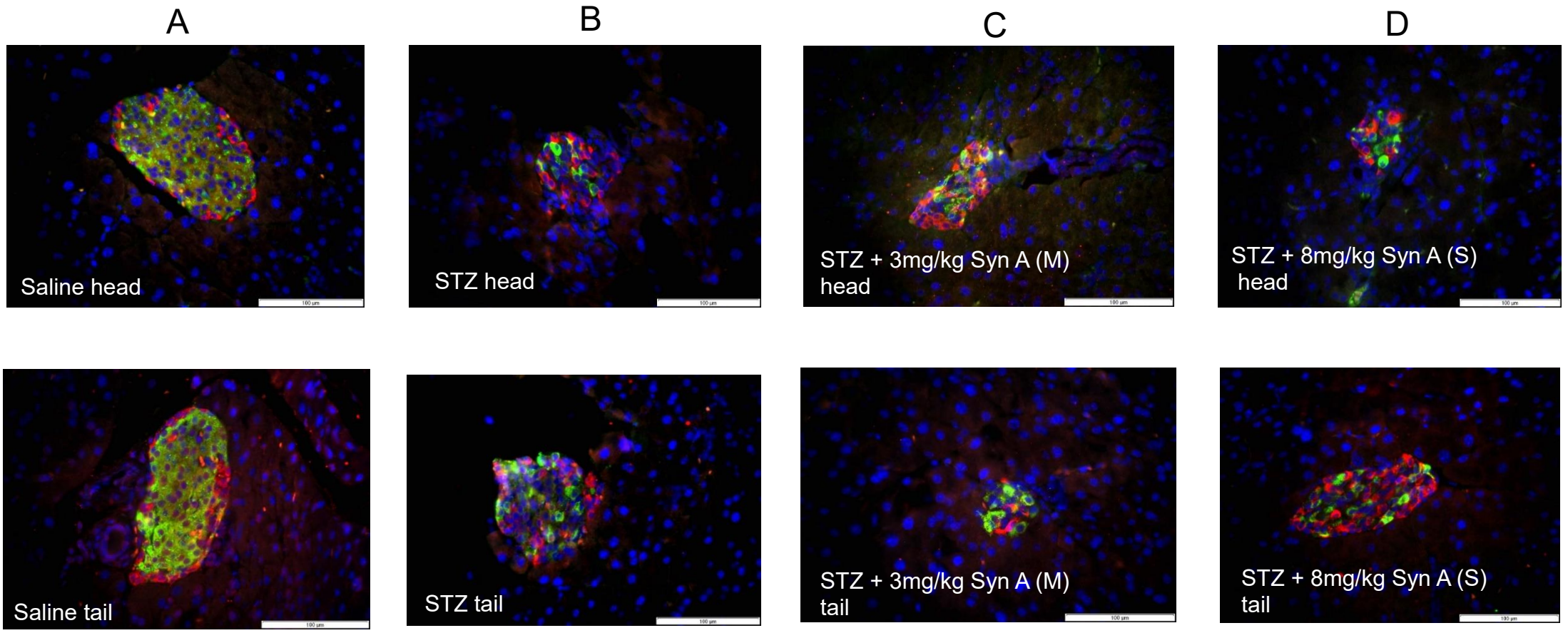

Islet morphology was evaluated at the end of the 15-day study of male Glu^{Cre} mice on 5-7µm sections. Saline (A), STZ (B), STZ+ 3mg/kg Syn A (C), and STZ+ 8mg/kg Syn A (D) islets in the tail of the pancreas. Insulin is represented in green, glucagon in red, and DAPI in blue. Photos imaged at 40x. Total number of 150 islets were analysed per treatment group.

Figure 6.12 Effects of single or multiple dose of Syn A on GFP positive, insulin positive cells in the head (A), tail (B), and whole (C) pancreas in male Glu^{Cre} Rosa mice with multiple low dose STZ diabetes after 15 days.

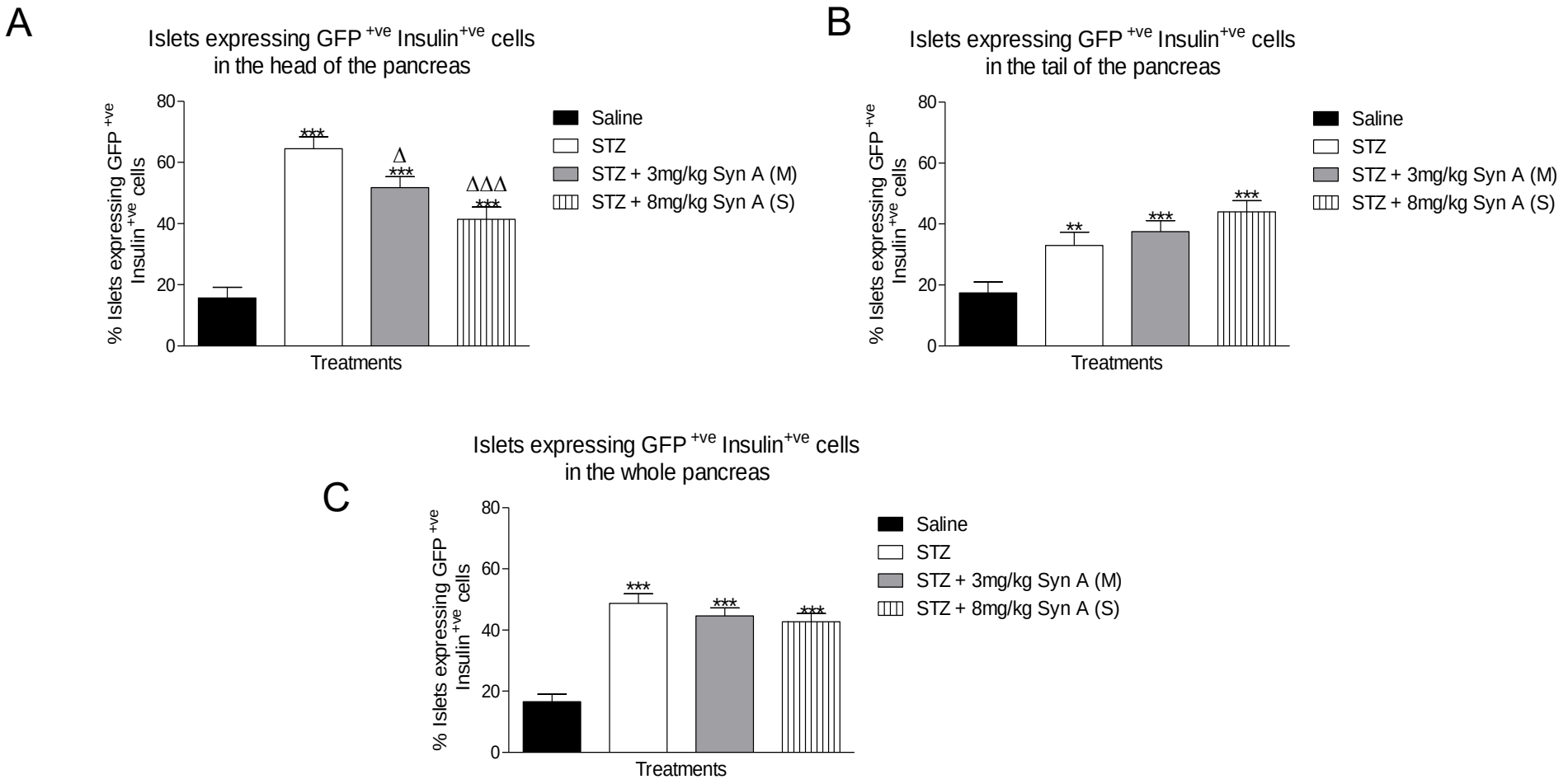

Percentage of islets expressing GFP^{+ve}, insulin^{+ve} cells in the head (A), tail (B), and whole (C) pancreas. STZ (50mg/kg) administered by i.p. on days 1-5, 3mg/kg Syn A (m) administered on days10-14, and 8mg/kg (s) administered on day 10. Values are mean ± SEM (n=6 mice). Changes were deemed significant when p values were **p<0.01 or ***p<0.001 when compared with saline. $^{\Delta}$p<0.05 or $^{\Delta\Delta}$p<0.001when STZ was compared with Syn A treated mice.

Figure 6.13 Representative images of saline (A), STZ (B), STZ+ 3mg/kg Syn A (C), and STZ+ 8mg/kg Syn A (D) islets from the head and the tail of the pancreas in male Glu^{Cre} mice.

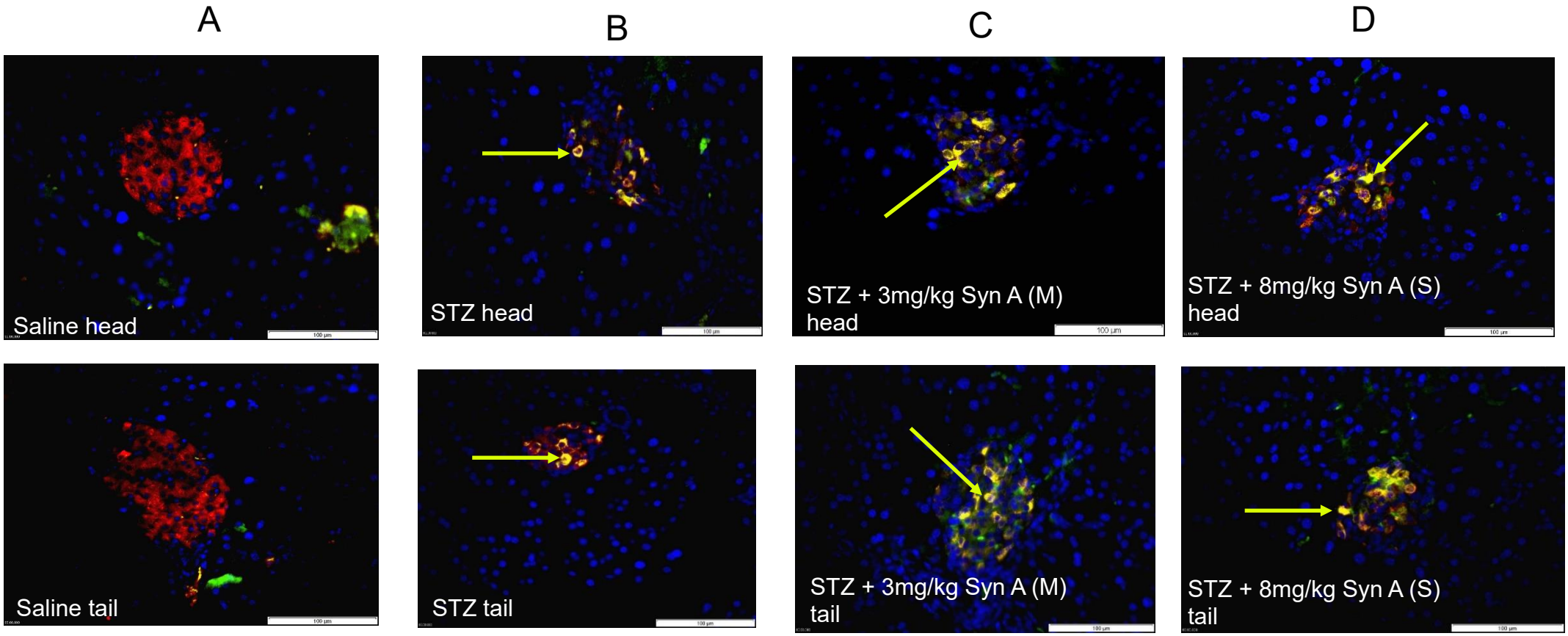

Percentage of transdifferentiation was determined by the islets expressing GFP^{+ve}, insulin^{+ve} cells. Insulin is represented in red, GFP in green, and DAPI in blue. Yellow arrows are pointing to GFP^{+ve}, insulin^{+ve} cells. Images were taken at 20x or 40x objective lens. Total number of 100 islets were analysed per treatment group.

Figure 6.14 Effects of single or multiple dose of Syn A on GFP positive, insulin negative cells in the head (A), tail (B), and whole (C) pancreas in male Glu^{Cre} Rosa mice with multiple low dose STZ diabetes after 15 days.

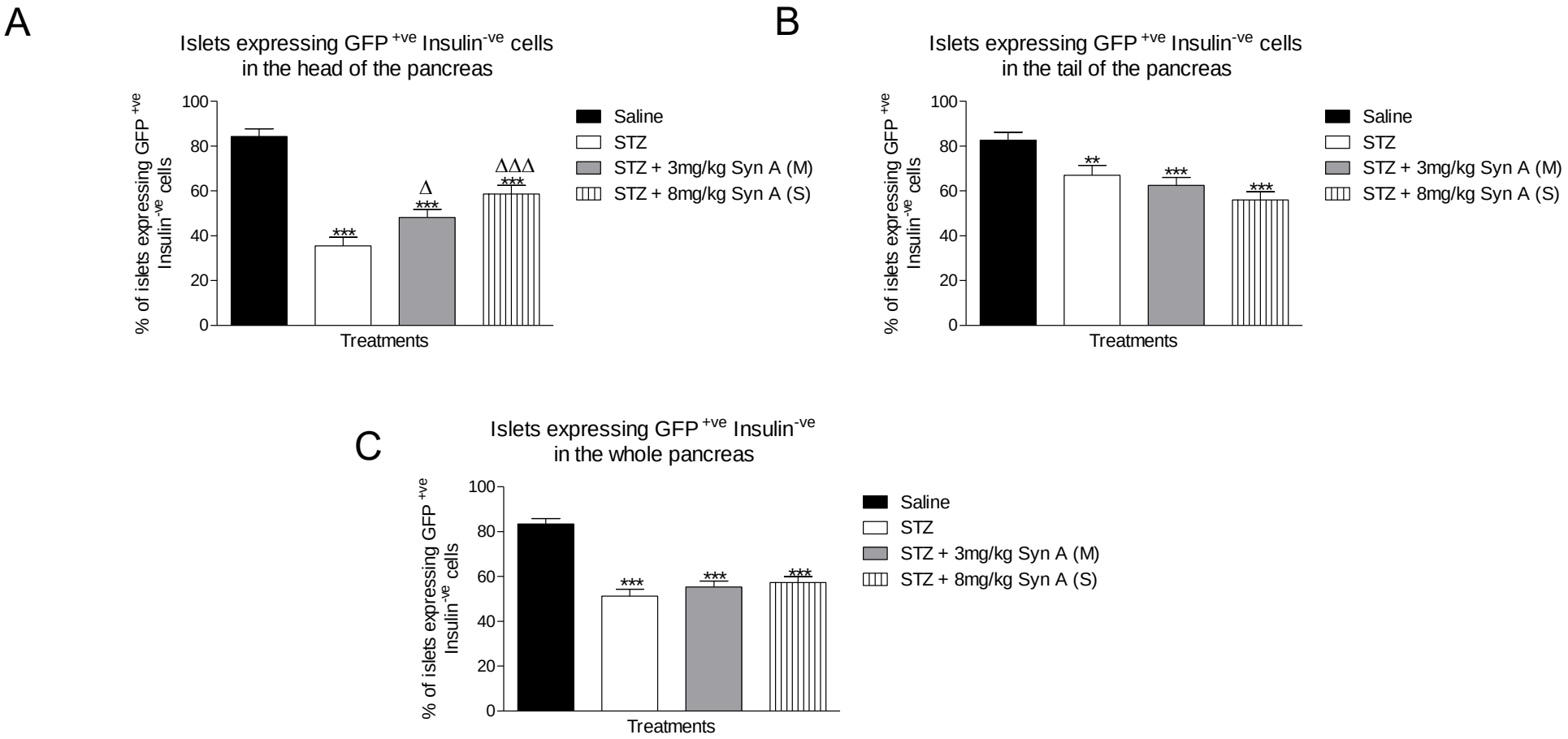

Percentage of islets expressing GFP^{+ve}, insulin^{-ve} cells in the head (A), tail (B), and whole (C) pancreas. STZ (50mg/kg) administered by i.p. on days 1-5, 3mg/kg Syn A (m) administered on days10-14, and 8mg/kg (s) administered on day 10. Values are mean ± SEM (n=6 mice). Changes were deemed significant when p values were *p<0.05, **p<0.01, or ***p<0.001 when compared with saline. $^{\Delta}$p<0.05 or $^{\Delta\Delta\Delta}$p<0.001 when STZ was compared with Syn A treated mice.

Figure 6.15 Representative images of saline (A), STZ (B), STZ+ 3mg/kg Syn A (C), and STZ+ 8mg/kg Syn A (D) islets from the pancreas in male Glu^{Cre} mice.

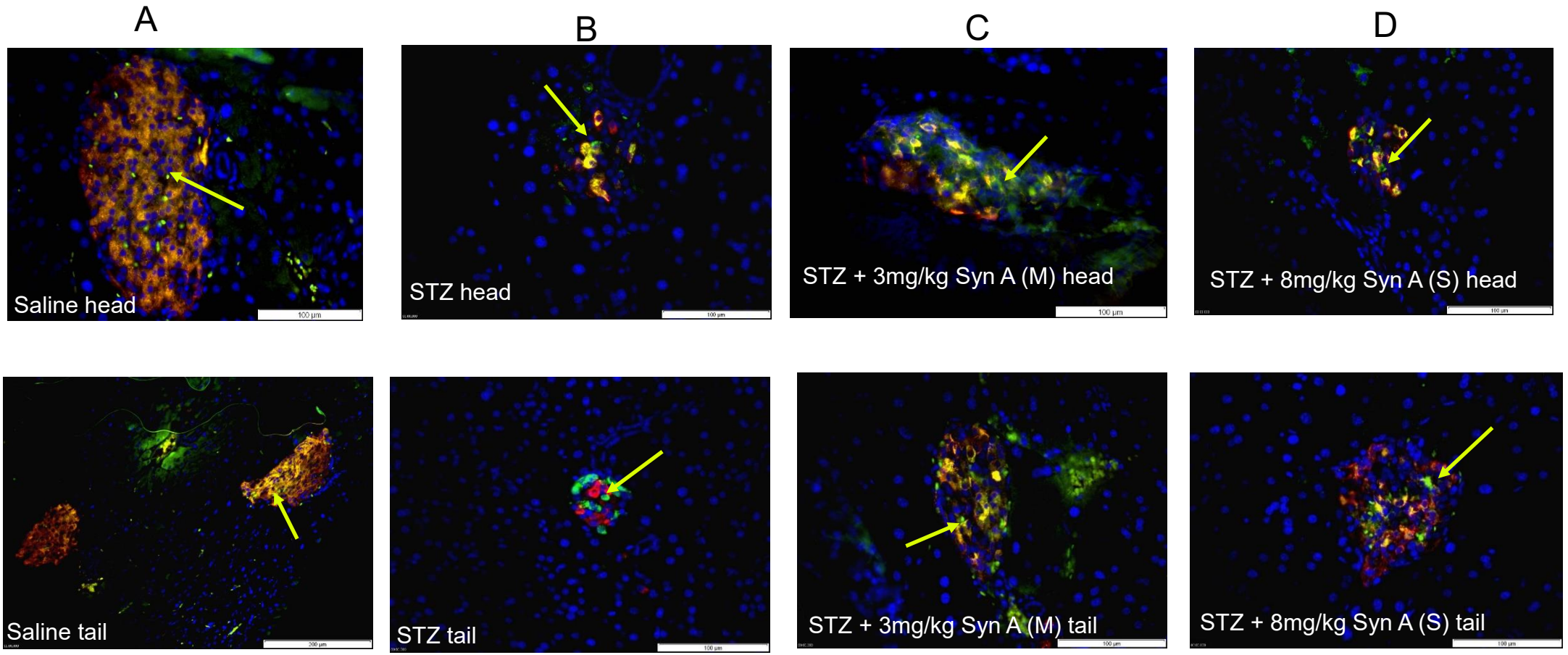

Percentage of transdifferentiation was determined by the islets expressing GFP^{+ve}, insulin^{-ve} cells. Insulin is represented in red, GFP in green, and DAPI in blue. Yellow arrows are point to GFP^{+ve}, insulin^{+ve} cells. Images were taken at 20x and 40x objective lens. Total of 100 islets were analysed. Total number of 100 islets were analysed per treatment groups.

Figure 6.16 Effects of single or multiple dose of Syn A on GFP positive, glucagon positive cells in the head (A), tail (B), and whole (C) pancreas in male Glu^{Cre} Rosa mice with multiple low dose STZ diabetes after 15 days.

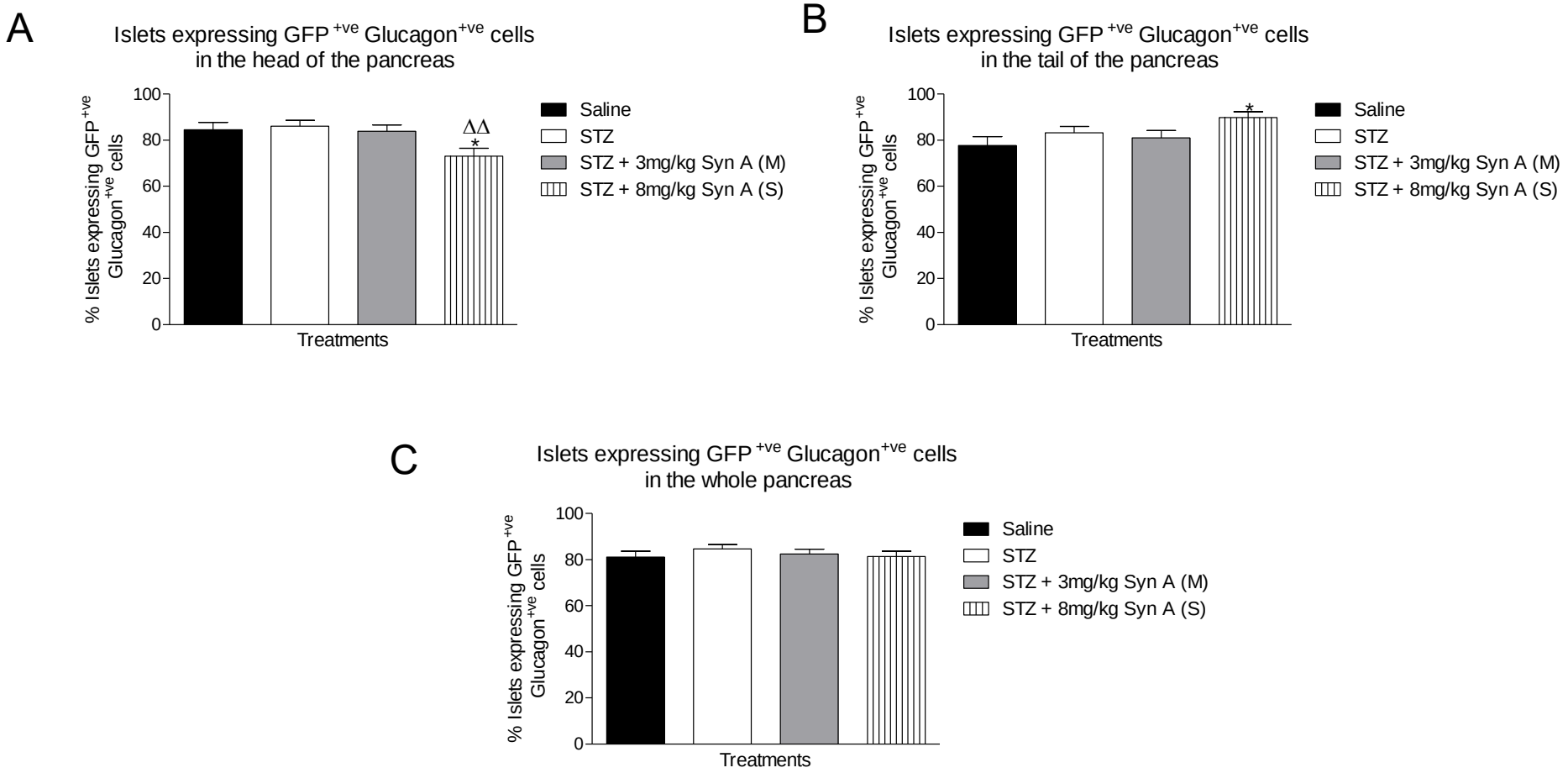

Percentage of islets expressing GFP^{+ve}, glucagon^{+ve} cells in the head (A), tail (B), and whole (C) pancreas. STZ (50mg/kg) administered by i.p. on days 1-5, 3mg/kg Syn A (m) administered on days10-14, and 8mg/kg (s) administered on day 10. Values are mean ± SEM (n=6 mice). Changes were deemed significant when p values were *p<0.05, ** p<0.01, or ***p<0.001 when compared with saline. $^{\Delta\Delta}$p<0.01 when STZ was compared with Syn A treated mice.

Figure 6.17 Representative images of saline (A), STZ (B), STZ+ 3mg/kg Syn A (C), and STZ+ 8mg/kg Syn A (D) islets from the pancreas in male Glu^{Cre} mice.

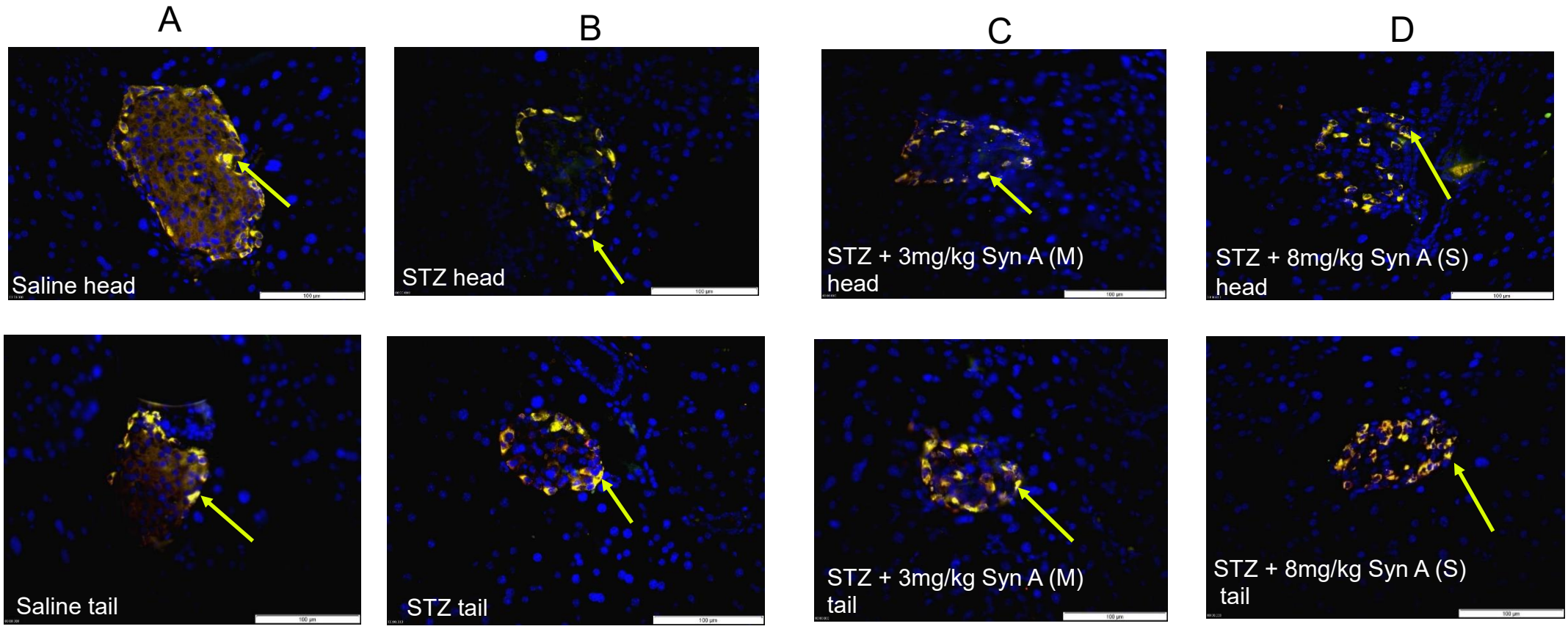

Percentage of dedifferentiation was determined by the islets expressing GFP^{+ve}, glucagon^{+ve} cells. Glucagon is represented in red, GFP in green, and DAPI in blue. Yellow arrows are point to GFP^{+ve}, glucagon^{+ve} cells Images were taken at 40x.Total number of 100 islets were analysed per treatment group.

Figure 6.18 Effects of single or multiple dose of Syn A on GFP positive, glucagon negative cells in the head (A), tail (B), and whole (C) pancreas in male Glu^{Cre} Rosa mice with multiple low dose STZ diabetes after 15 days.

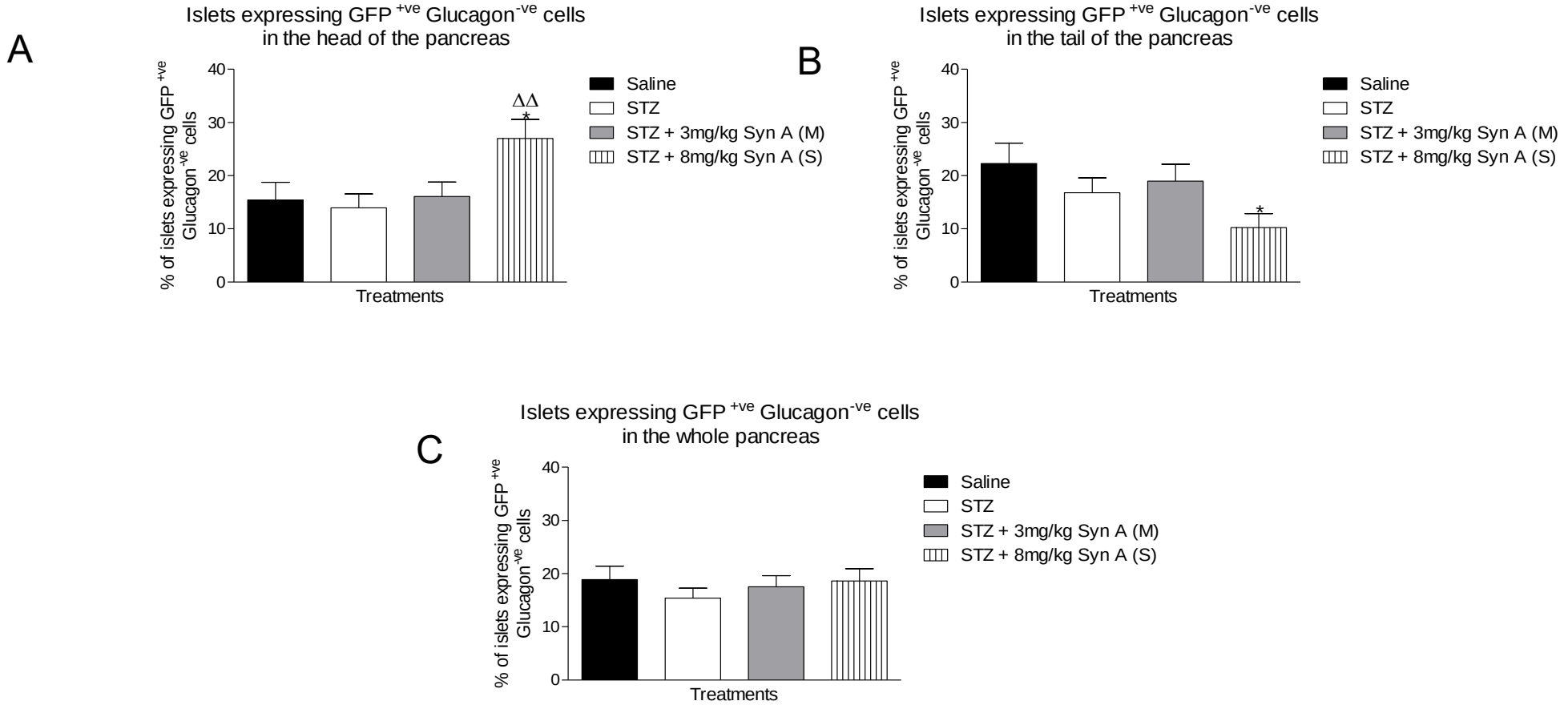

Percentage of islets expressing GFP^{+ve}, glucagon^{-ve} cells in the head (A), tail (B), and whole (C) pancreas. STZ (50mg/kg) administered by i.p. on days 1-5, 3mg/kg Syn A (m) administered on days10-14, and 8mg/kg (s) administered on day 10. Values are mean ± SEM (n=6 mice). Changes were deemed significant when p values were ** $p<0.01$ or ***$p<0.001$ when compared with saline. $^{\Delta\Delta}p<0.01$ when STZ was compared with Syn A treated mice.

Figure 6.19 Representative images of saline (A), STZ (B), STZ+ 3mg/kg Syn A (C), and STZ+ 8mg/kg Syn A (D) islets from the pancreas in male Glu^{Cre} mice.

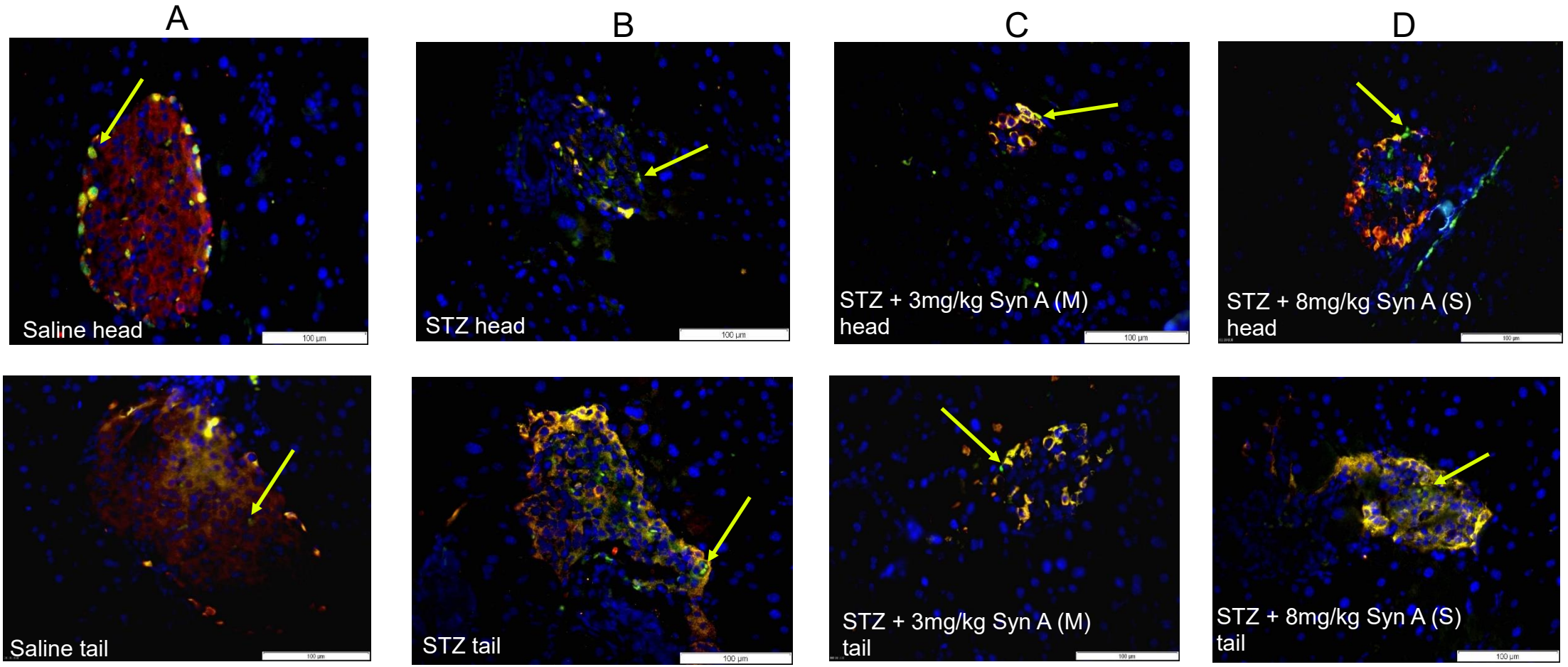

Percentage of dedifferentiation was determined by the islets expressing GFP^{+ve}, $glucagon^{-ve}$ cells. Glucagon is represented in red, GFP in green, and DAPI in blue. Yellow arrows are pointing to GFP^{+ve}, $glucagon^{-ve}$ cells Images were taken at 40x.Total number of 100 islets were analysed per treatment group.

Figure 6.20 Effects of single or multiple dose of Syn A on Ki67 positive, insulin positive cells in the head (A-C) of the pancreas in male Glu^{Cre} Rosa mice with multiple low dose STZ diabetes after 15 days.

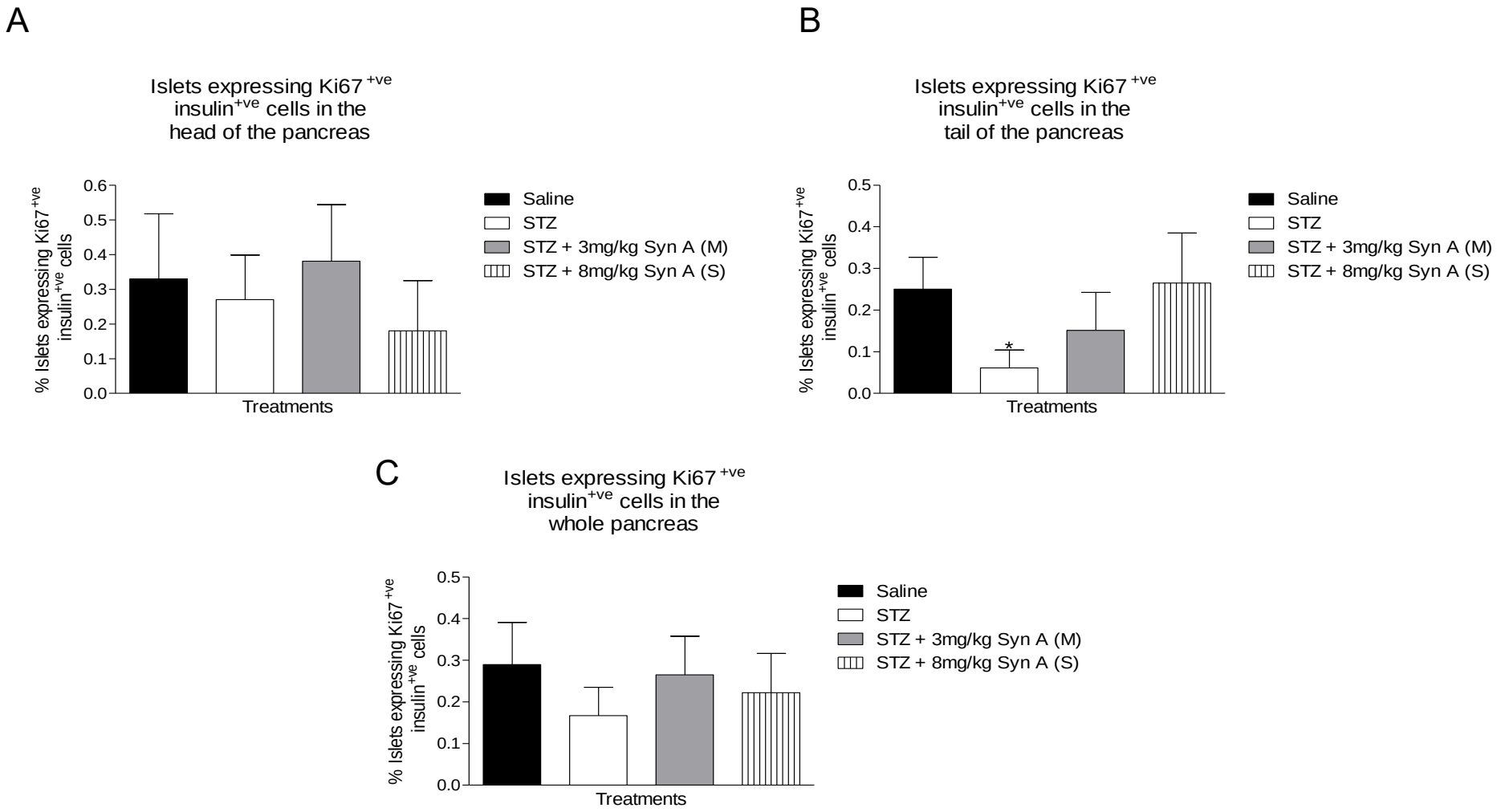

Percentage of islets expressing Ki67^{+ve}, insulin^{+ve} cells in the head (A), tail (B), and whole (C) of the pancreas. STZ (50mg/kg) administered by i.p. on days 1-5, 3mg/kg Syn A (m) administered on days10-14, and 8mg/kg (s) administered on day 10. Values are mean ± SEM (n=6 mice). Changes were deemed significant when p values were *p<0.05 when compared with saline.

Figure 6.21 Representative images of saline (A), STZ (B), STZ+ 3mg/kg Syn A (C), and STZ+ 8mg/kg Syn A (D) islets from the pancreas in male Glu^{Cre} mice.

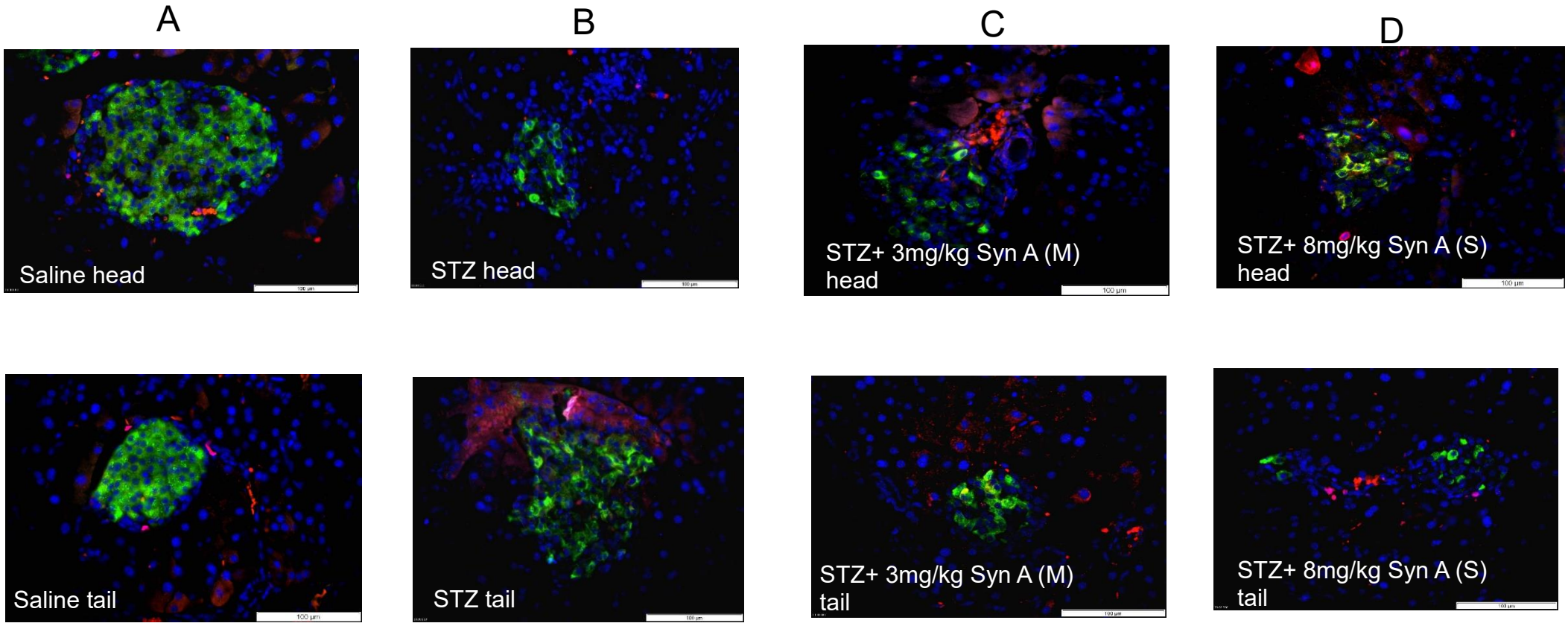

Percentage of beta cell proliferation was determined by the islets expressing $Ki67^{+ve}$, $insulin^{+ve}$ cells in the pancreas. Insulin is represented in green, Ki67 in red, and DAPI in blue. Images were taken at 20x and 40x objective lens. Total number of 100 islets per treatment group were analysed.

Figure 6.22 Effects of single or multiple dose of Syn A on Ki67 positive, glucagon positive cells in the head (A), tail (B), and whole (C) pancreas in male Glu^{Cre} Rosa mice with multiple low dose STZ diabetes after 15 days.

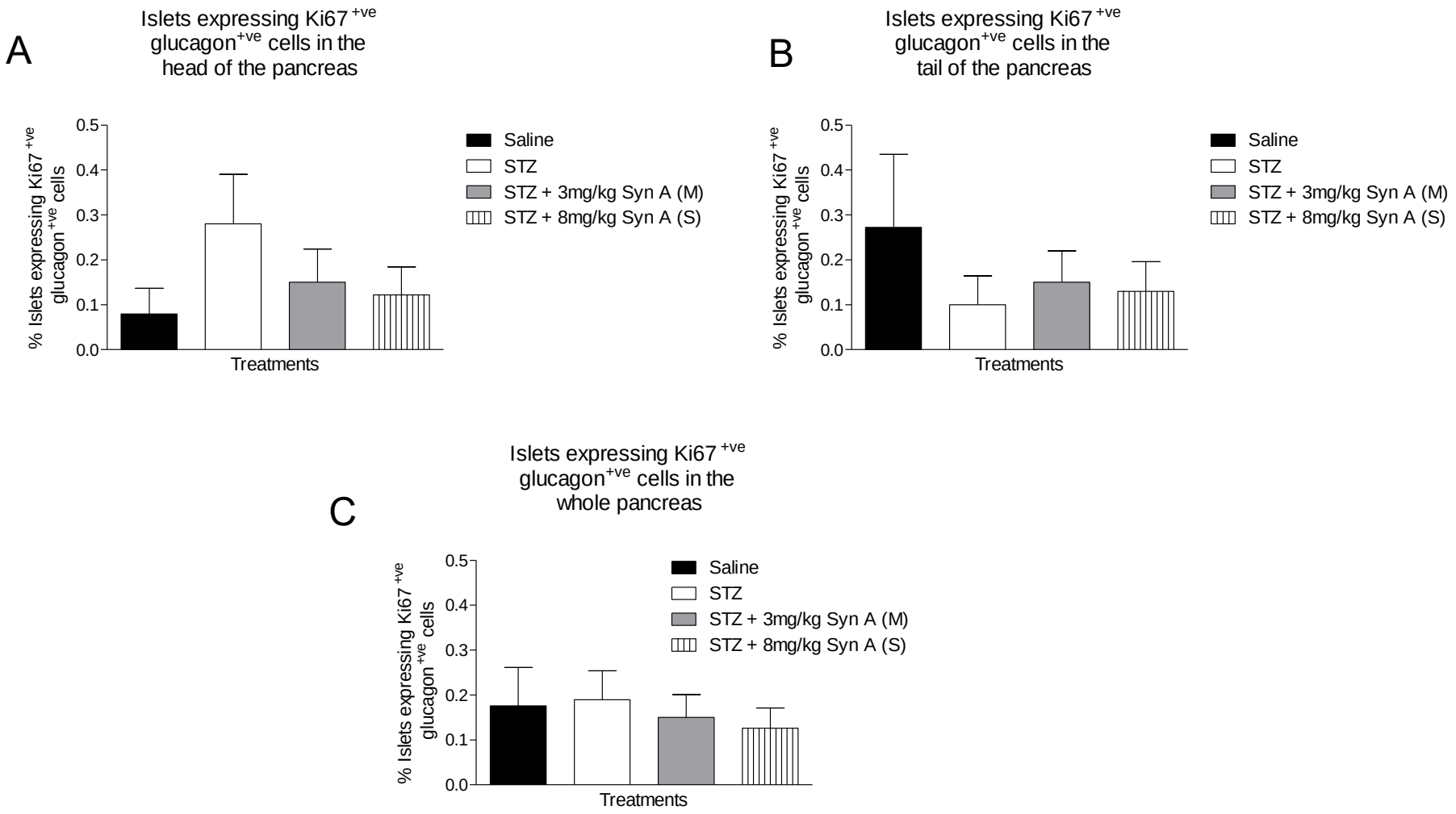

Percentage of islets expressing Ki67^{+ve}, glucagon^{+ve} cells in the head (A), tail (B), and whole (C) pancreas. STZ (50mg/kg) administered by i.p. on days 1-5, 3mg/kg Syn A (m) administered on days10-14, and 8mg/kg (s) administered on day 10. Values are mean ± SEM (n=6 mice). Changes were deemed significant when p values were $p<0.05$.

Figure 6.23 Representative images of saline (A), STZ (B), STZ+ 3mg/kg Syn A (C), and STZ+ 8mg/kg Syn A (D) islets from the pancreas in male Glu^{Cre} mice.

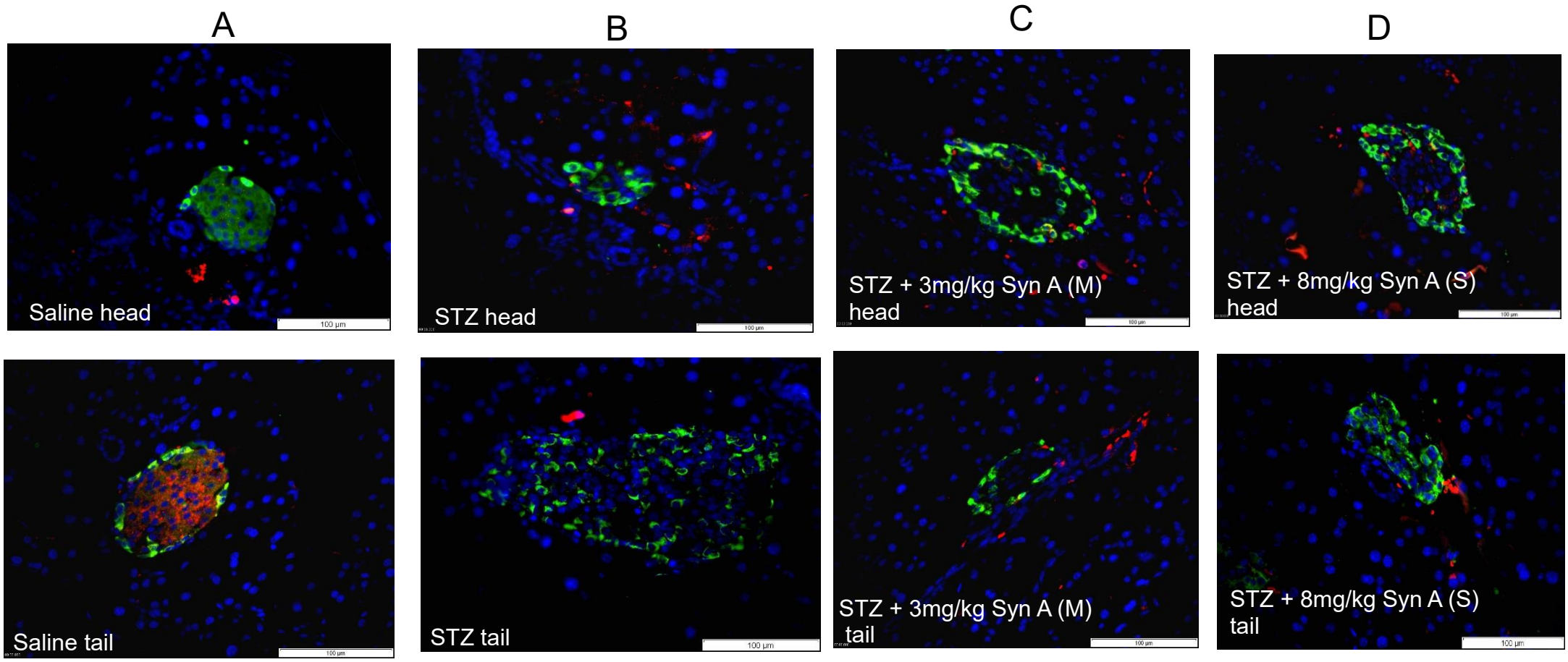

Percentage of alpha cell proliferation was determined by the islets expressing Ki67^{+ve}, glucagon^{+ve} cells in the pancreas. Glucagon is represented in green, Ki67 in red, and DAPI in blue. Images were taken at 40x. Total number of 100 islets were analysed per treatment group.

Figure 6.24 Effects of single or multiple dose of Syn A on Tunel positive, insulin positive cells in male Glu^{Cre} Rosa mice with multiple low dose STZ diabetes after 15 days.

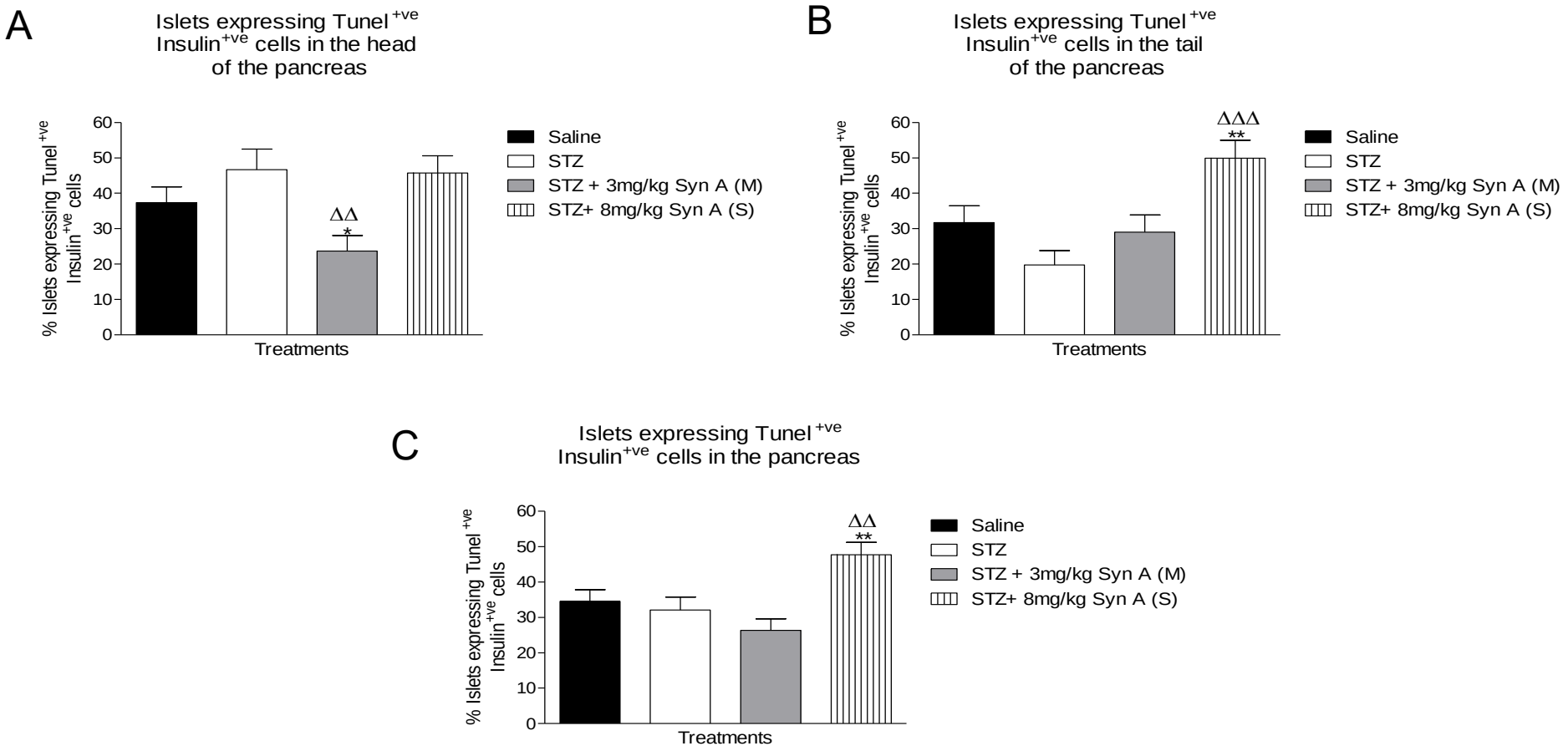

Percentage of islets expressing Tunel^{+ve}, insulin^{+ve} cells in the head (A), tail (B), and whole (C) pancreas. STZ (50mg/kg) administered by i.p. on days 1-5, 3mg/kg Syn A (m) administered on days10-14, and 8mg/kg (s) administered on day 10. Values are mean ± SEM (n=6-7 mice). Changes were deemed significant when p values were *p<0.05 or **p<0.01 when compared with saline treated mice. $^{\Delta\Delta}$ p <0.01 or $^{\Delta\Delta\Delta}$ p <0.001 when STZ was compared with Syn A treated mice.

Figure 6.25 Representative images of saline (A), STZ (B), STZ+ 3mg/kg Syn A (C), and STZ+ 8mg/kg Syn A (D) Tunel^{+ve}, insulin^{+ve} islets from the pancreas in male Glu^{Cre} mice.

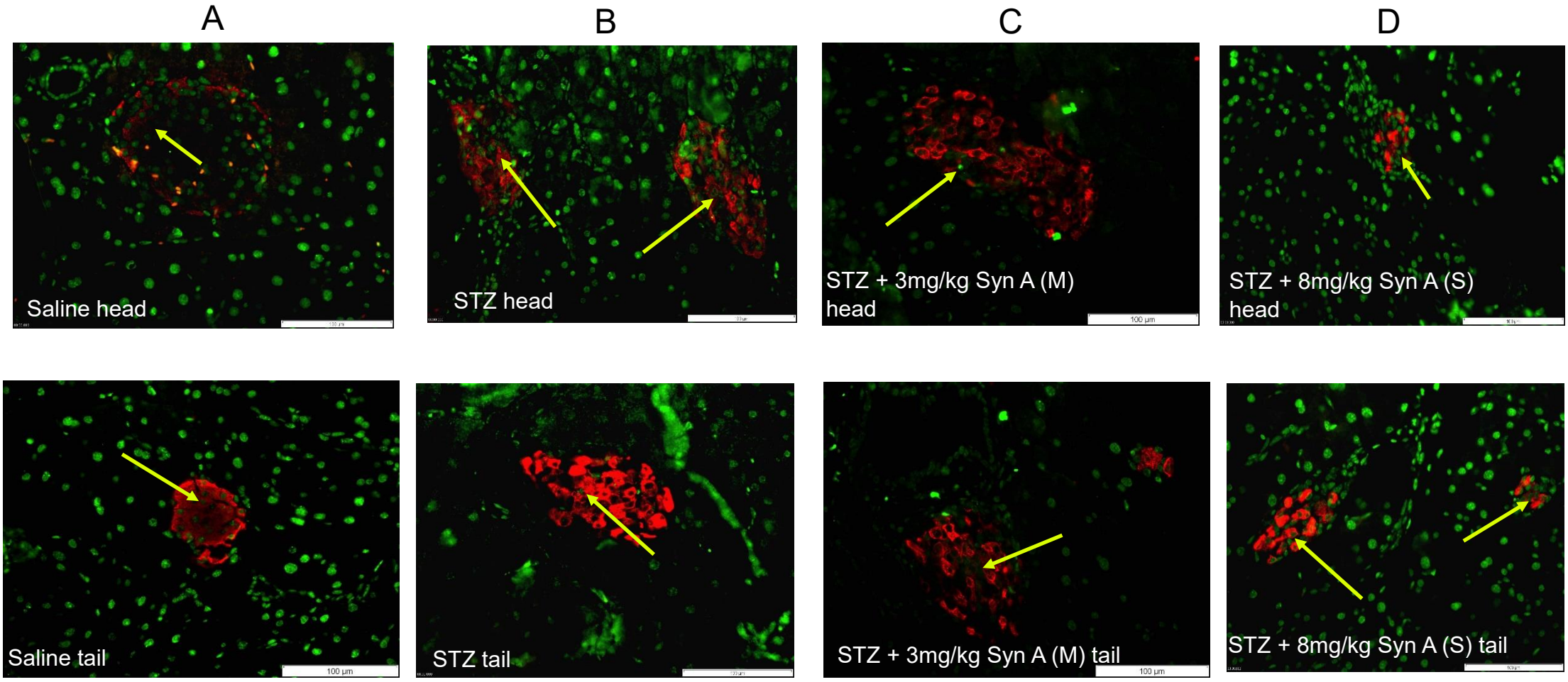

Beta cell apoptosis was determined by the islets expressing Ki67^{+ve}, insulin^{+ve} cells in the pancreas. Saline (A), STZ (B), STZ+ 3mg/kg Syn A (C), and STZ+ 8mg/kg Syn A (D) islets. Tunel is represented in green and insulin in red. The yellow arrows are pointing to Ki67^{+ve}, glucagon^{+ve} cells. Photos imaged at 40x. Total number of 80+ islets were analysed per treatment group.

Figure 6.26 Effects of single or multiple dose of Syn A on Tunel positive, glucagon positive cells in male Glu^{Cre} Rosa mice with multiple low dose STZ diabetes after 15 days.

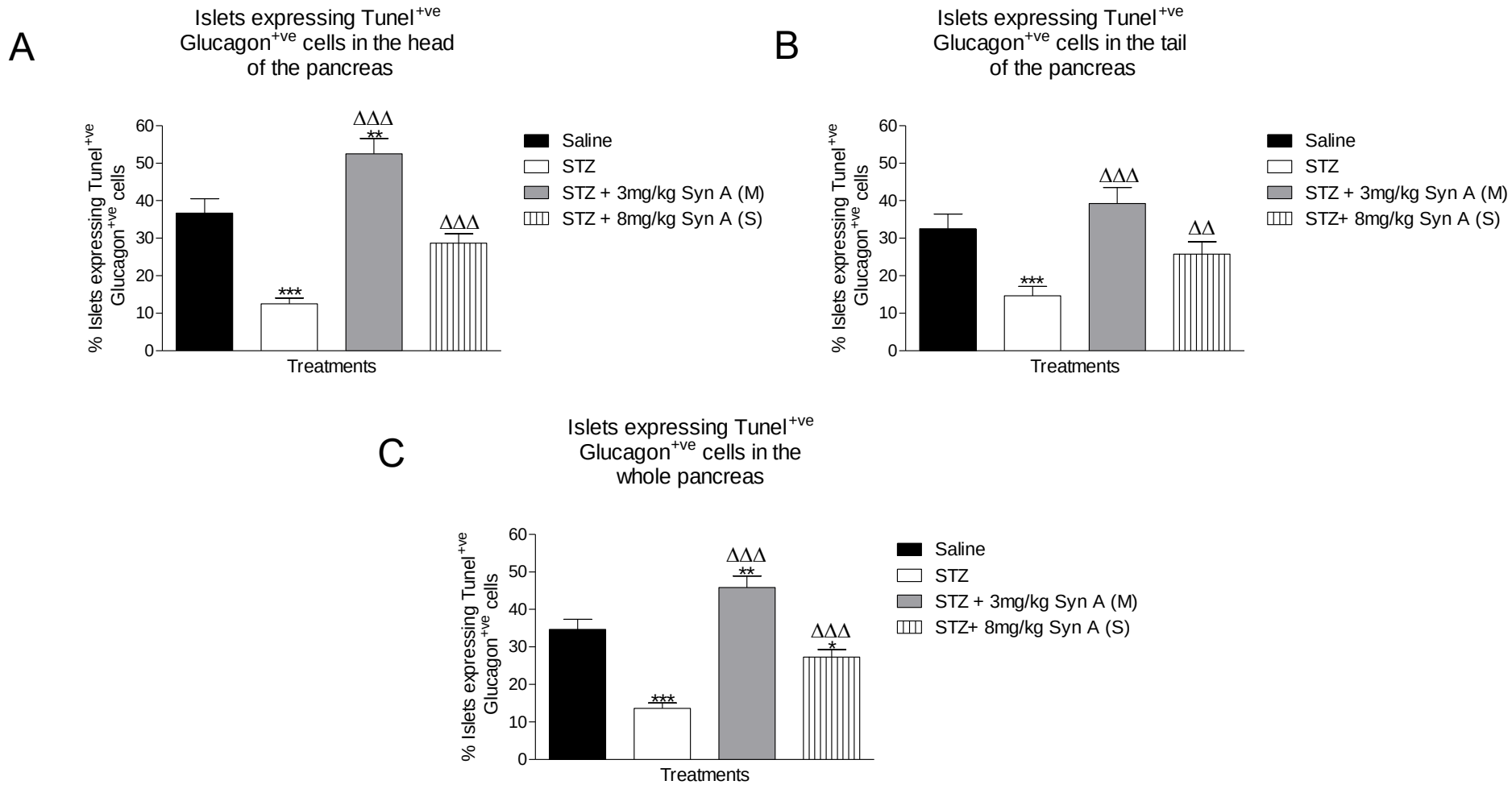

Percentage of islets expressing Tunel^{+ve}, glucagon^{+ve} cells in the head (A), tail (B), and whole (C) pancreas. STZ (50mg/kg) administered by i.p. on days 1-5, 3mg/kg Syn A (m) administered on days10-14, and 8mg/kg (s) administered on day 10. Values are mean ± SEM (n=6-7 mice). Changes were deemed significant when p values were ***p<0.001 when compared saline. $^{\Delta\Delta}$ p <0.01 or $^{\Delta\Delta\Delta}$ p <0.001 when STZ was compared with Syn A treated mice.

Figure 6.27 Representative images of saline (A), STZ (B), STZ+ 3mg/kg Syn A (C), and STZ+ 8mg/kg Syn A (D) Tunel^{+ve}, glucagon^{+ve} islets from the pancreas in male Glu^{Cre} mice.

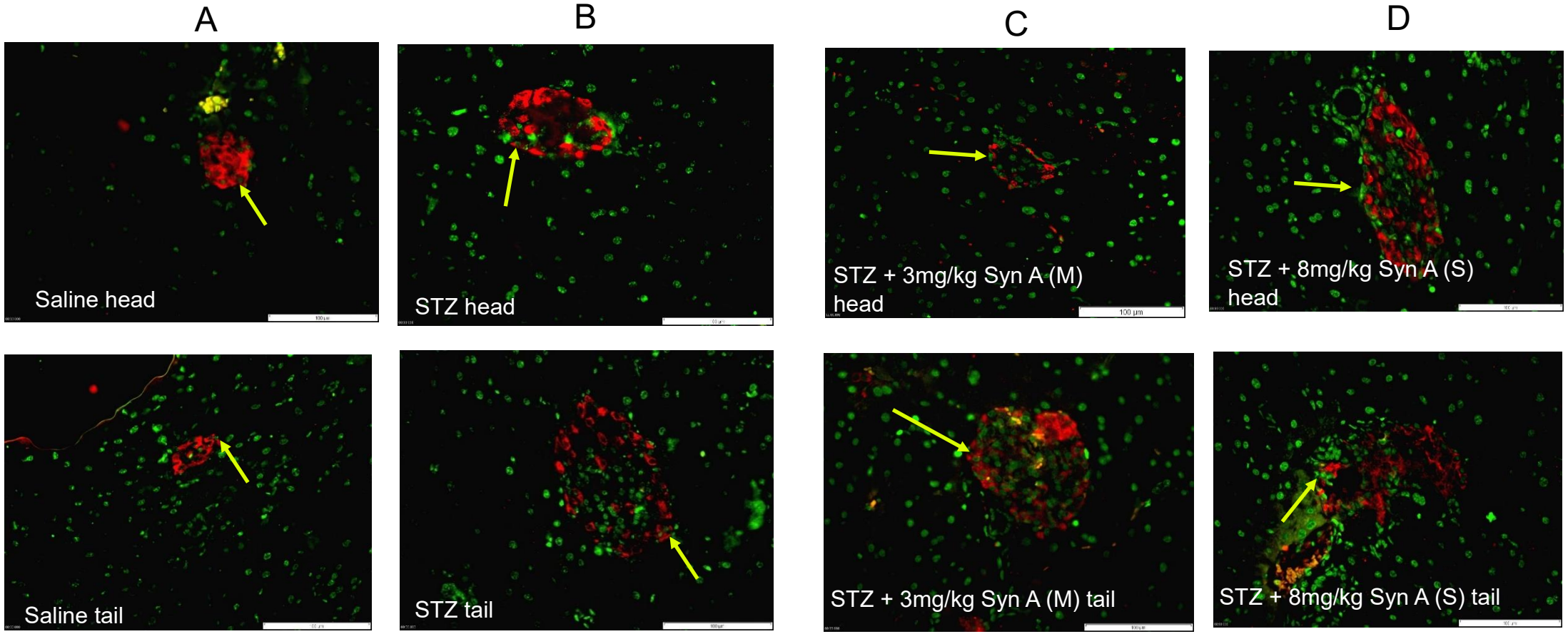

Alpha cell apoptosis was determined by the islets expressing Ki67^{+ve}, glucagon^{+ve} cells in the pancreas. Saline (A), STZ (B), STZ+ 3mg/kg Syn A (C), and STZ+ 8mg/kg Syn A (D) islets. Tunel is represented in green and glucagon in red. The yellow arrows are pointing to Ki67^{+ve}, glucagon^{+ve} cells. Photos imaged at 40x. Total number of 80+ islets were analysed per treatment group.

Figure 6.28 Effects of single or multiple dose of Syn A on body weight (A), weight change (B), and blood glucose (C) in female Glu^{Cre} Rosa mice with multiple low dose STZ diabetes over 23 days.

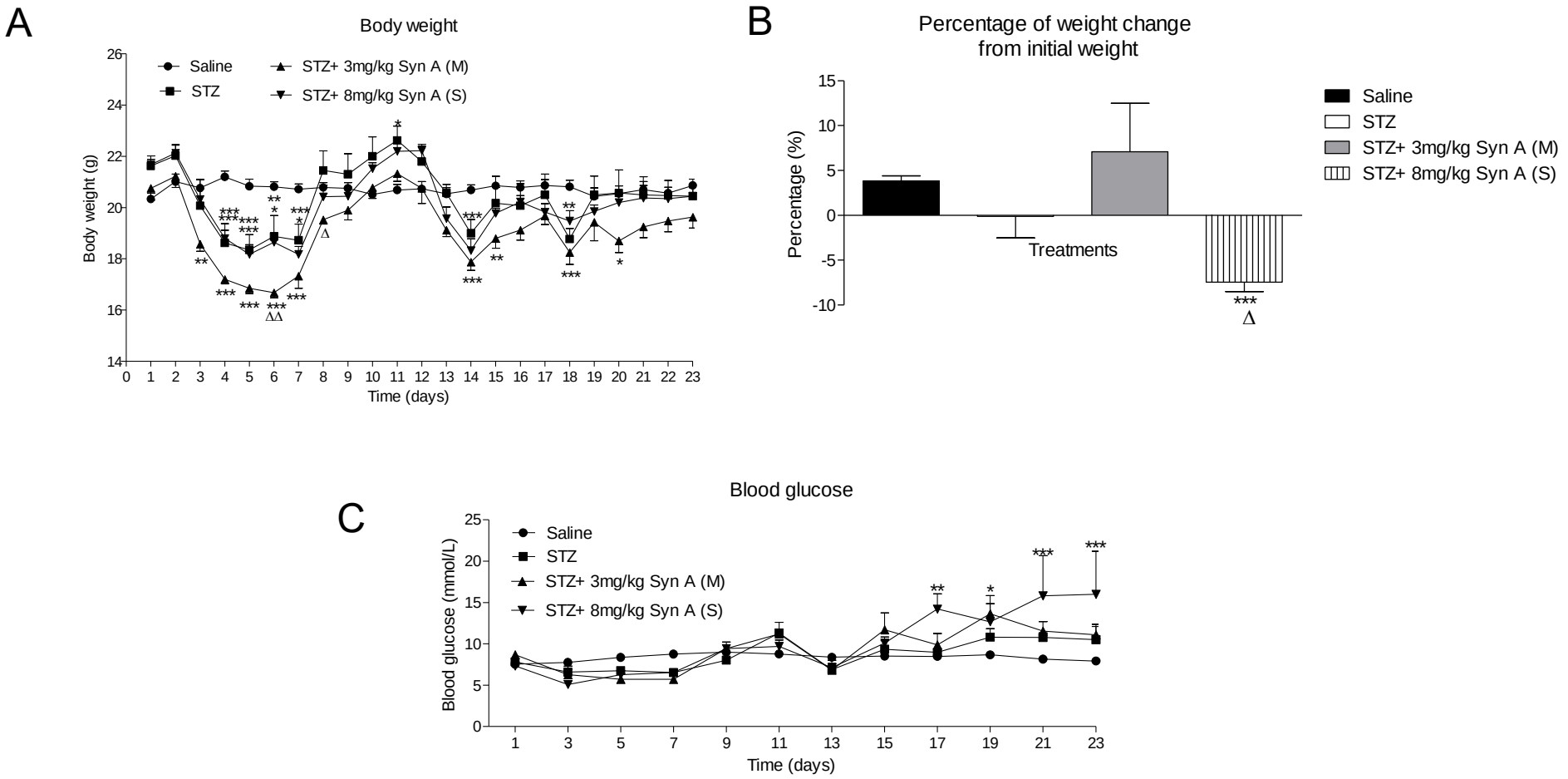

Body weight (A), percentage of body weight change (B), and blood glucose (C) over the course of 23 days in female Glu^{Cre} mice. STZ (50mg/kg) administered by i.p. on days 1-5, STZ (150mg/kg) administered on day 12, and STZ (200mg/kg) administered on day 15. 3mg/kg Syn A (m) administered on days18-22, and 8mg/kg (s) administered on day 15. Values are mean ± SEM (n=4-6 mice). Changes were deemed significant when p values were *p<0.05, **p <0.01, or ***p<0.001 when compared with saline. $^{\Delta}$ p<0.05 or $^{\Delta\Delta}$ p<0.01 when STZ was compared with Syn A treated mice.

Figure 6.29 Effects of single or multiple dose of Syn A on food (A) and fluid (B) intake in female Glu^{Cre} Rosa mice with multiple low dose STZ diabetes over 23 days.

A

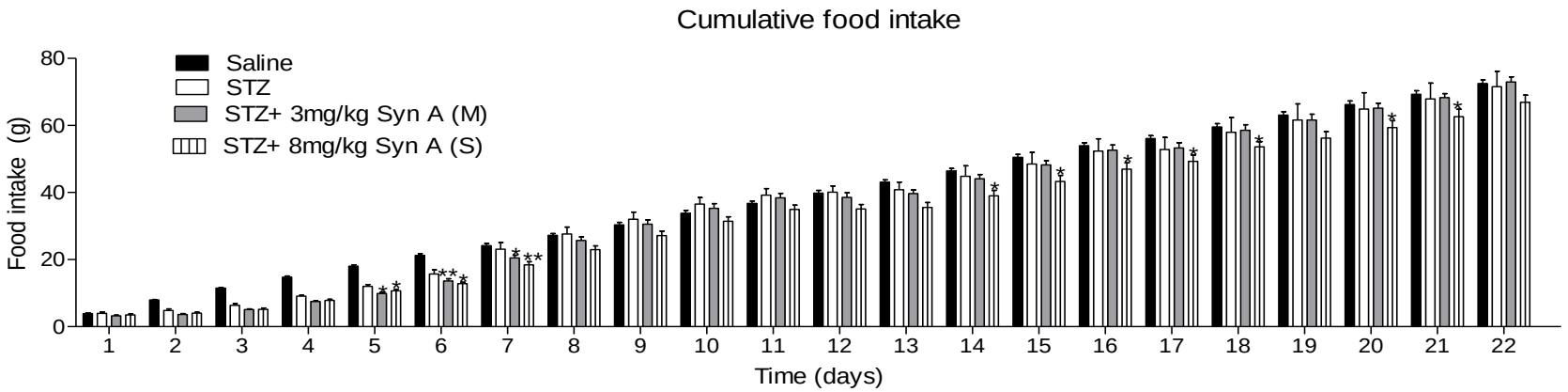

B

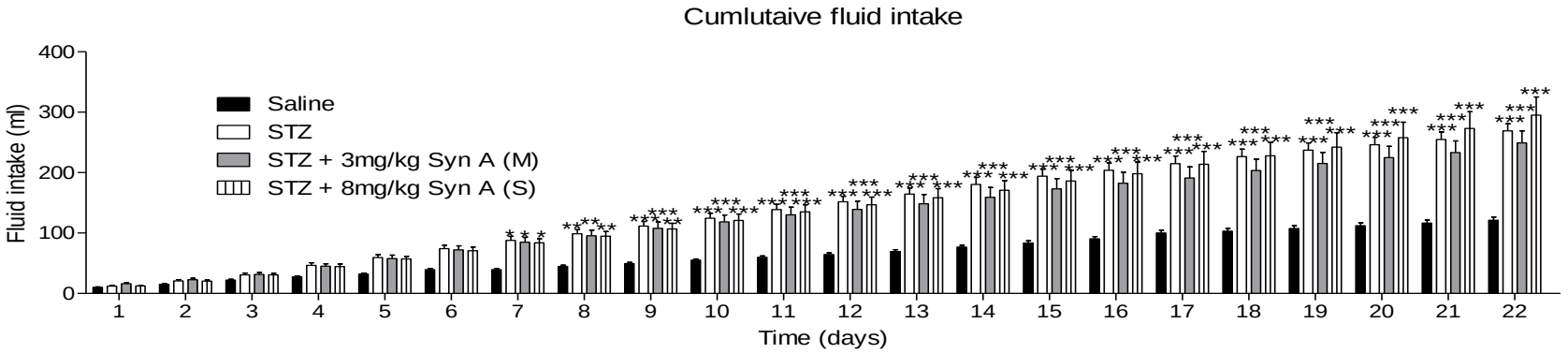

Cumulative food (A) and fluid (B) intake over the course of 23 days in female Glu^{Cre} Rosa mice. STZ (50mg/kg) administered by i.p. on days 1-5, STZ (150mg/kg) administered on day 12, and STZ (200mg/kg) administered on day 15. 3mg/kg Syn A (m) administered on days18-22, and 8mg/kg (s) administered on day 15. Values are mean ± SEM (n=4-6 mice). Changes were deemed significant when p values were *p<0.05, **p <0.01, or ***p<0.001 when compared with saline.

Figure 6.30 Effects of single or multiple dose of Syn A on nonfasting (A) and fasting (B) plasma in female Glu^{Cre} mice with multiple low dose STZ diabetes on the final day of the study.

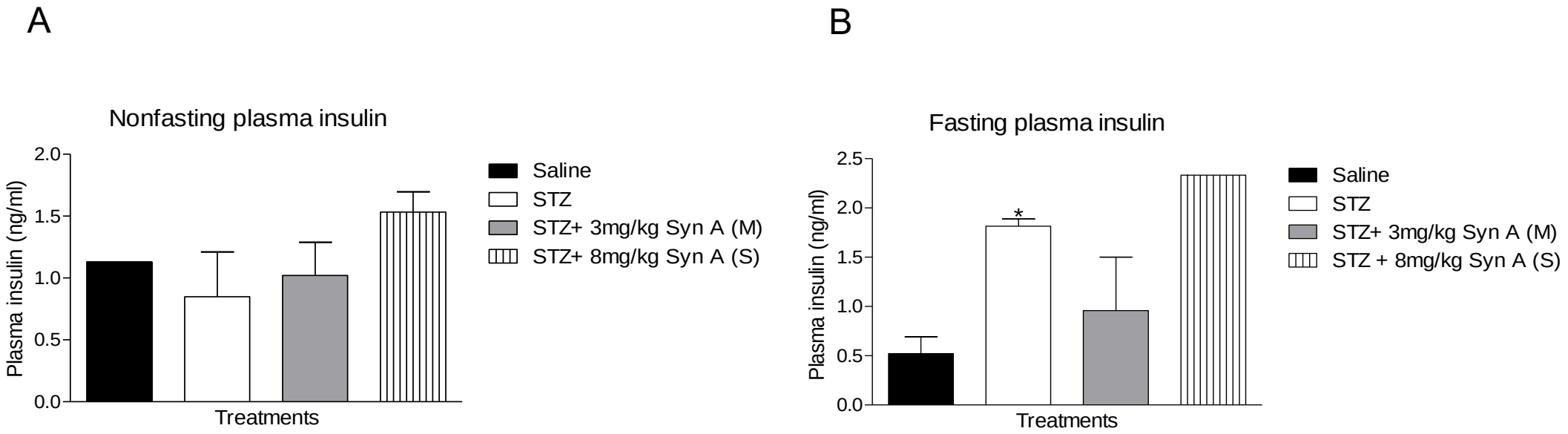

Nonfasting (A) and fasting (B) blood was taken at the end of the study. STZ (50mg/kg) administered by i.p. on days 1-5, STZ (150mg/kg) administered on day 12, and STZ (200mg/kg) administered on day 15. 3mg/kg Syn A (m) administered on days18-22, and 8mg/kg (s) administered on day 15. Plasma insulin was measured by RIA. Values are mean ± SEM (n= 4-6 mice). Changes were deemed significant when p values were *p <0.05 when compared with saline.

Figure 6.31 Effects of single or multiple dose of Syn A on pancreatic insulin content from the head (A), tail (B), and whole (C) pancreas in female Glu^{Cre} mice with multiple low dose STZ diabetes after 23 days.

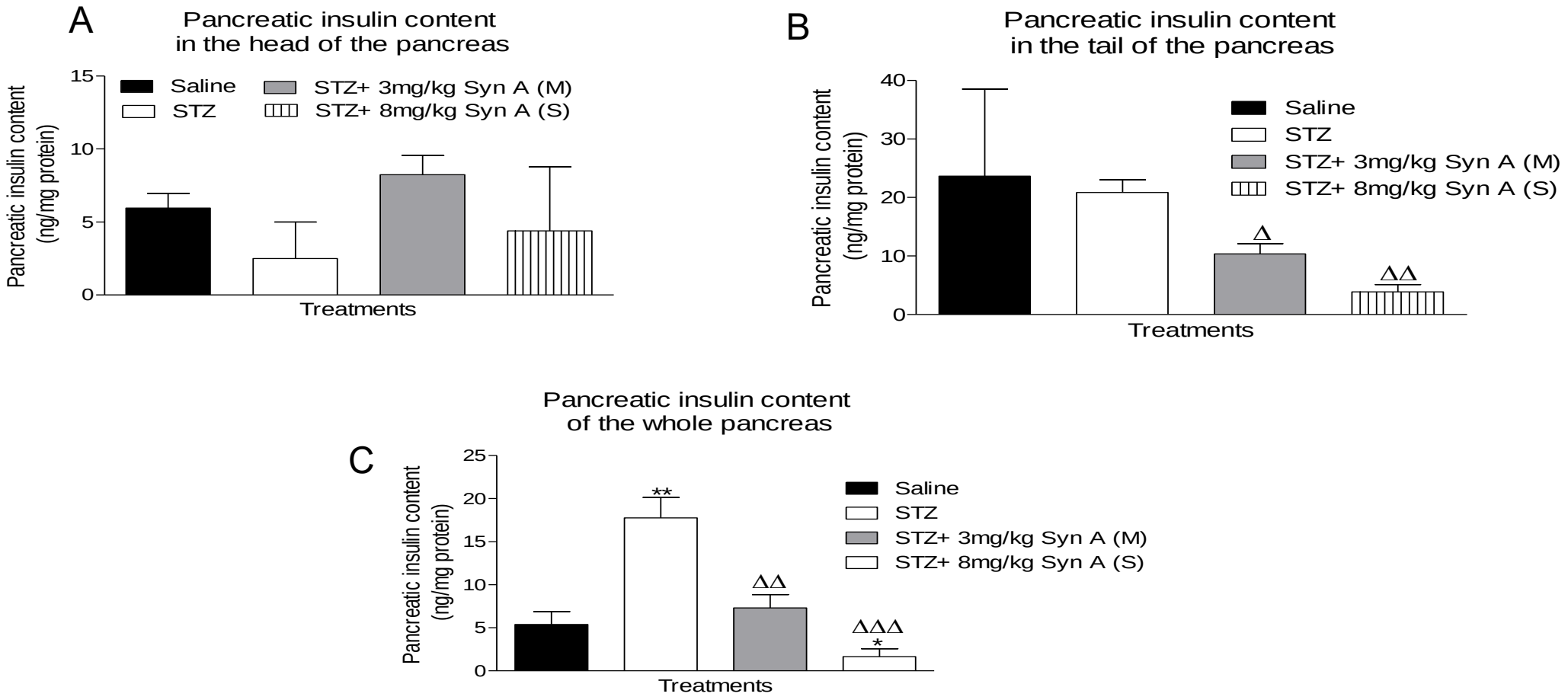

Pancreatic insulin content from the head (A), tail (B), and whole (C) flash frozen pancreas. STZ (50mg/kg) administered by i.p. on days 1-5, STZ (150mg/kg) administered on day 12, and STZ (200mg/kg) administered on day 15. 3mg/kg Syn A (m) administered on days18-22, and 8mg/kg (s) administered on day 15. Values are mean ± SEM (n=4- 6 mice). Changes were deemed significant when p values were *p <0.05 or **p<0.01 when compared with saline. $^{\Delta}$ p<0.05, $^{\Delta\Delta}$ p<0.01, or $^{\Delta\Delta\Delta}$ p<0.001 when STZ was compared with Syn A treated mice.

Figure 6.32 Effects of single or multiple dose of Syn A on number of islets (A), islet area (B), and islet size distribution (C) in the head of the pancreas of female Glu^{Cre} Rosa mice with multiple low dose STZ diabetes after 23 days.

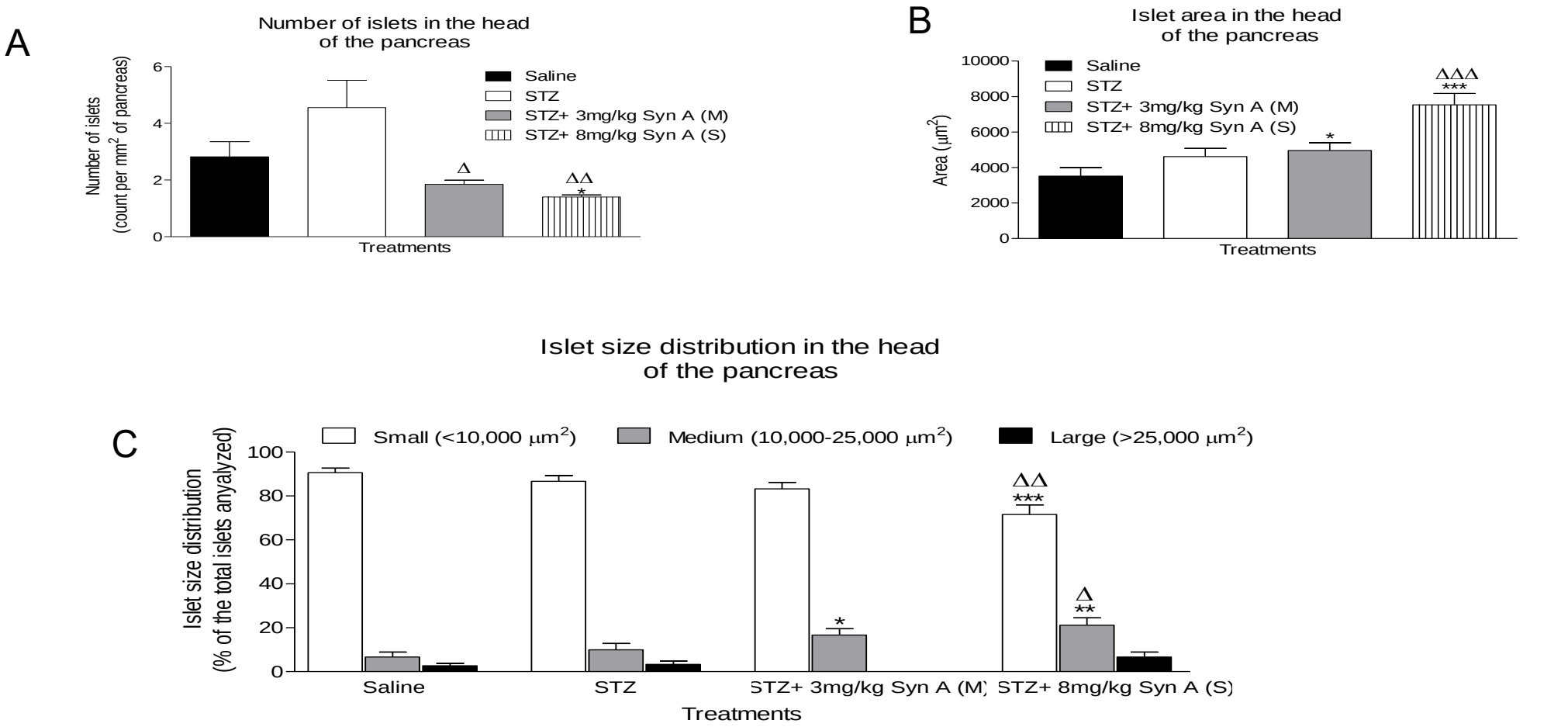

Number of islets (A), islet area (B), and islet size distribution (C) per pancreas in female Glu^{Cre} Rosa mice. STZ (50mg/kg) administered by i.p. on days 1-5, STZ (150mg/kg) administered on day 12, and STZ (200mg/kg) administered on day 15. 3mg/kg Syn A (m) administered on days18-22, and 8mg/kg (s) administered on day 15. Values are mean ± SEM (n=4-6 mice). Changes were deemed significant when p values were *p <0.05, **p<0.01, or ***p<0.001 when compared with saline. $^{\Delta}$p<0.05, $^{\Delta\Delta}$p<0.01, or $^{\Delta\Delta\Delta}$ p<0.001 when STZ was compared with Syn A treated mice.

Figure 6.33 Effects of single or multiple dose of Syn A on number of islets (A), islet area (B), and islet size distribution (C) in the tail of the pancreas of female Glu^{Cre} Rosa mice with multiple low dose STZ diabetes after 23 days.

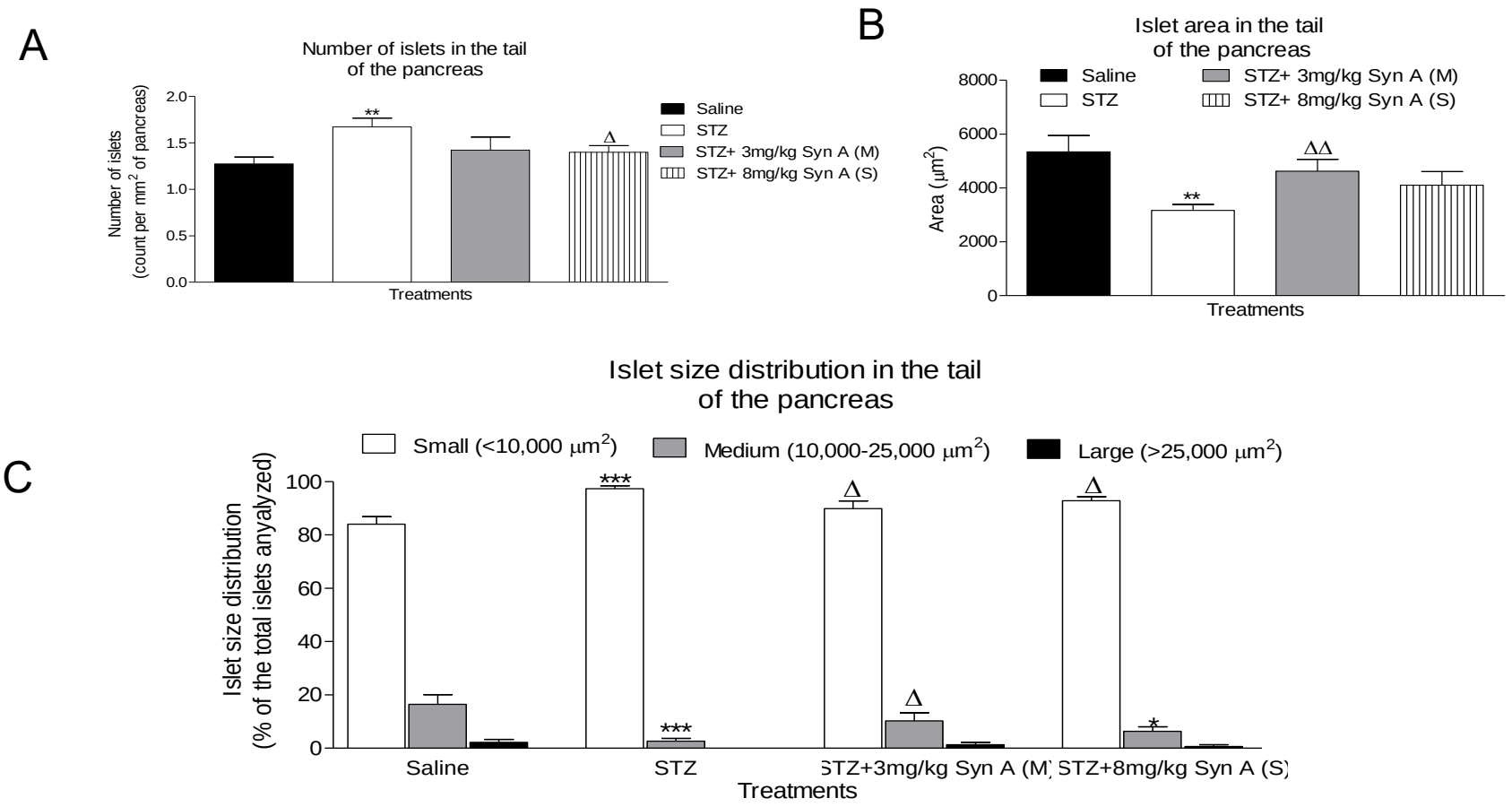

Number of islets (A), islet area (B), and islet size distribution (C) per pancreas in female Glu^{Cre} Rosa mice. STZ (50mg/kg) administered by i.p. on days 1-5, STZ (150mg/kg) administered on day 12, and STZ (200mg/kg) administered on day 15. 3mg/kg Syn A (m) administered on days18-22, and 8mg/kg (s) administered on day 15. Values are mean ± SEM (n=4-6 mice). Changes were deemed significant when p values were *p <0.05, **p<0.01, or ***p<0.001 when compared with saline. $^{\Delta}$ p<0.05 or $^{\Delta\Delta}$p<0.01 when STZ was compared with Syn A treated mice.

Figure 6.34 Effects of single or multiple dose of Syn A on number of islets (A), islet area (B), and islet size distribution (C) in the whole pancreas of female Glu^{Cre} Rosa mice with multiple low dose STZ diabetes after 23 days.

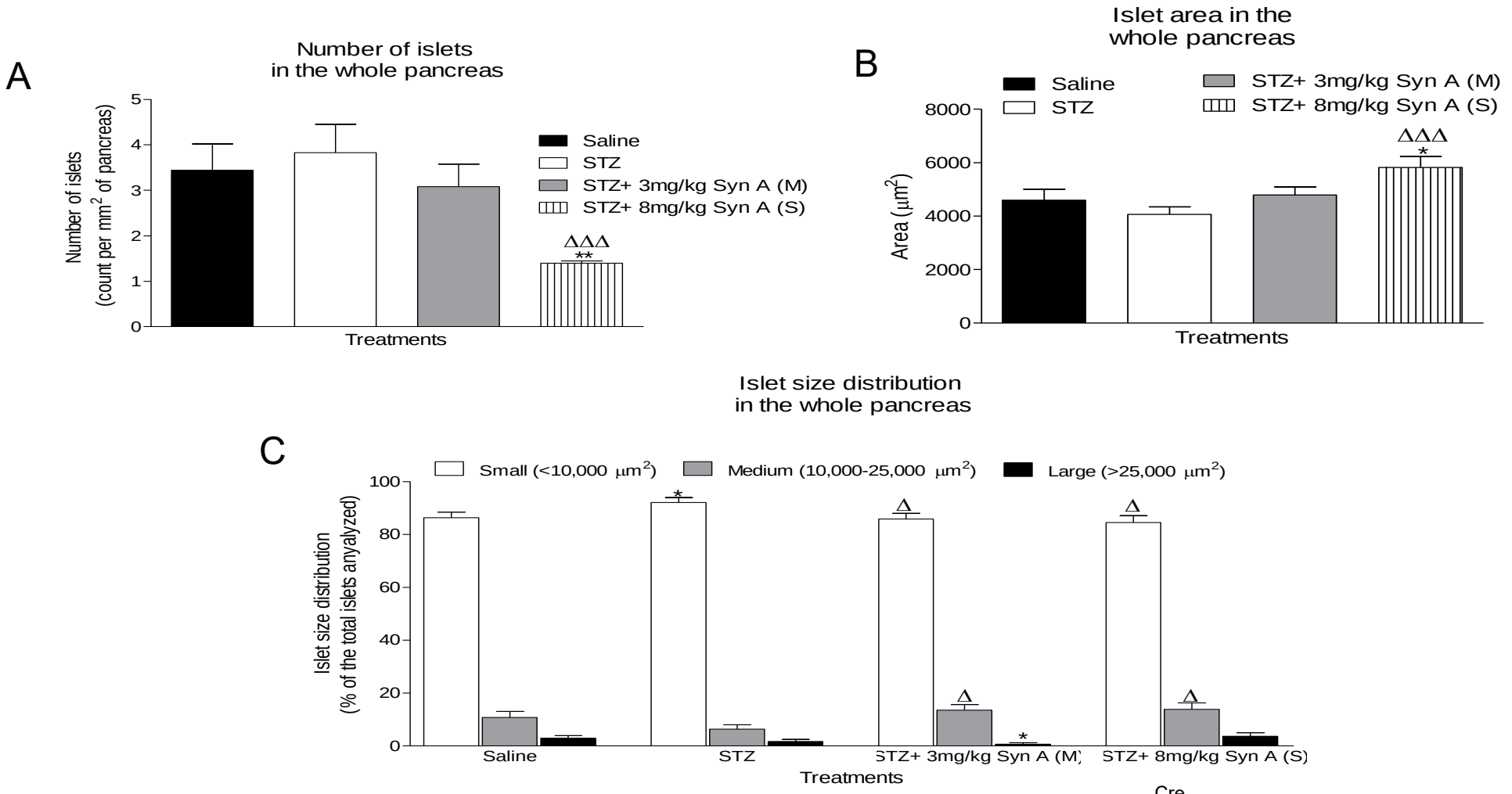

Number of islets (A), islet area (B), and islet size distribution (C) per pancreas in female Glu^{Cre} Rosa mice. STZ (50mg/kg) administered by i.p. on days 1-5, STZ (150mg/kg) administered on day 12, and STZ (200mg/kg) administered on day 15. 3mg/kg Syn A (m) administered on days18-22, and 8mg/kg (s) administered on day 15. Values are mean ± SEM (n=4-6 mice). Changes were deemed significant when p values were *p <0.05, **p<0.01, or ***p<0.001 when compared with saline. $^{\Delta}$ p<0.05 or $^{\Delta\Delta\Delta}$ p<0.001 when STZ was compared with Syn A treated mice.

Figure 6.35 Effects of single or multiple dose of Syn A on alpha cell area and percentage (A and B) and beta cell area and percentage (C and D) in the head of the pancreas of female Glu^{Cre} Rosa mice with multiple low dose STZ diabetes after 23 days.

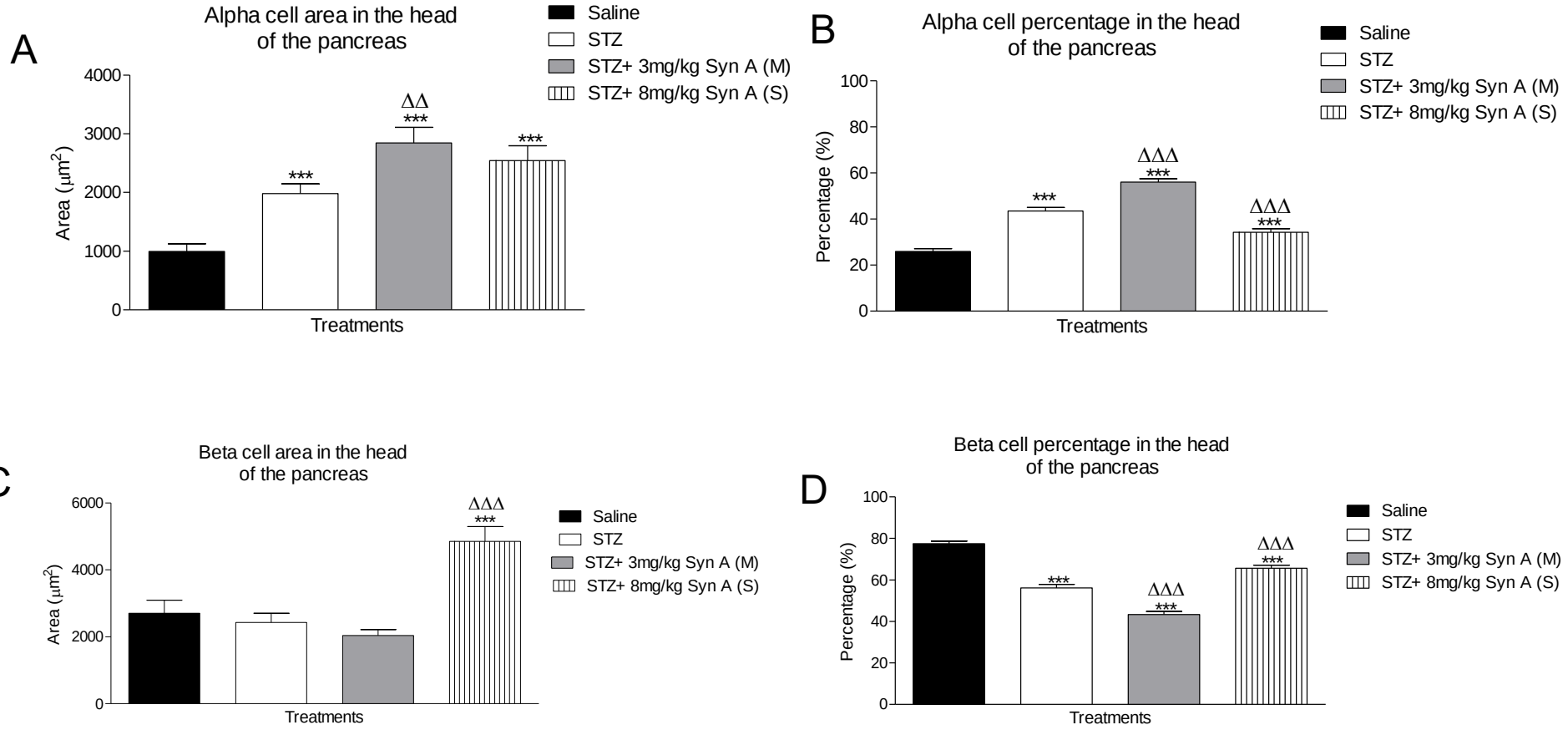

Alpha cell area and percentage (A and B) and beta cell area and percentage (C and D) per pancreas in female Glu^{Cre} Rosa mice. STZ (50mg/kg) administered by i.p. on days 1-5, STZ (150mg/kg) administered on day 12, and STZ (200mg/kg) administered on day 15. 3mg/kg Syn A (m) administered on days18-22, and 8mg/kg (s) administered on day 15. Values are mean ± SEM (n=4-6 mice). Changes were deemed significant when p values were ***$p<0.001$ when compared with saline. $^{\Delta\Delta}p<0.01$ or $^{\Delta\Delta\Delta}p<0.001$ when STZ was compared with Syn A treated mice.

Figure 6.36 Effects of single or multiple dose of Syn A on alpha cell area and percentage (A and B) and beta cell area and percentage (C and D) in the tail of the pancreas of female Glu^{Cre} Rosa mice with multiple low dose STZ diabetes after 23 days.

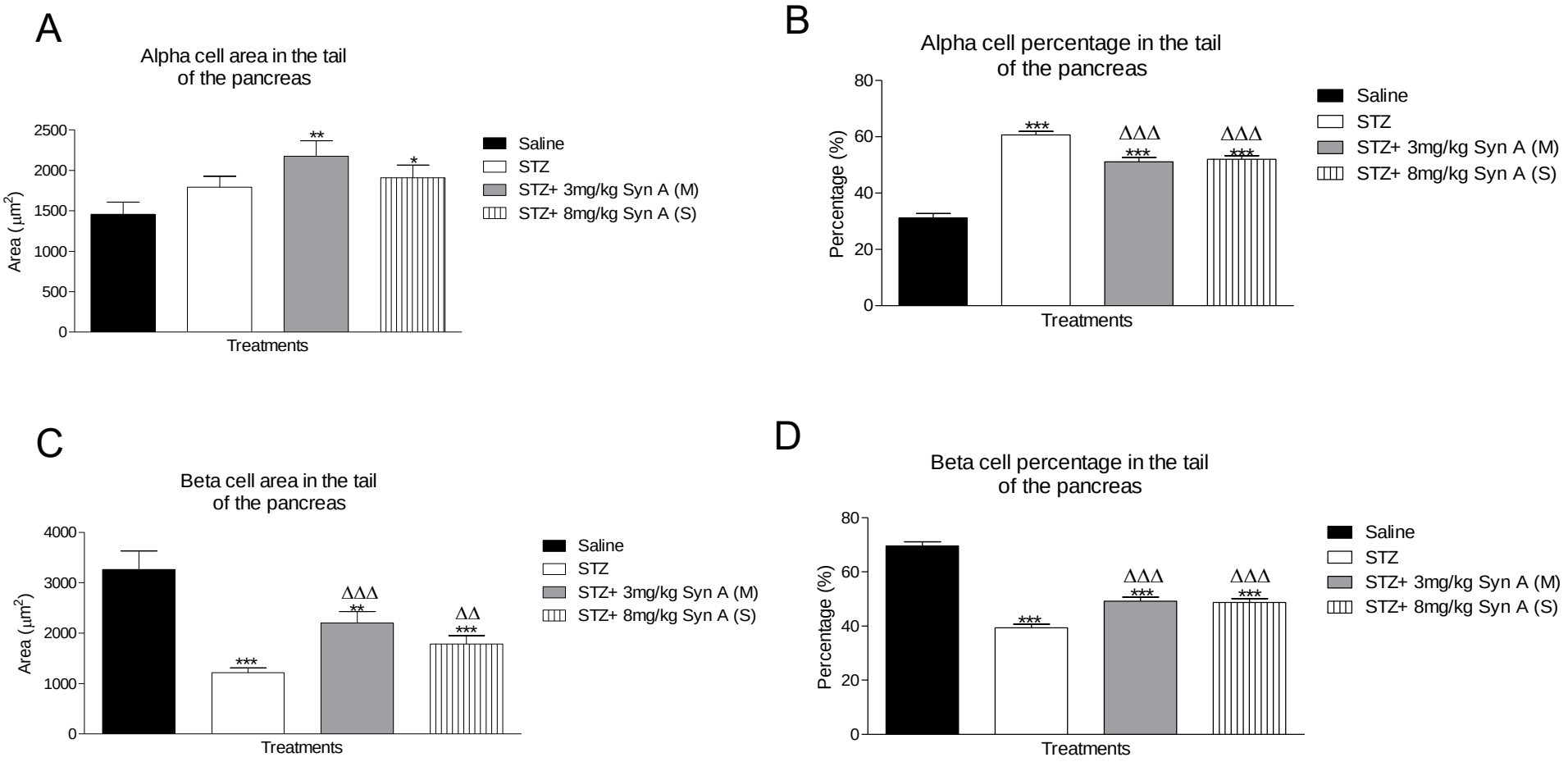

Alpha cell area and percentage (A and B) and beta cell area and percentage (C and D) in tail of pancreas in female Glu^{Cre} Rosa mice. STZ (50mg/kg) administered by i.p. on days 1-5, STZ (150mg/kg) administered on day 12, and STZ (200mg/kg) administered on day 15. 3mg/kg Syn A (m) administered on days18-22, and 8mg/kg (s) administered on day 15. Values are mean ± SEM (n=4-6 mice). Changes were deemed significant when p values were *p<0.05, **p<0.01, or ***p<0.001 when compared with saline. $^{\Delta\Delta}$ p<0.01 or $^{\Delta\Delta\Delta}$ p<0.001 when STZ was compared with Syn A treated mice.

Figure 6.37 Effects of single or multiple dose of Syn A on alpha cell area and percentage (A and B) and beta cell area and percentage (C and D) in the whole pancreas of female Glu^{Cre} Rosa mice with multiple low dose STZ diabetes after 23 days.

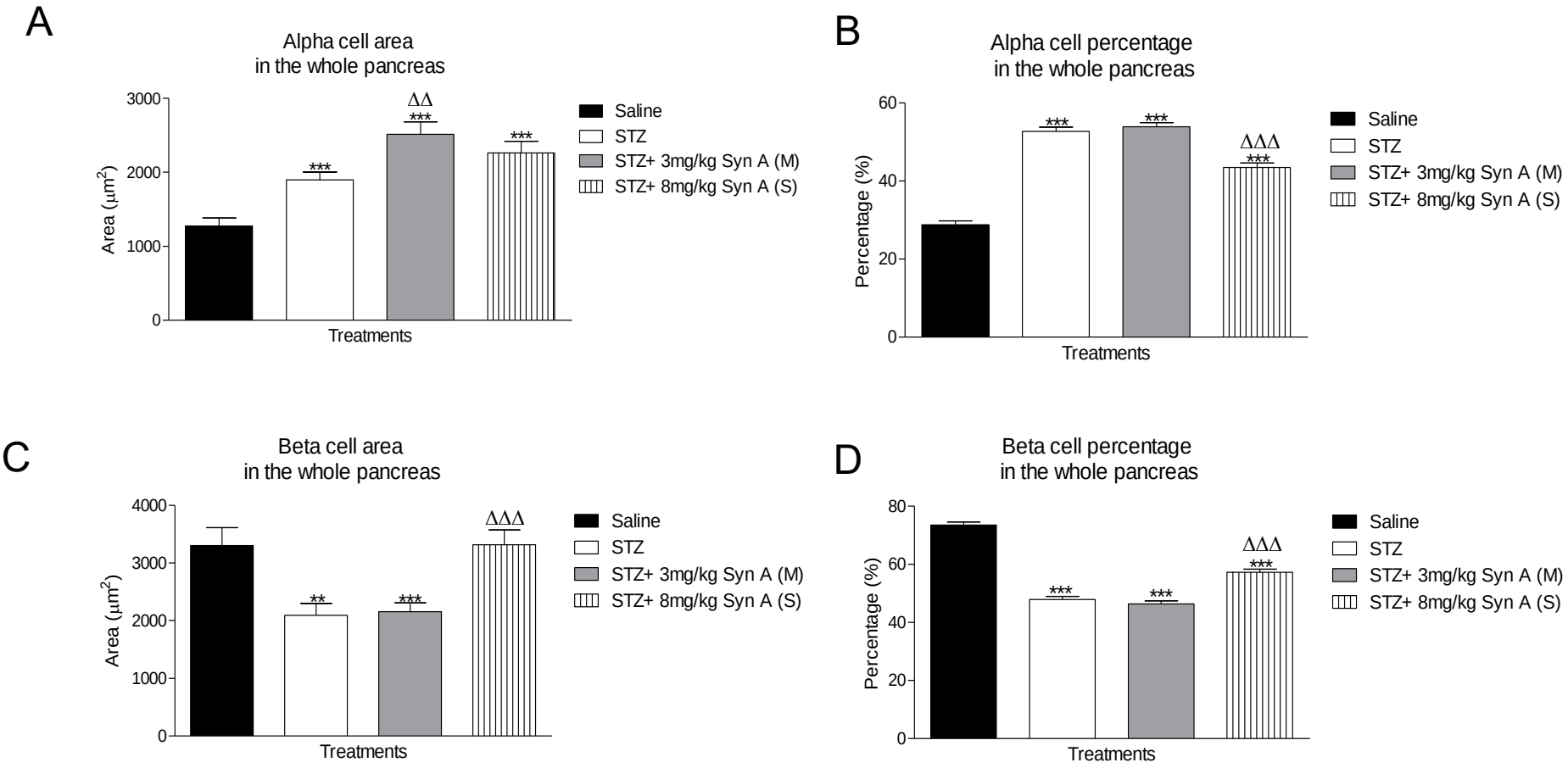

Alpha cell area and percentage (A and B) and beta cell area and percentage (C and D) per pancreas in female Glu^{Cre} Rosa mice. STZ (50mg/kg) administered by i.p. on days 1-5, STZ (150mg/kg) administered on day 12, and STZ (200mg/kg) administered on day 15. 3mg/kg Syn A (m) administered on days18-22, and 8mg/kg (s) administered on day 15. Values are mean ± SEM (n=4-6 mice). Changes were deemed significant when p values were **p<0.01 or ***p<0.001 when compared with saline. $^{\Delta\Delta}$p<0.01 or $^{\Delta\Delta\Delta}$ p<0.001 when STZ was compared with Syn A treated mice.

Figure 6.38 Representative images of saline (A), STZ (B), STZ+ 3mg/kg Syn A (C), and STZ+ 8mg/kg Syn A (D) islets from the pancreas in female Glu^{Cre} mice.

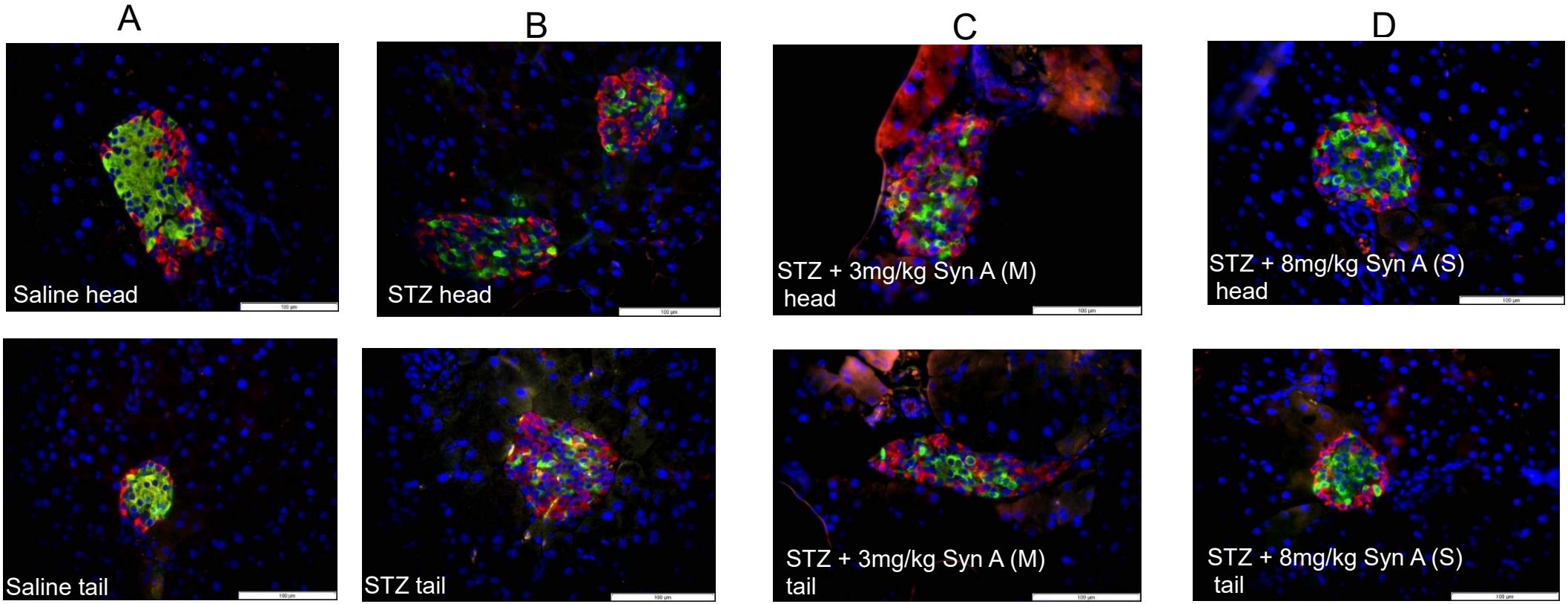

Islet morphology was evaluated at the end of the 23-day study on 5-7µm sections. Islet morphology. Saline (A), STZ (B), STZ+ 3mg/kg Syn A (C), and STZ+ 8mg/kg Syn A (D) islets. Insulin is represented in green, glucagon in red, and DAPI in blue. Photos imaged at 40x. Total of 150 islets were analysed per treatment group.

Figure 6.39 Effects of single or multiple dose of Syn A on GFP positive, insulin positive cells in the head (A), tail (B), and whole (C) pancreas in female Glu^{Cre} Rosa mice with multiple low dose STZ diabetes after 23 days.

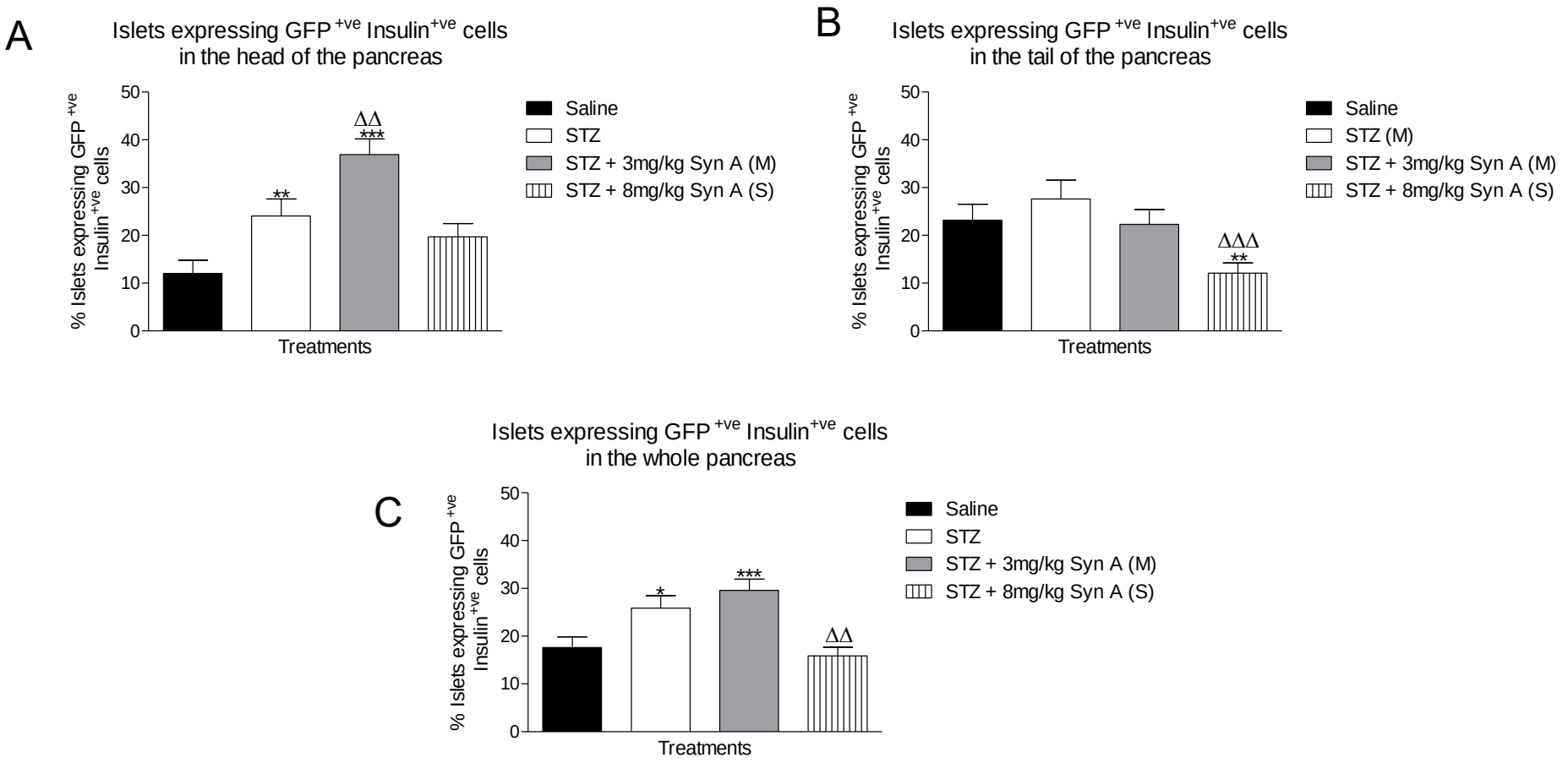

Percentage of islets expressing GFP^{+ve}, insulin^{+ve} cells in the head (A), tail (B), and whole (C) pancreas. STZ (50mg/kg) administered by i.p. on days 1-5, STZ (150mg/kg) administered on day 12, and STZ (200mg/kg) administered on day 15. 3mg/kg Syn A (m) administered on days18-22, and 8mg/kg (s) administered on day 15. Values are mean ± SEM (4-6 mice). Changes were deemed significant when p values were *p<0.05, **p<0.01, ***p<0.001 when compared with saline. $^{\Delta\Delta}$p<0.01 or $^{\Delta\Delta\Delta}$p<0.001 when STZ was compared with Syn A treated mice.

Figure 6.40 Representative images of saline (A), STZ (B), STZ+ 3mg/kg Syn A (C), and STZ+ 8mg/kg Syn A (D) islets from the pancreas in female Glu^{Cre} mice.

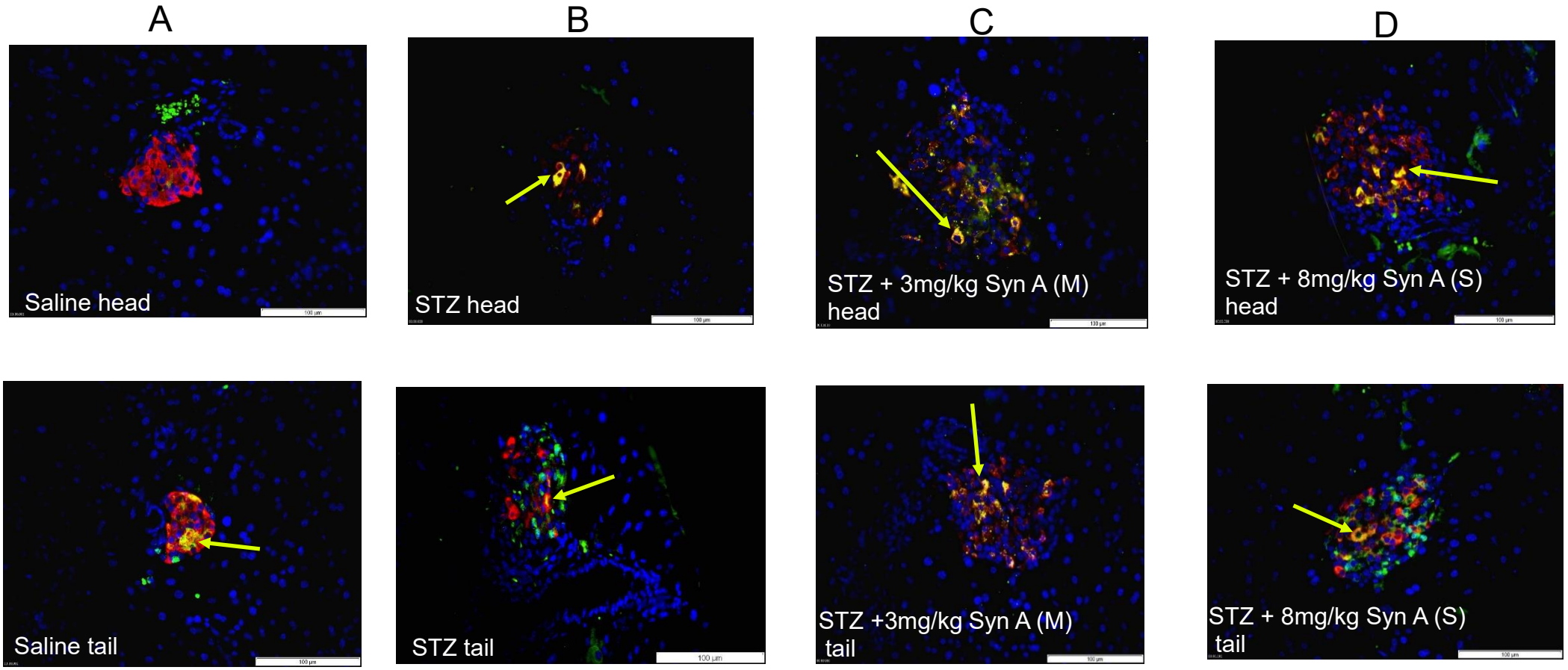

Percentage of transdifferentiation was determined by the islets expressing GFP^{+ve}, insulin^{+ve} cells. Insulin is represented in red, GFP in green, yellow represents GFP^{+ve}, insulin^{+ve} cells, and DAPI in blue. The yellow arrows are pointing to GFP^{+ve}, insulin^{+ve} cells. Images were taken at 40x. Total number of 100 islets were analysed per treatment group.

Figure 6.41 Effects of single or multiple dose of Syn A on GFP positive, insulin negative cells in the head (A), tail (B), and whole (C) pancreas in female Glu^{Cre} Rosa mice with multiple low dose STZ diabetes after 23 days.

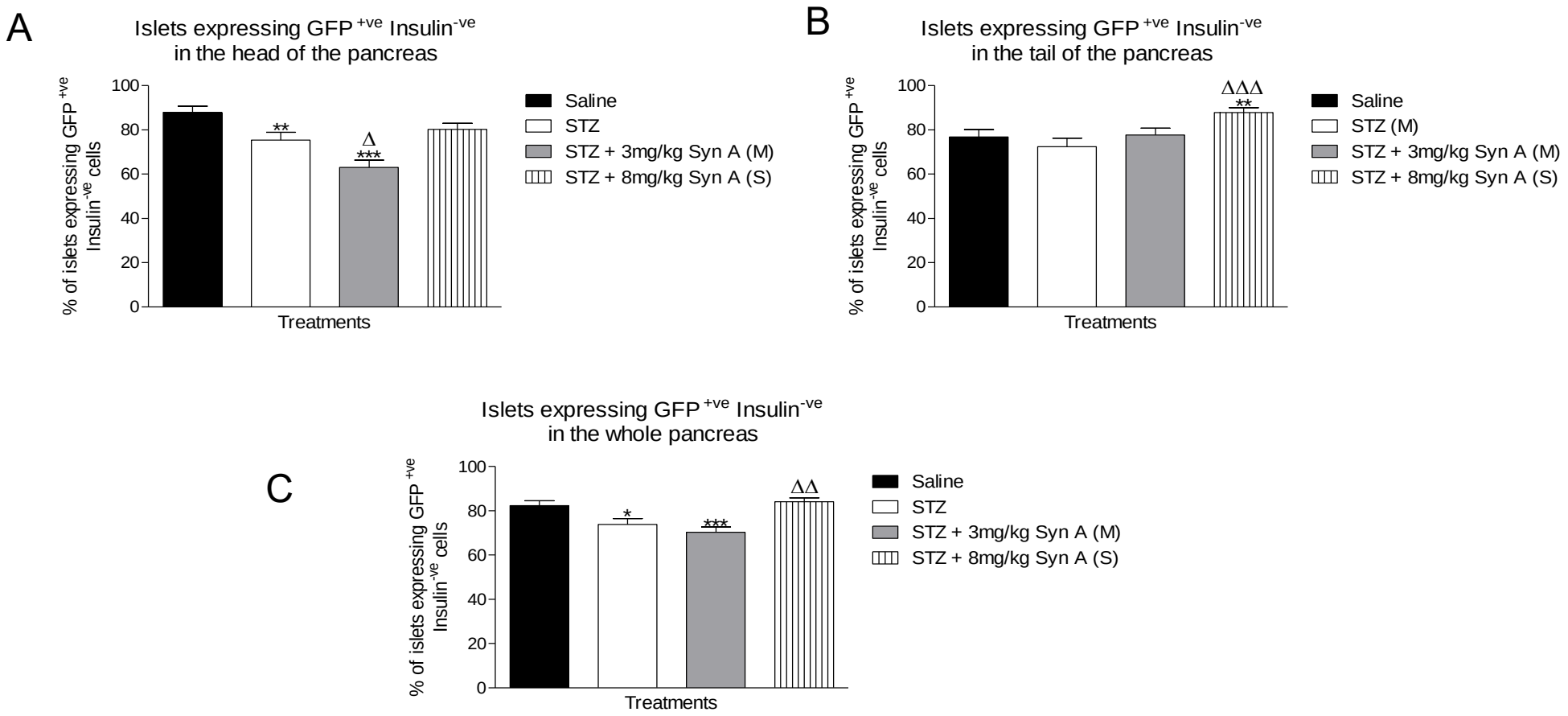

Percentage of islets expressing GFP^{+ve}, insulin^{-ve} cells in the head (A), tail (B), and whole (C) pancreas. STZ (50mg/kg) administered by i.p. on days 1-5, STZ (150mg/kg) administered on day 12, and STZ (200mg/kg) administered on day 15. 3mg/kg Syn A (m) administered on days18-22, and 8mg/kg (s) administered on day 15. Values are mean ± SEM (4-6 mice). Changes were deemed significant when p values were *p<0.05, **p<0.01, ***p<0.001 when compared with saline. $^{\Delta}$p<0.05, $^{\Delta\Delta}$p<0.01, $^{\Delta\Delta\Delta}$p<0.001 when STZ was compared with Syn A treated mice.

Figure 6.42 Representative images of saline (A), STZ (B), STZ+ 3mg/kg Syn A (C), and STZ+ 8mg/kg Syn A (D) islets from the pancreas in female Glu^{Cre} mice.

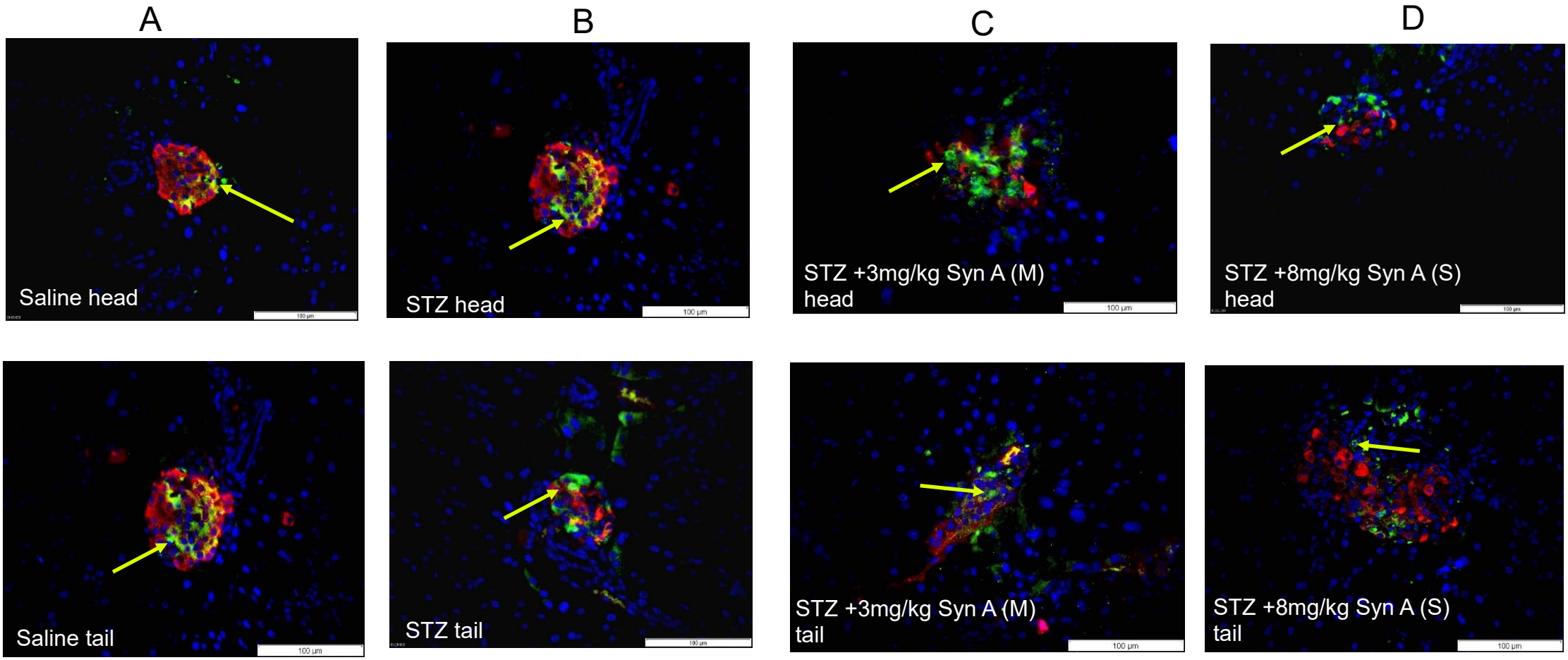

Percentage of transdifferentiation was determined by the islets expressing GFP^{+ve}, $insulin^{-ve}$ cells. Insulin is represented in red, GFP in green, yellow represents GFP^{+ve}, $insulin^{-ve}$ cells, and DAPI in blue. The yellow arrows are pointing to GFP^{+ve}, $insulin^{-ve}$ cells. Images were taken at 40x. Total number of 100 islets were analysed per treatment group.

Figure 6.43 Effects of single or multiple dose of Syn A on GFP positive, glucagon positive cells in the head (A), tail (B), and whole (C) pancreas in female Glu^{Cre} Rosa mice with multiple low dose STZ diabetes after 23 days.

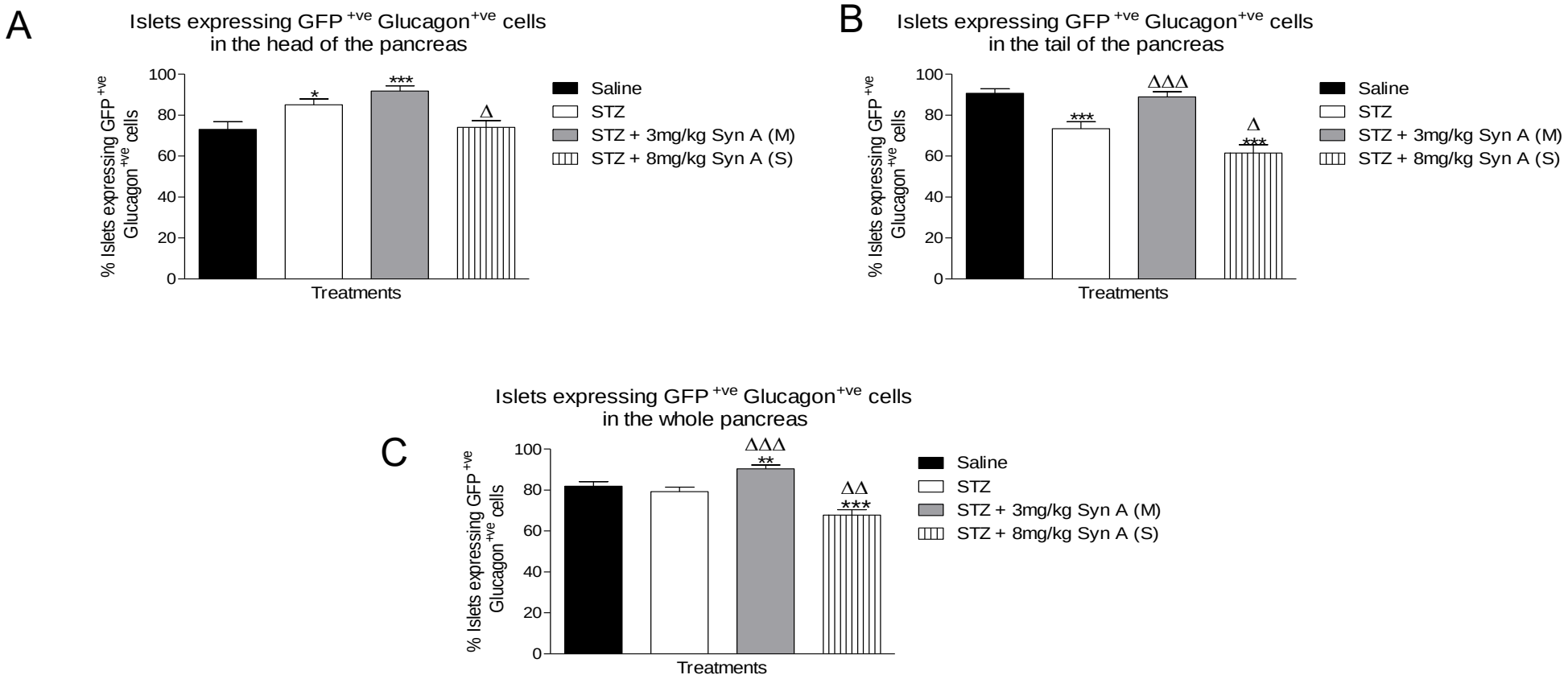

Percentage of islets expressing GFP^{+ve}, glucagon^{+ve} cells in the head (A), tail (B), and whole (C) pancreas. STZ (50mg/kg) administered by i.p. on days 1-5, STZ (150mg/kg) administered on day 12, and STZ (200mg/kg) administered on day 15. 3mg/kg Syn A (m) administered on days18-22, and 8mg/kg (s) administered on day 15. Values are mean ± SEM (4-6 mice). Changes were deemed significant when p values were *p<0.05, **p<0.01, or ***p<0.001 when compared with saline. $^{\Delta}$p<0.05, $^{\Delta\Delta}$p<0.01, $^{\Delta\Delta\Delta}$p<0.001 when STZ was compared with Syn A treated mice.

Figure 6.44 Representative images of saline (A), STZ (B), STZ+ 3mg/kg Syn A (C), and STZ+ 8mg/kg Syn A (D) islets from the pancreas in female Glu^{Cre} mice.

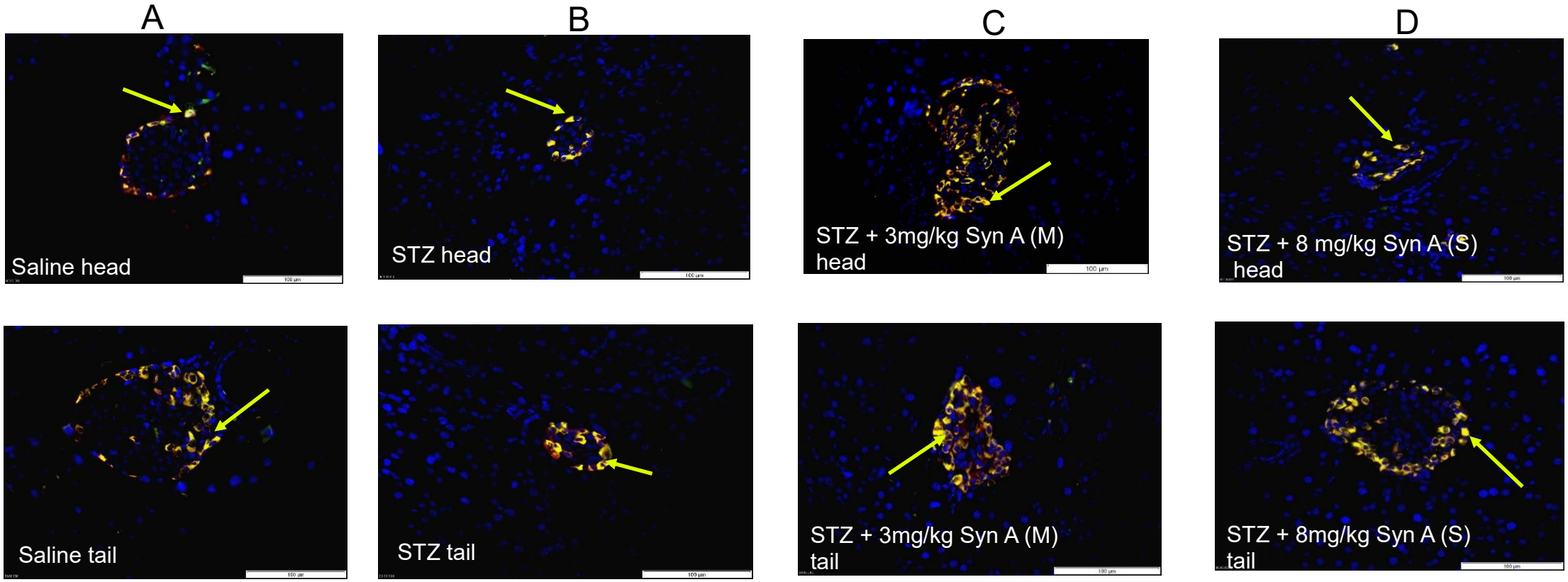

Percentage of dedifferentiation was determined by the islets expressing GFP^{+ve}, $glucagon^{+ve}$ cells. Insulin is represented in red, GFP in green, yellow represents GFP^{+ve}, $glucagon^{+ve}$ cells, and DAPI in blue. The yellow arrows are pointing to GFP^{+ve}, $glucagon^{+ve}$ cells. Images were taken at 40x.Total number of 100 islets were analysed per treatment group.

Figure 6.45 Effects of single or multiple dose of Syn A on GFP positive, glucagon negative cells in the head (A), tail (B), and whole (C) pancreas in female Glu^{Cre} Rosa mice with multiple low dose STZ diabetes after 23 days.

A

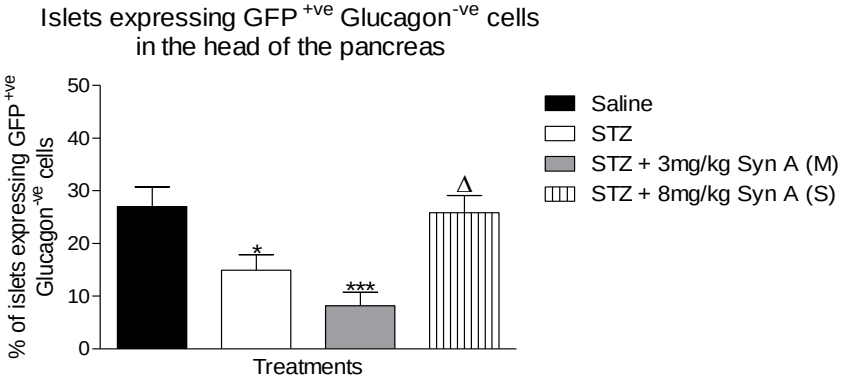

B

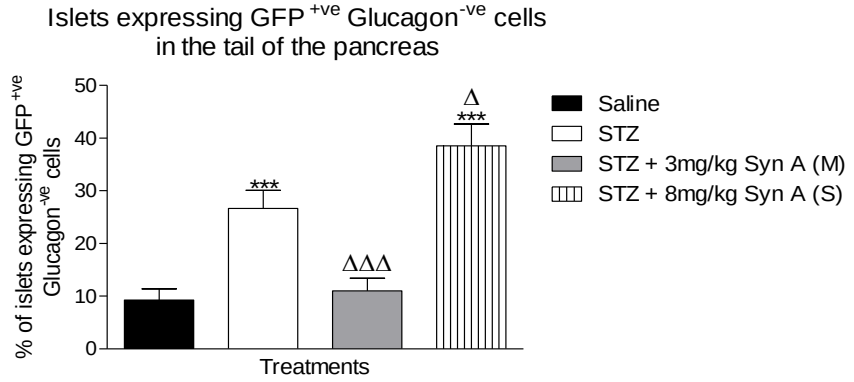

C

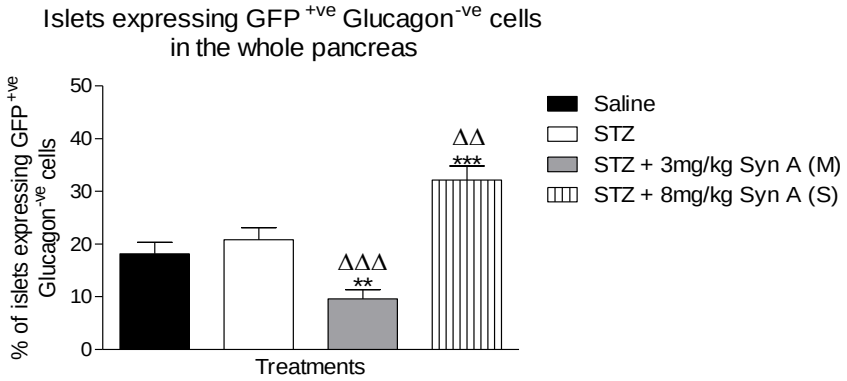

Percentage of islets expressing GFP^{+ve}, glucagon^{-ve} cells in the head (A), tail (B), and whole (C) pancreas. STZ (50mg/kg) administered by i.p. on days 1-5, STZ (150mg/kg) administered on day 12, and STZ (200mg/kg) administered on day 15. 3mg/kg Syn A (m) administered on days18-22, and 8mg/kg (s) administered on day 15. Values are mean ± SEM (4-6 mice). Changes were deemed significant when p values were *p<0.05, **p<0.01, or ***p<0.001 when compared with saline. $^{\Delta}$p<0.05, $^{\Delta\Delta}$p<0.01, or $^{\Delta\Delta\Delta}$ p<0.001 when STZ was compared with Syn A treated mice.

Figure 6.46 Representative images of saline (A), STZ (B), STZ+ 3mg/kg Syn A (C), and STZ+ 8mg/kg Syn A (D) islets from the pancreas in female Glu^{Cre} mice.

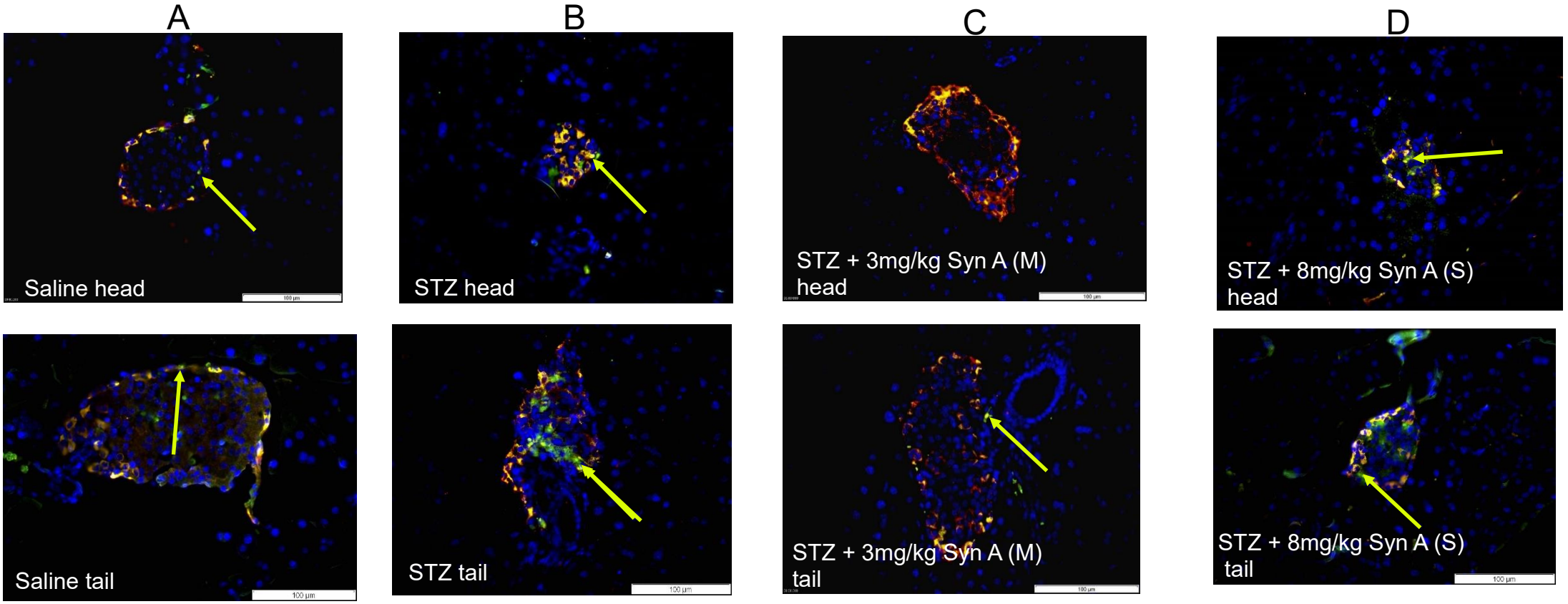

Percentage of dedifferentiation was determined by the islets expressing GFP^{+ve}, $glucagon^{-ve}$ cells. Insulin is represented in red, GFP in green, yellow represents GFP^{+ve}, $glucagon^{-ve}$ cells, and DAPI in blue. The yellow arrows are pointing to GFP^{+ve}, $glucagon^{-ve}$ cells. Images were taken at 40x.Total number of 100 islets were analysed.

Figure 6.47 Effects of single or multiple dose of Syn A on Ki67 positive, insulin positive cells in the head (A), tail (B), and whole (C) pancreas in female Glu^{Cre} Rosa mice with multiple low dose STZ diabetes after 23 days.

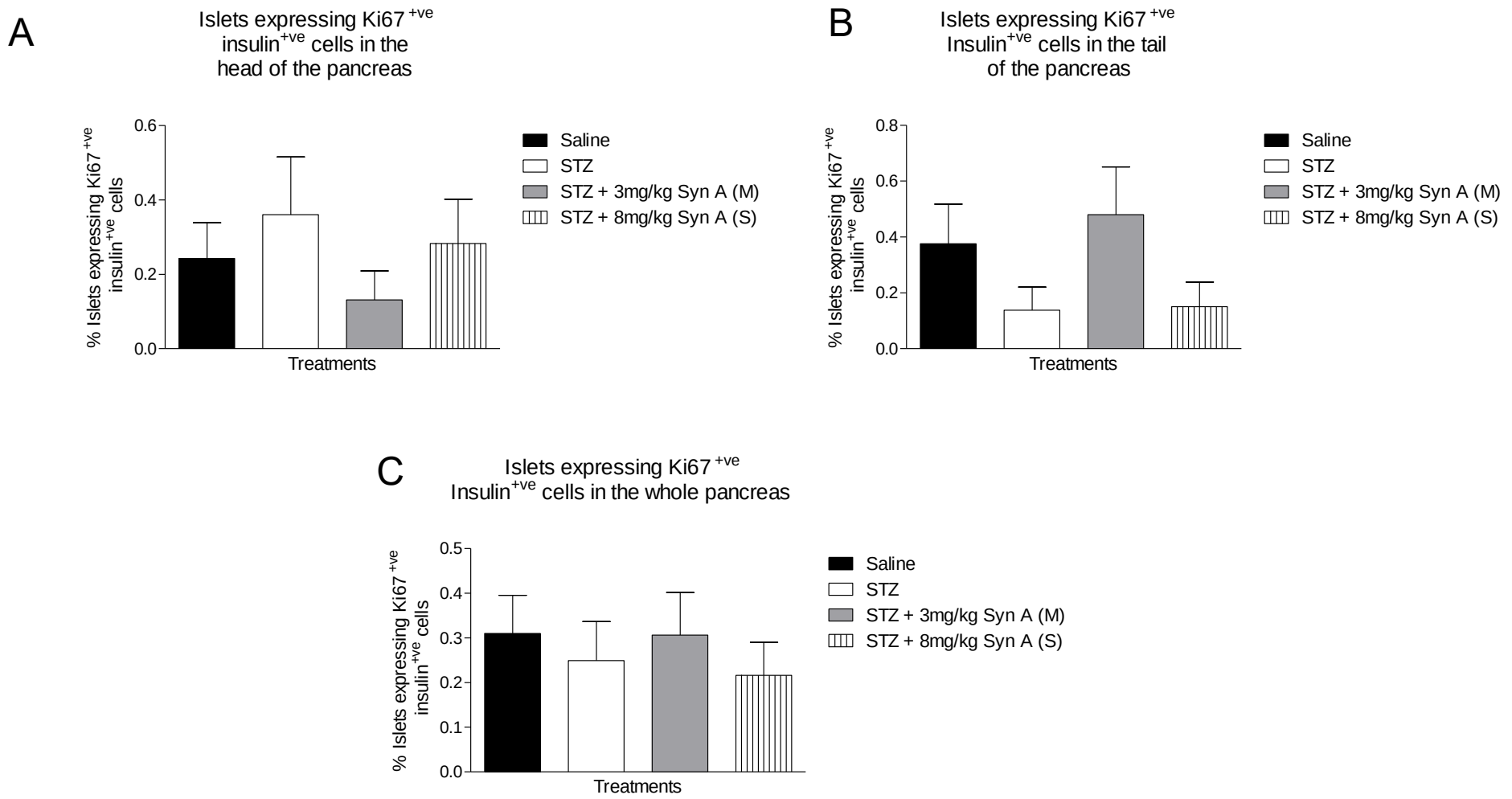

Percentage of islets expressing Ki67^{+ve}, insulin^{+ve} cells in the head (A), tail (B), and whole (C) pancreas. STZ (50mg/kg) administered by i.p. on days 1-5, STZ (150mg/kg) administered on day 12, and STZ (200mg/kg) administered on day 15. 3mg/kg Syn A (m) administered on days18-22, and 8mg/kg (s) administered on day 15. Values are mean ± SEM (n=4-6 mice). Changes were deemed significant when p values were <0.05.

Figure 6.48 Representative images of saline (A), STZ (B), STZ+ 3mg/kg Syn A (C), and STZ+ 8mg/kg Syn A (D) islets from the pancreas in female Glu^{Cre} mice.

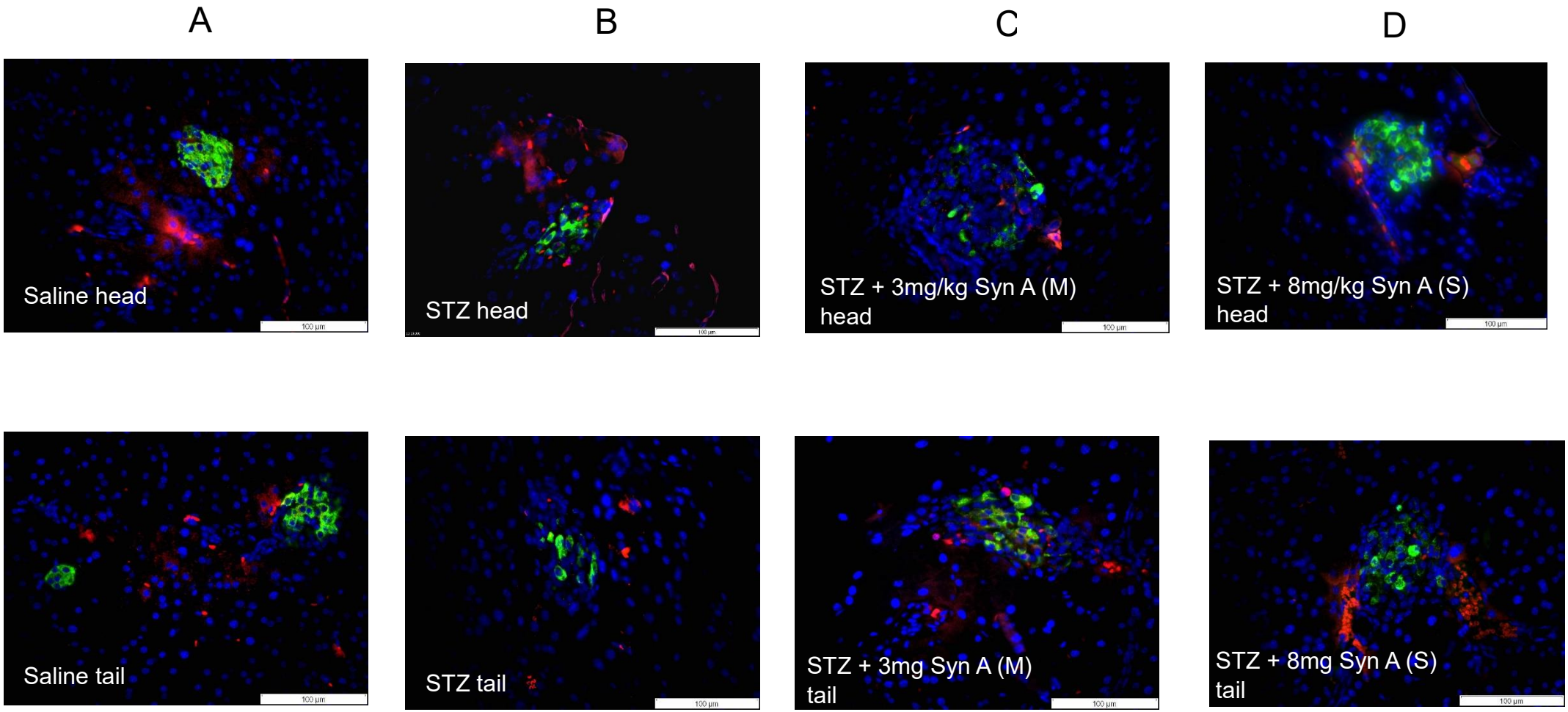

Percentage of beta cell proliferation was determined by the islets expressing Ki67^{+ve}, insulin^{+ve} cells in the pancreas. Insulin is represented in green, Ki67 in red, and DAPI in blue. Images were taken at 40x. Total number of 100 islets were analysed per treatment group.

Figure 6.49 Effects of single or multiple dose of Syn A on Ki67 positive, glucagon positive cells in the head (A), tail (B), and whole (C) pancreas in female Glu^{Cre} Rosa mice with multiple low dose STZ diabetes after 23 days.

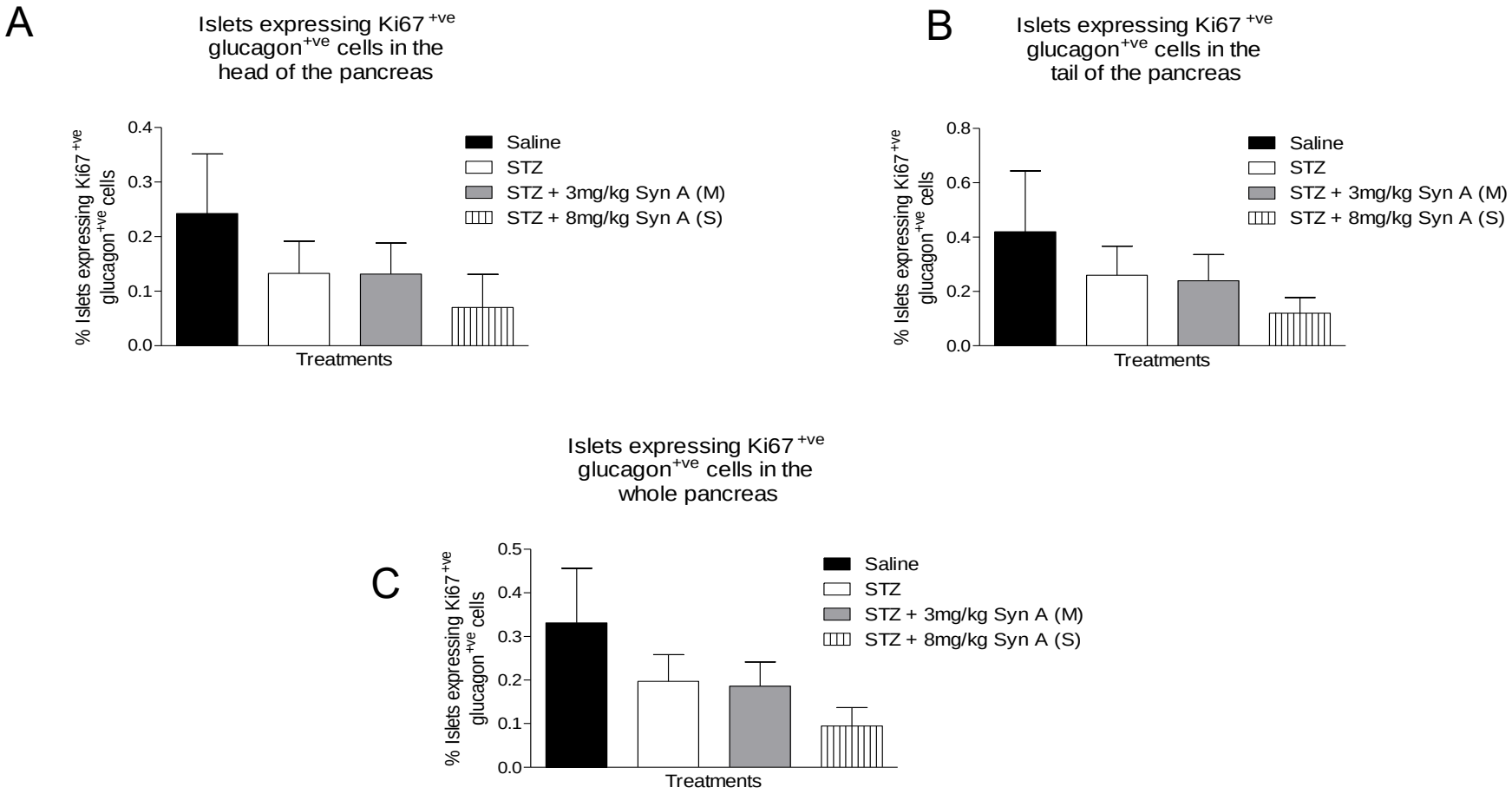

Percentage of islets expressing Ki67^{+ve}, glucagon^{+ve} cells in the head (A), tail (B), and whole (C) pancreas. STZ (50mg/kg) administered by i.p. on days 1-5, STZ (150mg/kg) administered on day 12, and STZ (200mg/kg) administered on day 15. 3mg/kg Syn A (m) administered on days18-22, and 8mg/kg (s) administered on day 15. Values are mean ± SEM (n=4-6 mice). Changes were deemed significant when p values were <0.05.

Figure 6.50 Representative images of saline (A), STZ (B), STZ+ 3mg/kg Syn A (C), and STZ+ 8mg/kg Syn A (D) islets from the pancreas in female Glu^{Cre} mice.

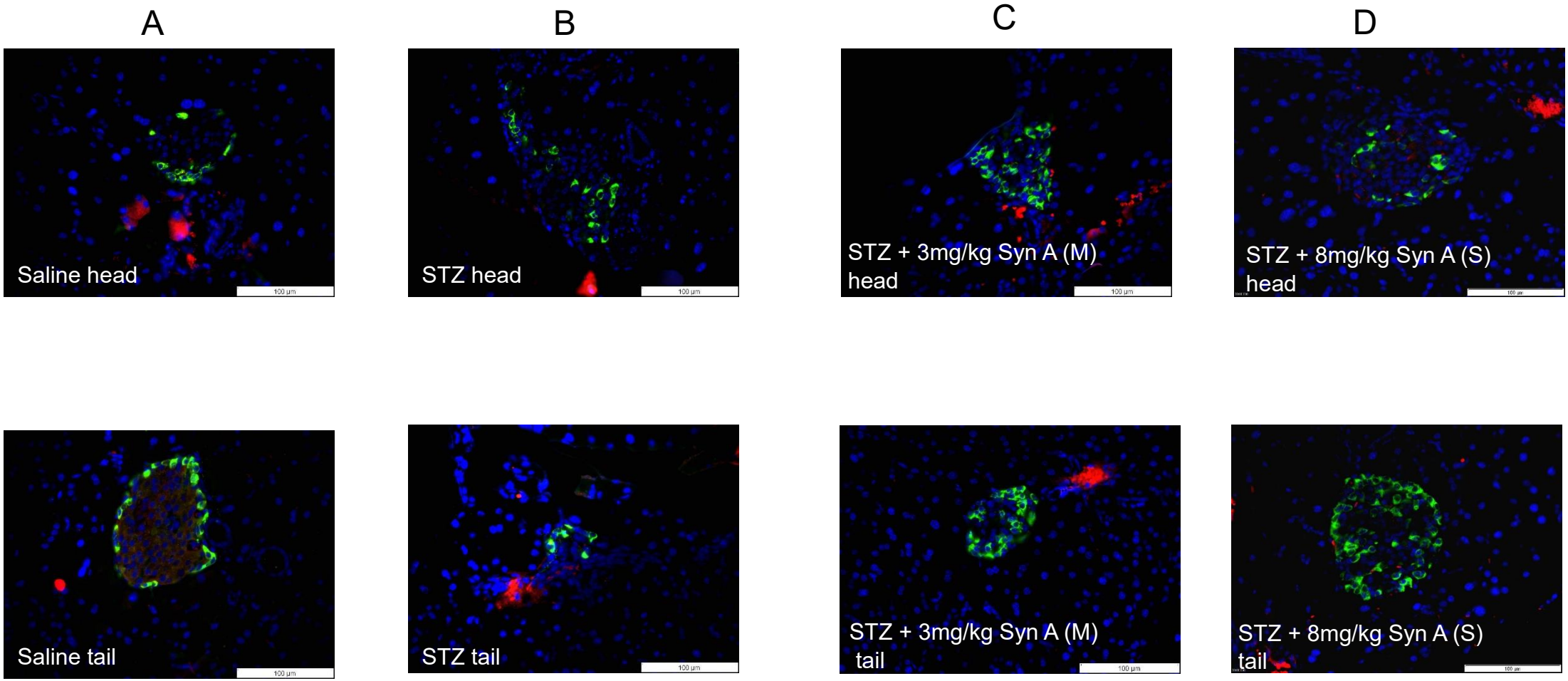

Percentage of alpha cell proliferation was determined by the islets expressing Ki67^{+ve}, glucagon^{+ve} cells in the pancreas. Glucagon is represented in green, Ki67 in red, and DAPI in blue. Images were taken at 20X and 40x objective lens. Total number of 100 islets were analysed per treatment group.

Chapter 7

The effects of cobalt chloride on glucose homeostasis and islet morphology in Glu^{Cre} mice

7.1 Summary

Cobalt chloride is believed to be a pancreatic alpha cell toxin. To confirm the islet toxicity of this drug, bioanalysis and histological analysis were conducted in the study below. A single low dose of 3mg/kg cobalt and a single high dose of 15m/kg cobalt were given to 19 normal transgenic mice with assessment over the following 8 days. Blood glucose was not affected by either dose during the study. Body weight loss was observed in the two cobalt treatment groups together with increases in food and fluid consumption. Histologically, the numbers of islets were significantly decreased in the head of the pancreas. The tail of the pancreas contained similar number of islets in the cobalt treated mice. Islet area was increased in the higher dose of cobalt treated mice in the tail of the pancreas, resulting in more islets being classified as large. The pancreas head and tail were both affected, showing a significant decrease of alpha cells in both regions. Beta cell proliferation was increased in the low dose cobalt treated mice in the head and tail of the pancreas. Alpha cell proliferation was greater in the tail of the pancreas in both groups of cobalt treated mice. Transdifferentiation and dedifferentiation of the alpha cells were observed within the head of the pancreas in mice treated with 3mg/kg cobalt. Anatomically, the kidneys, heart, and liver appeared to display a colour change in the mice treated with cobalt.

7.2 Introduction

Cobalt chloride is an alpha cell toxin, like Synthalin A (Syn A), which is deemed to be more effective in some species more than others (Eaton, 1973; Van Campenhout and Cornelis, 1960; Hultquist, 1956). Most of the research conducted on this toxin was carried out in the 1950's and rarely used rodents. Past research in rabbits' states that the effects of cobalt are as toxic to alpha cells as alloxan is to beta cells but does not have any effect on the surrounding cells in the gastric mucosa (Rao and De, 1955). One study found that when examining the nucleus area of the cells from rats treated with cobalt, the beta cells nucleus were affected and not the alpha cells nucleus. This was true for both the male and female rats. However, unlike males, the female rats did not reach hypoglycaemia 6-12 hours after an

injection of the same amount (Hultquist, 1959). This suggests that there are two possible actions through which cobalt chloride works (Volk *et al.* 1953). First, cobalt damages the alpha cells causing a hyperglycaemic phase and second, that the hyperglycaemic effects caused by the alpha cell damage are independent of one another suggesting it comes from outside of the pancreas. They also reported that daily administration of cobalt did not increase the anatomical changes that were observed after a single dose, and that histologically the alpha cells in the diabetic rabbits were more destroyed than the control animals (Volk *et al.* 1953). This contradicts with the results found in another rabbit study that showed damage to the alpha cells was observed one hour after a single treatment of cobalt, and after four hours, no alpha cells were present (Caren and Carbo, 1955).

In studies using obese mice injected with cobalt chloride, extreme hyperglycaemia was observed two hours after the initial injection and started to return to normal around days 4-7 (Mayer *et al.* 1953). Alpha and beta cell mass was also increased in these mice. It was also noted that when the control mice were given the same amount of cobalt chloride, they did not survive, perhaps leading to the hypothesis that obesity in this case was a protective factor (Mayer *et al.* 1953). In other animal studies investigating various doses of cobalt chloride, the alpha cells in rabbits began to regenerate after 5 or 6 days of exposure to cobalt and were completely regenerated by day 10 (Caren and Carbo, 1955; Volk *et al.* 1953).

The aim of this Chapter was to investigate the effects of cobalt chloride compared to the alpha cell toxin, Synthalin A (Syn A). Both toxins have been neglected in recent years and there is a lack of recent information. Experiments using these alpha cell toxins in transgenic mice that have fluorescently labelled alpha cells, will potentially provide key information on their mechanism of action, and if cobalt chloride is driving alpha to beta, or beta to alpha cell transdifferentiation.

7.3 Materials and methods

All materials and methods for this study have been summarised in 7.3.1 to 7.3.3. A detailed description of the materials and methods can be found in Chapter 2.

7.3.1 Glu^{Cre} Rosa mice treated with Cobalt Chloride

Nineteen 3-month-old male mice were bred in house at the BBRU in Coleraine at Ulster University. All three groups (n=6 or 7 mice) were injected with 7mg of Tamoxifen prior to the start of the study. The first set of mice were treated with saline, the second group was treated with a single dose of 3mg/kg of cobalt chloride, and the third group was treated with 15mg/kg of cobalt chloride.

7.3.2 Immunohistochemistry

Tissue blocks were cut at 5-7µm thick and left to dry overnight on coated slides. Slides were double stained using in house guinea-pig anti-glucagon 1:400, mouse anti-insulin 1:400; anti rabbit- Ki67 1:500 (ab15580) and anti-goat GFP polyclonal antibodies (ab 5450). Secondary antibodies for immunohistochemistry included Alexa Fluor 488 or Alexa Fluor 594 goat anti mouse, IgG- 1:400, Alexa Fluor 488 or Alexa Fluor 594 goat anti guinea pig, IgG- 1:400, Alexa Fluor 594 goat anti rabbit, IgG- 1:400, and Alexa Fluor 488 donkey anti goat, IgG- 1:400. DAPI was added as a nuclei marker. A 50:50 mixture of glycerol and PBS was used to mount coverslips to the slides. Images were analysed using the Olympus fluorescent microscope fitted with DAPI (350nm) FITC (488nm) and TRITC (594nm) filters and a DP70 camera adapter system using Cell^F program.

7.3.3 Statistics

The graphs and results were all generated and analysed using GraphPad Prism 5 and Image J. The results below expressed as comparisons between two groups with $p<0.05$ displaying statistical significance. A two-way Repeated Measures ANOVA statistical test with Bonferroni Multiple Comparison Test or an unpaired student t-test.

7.4 Results

7.4.1 Effects of a single low and high dose of cobalt chloride on body weight, weight change, and blood glucose in male Glu^{Cre} Rosa mice.

As seen in Figure 7.1A, no significance was observed regarding body weight. When examining body weight change, the 3mg/kg group to the saline group, only a small significance was found ($p<0.05$) (Figure 7.1B). The 15mg/kg cobalt treated mice, compared to saline, had a much larger change in percentage of weight change ($p<0.01$). No significance was observed regarding blood glucose levels (Figure 7.1C).

7.4.2 Effects of a single low and high dose of cobalt chloride on food and fluid intake in male Glu^{Cre} Rosa mice.

Both cobalt treated groups consumed similar amounts of food throughout the study (Figure 7.2A). A significant increase was observed starting from day 4 ($p<0.05$) when both cobalt groups were compared to saline. On day 6, the 15mg/kg treated mice, compared to saline, displayed a higher significance ($p<0.01$) than the previous days. The same was true for the 3mg/kg mice on the last two days of the study. As shown in Figure 7.2B, the two cobalt treated mice groups showed a significant increase in the fluid intake over the 8-day study. The significance ($p<0.05$) of the 3mg/kg group when compared to the saline group continued to increase to a larger significance ($p<0.001$) from day 4 that continued till the end of the study. The 15mg/kg cobalt mice fluid intake was increased ($p<0.01$) from day 4 till the end when compared to saline.

7.4.3 Effects of a single low and high dose of cobalt chloride on nonfasting and fasting plasma insulin in male Glu^{Cre} Rosa mice.

When looking at nonfasting plasma insulin levels in the three treatment groups, the 15mg/kg cobalt group had significantly lower insulin ($p<0.001$) when compared to the saline mice (Figure 7.3A). However, the opposite occurred when examining the plasma insulin levels

taken from fasting mice (Figure 7.3B). Both groups showed a significant increase ($p<0.05$) when compared to saline.

7.4.4 Effects of a single low and high dose of cobalt chloride on pancreatic insulin content from the head, tail, and the whole pancreas in male Glu^{Cre} Rosa mice.

Figure 7.4A, shows the pancreatic insulin content in the head of the pancreas in all three groups. No significance was found regarding the insulin content from the head of the pancreas. Pancreatic insulin content significantly decreased ($p<0.01$) in the tail of the pancreas in the mice treated with 15mg/kg cobalt (Figure 7.4B). When looking at the whole pancreas, mice treated with the 15mg/kg exhibited a significant decrease ($p<0.05$) in pancreatic insulin content (Figure 7.4C).

7.4.5 Effects of a single low and high dose of cobalt chloride on number of islets, islet area, and islet size distribution in the head of the pancreas in male Glu^{Cre} Rosa mice.

As shown in Figure 7.5A, the number of islets varied between each of the groups. The 3mg/kg group displayed a large decrease ($p<0.001$) in the number of islets in the head of the pancreas compared to saline. Mice treated with 15mg/kg showed a slight decrease ($p<0.05$) in the number of islets in the pancreatic head when compared to saline. No significance was found regarding islet area (Figure 7.5B). Interestingly, when grouping the islets by size, the saline and the 15mg/kg treated mice contained no large islets (Figure 7.5C). No significance was found regarding islet size distribution.

7.4.6 Effects of a single low and high dose of cobalt chloride on number of islets, islet area, and islet size distribution in the tail of the pancreas in male Glu^{Cre} Rosa mice.

The number of islets statistically decreased ($p<0.001$) in the two cobalt treatment groups when compared to saline (Figure 7.6A). There was a slight increase ($p<0.05$) in the islet area in the

3mg/kg treated mice, and a larger increase ($p<0.001$) in the 15mg/kg treated mice in comparison to saline treated islets (Figure 7.6B). When examining the islet size distribution, mice treated with 15mg/kg showed a significantly decreased ($p<0.001$) small islet percentage when compared to the saline islets (Figure 7.6C) The 15mg/kg treated mice displayed a significant increase in the percentage of larger number of islets ($p<0.001$) when compared to the saline group.

7.4.7 Effects of a single low and high dose of cobalt chloride on number of islets, islet area, and islet size distribution in the whole pancreas in male Glu^{Cre} Rosa mice.

Figure 7.7A shows that the mice treated with 3mg/kg group displayed decrease ($p<0.05$) in the number of islets per mm^2 when compared to the saline group. The islet area in the whole pancreas showed an increase in size when looking at the two treatment groups ($p<0.05$; $p<0.01$) when compared to the saline group (Figure 7.7B). Figure 7.7C shows the islet size distribution within the whole pancreas. When compared to saline, the small islets decreased ($p<0.01$) in the 15mg/kg whereas the percentage of islets classified as large increased ($p<0.01$).

7.4.8 Effects of a single low and high dose of cobalt chloride on alpha cell area and percentage and beta cell area and percentage in the head of the pancreas in male Glu^{Cre} Rosa mice.

The alpha cell area ($p<0.01$; $p<0.001$) and percentage ($p<0.001$) in the head of the pancreas decreased in the two cobalt treated groups when compared to saline (Figure 7.8A and B). When looking at the beta cell area and percentage there was an overall increase among the groups (Figure 7.8C and D). Specifically looking at the beta cell percentage, the two cobalt groups showed a significant increase ($p<0.001$) when compared to the saline treated mice.

7.4.9 Effects of a single low and high dose of cobalt chloride on alpha cell area and percentage and beta cell area and percentage in the tail of the pancreas in male Glu^{Cre} Rosa mice.

No significance was observed regarding alpha cell area in the pancreatic tail (Figure 7.9A). The percentage of alpha cells was decreased in the two cobalt treatment groups ($p<0.001$) when compared to saline (Figure 7.9B). However, when looking at the beta cell area in the tail of the pancreas, both cobalt groups were largely increased ($p<0.01$; $p<0.001$) when compared to the saline group (Figure 7.9C). Figure 7.9D shows the statistically significant increase ($p<0.001$) in the cobalt treated mice compared to saline when examining the beta cell percentage in the tail portion of the pancreas.

7.4.10 Effects of a single low and high dose of cobalt chloride on alpha cell area and percentage and beta cell area and percentage in the whole pancreas in male Glu^{Cre} Rosa mice.

No significance was observed regarding the alpha cell area (Figure 7.10A). Alpha cell percentage was significantly decreased ($p<0.001$) in the two cobalt groups when compared to the saline group (Figure 7.10B). Beta cell area increased ($p<0.01$; $p<0.001$) in the two cobalt groups when compared to the whole pancreas of the saline group (Figure 7.10C). Both cobalt treatment groups had a significant increase ($p<0.001$) in the percentage of beta cells in the whole pancreas (Figure 7.10D). Photo representation is seen in Figure 7.11A-C. Glucagon is represented in red, insulin in green, and DAPI in blue.

7.4.11 Effects of a single low and high dose of cobalt chloride on GFP positive, insulin positive cells in the head, tail, and whole pancreas in male Glu^{Cre} Rosa mice.

When looking at transdifferentiation in the islets, Figure 7.12A shows a significant increase ($p<0.001$) in GFP positive, insulin positive cells in the head of both cobalt groups when compared to saline. In the tail portion of the pancreas, mice treated with 3mg/kg cobalt

(p<0.01) and 15mg/kg cobalt (p<0.001) group showed a significant increase when compared to saline (Figure 7.12B). Both cobalt treatment groups exhibited a significant increase (p<0.001) in positive cells when compared to saline (Figure 7.12C). Photos are represented in Figure 7.13A-C. Insulin is represented in red, GFP in green, and DAPI in blue.

7.4.12 Effects of a single low and high dose of cobalt chloride on GFP positive, insulin negative cells in the head, tail, and whole pancreas in male Glu^{Cre} Rosa mice.

As seen in Figure 7.14A, both cobalt treated mice showed a significant decrease (p<0.001) in GFP positive, insulin negative cells in the head of the pancreas. When looking at the tail section, there was a significant decrease in insulin negative cells the 3mg/kg group (p<0.01) and in the 15mg/kg (p<0.001) group when compared to saline (Figure 7.14B). Both cobalt groups displayed a large decrease in negative cells (p<0.001) when compared to saline (Figure 7.14C). Photos are represented in Figure 7.15A-C. Insulin is represented in red, GFP in green, and DAPI in blue.

7.4.13 Effects of a single low and high dose of cobalt chloride on GFP positive, glucagon positive cells in the head, tail, and whole pancreas in male Glu^{Cre} Rosa mice.

Figure 7.16A shows a decrease in the percentage of islets expressing GFP positive, glucagon positive cells in the head of the pancreas in mice treated with 3mg/kg (p<0.01) and 15mg/kg cobalt (p<0.001). No significance was observed regarding positive cells in the tail of the pancreas (Figure 7.16B). When examining the whole pancreas, both cobalt treatment groups showed a statistically significant decrease (p<0.05; p<0.01) when compared to saline (Figure 7.16C). Photos are represented in Figure 7.17A-C. Glucagon is represented in red, GFP is represented in green, and DAPI is represented in blue.

7.4.14 Effects of a single low and high dose of cobalt chloride on GFP positive, glucagon negative cells in the head, tail, and whole pancreas in male Glu^{Cre} Rosa mice.

As seen in Figure 7.18A, mice treated with 3mg/kg ($p<0.01$) and 15mg/kg cobalt ($p<0.001$) displayed an increase in GFP positive, glucagon negative cells in the pancreatic head. In the tail of the pancreas, no significance was observed regarding GFP positive, glucagon negative cell expression (Figure 7.18B). When examining the pancreas as a whole, an increase of GFP positive, glucagon negative cell expression in mice treated with 3mg/kg ($p<0.05$) and 15mg/kg cobalt ($p<0.01$) was noted (Figure 7.18C). Photo representation can be seen in Figure 7.19 A-C. Glucagon is represented in red, GFP is represented in green, and DAPI is in blue.

7.4.15 Effects of a single low and high dose of cobalt chloride on Ki67 positive, insulin positive cells in the head, tail, and whole pancreas in male Glu^{Cre} Rosa mice.

As seen in Figure 7.20A-C, no statistical significance was observed regarding beta cell proliferation in the three areas of the pancreas. Photo representation can be seen in Figure 7.21A-C. Insulin is represented in green, Ki67 is represented in red, and DAPI is represented in blue.

7.4.16 Effects of a single low and high dose of cobalt chloride on Ki67 positive, glucagon positive cells in the head, tail, and whole pancreas in male Glu^{Cre} Rosa mice.

No statistical significance was observed regarding alpha cell proliferation in the three pancreatic sections (Figure 22A-C). Photo representation can be seen in Figure 7.23A-C. Glucagon is represented in green, Ki67 is represented in red, and DAPI is represented in blue.

7.5 Discussion

According to Mayer *et al.* (1953), the non-obese mice that were given the same dosage, 2.5 to 10mg, of cobalt as the obese mice in the study, did not survive 24 hours after injection. However, the mice in the present study with lean body mass survived the 8-day study. All of the mice in the 1953 study showed hyperglycaemia up to 2 hours after injection (Mayer *et al*. 1953). Blood glucose was taken on alternating days in the present study, but hyperglycaemia was not observed. It was noted that in the past study, blood glucose levels decreased from days 4 to 7, before a second injection of cobalt. Although, we only administered cobalt chloride once in the 8 days, there was a decrease in blood glucose levels on day 2 and 4. Hultquist (1959), found that only the male rats treated with 20 and 45mg/kg of cobalt, caused blood glucose levels to decrease 6-12 hours after the initial injection. However, after an injection amount of 35 or 40mg/kg of cobalt, the rats showed elevated blood glucose levels. Following a second or third injection of cobalt, the blood glucose in rabbits returned to the same levels as before they were treated (Volk *et al.* 1953). This is consistent with the blood glucose in the mice we treated with cobalt. After day 4, the blood glucose returned to the same level as the saline mice, however it did not reach the starting values. In Volk *et al.* (1953), none of the rabbits that were injected with cobalt exacerbated hypoglycaemia, which confirms our observations with the Glu^{Cre} male mice.

Most of the past animal studies involving cobalt focused on blood glucose and histology of the alpha cells and the liver. Of these past animal studies that were located, there are none that examined food or fluid intake. Both cobalt treatment groups displayed an increase in food and fluid intake over the course of the study.

We found significant decreases in the nonfasting insulin levels and significant increases in fasting mice treated with cobalt when compared to the saline treated mice. However, in a previous study with rats, the authors found that the levels of serum insulin after cobalt treatment was the same the saline controls (Eaton, 1973). This study also states that hyperglycaemia was not attained in the rats that were treated with cobalt, which is consistent

with our findings. This research suggests that the blood glucose in these treated rats did not rise due to the inhibitory action of cobalt on cells in the liver (Eaton, 1973).

Histologically, the morphology of the alpha cells in rabbits appeared damaged only for 10 days before they started to regenerate (Volk *et al.* 1953). Our study finished before 10 days and the damage was noticeable. Decrease in the alpha area in the pancreatic tail was noticed, which could be because the alpha cells have started to regenerate like they do in rabbits starting on day 6. Nevertheless, regeneration of the alpha cells after a cobalt treatment in mice has yet to be documented. Perhaps if alpha cell regeneration did take place in the mice after day 6, this could be the cause of why the alpha cells in the tail of the pancreas did not display the same changes as the head of the pancreas. One study dissected the rabbit pancreas into three sections: the head, body, and tail. These two animals that were killed shortly after a single injection, found that the alpha cells were already affected, and the beta cells remained intact. They documented that the alpha cells were degranulated and swollen in the all three sections of the pancreas (Boyd and Maclean, 1959). We documented alpha cell changes in the head and the tail of the pancreas in the mice. A study that examined pancreases from guinea pigs treated with cobalt, found that the number alpha cells, islet area, and total number of islets increased compared to the control animals (Hultquist and Sundqvist, 1961). We can confirm these findings. Mice treated with 15mg/kg cobalt displayed an increase in the number of islets in the head of the pancreas and an increase in islet area within the pancreatic tail. We did not observe an increase in alpha cells.

The increase of GFP positive, insulin positive/negative cells that was observed in the head and the tail of the pancreas in mice treated with 3mg/kg or 15mg/kg cobalt show that the alpha cells are transdifferentiating to beta cells. When looking at the GFP positive, glucagon positive/negative cells in the head of the pancreas, the changes in the cobalt treatment groups show that the cobalt treatment is causing alpha cell dedifferentiation. However, in the tail of the pancreas shows that cobalt had no effect on transdifferentiation/dedifferentiation. In a study that examined kidney cells in conjunction with cobalt in a study on renal fibrosis, found

that the hypoxic conditions cobalt created caused the fibroblasts to transdifferentiate from tubular cells (Manotham *et al*. 2004). In another renal study, hypoxic conditions caused the epithelial-mesenchymal cells to transdifferentiate to myofibroblasts (Nangaku and Eckardt, 2007). In a study that examined pancreatic cancer with cobalt chloride, it was found that the hypoxia from the cobalt resulted in dedifferentiation of tumour cells resulting in the tumours becoming more aggressive (Angst *et al*. 2006; Helczynska *et* al. 2003; Unruh *et al*. 2003; Jögi *et al*. 2002; Reynolds *et al*. 1996). There was a lack of studies regarding transdifferentiation or dedifferentiation within the pancreas with a treatment of cobalt. However, the studies that examined transdifferentiation and dedifferentiation in conjunction with cobalt, referred to the change in cells due to the hypoxic conditions caused by cobalt.

Beta cell and alpha cell proliferation were not present in the cobalt treated mice. Unfortunately, we were unable to perform the TUNEL assay, to detect any apoptosis, on these animals due to the cobalt within the kit reacting with the cobalt treated pancreases. One study started that during insulin secretion in the beta cells, large amounts of oxygen are consumed causing these cells to be sensitive to hypoxia (Zheng *et al*. 2012). This could account for the changes we observed in the beta cells in mice treated with cobalt.

Anatomically, we only looked at the outside of other organs. Boyd and MaClean (1959), took the necropsy further and evaluated dissections to reveal the inside of the organs of the rabbits. They found that the loop of Henle in the kidneys displayed degenerative changes as well as necrosis. They also observed a large quantity of fat around the capillaries and the renal veins. In the heart, there appeared to be tiny thrombi along the blood vessels as well as some degeneration and necrosis. The lungs showed some congestion and swelling. The adrenal glands displayed a lack of cortical lipids and the submaxillary glands also displayed signs of necrosis. The liver, kidneys, and heart displayed severe signs of toxicity (Boyd and MaClean, 1959). When we examined the organs of the cobalt treated mice, the kidneys, heart, and liver all appeared darker in colour than the saline treated mice. This could be due to the fact that cobalt is accumulated in these organs, as well as others, such as the pancreas (Simonsen *et*

al. 2012). Unlike the mice we have treated with Syn A, there were no blood clots present. Boyd and McClean (1959) state that the toxicity from cobalt on the organs may not always be identifiable microscopically.

A few limitations arose in this study, such as the number of days and the treatment amounts. It would have been beneficial to also include a multiple dose of cobalt to review the effects on the organs and the islets within the mice. This would have been a better comparison against the mice that were given a single dose and multiple dose of Syn A.

In conclusion, cobalt is similar to Syn A in the fact that it does affect they alpha cells. We can conclude that cobalt drives alpha to beta cell transdifferentiation as well as dedifferentiation. This study also provided a deeper understanding of the effects cobalt has on the bioanalysis, islet morphology , and different anatomical structures.

Figure 7.1 Effects of a single low and high dose of cobalt chloride on body weight (A), weight change (B), and blood glucose (C) in male Glu^{Cre} Rosa mice over 8 days following injection.

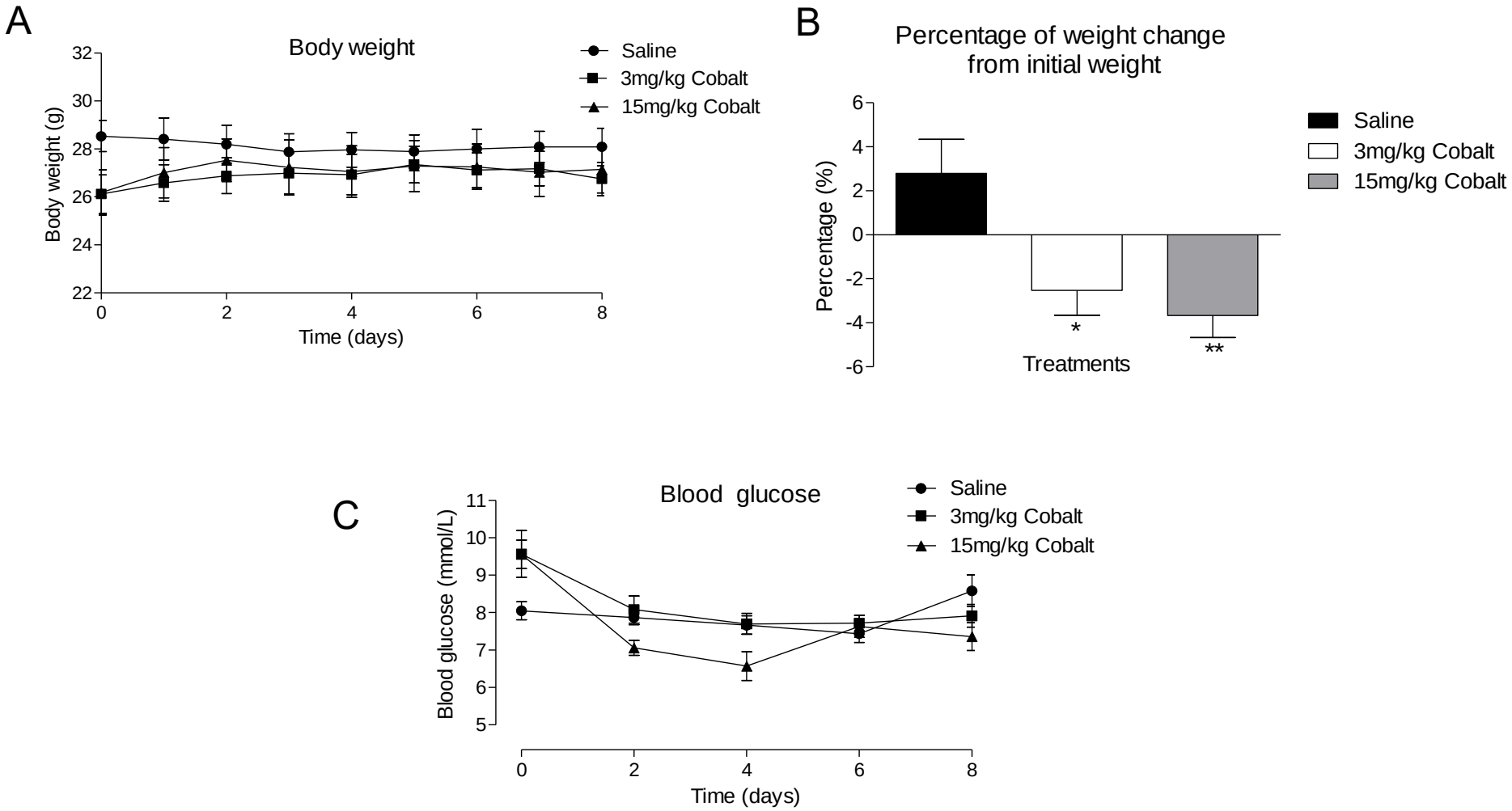

Body weight (A), percentage of body weight change (B), and blood glucose (C) over the course of 8 days in Glu^{Cre} mice. A single dose of either 3mg/kg or 15mg/kg of cobalt was administered by i.p. on day 2. Values are mean ± SEM (n=6-7 mice). Changes were deemed significant when p values were *p<0.05, or **p <0.01 when compared to the saline treated mice.

Figure 7.2 Effects of a single low and high dose of cobalt chloride on food (A) and fluid (B) intake in male Glu^{Cre} Rosa mice over 8 days following injection.

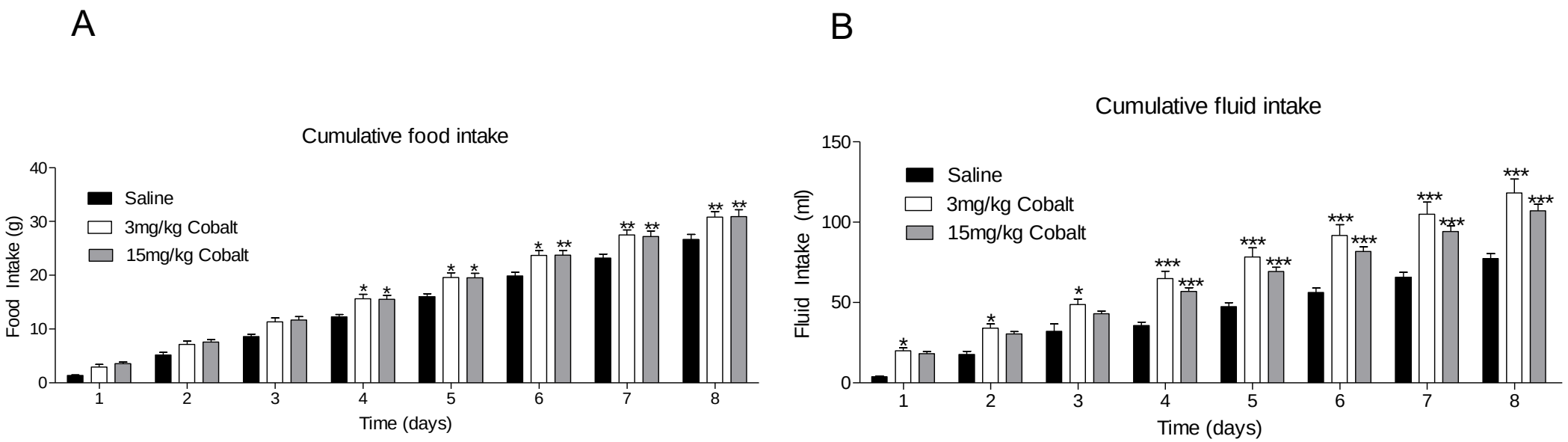

Cumulative food (A) and fluid (B) intake over the course of 8 days in Glu^{Cre} Rosa mice. A single dose of either 3mg/kg or 15mg/kg of cobalt was administered by i.p. on day 2. Values are mean ± SEM (n=6-7 mice). Changes were deemed significant when p values were **p <0.01 or ***p<0.001 when compared to the saline treated mice.

Figure 7.3 Effects of a single low and high dose of cobalt chloride on nonfasting (A) and fasting (B) plasma insulin in male Glu^{Cre} mice on the final day of the study.

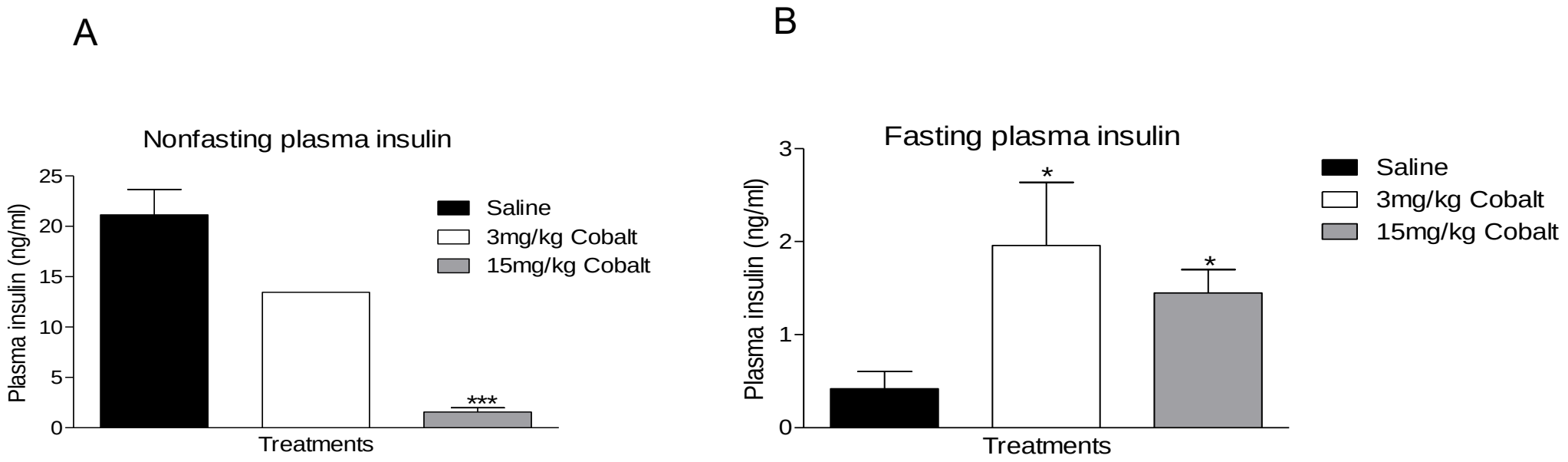

Nonfasting (A) and fasting (B) blood was taken at the end of the study. Plasma insulin levels were measured by RIA. A single dose of either 3mg/kg or 15mg/kg of cobalt was administered by i.p. on day 2. Values are mean ± SEM (n= 6-7 mice). Changes were deemed significant when p values were *p <0.05 or ***p<0.001 when saline was compared with the respective treated mice.

Figure 7.4 Effects of a single low and high dose of cobalt chloride on pancreatic insulin content from the head (A), tail (B), and the whole (C) pancreas in male Glu^{Cre} mice over 8 days following injection.

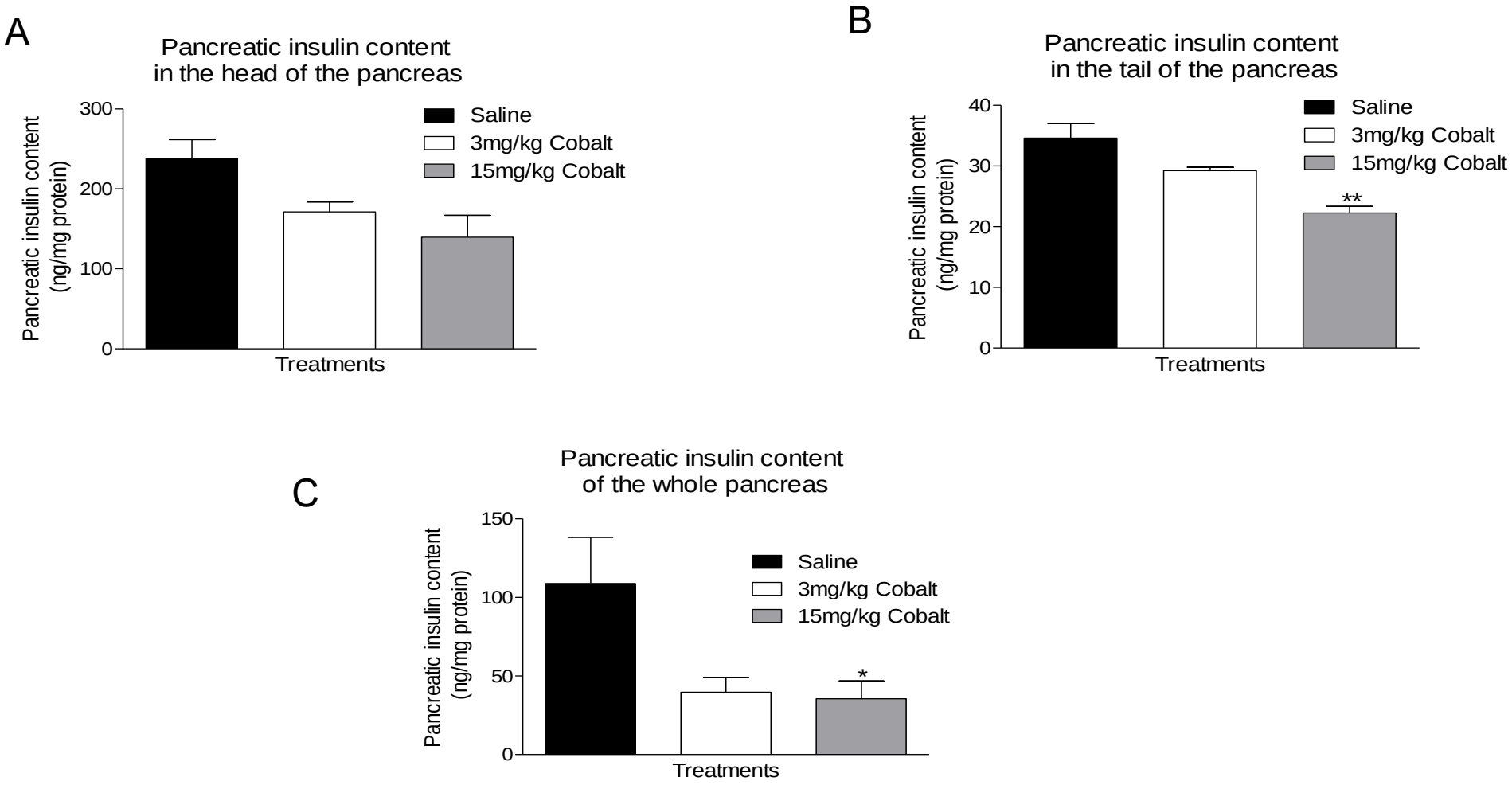

Pancreatic insulin content from the head (A), tail (B), and whole (C) flash frozen pancreas. A single dose of either 3mg/kg or 15mg/kg of cobalt was administered by i.p. on day 2. Values are mean ± SEM (n= 6-7 mice). Changes were deemed significant when p values were *p <0.05 or **p<0.01 when saline was compared with the respective treated mice.

Figure 7.5 Effects of a single low and high dose of cobalt chloride on number of islets (A), islet area (B), and islet size distribution (C) in the head of the pancreas of male Glu^{Cre} Rosa mice over 8 days following injection.

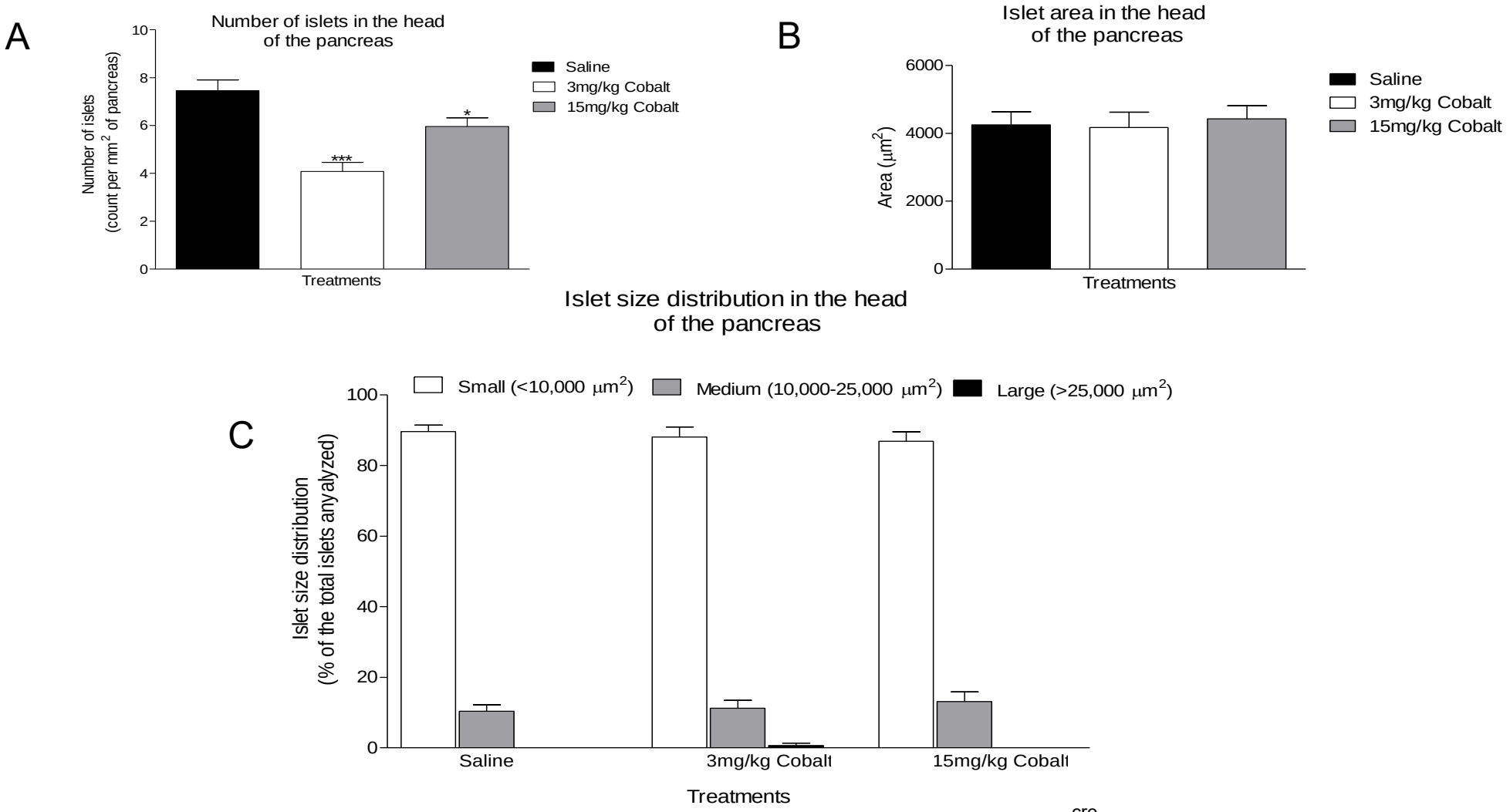

Number of islets (A), islet area (B), and islet size distribution (C) per pancreas in male Glu^{cre} Rosa mice. A single dose of either 3mg/kg or 15mg/kg of cobalt was administered by i.p. on day 2. Values are mean ± SEM (n=6-7 mice). Changes were deemed significant when p values were *p <0.05, or ***p<0.001 when compared to the saline treated mice.

Figure 7.6 Effects of a single low and high dose of cobalt chloride on number of islets (A), islet area (B), and islet size distribution (C) in the tail of the pancreas of male Glu^{Cre} Rosa mice over 8 days following injection.

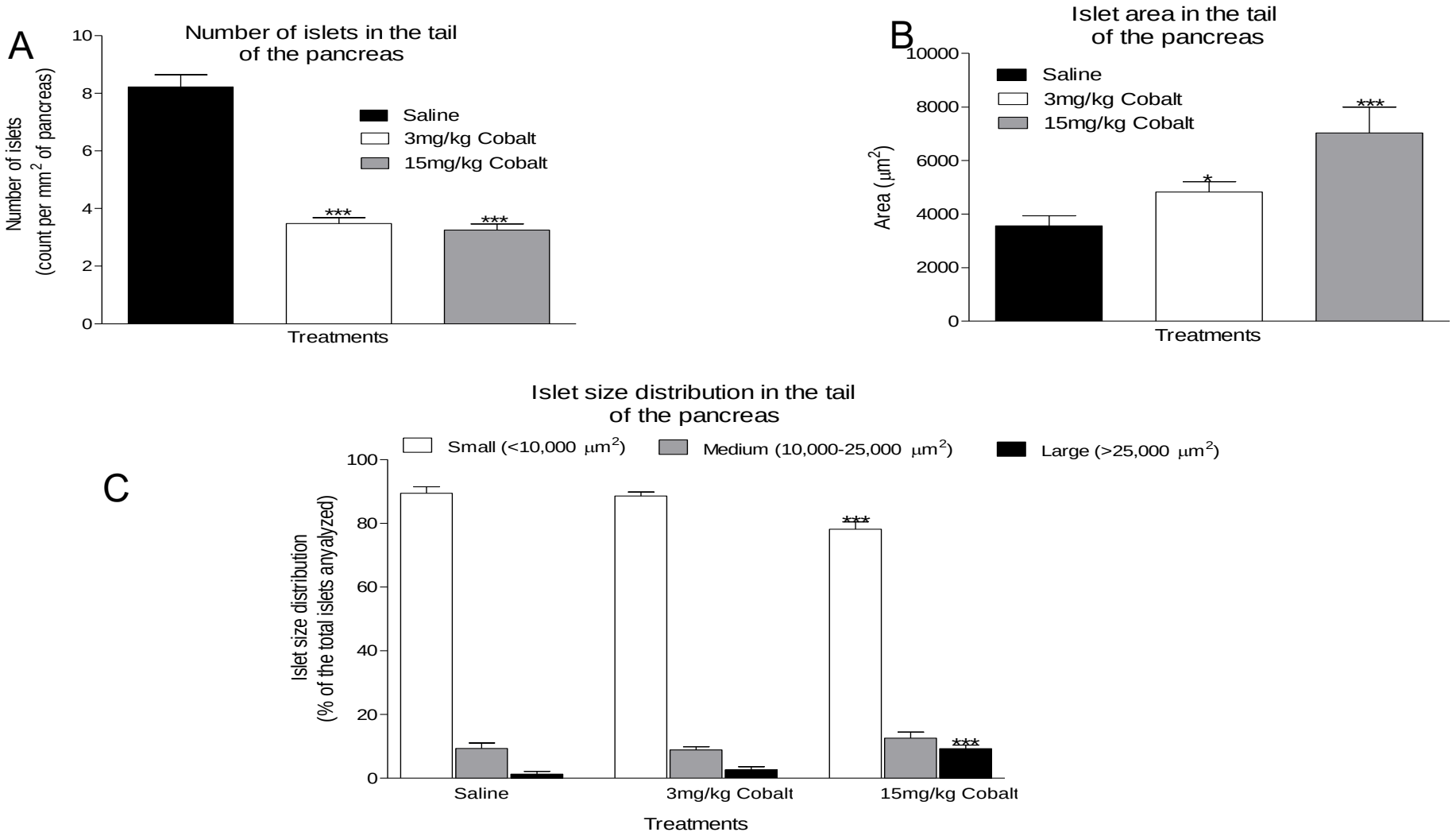

Number of islets (A), islet area (B), and islet size distribution (C) per pancreas in male Glu^{Cre} Rosa mice. A single dose of either 3mg/kg or 15mg/kg of cobalt was administered by i.p. on day 2. Values are mean ± SEM (n=6-7 mice). Changes were deemed significant when p values were *p <0.05, or ***p<0.001 when compared to the saline treated mice.

Figure 7.7 Effects of a single low and high dose of cobalt chloride on number of islets (A), islet area (B), and islet size distribution (C) on the whole pancreas of male Glu^{Cre} Rosa mice over 8 days following injection.

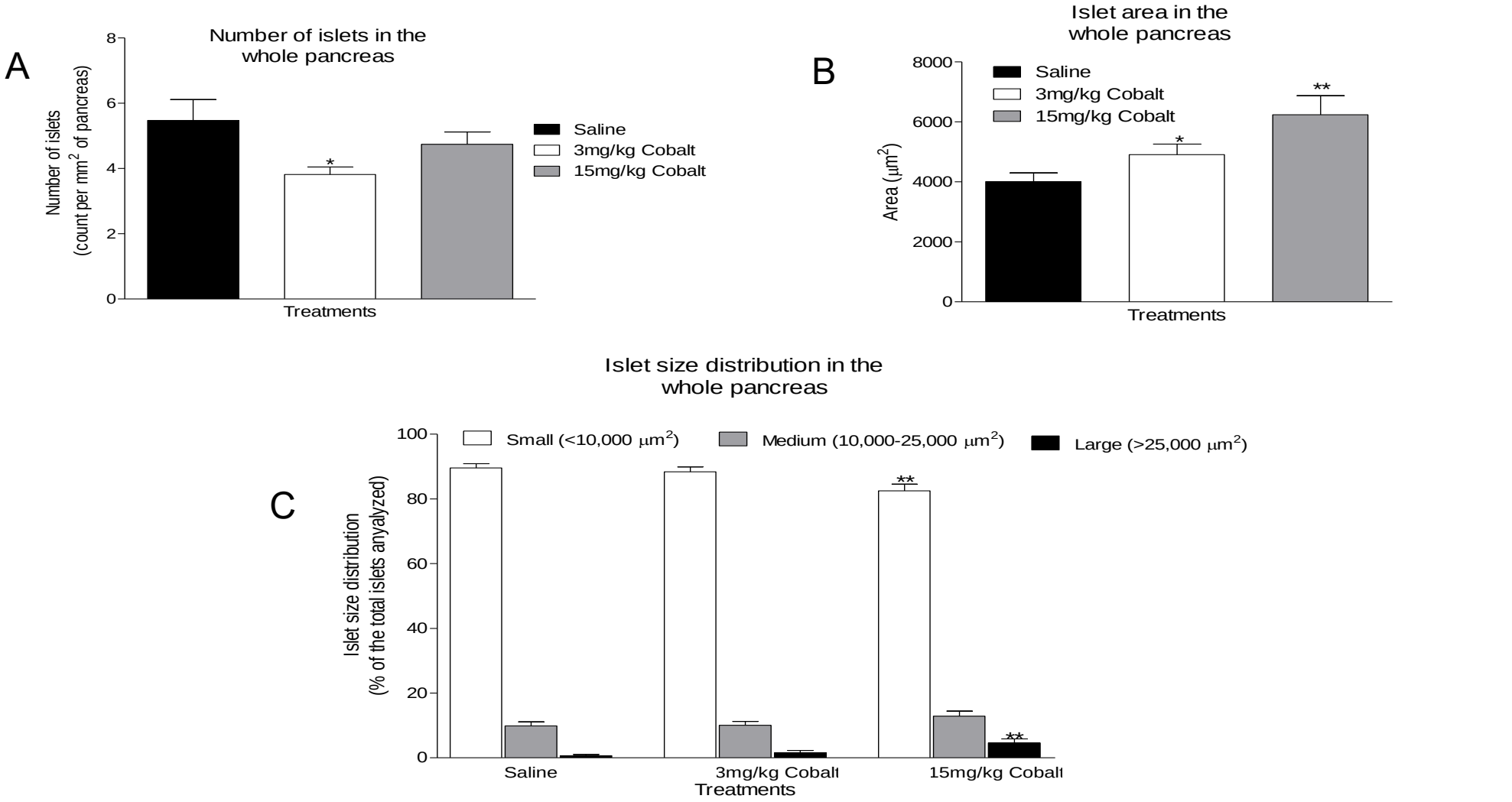

Number of islets (A), islet area (B), and islet size distribution (C) per pancreas in male Glu^{Cre} Rosa mice. A single dose of either 3mg/kg or 15mg/kg of cobalt was administered by i.p. on day 2. Values are mean ± SEM (n=6-7 mice). Changes were deemed significant when p values were *p <0.05, or **p<0.01 when compared to the saline treated mice.

Figure 7.8 Effects of a single low and high dose of cobalt chloride on alpha cell area and percentage (A and B) and beta cell area and percentage (C and D) in the head of the pancreas of male Glu^{Cre} Rosa mice over 8 days following injection.

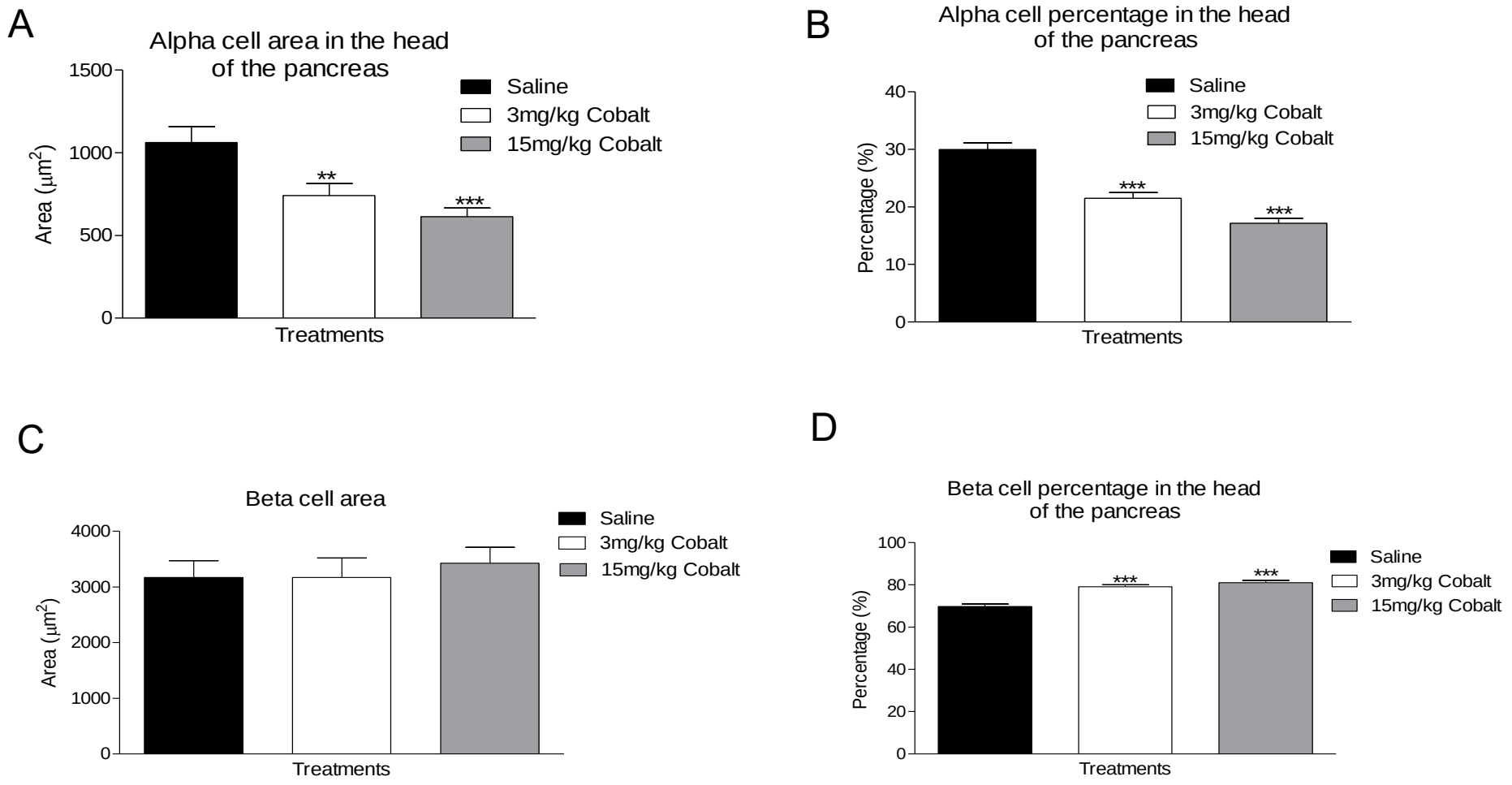

Alpha cell area and percentage (A and B) and beta cell area and percentage (C and D) per pancreas in male Glu^{Cre} Rosa mice. A single dose of either 3mg/kg or 15mg/kg of cobalt was administered by i.p. on day 2. Values are mean ± SEM (n=6-7 mice). Changes were deemed significant when p values were **p<0.01 or ***p<0.001 when compared to the saline treated mice.

Figure 7.9 Effects of a single low and high dose of cobalt chloride on alpha cell area and percentage (A and B) and beta cell area and percentage (C and D) in the tail of the pancreas of male Glu^{Cre} Rosa mice over 8 days following injection.

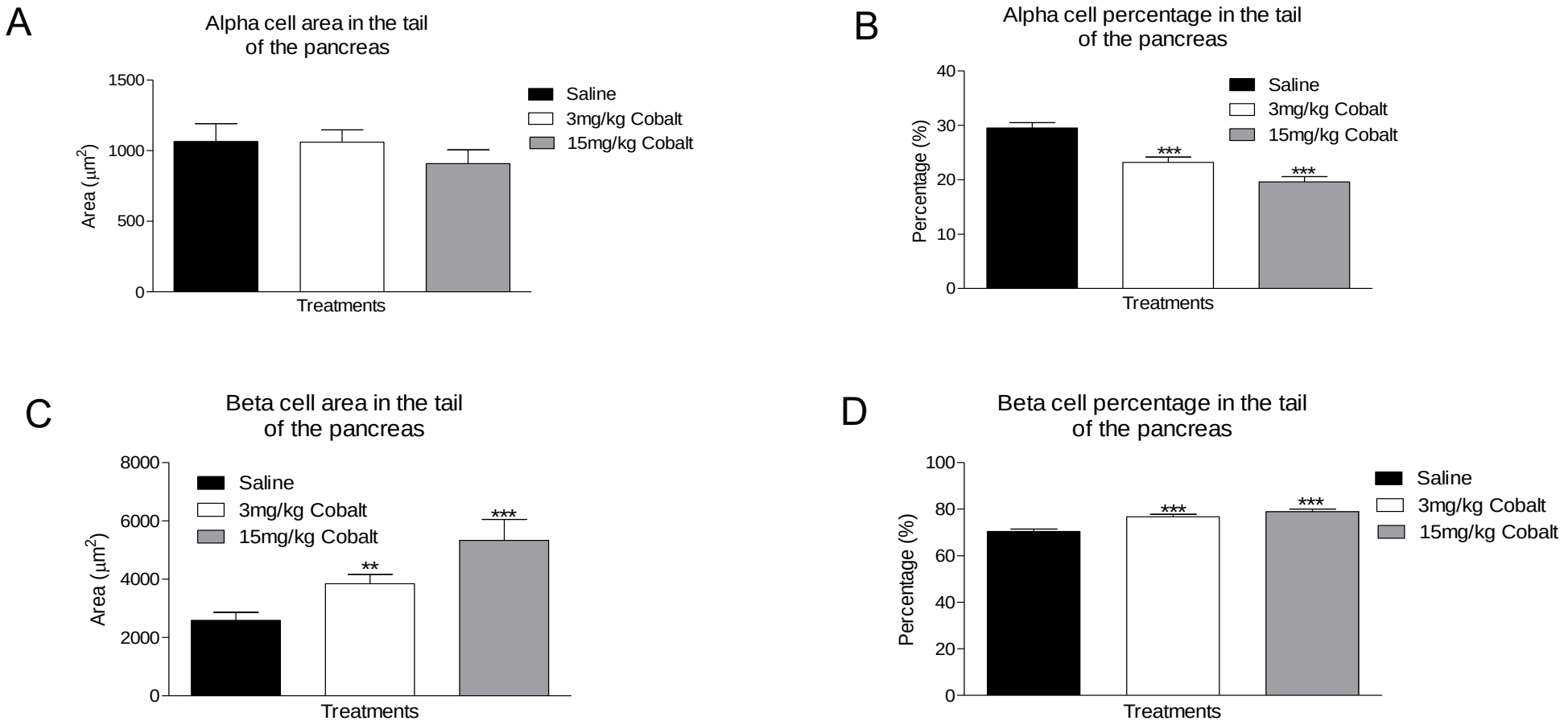

Alpha cell area and percentage (A and B) and beta cell area and percentage (C and D) per pancreas in male Glu^{Cre} Rosa mice. A single dose of either 3mg/kg or 15mg/kg of cobalt was administered by i.p. on day 2. Values are mean ± SEM (n=6-7 mice). Changes were deemed significant when p values were **p<0.01 or ***p<0.001 when compared to the saline treated mice.

Figure 7.10 Effects of a single low and high dose of cobalt chloride on alpha cell area and percentage (A and B) and beta cell area and percentage (C and D) in the whole pancreas of male Glu^{Cre} Rosa mice over 8 days following injection.

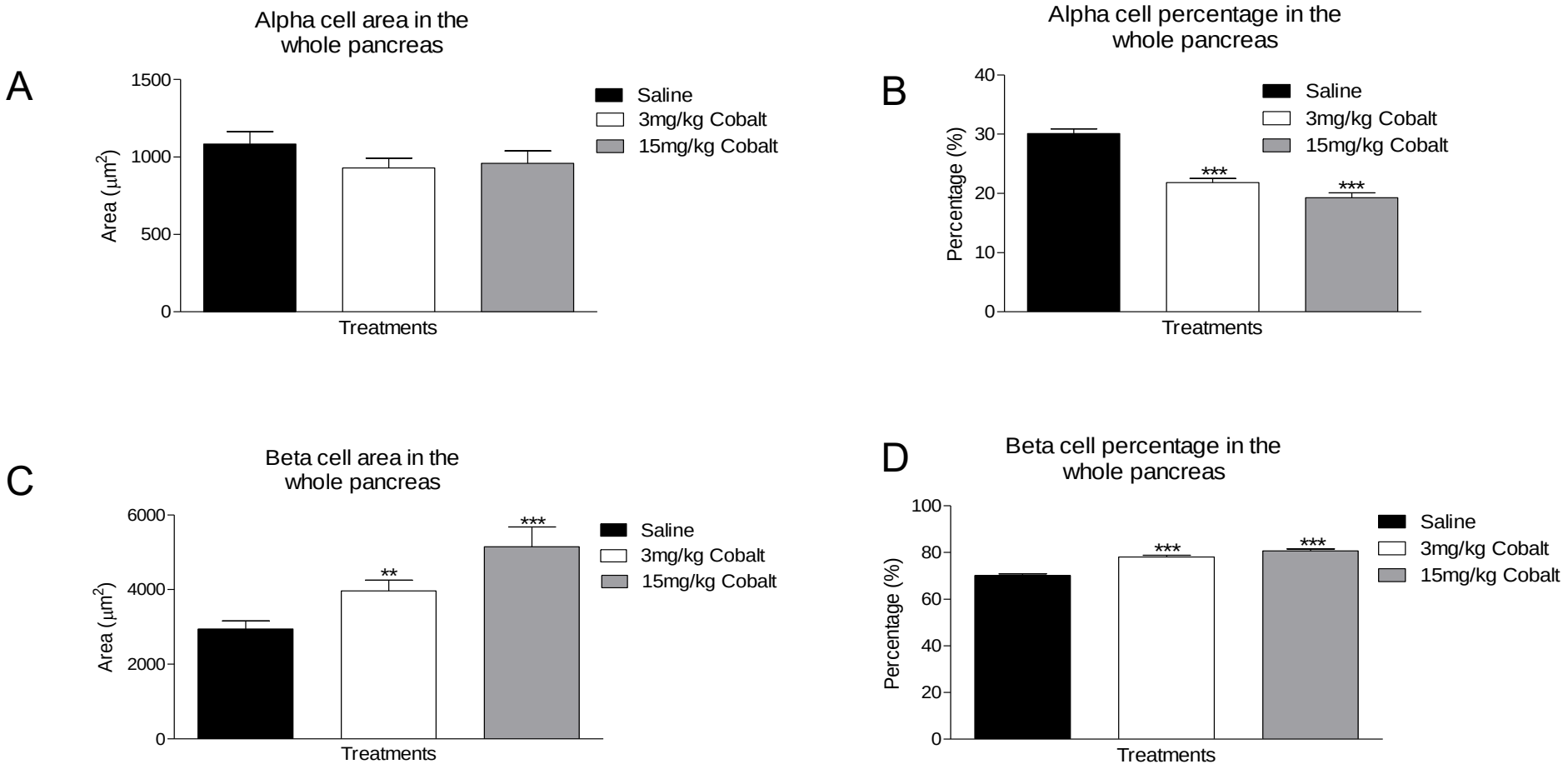

Alpha cell area and percentage (A and B) and beta cell area and percentage (C and D) per pancreas in male Glu^{Cre} Rosa mice. A single dose of either 3mg/kg or 15mg/kg of cobalt was administered by i.p. on day 2. Values are mean ± SEM (n=6-7 mice). Changes were deemed significant when p values were **p<0.01 or ***p<0.001 when compared to the saline treated mice.

Figure 7.11 Representative images of saline (A), 3 mg/kg cobalt chloride (B), and 15 mg/kg cobalt chloride (C) islets from the pancreas in male Glu^{Cre} mice over 8 days following injection.

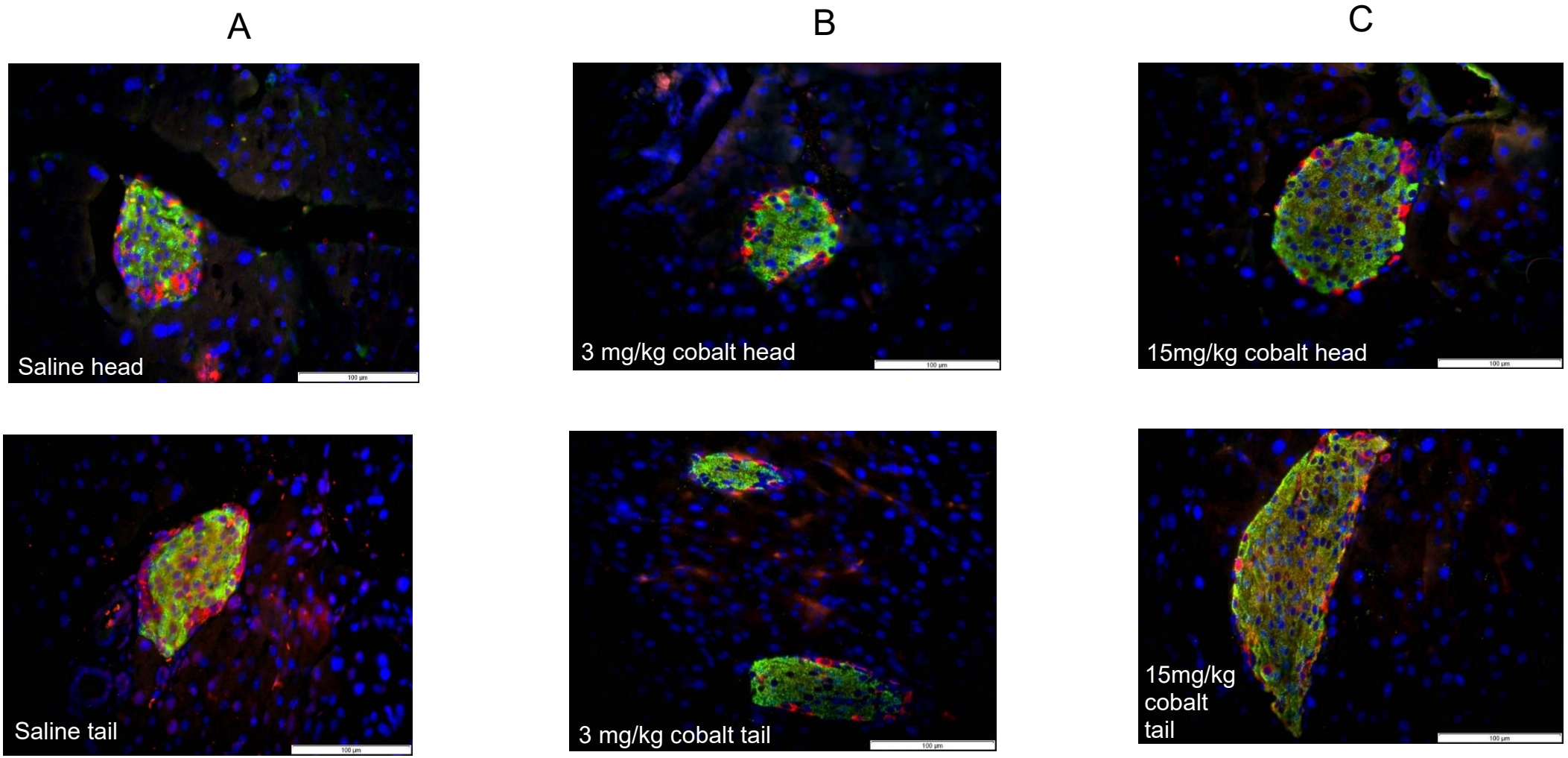

Islet morphology was evaluated at the end of the 8-day study using 5-7 µm tissue sections. Saline (A), 3 mg/kg cobalt chloride (B), and 15 mg/kg cobalt chloride (C) islets from the pancreas of Glu^{cre} male mice. Insulin is represented in green, glucagon in red, and DAPI in blue. Photos imaged at 40x objective lens. Total number of 150 islets were analysed per treatment group.

Figure 7.12 Effects of a single low and high dose of cobalt chloride on GFP positive, insulin positive cells in the head (A), tail (B), and whole (C) pancreas in male Glu^{Cre} Rosa mice over 8 days following injection.

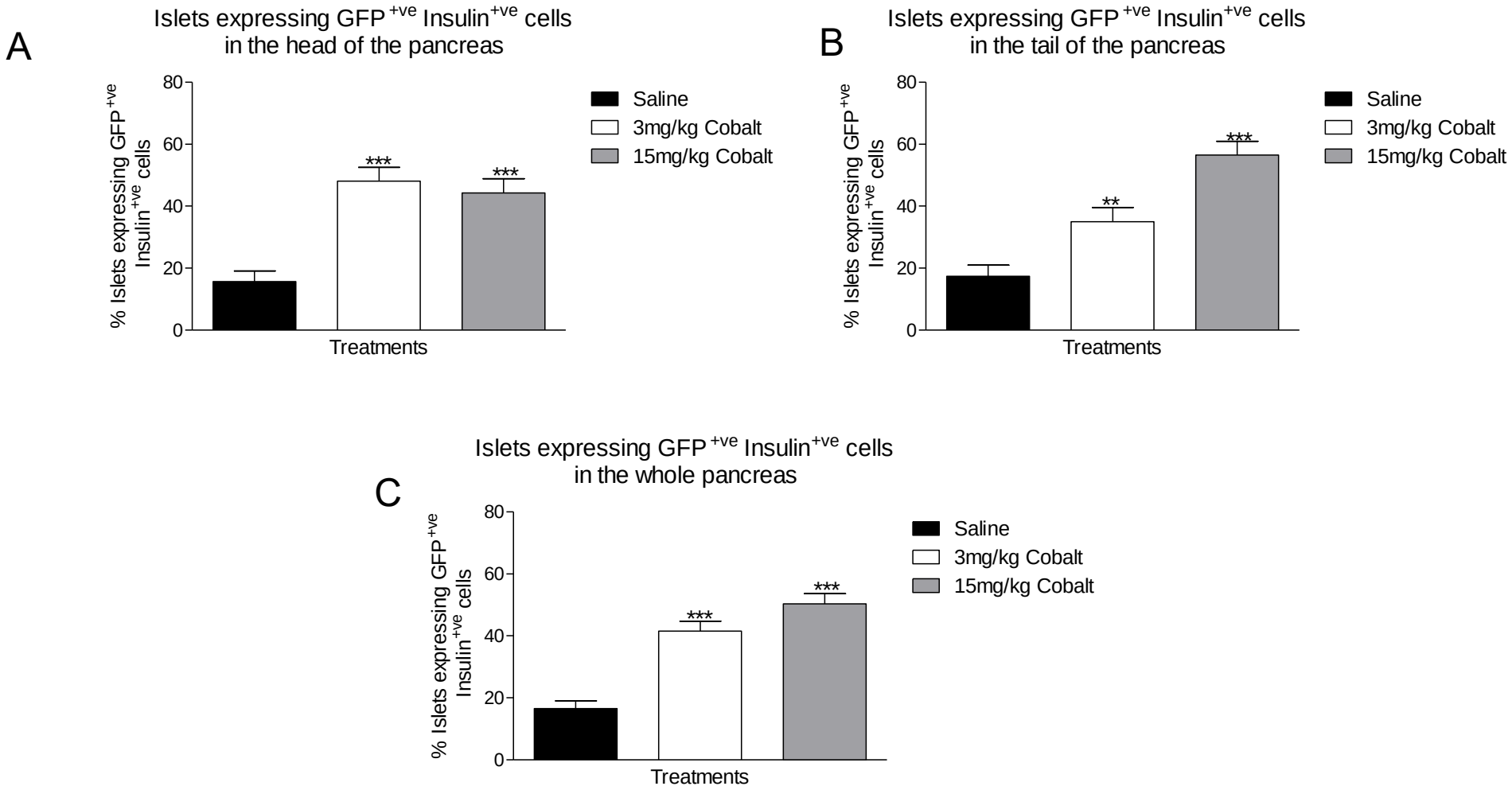

Percentage of alpha to beta cell transdifferentiation was determined by islets expressing GFP^{+ve}, insulin^{+ve} cells in the head (A), tail (B), and whole (C) pancreas. A single dose of either 3mg/kg or 15mg/kg of cobalt was administered by i.p. on day 2. Values are mean ± SEM (n=6-7 mice). Changes were deemed significant when p values were *p<0.05, **p<0.01, or ***p<0.001 when compared with saline.

Figure 7.13 Representative images of saline (A), 3mg/kg cobalt (B), and 15mg/kg cobalt (C) islets from the pancreas in male Glu^{Cre} mice over 8 days following injection.

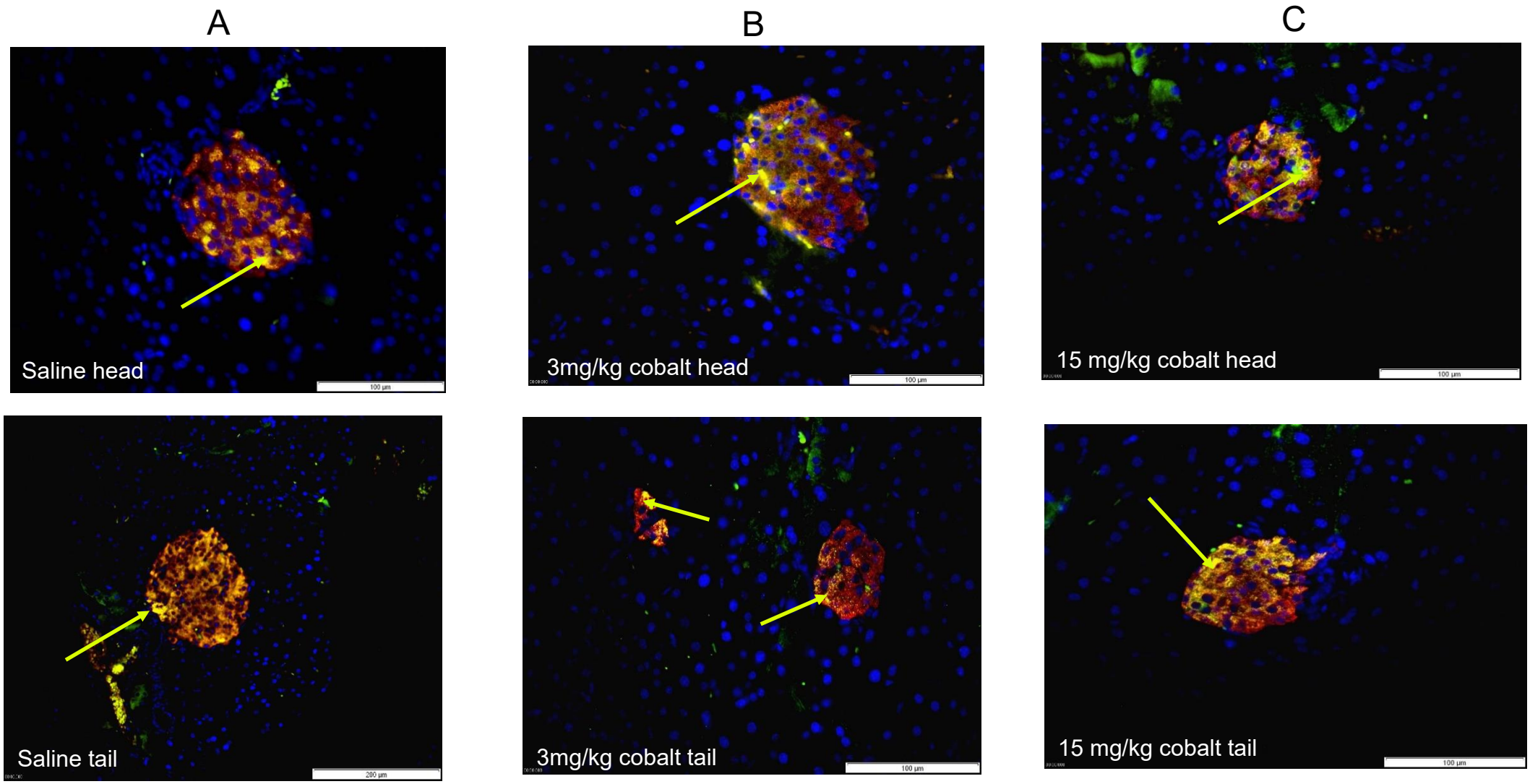

Photo representation of male Glu^{Cre} pancreatic GFP^{+ve}, insulin^{+ve} cells. Insulin is represented in red, GFP in green, and DAPI in blue. The yellow arrows are pointing to GFP^{+ve}, insulin^{+ve} cells. Images were taken at 40x objective lens. Total number of 100 islets were analysed per treatment group.

Figure 7.14 Effects of a single low and high dose of cobalt chloride on GFP positive, insulin negative cells in the head (A), tail (B), and whole (C) pancreas in male Glu^{Cre} Rosa mice over 8 days following injection.

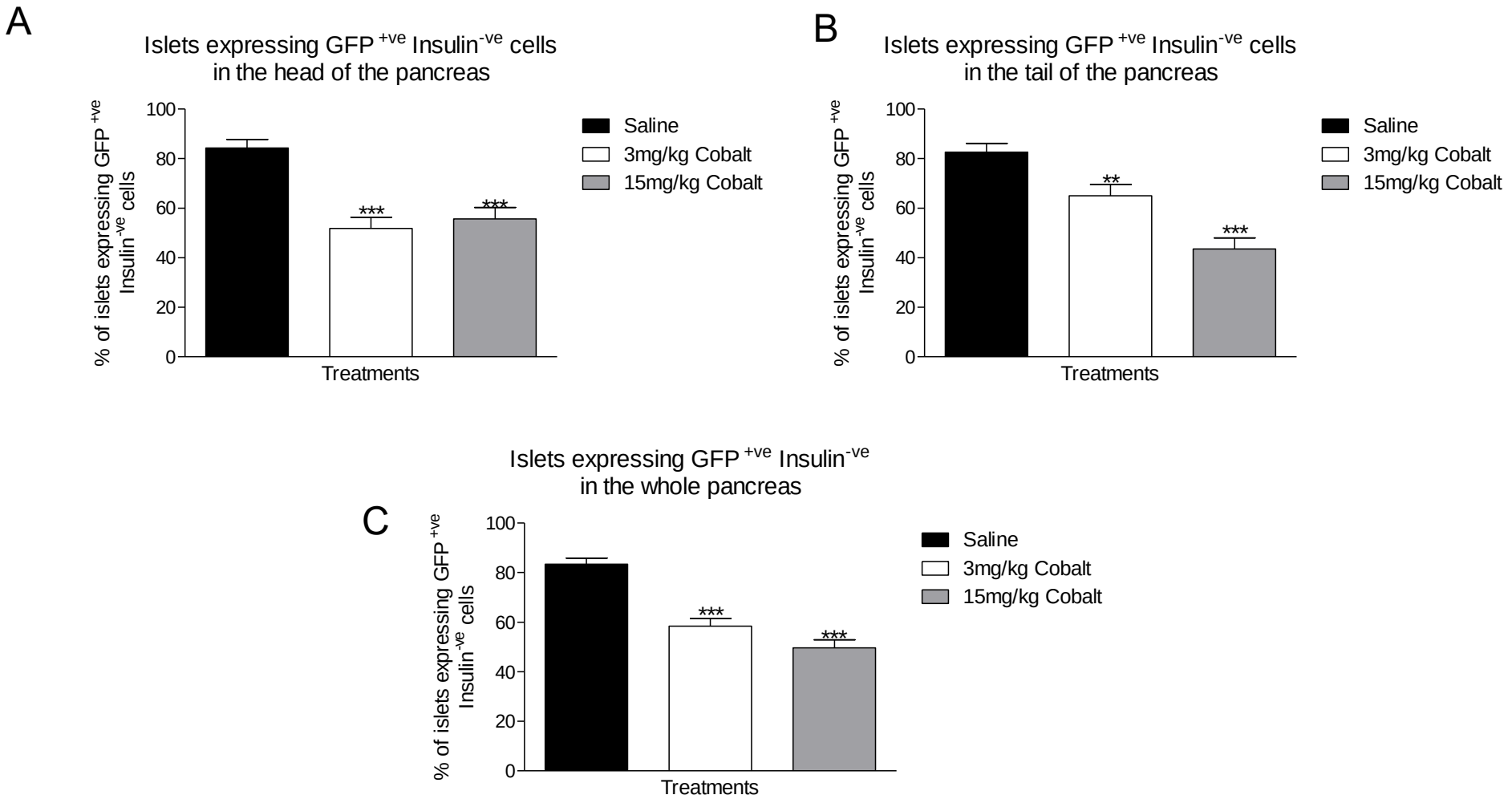

Percentage of alpha to beta cell transdifferentiation was determined by islets expressing GFP^{+ve}, insulin^{-ve} cells in the head (A), tail (B), and whole (C) pancreas. A single dose of either 3mg/kg or 15mg/kg of cobalt was administered by i.p. on day 2. Values are mean ± SEM (n=6-7 mice). Changes were deemed significant when p values were *p<0.05, **p<0.01, or ***p<0.001 when saline was compared with the respective treated mice.

Figure 7.15 Representative images of saline (A), 3mg/kg cobalt (B), and 15mg/kg cobalt (C) islets from the pancreas in male Glu^{Cre} mice over 8 days following injection.

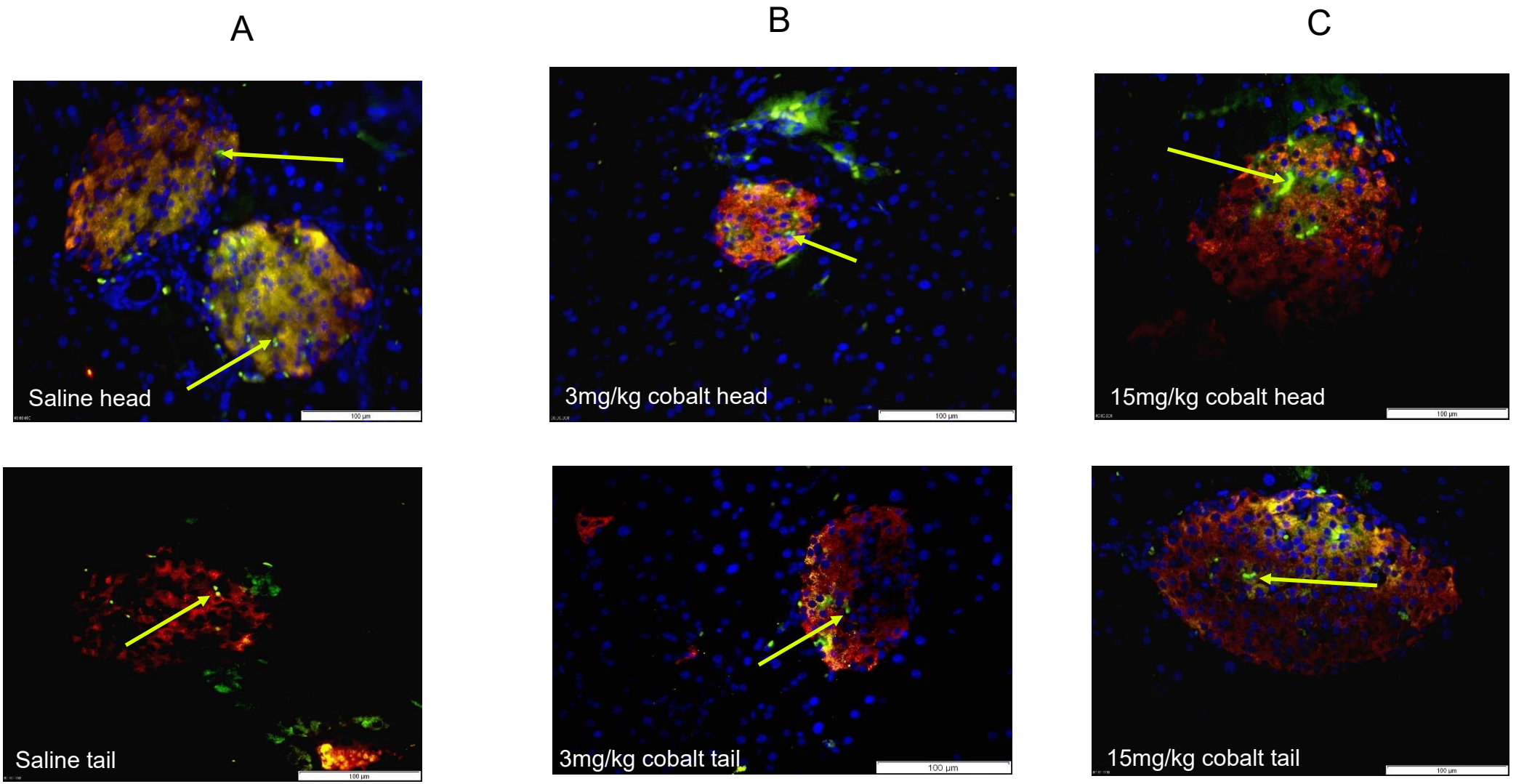

Photo representation of male Glu^{Cre} pancreatic GFP^{+ve}, insulin^{-ve} cells. Insulin is represented in red, GFP in green, and DAPI in blue. The yellow arrows are pointing to GFP^{+ve}, insulin^{-ve} cells. Images were taken at 40x objective lens. Total number of 100 islets were analysed per treatment group.

Figure 7.16 Effects of a single low and high dose of cobalt chloride on GFP positive, glucagon positive cells in the head (A), tail (B), and whole (C) pancreas in male Glu^{Cre} Rosa mice over 8 days following injection.

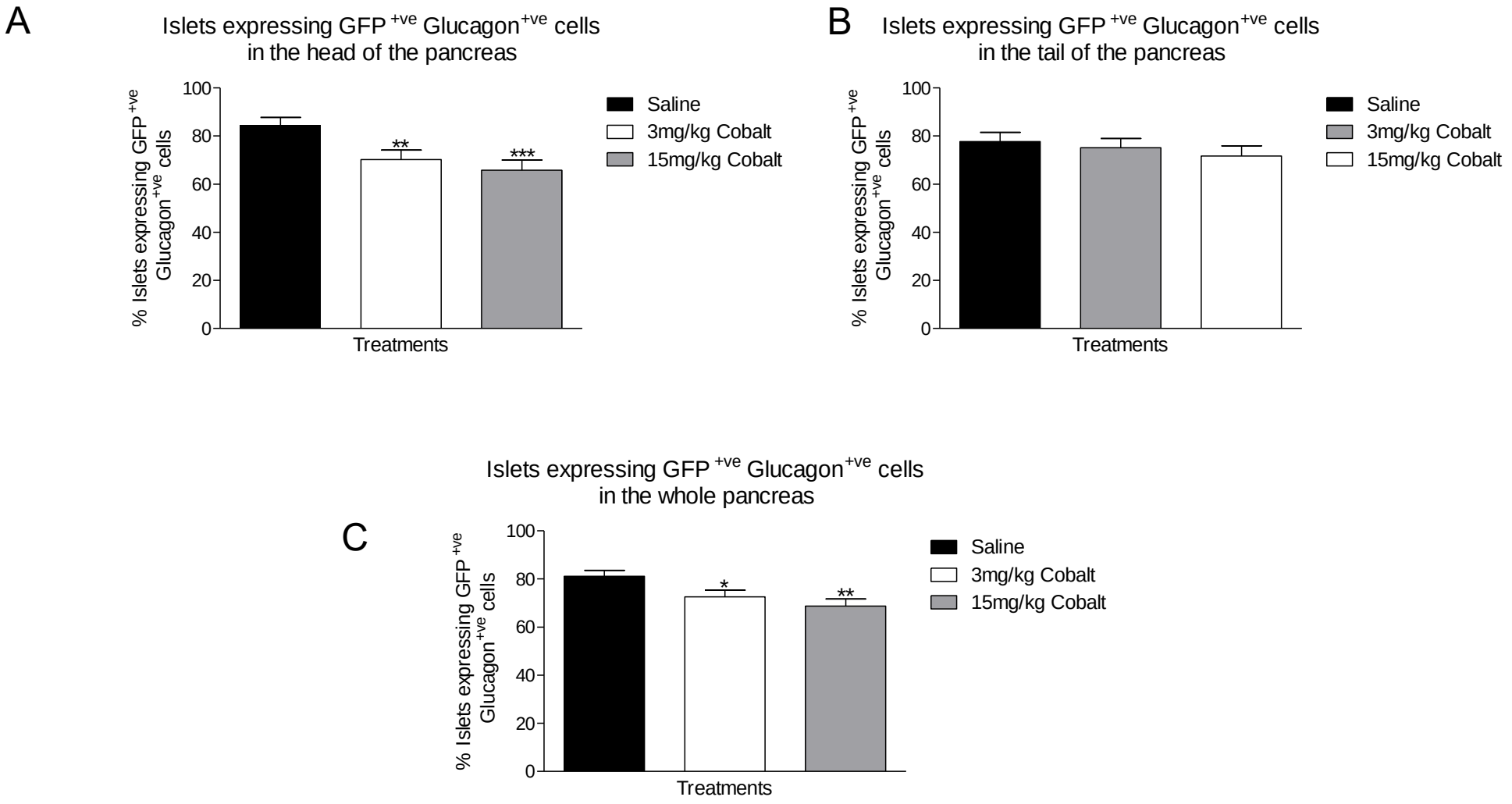

Percentage of alpha to beta cell dedifferentiation was determined by islets expressing GFP^{+ve}, glucagon^{+ve} cells in the head (A), tail (B), and whole (C) pancreas. A single dose of either 3mg/kg or 15mg/kg of cobalt was administered by i.p. on day 2. Values are mean ± SEM (n=6-7 mice). Changes were deemed significant when p values were *p<0.05, **p<0.01, or ***p<0.001 when saline was compared with the respective treated mice.

Figure 7.17 Representative images of saline (A), 3mg/kg cobalt (B), and 15mg/kg cobalt (C) islets from the pancreas in male Glu^{Cre} mice over 8 days following injection.

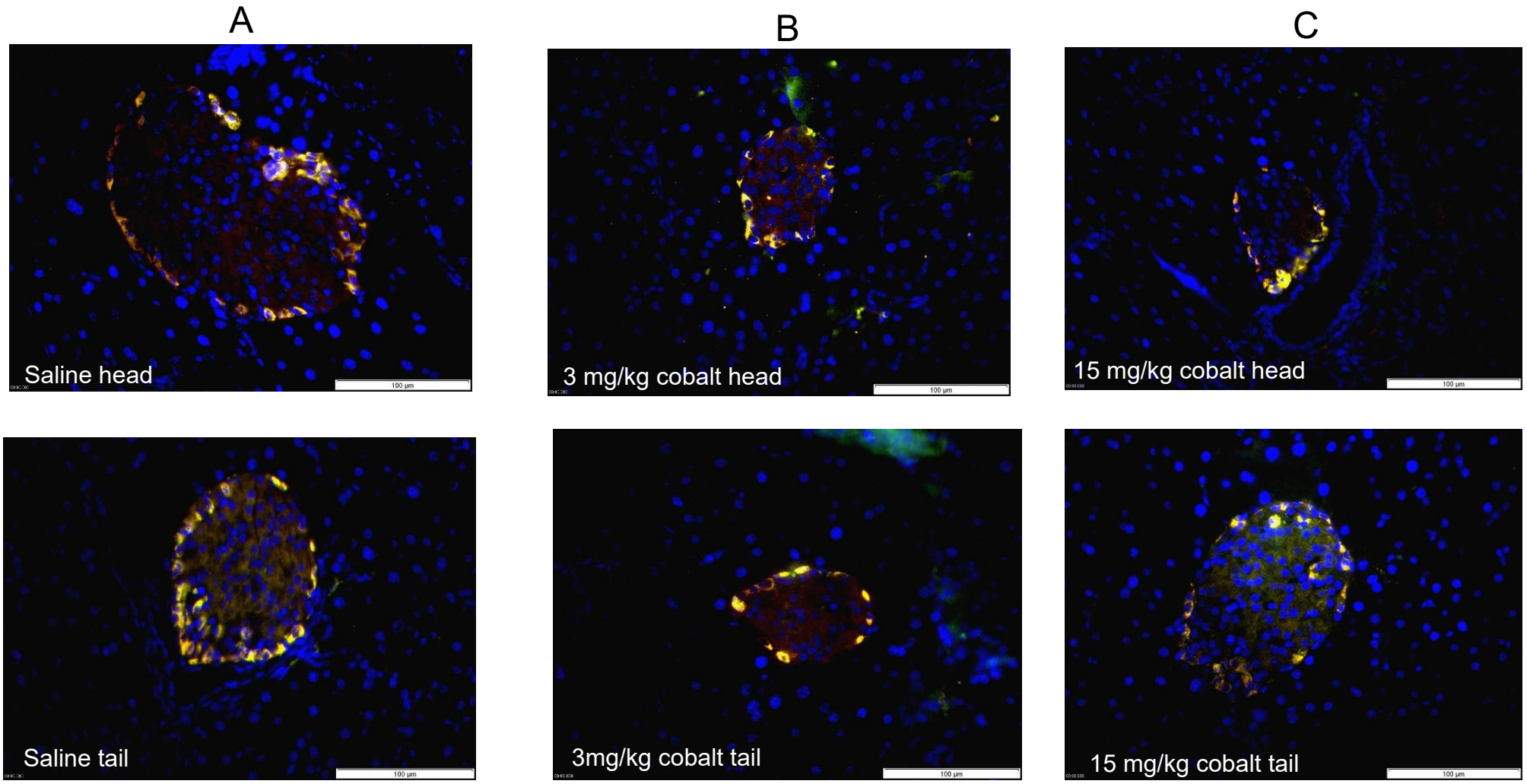

Photo representation of male Glu^{Cre} pancreatic GFP^{+ve}, glucagon^{+ve} cells. Glucagon is represented in red, GFP in green, and DAPI in blue. Yellow arrows are pointing to GFP^{+ve}, glucagon^{+ve} Images were taken at 40x objective lens. Total of 100 islets were analysed per treatment group.

Figure 7.18 Effects of a single low and high dose of cobalt chloride on GFP positive, glucagon negative cells in the head (A), tail (B), and whole (C) pancreas in male Glu^{Cre} Rosa mice over 8 days following injection.

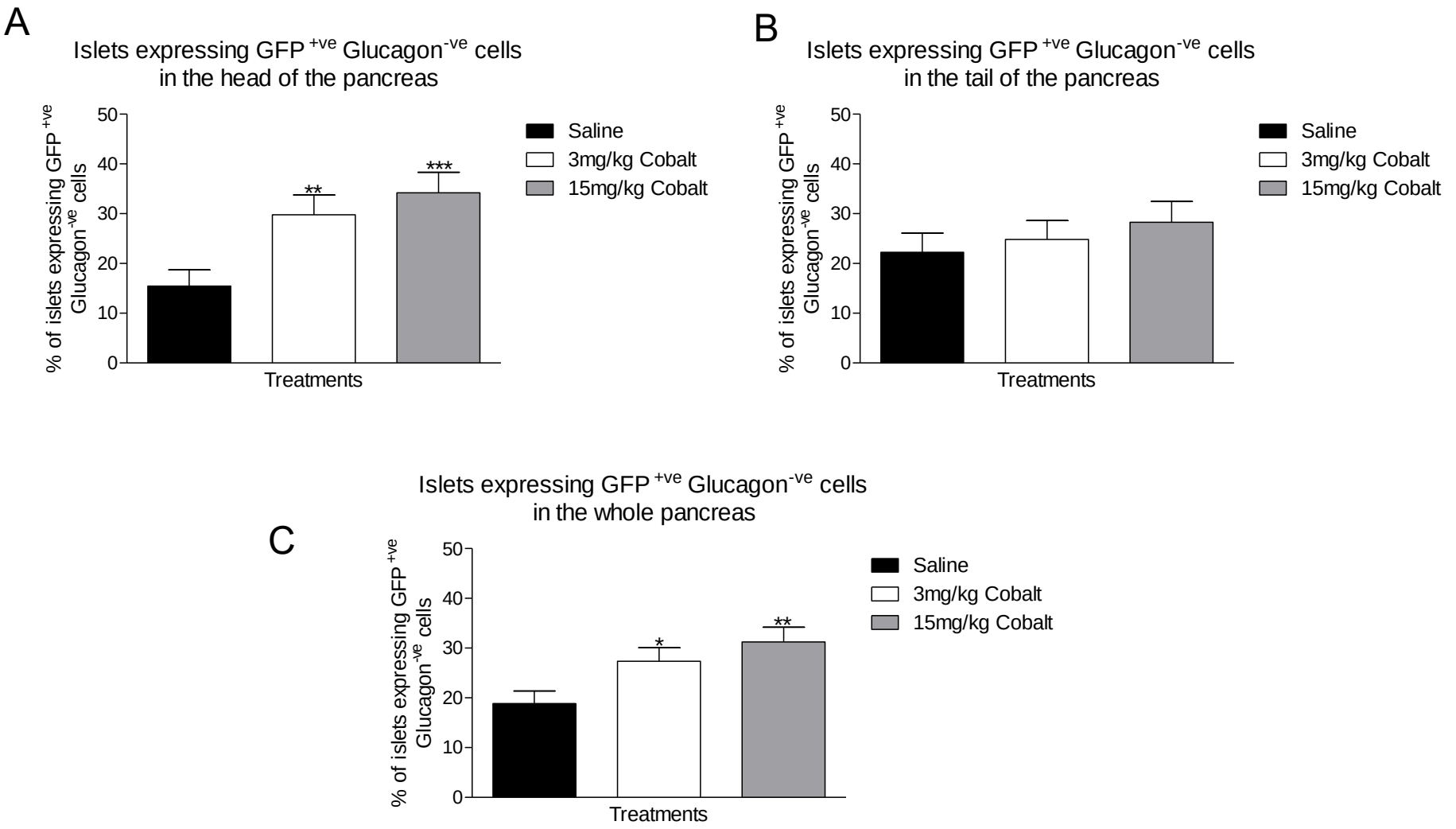

Percentage of alpha to beta cell dedifferentiation was determined by islets expressing GFP^{+ve}, glucagon^{-ve} cells in the head (A), tail (B), and whole (C) pancreas. A single dose of either 3mg/kg or 15mg/kg of cobalt was administered by i.p. starting at day 2. Values are mean ± SEM (n=6-7 mice). Changes were deemed significant when p values were *p<0.05, **p<0.01, or ***p<0.001 when saline was compared with the respective treated mice.

Figure 7.19 Representative images of saline (A), 3mg/kg cobalt (B), and 15mg/kg cobalt (C) islets from the pancreas in male Glu^{Cre} mice over 8 days following injection.

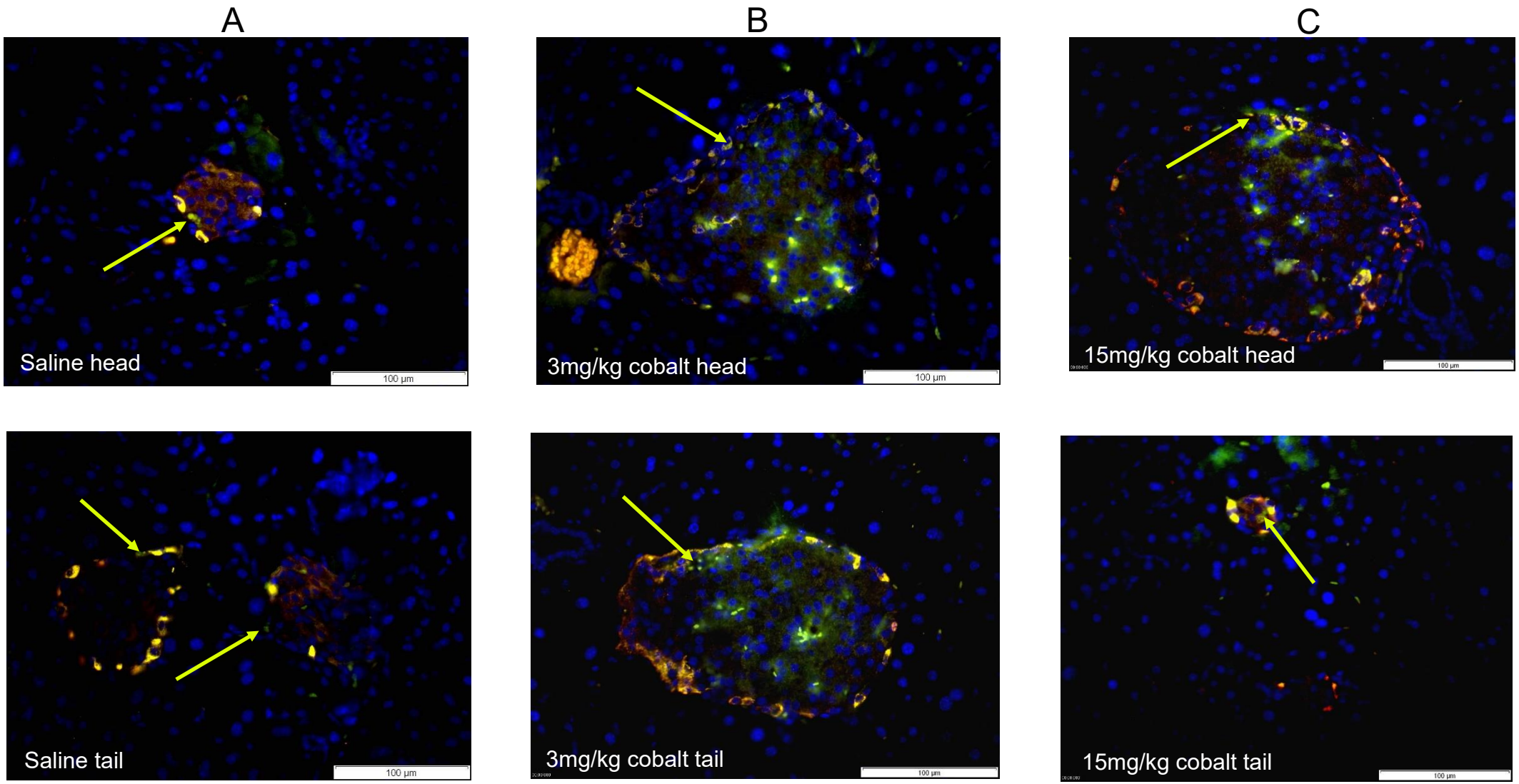

Photo representation of male Glu^{Cre} pancreatic GFP^{+ve}, glucagon^{-ve} cells. Glucagon is represented in red, GFP in green, and DAPI in blue. The yellow arrows are pointing to GFP^{+ve}, glucagon^{-ve}. Images were taken at 40x objective lens. Total of 100 islets were analysed per treatment group.

Figure 7.20 Effects of a single low and high dose of cobalt chloride on Ki67 positive, insulin positive cells in the head (A), tail (B), and whole (C) pancreas in male Glu^{Cre} Rosa mice over 8 days following injection.

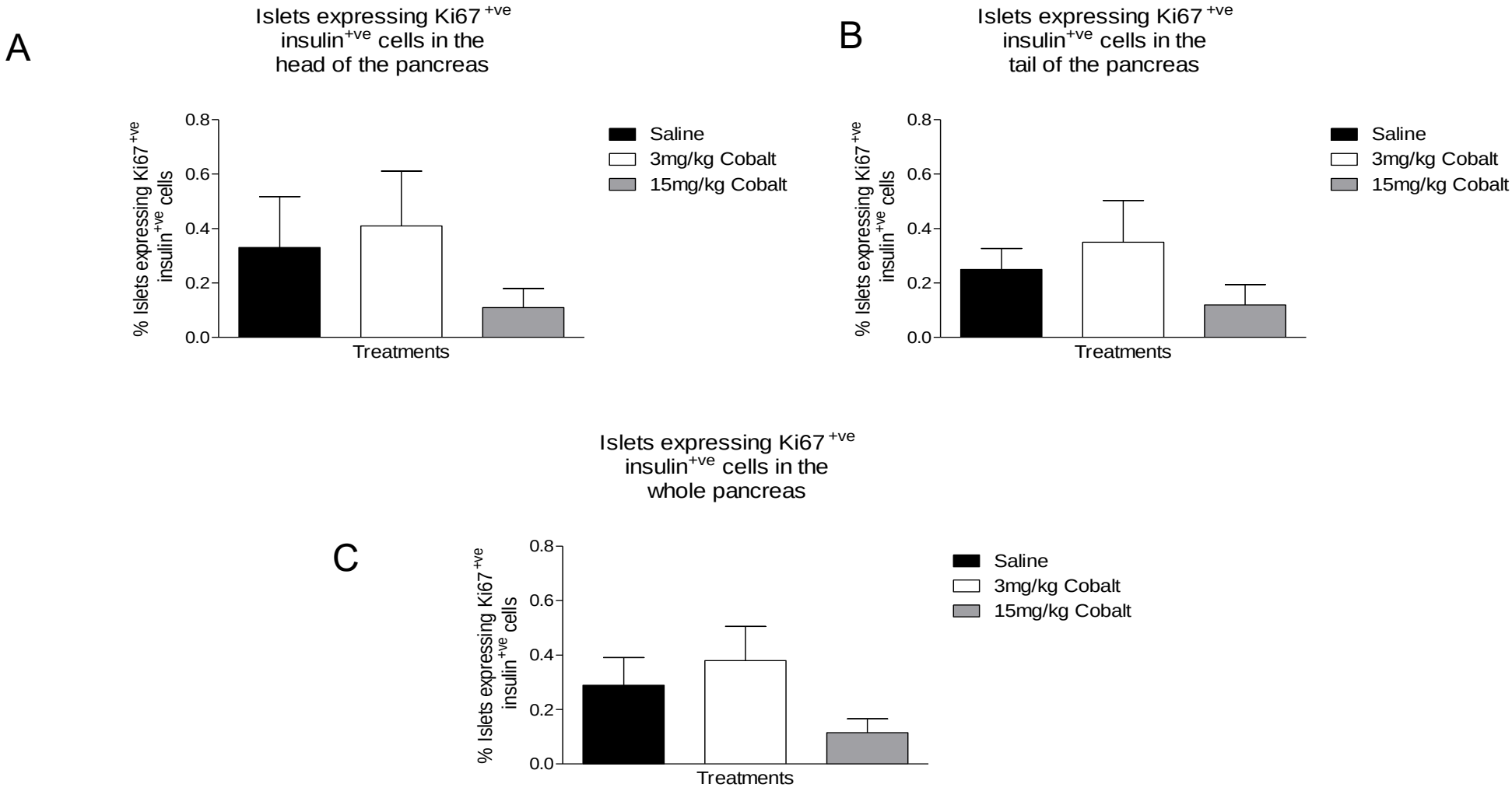

Percentage of beta cell proliferation was determined by islets expressing Ki67^{+ve}, insulin^{+ve} cells in the head (A), tail (B), and whole (C) pancreas. A single dose of either 3mg/kg or 15mg/kg of cobalt was administered by i.p. starting at day 2. Values are mean ± SEM (n=6-7 mice). Changes were deemed significant when p values were $p<0.05$.

Figure 7.21 Representative images of saline (A), 3mg/kg cobalt (B), and 15mg/kg cobalt (C) islets from the pancreas in male Glu^{Cre} mice over 8 days following injection.

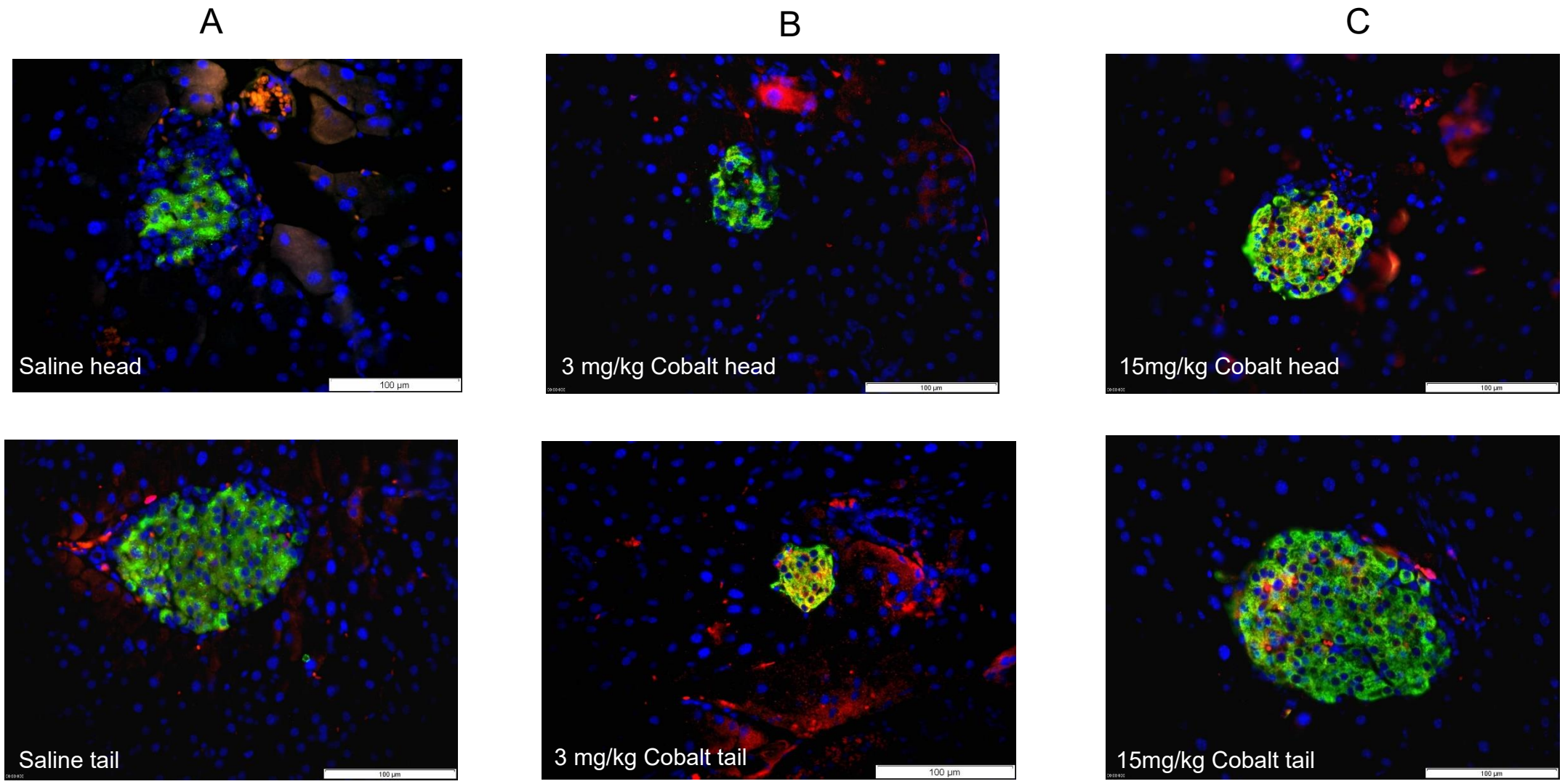

Insulin is represented in green, Ki67 in red, and DAPI in blue. Images were taken at 40x objective lens. Total of 100 islets were analysed per treatment group.

Figure 7.22 Effects of a single low and high dose of cobalt chloride on Ki67 positive, glucagon positive cells in the head (A), tail (B), and whole (C) pancreas in male Glu^{Cre} Rosa mice over 8 days following injection.

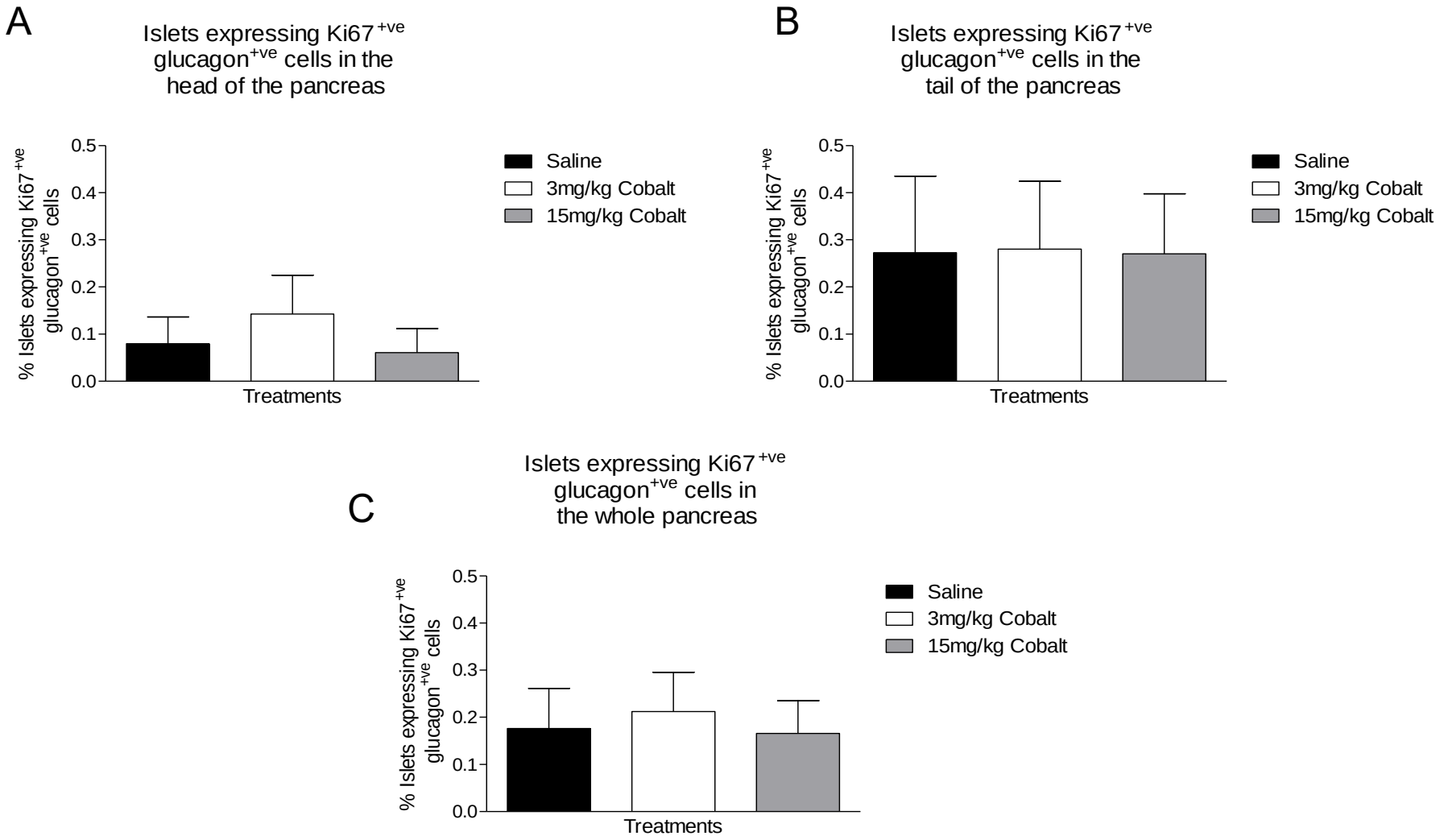

Percentage of alpha cell proliferation was determined by islets expressing Ki67^{+ve}, glucagon cells in the head (A), tail (B), and whole (C pancreas. A single dose of either 3mg/kg or 15mg/kg of cobalt was administered by i.p. starting at day 2. Values are mean ± SEM (n= 7 mice). Changes were deemed significant when p values were $p<0.05$.

Figure 7.23 Representative images of saline (A), 3mg/kg cobalt (B), and 15mg/kg cobalt (C) islets from the pancreas in male Glu^{Cre} mice over 8 days following injection.

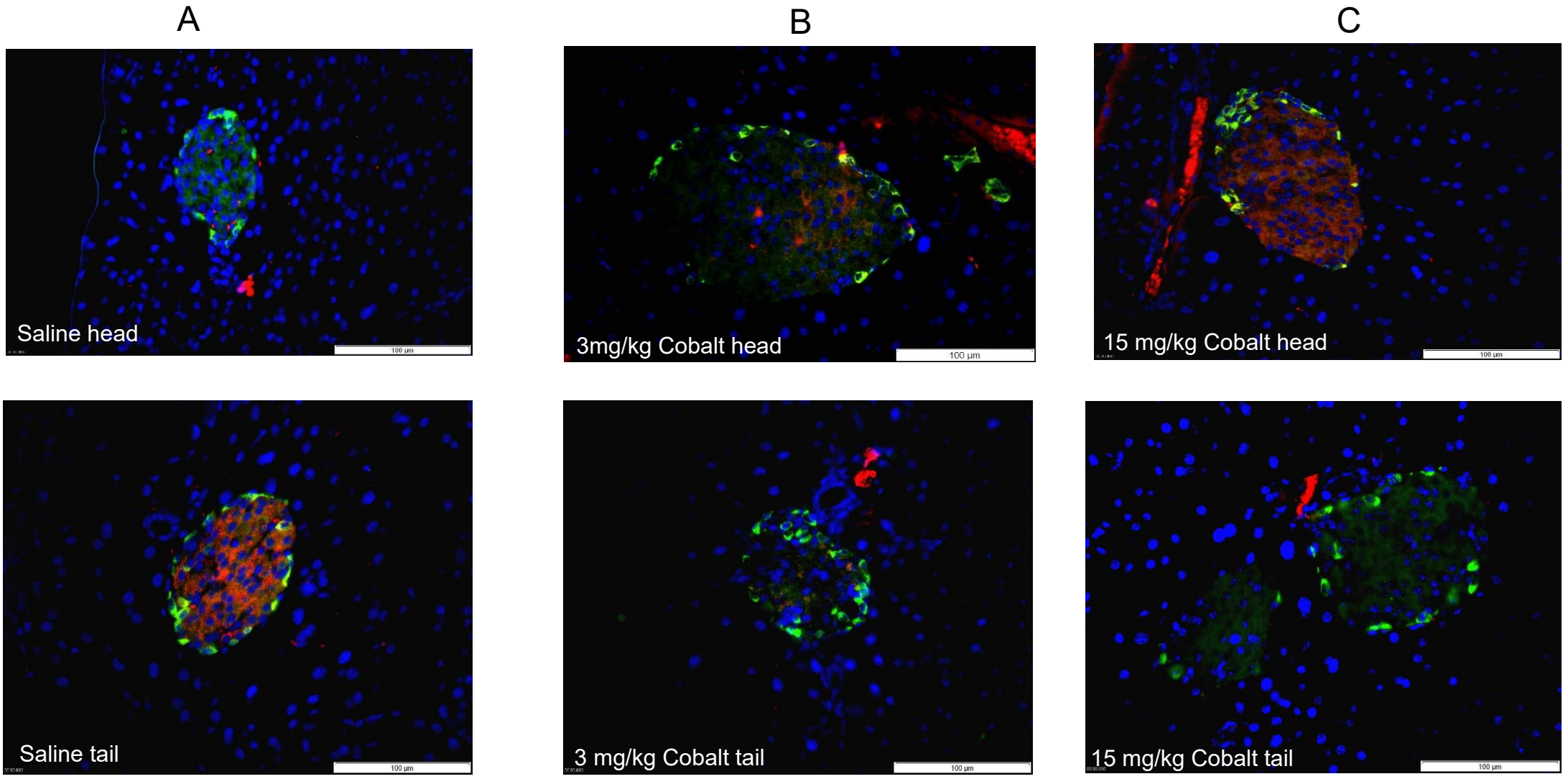

Photo representation of male Glu^{Cre} pancreatic islet proliferation. Glucagon is represented in green, Ki67 in red, and DAPI in blue. Images were taken at 40x objective lens. Total of 100 islets were analysed per treatment group.

Chapter 8

Effects of Synthalin A and cobalt chloride on viability and gene expression in alpha TC cells, Min-6 cells, and GLUTag cells

8.1 Summary

Alpha TC cells are a clonal cell line that secrete glucagon which is an essential hormone for blood glucose control. Several assays were performed using alpha TC cells after exposure to Synthalin A (Syn A) or cobalt chloride to test cellular viability, gene expression, proliferation, and apoptosis of alpha TC cells. Hydrogen peroxide was also introduced as a general cytotoxin to compare against the specific alpha cell toxins. Viability of this cell line, as well as Min-6 and GLUTag cells (beta and L-cell lines, respectively), showed different levels of toxicity depending on incubation time and media composition. Hydrogen peroxide showed toxicity in all the assays conducted. Both alpha cell toxins, Synthalin A (Syn A) and cobalt chloride, had a negative effect on proliferation, apoptosis, and necrosis. However, these tests showed that cobalt chloride is more toxic than Syn A in regard to alpha cells.

8.2 Introduction

There are very few studies that look at the cellular activity following exposure to Syn A or cobalt. As stated previously, a study in 1983 was carried out looking at incubated islets of guinea pigs. It was concluded that when Syn was given at the highest dose of 500µg/ml, glucagon secretion was three times greater than the secretion in control islets. This *in vitro* study showed that suppression of the glucose oxidation rates was observed in both alpha and beta cells in islets by Syn A. Together with the present results, the guinea pig study on isolated islets provides an insight on what is to be expected in the future tests that will be performed. Cellular morphology was observed within this study, showing that the alpha cells became hydropic, cytoplasmic vacuolation, and showed disruption to the nucleus. Given the research that has previously been conducted on incubated guinea pig islets (Östenson, 1983), one can suspect that Syn will have a cytotoxic effect on the present study of the glucagon secreting cells, alpha TC cells.

Cobalt has been documented to be toxic to alpha cells when treated with large doses or smaller doses for a long period of time (Simonsen *et* al. 2012). Previously, it was stated that,

administration of cobalt results in the alpha cells to become over stimulated causing degeneration. However, this was disproven in past animal studies. This observation conclusion was made using histology, and not cytology (Koch, 1955). Some recent studies have found that cobalt chloride is a hypoxic mimicking agent and can alter cellular activity as well as gene expression (Simonsen *et* al. 2012; Okail, 2010; Grasselli *et al*. 2005; Vengellur *et al*. 2003; *Epstein et al*. 2001; Lee *et al*. 2001; Badr *et al*. 1999; Wang and Semenza, 1993; *Goldberg et* al. 1988). In terms of gene expression, cobalt has been documented as causing oxidative DNA damage (Simonsen *et al*. 2012). High levels of cobalt can cause cellular and tissue damage. Cellular toxicity from cobalt depends on cobalt being ionized (Simonsen *et al*. 2012; Rossner *et al*. 2001).

Mice derived cell lines, alpha TC, Min-6, and GLUTag cells, were used in a MTT assay with Syn A and cobalt chloride. An MTT assay examines the activity of the mitochondrial dehydrogenases within the cell (Gare *et al*. 2007). We examined the insulin secreting Min-6 cells and GLUTag cells for an L-cell model to see if the two toxins had an effect on other cells besides alpha cells. Alpha TC cells were the primary focus for the follow up assays: staining, apoptosis, and PCR. Cellular viability can be described as the number of healthy cells within an experiment (Stoddart, 2011). An MTT assay was carried out to determine the percentage of cellular viability and proliferation when looking at two cytotoxins, Syn A and cobalt chloride (Sylvester, 2011; Liu *et al*. 1997). The MTT color change from clear to purple indicates viable cells with active metabolisms (Riss *et al*. 2016) ATP, which is produced through glycolysis, has been documented to be the result of the cause of the MTT reduction (Liu *et al*. 1997; Vistica *et al*. 1991).

Alpha TC cells secrete glucagon, and since Syn A and cobalt are known as alpha cell toxins, it can be hypothesized that the alpha TC cells will be greatly affected by the treatment. Min-6 cells secrete insulin, and therefore it is hypothesized that Syn A and cobalt will have seldom effect on this beta cell line as well as on the GLP-1 secreting GLUTag cell line (Whalley *et al.* 2011; Baggio and Drucker, 2007; Kjems *et al*. 2003). However, due to the limited research

on these alpha cell toxins, there is no previous study that examines the effects of these alpha cell toxins on beta and GLP-1 producing cells, which is why these assays were performed. There has been previous research that examined the effects of Syn A and cobalt in reference to the stomach at an anatomical level, but not hormonal. Therefore, testing to see if the alpha cell toxins have an effect on the intestinal cells producing GLP-1 which acts to prevent glucagon release could be interesting in future studies (Whalley *et al.* 2011; Jin, 2008; Baggio and Drucker, 2007; Kjems *et al*. 2003; Nauck *et al*. 2003; Drucker, 2002; Drucker, 1998; Ahen *et al.* 1997; Rachman *et al*. 1997; Nauck *et al*. 1996; Gutniak *et al*. 1994). Using the three different cell lines and determining the viability of cells after the two toxic agents will provide insight into the mechanism of action of Syn A and cobalt and why past research says it is only toxic to alpha cells.

The aim of this study was to determine the direct effects and mechanism of action of Syn A and cobalt. It also attempted to determine why alpha cells are affected, but beta cells remain stable. As part of this, we also determined which genes were affected by the toxins in alpha cells and which inhibitors, as laid out by Flatt *et al*. 1987, could possibly prevent deleterious effects of the two toxins.

8.3 Materials and methods

All materials and methods for this study have been summarised in 8.3.1 to 8.3.9. A detailed description of the materials and methods can be found in Chapter 2.

8.3.1 Cell culture and treatments

Under aseptic conditions, three cell lines, Alpha TC, GLUTag, and Min-6 cells, were cultured in high glucose DMEM (25mM) media containing 10% foetal bovine serum (FBS) and 1% penicillin-streptomycin antibiotics. For Min 6 cells, an additional 200µM of 2-mercaptoethenol was supplemented to the DMEM media used to culture the cells. For the MTT assay, Syn A and cobalt were added to seeded cells for 2 or 8 hours at different concentrations in high glucose media with and without FBS. For PCR, MTT with inhibitors, immunocytochemistry,

and apoptosis, alpha TC cells were seeded overnight and then treated with a specific concentration of Syn A, cobalt, and hydrogen peroxide for 2 or 8 hours in DMEM high glucose media containing FBS.

8.3.2 Cellular viability using the MTT assay

Treated cells were incubated at different time intervals, 2 and 8 hours, and treatments were serial diluted starting from 5 mM or 10mM (Vasu *et al*. 2015). This cellular viability assay was also repeated with the addition of inhibitors. The inhibitors, that inhibit DNA strand breaks, concentrations that were used are as followed: nicotinamide (10mM), theophlylline (5mM), benzamide (1mM), and the inhibitors that scavenge OH radicals; high glucose (20mM), sodium benzoate (50mM), DMSO (28mM), butanol (22mM), superoxide dismutase (2000u/ml), and catalase (250u/ml). Data was used to generate cellular viability as well as to determine where the lethal dose 50 (LD 50) occurred within the specific treatments. Analysis of the well plates occurs using the Softmax Pro computer program and plates were read at a wavelength of 570nm. To generate statistical analysis outcomes, the Graphpad program, Prism was used.

8.3.3 RNA extraction and cDNA conversion

Cells were seeded in 6 well plates at a density of 500,000 cells and incubated overnight. The toxins were added to the alpha cells for two hours, washed with HBSS and ice cold Trizol was added. Eppendorf's were then place in the centrifuge for 10 minutes at 12,000 RPM at 4°C. Chloroform was added and placed back in the centrifuge to create three layers within the mixture. Isopropanol was added placed back in the centrifuge resulting in an RNA pellet to form at the bottom of the tube and washed with ethanol. The NanoDrop ND-1000 UV/Vi spectrophometer to determine the quantity and quality of RNA. OligoDT was mixed with the RNA samples and placed in the thermocycler which heated them to 70°C. A master mix was added to the samples and placed back in the thermocycler to heat the mixture. Samples were then stored at -20°C until qPCR was ready to be performed.

8.3.4 Real Time Polymerase Chain Reaction (RT-PCR)

A master mix containing SYBR green and RNA free water was created and added to the forward and reverse primers. The master mix was then added into each well of a 96 well plate along with 1µL of cDNA. Plates were centrifuged and placed in the Light Cycler 480 (Roche Diagnostics Ltd., Switzerland) for further analysis.

8.3.5 Proliferation

Cells were seeded at a density of 40,000 for 24 to 48 hours in a 12 well plate containing sterilised 19mm round coverslips. The following day cells were treated with specific treatments for 2 hours in DMEM media containing FBS. Cells were stained using anti-guinea pig glucagon primary antibody, goat anti-guinea pig secondary antibody, and goat anti- rabbit Ki67 primary antibody. Analysis was carried out using Image J cell counter (Moffett, 2012; Abràmoff, 2004).

8.3.6 Trypan blue staining

Alpha TC cells were cultured and seeded overnight in a 6-well plate in DMEM media containing FBS. Wells were then treated with either hydrogen peroxide (0.25mM), Syn A or cobalt at 2.5mM for two hours. Cells were analysed using the histocytomere and percentages of living and dead cells were calculated. This was also repeated with a few inhibitors to assess

8.3.7 Apoptosis and Necrosis using Flow cytometry

Alpha TC cells were grown overnight in a 6-well plate, one plate per treatment. Treatments were added to the wells and incubated for 8 hours. 1X annexin-binding buffer and a 5µl of propidium iodide (PI) stock was prepared and cells were resuspended in this buffer. Next, Alexa Fluor 488 annexin V and 1 µlg/ml of PI was added to the cells and they were incubated at room temperature for 15 minutes. The 1X annexin- buffer was added once again and kept on ice. Flow cytometry was performed as soon as possible and viewed under a fluorescent microscope using the FITC filter (Olympus system microscope, model BX51) and photographed using the DP70 digital camera adapter system (ThermoFisher Scientific, United

Kingdom).

8.3.8 Statistics

The graphs and results were all generated and analysed using GraphPad Prism 5. The appropriate statistical tests were conducted for these experiments: one-way ANOVA followed by a Newman-Keuls Multiple Comparison Test, or an unpaired t-test. Comparisons of two groups with $p<0.05$ were statistically significant.

8.4 Results

8.4.1 Effects of Syn A treatment on alpha TC cellular viability at 2- and 8-hour incubation with and without FBS as detected by MTT assay.

Figure 8.1A, shows that there was a slight decrease in alpha cells treated with 1mM ($p<0.01$) Syn A cells when compared to control cells. The 2.5mM and 5mM ($p<0.001$) Syn A concentrations showed a significant decrease when compared to control cells when treated in serum free media. Syn A concentrations of 1mM, 2.5mM, and 5mM ($p<0.001$) show a significant decrease when compared to control cells (Figure 8.1B). As seen in Figure 8.1C, the alpha cells incubated for 8 hours in FBS rich media, when compared to the control cells, show all concentrations of Syn A treated cell viability is significantly decreased ($p<0.001$). Compared to the control cells, cells incubated for 8 hours in serum free media with Syn A had significantly decreased cell viability at all concentrations that were tested ($p<0.001$) (Figure 8.1D).

8.4.2 The LD 50 of Syn A treated alpha TC cells at 2- and 8-hour incubation as detected by MTT assay.

In the 2-hour incubation cellular viability assay, the LD 50 was observed only in the alpha TC cells treated at 5mM in media containing no FBS (Figure 8.2A). However, in the FBS free media, LD 50 was observed at the concentration 1mM Syn A after 8 hours (Figure 8.2B)

8.4.3 Effects of cobalt chloride treatment on alpha TC cellular viability at 2- and 8-hour incubation with and without FBS as detected by MTT assay.

As seen in Figure 8.3A, there was a decrease in cellular viability in all of the cobalt treatment concentrations ($p<0.001$) after 2 hours, except the 0.25mM when compared to control cells in normal media. When analysing the cells incubated for 2 hours in FBS free media, cells treated with all of the cobalt concentrations, except 0.25mM exhibited a decrease ($p<0.001$) in cellular viability when compared to control cells (Figure 8.3B). When looking at the control cells incubated in media containing FBS for 8 hours, the 0.25mM ($p<0.01$) cobalt treated cells show a slight decline in viability (Figure 8.3C). The cobalt treatment concentrations of 0.5mM, 1mM, 2.5mM, 5mM, and 10mM showed a decrease ($p<0.001$) in cellular viability when compared to control cells. Figure 8.3D, shows a significant decrease in viability in the 0.5mM, 1mM, 2.5mM, 5mM, and 10mM ($p<0.001$) cobalt treatment when compared to control cells.

8.4.4 The LD 50 of cobalt chloride treated alpha TC cells at 2- and 8-hour incubation as detected by MTT assay.

As seen in Figure 8.4A, the LD 50 was observed at the 2.5mM concentration in cells incubated for 2 hours in FBS rich media. However, the LD 50 in cells incubated in FBS free media for 2 hours was in a concentration below 1mM. When looking at the alpha cells incubated for 8 hours with and without FBS, a concentration below 1mM showed the LD 50 of this assay (Figure 8.4B).

8.4.5 Effects of Syn A treatment on Min-6 cellular viability at 2- and 8-hour incubation with and without FBS as detected by MTT assay.

As seen in Figure 8.5A, when compared to media only control cells, the treatment concentrations of 0.5mM ($p<0.05$) decreased viability. The Min-6 cells with the greatest decrease in cellular viability, compared to the media only control cells, were the 2.5mM and 5mM ($p<0.001$) treated cells. There was a slight decrease in viability of cells treated with 1mM ($p<0.01$ and a significant decrease in 2.5mM and 5mM ($p<0.001$) concentrations of Syn A

(Figure 8.5B). When examining the cells that were incubated for 8 hours in media with FBS, compared to the control cells, all of the Syn A concentrations displayed a significant decrease in viability ($p<0.001$) (Figure 8.5C). As seen in Figure 8.5D, all Syn A concentrations showed a significantly decreased ($p<0.001$) cellular viability in serum free media.

8.4.6 The LD 50 of Syn A treated Min-6 cells at 2- and 8-hour incubation as detected by MTT assay.

As seen in Figure 8.6A, when looking at the cells incubated in media containing FBS for 2 hours, there was no treatment concentration that produced a 50% cellular death percentage. However, when examining the cells incubated in media with no FBS for 2 hours, the Syn A 5mM concertation cells displayed the LD for this 2-hour assay. The 50% cellular death rate was present at the 5mM concertation in Min-6 cells incubated for 8 hours in FBS rich media (Figure 8.6B). The LD 50 was documented at the 1mM Syn A treatment concentration in the cells incubated for 8 hours in FBS free media.

8.4.7 Effects of cobalt chloride treatment on Min-6 cellular viability at 2- and 8-hour incubation with and without FBS as detected by MTT assay.

When compared to the media only control cells, cobalt treatment concentrations of 0.25mM and 0.5mM ($p<0.01$) show a decline in viable cell percentage when incubated in media containing FBS for 2 hours (Figure 8.7A). Cobalt concentrations of 1mM, 5mM, and 10mM ($p<0.001$) when incubated in serum free media showed a significant decline in cellular viability when compared to control cells. As seen in Figure 8.7B, cellular viability was significantly decreased in the 0.5mM, 1mM, 2.5mM, 5mM, and 10mM ($p<0.001$) when compared to control cells. Control cells compared to 0.25mM and 0.5mM ($p<0.01$) showed a decrease in viable cells when incubated in normal media for 8 hours (Figure 8.7C). When compared to the control cells, there was a significant decrease in cellular viability in the 1mM, 5mM, and 10mM ($p<0.001$) cobalt treated cells. Figure 8.7D, shows that when compared to control cells, there was a slight decrease in cellular viability in the 0.25mM ($p<0.01$) cobalt treatment, whereas

concentrations of 0.5mM to 10mM ($p<0.001$) all exhibited significant decreases in cellular viability after 8 hours in serum free media.

8.4.8 The LD 50 of cobalt chloride treated Min-6 cells at 2- and 8-hour incubation as detected by MTT assay.

The LD 50 of cells incubated for 2 hours in FBS rich media is observed between the 1mM and 2.5mM (Figure 8.8A). However, the LD 50 in cells incubated for 2 hours in FBS free media can be seen at the concentrations smaller than 1mM. In Figure 8.8B, the LD 50 for cells incubated at 8 hours with FBS can be seen in 1mM, but the LD50 of cells without FBS is in the concentrations below 1mM.

8.4.9 Effects of Syn A treatment on GLUTag cellular viability at 2- and 8-hour incubation with and without FBS as detected by MTT assay.

Figure 8.9A, shows the viability of GLUTag cells treated with Syn A and incubated in normal media for 2 hours. Slight significance was observed in the 2.5mM of Syn A ($p<0.05$) when compared to the control cells. The highest concentration of Syn A, 5mM ($p<0.001$), showed the greatest decrease in viable cells compared to the control cells. All 5 of the Syn A concentrations reduced cell viability ($p<0.001$) when compared to media only cells treated without FBS for 2 hours (Figure 8.9B). As seen in Figure 8.9C, the GLUTag cells were incubated for 8 hours in media containing FBS. When compared to the media only cells those treated with 0.25mM and 0.05mM ($p<0.05$) Syn A showed a slight decline in cellular viability. A significant decrease in the percentage of viable cells was observed at 1mM, 2.5mM, and 5mM ($p<0.001$) Syn A. An even greater decrease was observed in the treatment concentrations when incubated for 8 hours without FBS (Figure 8.9D). When compared to the control cells, all of the different concentrations of Syn A, significantly decreased viability ($p<0.001$).

8.4.10 The LD 50 of Syn A treated GLUTag cells at 2- and 8-hour incubation as detected by MTT assay.

As seen in Figure 8.10A, the cells incubated for 2 hours with FBS, show that the lethal dose 50 (LD 50) is with cells treated with 5mM Syn A. There was no LD 50 observed in the 2-hour incubation without FBS. However, when the cells were incubated for 8 hours, 50% of the cells in both media conditions, show the LD 50 starts at 1mM of Syn A (Figure 8.10B).

8.4.11 Effects of cobalt chloride treatment on GLUTag cellular viability at 2- and 8-hour incubation with and without FBS as detected by MTT assay.

When compared to the control cells incubated at 2 hours with FBS, viability was significantly decreased in the 0.25mM ($p<0.05$) and an even greater decrease ($p<0.001$) in the remainder of the concentrations in cobalt treated GLUTag cells (Figure 8.11A). Figure 8.11B shows the GLUTag cells incubated for 2 hours in media containing no FBS. When compared to control cells, there was a significant decrease in viability for all of the different concentrations of cobalt ($p<0.001$). As seen in Figure 8.11C, when compared to the media only control cells, there was a large decrease in cellular viability within all of the different concentrations of cobalt ($p<0.001$). When examining the cells incubated for 8 hours without FBS, all of the concentrations of cobalt exhibited a significant decrease ($p<0.001$) in viability (Figure 8.11 D).

8.4.12 The LD 50 of cobalt chloride treated GLUTag cells at 2- and 8-hour incubation as detected by MTT assay.

Figure 8.12A and B, shows the LD 50 percentage of cells treated with and without FBS for 2 and 8 hours, was smaller than 1mM.

8.4.13 The effects of hydrogen peroxide, Syn A, and cobalt chloride on alpha TC cellular viability alone and with inhibitors following a 2-hour incubation as detected by MTT assay.

Figure 8.13 displays the alpha cell viability with the addition of inhibitors. Figure 8.13A, shows the effects of the inhibitors when compared to KRBB treated alpha cells incubated for two

hours. There was a significant increase in MTT absorbance in the alpha cells when treated with the addition of KRBB + high glucose, KRBB + theophylline, KRBB + sodium benzoate, and KRBB + DMSO ($p<0.001$) when compared to the control. A small significant increase was observed in the alpha cells treated with KRBB + catalase ($p<0.05$). KRBB + benzamide ($p<0.001$) showed a significant increase in absorbance when compared to KRBB only treated cells. When compared to peroxide+ KRBB treated cells, peroxide + nicotinamide, peroxide + superoxide dismutase, peroxide + catalase, and peroxide + benzamide ($p<0.001$) displayed an increase in absorbance (Figure 8.13B). Peroxide + sodium benzoate and peroxide + DMSO showed an increase ($p<0.01$) in absorbance when compared to peroxide + KRBB cells. Peroxide + butanol ($p<0.05$) exhibited a slight increase when compared to peroxide+ KRBB.

Figure 8.13C shows the alpha cells treated with Syn A plus inhibitors were affected. Syn A + high glucose and Syn A + superoxide dismutase exhibited an increase in absorbance when compared to KRBB + Syn A cells. Syn A+ nicotinamide, Syn A + theophylline, and Syn A + butanol ($p<0.01$) displayed an increase when compared to Syn A + KRBB treated cells. Syn A + sodium benzoate, Syn A + DMSO, and Syn A + benzamide ($p<0.001$) show a greater increase in absorbance when compared to Syn A + KRBB treated cells. When compared to cobalt + KRBB cells, cobalt + nicotinamide, cobalt + sodium benzoate, and cobalt +catalase ($p<0.05$), display an increase in absorbance. Cobalt + butanol ($p<0.001$) displayed a significant decrease when compared to cobalt + KRBB treated cells. Cobalt + high glucose, cobalt + theophylline, cobalt + DMSO, cobalt + superoxide dismutase, and cobalt + benzamide ($p<0.001$) exhibit an increase when compared to cobalt + KRBB treated cells (Figure 8.13D).

8.4.14 The effects of KRBB, hydrogen peroxide, Syn A, and cobalt chloride treated alpha TC cellular viability with inhibitors at 8-hour incubation as detected by MTT assay.

Figure 8.14A shows when compared to KRBB only treated cells, KRBB + benzamide exhibited an increase in absorbance. An increase in absorbance was shown in cells treated with KRBB + nicotinamide, KRBB + high glucose, KRBB + theophylline, and KRBB + sodium benzoate

($p<0.001$) when compared to KRBB only treated cells. Peroxide + high glucose ($p<0.05$), peroxide + theophylline, and peroxide + sodium benzoate ($p<0.01$) show a significant increase when compared to peroxide + KRBB treated cells (Figure 8.14B). Peroxide + nicotinamide, peroxide + butanol, peroxide + catalase, and peroxide + benzamide ($p<0.001$) show an increase when compared to peroxide + KRBB treated cells.

As seen in Figure 8.14C, when compared to Syn A + KRBB cells, Syn A + superoxide dismutase ($p<0.05$) and Syn A + high glucose, Syn A + sodium benzoate, and Syn A + butanol ($p<0.01$) are significantly increased. Syn A + nicotinamide, Syn A + theophylline, Syn A + DMSO, and Syn A + benzamide ($p<0.001$) exhibit an increase when compared to Syn A + KRBB treated cells. Cobalt + superoxide dismutase shows a decrease ($p<0.05$) and cobalt + benzamide ($p<0.05$) shows a small increase when compared to cobalt + KRBB treated cells (Figure 8.14D). Cobalt + butanol ($p<0.01$), cobalt + high glucose, and cobalt + theophylline ($p<0.001$) show an increase when compared to cobalt + KRBB treated cells.

8.4.15 Effects of hydrogen peroxide, Syn A, and cobalt on expression of genes involved in secretion function in alpha TC cells.

When looking at the control cells, peroxide and Syn A treated cells($p<0.001$) showed a significant increase in the Pcsk 1 (PC 1/3) gene expression (Figure 8.15A). When compared to the control cells, there was a significant decrease in the gene expression in the cobalt treated cells ($p<0.001$). Figure 8.15B, shows that when compared to the control cells, the peroxide treated cells ($p<0.01$) had increased expression of the Pcsk 2 (PC 2) gene. Cells treated with Syn A and cobalt ($p<0.001$) showed significant decreases in the gene expression. When compared to the control cell, cobalt treated cells ($p<0.001$) showed a significant decrease in expression of Gcg (proglucagon) gene (8.15C). As seen in Figure 8.15D, a significant decrease in Scl2a2 gene expression was observed in the cobalt treated cells ($p<0.001$) when compared to control cells.

8.4.16 Effects of hydrogen peroxide, Syn A, and cobalt on expression of genes involved in proliferation in alpha TC cells.

When compared with the control cells, Syn A treated cells ($p<0.001$) exhibit a significant increase in Erk1 gene expression (Figure 8.16A). Cobalt treated cells ($p<0.001$) displayed a significant decrease in gene expression when compared to the control cells. When looking at the Erk 2 (extracellular signal-regulate kinases) gene expression in comparison to the control cells, Syn A ($p<0.01$) treated cells displayed a significant increase whereas the cobalt ($p<0.001$) treated cells showed a significant decrease when compared to the control cells (Figure 8.16B).

8.4.17 Effects of hydrogen peroxide, Syn A, and cobalt on expression of genes involved in apoptosis in alpha TC cells.

Figure 8.17A shows that, when compared to the control cells, Syn A treated cells displayed a significant decrease ($p<0.01$) and cobalt treated cells ($p<0.001$) showed a significant increase in the Bax (BCL2-associated X Protein) gene expression. When compared to the control cells, the peroxide treated cells ($p<0.001$) show a large increase in the Bcl 2 (B cell lymphoma 2) gene expression (Figure 8.17B). A significant decrease in the gene expression in the cobalt treated cells ($p<0.001$) was observed when compared to control cells. When compared to the control cells, the Syn A ($p<0.01$) and cobalt ($p<0.001$) treated cells, show a significant decrease in Nos 2 (Nitric oxide Synthase 2, inducible) gene expression (Figure 8.17C). Figure 8.17D, shows how the treated cells expressed the Nxfb1 (nuclear factor of κ light polypeptide gene enhancer in B cells 1). When compared to the control cells, the peroxide treated cells ($p<0.05$) show an increase in gene expression. Cobalt treated cells ($p<0.001$) displayed a significant decrease when compared to the control cells.

8.4.18 Effects of hydrogen peroxide, Syn A, and cobalt treated on expression of genes involved in antioxidant defence in alpha TC cells.

When compared to control cells, the peroxide treated cells ($p<0.001$) display a significant increase in the cat (catalase) gene expression (Figure 8.18A). Cobalt treated cells ($p<0.001$) displayed a significant decrease in the cat gene expression. Figure 8.18B, when compared to control cells, shows that the peroxide treated cells ($p<0.01$) had a significant increase in the GPX-1 (glutathione peroxidase 1) gene expression. Syn A and cobalt treated cells ($p<0.001$) displayed a significant decrease when compared to control cells.

Sod 1 (superoxide dismutase, soluble) gene expression in peroxide treated cells ($p<0.05$) show an increase when compared to control cells (Figure 8.18C). Syn A and cobalt ($p<0.001$) treated cells show a significant decrease in gene expression. Sod 2 (superoxide dismutase 2, mitochondrial) gene expression, when compared to control cells, shows a significant increase in peroxide treated cells ($p<0.001$) (Figure 8.18D). Syn A and cobalt treated cells ($p<0.001$), displayed a significant increase in Sod 2 gene expression when compared to control cells.

8.4.19 Effects of hydrogen peroxide, Syn A, and cobalt on expression of genes involved in ER stress in alpha TC cells.

As seen in Figure 8.19A, compared to control cells, Syn A treated cells ($p<0.001$) show a significant increase in Hspa 4 (Hsp 70, heat shock 70-kd protein 4) gene expression. Cobalt treated cells ($p<0.001$) display a significant decrease in gene expression compared to the control cells. However, when compared to the control cells, peroxide treated cells ($p<0.001$) show a significant increase in the expression of Hspa 5 (BiP, heat shock 70-kd protein 5) (Figure 8.19B). Cobalt treated cells ($p<0.001$) showed a significant decrease when compared to control cells.

8.4.20 Effects of hydrogen peroxide, Syn A, and cobalt on expression of genes involved in alpha cell markers in alpha TC cells.

The alpha cell marker, Arx (aristaless- related homeobox), gene expression, when compared to control cells was significantly increased in peroxide and Syn A ($p<0.001$) treated cells (Figure 8.20A). However, when compared to controls, cobalt treated cells ($p<0.001$) show a significant decrease in gene expression. When compared to control cells, the peroxide treated cells ($p<0.01$) display a slight increase in Pax 6 (paired box gene 6) gene expression (Figure 8.20B). Syn A treated cells ($p<0.05$) show an increase while cobalt treated cells ($p<0.001$) exhibited a decrease in gene expression.

8.4.21 Effects of hydrogen peroxide, Syn A, and cobalt on expression of genes involved in beta cell markers in alpha TC cells.

When compared to the control cells, Syn A treated cells ($p<0.01$) show a large significant increase in Glut 2 (glucose transporter 2) gene expression (Figure 8.21A). Cobalt treated cells ($p<0.001$), display a significant decrease in gene expression when compared to control cells. The ins 1 (insulin) beta cell marker gene expression, when compared to the control cells, peroxide and Syn A ($p<0.001$) treated cells show an increase in gene expression (Figure 8.21B). Cobalt treated cells ($p<0.001$) show a significant decrease in gene expression. When compared to control cells, there was a slight increase in peroxide treated cells ($p<0.05$) in Pdx 1 (pancreatic duodenal homeobox 1) gene expression (Figure 8.21C). Syn A treated cells ($p<0.001$) show a significant increase in gene expression compared to control cells. A significant decrease in gene expression was observed in cobalt treated cells ($p<0.001$) when compared against control cells.

8.4.22 Effects of hydrogen peroxide, Syn A, and cobalt chloride on Ki67 positive, glucagon positive in alpha TC cells.

Figure 8.22A, shows proliferation of the alpha TC cells after a 2-hour incubation. When compared to media only control cells, there was a significant decrease in all three treatment

groups ($p<0.001$). Photo representation is seen in Figure 8.22 B-E. Green represents glucagon and red represents Ki67.

8.4.23 Effects of hydrogen peroxide, Syn A, and cobalt chloride treatment on alpha TC cell viability assed by trypan blue staining.

When compared to the viable control cells, there was a significant decrease in cellular viability in the peroxide cells ($p<0.001$) in the analysis of trypan blue staining (Figure 8.23A). Surprisingly, the Syn A treated cells ($p<0.01$) and cobalt treated cells ($p<0.001$) show only a slight decrease in comparison to the control cells. Nonviable cells after a 2-hour incubation can be seen in Figure 8.23B. When compared to the control cells, there was a significant increase in nonviable peroxide cells ($p<0.001$). There was a slight increase in nonviable cells in the Syn A ($p<0.01$) and cobalt treated cells ($p<0.001$) treatment in comparison to control cells. Figure 8.23C shows the viable and nonviable alpha cell viability in a combination graph.

8.4.24 Effects of inhibitors incubated for 2 hours on KRBB, hydrogen peroxide, Syn A, and cobalt chloride treated alpha TC cell viability stained with trypan blue.

As seen in Figure 8.24A, the viable treated alpha cells incubated in KRBB with inhibitors. When compared to culture media, the cells treated with KRBB and KRBB + superoxide dismutase ($p<0.05$) displayed a slight increase in viable cells. Cells incubated with KRBB + nicotinamide ($p<0.05$) displayed a significant decrease when compared only to KRBB treated cells. When compared to media treated cells, peroxide + nicotinamide ($p<0.05$), peroxide and peroxide + superoxide dismutase ($p<0.01$) treated cells significantly decreased in viability (Figure 8.24B). When compared to media only treated cells, cells treated with Syn A + superoxide dismutase ($p<0.01$) show a slight decrease in viability (Figure 24.C). As seen in Figure 8.24D, when compared to media only treated cells, cells treated with Syn + superoxide dismutase ($p<0.01$), cobalt + nicotinamide, and cobalt + catalase ($p<0.001$) show a decrease in viability.

Figure 8.25A shows the nonviable alpha cells when treated with KRBB. When compared with the control, media only treated cells, KRBB + catalase ($p<0.01$), KRBB only, and KRBB + superoxide dismutase ($p<0.001$) showed a significant decrease in the nonviable cells. Compared against media treated cells, only peroxide and peroxide + nicotinamide ($p<0.05$) treated cells and peroxide + superoxide dismutase ($p<0.01$) showed an increase in the percentage of nonviable cells (Figure 8.25B). As displayed in Figure 8.25C, Syn A + superoxide dismutase treated cells ($p<0.01$) showed a significant increase in nonviable cells when compared with media only treated cells. Cobalt + superoxide dismutase ($p<0.05$) increased in nonviable cells when compared to media only and cobalt only treated cells (Figure 8.25D). Figure 8.26A and B shows viable and nonviable cells together within KRBB and peroxide treatments. Figure 8.27A and B show the viable and nonviable cell viability percentages within Syn A and cobalt treatments.

8.4.25 Effects of hydrogen peroxide, Syn A, and cobalt chloride on alpha TC cell apoptosis and necrosis levels as determined using Flow cytometry.

Flow cytometer was used to establish the different levels of apoptosis and necrosis in the 8-hour incubated alpha TC cells treated with media, hydrogen peroxide, Syn A, and cobalt. When compared to the control cells, peroxide treated cells ($p<0.001$) decreased in living cell percentage (Figure 8.28A). There was an increase in the percentage of living cells in the Syn A treatment group ($p<0.01$) when compared to the control cells. Cobalt treated cells ($p<0.01$) displayed a slight decrease in the percentage of living cells, when compared to the control cells. While looking at the early apoptosis stage and the control cells, the peroxide treated cells ($p<0.001$) show a significant increase in the percentage of cells observed within the early apoptosis phase (Figure 8.28B). Syn A treated cells ($p<0.001$) show a decrease in early apoptotic cells, whereas cobalt treated cells ($p<0.01$) show an increase when compared to control cells. As seen in Figure 8.28C, when compared to the control cells, the peroxide treated cells ($p<0.01$) show a significant increase in cells observed in the late apoptosis cell cycle. Syn A treated cells ($p<0.01$) display an increase in necrotic cells, whereas the cells

treated with cobalt ($p<0.01$) show a significant decrease when compared to control cells (Figure 8.28D).

8.5 Discussion

8.5.1 MTT assay

FBS was introduced to cell media to allow the cells to proliferate and grow (Van der Valk *et al*. 2018; Brunner *et al*. 2010; Puck *et al*. 1958). According to the company website, FBS is used to provide nutrients to the cells, enable growth, adherence, and protection from apoptosis and oxidative damage (Sigma-Aldrich, 2019). This could explain why during the MTT assays using media rich in FBS did not affect the cells as cells incubated without FBS. Using two different incubation medias has provided insights into measure of protective factors against the two different cytotoxins. According to Vasu *et al*. (2015) the LD_{50} was higher in the alpha TC cells than GLUTag and Min-6 cell lines when looking at the beta cell toxin, streptozotocin (STZ). Table 8.1 and 8.2 shows the minimal significance of the inhibitory concentration and the LD50 values for each of the three cell lines incubated for 2 and 8 hours with Syn A. Table 8.3 and 8.4 shows the minimal significance of the inhibitory concentration and the LD_{50} values for each of the three cell lines incubated for 2 and 8 hours with cobalt chloride. However, no LD_{50} was observable in the alpha TC and Min 6 cell line during the 2-hour incubation with FBS. LD_{50} was not observed in GLUTag in cells incubated in FBS depleted media for 2 hours. Syn A appears to be more toxic to the GLUTag cells from 8 hours onward. It is clear that cobalt had a more toxic effect on GLUTag cells then the other cell lines. However, when examining the LD_{50} for cells treated with cobalt, the alpha TC and GLUTag cells showed a quick response in killing off more than 50% of the cells. Cells were destroyed at the lowest concentration of 0.25mM. In Min-6 cells, 50% cell viability was not seen until the 1mM, for 2-hour incubation without FBS and both 8-hour assays or the 2.5mM concentration at 2 hours with FBS.

Table 8.1 Effects of Syn A on the minimal significance of the inhibitory concentration and the LD50 of cells incubated for 2 hours as determined by the MTT assay

Cell lines	**Minimal inhibitory concentration**		**LD_{50}**	
	With FBS	**Without FBS**	**With FBS**	**Without FBS**
Alpha TC	1mM ($p<0.01$)	1mM ($p<0.01$)	N/A	5mM
Min-6	0.5mM ($p<0.05$)	1mM ($p<0.01$)	N/A	5mM
GLUTag	2.5mM ($p<0.05$)	0.25mM ($p<0.001$)	5mM	N/A

Table 8.1 Cells incubated for 2 hours with Syn A. Changes were deemed significant when p values were *$p<0.05$, **$p<0.01$, or ***$p<0.001$. N/A shows that there were more than 50% of living cells at every concentration.

Table 8.2 Effects of Syn A on the minimal significance of the inhibitory concentration and the LD50 of cells incubated for 8 hours as determined by the MTT assay

Cell lines	**Minimal inhibitory concentration**		**LD_{50}**	
	With FBS	**Without FBS**	**With FBS**	**Without FBS**
Alpha TC	0.25mM ($p<0.001$)	0.25mM ($p<0.001$)	NA	> 1mM
Min-6	0.25mM ($p<0.001$)	0.25mM ($p<0.001$)	5mM	>1mM
GLUTag	0.25mM ($p<0.05$)	0.25mM ($p<0.001$)	1mM	1mM

Table 8.2 Cells incubated for 8 hours with Syn A. Changes were deemed significant when p values were *$p<0.05$ or ***$p<0.001$. N/A shows that there were more than 50% of living cells at every concentration.

Table 8.3 Effects of cobalt chloride on the minimal significance of the inhibitory concentration and the LD50 of cells incubated for 2 hours as determined by the MTT assay

Cell lines	**Minimal inhibitory concentration**		**LD_{50}**	
	With FBS	**Without FBS**	**With FBS**	**Without FBS**
Alpha TC	0.05mM (p<0.001)	0.05mM (p<0.001)	2.5mM	>1mM
Min-6	0.25mM (p<0.01)	0.5mM (p<0.001)	> 2.5mM	>1mM
GLUTag	0.25mM (p<0.05)	0.25mM (p<0.05)	>1mM	>1mM

Table 8.3 Cells incubated for 2 hours with cobalt chloride. Changes were deemed significant when p values were *p<0.05 or ***p <0.001. N/A shows that there were more than 50% of living cells at every concentration.

Table 8.4 Effects of cobalt chloride on the minimal significance of the inhibitory concentration and the LD50 of cells incubated for 8 hours as determined by the MTT assay

Cell lines	**Minimal inhibitory concentration**		**LD_{50}**	
	With FBS	**Without FBS**	**With FBS**	**Without FBS**
Alpha TC	0.25mM (p<0.01)	0.5mM (p<0.001)	>1mM	>1mM
Min-6	0.25mM (p<0.01)	0.25mM (p<0.01)	1mM	>1mM
GLUTag	0.25mM (p<0.001)	0.25mM (p<0.001)	>1mM	>1mM

Table 8.4 Cells incubated for 8 hours with cobalt chloride. Changes were deemed significant when p values were *p<0.05 or ***p <0.001. N/A shows that there were more than 50% of living cells at every concentration.

The inhibitors used in the second set of cell viability assays, were determined based on the research from Flatt *et al*. (1987). We examined peroxide treated alpha cells with inhibitors and found that catalase and benzamide protected the cells. According to the past research, the inhibitors used in both assays were used because of their ability to protect cells against pancreatic cells. Although the past research showed that the inhibitors protected the pancreatic beta cells against beta cell toxins, it was our hope that these inhibitors would provide the same protection for alpha cells against alpha cell toxins. Li *et al*. (2014) looked at cobalt treated Min-6 cells and an isoflavone that protected the cells against cobalt toxicity. Their research showed that the isoflavone, puerarin, protected the beta cells from apoptosis due to puerarins' anti-apoptotic properties. However, we did not look at this isoflavone, which can perhaps provide the same protection to alpha cells treated with Syn A and cobalt. Although, cobalt is an alpha cell toxin, we found that cobalt also influenced the Min-6 cells, especially when incubated in FBS free media. Perhaps, introducing puerarin, would help prevent the pancreatic cells from becoming apoptotic. With pancreatic cells treated with hydrogen peroxide, puerarin was found to help the cells from going into apoptosis (Li, 2014; Zhou *et al*. 2014).

8.5.2 Immunocytology

Alpha TC cells were stained with Ki67 and glucagon to assess alpha cell proliferation. As expected, all three toxins showed a decrease in alpha cell proliferation. Trypan blue staining was also used to look at cell viability. Trypan blue dyes the dead cells because the living cells have an intact membrane that the dye cannot penetrate (Fang and Trewyn, 2012; Strober, 2001). When specifically looking at the alpha TC cells and the two alpha cell toxins at 2.5mM, cellular viability was greater than 50% in both toxins when incubated in FBS for 2 hours and then analyzed with trypan blue staining. Cell death for these two toxins was below 40%. This shows that even against the alpha cell toxin in alpha cells, the FBS provided a level of protection.

8.5.3 Gene expression

When looking at the treatments that effected gene secretion expression, hydrogen peroxide expressed the Pcsk1 and Pcsk2 gene the most. Syn A was upregulated by the Pcsk1 and down regulated by the Pcsk2 gene. Cobalt showed a down regulation of the following genes: Pcsk1, Pcsk2, Gcg, and Slc2a2. Syn A also showed high levels of expression in proliferation regarding the ERK 1 and 2 genes. However, when compared to the Ki67 proliferation staining on alpha cells, the Syn A treated cells were significantly decreased when compared to the control. Cobalt displayed significant deregulation within the two genes tested for proliferation expression. When looking at the genes for apoptosis, cobalt showed high levels upregulation of apoptosis when tested against the Bax gene expression. Syn A showed the opposite and displayed a deregulation action when compared with the control. Hydrogen peroxide treated cells were upregulated within the Bcl2 gene, whereas cobalt was significantly deregulated. Syn A and cobalt both showed a deregulation of the Nos 2 gene. Peroxide was increased, whereas cobalt was decreased in the expression of the Nxfb1 gene. The four antioxidant genes: Cat, GPX-1, Sod 1, and Sod 2, were greatly increased in the alpha cells treated with hydrogen peroxide, however these genes showed deregulation in the cells treated with cobalt. Syn A treated cells also showed deregulation in GPX-1, Sod1 and Sod2. Like the ERK 1 gene, Syn A exhibited high levels of Hspa 4 gene regulation expression. However, Hspa 5 was only upregulated with the peroxide treated cells and deregulated with cobalt treated cells.

Alpha cell marker, Arx, displayed an increase in gene expression in the cells treated with hydrogen peroxide and Syn A and a significant decrease in cobalt treated cells. In the past research, it states that the Arx gene is known to determine what will happen to the alpha cell as well as being the start for alpha to beta cell transdifferentiation while suppressing beta cell function (Courtney *et al*. 2013; Collombat *et* al. 2005; Collombat *et al*. 2003). This could account for the transdifferentiation that was detected in the Glu^{cre} Rosa mice. Pax 6 also was increased in cells treated with peroxide and Syn A. Cobalt treated cells exhibited deregulation of the Arx and Pax 6 gene. All three of the beta cell markers: Glut 2, Ins, and Pdx 1 showed

increased expression in the cells treated with Syn A. Past studies found that epigenetic changes within the PDX1 and Ins 1 genes affect beta cell function with alterations to the methylation of DNA (Halban *et al*. 2014). With the increase in gene expression in those genes, it can be speculated that Syn A and peroxide works on the DNA methylation of the cells. Although, we did not look at GLUT 1 gene expression, research in the past found that the hypoxic effect of cobalt mimicked the gene expression of GLUT 1 (Ybarra *et al*. 1997). This is not true for the GLUT 2 gene expression that we examined. Cobalt had very little effect on the GLUT 2 gene we tested. Overall, cobalt showed a decrease in gene expression in all, but one gene tested.

8.5.4 Flow cytometry

While the past research on incubated islets focused on a mass of cells, the experiment involving the flow cytometry focused on the single cells to confirm necrosis (Östenson, 1983) Flow cytometry is used to detect DNA fragmentation causing apoptosis through DNase II- like enzymes (Lecoeur, 2002). We observed that the number of living cells after an 8-hour incubation was increased in the 2.5mM Syn A treated cells. This percentage is similar to the number of healthy cells when the LD50 was calculated (Table 8.1). However, the 2.5mM cobalt treated living cells showed a higher percentage in the flow cytometry versus the LD50 and the MTT assay (Table 8.3). It has been said that DNase II, could possibly mediate the breakup of DNA during random apoptosis of certain cells (Lecoeur, 2002; Gottlieb *et al*. 1995) The purpose of this assay was to determine if Syn A and cobalt toxicity cause DNA fragmentation. Within the animal Chapters, TUNEL assay was used to detect apoptosis, however, it does not identify the apoptotic cells with 3'P DNA ends that have been damaged (Lecoeur, 2002). Those results showed that the animals that were treated with Syn A showed high levels of apoptosis. In a study that looked at the beta cell toxin, STZ, it is stated that the beta cells become apoptotic, and then they die, causing an increase in alpha cells (Tanday, 2019; Vasu *et al.* 2015; O'Brien *et al*. 1996). Perhaps, Syn A functions in a similar way regarding alpha cells. Syn A and cobalt treated cells possibly proliferate and then go into an

apoptotic state resulting in an increased beta cell mass (Caren and Carco, 1955). Simonsen *et al*. (2012) showed that when cobalt was given at larger doses, apoptosis was induced, and the necrosis rates of pancreatic cells were higher. Past research has stated that, given the assay reagent being used, the results will vary on the cytotoxicity (Grare *et al*. 2007; Fortakis and Timbrell, 2006; Weyerman *et al*. 2005). Our results confirm this when examining cell viability using the MTT, cellular death with trypan blue, and necrosis using flow cytometry. Metabolic activity, DNA damage, and cell death assays allowed us to see the mechanism of action of Syn A and cobalt.

Overall, the past research on Syn A or cobalt treated cells is limited, and the research that was produced did not examine the same assays as this current project. In a study that researched rat livers and the effects of Syn A, they concluded that this toxin did not have any effect on cellular mitochondrial swelling. They also concluded that the function of Syn A is aerobic and produces high energy (Bhuvaneswaran and Dakshinamurti, 1970). In another study that looked at the mitotic rate of the alpha and beta cells from rats, it was found that a decrease in the mitotic frequency was observed in the rats treated with Syn A. They also observed a shrinkage in the nucleus during the stages of prophase and metaphase (Ferner and Runge, 1955). We found that when we stained for proliferation in these alpha TC cells, the nucleus was like the control, however, the cell appeared bigger than the cells treated only with media. Perhaps these alpha cells that we treated with Syn A became vacuolated giving it a bigger appearance. This would confirm the results seen in Gunnarsson *et al*. (1969). These researchers found that the alpha cells in guinea pigs treated with Syn A showed signs of vacuolation, swelling, enlarged nuclei, and degranulation (Gunnarsson *et al*.1969).

It has been suggested that instead of a toxic effect on the alpha cells, perhaps the cells increase in activity and become exhausted (Gunnarsson *et al*. 1969; Creutzfeldt, 1960; Hultquist, 1959). Research states that the changes on the alpha cells from Syn A are species specific as studies on ducks showed no cytological changes when given large doses of the toxin (Lansglow *et al.* 1973; Kern, 1971; Müller *et al.* 1956). Like the animal necropsy results

and the effects of Syn A on the other tissues, it is possible that the alpha cells are not the primary site of action (Lansglow and Freeman, 1973, Langslow *et al.* 1973; Beekman 1956). However, Davis (1952) suggests that the damage to alpha cells is the direct result of the Syn A and suggests that the cells are exhausted and cause the alpha cells to become hydropic. Not only were the alpha cells hydropic, but in some cases the beta cells were also affected in rabbits treated with Syn A (Davis, 1952). Östenson (1983), found that, at lower concentrations of Syn A, the islets remained intact but with some vacuolation, at higher doses, both alpha and beta cells became degranulated. Some of the cells at a higher concentration also become necrotic and decreased in number, as well as a reduction in the oxidation rate of glucose (Östenson, 1983). Our results during the cell viability of the Min-6 cells confirm that the beta cells are also affected by the treatment of Syn A, although, just not as much as the alpha cells.

Similarly, to the cells treated with Syn A, cobalt treated cells, pancreatic cells also displayed signs of vacuolation and severe degranulation (Bencosme and Frei, 1955). When looking at the image results from the proliferation staining, the alpha cells treated with cobalt did not show as much swelling as they did in the Syn A treatment. Like Syn A, cobalt is said to be species specific regarding alpha cell damage, as some past research states that they were only able to detect cytological changes in guinea pigs, but not rats or rabbits (van Campenhout, 1955; Creutzfeldt and Schmidt, 1954). In a study that looked at fish and cobalt treated alpha cells, three types of cells were described with-in the pancreas, and the cobalt effect the alpha cells as well as the third type. The third type was not stated, but it was hypothesized as arising from beta cells or perhaps alpha cells with altered functionality. Within this third type, there was no sign of damage to these cells, and no changes were detected in the beta cells (Mosca, 1956). When looking at the alpha cells treated with cobalt, past research states that cell death was only observable on occasion and that when abnormal stress is occurring the alpha cell changes and the beta cell becomes hydropic. With the beta cells being affected, it was documented as a secondary degeneration occurs in response to metabolic disturbances (Creutzfeldt, 1957; Creutzfeldt and Schmidt, 1954).

Fodden (1956), states that once cobalt is administered there are morphologic changes to the alpha cells that mimic the destruction of beta cells once an alloxan is introduced. In a study that examined the alpha cells after the administration of cobalt in female rabbits, researchers found that the cells became cloudy, swollen, degranulated, hydropic, as well as the disappearance of the nuclei (Fodden, 1956; van Campenhout, 1955). This can be confirmed in our proliferation study, as some of the nuclei were faint and could not be seen as clear as the other treatment groups. Photo representation can be found in Figure 8.2 B-E. In a study that looked at the cytological effects of cobalt on alpha cells in guinea pigs, researchers found endocrine islands appeared and increased in size, scattered beta cells, and alpha cell degranulation (Fodden, 1956; van Campenhout, 1955). The small islands containing alpha cell damage were also observed in Rhesus monkeys and dogs. However, in the dogs, there was a destruction of the dying cell nucleus as well as a reduction in beta cell granulation. When looking at alpha cells from a cat, researchers found that the viability of the cells were not dramatically changed in long time periods (Fodden, 1956). Our 2 hour and 8-hour cell viability assay with both toxins did not confirm these results. There was a reduction in cellular viability in the GLUTag cells when incubated with FBS compared to the cells incubated without FBS. The Min-6 cells only displayed a drastic change in the higher doses: 1mM to 10mM in both incubation conditions. As for the alpha cells, there was a drastic change in cellular viability in both media conditions when comparing the 2-and 8-hour incubation period. Fodden (1956) also examined the phosphatase within the islets treated with cobalt. The beta cells displayed signs of destruction and hypogranular at the early stages of toxicity.

In the future, it would be useful to repeat the assays in this Chapter to test if the effects on proliferation, gene expression, and apoptosis in alpha cells incubated in FBS depleted media. This would allow determination of the advantages or disadvantages of FBS in the cell culture media. It would also be beneficial to stain the alpha TC cells using the TUNEL assay kit to detect the differences between this assay and flow cytometry. Further investigations into these specific genes are need in order to identify the pathway that the toxin is following to cause the

upregulation or deregulation. Due to the two alpha cell toxins being species specific, it would be beneficial to treat different cell lines derived from different species to confirm this past research.

In conclusion, both alpha cell toxins not only affect the alpha TC cells, but also the Min-6 and GLUTag cells. We can also conclude that some inhibitors as well as FBS provided protection to the toxin treated cells. Through the genes that we did look at we can conclude that cobalt only upregulates one, Bax. We were also able to conclude that alpha cell proliferation was hindered by these toxins, which verifies the immunohistochemistry performed in the *in vivo* models.

Figure 8.1 Effects of Syn A on alpha TC cellular viability after incubation for 2 hours (A and B) or 8 hours (C and D) with and without FBS.

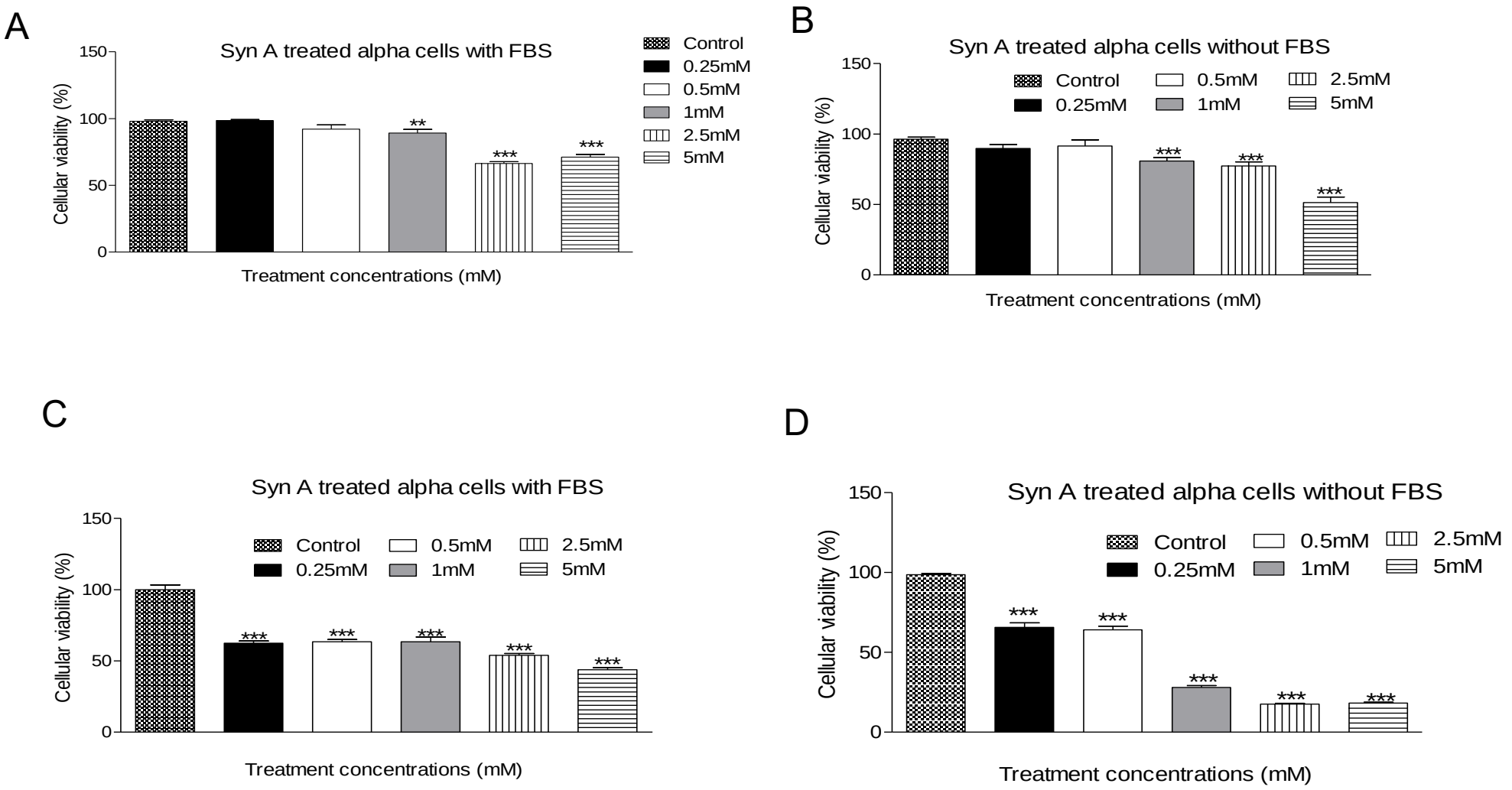

Alpha TC cellular viability after incubation for 2 hours (A and B) or 8 hours (C and D). Viability was determined by an MTT assay. Values are mean ± SEM (n= 6 treatments). Changes were deemed significant when p values were *p<0.05, **p<0.01, or ***p <0.001 when media only control was compared with the respective concentrations of Syn A.

Figure 8.2 The lethal dose 50 of Syn A treated alpha cells at 2 (A) and 8 (B) hour incubation as detected by the MTT assay.

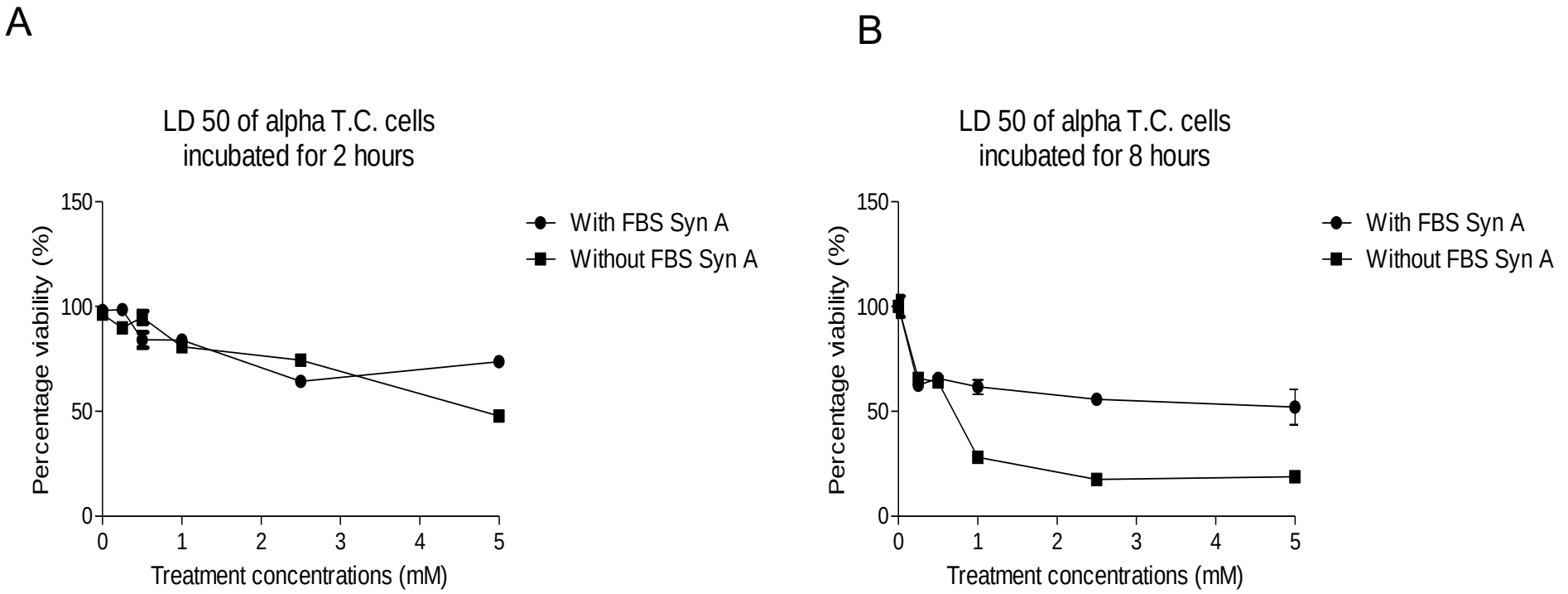

LD 50. Syn A on Alpha TC cells incubated for 2 hours (A) and 8 hours (B). Values are mean ± SEM (n= 6 treatments).

Figure 8.3 Effects of cobalt chloride on alpha TC cellular viability after incubation for 2 hours (A and B) or 8 hours (C and D) with and without FBS.

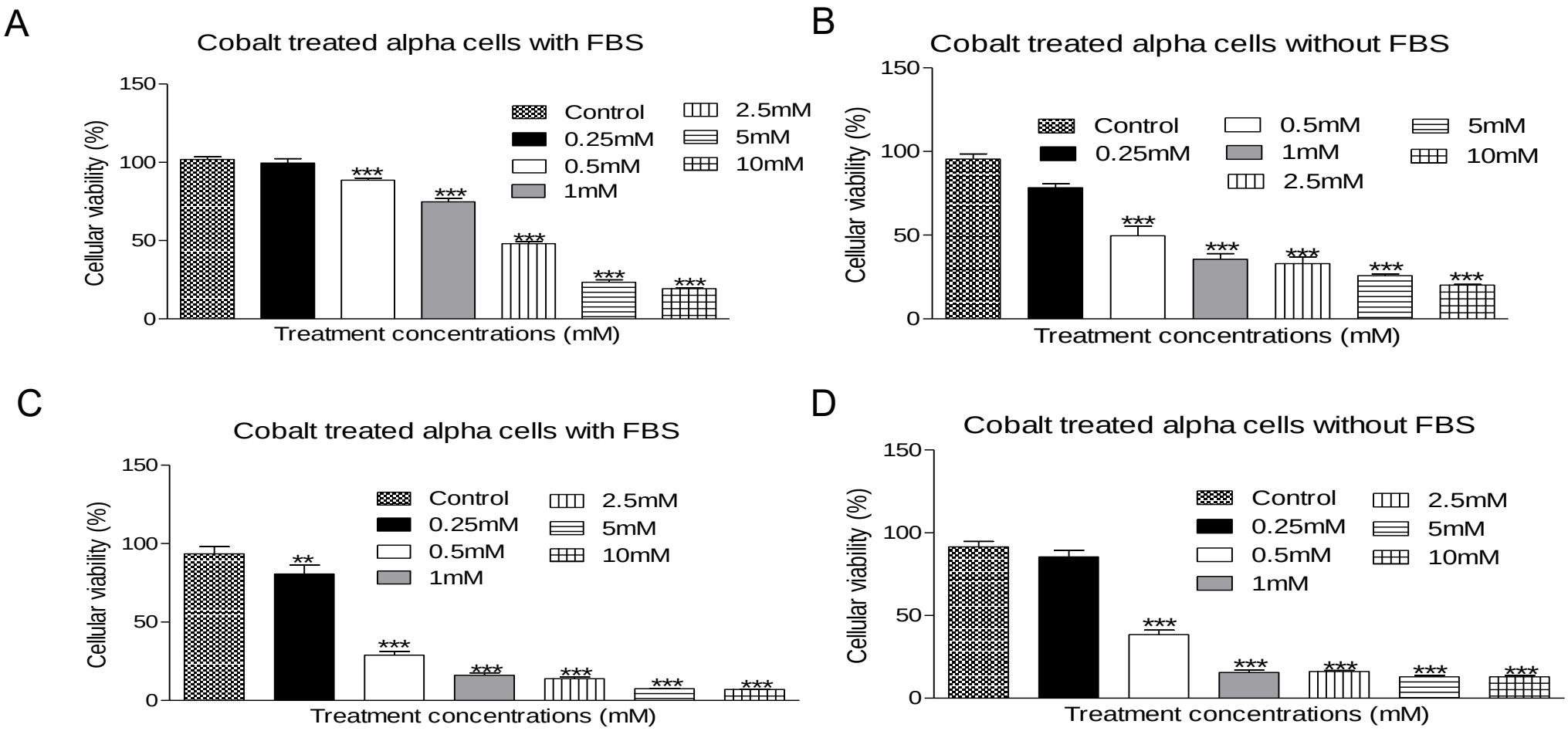

Alpha TC cellular viability after incubation for 2 hours (A and B) or 8 hours (C and D). Viability was determined by an MTT assay. Values are mean ± SEM (n= 7 treatments). Changes were deemed significant when p values were **p<0.01 or ***p <0.001 when media only control was compared with the respective concentrations of cobalt chloride.

Figure 8.4 The lethal dose 50 of cobalt chloride treated alpha cells at 2 (A) and 8 (B) hour incubation as detected by the MTT assay.

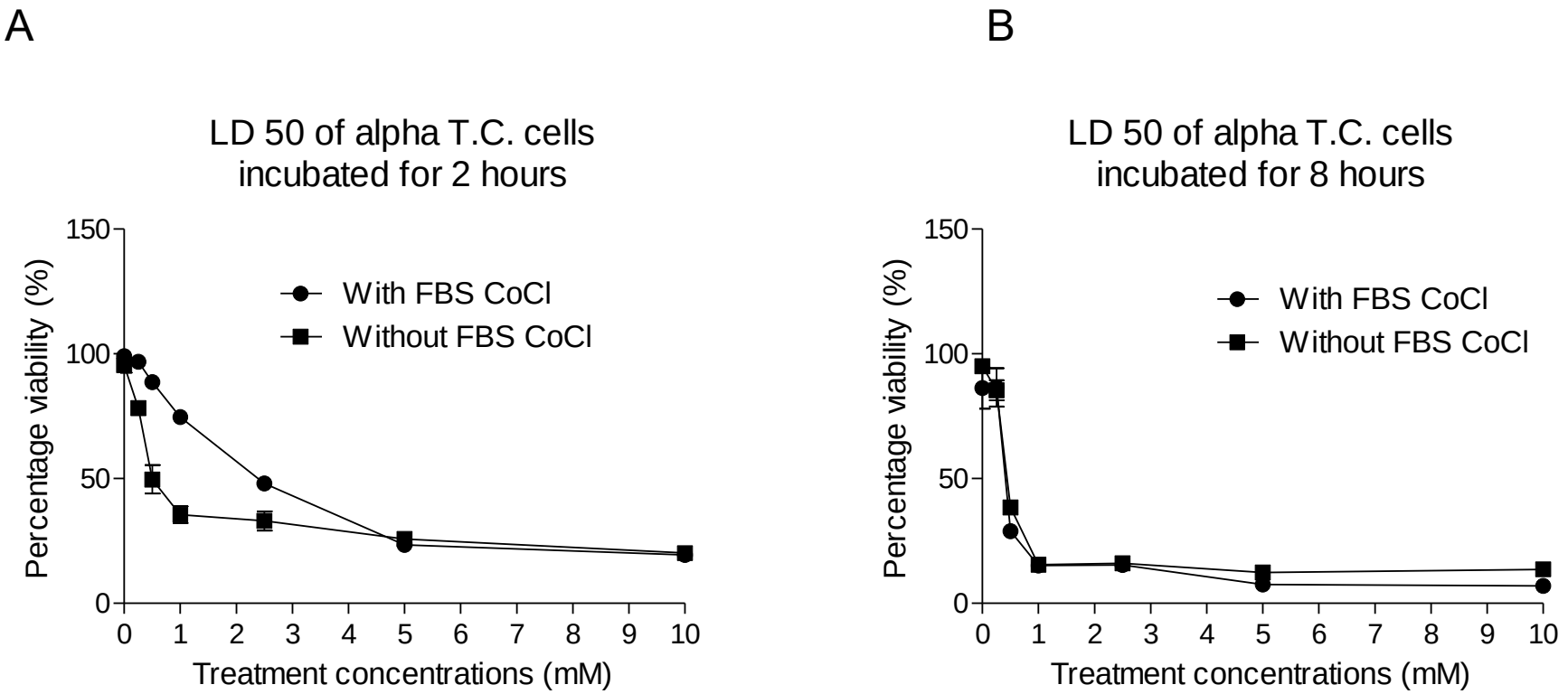

LD 50. Cobalt chloride on Alpha TC cells incubated for 2 hours (A) and 8 hours (B). Values are mean ± SEM (n= 7 treatments).

Figure 8.5 Effects of Syn A on Min-6 cellular viability after incubation for 2 hours (A and B) or 8 hours (C and D) with and without FBS.

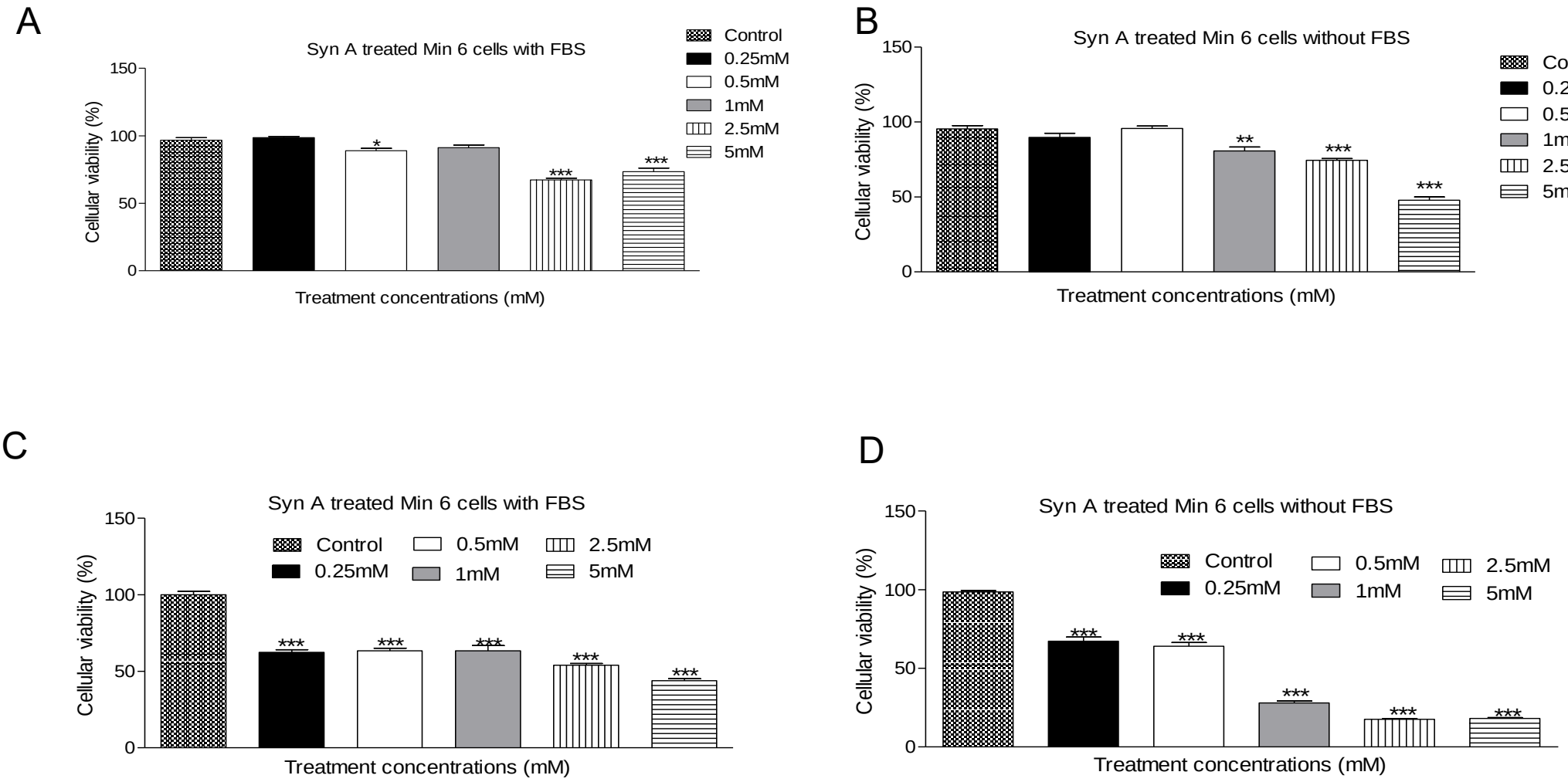

Min-6 cellular viability after incubation for 2 hours (A and B) or 8 hours (C and D). Viability was determined by an MTT assay. Values are mean ± SEM (n= 6 treatments). Changes were deemed significant when p values were *p<0.05, **p<0.01, or ***p <0.001 when media only control was compared with the respective concentrations of Syn A.

Figure 8.6 The lethal dose 50 of Syn A treated Min-6 cells at 2 (A) and 8 (B) hour incubation as detected by the MTT assay.

A

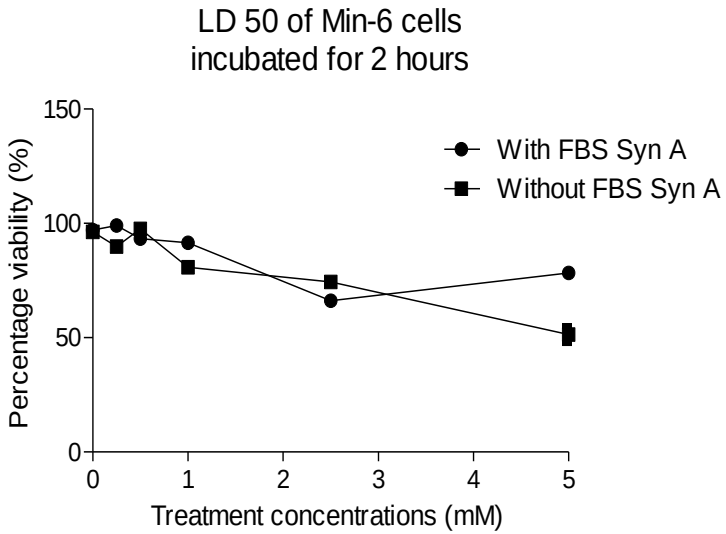

B

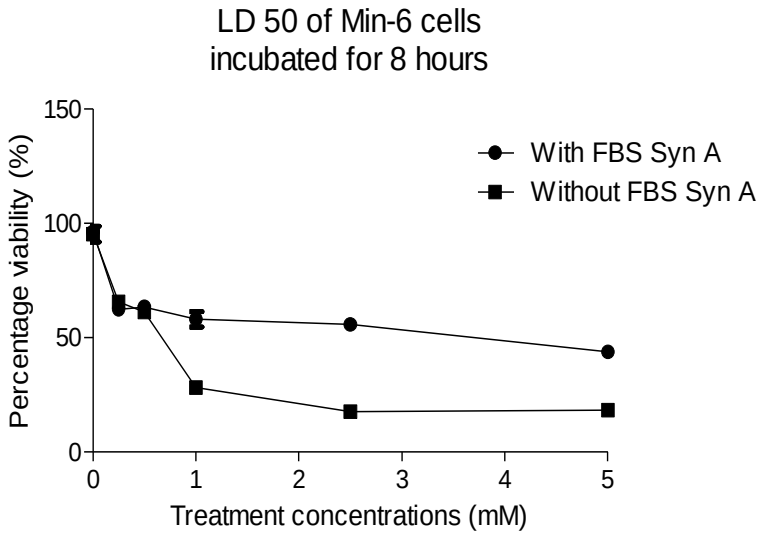

LD 50. Syn A on Min-6 cells incubated for 2 hours (A) and 8 hours (B). Values are mean ± SEM (n= 6 treatments).

Figure 8.7 Effects of cobalt chloride on Min-6 cellular viability after incubation for 2 hours (A and B) or 8 hours (C and D) with and without FBS.

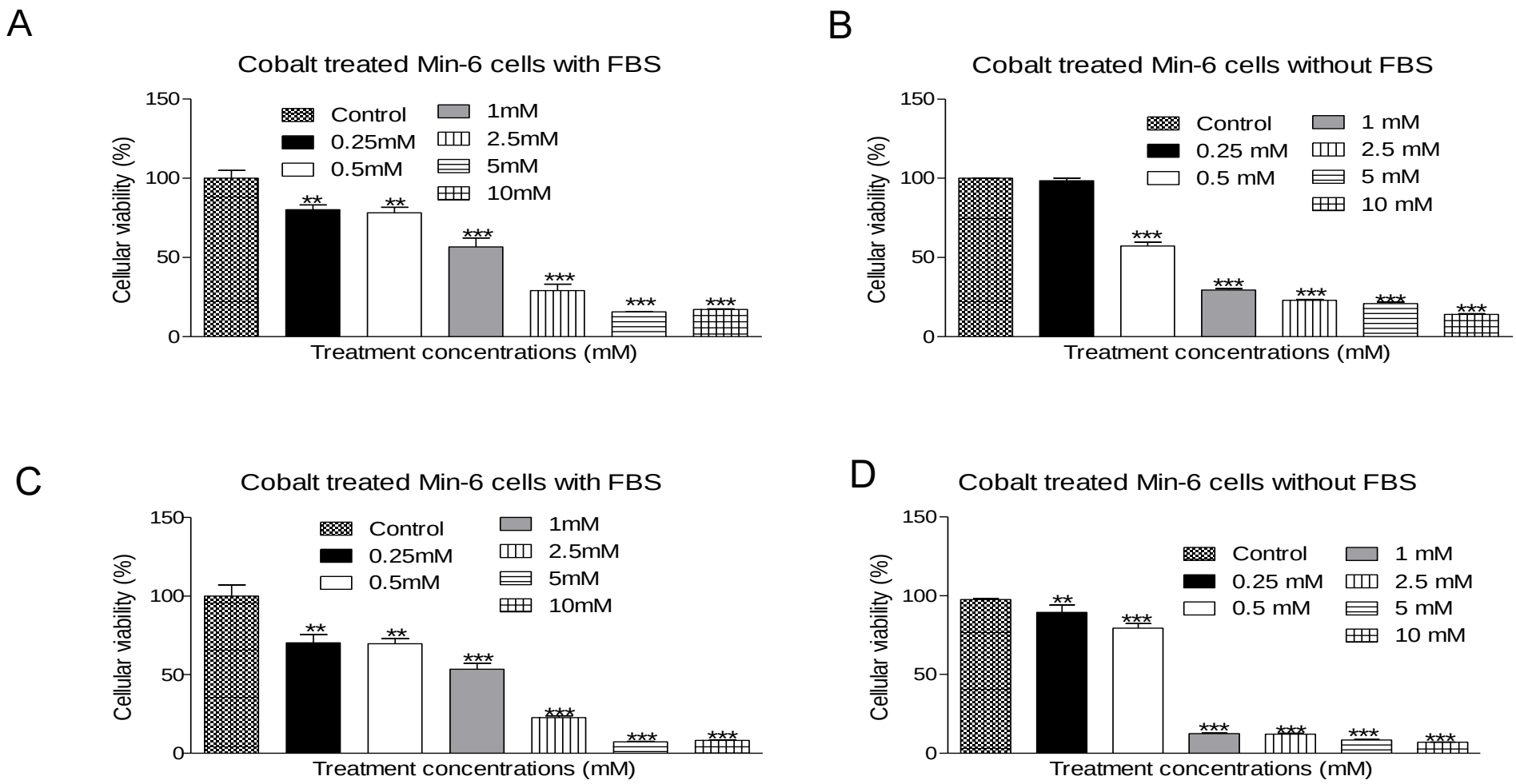

Min-6 cellular viability after incubation for 2 hours (A and B) or 8 hours (C and D). Viability was determined by an MTT assay. Values are mean ± SEM (n= 7 treatments). Changes were deemed significant when p values were **p<0.01 or ***p <0.001 when media only control was compared with the respective concentrations of cobalt chloride.

Figure 8.8 The lethal dose 50 of cobalt chloride treated Min-6 cells at 2 (A) and 8 (B) hour incubation as detect the MTT assay.

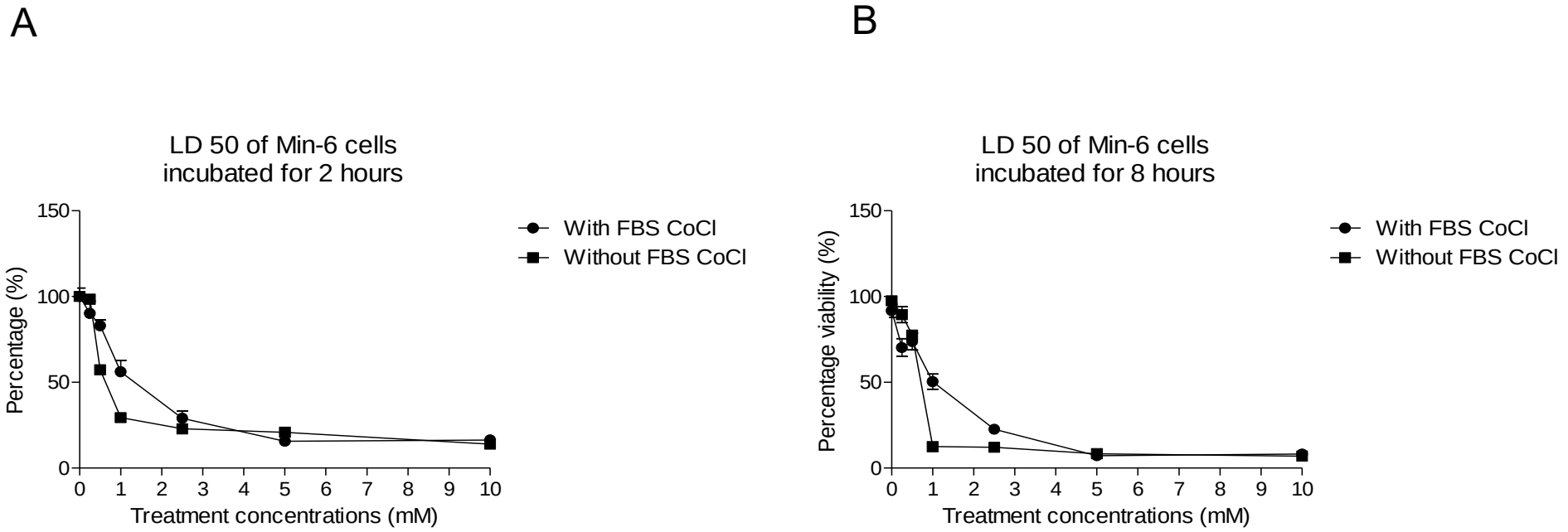

LD 50. Cobalt chloride on Min-6 cells incubated for 2 hours (A) and 8 hours (B). Values are mean ± SEM (n= 7 treatments).

Figure 8.9 Effects of Syn A on GLUTag cellular viability after incubation for 2 hours (A and B) or 8 hours (C and D) with and without FBS.

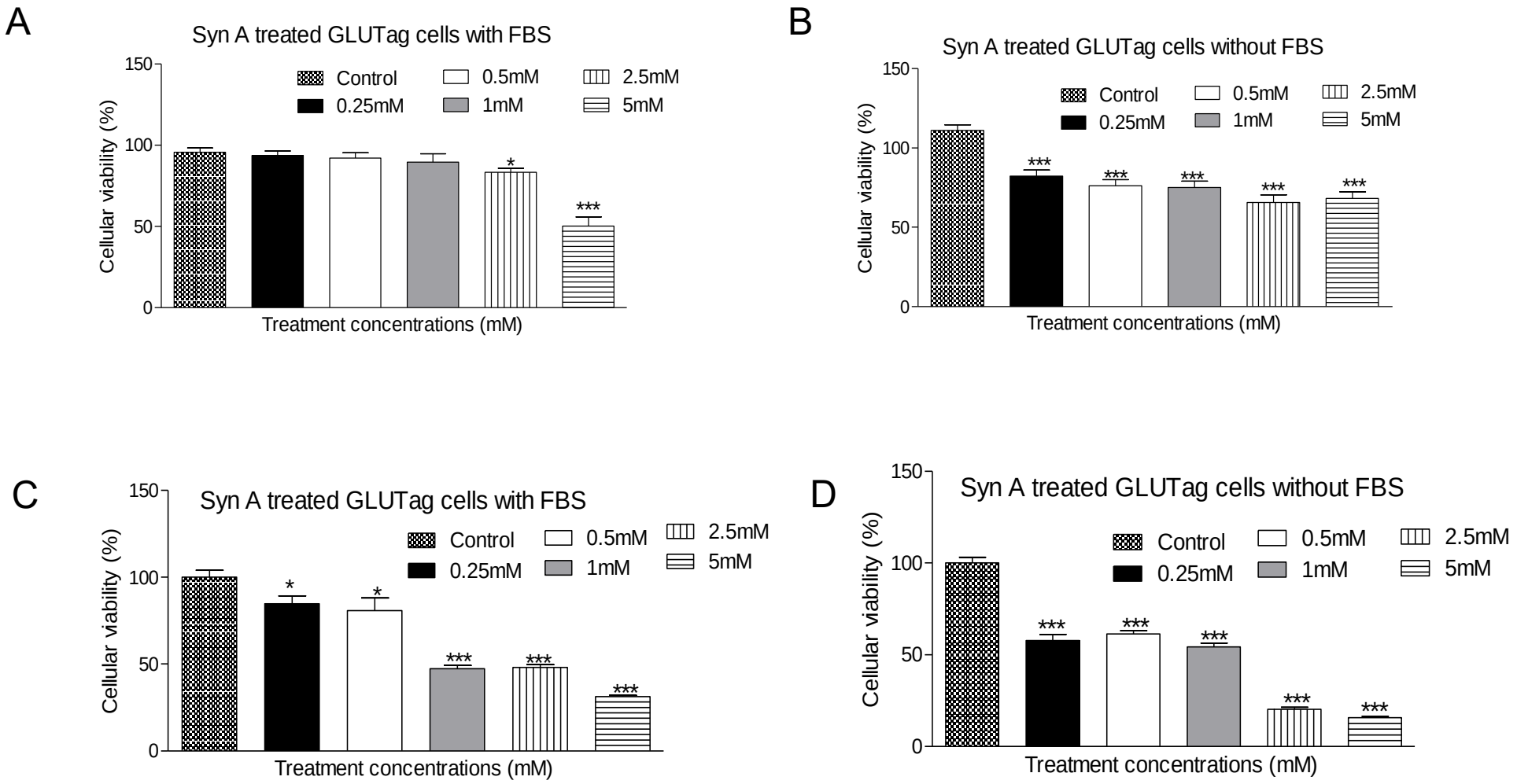

GLUTag cellular viability after incubation for 2 hours (A and B) or 8 hours (C and D). Viability was determined by an MTT assay. Values are mean ± SEM (n= 6 treatments). Changes were deemed significant when p values were *p<0.05 or ***p <0.001 when compared with control.

Figure 8.10 The lethal dose 50 of Syn A treated GLUTag cells at 2 (A) and 8 (B) hour incubation as detected by the MTT assay.

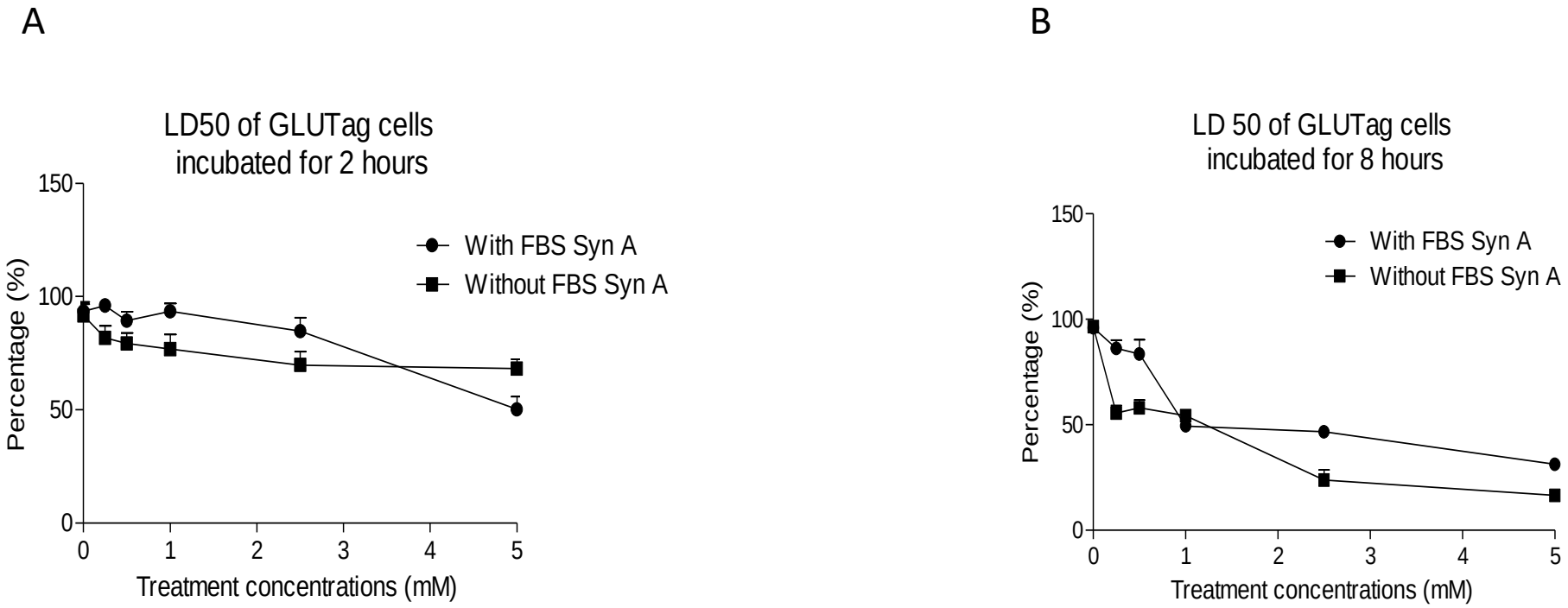

Lethal Dose (LD) 50. Syn A on GLUTag cells incubated for 2 hours (A) and 8 hours (B). Values are mean ± SEM (n= 6 treatments).

Figure 8.11 Effects of cobalt chloride on GLUTag cellular viability after incubation for 2 hours (A and B) or 8 hours (C and D) with and without FBS.

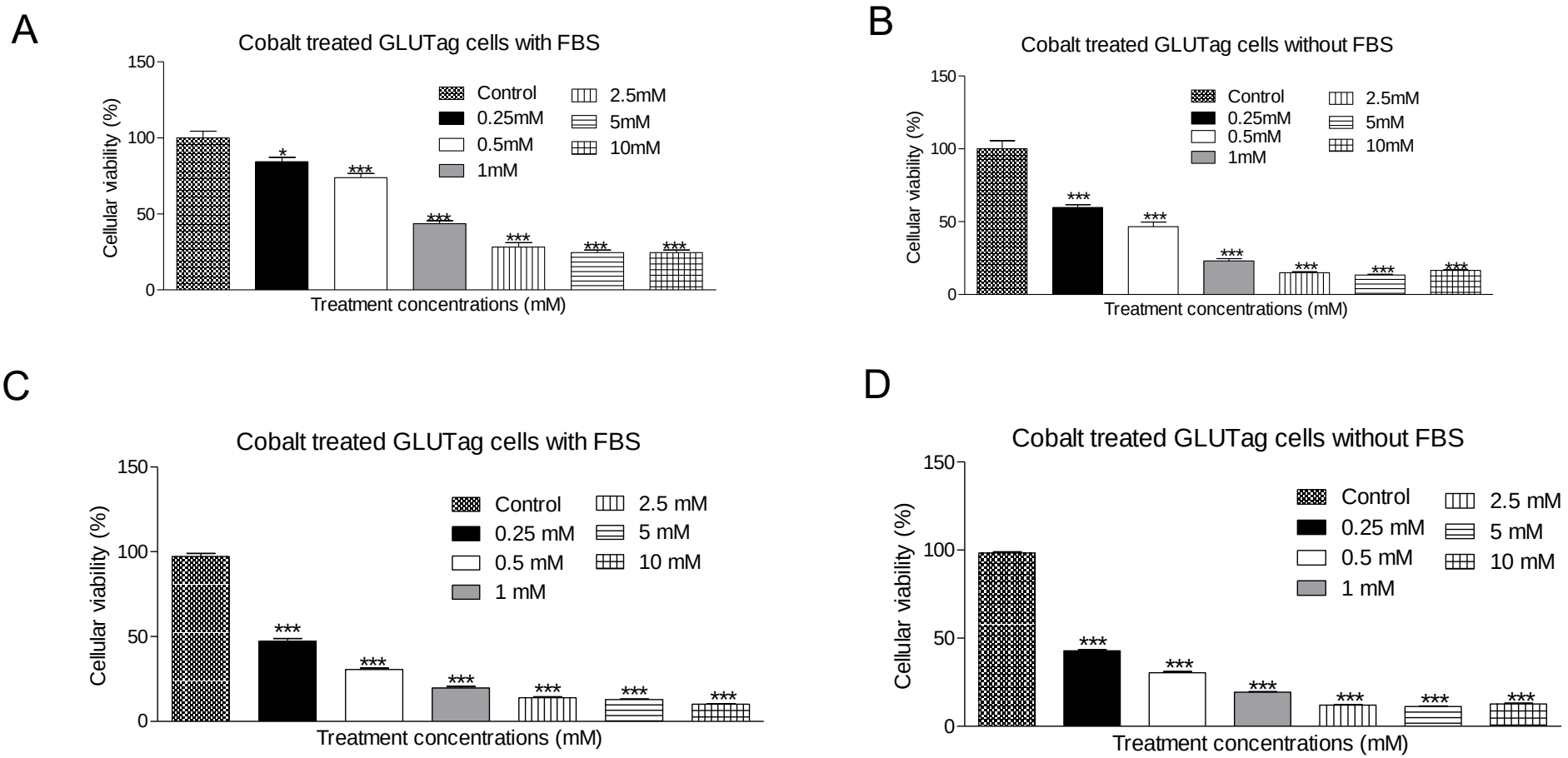

GLUTag cellular viability after incubation for 2 hours (A and B) or 8 hours (C and D). Viability was determined by an MTT assay. Values are mean ± SEM (n= 7 treatments). Changes were deemed significant when p values were **p<0.01 or ***p <0.001 when media only control was compared with the respective concentrations of cobalt chloride.

Figure 8.12 The lethal dose 50 of cobalt chloride treated GLUTag cells at 2 (A) and 8 (B) hour incubation as detected by the MTT assay.

A

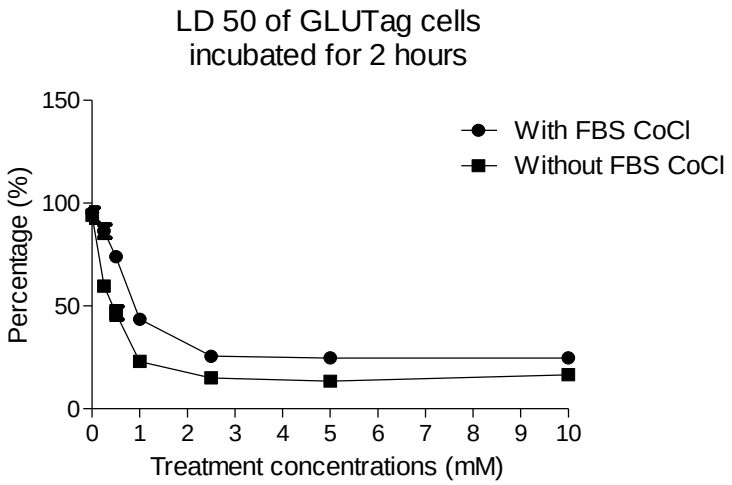

B

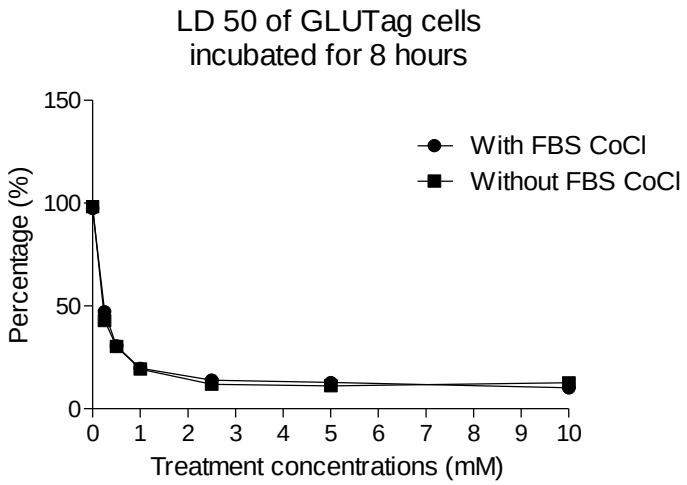

LD 50. Cobalt chloride on GLUTag cells incubated for 2 hours (A) and 8 hours (B). Values are mean ± SEM (n= 7 treatments).

Figure 8.13 Effects inhibitors incubated for 2 hours with KRBB (A), hydrogen peroxide (B), Syn A (C), and cobalt chloride (D) on alpha TC cell viability.

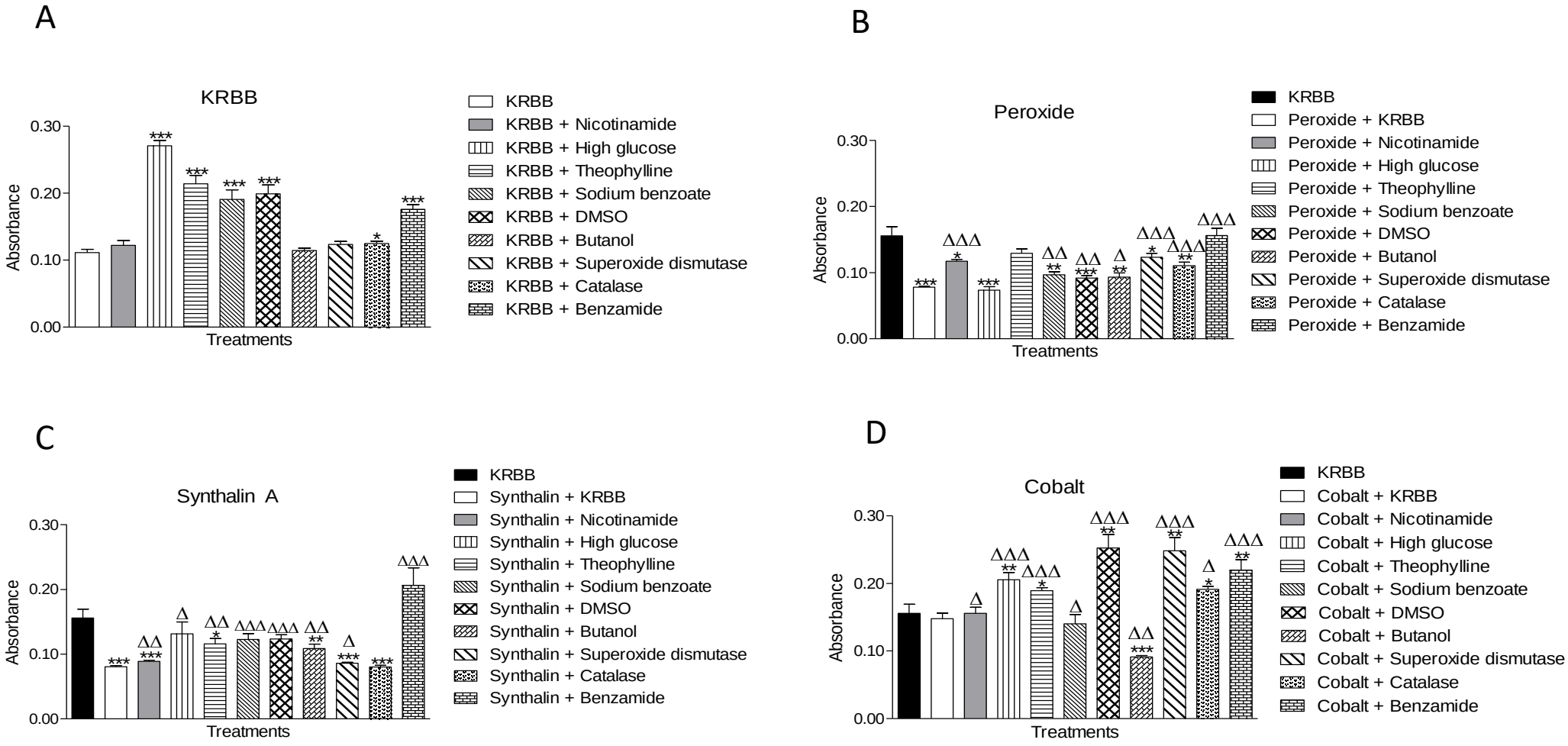

Alpha TC cellular viability assay incubated for 2 hours. Viability was determined by an MTT assay. Values are mean ± SEM (n= 6 wells). Changes were deemed significant when p values were *p<0.05, **p<0.01, or ***p <0.001 when compared with KRBB alone. $^{\Delta}$p<0.05, $^{\Delta\Delta}$p<0.01, or $^{\Delta\Delta\Delta}$p<0.001 when compared with treatment + KRBB.

Figure 8.14 Effects inhibitors incubated for 8 hours with KRBB (A), hydrogen peroxide (B), Syn A (C), and cobalt chloride (D) on alpha TC cell viability.

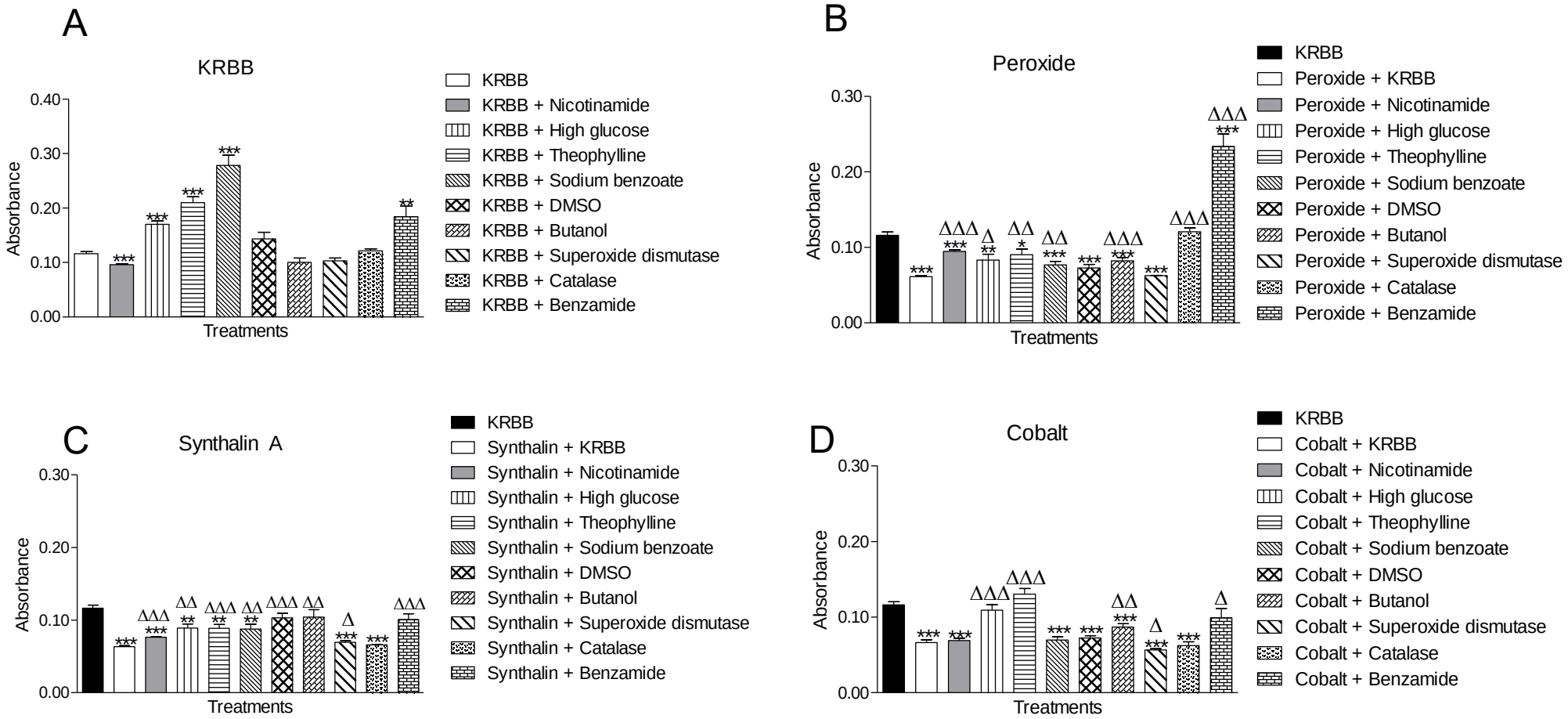

Alpha TC cellular viability assay incubated for 8 hours. Viability was determined by an MTT assay. Values are mean ± SEM (n= 6 wells). Changes were deemed significant when p values were *p<0.05, **p<0.01, or ***p <0.001 when compared with KRBB alone. $^{\Delta}$p<0.05 or $^{\Delta\Delta}$p<0.01, or $^{\Delta\Delta\Delta}$ p<0.001 when compared with treatment + KRBB.

Figure 8.15 Effects of 2-hour exposure to alpha TC cells to hydrogen peroxide, Syn A, and cobalt chloride on secretion function genes expression.

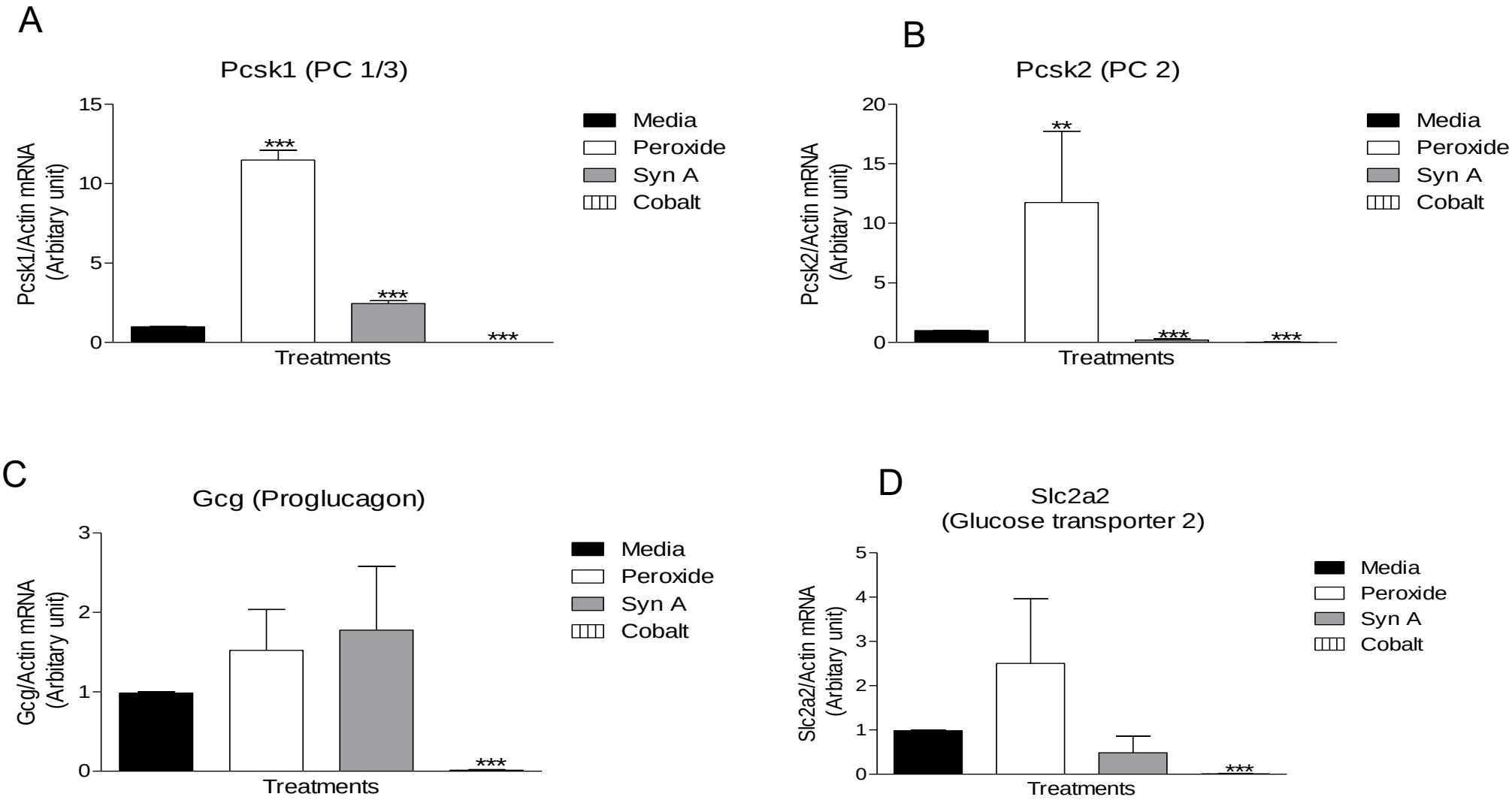

Secretion function genes expression in Alpha TC cells. Pcsk 1 (A), Psck 2 (B), Gcg (C), and Slc2a2 (D) following a 2-hour culture with media, peroxide, Syn A, and cobalt chloride. Gene expression was normalized to Actin gene expression. Gene expression was determined by RT-PCR. Values shown are mean ± SEM (n=3 replications). Changes were deemed significant when p values were **p<0.01 or ***p<0.001 when compared with media.

Figure 8.16 Effects of 2-hour exposure to alpha TC cells to hydrogen peroxide, Syn A, and cobalt chloride on proliferation function genes expression.

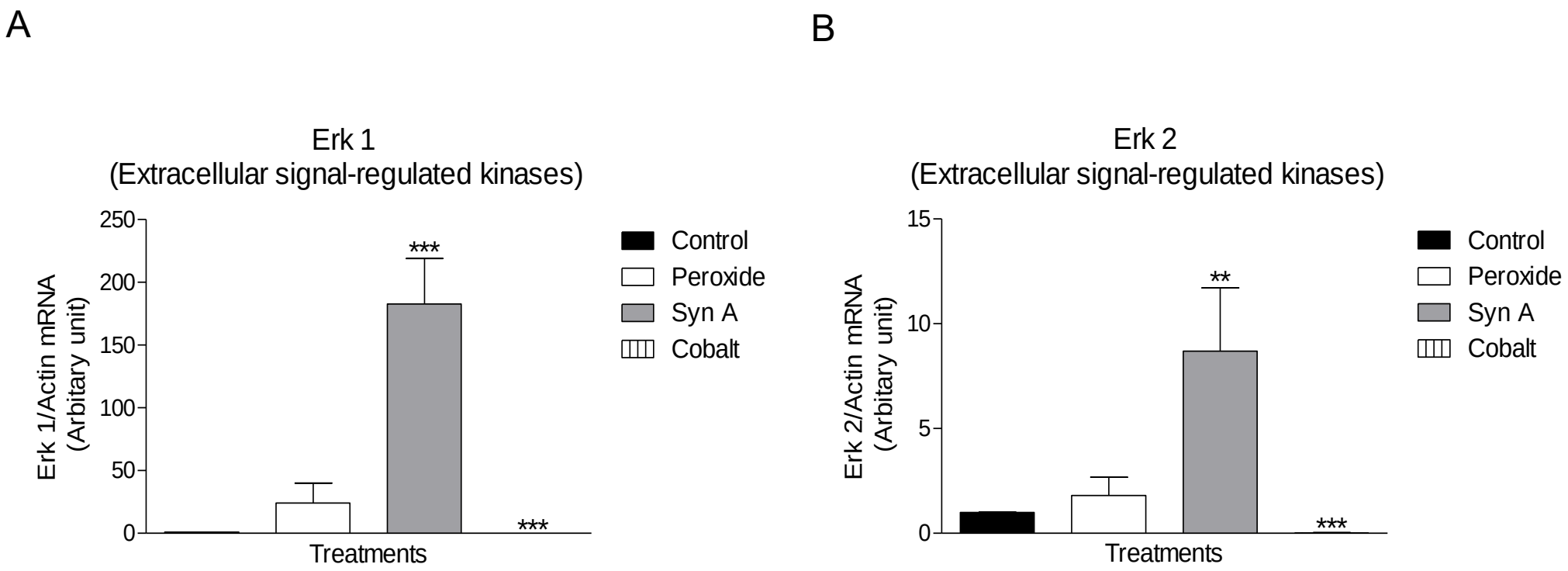

Proliferation genes expression in alpha TC cells. Erk1 (A) and Erk2 (B) genes following a 2-hour culture with media, peroxide, Syn A, and cobalt chloride. Gene expression was normalized to Actin gene expression. Gene expression was determined by RT-PCR. Values shown are mean ± SEM (n=3 replications). Changes were deemed significant when p values were **p<0.01 ***p<0.001 when compared with media.

Figure 8.17 Effects of 2-hour exposure to alpha TC cells to hydrogen peroxide, Syn A, and cobalt chloride on apoptosis genes expression.

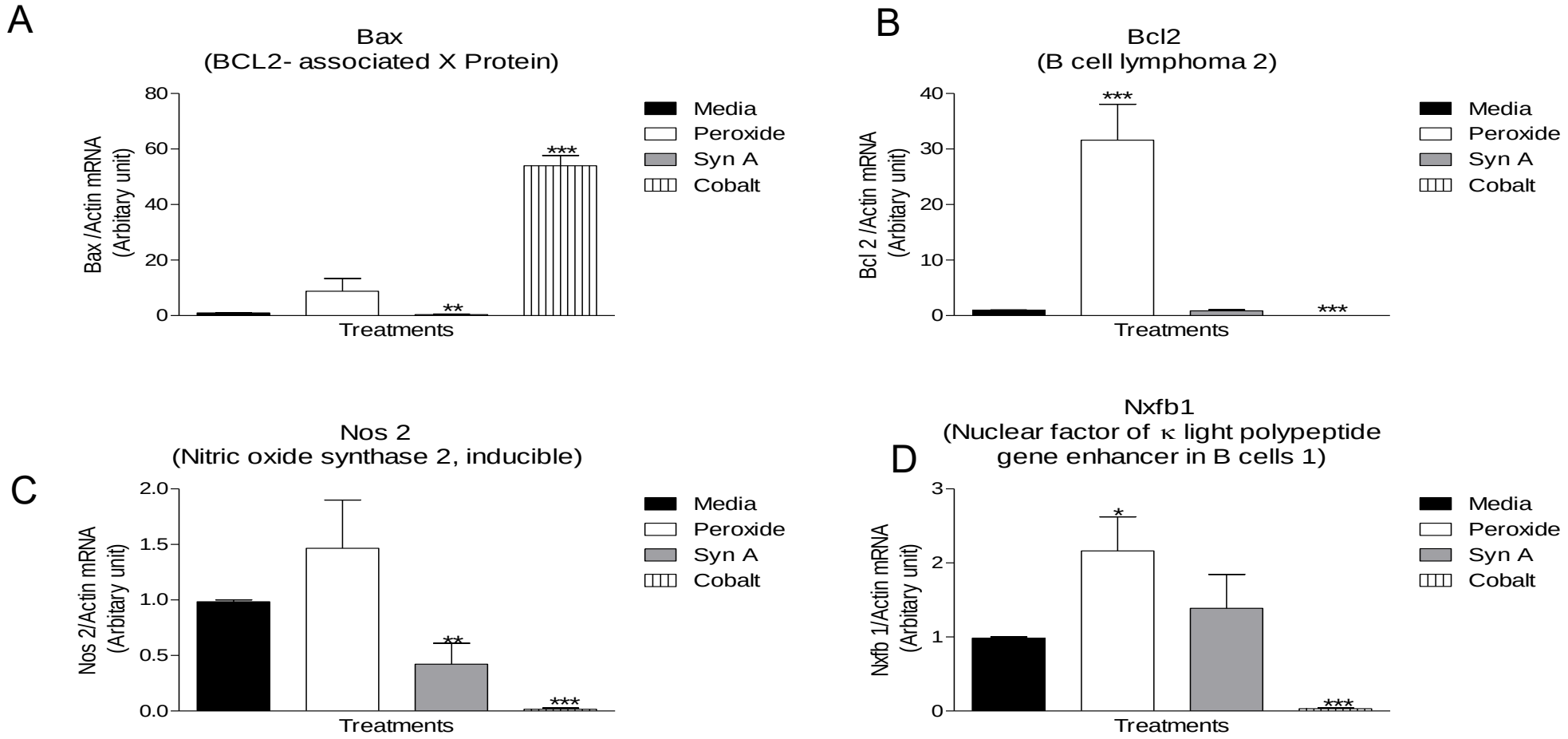

Apoptosis genes expression in alpha TC cells. Bax (A), Bcl2 (B), Nos 2 (C), and Nxfb 1 (D) genes following a 2-hour culture with media, peroxide, Syn A, and cobalt chloride. Gene expression was normalized to Actin gene expression. Gene expression was determined by RT-PCR. Values shown are mean ± SEM (n=3 replications). Changes were deemed significant when p values were *p<0.05, **p<0.01, or ***p<0.001 when compared with media. 293

Figure 8.18 Effects of 2-hour exposure to alpha TC cells to hydrogen peroxide, Syn A, and cobalt chloride on antioxidant defence genes expression.

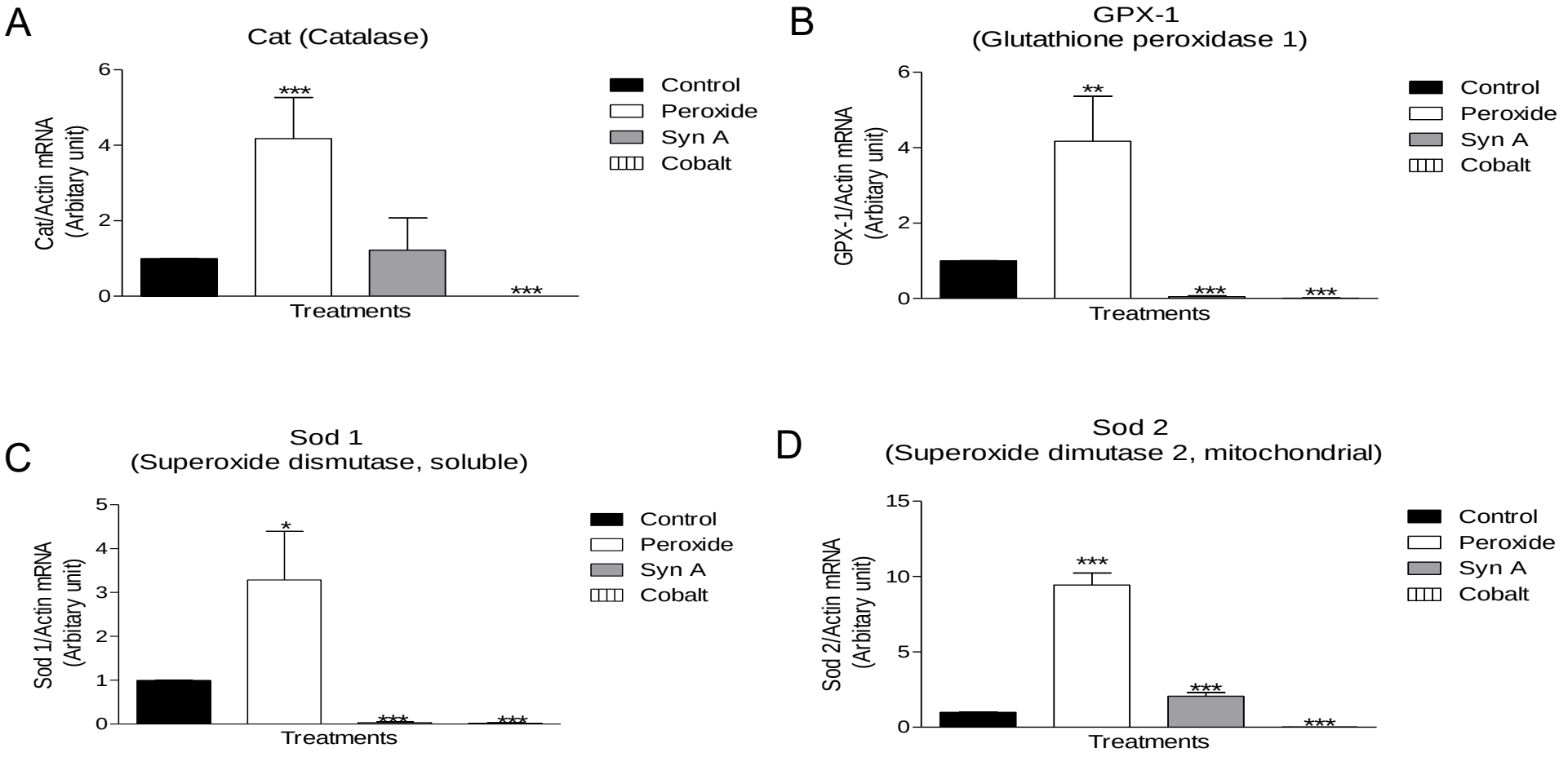

Antioxidant defence genes expression in alpha TC cells. Cat (A), GPX-1 (B), Sod1 (C), and Sod 2 (D) genes following a 2-hour culture with media, peroxide, Syn A, and cobalt chloride. Gene expression was normalized to Actin gene expression. Gene expression was determined by RT-PCR. Values shown are mean ± SEM (n=3 replications). Changes were deemed significant when p values were ***p<0.001 when compared with control.

Figure 8.19 Effects of 2-hour exposure to alpha TC cells to hydrogen peroxide, Syn A, and cobalt chloride on ER stress genes expression.

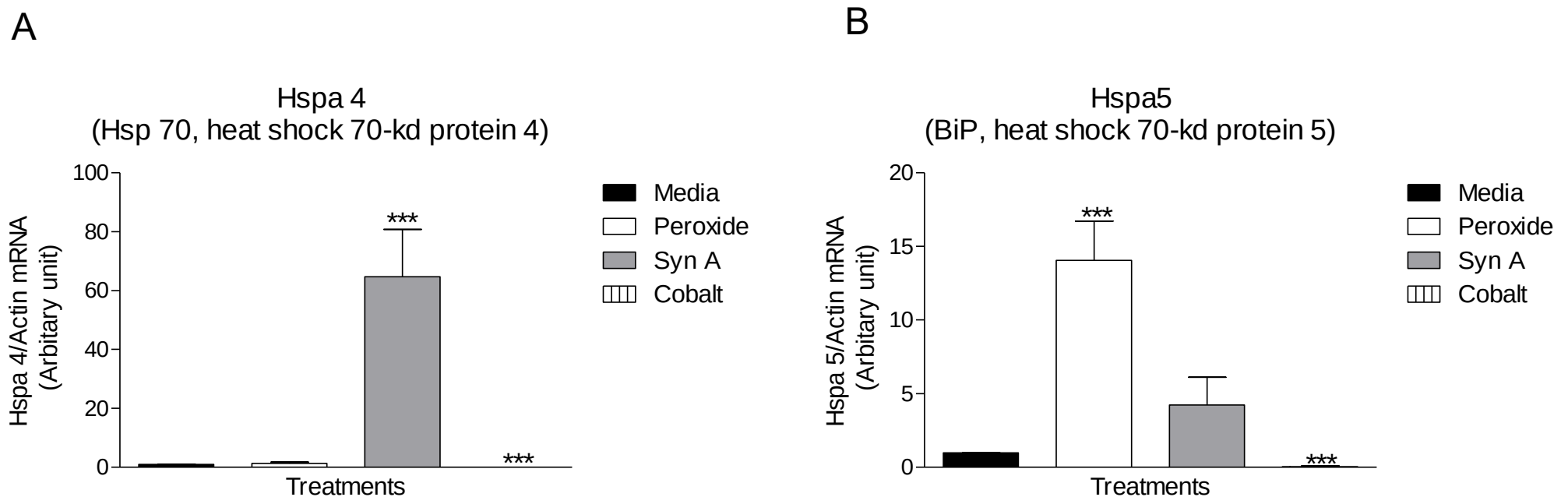

ER stress genes expression in alpha TC cells. Hspa 4 (A), and Hspa 5 (B) genes following a 2-hour culture with media, peroxide, Syn A, and cobalt chloride. Gene expression was normalized to Actin gene expression. Gene expression was determined by RT-PCR. Values shown are mean ± SEM (n=3 replications). Changes were deemed significant when p values were ***$p<0.001$ when compared with media.

Figure 8.20 Effects of 2-hour exposure to alpha TC cells to hydrogen peroxide, Syn A, and cobalt chloride on alpha cell marker genes expression.

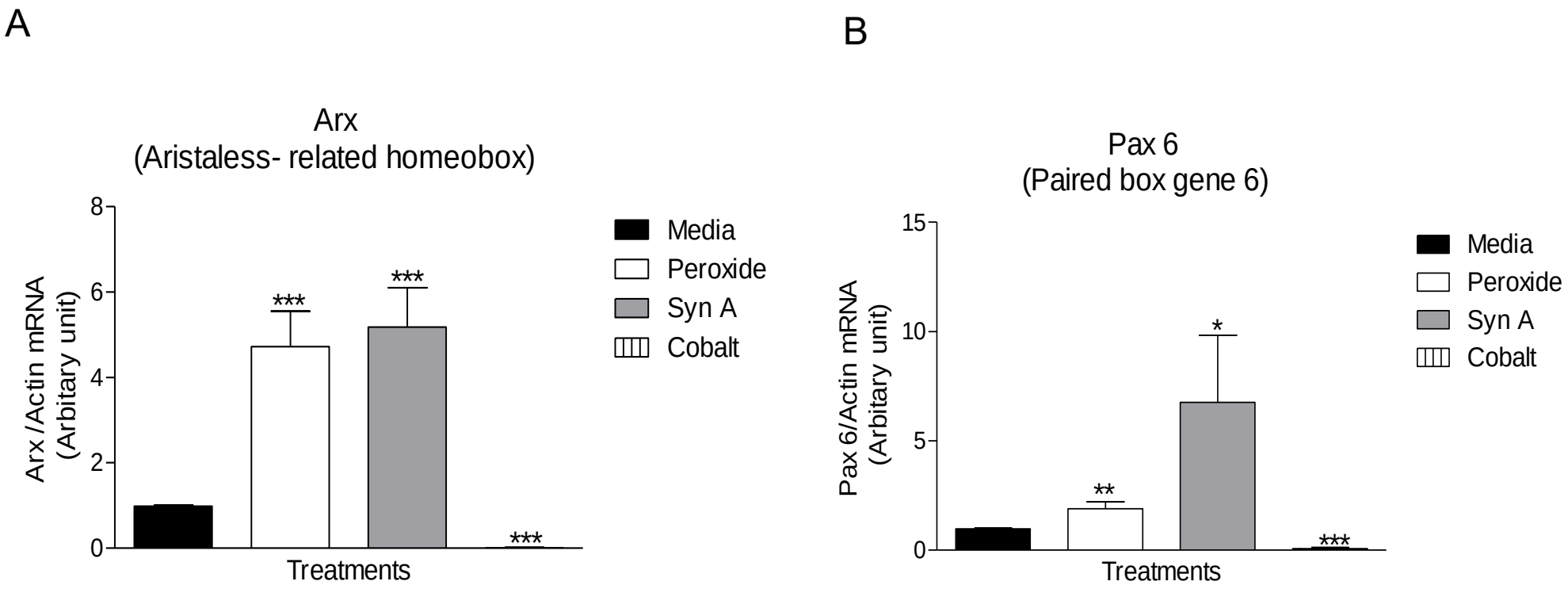

Alpha cell markers genes expression in alpha TC cells. Pax 6 (A), and Arx (B) genes following a 2-hour culture with media, peroxide, Syn A, and cobalt chloride. Gene expression was normalized to Actin gene expression. Gene expression was determined by RT-PCR. Values shown are mean ± SEM (n=3 replications). Changes were deemed significant when p values were *p<0.05, **p<0.01, or ***p<0.001 when compared with media.

Figure 8.21 Effects of 2-hour exposure to alpha TC cells to hydrogen peroxide, Syn A, and cobalt chloride on beta cell marker gene expression.

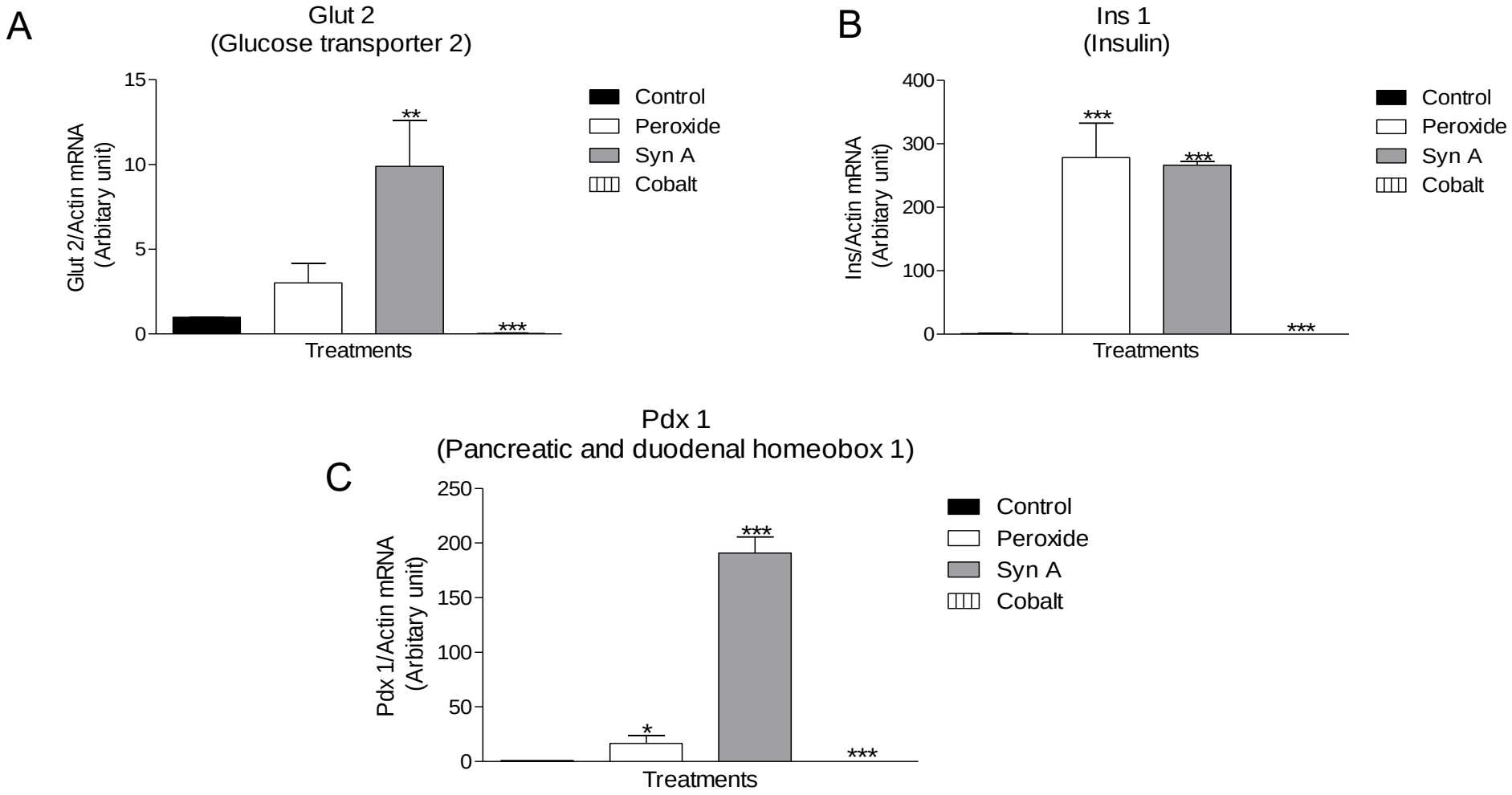

Beta cell markers gene expression in alpha TC cells. Glut 2 (A), Ins (B), and Pdx1 (C) genes following a 2-hour culture with media, peroxide, Syn A, and cobalt chloride. Gene expression was normalized to Actin gene expression. Gene expression was determined by RT-PCR. Values shown are mean ± SEM (n=3 replications). Changes were deemed significant when p values were *p<0.05 or ***p<0.001 when compared with media.

Figure 8.22 Effects of hydrogen peroxide, Syn A, and cobalt chloride on Ki67 positive, glucagon positive alpha TC cells.

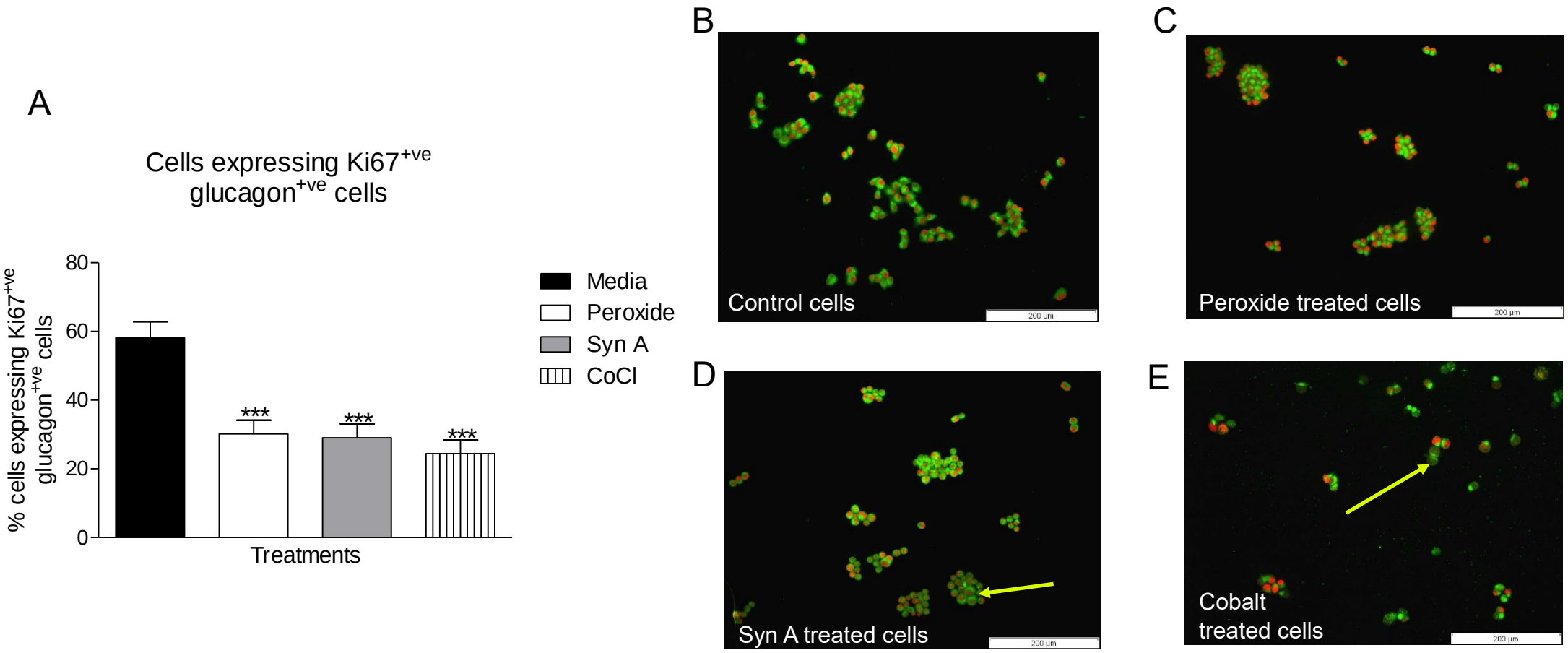

Alpha cell proliferation determined by cells expressing Ki67^{+ve}, glucagon^{+ve} cells. Values shown are ± SEM (n= 6 wells). Changes were deemed significant when p values were ***p<0.001 when compared with media. Control (B), peroxide (C), Syn A (D), and Cobalt (E) are represented in photos. Green represents glucagon and red represents Ki67. The yellow arrows are pointing to faint nuclei. Photos were imaged with a 20x objective lens with a total of 90 + alpha cells counted per treatment.

Figure 8.23 Effects on cellular viability of hydrogen peroxide, Syn A, and cobalt chloride treated alpha TC cells incubated for 2 hours in normal culture media stained with trypan blue.

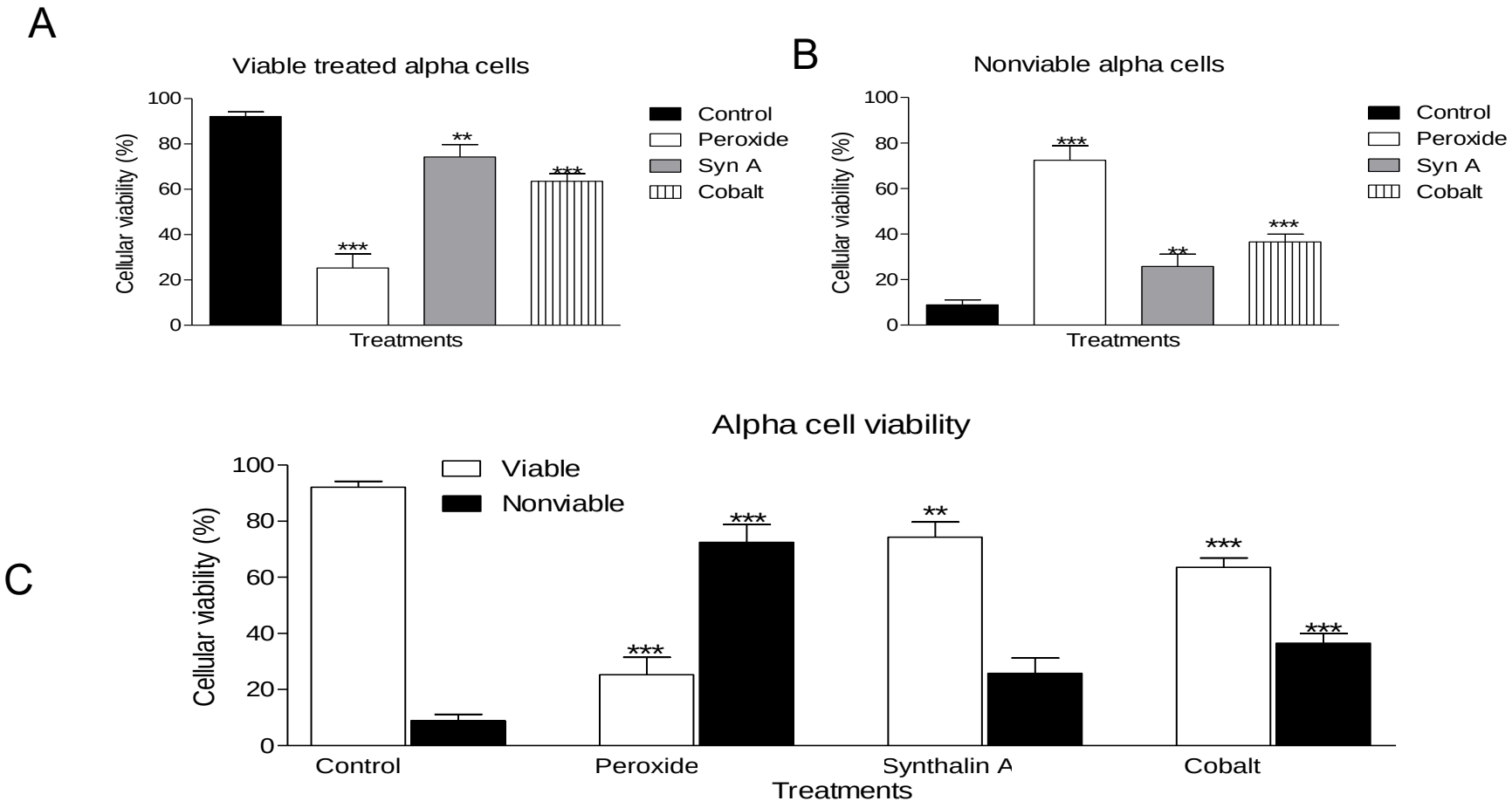

Alpha TC cellular viability determined by trypan blue staining. Alpha TC cells incubated for 2 hours in normal culture media to determined viable (A and C), and nonviable (B and C). Values are mean ± SEM (n= 12 counts). Changes were deemed significant when p values were **p<0.01 or ***p <0.001 when compared with media.

Figure 8.24 Effects of inhibitors incubated with KRBB (A), hydrogen peroxide (B), Syn A (C), and cobalt chloride (D) treated alpha TC cells incubated for 2 hours in normal culture media stained with trypan blue.

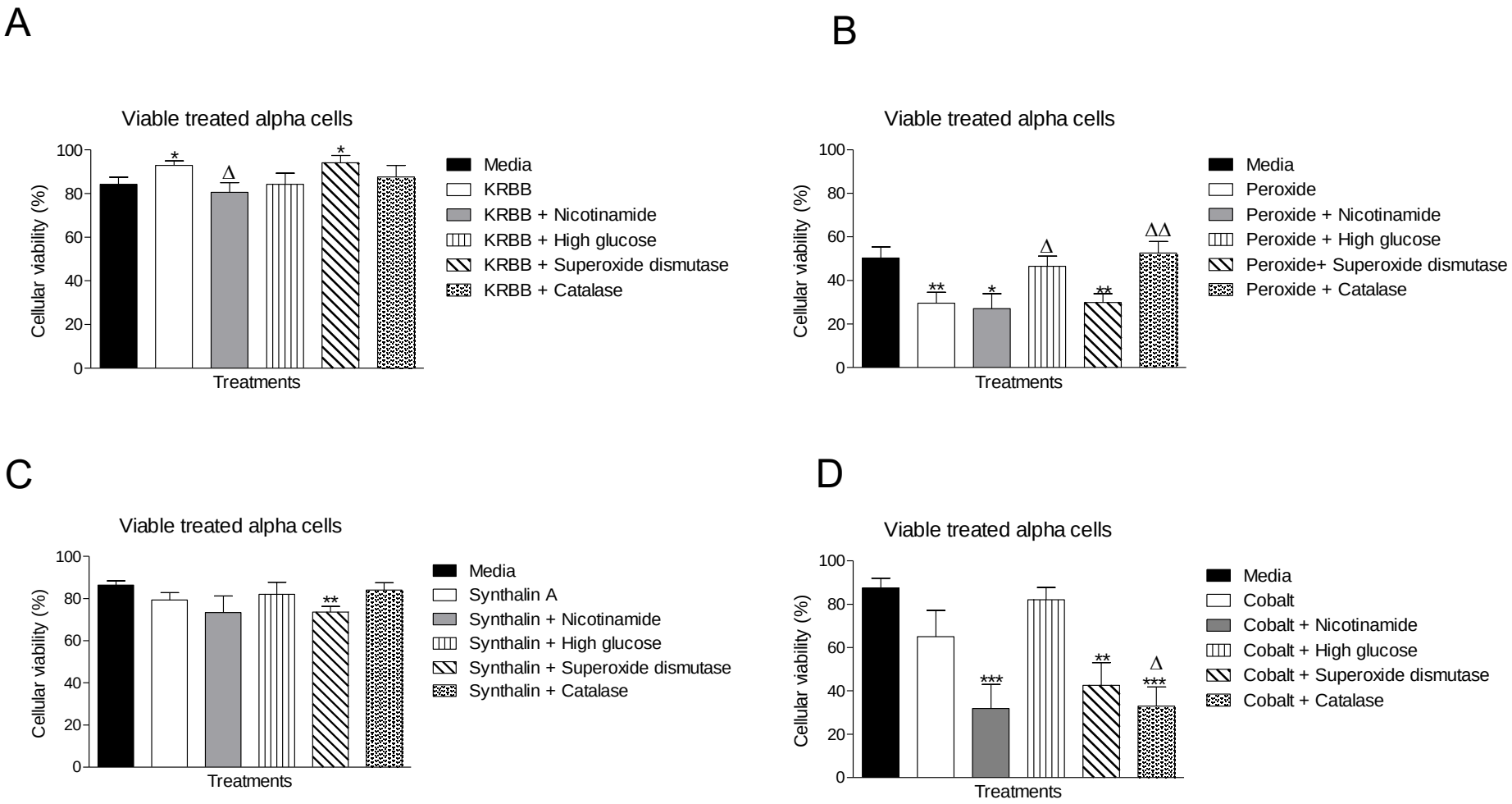

Alpha TC cellular viability determined by trypan blue staining. Alpha TC cells incubated for 2 hours in normal culture media. Values are mean ± SEM (n= 12 counts). Changes were deemed significant when p values were *p<0.05, **p<0.01, or ***p <0.001 when compared media. $^{\Delta}$p<0.05 or $^{\Delta\Delta}$p<0.01 when compared with treatment + inhibitor.

Figure 8.25 Effects of inhibitors incubated with KRBB (A), hydrogen peroxide (B), Syn A (C), and cobalt chloride (D) treated alpha TC cells incubated for 2 hours in normal culture media stained with trypan blue.

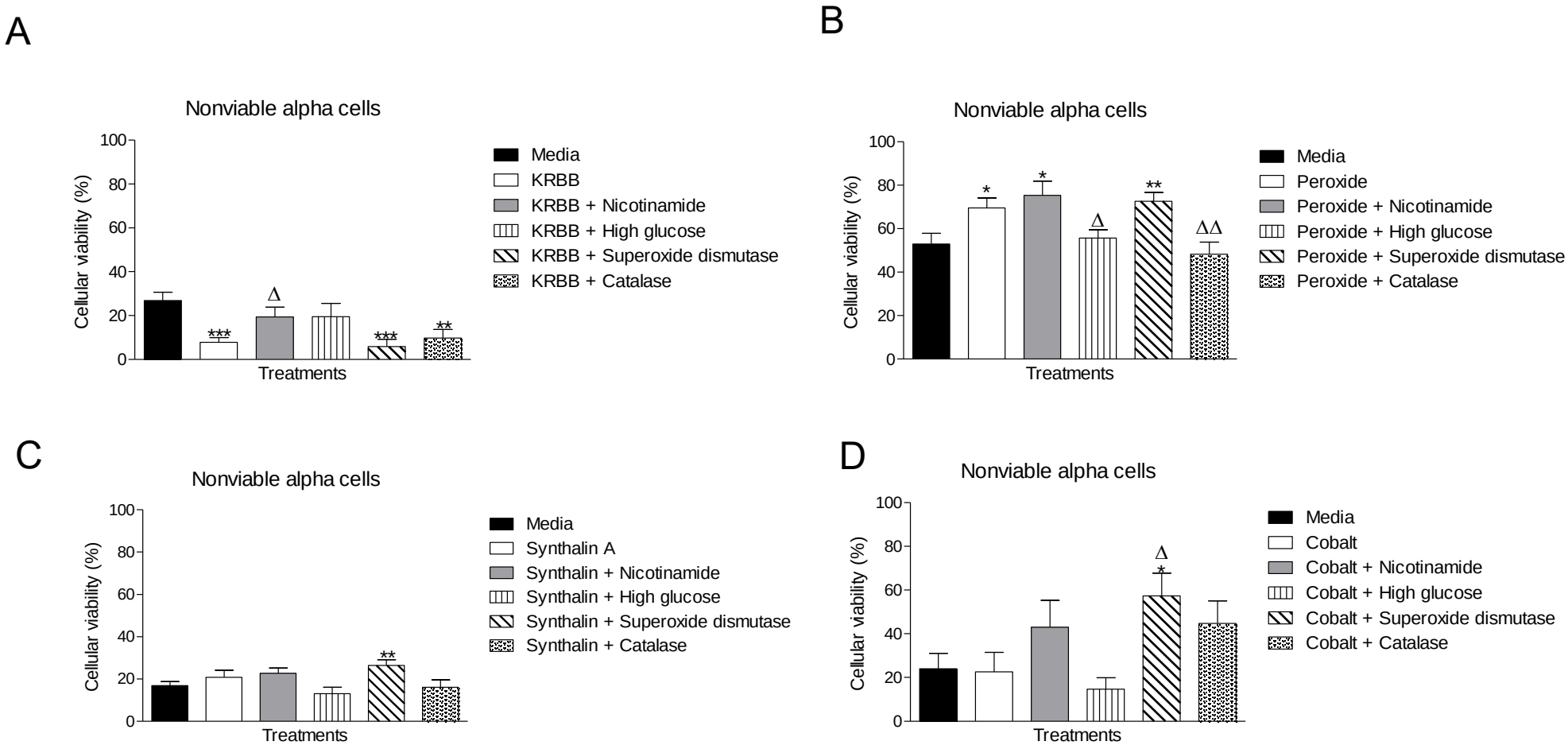

Alpha TC cellular viability determined by trypan blue staining. Alpha TC cells incubated for 2 hours. Values are mean ± SEM (n= 12 counts). Changes were deemed significant when p values were *p<0.05, **p<0.01, or ***p <0.001 when compared with media. $^{\Delta}$p<0.05 or $^{\Delta\Delta}$p<0.01 when compared with treatments + inhibitor.

Figure 8.26 Effects of inhibitors incubated for 2 hours on KRBB (A) and hydrogen peroxide (B) treated alpha TC cell viability stained with trypan blue.

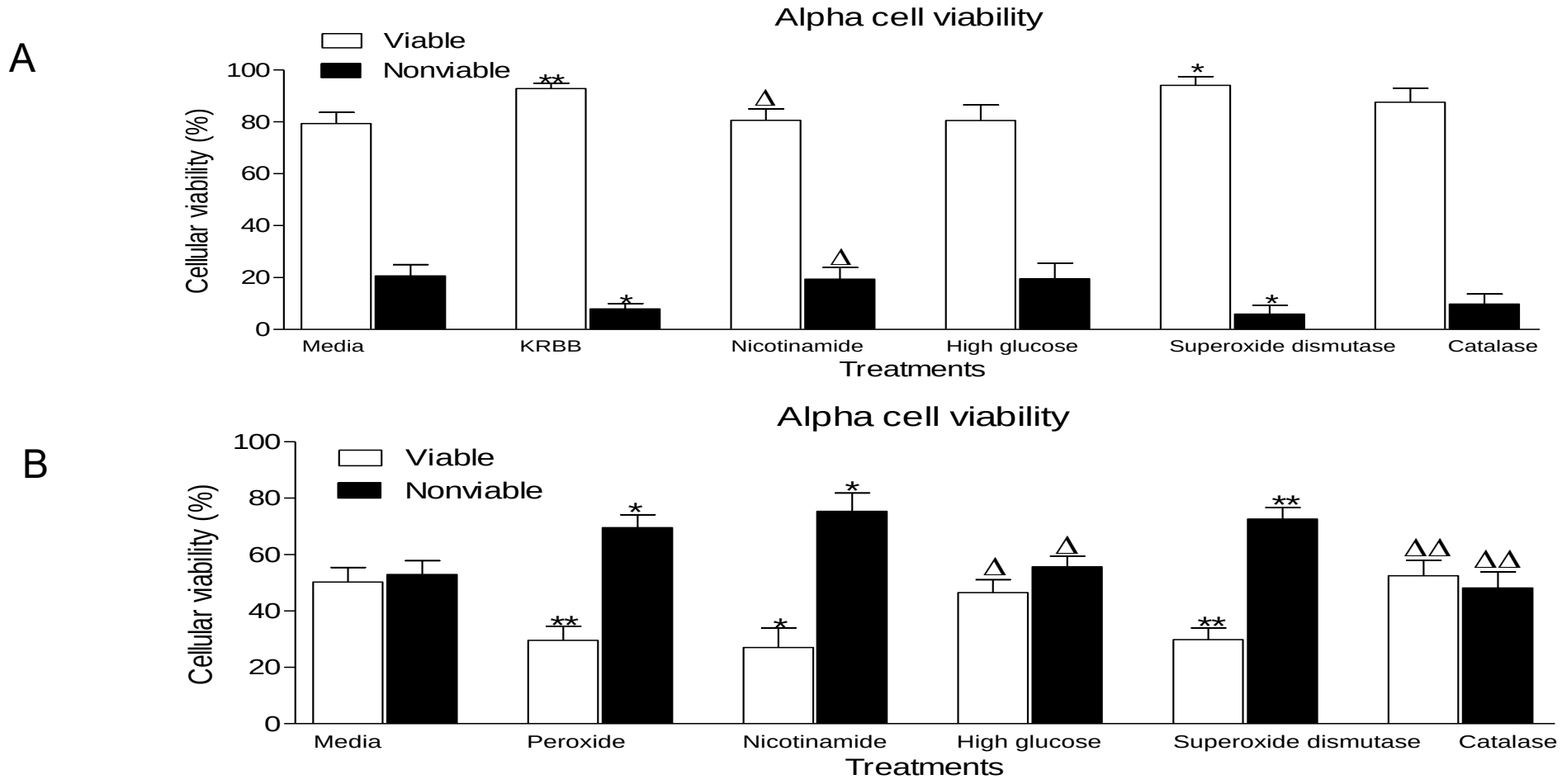

Alpha TC cellular viability determined by trypan blue staining. Alpha TC cells incubated for 2 hours. Values are mean ± SEM (n= 12 counts). Changes were deemed significant when p values were *p<0.05, **p<0.01, or ***p <0.001 when compared with media. $^{\Delta}$p<0.05 or $^{\Delta\Delta}$p<0.01 when compared with treatments +inhibitor.

Figure 8.27 Effects of inhibitors incubated for 2 hours on Syn A (A) and cobalt chloride (B) treated alpha TC cell viability stained with trypan blue.

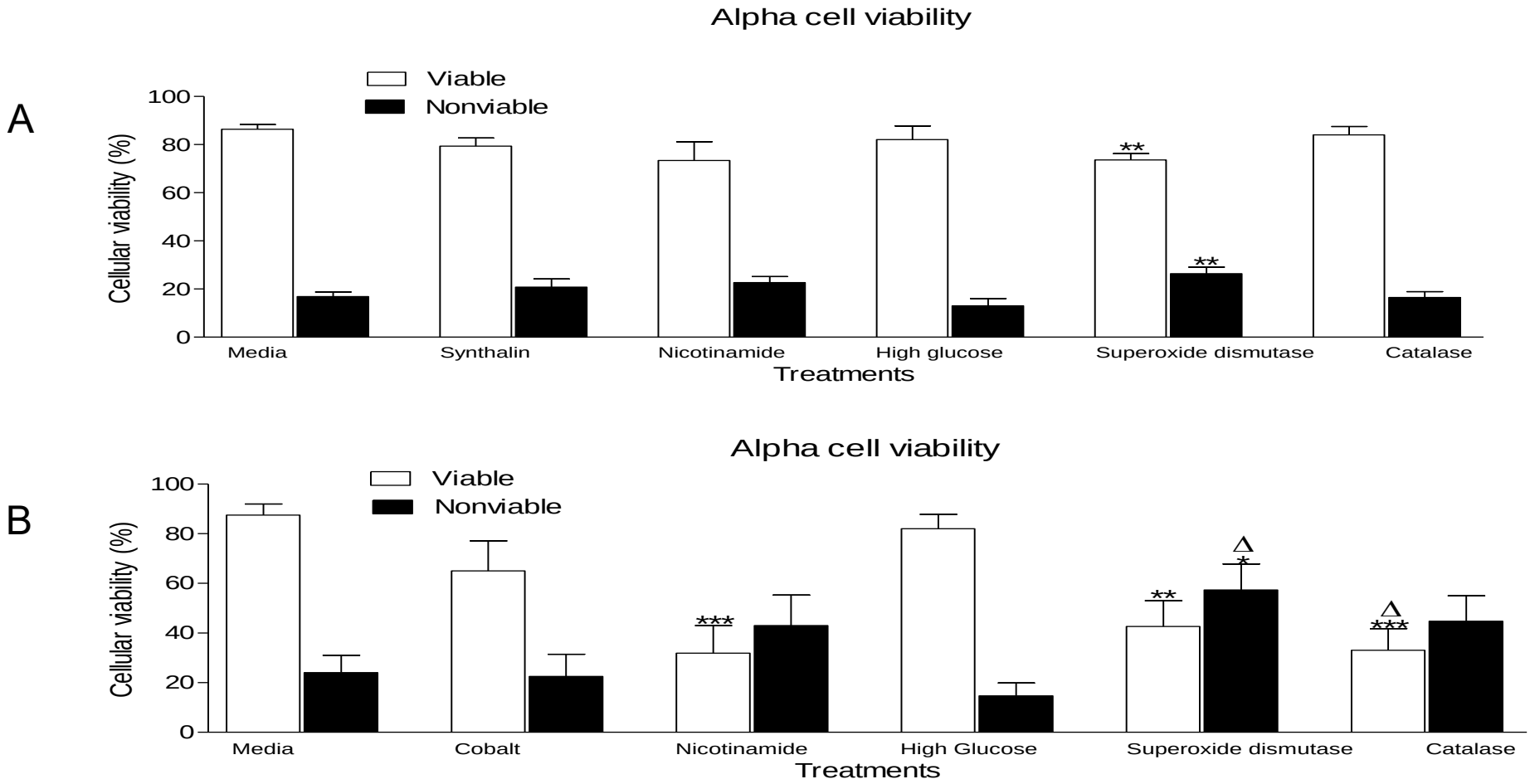

Trypan blue cellular viability. Alpha TC cells incubated for 2 hours. Values are mean ± SEM (n= 12 counts). Changes were deemed significant when p values were *p<0.05, **p<0.01, or ***p <0.001 when compared with media. $^{\Delta}$p<0.05 or $^{\Delta\Delta}$p<0.01 when compared with treatments + inhibitor.

Figure 8.28 Effects of hydrogen peroxide, Syn A, and cobalt chloride on alpha TC cell apoptosis and necrosis levels as determined using Flow cytometry.

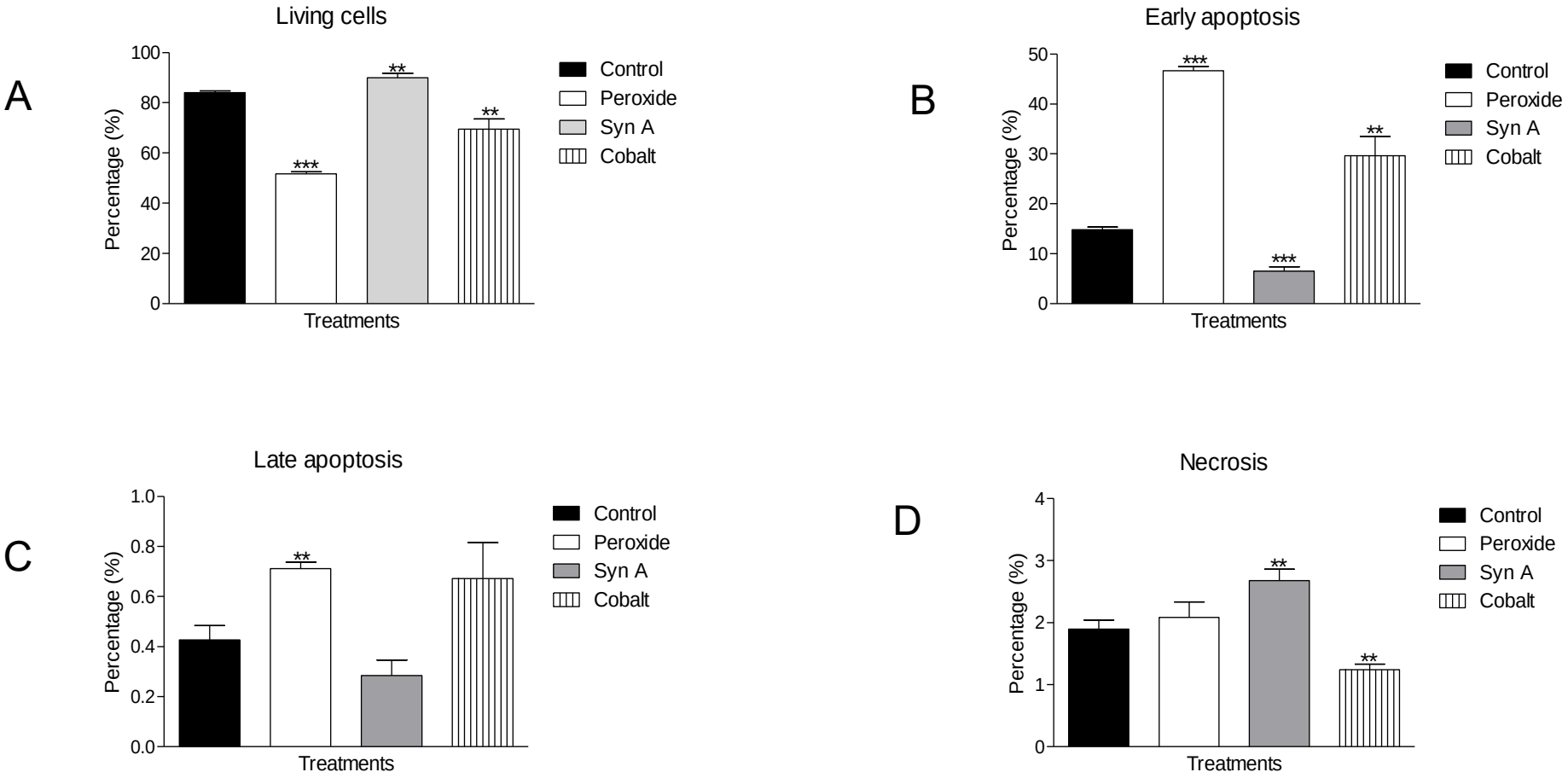

Alpha TC cellular viability determined by Flow cytometry. Alpha TC cells incubated with treatments for 8 hours. Living (A), early apoptosis (B), late apoptosis (C), and necrosis (D). Values are mean ± SEM (n=6). Changes were deemed significant when p values were *p<0.05 or **p<0.01 when compared with media.

Chapter 9
General discussion

9.1 Diabetes Mellitus

Diabetes is a bi-hormonal metabolic disorder and can be broken down to two main types: type 1 (T1D) and type 2 (T2D). The prevalence of diabetes is increasing worldwide and within the United Kingdom (UK). In 2015, roughly 3.5 million people were living with diabetes in the UK whereas the number increased to 3.8 million in 2018 (Diabetes UK, 2019; Diabetes UK, 2018a and 2016b). Within this disease, the insulin levels within the blood are decreased and glucose levels are increased (Henquin and Rahier, 2011; Parker *et al.*2002). In both main types of diabetes, genetic and environmental factors can lead to beta cell decrease, resulting in increased blood glucose. This was observed in the animal models that we induced diabetes with the beta cell toxin, streptozotocin (STZ).

9.2 Pancreatic islets

Beta cells are predominantly within the head of the mouse pancreas (Liggitt and Dintzis, 2018; Dolenšek *et al.*2015; Moffett, 2013; Hörnblad *et al.*2011; Trimble *et al.*1982). These cells secrete insulin, which is a hormone that has the capability to lower an individual's blood glucose levels (Rorsman and Renström, 2003). These cells are often destroyed in T1D and a progressive loss of the insulin secretion from the beta cells in T2D is observed (American Diabetes Association, 2019). We were able to mimic this destruction of beta cells using the toxin STZ. As expected, the blood glucose levels increased, as well as the fluid intake in this animal model. When the islets were analysed through histology. We could see that the beta cell area and percentage were decreased in the mice treated with STZ.

Alpha cells are predominant in the tail of the mouse pancreas and secrete the hormone glucagon. When secreted, glucagon functions to help balance out the blood glucose level affected by insulin (Chiras, 2015; Martini *et al.* 2015; Conarello *et al.* 2007; Sørensen *et al.* 2006; Gelling *et al.* 2003; Lefèbvre, 1995). We were able to cause alpha cell destruction to confirm past research results. This was done by the treatment with Synthalin A (Syn A) and cobalt. We observed that once the alpha cells were destroyed, blood glucose levels

decreased. We found that these two toxins were in fact affecting the alpha cells and observed a decrease in alpha cell area and percentage in the mice treated with both toxins. Alpha cell viability was also determined by cellular viability assays, and the results confirmed that these compounds decreased the number of living cells, specifically at higher concentrations.

9.3 Synthalin A

As stated previously, Syn A was discovered in the 1920's by Frank, Nothmann, and Wagner. They believed Syn A could not be a complete substitute for insulin, and it reacts slower than the peptide hormone (Frank *et al*. 1926). They suggested that the treatment involving Syn A will be different from insulin in the sense that it does not need to be injected and should only be used when the patient does not respond to insulin (Frank *et al.* 1926). It was also stated that the individuals who could tolerate insulin could tolerate Syn A with no difficulty. They found that once Syn A was introduced as a treatment, the sugar in the urine of diabetics would decrease as well as a decrease in urine output. They suggested that the best way for Syn A to be taken was in variation with one to two day breaks in-between doses and with a pre-treatment of dietary change. In comparison, the pure form of insulin was believed to be 75 times stronger than Syn A. This Syn A study was done in humans and researchers found that acidosis and other symptoms disappeared, blood glucose decreased, but some patients ended up with blisters on their skin due to the drug (Frank *et al.*1926). We confirmed this with the experiments in animal models, that Syn A does, in fact, decrease the blood glucose levels, however, no skin issues in rodents were detected. Frank *et al.* (1926) concluded that more tests needed to be carried out on this drug, and it required rigorous testing to confirm the beneficial effects. We have carried out several different experiments using animal models as well as cell assays, to show the effects of Syn A. Although we have proved it is toxic to the alpha cells, it does have a mild impact on the beta cells. We have also shown that Syn A affects other organs, such as the lungs and liver, by the blood clots we observed during the necropsy.

There are two different suggestions on why Syn A was discontinued. Some research states that it was discontinued and removed from consideration as a potential for diabetes due to the toxic effects that it caused on the organs (Langslow *et al.* 1973; Creutzfeldt, 1960 and 1957; Fodden and Read, 1953; Davis, 1952; Karr *et al.* 1929; Bodo and Marks, 1928; Watanabe, 1918). We can confirm this level of toxicity, only within the pancreatic islets. We saw a decrease in alpha cells when looking at the histological sections as well as the cellular viability assays. While Syn A was decreasing in potential clinical use due to the toxic effects, insulin was discovered which resulted in Syn A being removed from further consideration (Krishnarth *et al.* 2013; Bailey and Day, 2004; Dey *et al.* 2002; Dale 1927). Past research states that when humans were taking insulin, once Syn A was added, the need for insulin decreased (Joslin, 1927). Perhaps in the future, Syn A, as well as cobalt, could be tested in conjunction with glucose or insulin treatments once the blood glucose levels reached hypoglycaemic state to see if blood glucose levels could return to normal. It has been reported that Syn A is more toxic than cobalt. Research states that when examining alpha cell destruction, more damage was caused by Syn A (Ito *et al*. 1958). We performed more studies using Syn A, but within the cellular experiments we can dispute the previous findings that Syn A is more toxic.

9.4 Cobalt chloride

Unlike Syn A, cobalt is a mineral that can be found in the human body (Vasudevan and McNeil, 2006). Cobalt is a vital component of vitamin B12 (Okail, 2010; Roessner *et al*. 2001). It has been stated that cobalt has the ability to decrease blood glucose (Vasudevan and McNeil, 2006; Ybarra *et al*. 1997). Cobalt was first used in therapeutic state to help with anaemia caused by renal failure. According to a review on toxic metals, cobalt creates strand breaks in the DNA in mammalian cells, but not in bacteria (Beyersmann and Hartwig, 2008; De Boeck *et al*. 2003). Past research also found that the oxidative DNA damage in the kidneys, lungs, and liver in rats treated with cobalt (Beyersmann and Hartwig, 2008; Kasprazak *et al*. 1994). Outside of those three organs, cobalt also accumulates in the pancreas, heart, and muscles (Simonsen *et al*. 2012). Although cobalt appeared to be toxic to specific organs, the effects

seemed to be short lived and the kidneys, thyroid and the central nervous system returned to normal after the discontinuation of the drug (Schirrmacher, 1967). There is no clear discontinuation of cobalt in diabetic studies, since cobalt is still being used as an essential trace element, especially in vitamins.

9.5 Other studies regarding Synthalin

In a study that looked at the parasite that caused African sleeping sickness, research found that the strain of *Trypsonoma: T. rhodesiene* showed that, when given the maximum dosage of Syn A, the signs of the disease disappeared. However, the symptoms returned shortly afterwards. This test was performed in rabbits and they eventually died due to the toxic effects of this drug (Lourie and Yorkie, 1938). In the experiments we conducted using rodents, we confirmed that the elevated blood sugar levels in diabetes, did decrease with the use of Syn A. However, it would have been beneficial to see if there was an increase in blood glucose once Syn A was stopped. This was only observed in the rats that were injected with 2mg/kg of Syn A. Their blood glucose levels increased at the end of the study, several days after the initial injection. Past research also stated that after the fourth course of treatment with Syn A, the symptoms of the disease increased in mice (Lourie and Yorkie, 1938). We can confirm these results in our mice studies using the Swiss TO and Glu^{Cre} mice. In the Swiss TO mice, some animals administered the higher dose did not survive, therefore confirming that after several days of treatment symptoms did not go away. In the Glu^{Cre} mice, symptoms of diabetes did not go away, but instead the blood glucose increased as well as the food and fluid intake in the higher dose Syn A mice.

9.6 Up to date literature for Synthalin and cobalt

Syn A has not been used in diabetic studies since the late 1950's. In the past few years, Syn A was researched in chemotherapy, microbiological settings, and in sleeping sickness (Grare *et al*. 2007). Syn A was used in these studies due to the anti-trypanosomal activity. In a study that looked at antimicrobial agents and antibacterial activity, Syn A had little to no effect

against all the bacterial strains and remained inactive against clinical isolates. However, after exposure for 168 hours, cytotoxicity occurred in human keratinocytes, but it was concluded that Syn A was not administered in a dose sufficient for antibacterial activity (Grare *et al*. 2007). This extended exposure confirms what we saw in the *in vitro* assays when comparing 2 and 8 hours. We concluded that the longer exposure was more toxic on the cells compared to the 2 hours. Syn A has seldomly been used acutely in diabetes research ever since the agent was lost. The latest research examines metformin, Syn A, and phenformin on liver toxicity. This study concluded that Syn A had effects on AMP- activated protein kinase (AMPK), acetyl-CoA carboxylase, and S6 phosphorylation and the increased activity of AMPK was like metformin when used at lower concentrations. Within this experiment the authors also concluded that Syn A suppressed oxygen consumption of intact mitochondria, in a similar way to metformin (Cameron *et al*. 2018; Zhou *et al*. 2001). This study also documented that alkylguanidines with similar length of chain as Syn substantially inhibit the mitochondria of the cell even more than diguanides and biguanides (Cameron *et al*. 2018; Pressman, 1962).

Cobalt chloride is still being researched, specifically in cardiac studies. Studies concluded that after excess amount of cobalt, severe hypoxia, intoxication, and heart problems occurred (Sataieva *et al*. 2019). In terms of diabetes research, interest appears to be on going, unlike Syn A. One study that examined oxidative stress in relation to type 1 diabetes in female rats, concluded that the glucose transporter 1 (GLUT 1) was increased when gluconeogenesis was inhibited (Ali *et al*. 2019; Saker *et al*. 1998). This study also concluded that with type 2 diabetes, cobalt levels became deficient (Ali *et al*. 2019). Although we did not look at GLUT 1, and we should perhaps take that into consideration for future studies, GLUT 2 displayed a decrease in gene expression in the alpha cells treated with cobalt. It may be beneficial to consider this in the future, and test cobalt chloride in normal and transgenic mice with STZ induced diabetes, as well as an obesity model to examine if treatment of additional cobalt can prevent cobalt deficiency.

9.7 Scope for future studies in diabetes

Further studies need to be carried out using diabetic models to determine the effects of Syn A on beta cells. However, because STZ and obesity have little to no effect on Gcg rec null mice it would be interesting to see if the mice started to gain a little weight, what Syn A would do to the body weight as well as the pancreatic islets (Conarello *et al*. 2007; Lee *et al.* 2014). It would also be beneficial to look at Gcg rec null mice to see if cobalt chloride has a similar effect on those mice as syn A did.

Multiple doses of Syn A should also be considered, as well as using high fat fed or diabetic rats. Hultquist (1956), examined other organs which an area of interest, such as the liver and kidneys. Perhaps it would be useful to look at the liver after a treatment of Syn A to examine further effects to the levels of glucagon within the body. Another area of interest would be to look at the effects of Syn A in rats during feeding studies. This would provide more insight to the effects of Syn A and food and fluid intake in relation to rodents. It would also be beneficial to perform the same cellular assays previously used on a rat cell line, such as BRIN BD11 cells.

For future studies, it might be worthwhile to use Syn A in the dosage pattern laid out by Frank, Nothmann, and Wagner (Joslin, 1927; Frank *et al*. 1926). This would allow us to see if the blood glucose levels decrease and stay decreased, once an injection of Syn A has been stopped and reintroduced. The liver, kidneys or other organs, should be looked at histologically and cytologically to see the effects of Syn A on other organs, since past research states that the pancreas may not be the primary site of action (Langslow and Freeman 1973; Langslow *et al*. 1973; Beekman 1956). Further studies need to be carried out, to see the effects on other animal models, such as transgenic mice, female mice, and animals fed a high-fat fed diet, as well as looking at different doses to find which one works the best. However, the current data and previous research suggest that Syn A has a strong influence on the alpha cells as well as on glucose levels.

When comparing male and female mice, one consideration to think about is treating the female with a higher dose of STZ at the start of a study to avoid different groups being treated with different amounts or treat female mice with Syn A, to see if the oestrogen has a similar effect when the alpha cells are only targeted. Another way to test the effects of these toxins on the female hormones would be to test on ovariectomized mice. Further studies need to be carried out to see how quickly the Syn A reacts. Perhaps by sacrificing the mice at different time points after the injections of Syn A would provide an understanding of how rapidly Syn A takes effect after the beta cells have been destroyed by STZ.

When treating with cobalt, perhaps a pre-treatment of STZ or a high fat diet should be considered, prior to administering cobalt. Hultquist (1956), stated that cobalt protects against diabetes. If the mice were injected with STZ first, then cobalt, blood glucose could be evaluated to see the effect cobalt has on the diabetic mice. (Hultquist 1956). A longer study, as well as culling of the mice at different time points, would help to see if the alpha cells regenerate after 10 days like rabbit alpha cells. It might confirm that the drug is species specific and the alpha cells only regenerate in rabbits. Another consideration to think about would be treating non-transgenic mice with cobalt, single and multiple doses to compare against the transgenic mice and mice treated with Syn A.

In early studies, it was reported that starved birds treated with Syn A did not have an extreme toxic effect (Langslow and Freeman, 1973; Langslow *et al*. 1973). This should be considered in future studies involving Syn A and cobalt. Even though both are species specific and may not have the same effect on starved mice or rats, perhaps it will also provide a slightly less toxic activity in the rodents. It would also be beneficial to examine the differences in route of administration. It was stated that when delivered orally, blood glucose decreased at a steady rate (Bodo and Marks, 1928). We only tested Syn A when given with i.p. injections, and most studies mention an immediate reaction depending on the dose amount.

When looking at islet cell lines treated with the toxins, it would be useful to test a liver cell line. This would give a better understanding why Syn A has been said to cause toxic effects on the

liver. It would be beneficial to carry out more cellular assays on the pancreatic beta cell line, Min-6, or primarily rodent islets. This could possibly provide more insight to the destruction of the beta cells as well as the alpha cells. For future studies, it would be beneficial to examine the pancreatic cell lines, and other cell lines in different conditions, such as low glucose, long and short incubation time, and with the addition of FBS and without. It would also be beneficial to stain with TUNEL on the cellular lines to view cellular apoptosis compared to the single/multiple dose treatment in the mice tissue. It would be helpful if glucagon levels could be measured in a similar way insulin was by RIA to provide more detail on the effects of these drugs.

In regard to both animal and cellular models, it may be beneficial to test these two drugs with the isoflavone, puerarin. As discussed in Chapter 8, puerarin protected the beta cells from the toxicity of cobalt. It may be beneficial to see the protective effects of this isoflavone when treated with the alpha cell toxins, Syn A and cobalt (Li *et al*. 2014; Zhou *et al*. 2014). It would raise the questions regarding pancreatic alpha cell protection, or is it just a beta cell protector? There appears to be little research done on puerarin and alpha cells, so it would be interesting to see if the alpha cells histologically and cytologically are protected as well when treated with this isoflavone coupled with these alpha cell toxins.

9.8 Concluding remarks

This thesis has evaluated the toxicity of Syn A and cobalt on alpha pancreatic cells. This has been achieved through numerous animal and cytology studies. The toxicity on the alpha cell, is likely the cause hypoglycaemia that the mice experienced in most of the studies. This could be accounted for by the decreased viability of alpha cells when viewed histologically. In the cellular assays, it appeared that the alpha TC cells treated with Syn A proliferate before dying when looking at the Flow cytometry results. If the toxicity could be reduced and only targeted to the pancreas, then it is possible that these two drugs could provide short term treatment for diabetes by countering the counter-regulatory hyperglucagonemia. These two toxins could also be used in the future for diabetic treatments if the delivery could be aimed at a specific

number of alpha cells to reduce the number to a safe amount while sparing other pancreatic cells. Further studies on the possible treatment of diabetes using alpha cell toxins to decrease circulating glucagon could lead to useful approaches to the treatment in T1D and T2D in humans.

Chapter 10
References

Abràmoff, M.D., Magalhães, P.J., and Ram, S.J. (2004). Image processing with imageJ. *Biophotonics International*, 11(7), pp. 36-42.

Ahrén, B., Larsson, H., and Holst, J.J. (1997). Effects of glucagon-like peptide-1 on islet function and insulin sensitivity in noninsulin-dependent diabetes mellitus. *Journal of Clinical Endocrinology and Metabolism*, 82, pp. 473-478.

Ali, S.K., Mahdi, E.A., Kareem, Z.K., Ali, M.K., and Ali, A.K. (2019). Evaluation of some trace elements status in females type 1 diabetics patients and its relationship with oxidative stress. *International Journal of Research in Pharmaceutical Sciences*, 10(4), 2792-2799.

American Diabetes Association. (2019). Classification and diagnosis of diabetes: Standards of medical care in diabetes- 2019. *Diabetes Care*, 42(Suppl. 1), pp. S13-S28.

Angst, E., Sibold, S., Tiffon, C., Weimann, R., Gloor, B., Candinas, D., and Stroka, D. (2006). Cellular differentiation determines the expression of the hypoxia-inducible protein NDRG1 in pancreatic cancer. *British Journal of Cancer*, 95, pp. 307-313.

Ashcroft, F.M. and Rorsman, P. (2012). Diabetes mellitus and the B cell: The last ten years. *Cell*, 148, pp. 1160-1171.

Arora, S., Ojha, S.K., and Vohora, D. (2009). Characteristics of streptozotocin induced diabetes mellitus in Swiss albino mice. *Global Journal of Pharmacology*, 3(2), pp. 81-84.

Avezzu, G. and Luise, R. (1951). Action of cobalt chloride in alloxan diabetes of the rabbit. *Journal of Biological Research- Bollettino della Società Italiana di Biologia Sperimentale*, 27(9-11), pp. 1515-1517.

Badr, G.A., Zhang, J-Z., Tang, J., Kern, T.S., and Ismail-Beigi, F. (1999). Glut1 and Glut3 expression, but not capillary density, is increase by cobalt chloride in rat cerebrum and retina. *Molecular Brain Research*, 64(1), pp. 24-33.

Baetens, D., Malaisse-Lagae, F., Perrelet, A., and Orci, L. (1979). Endocrine pancreas: Three- dimensional reconstruction shows two types of islets of Langerhans. *Science*, 206(4424), pp. 1323-1325.

Bagger, J.I., Knop, F.K., Holst, J.J., and Visbøll, T. (2011). Glucagon antagonism as a potential therapeutic target in type 2 diabetes. *Diabetes, Obesity, and Metabolism*, 13, pp. 965-971.

Baggio, L.L. and Drucker, D.J. (2007). Biology of incretins: GLP-1 and GIP. *Gastroenterology*, 132(6), pp. 2131-2157.

Bailey, C. and Day, C. (2004). Metformin: Its botanical background. *Practical Diabetes International*, 21(3), pp. 115-117.

Beekman, B.E. (1956). The effect of Synthalin A on blood sugar and pancreatic alpha islet cells of the fowl. *Endocrinology*, 59(6), pp. 708-712.

Bencosme, S. A. and Feri, J. (1955). Relation of glucagon to A cells of the pancreas. *Proceedings of the society for Experimental Biology and Medicine*, 91(4), pp. 589-592.

Beyersmann, D. and Hartwig, A. (2008). Carcinogenic metal compounds: recent insight into molecular and cellular mechanisms. *Archives of Toxicology*, 82(8), pp. 493-512.

Bhuvaneswaran, D. and Dakshinamurti,K. (1970). Effects of guanidine derivatives and

oligomycin on swelling of rat liver mitochondria. *Biochemistry*, 9(26), pp. 5070-5076.

Bodo, R. and Marks, H.P. (1928). The relation of Synthalin to carbohydrate metabolism. *The Journal of Physiology*, 65(1), pp. 83-99.

Bonnevie-Nielsen, V., Steffes, M.W., and Lernmark, Å. (1981). A major loss in islet mass and B-cell function precedes hyperglycemia in mice given multiple low doses of streptozotocin. *Diabetes*, 30(5), pp. 424-429.

Bourne, R.R.A., Stevens, G.A., White, R.W., Smith, J.L., Flaxman, S.R., Price, H., Jonas, J.B., Keeffe, J., Leasher, J., Naidoo, K., Pseudos, K., Resinkoff, S., Taylor, H.R., and Vision Loss Expert Group. (2013). Causes of vision loss worldwide, 1990–2010: a systematic analysis. *The Lancet Global Health*, 1(6), pp. e339-e349.

Bouwens, L. and Blay, E.D. (1996). Islet morphogenesis and stem cell markers in rat pancreas. *Journal of Histochemistry and Cytochemistry,* 44, pp. 947-951.

Boyd, G.S., and MaClean, N. (1959). Observations on the metabolic and histological effects of cobalt chloride in the rabbit, with particular reference to cobalt-induced hypercholesterolemia. *Quarterly Journal of Experimental Physiology & Cognate Medical Sciences,* 44(4), pp/ 394-403.

Boyland, E. (1938). Experiments on the chemotherapy of cancer: the effect of certain antibacterial substances and related compounds. *Biochemical Journal*, 32(7), pp. 1207-1213.

Brand, C.L., Hansen, B., Gronnemann, S., Boysen, M., Holst, J.J. (2000). Sub-chronic glucagon neutralisation improves diabetes in ob/ob mice, *Diabetes*, 49(5), pp. A81-A81.

Brand, C.L., Rolin, B., Jørgensen, P.N., Svendsen, I., Kristensen, J.S., and Holst, J.J. (1994). Immunoneutralization of endogenous glucagon with monoclonal glucagon antibody normalizes hyperglycaemia in moderately streptozotocin-diabetic rats. *Diabetologica*, 37(10), pp. 985-993.

Brissova, M., Fowler, M.J., Nicholson, W.E., Chu, A., Hirshberb, B., Harlan, D.M., and Powers A.C. (2005). Assessment of human pancreatic islet architecture and composition by laser scanning confocal microscopy. *Journal of Histochemistry and Cytochemistry*, 53, pp. 1087-1097.

Brunner, D., Frank, J., Appl, H., Schöffl, H., Pfaller, W., Gastraunthaler, G. (2010). Serum-free cell culture: the serum-free media interactive online database. *ALTEX: Alternatives to Animal Experimentation*, 27(1), pp. 53-62.

Burcelin, R., Katz, E.B., and Charron, M.J. (1996). Molecular and cellular aspects of the glucagon receptor: role in diabetes and metabolism. *Diabetes and Metabolism,* 22, pp. 373-396.

Cabrerra, O., Berman, M., Kenyon, N.S., Ricordi C., Berggren, P., and Caicedo, A. (2006). The unique cytoarchitecture of human pancreatic islets has implications for islet cell function. *Proceedings of the National Academy of Sciences of the United States of America (PNAS)*, 103, pp. 2334-2339.

Cameron, A.R., Logie, L., Patel, K., Erhardt, S., Bacon, S., Middleton, P., Harthill, J., Forteath, C., Coats, J.T., Kerr, C., Curry, H., Stewart, D., Sakamoto, K., Repiščak, P., Paterson, M.J., Hassinen, I., McDougall, G., and Rena, G. (2018). Metformin selectively targets redox control of complex I energy transduction. *Redox Biology*, 14, pp. 187-197.

Cameron, A.T. (1928). Glukhorment and Synthalin. *Canadian Medical Association journal*, 18(2), pp. 196-197.

Cantini, G., Mannucci, E., and Luconi, M. (2016). Perspectives in GLP-1 research: New targets, new receptors. *Trends in Endocrinology and Metabolism*, 27(6), pp. 1-12.

Caren, R. and Carbo, L. (1955). Pancreatic alpha-cell function in relation to cholesterol metabolism. *The Journal of Clinical Endocrinology & Metabolism,* 16(4), pp. 507-516.

Chiang, Y.A., Ip, W., and Jin, T. (2012). The role of the Wnt signalling pathway in incretin hormone production and function. *Frontiers in Physiology*, 3(273), pp. 1-14.

Chiras, D.D. (2015). *Nutrition and Digestion. In:* Human Biology. 8th edition, Jones and Bartlett Publishers, pp. 131-164.

Chung, C.H., Hao, E., Piran, R., Keinan, E., and Levine, F. (2010). Pancreatic β-cell neogenesis by direct conversion from mature α-cells. *Stem Cells*, 28(9), pp. 1630-1638.

Collomburt, P., Hecksher-Sørensen, J., Broccoli, V., Krull, J., Ponte, I., Mundiger, T., Smith, J., Gruss, P., Serup, P, and Mansouri, A. (2005). The simultaneous loss of Arx and Pax4 genes promotes a somatostatin-producing cell fate specification at the expense of the alpha-and-beta- cell lineages in the mouse endocrine pancreas. *Development*, 132(13), pp. 2969-2980.

Collombart, P., Mansouri, A., Hecksher-Sørensen, J., Serup, P., Krull, J., Gradwohl, G., and Gruss, P. (2003). Opposing actions of Arx and Pax4 in endocrine pancreas development. *Genes and Development*, 17(20), pp. 2591-2603.

Conarello, S.L., Jing, G., Mu, J., Li, Z., Woods, J., Zycband, E., Ronan, J., Liu, F., Roy, R.S., Zhu, L., Charron, M.J., and Zhang, B.B. (2007). Glucagon receptor knockout mice are resistant to diet-induced obesity and streptozotocin-mediated beta cell loss and hyperglycemia. *Diabetologia*, 50, pp. 142-150.

Courtney, M., Gjernes, E., Druelle, N., Ravaud, C., Vieira, A., Ben-Othman, N., Pfeifer, A., Avolio, F., Leuckx, G., Lacas-Gervals, S., Burel-Vandenbos, F., Ambrosetti, D., Hecksher-Sørensen, J., Ravassard, P., Heimberg, H., Mansouri, A., and Collombart, P. (2013). The inactivation of *Arx* in pancreatic α-cells triggers their neogenesis and conversion into functional β-like cells. *PLOS Genetics*, 9(10), pp. 1-18.

Creutzfeldt, W. (1960). Alpha cell cytotoxins. *In*: Williams, R.H. *Diabetes*, York: Hoeber Inc., pp. 51-63.

Creutzfeldt, W. (1957). Alpha cell cytotoxins: Their influence on carbohydrate metabolism and the effect of the oral blood glucose reducing sulfonamides on the islet cells. *Diabetes*, 6(2), pp. 135-145.

Creutzfeldt, W. and Schmidt, W. (1954). Über die wikung von kobaltchlorid auf den blutzucker und die pankreasinseln bei verschiedenen nagetieren. *Naunyn-Schmiedebergs Archiv für Experimentelle Pathologie und Pharmakologie*, 222, pp. 487-512.

Dale, H.H. (1927). Discussion on the action of Synthalin. *In*: Gunn, J.A. *Section of Therapeutics and Pharmacology*, Royal Society of Medicine, pp. 528-531.

Davis, J.C. (1952). Hydropic degeneration of the α cells of the pancreatic islets produced by Synthalin A. *The Journal of Pathology and Bacteriology*, 64(3), pp. 575-584.

Davis, J.C. (1958). Lesions in the rabbit liver produced by Synthalin. *The Journal of Pathology and Bacteriology*, 76(1), pp. 97-109.

De Boeck, M., Lombaert, N., de Backer, S., Finsy, R., Lison, D., Kirsch-Volders, M. (2003). In vitro effects of different combinations of cobalt and metallic carbide particles. *Mutagenesis*, 18, pp. 177-186.

Deeds, M.C., Anderson, J.M., Armstrong, A.S., Gastineau, D.A., Hiddinga, H.J., Jahangir, A., Eberhardt, N.L., and Kudva, Y.C. (2011). Single dose streptozotocin induced diabetes: Considerations for study design in islet transplantation models. *Laboratory Animals*., 45(3), pp. 131-140.

Dey, L., Attele, A.S., Yuan, C-S. (2002). Alternative therapies for type 2 diabetes. *Alternative Medicine Review,* 7(1), pp. 45-58.

Diabetes UK. (2016a). *Diabetes UK: Diabetes in Northern Ireland*. Available at: https://www.diabetes.org.uk/In_Your_Area/N_Ireland/Diabetes_in_Northern_Ireland/ [Accessed 17 Sep. 2016].

Diabetes UK (2016b). *Diabetes UK: Diabetes Prevalence 2015 (November 2015).* Available at: https://www.diabetes.org.uk/About_us/What-we-say/Statistics/diabetes-prevalence-2015/ [Accessed 17 Sep. 2016].

Diabetes UK (2018a). *Diabetes UK: Diabetes prevalence 2018 (2018).* Available at: https://www.diabetes.org.uk/professionals/position-statements-reports/statistics/diabetes-prevalence-2018 [Accessed 20 Nov. 2019].

Diabetes UK (2018b). *Diabetes UK: Number of people with diabetes in Northern Ireland increases by 62.5% in a decade (February 2018).* Available at: https://www.diabetes.org.uk/in_your_area/n_ireland/news/number-of-people-living-with-diabetes-jumps [Accessed 20 Nov. 2019].

Diabetes UK (2019). *Diabetes UK: Number of people with diabetes reaches 4.7 million (February 2019).* Available at: https://www.diabetes.org.uk/about_us/news/new-stats-people-living-with-diabetes [Accessed 25 Nov. 2019].

Dolenšek, J., Rupnik, M.S., and Stožer, A. (2015). Structural similarities and differences between the human and the mouse pancreas. *Islets*, 7(1), pp.1-16.

Drucker, D. J. (1998). Perspectives in diabetes: glucagon-like peptides. *Diabetes*, 47(2), pp. 159-169.

Drucker, D.J. (2002). Biological actions and therapeutic potential of the glucagon-like peptide. *Gastroenterology*, 122(2), pp. 531-544.

Drucker, D.J. and Nauck, M.A. (2006). The incretin system: glucagon-like peptide-1 receptor agonists and dipeptidyl peptidase-4 inhibitors in type 2 diabetes. *The Lancet*, 368, pp. 1696-1705.

Dusaulcy, R., Handgraaf, S., Heddad-Masson, M., Visentin, F., Vesin, C., Reimann, F., Gribble, F., Philippe, J., and Gosmain, Y. (2016). A-Cell dysfunctions and molecular alterations in male insulinopenic diabetic mice are not completely corrected by insulin. *Endocrinology*, 157(2), pp. 536-547.

Eaton, R.P. (1973). Glucagon secretion and activity in the cobalt chloride-treated rat. *American Journal of Physiology*, 225(1), pp. 67-72.

Elayat, A. A., el-Naggar, M. M., & Tahir, M. (1995). An immunocytochemical and morphometric study of the rat pancreatic islets. *Journal of anatomy*, *186*(Pt 3), 629.

Emerging Risk Factors Collaboration, Sarwar, N., Gao, P., Seshassi, S.R., Gobin, R., Kaptoge, S., Di Angelantonio, E., Ingelsson, E., Lawlor, D.A., Selvin, E., Stampfer, M., Stehouwer, C.D., Lewington, S., Pennells, L., Thompson, A., Sattar, N., White, I.R., Ray, K.K., and Danesh, J. (2010). Diabetes mellitus, fasting blood glucose concentration, and risk of vascular disease: a collaborative meta-analysis of 102 prospective studies. *The Lancet*, 375(9733), pp. 2215-2222.

Epple, A. (1968). Comparative studies on the pancreatic islets. *Endocrinologia Japonica*, 15(1), pp. 107-122.

Epple, A. and Farner, D.S. (1967). The pancreatic islets of the white-crowned sparrow *Zonotrichia leucophrys gambelii*, during its annual cycle and under experimental conditions. *Zeitscrift für Zellforshung und Mikroskopische Anatomie*, 79(2), pp. 185-197.

Epstein, A.C.R., Gleadle, J.M., McNeil, L.A., Hewitson, K.S., O'Rourke, J., Mole, D.R., Mukherji, M., Metzen, E., Wilson, M.I., Dhanda, A., Tian, Y-M., Masson, N., Hamilton, D.L., Jaakkola, P., Barstead, R., Hodgkin, J., Maxwell, P.H., Pugh, C.W., Ratcliffe, P.J. (2001). C. *elegans* EGL-9 and mammalian homologs define a family of dioxygenases that regulate HIF by prolyl hydroxylation. *Cell*, 107(1), pp. 43-54.

Fang, I-J. and Trewyn, B.G. (2012). Nanomedicine: The purpose of trypan blue. In: *Methods in Enzymology*, 508, pp. 41-59.

Ferner, H. and Runge, W. (1955). Synthalin A as selective mitotic poison acting on alpha-cells of the islets of Langerhans. *Science,* 122(3166), pp. 420.

Flatt, P.R. and Bailey, C.J. (1981). Abnormal plasma glucose and insulin response in heterozygous lean (ob/+) mice. *Diabetologia*, 42, pp. 670-674.

Flatt, P.R., Swanston-Flatt, S.K., Tan, K. S., Marks, V. (1987). Effects of cytotoxic drugs and inhibitors of insulin secretion on a serially transplantable rat insulinoma and cultured rat insulinoma cells. *General Pharmacology: The Vascular System*, 18(3), pp. 293-297

Fodden, J.H. (1956). Cytopathologic effects of cobalt on pancreatic islets of many species. *A.M.A. Archives of Pathology*, 61(1), pp. 65-75.

Fodden, J.H. and Read, W.O. (1953). The activity of extracted pancreatic hyperglycemic-glycogenolytic factor after cobaltous chloride and Synthalin A. *Endocrinology*, 54(3), pp. 303-310.

Fortakis, G. and Timbell, J.A. *In vitro* cytotoxicity assays: comparison of LDH, neutral red, MTT, and protein assay in hepatoma cell lines following exposure to cadmium chloride. *Toxicology Letters*, 160(2), pp. 171-177.

Frank, E., Nothmann, M., and Wagner, A. (1926). Über Synthetisch dargestelle Körper mit insulinartiger wirkung auf den normalen und diabetishen organisms. *Journal of Molecular Medicine*, 5(45), pp. 2100-2107.

Furuzawa, Y., Ohmori, Y., and Watanabe, T. (1992). Immunohistochemical morphometry of pancreatic islets in the cat. *Journal of Vetinary Medicine*, 54, pp. 1165-1173.

Gatineau, M., Hancock, C., Holman, N., Outhwaite, H., Oldridge, L., Christie, A., and Ellis, L.

(2014). *Adult obesity and type 2 diabetes.* Available at: https://www.gov.uk/government/uploads/system/uploads/attachment_data/file/338934/Adult_obesity_and_type_2_diabetes_.pdf [Accessed 18 Sep. 2016].

Gelling, R.W., XQ, D., Dichmann, D.S., Rømer, J., Huang, H., Cui, L., Obici, S., Tang, B., Holst, J.J., Fledelius, C., Johansen, C., Rossetti, L., Jelicks, L.A., Serup, P., Nishimura, E., and Charron, M.J. (2003). Lower blood glucose, hyperglucagonemia, and pancreatic alpha cell hyperplasia in glucagon receptor knockout mice. *Proceedings of the National Academy of Sciences*, 100(3), pp. 1438-1443.

Goldberg, M., Dunning, S., and Bunn, H. (1988). Regulation of the erythropoietin gene: evidence that oxygen sensor is a heme protein. *Science*, 242(4884), pp. 1412-1435.

Goldsmith, P.C., Rose, J.C., Arimura, A., and Ganong, W.F. (1975). Ultrastructural localization of somatostatin in pancreatic islets of the rat. *Endocrinology*, 97, pp. 1061-1064.

Goldner, M.G., Volk, B.W., and Lazarus, S.S. (1953). Effect of alpha-cell destruction on the HGF content of the canine pancreas. *The Journal of Clinical Endocrinology and Metabolism*, 14(2), pp. 184-192.

Gottlieb, R.A., Giesing, H.A., Engler, R.L., and Babior, B.M. (1995). The acid deoxyribonuclease of neutrophils: a possible participant in apoptosis-associated genome destruction. *Blood*, 86(6), pp. 2414-2418.

Graf, T., and Enver, T. (2009). Forcing cells to change lineages. *Nature, 462 (7273)*, pp. 587-594.

Graham, G. (1927). Discussion on the action of Synthalin. *In*: Gunn, J.A. *Section of Therapeutics and Pharmacology*, Royal Society of Medicine, pp. 531-534.

Grare, M., Mourer, M., Fontanay, S., Regnouf-de-Vains, J.B., Finance, C. and Duval, R.E. (2007). *In vitro* activity of para-guanidinoethylcalix[4]arene against susceptible and antibiotic-resistant Gram-negative and Gram-positive bacteria. *Journal of Antimicrobial Chemotherapy*, 60(3), pp. 575-581.

Grasselli, F., Basini, G., Bussolati, S., and Bianco, F. (2005). Cobalt chloride, a hypoxia-mimicking agent, modulates redox status and functional parameters of cultured swine granulosa cells. *Reproduction, Fertility, and Development*, 17(7), 99.715-720.

Grube, D., and Bohn, R. (1983). The microanatomy of human islets of Langerhans, with special reference to somatostatin (D-) cells. *Archivum Histologicum Japonicum= Nihon Soshikigaku Kiroku*, pp. 327-353.

Gunnarsson, R., Petersson, B., and Hellerstrom, C. (1969). The two types of a-cells in the islets of langerhans of normal and Synthalin-treated guinea-pigs. *Acta Pathologica Microbiologica Scandinavica,* 76(2), pp. 184-192.

Gupta, Y.K. and Kumar, S. (1980). Islets of Langerhans in the parakeet, Psittacula krameri. *Anatomischer Anzeiger*, 147(1), pp. 51-59.

Gutniak, M.K., Linde, B., Holst, J.J., and Efendić, S. (1994). Subcutaneous injection of the incretin hormone glucagon-like peptide 1 abolishes postprandial glycemia in NIDDM. *Diabetes Care*, 17(9), pp. 1039-1044.

Halban, P.A., Polonsky, K.S., Bowden, D.W., Hawkins, M.A., Ling, C., Mather, K.J., Powers, A.C., Rhodes, C.J., Sussel, L., and Weir, G. (2014). β-cell failure in type 2 diabetes: Postulated mechanisms and prospects for prevention and treatment. *Diabetes Care*, 37(6), pp. 1751-1758.

Hawley, J.A. and Lessard, S.J. (2008). Exercise training-induced improvements in insulin action. *Acta Physiologica*, 192(1), pp. 127-135.

Helczynska, K., Kronblad, Å., Jögi, A. Nilsson, E., Beckman, S., Landberg, G., and Påhlman, S. (2003). Hypoxia promotes a dedifferentiated phenotype in duct breast carcinoma *in situ*. *Cancer Research 63*, pp. 1441-1444.

Henquin, J.C. and Rahier, J. (2011). Pancreatic alpha cell mass in European subjects with type 2 diabetes. *Diabetologia*, 54(7), pp. 1720-1725.

Herbertson, B.M. (1958). The effects of Synthalin on the liver of guinea-pigs. *The Journal of Pathology and Bacteriology*, 75(1), pp. 183-188.

Hörnblad, A., Eriksson, A.U., Sock, E., Hill, R.E. and Ahlgren, U. (2011). Impaired spleen formation perturbs morphogenesis of the gastric lobe of the pancreas. *PloS One,* 6(6), pp. 1-8.

Hornung, S. (1928). Synthalin und Leberschädigung. *Journal of Molecular Medicine*, 7(2), pp. 69-70.

Hoyt, E.C., Lund, P.K., Winesett, D.E., Fuller, C.R., Ghatei, M.A., Bloom, S.R., Ulshen, M.H., (1996). Effects of fasting, refeeding, and intraluminal triglyceride on proglucagon expression in jejunum and ileum. *Diabetes*, 45(4), pp. 434-439.

Hruban, R.H. and Iacobuzio-Donahue, C.A. (2015) The Pancreas. *In***:** Kumar, V., Abbas, A.K., Fausto, N., and Aster, J.C. *Robbins and Cortan pathologic basis of disease*. 9th Edition. Philadelphia, PA: Elseview, pp. 883-896.

Huang, Y.H., Sun, M.J., Jiang, M., and Fu, B.Y. (2009). Immunohistochemical localization of glucagon and pancreatic polypeptide on rat endocrine pancreas: coexistence in rat islet cells. *European Journal of Histochemistry,* 53(2), pp. 81-86.

Hultquist, G.T. (1956). The effect of cobalt chloride and Synthaline A on reduced glutathione in blood and tissues in rats with partial pancreatic duct ligation. *British Journal of Experimental Pathology*, 37(4), pp. 357-360.

Hultquist, G.T. (1959). Effect of cobaltous chloride on the blood sugar level and the islet cells in rats. *Experientia*, 15, pp. 340-342.

Hultquist, G.T. and Sundqvist, U.B. (1961). On the nature of cobalt-induced changes in the alpha cells of the islets of Langerhans in the guinea pig. *Acta Pathologica Microbiologica Scandinavia,* pp. 155-162.

International Diabetes Federation (2019a). *Diabetes: Facts and Figures.* Available at: https://www.idf.org/aboutdiabetes/what-is-diabetes/facts-figures.html [Accessed 3 March. 2020].

International Diabetes Federation (2019b). *Demographics and Geographic outline.* Available at: https://diabetesatlas.org/en/sections/demographic-and-geographic-outline.html [Accessed 3 March. 2020].

Inzucchi, Silvio E. *Diabetes*. Montvale, N.J.: Physicians' Desk Reference, 2009. Print. 1st edition, pp. 9 and 36.

Ito, S., Yamada, Y., Hayashi, M., Mastsubara, Y. (1978). Somatostatin-containing cells in the rat and horse pancreatic islets. *The Tohoku Journal of Experimental Medicine*, 124, pp. 57-64.

Ito, Y., Kobatashi, B., Kim, Y.E., Ui, M., and Moriwaki, C. (1958). Extracted glucagon from dog pancreas treated with alloxan, Synthalin A and cobaltous chloride. *Endocrinologia Japonica*, 5(1), pp. 1-10.

Jin, T. (2008). Mechanisms underlying proglucagon gene expression. *Journal of Endocrinology*, 198(1), pp. 17-28.

Jögi, A., Øra, I., Nilsson, H., Lindeheim, Å., Makino, Y., Poellinger, L., Axelson, H., and Påhlman, S. (2002). Hypoxia alters gene expression in human neuroblastoma cells toward an immature and neural crest-like phenotype. *Proceedings of the National Academy of Sciences of the United States of America (PNAS)*, 99(10), pp. 7021-7026.

Johnson, D.G., Goebel, C.U., Hruby, V.J., Bregman, M.D., and Trivedi, D. (1982). Hyperglycemia of diabetic rats decreased by a glucagon receptor antagonist. *Science*, 215(4536), pp. 1115-1116.

Jonas, J.-C., Sharma, A., Hasenkamp, W., Ilkova, H., Patanè, G., Laybutt, R., Bonner-Weir, S., and Weir, G.C. (1999). Chronic hyperglycemia triggers loss of pancreatic β cell differentiation in an animal model of diabetes. *Journal of Biological Chemistry*, 274(20), pp. 14112-14121.

Jörns, A., Barklage, E., and Grube, D. (1988). Heterogeneities of the islets in the rabbit pancreas and the problem of “paracrine” regulation of islet cells. *Anat Embryol*, 178, pp. 297-307.

Joslin, E. (1927). Synthalin: Proceedings of the Nineteenth Annual Meeting of the American Society for Clinical Investigation. *Journal of Clinical Investigation,* 4(3), pp. 435-436.

Karr, W.G., Belk, W.P., and Petty, O.H. (1929). The toxicity of Synthalin. *Journal of Pharmacology and Experimental Therapeutics,* 36(4), pp. 611-618.

Karunanayake, E.H., Baker, J.R.J, Christian, R.A., Hearse, D.J., and Mellows, G. (1976). Autoradiographic study of the distribution and cellular uptake of (^{14}C)- streptozotocin in the rat. *Diabetologia*, 12, pp. 123-128

Kasprzak, K.S., Zatawny, T.H., North, S.L., Riggs, C.W., Diwan, B.A., Rice, J.M., and Dizaroglu, M. (1994). Oxidative DNA base damage in renal, hepatic, and pulmonary chromatin of rats after intraperitoneal injection of cobalt (II) acetate. *Chemical Research in Toxicology*, 7(3), pp. 329-335.

Kern, H.F. (1970). The fine structure of pancreatic α-cells under normal and experimental conditions. *Wenner-Gren Center International Symposium Series—The Structure and Metabolism of the Pancreatic Islets*, 16, pp. 99-107.

Kharouta, M., Miller, K., Kim, A. Wojcik, P., Kilmnik, G., Dey, A. (2009). No mantle formation in rodent islets- the prototype of islet revisited. *Diabetes Research and Clinical Practice*, 85, pp. 252-257.

Kim, A., Miller, K., Jo, J., Kilimnik, G., Wojcik, P., and Hara, M. (2009). Islet architecture: a comparative study. *Islets*, 1, pp. 129-136.

Kjems, L.L., Holst, J.J., Volund, A., and Madsbad, S. (2003). The influence of GLP-1 on glucose-stimulated insulin secretion: effects on β-cell sensitivity in type 2 and nondiabetic subjects. *Diabetes*, 52, pp. 380-386.

Koch, J.H. (1955). Cobalt chloride and the alpha-cells of the pancreas. *Nature*, 175(4463), pp. 856-857.

Koh, Y., Bidstrup, H., and Nichols, D.L. (2014). Niacin increased glucose, insulin, and C-peptide levels in sedentary nondiabetic postmenopausal women. *International Journal of Women's Health*, 6, pp. 913-920.

Kramer, J.W., Nottingham, S., Robinette, J., Lenz, G, Sylvester, S., and Dessouky, M.I. (1980). Inherited, early onset, insulin-requiring diabetes mellitus of Keeshond dogs. *Diabetes*, 29, pp. 558-565.

Krishnarth, N., Bisht, A., Verma, S. and Sharma, B. (2013). Design, Synthesis of guanidine derivatives and their anti-hyperglycemic evaluation. *Der Pharma Chemica*, 5(2), pp. 59-66.

Kruger, F.A., Skillman, T.G., Hamwi, G.J., Grubbs, R.C., and Danforth, N. (1959). The mechanism of action of hypoglycemic guanidine derivatives. *Diabetes*, 9(3), pp. 170-173.

Ku, S.K., and Lee, H.S. (2006). An immunohistochemical study of the pancreatic endocrine cells of the nude mouse, Balb/c-nu/nu. *European Journal of. Histochemistry*, 50, pp. 61-68.

Kumar, R.B., Gupta, M., and Feldman, B.J. (2015). The development of next-generation screening and diagnostic platforms will change diabetes care. *Expert Review of Molecular Diagnostics*, 15(3), pp. 291-294.

Kyrylkova, K., Kyryachenko, S., Leid, M., Kioussi, C. (2012). Detection of apoptosis by TUNEL assay. In: Kioussi, C (eds) *Odontogenesis. Methods in Molecular Biology (Methods and Protocols)*, volume 887, Humana Press, pp. 41-47.

Langslow, D.R. and Freeman, B.M. (1973). Investigations into the mode of action of Synthalin A in *Gallus domesticus*. *Comparative Biochemistry and Physiology Part A: Physiology.* 46(3), pp. 447-462.

Langslow, D.R., Freeman, B.M., and Buchanan, K.D. (1973). Responses of plasma glucose, free fatty acids, glucagon and insulin to Synthalin A by *Gallus domesticus*. *Comparative Biochemistry and Physiology Part A: Physiology.* 46(3), pp. 437-445.

Lawrence, R.D. (1927). Discussion on the action of Synthalin. *In*: Gunn, J.A. *Section of Therapeutics and Pharmacology*, Royal Society of Medicine, pp. 534-535.

Le May, C., Chu, K., Hu, M. (2006). Estrogens protect pancreatic beta-cells from apoptosis and prevent insulin-deficient diabetes mellitus in mice. *Proceedings of the National Academy of Sciences of the United States of America (PNAS)*, 103(24), pp. 9232-9237.

Lecoeur, H. (2002). Nuclear apoptosis detection by flow cytometry: influence of endogenous endonucleases. *Experimental Cell Research*, 277, pp. 1-14.

Lee, S.G., Lee, H., and Rho, H.M. (2001). Transcriptional repression of the human *p53* gene by cobalt chloride mimicking hypoxia. *FEBS Letters*, 507(3), pp. 259-263.

Lee, Y., Berglund, E.D., Yu, X., Wang, M.Y., Evans, M.R., Scherer, P.E., Holland, W.L., Charron, M.J., Roth, M.G., and Unger, R.H. (2014). Hyperglycemia in rodent models of type 2 diabetes requires insulin-resistant alpha cells. *Proceedings of the National Academy of Sciences of the United States of America (PNAS),* 111(36), pp. 13217-13222.

Lefèbvre, P.J. (1995). Glucagon and its family revisited. *Diabetes Care*, 18(5), pp. 715-730.

Leiter, E.H. (1982). Multiple low-dose streptozotocin-induced hyperglycemia and insulitis in C57BL mice: Influence of inbred background, sex, and thymus. *Proceedings of the National Academy of Sciences of the United States of America (PNAS),*79(2), pp. 630-634.

Lenzen, S. (2008). The mechanisms of alloxan-and streptozotocin-induced diabetes. *Diabetologia*, 51(2), pp. 216-226.

Li, Z., Shangguan, Z., Liu, Y., Wang, J., Li, X., Yang, S., and Liu, S. (2014). Puerarin protects pancreatic β- cell survival via P13K/Akt signalling pathway. *Journal of Molecular Endocrinology*, 51(3), pp. 71-79.

Liggitt,D. and Dintzis, S.M. (2018). *Pancreas. In:* Comparative Anatomy and Histology: A mouse, rat, and human atlas. 2nd edition. London: Academic Press, an imprint of Elsevier, pp. 241-250.

Like, A.A. and Rossini, A.A. (1976). Streptozotocin-induced pancreatic insulitis: new model of diabetes mellitus. *Science,* 193(4251), pp. 415-417.

Liu, Y., Peterson, D.A., Kimura, H., and Schubert, D. (1997). Mechanism of cellular 3-(4,5 dimethylthiazol-2-yl)-2,5-diphenyltetrazolium bromide (MTT) reduction. *Journal of Neurochemistry*, 69(2), pp. 581-593.

Lourie, E.M. and Yorkie, W. (1938). The preparation of strains of trypanosomes resistant to Synthalin and undecane diamidine, and an analysis of their characters. *Annals of Tropical Medicine and Parasitology*, 32(2), pp. 201-213.

Lundbaek, K. and Nielsen, K. (1958). A comparative study of the action of three hypoglycemic compounds on the blood sugar and the islet cells of the pancreas in the rat. *Acta Endocrinologia*, 27, pp. 325-338.

Maclaren, N.K., Neufeld, M., McLaughlin, J. V., and Taylor, G. (1980). Androgen sensitization of streptozotocin-induced diabetes in mice. *Diabetes*, 29(9), pp. 710-716.

Manotham, K., Tanka, T., Matsumoto, M., Ohse, T., Inagi, R., Miyata, T., Kurokawa, K., Fujita, T., Ingelfinger, J.R., and Nangaku, M. (2004). Transdifferentiation of cultured tubular cells induced by hypoxia. *Kidney International*, 65(3), pp. 871-880.

Mansur, S.A., Mieczkowska, A., Bouvard, B., Flatt, P.R., Chappard, D., Irwin, N., and Mabilleau, G. (2015). Stable incretin mimetics counter rapid deterioration of bone quality in type 1 diabetes mellitus. *Journal of Cellular Physiology*, 230(12), pp. 3009-3018.

Martini, F.H., Narth, J.L. and Bartholomew, E.F. (2015). *The Endocrine System. In:* Fundamentals of Human Anatomy and Physiology, 9th edition. Boston, Massachusetts:

Benjamin Cummings, pp. G10, 620-622.

Marieb, E.N. and Hoehn, K. (2013). *The Endocrine System. In*: Human Anatomy and Physiology. 9th edition, Pearson Education, Glenview, IL., pp. 591-630.

Mathers, C.D. and Loncar, D. (2006). Projections of Global Mortality and Burden of Disease from 2002 to 2030. *PLOS Med*, 3(11), pp. 2011-2030.

Mayer, J., Andrus, S.B., and Silides, D.J. (1953). Effect of diethyldithiocarbamate and other agents of mice with these obese-hyperglycemic Syndrome. *Endocrinology*, 53(5), pp. 572-581.

McEvoy, R.C., Andersson, J., Sandler, S., Hellerström, C. (1984). Multiple low-dose streptozotocin-induced diabetes in the mouse. Evidence for stimulation of a cytotoxic cellular immune response against an insulin-producing beta cell line. *The Journal of Clinical Investigation*, 74(3), pp. 715-722.

Mieczkowska, A., Mansur, S.A., Irwin, N., Flatt, P.R., Chappard, D., and Mabilleau, G. (2015). Alteration of the bone tissue material properties in type 1 diabetes mellitus: A Fourier transform infrared microspectroscopy study. *Bone*, 76, pp. 31-39.

Mihich, A., Mulhern, A.I., and Hornung, N. (1959). Inhibitory effect of Decamethylene-diguanide (Synthalin) against Leukaemia L1210 and Sarcoma 180 (Ascites). *Cancer Research*, 20(5 part 1), pp. 609-612.

Miller, M.R. and Wurster, D.H. (1958). Further studies on the blood glucose and pancreatic islets of lizards. *Endocrinology*, 63(2), pp. 191-200.

Mixner, J.P., Lennon, H.D., and Robertson, W.G. (1957). Effect of Synthalin A on blood glucose levels and liver function in dairy bull calves. *Journal of Dairy Science,* 40(8), pp. 973-976.

Modak, M., Dixit, P., Londhe, J., Ghaskadbi, S., Devasgayam, T.P.A. (2007). Indian herbs and herbal drugs used for the treatment for diabetes. *Journal of Clinical Biochemistry and Nutrition*, 40(3), pp. 163-173.

Moffett, R.C.R. (2013). Effects of gut hormones on metabolism and the morphology and function of pancreatic islets in pregnancy, obesity, and diabetes. Ph.D. University of Ulster.

Moin, A.S.M. and Butler, A.E. (2019). Alterations in beta cell identity in type 1 and type 2 diabetes. *Current diabetes reports*, 19(83), pp. 1-12.

Mosca, L. (1956). An experimental study of the cytology of pancreatic islets. *Quarterly Journal of Experimental Physiology and Cognate Medical Sciences*, 42(1), pp. 49-55.

Muranishi, T., Takehana, K., Hiratsuka, T., Kobayashi, A., Eerdunchaolu, I.K., and Mitsuo, ABE. (1999). An investigation of the relationship between duct system and A cell-rich and PP. cell-rich pancreatic islets in the canine pancreas. *Journal of Veterinary Medical Science*, 61, pp. 737-742.

Nangaku, M. and Eckardt, K.U. (2007). Hypoxia and the HIF system in kidney disease. *Journal of Molecular Medicine*, 85, pp. 1325-1330.

Nauck, El-Ouaghlidi, A., Hompesch, M., Jacobsen, J., Elbrønd, B. (2003). No impairment of

hypoglycemia counterregulation via glucagon with NN2211, a GLP-1 derivative, in subjects with type 2 diabetes. *Diabetes*, 52(suppl 1), pp. A128

Nauck, M.A., Wollschlager, D., Werner, J., Holst, J.J., Ørskov, C., Creutzfeldt, W., and Willms, B. (1996). Effects of subcutaneous glucagon like peptide 1 (GLP-1[7-36 amide]) in patients with NIDDM. *Diabetologia*, 39(12), pp. 1546-1553.

NICE: National Institute for Health and Care Excellence. (2012). Type 2 diabetes: prevention in people at high risk. Available at: https://www.nice.org.uk/guidance/ph38/chapter/1-recommendations#recommendation-12-providing-tailored-advice-on-physical-activity [Accessed on 26 Sep. 2016].

O' Brien, B.A., Harmon, B.V., Cameron, D.P., and Allan, D.J. (1996). Beta-cell apoptosis is responsible for the development of IDDM in the multiple low-dose streptozotocin model. *The Journal of Pathology*, 178(2), pp. 176-181.

Okail, M.S. (2010). Cobalt chloride, a chemical inducer of hypoxia-inducible factor-1α in U251 human glioblastoma cell line. *Journal of Saudi Chemical Society*, 14(2), pp. 197-201.

Östenson, C.-G. (1983). Effects of the biguanide Synthalin A on the pancreatic A2-cell of the guinea pig. *Experimental and Clinical Endocrinology and Diabetes*, 81(03), pp. 255-262.

Paik, S.-G., Michelis, M.A., Kim, Y.T., and Shin, S. (1982). Induction of insulin-dependent diabetes by streptozotocin inhinition by estrogens and potentiation by androgens. *Diabetes*, 31(8), pp. 724-729.

Park, I. and Bendayan, M. (1992). Coexistence of glucagon and pancreatic polypeptide in human and rat pancreatic endocrine cells. Endocrine Pathology, 3, pp. 134-43.

Parker, J.C., Andrews, K.M., Allen, M.R., Stock, J.L., and McNeish, J.D. (2002). Glycemic control in mice with targeted disruption of the glucagon receptor gene. *Biochemical and Biophysical Research Communications*, 290(2), pp. 839-843.

Parker, J.C., McPherson, R.K., Andrews, K.M., Levy, C.B., Dubins, J.S., Chin, J.E., Perry, P.V., Hulin, B., Perry, D.A., Inagaki, T., Dekker, K.A., Tachikawa, K., Sugie, Y., and Treadway, J.L. (2000). Effects of skyrin, a receptor-selective glucagon antagonist, in rat and human hepatocytes. *Diabetes*, 49(12), pp. 2079-2086

Pocock G. and Richards, C. (2009). *The Endocrine System. In:* The Human Body: An introduction for the Biomedical and Health Sciences. Oxford: Oxford University Press, pp. 283-326.

Pressman, B.C. (1962). The effects of guanidine and alkylguanidines on the energy transfer reactions of mitochondria. *Journal of Biological Chemistry*, 238(1), pp. 401-409.

Puck, T.T., Cieciura, S.J., Robinson, A. (1958). Genetics of somatic mammalian cells. III. Long-term cultivation of euploid cells from human and animal subjects. *The Journal of Experimental Medicine*, 108(6), pp. 945-956.

Quesada I., Tudurí, E., Ripoll, C., Nadal, Á. (2008). Physiology of the α-cell and glucagon secretion: role in glucose homeostasis and diabetes. *Journal of Endocrinology*, 199, pp. 5-19.

Quoix, N., Cheng-Xue, R., Guiot, Y., Herrera, P.L., Henquin, J.C., and Gilon, P. (2007). The GluCre-ROSA26EYFP mouse: a new model for easy identification of living pancreatic α-cells. *FEBS Letters*, 581 (22), pp. 4235-4240.

Rabinowitch, I.M. (1927). Observations on the use of Synthalin in the treatment of diabetes mellitus. *Canadian Medical Association Journal*, 17(8), pp. 901-904.

Rachman, J., Barrow, B.A., Levy, J.C., and Turner, R.C. (1997). Near-normalisation of diurnal glucose concentrations by continuous administration of glucagon like peptide-1 (GLP-1) in subjects with NIDDM. *Diabetologia*, 40(2), pp. 205-211.

Rall, L.B., Pictet, R.L., Williams, R.H., and Rutter, W.J. (1973). Early differentiation of glucagon-producing cells in embryonic pancreas: A possible developmental role for glucagon. *Proceedings of the National Academy of Sciences of the United States of America (PNAS),* 70, pp. 3478-3482.

Rao, M.R.R. and De, N.N. (1955). Studies on the origin of the hyperglycemic glycogenolytic factor (HGF). *Acta Endocinologica,* 18, pp. 293-298.

Reddy, S., Bibby, N.J., Elliott, R.B. (1985). Cellular distribution of insulin, glucagon, pancreatic polypeptide hormone and somatostatin in the fetal and adult pancreas of the guinea pig: a comparative immunohistochemical study. *Eur J Cell Biol*, 38, pp. 301-305.

Reynolds, T.Y., Rockwell, S., and Glazer, P.M. (1996). Genetic instability induced by the tumor microenvironment. *Cancer Research*, 56, pp. 5754-5757.

Riss, T.L., Moravec, R.A., Niles, A.L., Duellman, S., Benink, H.A., Worzella, T.J., and Minor, L. (2016). *Cell viability assays.* In: Assay Guidance Manual. Bethesda, Maryland, Eli Lilly and Company and the National Center for Advancing Translational Sciences; 2020, pp. 295-320.

Rivas, E., Newmire, D.E., Crandall, C.G., Hooper, P.L., and Ben-Ezra, V. (2016). An acute bout of whole passive hyperthermia increases plasma leptin, but does not alter glucose or insulin responses in obese type 2 diabetics and healthy adults. *Journal of Thermal Biology*, 59, pp. 26-33.

Roessner, C.A., Santander, P.J., and Scott, A.I. (2001). Multiple bioSynthetic pathways for vitamin B_{12}: variations on a central theme. *Vitamins and Hormones*, 61, pp. 267-297.

Rorsman, P. and Renström, E. (2003). Insulin granule dynamics in pancreatic beta cells. *Diabetologia*, 46(8), pp. 1029-1045.

Rossini, A.A., Williams, R.M., Appel, M.C., and Like, A.A. (1978). Sex differences in the multiple-dose streptozotocin model of diabetes. *Endocrinology*, 103(4), pp. 1518-1520.

Sacchi, T.B. and Bani, D. (1985). New views on the identification of the various cell types in the pancreatic islets of the rat. An ultrastructural and morphometrical study. *Acta Anatomica (Basel)*, 122(1), pp. 1-17.

Saker, F., Ybarra, J., Leahy, P., Hanson, R. W., Kalhan, S.C., and Ismail-Beigi, F. (1998). Glycemia-lowering effect of cobalt chloride in the diabetic rat: role of decreased gluconeogenesis. *American Journal of Physiology-Endocrinology and Metabolism*, 274(6),

pp. E984-E991.

Sataieva, T.P., Zadnipryany, I.V., and Zukow, W. (2019). Toxic cardiac effect of cobalt chloride excessive chronic consumption in male Winstar rats. *Ecological Questions*, 30, pp. 25-32.

Schnedl, W.J., Ferber, S., Johnson, J.H., and Newgard, C.B. (1994). STZ transport and cytotoxicity: specific enhancement in GLUT2-expressing cells. *Diabetes*, 43(11), pp. 1326-1333.

Schirrmacher, U.O. (1967). Case of cobalt poisoning. *British Medical Journal*, 1(5539), pp. 544-545.

Seaquist, E.R. (2004). Pancreatic Islet Hormones, Diabetes Mellitus, and Hypoglycemia. *In:* Niewoehner, C.B. *Endocrine Pathophysiology*. 2nd Edition. Raleigh, North Carolina: Hayes Barton Press, pp163-195.

Sigma-Aldrich (2019). Fetal Bovine Serum. Available at: https://www.sigmaaldrich.com/catalog/product/sigma/f8067?lang=en&region=GB. [Accessed on 1 November 2019].

Simonsen, L.O., Harbak, H., and Bennekou, P. (2012). Cobalt metabolism and toxicology- A brief update. *Science of the Total Environment,* 432, pp. 210-215.

Sørensen, H., Winzell, M.S., Brand, C.L., Fosgerau, K., Gelling, R.W., Nishimura, E., and Steiner, D.J., Kim, A., Miller, K., and Hara, M. (2010). Pancreatic islet plasticity: Interspecies comparison of islet architecture and composition. *Islets*, 2(3), pp. 135-145.

Steiner, D.J., Kim, A., Miller, K., and Hara, M. (2010). Pancreatic islet plasticity: Interspecies comparison of islet architecture and composition. *Islets,* 2(3), pp. 135-145.

Stoddart, M.J. (2011). Cell viability assays: introduction. *Mammalian Cell Viability.* In: *Methods in Molecular Biology*, 740, pp. 1-6.

Strober, W. (2001). Trypan blue exclusion test of cell viability. *Current Protocols in Immunology*, 21(1), pp. A.3B.1-A.3B.2.

Sundler, F., Hakanson, R., Lundquist, I., and Larrson, LI. (1977). Effect of alloxan on rat pancreatic polypeptide (PP) cells. *Cell and Tissue Research*, 178(3), pp. 307-312.

Sylvester, P.W. (2011). Optimization of the tetrazolium dye (MTT) colometric assay for cellular growth and viability. *Drug Design and Discovery.* In: *Methods in Molecular Biology*, 716, pp. 157-168.

Szkudelski, T. (2001). The mechanism of alloxan and streptozotocin actin in B cells of the rat pancreas. *Physiological Research*, 50(6), pp. 536-546.

Talchai, C., Xuan, S., Lin, H.V., Sussel, L., and Accili, D. (2012). Pancreatic β cell dedifferentiation as a mechanism of diabetic β cell failure. *Cell*, 150(6), pp. 1223-1234.

Takeda, Y., Fujita, Y., Honjo, J., Yanagimachi, T., Sakagami, H., Takiyama, Y., Makino, Y., Abiko, A., Kieffer, T.J., and Haneda, M. (2012). Reduction of both beta cell death and alpha

cell proliferation by dipeptidyl peptidase-4 inhibition in a streptozotocin induced model of diabetes in mice. *Diabetologia*, 55, pp. 404-412.

Tanday, N. (2019). Pharmacological modulation of pancreatic beta-to-alpha cell transdifferentiation in diabetes. Ph.D. University of Ulster.

Telib, M. (1972). Effects of cobaltous chloride in laboratory animals: The histological and electron microscopic changes in the islets of rabbits. *Endokrinologie*, 60(1), pp. 81-102.

Thaler, J.P. and Cummings, D.E. (2009). Hormonal and metabolic mechanisms of diabetes remission after gastrointestinal surgery. *Endocrinology*, 150(6), pp. 2518-2525.

Thomson, A.P., Gittins, R.J., and Thomas, G. (1932). Synthalin in the treatment of diabetes. *British Medical Journal*, 1, pp. 322-325.

Thorel, F., Damond, N., Chera, S., Wiederkehr, A., Thorens, B., Meda, P., Wollheim, C.B., and Herra, P.L. (2011). Normal glucagon signaling and β-cell function after near-total α-cell ablation in adult mice. *Diabetes*, 60(11), pp. 2872-2882.

Thorel, F., Népote, V., Avril, I., Kohno, K. Desgraz, R., Chera, S., and Herrera, P.L. (2010). Conversion of adult pancreatic α-cells to β-cells after extreme β-cell loss. *Nature*, 464(7292), pp. 1149-1154.

Thulesen, J., Ørskov, C., Holst, J.J., and Poulsen, S.S. (1997). Short term insulin treatment prevents the diabetogenic action of streptozotocin in rats. *Endocrinology*, 138(1), pp. 62-68.

Tjälve, H., Wilander, E., and Johansson, E.B. (1976). Distribution of labelled streptozotocin in mice: uptake and retention in pancreatic islets. *Journal of Endocrinology*, 69(3), pp. 455-456.

Trimble, E.R., Halban, P.A., Wollheim, C.B., and Renold, A.E. (1982). Functional differences between rat islets of ventral and dorsal pancreatic origin. *The Journal of Clinical Investigation*, 69(2), pp. 405-413.

Unruh, A., Ressel, A., Mohamed, H.G., Johnson, R.S., Nadrowitz, R., Richter, E., Katschinski, D.M., and Wenger, R.H. (2003). The hypoxia-inducible factor-1α is a negative factor for tumor therapy. *Oncogene*, 22, pp. 3213-3220.

USRDS: United States Renal Data System (2014). *2014 ADR Chapters.* Available at: https://www.usrds.org/2014/view/Default.aspx [Accessed 17 Sep. 2016].

Van Campenhout, E. (1955). The cytotoxic effect of cobalt salts on the alpha cells of the islands of Langerhans. *Journal of Experimental Zoology*, 129(3), pp. 535-559.

Van Campenhout, E. and Cornelis, G. (1960). Destruction experimentale der cellular alpha der ilots endocriner du pancreas chez le cabaze. *Compt. Rend. Soc. Biol.*, 145, pp. 933-935.

Van Campenhout, E. and Cornelis, G. (1951). Destruction expérimentale des cellules alpha des ilots endocrines du pancreas chez le cobaye. *Comptes Rendus Biologies*, 145, pp. 933-935.

Van der Meulen, T. and Huising, M.O. (2015). Role of transcription factors in the

transdifferentiation of pancreatic islet cells. *Journal of Molecular Endocrinology*, 54(2), pp. R103-R117.

Van der Valk, J., Bieback, K., Buta, C., Cochrane, B., Dirks, W.G., Fu, J., Hickman, J.J., Hohensee, C., Kolar, R., Liebsch, M., Pistollato, F., Schulz, M., Thieme, D., Weber, T., Wiest, J., Winkler, S., and Gstraunthaler, G. (2018). Fetal bovine serum (FBS): past-present-future. *ALTEX: Alternatives to animal experimentation*, 35(1), pp. 99-118.

Vasu, S., Moffett, R.C., Thorens, B., and Flatt, P.R. (2014). Role of endogenous GLP-1 and GIP in beta cell compensatory responses to insulin resistance and cellular stress. PloS One, 9(6), pp. 1-9.

Vasu, S., Moffett, R.C., McClenaghan, N.H., and Flatt, P.R. (2015). Responses of GLP1-secreting L-cells to cytotoxicity resemble pancreatic β-cells but not α-cells. *Journal of Molecular Endocrinology*, 54(1), pp. 91-104.

Vasudevan, H. and McNeil J.H. (2006). Chronic cobalt treatment decreases hyperglycemia in streptozotocin- diabetic rats. *BioMetals*, 20, pp. 129-134.

Vengellur, A., Woods, B.G., Ryan, H.E., Johnson, R.S., and Lapres, J.J. (2003). Gene expression profiling of the hypoxia signaling pathway in hypoxia-inducible factor 1α null mouse embryonic fibroblasts. *Gene Expression: The Journal of Liver Research*, 11(3-4), pp. 181-197.

Vistica, D.T., Skehan, P., Scudiero, D., Monks, A., Pittman, A., and Boyd, M.R. (1991). Tetrazolium-based assays for cellular viability: a critical examination of selected parameters affecting formazan production. *Cancer Research*, 51(10), pp. 2515-2520.

Volk, B.W., Lazarus, S.S., and Goldner, M.G. (1953). Alpha cell damage and blood sugar changes in rabbits after administration of cobalt. *Experimental Biology and Medicine/Society for Experimental Biology and Medicine,* 82(3), pp. 406-411.

Wang, G.L., and Semenza, G.L. (1993). Characterization of hypoxia-inducible factor 1 and regulation of DNA binding activity by hypoxia. *Journal of Biological Chemistry*, 268(29), pp. 21513-21518.

Wang, Z., York, N.W., Nichols, C.G., and Remedi, M.S.(2014). Pancreatic β cell dedifferentiation in diabetes and redifferentiation following insulin therapy. *Cell Metabolism*, 19(5), pp. 872-882.

Watanabe, C.K. (1918). Studies in the metabolic changes induced by administration of guanidine bases. *The Journal of Biological Chemistry*, 33, pp. 253-265.

Weir, G.C., Goltsos, P.C., Steinberg, E.P., and Patel, Y.C. (1976). High concentration of somatostatin immunoreactivity in chicken pancreas. *Diabetologia,* 12, pp. 129-132.

Weyerman, J., Lochmann, D., Zimmer, A. (2005). A practical note on the use of cytotoxicity assays. *International Journal of Pharmaceutics*, 288(2), pp. 369-376.

Whalley, N.M., Pritchard, L.E., Smith, D.M.m, and White, A. (2011). Processing of proglucagon to GLP-1 in pancreatic α-cells: is this a paracrine mechanism enabling GLP-1 to act on β-cells? *Journal of Endocrinology*, 211(1), pp. 99-106.

WHO: The World Health Organization. (2016). *Diabetes: Key Facts.* Available at: http://www.who.int/mediacentre/factsheets/fs312/en/ [Accessed 18 Sep. 2016].

Wieczorek, G., Pospischil, A., and Perentes, E. (1998). A comparative immunohistochemical study of pancreatic islets in laboratory animals (rats, dogs, minipigs, nonhuman primates). *Experimental and Toxicologic Pathology*, 50, pp. 5-19.

Wojtaszewski, J.F., Hansen, B.F., Kiens, B., Markuns, J.F., Goodyear, L.J., and Richter, E.A. (2000). Insulin signaling and insulin sensitivity after exercise in human skeletal muscle. *Diabetes*, 49(3), pp. 325-331.

Wright, P.H. (1959). The effect of insulin antibodies on glucose uptake by the isolated rat diaphragm. *Biochemical Journal*, 71(4), pp. 633-638.

Ybarra, J., Behrooz, A., Gabriel, A., Koseoglu, M.H., and Ismail-Beigi, F. (1997). Glycemia-lowering effect of cobalt chloride in the diabetic rat: increased GLUT1 mRNA expression. *Molecular and Cellular Endocrinology*, 133(2), pp. 151-160.

Ye, L., Robertson, M.A., Hesselson, D., Stainer, D.Y.R., and Anderson, R.M. (2015). Glucagon is essential for alpha cell transdifferentiation and beta cell neogenesis. *Development*, 142(8), pp. 1407-1417.

Zheng, X., Zheng, X., Wang, X., Ma, Z., Sunkari, V.G., Botusan, I., Takeda, T., Björklund, A., Inoue, M., Catrina, S-B., Brismar, K., Poellinger, L., and Pereira, T.S. (2012). Acute hypoxia induces apoptosis of pancreatic B-cell by activation of the unfolded protein response and upregulation of CHOP. *Cell Death and Disease*, 3(e322), pp. 1-11.

Zhou, G., Myers, R., Li, Y. Chen, Y., Shen, X., Fenyl-Melody, J., Wu, M., Ventre, J., Doebber, T., Fujii, N., Musi, N., Hirshman, M.F., Goodyear, L.J., and Moller, D.E. (2001). Role of AMP-activated protein kinase in mechanism of metformin action. *The Journal of Clinical Investigation*, 108(8), pp. 1167-1174.

Zhou, Y-X., Zhang, H., and Peng, C. (2014). Puerarin: A review of pharmacological effects. *Phytotherapy Research*, 28(7), pp. 961-975.